Bioactive Secondary Metabolites from Medicinal Plants

(Bioaktive Sekundärmetabolite aus Medizinalpflanzen)

Inaugural dissertation

for the attainment of the title of doctor
in the Faculty of Mathematics and Natural Sciences
at the Heinrich Heine University Düsseldorf

presented by

Rini Muharini
from Pontianak, Indonesia

Düsseldorf, 09.2016

from the institute for Pharmaceutical Biology and Biotechnology
at the Heinrich Heine University Düsseldorf

Published by permission of the
Faculty of Mathematics and Natural Sciences at
Heinrich Heine-University Düsseldorf

Supervisor: Prof. Dr. Peter Proksch
Co-supervisor: Prof. Dr. Rainer Kalscheuer

Date of the oral examination: /10/2016

Declaration of Academic Honesty/Erklärung

Hiermit erkläre ich ehrenwörtlich, dass ich die vorliegende Dissertation mit dem Titel “Bioaktive Sekundärmetabolite aus Medizinalpflanzen“ selbst angefertigt habe. Außer den angegebenen Quellen und Hilfsmitteln wurden keine weiteren verwendet. Diese Dissertation wurde weder in gleicher noch in abgewandelter Form in einem anderen Prüfungsverfahren vorgelegt. Weiterhin erkläre ich, dass ich früher weder akademische Grade erworben habe, noch dies versucht habe.

Düsseldorf, den 07.09.2016

Rini Muharini

Acknowledgments

First of all, I would like to express my heartfelt appreciation and gratitude to Prof. Prof. h.c. Dr. rer. nat. Peter Proksch for giving me this precious opportunity to pursue my doctoral study in medicinal plants natural products with the excellent working condition and facilities at the Institute Pharmaceutical Biology and Biotechnology, Heinrich-Heine University, Duesseldorf. I wish to express my sincere gratitude and indebtedness to him for his admirable supervision, his patient guidance, his fruitful discussion, his constant encouragement, his remarkable support and affection during the period of my study and preparing of this thesis, in both work and life issues.

My sincere appreciation and gratitude to Prof. Dr. rer. nat. Rainer Kalscheuer (Institute of Pharmaceutical Biology and Biotechnology, Henrich-Heine University Duesseldorf) for conducting antimicrobial assays and for evaluating my doctorate study as second referee.

I would like to express my cordial thank to Prof. Dr. Wenhan Lin (National Research Laboratories of Natural and Biomimetic Drugs, Peking University, Health Science Center) for his fruitful discussion and constructive advises with regards to structure elucidation issues.

I would like to extend my special thank to Prof. Dr. Bingui Wang (Laboratory of Experimental Marine Biology, Institute of Oceanology, Chinese Academy of Science), and Prof. Haofu Dai (Institute of Chinese Academy, Haikou) for pleasant discussion and advises.

I extend my deep thanks to Prof. Dr. Tibor Kurtán for helping in CD measurement and calculation, and Prof. Dr. rer. nat. Werner E. G. Müller (Institute of Physiological Chemistry and Pathobiochemistry, University of Mainz) for carrying out cytotoxicity assays during my study.

I truly appreciate to Prof. Dr. Clauss Passreiter (Institute of Pharmaceutical Biology and Biotechnology, Henrich-Heine University Duesseldorf) for his support and help in safety work in the laboratory.

I want to express my sincere gratitute to Ms. Claudia Eckelskemper for her hospitality, kindness and administrative help whenever needed, to Mrs. Waltraud Schlag, Mrs. Simone Miljanovic, Mrs. Heike Goldbach-Gecke, Mrs. Katja Friedrich, Mrs. Eva Müller, Mr. Klaus Dieter Jansen, Mrs. Simone Mönninghoff-Pützer, and Ms. Linda Weigand for their kindness, nice conversations and all help in any technical problems encountered during lab work.

I wish to extend my special thank to Nidja Rehberg (Institute of Pharmaceutical Biology and Biotechnology, Henrich-Heine University Duesseldorf) for collaborating in microbial assays.

Acknowledgments

My deepest thanks to Dr. Peter Tommes, Mr. Ralf Bürgel, Ms. Maria Beuer, and Ms. Renata Steffen for all help in the measurement of ESI/HRESIMS and NMR as well as performing cytotoxicity assay, respectively.

My sincere thank to Dr. Rudolf Hartmann (Institute of Complex Systems (ICS-6), Forschungszentrum Jülich Gmb) for measuring NMR, nice discussion with regards to the structure elucidation of my substances and showing me around the NMR facilities in his Institute.

My profound gratitude to all former and recent postdocs at the institute, Dr. Amal Hassan, Dr. Abdessamad Debbab, Dr. Daowan Lai, Dr. Zhen Liu, Dr. Weaam Ebrahim, Dr. Georgios Daletos, Dr. Elena Ancheeva, Dr. Ramsay Kadeem and Dr. Rudiyansyah for scientific advises, fruitful discussion, sharing expertise and warm fellowship.

I truly appreciate Dr. Antonius Ola and his family, for welcoming me in their warm house in the first week of my staying in Duesseldorf and accompanying my PhD live journey for one and half year with their warmness and kindness. My sincere thank to Dr. Antonius Ola and Dr. Robert Bara, for guiding me before entering the institute until I can walk by myself and for giving away the stuff and cooking utensil, which I needed, for free.

I would like to profound my sincere thank and grateful to my former and recent colleagues at the institute, Heinrich-Heine University Duesseldorf: Dr. Robert Bara, Dr. Antonius R.B Ola, Dr. Mustapha ElAmrani, Dr. David Roensberg, Dr. Andreas Marmann, Dr. Cong-Dat Pham, Dr. Lena Hammerschmidt, Dr. Hendrik Niemann, Dr. Mousa Al Tarabeen, Dr. Raha S. Orfali, Dr. Huiqin Chen, Dr. Yang Liu, Dr. Sergi Herve Akone, Imke Form, Catalina Pérez Hempfill, Mi-Young Chung, Amin Mokhlesi, Arta Kuci, Ingo Kolb, Shuai Liu, Hao Wang, Marian Frank, Mariam Moussa, Haiqian Yu, Nam Michael Tran-Cong, Mohamed El-Naggar, Ferhat Oezkaya, Dr. Fang Lv, Dr. Yanbo Zeng, Dr. Blessing Omeukoli, Adriana Diaz, Dr. Festus B.C Okoye, Dr. Mario Tan, Catharine Bogner, Nihal Aktas, Tatiana Medvedeva, Houda, Fatima Kabbaj, Ilias Marmouzi, Sathishkumar Arumugam, Yaolong Liu, Dr. Edwin, Peter Eze, Nihad, Dr. Ken, Andrei Whaley, Lisa Anne Küppers, Jens Hagenow, Stefanie Kaßel, Paula-Oxana Giesa, Kathrin Papadopoulos, Pamela Namo, Linhong Meng, Dr. Justina, and Dr. Chika for sharing not only knowledge and skills, but also laugh and tears, maintaining a nice environment in and outside the laboratory work, and having all multicultural times together. I can still vaguely recall the memory with all of you one by one as I write your name. I really enjoy our treasure time together, thank you very much!!

Acknowledgments

My sincere thank to Dr. Chaidir Amin for broadening my horizontal view with regards to natural products research in Indonesia and introducing me with a wonderful family, kak Novi Pulungan and kak Timmy.

My special thank to all my friends in Kajian Muslimah Ruhr (KMR) and Perhimpunan Pelajar Indonesia (PPI) Duisburg-Essen for spending time together.

I would like to express my special thank to Ms. Natalia Celia Vich Redondo, Mrs. Marion Lahusen, Mr. Ruddy Lammert and Mrs. Gitta Lammert for opening their house and heart for me. I will remember all of you always.

I am feeling blessed to all my colleagues in the Department of Educational Chemistry, Tanjungpura University, for their understanding, their supporting and kind help with regards to administration needed for my carrier.

I am grateful to Directorate General of Higher Education, the Ministry of Research, Technology and Higher Education of the Republik of Indonesia, for financial support during my study in Germany

My heartfelt thank to my beloved parents, Abdul Gafar Sjamsu and Lisma Djuwita, my brothers Ferry Sagori and Gazali for continuous trusting and encouraging me. My father, who sincerely supported me to go study abroad even he knew that it would be far away from him, yet he was so ill and could not see when it is finally accomplished. Pa, this accomplishment is for you. I wish to extend my deep thanks to my parents in law, Arsjad Djamal and Azizah as well as to my sisters and brothers in law for their understanding, continuous encouragement, and spiritual support.

Last, but certainly not least, I would like to profound my deepest appreciation and gratitude to my dear husband, Dr. Rudiyansyah, for his continuous trusting and supporting, his valuable critics, advises and discussion, and for always be my side, spiritually and/or physically, as a husband, a friend or a colleague, in happy and difficult times.

To all of you, thank you very much!!!

Abstract

Natural products have been a reservoir of diverse structures that lead to pharmacologically active compounds, lead compounds or new chemical entities in drug discovery. At present, one quarter of all approved small molecular drugs are based on natural products or natural product derivatives. Terrestrial plants are a major source of natural products. Especially plants used in traditional medicine systems are mostly chosen as material for chemical investigation to discover pharmacologically active compounds. This dissertation describes secondary metabolites isolated from four medicinal plants including *Sarcotheca griffithii* and *Piper retrofractum* collected from Indonesia, *Talinum triangulare* collected from Nigeria and *Amorpha fruticosa* collected from Germany. The structure of the isolated compounds was unambiguously elucidated by one- and two-dimensional NMR spectroscopy, mass spectroscopy and by comparison with literature data. The absolute configurations were determined by ECD calculations or by comparison of optical rotation and CD with literature data. The isolated compounds were tested for their antifungal, antibacterial and cytotoxic activities. All obtained results were published or submitted for publication in respective international journals. This dissertation consists of the following parts:

Sarcotheca griffithii

This is the first report of secondary metabolites from the genus *Sarcotheca* (Oxalidacae). From the methanolic extract of leaves of *S. griffithii*, six flavonoid C-glucosides were isolated. Five of them are new compounds including chrysin 6-C-(2″-O-α-L-rhamnopyranosyl)-*β*-D-glucopyranoside (**1**), chrysin 6-C-(2″-O-α-L-rhamnopyranosyl)-*β*-D-glucopyranosyl-7-O-*β*-D-glucopyranoside (**2**), chrysin 6-C-(2″-O-α-L-rhamnopyranosyl)-β-L-fucopyranoside (**3**), chrysin 6-C-(2″-O-α-L-rhamnopyranosyl)-6′-deoxy-*ribo*-hexos-3-uloside (**4**), chrysin 6-C-*β*-boivinopyranosyl-7-O-*β*-L-glucopyranoside (**5**). The known compound isovitexin 2″-O-α-L-rhamnopyranoside (**6**) is the major compound. Their structures were elucidated by analysis of NMR and MS data as well as by comparison with literature data. The absolute configuration of glucose and rhamnose moieties were determined by acid hydrolysis and ester derivatization followed by TLC analysis and comparison of its Rf values with those of the authentic standards. Chemical investigation of *S.griffithii* led to the suggestion that chrysin C- glycosides seemed to be the chemotaxonomic marker of this species. The crude extract and fractions were found to not be active against the L5178Y mouse lymphoma cell line.

Abstract

Piper retrofractum

The genus *Piper* (Piperaceae) is known worldwide as an important spice and medicinal plant. For this study, the fruits of *P.retrofractum* were collected in Indonesia. Chromatographic separation of the methanolic extract gave three new amides, namely (2*E*,14*Z*)-*N*-isobutyleicosa-2,14-dienamide (**1**), dipiperamide F (**2**) and G (**3**), together with 30 known compounds. Their structures were determined by analysis of the obtained 1D and 2D NMR spectra as well as MS data and by comparison with literature data. The isolated compounds were classified as long chain alkylamides, methylenedioxyphenyl amides, cyclobutanamides and cyclohexenamides. Plausible biosynthetic pathwaysare discussed in this study. Preliminary assays of all isolated compounds against the fungus *Cladosporium cladosporioides* revealed that piperanine was active. All isolated compounds were also tested for their cytotoxicity against the L5178Y mouse lymphoma cell line. Three cyclobutanamides, dipiperamide F and G (**2** and **3**), nigramide R (**31**); one cyclohexenamide,chabamide (**30**); four methylenedioxyphenyl amide, dehydropipernonaline (**25**), guineensine (**22**), brachystamide B (**23**), retrofractamide C (**20**), and two alkylamides, pellitorine (**13**), pipericine (**14**) displayed considerable cytotoxicity with IC_{50} values of 10.0, 13.9, 11.6, 9.3, 8.9, 17.0, 16.4, 13.4, 28.3, and 24.3 μM, respectively. Structure-activity relationships of cytotoxic amides are discussed.

Talinum triangulare

Chromatographic investigation of the methanolic extract from the roots of *Talinum triangulare* (Portulacaceae) from Nigeria yielded two new *C*-methylated flavonoids, 5,6-dimethoxy-7-hydroxy-8-methyl-flavone (**1**), 5,6-dimethoxy-8-methyl-2-phenyl-7*H*-1-benzopyran-7-one (**2**), and one new α-pyrone derivative, 4-methoxy-6-(2-hydroxy-4-phenylbutyl)-2*H*-pyran-2-one (**3**), together with thirteen known compounds including nine amides (**4**-**12**), indole-3-carboxylic acid (**13**), *p*-hydroxy benzoic acid (**14**), and two steroids (**15**-**16**). Extensive analysis of NMR and MS data as well as comparison with literature data was performed to determine their structures. All isolated compounds were subjected to cytotoxic assay against the mouse lymphoma L5178Y cell line and antifungal assay against *Cladosporium cladosporioides*. However, none of them showed significant activity.

Abstract

Amorpha fruticosa

The dichloromethane-methanol extract of fruits of *Amorpha fruticosa* (Fabaceae) was separated using various chromatography techniques. Fourteen new natural products including 2-[(*Z*)-styryl]-5-geranyl-resorcin-1-carboxylic acid (**1**), amorfrutin D (**2**), demethoxyamorfrutin D (**3**), 8-geranyl-3,5,7-trihydroxyflavanone(**13**), 8-geranyl-3′,5,7-trihydroxy-4′-methoxyisoflavone(**14**), 6-geranyl-3′,5,7-trihydroxy-4′-methoxyisoflavone (**15**), 8-geranyl-3′,7-dihydroxy-4′-methoxyisoflavone (**16**), 3-demethoxydalbinol (**42**), 6a,12a-dehydro-3-demethoxyamorphigenin (**43**), (6a*R*,12a*R*,5′*R*)-amorphigenin (**44**), amorphispironone B−C (**45**−**46**), resokaempferol 3-O-*β*-D-glucopyranosyl-(1→2)-*β*-D-glucopyranoside-7-O-*α*-L-rhamnopyranoside (**51**), and daidzein 7-O-*β*-D-glucopyranosyl-(1→2)-*β*-D-glucopyranoside (**52**) as well as 40 known compounds were isolated. Their structures were unambiguously established by extensive 1D and 2D NMR spectroscopic analyses as well as by mass-spectrum data. CD calculations or comparison of CD with literature data were involved in determination of the absolute configuration of **11**, **42**, **44** and **45**. The sugar moieties were characterized using acid hydrolysis of the respective glycosides, derivatization, and HPLC analysis with comparison to authentic standards. All isolated compounds were tested for their antibacterial and cytotoxic activities. Compounds **1**, **4**, **5**, **7**, **8**, **12**−**15** displayed potent to modest antibacterial activities against several gram-positive bacteria. In addition, compounds **10**, **13**, **25**, **27**, **30**, **32**, **34**, **35**, **37**, **41**, **45**, **48** and **53** exhibited significant cytotoxicity against the L5178Y mouse lymphoma cell line. The structure-activity relationships of respective antibacterial and cytotoxic compounds are discussed. Plausible biosynthetic pathways leading to bibenzyl and rotenoids isolated in this study were proposed.

Zusammenfassung

Naturstoffe bieten eine große Vielfalt unterschiedlicher Strukturen, die zu pharmakologisch aktiven Substanzen, Leitstrukturen oder neuen chemischen Entitäten in der Medikamentensuche führen. Derzeit basieren ein Viertel aller zugelassenen Arzneimittel niedrigen Molekulargewichtes auf Naturstoffen oder deren Derivaten. Terrestrische Pflanzen stellen die Hauptquelle der Naturstoffe dar. Vor allem Pflanzen, welche in traditionellen medizinischen Systemen verwendet werden, werden als Material für chemische Untersuchungen, um pharmakologisch aktive Substanzen zu finden, ausgewählt. Diese Dissertation beschreibt Sekundärmetabolite, die aus vier medizinisch relevanten Pflanzen isoliert wurden, wie *Sarcotheca griffithii* und *Piper retrofractum* aus Indonesien, *Talinumtriangulare* aus Nigeria und *Amorpha fruticosa* aus Deutschland. Die Strukturen der isolierten Substanzen wurden eindeutig durch ein- und zwei dimensionale NMR-Spektroskopie, Massenspektroskopie und durch Vergleich mit Literaturstellen aufgeklärt. Die absolute Konfiguration wurde durch ECD Berechnungen oder durch Vergleich der optischen Drehung und CD Spektren mit Literaturdaten ermittelt. Die isolierten Substanzen wurden auf antimykotische, antibakterielle und zytotoxische Aktivitäten getestet. Alle erhaltenen Ergebnisse wurden publiziert oder für eine Veröffentlichung in internationalen Zeitschriften eingereicht. Diese Dissertation besteht aus folgenden Teilen:

Sarcothecagriffithii

Dies ist der erste Bericht über Sekundärmetabolite aus der Gattung *Sarcotheca* (Oxalidacae). Aus dem methanolischen Extrakt der Blätter von *S. griffithii* wurden sechs Flavonoid-C-Glukoside isoliert. Fünf von ihnen sind neue Substanzen wie Chrysin 6-C-(2″-O-α-L-Rhamnopyranosyl)-*β*-D-Glukopyranosid (**1**), Chrysin 6-C-(2″-O-α-L-Rhamnopyranosyl)-*β*-D-Glukopyranosyl-7-O-*β*-D-Glukopyranosid (**2**), Chrysin 6-C-(2″-O-α-L-Rhamnopyranosyl)-*β*-L-Fucopyranosid (**3**), Chrysin 6-C-(2″-O-α-L-rhamnopyranosyl)-6′-Deoxy-*ribo*-hexos-3-Ulosid (**4**), Chrysin 6-C-β-Boivinopyranosyl-7-O-*β*-L-Glukopyranosid (**5**). Die bekannte Substanz Isovitexin 2″-O-α-L-Rhamnopyranosid (**6**) ist die Hauptkomponente. Die Strukturen wurden mit Hilfe von NMR- und MS-Daten, sowie durch Vergleich mit Daten aus Literaturstellen verglichen und identifiziert. Die absolute Konfiguration der Glukose- und Rhamnose-Reste wurde mittels saurer Hydrolyse und Ester-Derivatisierung und anschließendem Vergleich der R_f-

Zusammenfassung

Werte von DC-Analysen mit authentischen Standards ermittelt. Die Chemischen Untersuchungen von *S. griffithii* legen nahe, dass Chrysin C-Glykoside der chemotaxonomische Marker dieser Spezies sind. Der Rohextrakt und die Fraktionen waren nicht aktiv gegenüber der Mauslymphomzelllinie L5178 Y.

Piper retrofractum

Die Gattung *Piper* (Piperaceae) ist weltweit als Gewürz und Medizinalpflanze bekannt. Die Früchte von *P. retrofractum* wurden in Indonesien gesammelt. Die chromatographische Auftrennung des methanolischen Extrakts ergab drei neue Amide, (2*E*,14*Z*)-*N*-isobutyleicosa-2,14-dienamid (**1**), dipiperamid F (**2**) and G (**3**), zusammen mit 30 bekannten Substanzen. Ihre Strukturen wurden weitgehend durch 1D- und 2D-NMR Spektroskopie sowie MS-Daten und Vergleich mit Literaturdaten ermittelt. Die isolierten Substanzen wurden als langkettige Alkylamide, Methylendioxyphenylamide, Cyclobutanamide und Cyclohexenamide klassifiziert. Plausible Biosynthesewege wurden in dieser Arbeit diskutiert. Alle isolierten Substanzen wurden auf ihre Toxizität gegenüber der Mauslymphomzelllinie L5178Y getestet. Drei Cyclobutanamide, Dipiperamid F und G (**2** und **3**), Nigramid R (**31**); ein Cyclohexenamide, Chabamid (**30**); vier Methylendioxyphenylamide, Dehydropipernonalin (**25**), Guineensin (**22**), Brachystamid B (**23**), Retrofractamid C (**20**), und zwei Alkylamide, Pellitorin (**13**), Pipericin (**14**) wiesen eine deutliche Zytotoxizität mit IC_{50}-Werten von 10,0; 13,9; 11,6; 9,3; 8,9; 17,0; 16,4; 13,4; 28,3 und 24,3 µM auf . Struktur-Wirkungsbeziehungen von zytotoxischen Amiden wurden diskutiert.

Talinumtriangulare

Chromatographische Untersuchungen des methanolischen Extrakts der Wurzeln von *Talinumtriangulare* (Portulacaceae) aus Nigeria erbrachten zwei neue *C*-methylierteFlavonoide, 5,6-Dimethoxy-7-Hydroxy-8-Methyl-Flavon (**1**), 5,6-Dimethoxy-8-Methyl-2-Phenyl-7H-1-Benzopyran-7-on (**2**), und ein neues α-Pyron-Derivat, 4-Methoxy-6-(2-Hydroxy-4-Phenylbutyl)-2*H*-Pyran-2-on (**3**), zusammen mit 13 bekannten Substanzen, unter denen sich neun Amide (**4-12**), Indol-3-Carbonsäure (**13**), *p*-Hydroxybenzoesäure (**14**), und zwei Steroide (**15-16**)befinden. Umfassende NMR- und MS-Datenanalysen sowie der Vergleich von Literaturdaten führten zur Ermittlung der Strukturen. Alle isolierten Substanzen wurden zytotoxischen Test gegen der

Mauslymphomzelllinie L5178 Y und antimykotischen Test gegen *Cladosporiumcladosporioides* unterzogen. Keine Substanz zeigte eine signifikante Aktivität.

Amorphafruticosa

Der Dichlormethan-Methanol Extrakt der Früchte von *Amorphafruticosa*(Fabaceae) wurden über verschiedene chromatographische Techniken aufgetrennt. Es wurden 14 neue Naturstoffe wie 2-[(*Z*)-Styrol]-5-Geranyl-Resorcin-1-Carbonsäure (**1**) Amorfrutin D (**2**), Demethoxyamorfrutin D (**3**), 8-Geranyl-3,5,7-Trihydroxyflavanon(**13**), 8-Geranyl-3′,5,7-Trihydroxy-4′-methoxyisoflavon(**14**), 6-Geranyl-3′,5,7-Trihydroxy-4′-Methoxyisoflavon (**15**), 8-Geranyl-3′,7-Dihydroxy-4′-Methoxyisoflavon (**16**), 3-Demethoxydalbinol (**42**), 6a,12a-Dehydro-3-Demethoxyamorphigenin (**43**), (6a*R*,12a*R*,5′*R*)-Amorphigenin (**44**), Amorphispironon B−C (**45**−**46**), Resokaempferol 3-O-*β*-D-Glukopyranosyl-(1→2)-*β*-D-Glukopyranosid-7-O-*α*-L-Rhamnopyranosid (**51**), und Daidzein 7-O-*β*-D-Glukopyranosyl-(1→2)-*β*-D-Glukopyranosid(**52**) sowie 40 bekannte Substanzen isoliert. Ihre Strukturen wurden eindeutig mit Hilfe umfassender 1D- und 2D NMR spektroskopischer Analysen sowie durch massenspektroskopische Daten aufgeklärt. CD Berechnungen oder der Vergleich von CD-Spektren mit Literaturdaten wurden zur Bestimmung der absoluten Konfiguration von **11**,**42**, **44** und **45** einbezogen. Die Zuckerreste wurden durch saure Hydrolyse der betreffenden Glykoside, Derivatisierung und HPLC Analyse mit entsprechenden Standards charakterisiert. Alle isolierten Substanzen wurden auf ihre antibakterielle und zytotoxische Aktivität getestet. Die Substanzen **1**, **4**, **5**, **7**, **8**, **12**−**15** wiesen potente bis moderate antibakterielle Aktivitäten gegen einige gram positive Bakterien auf. Die Substanzen **10**, **13**, **25**, **27**, **30**, **32**, **34**, **35**, **37**, **41**, **45**, **48** und **53** zeigten signifikante Zytotoxizitäten gegenüber der Mauslymphomzelllinie L5178Y. Die Struktur-Wirkungsbeziehungen der betreffenden antibiotischen und zytotoxischen Substanzen wurdendiskutiert. Plausible Biosynthesewege, die zu den isolierten Bibenzyl und Rotenoiden führen, wurden in dieser Arbeit vorgeschlagen

Contents

CONTENTS

1 Introduction 1
- 1.1 Significant of Study 2
- 1.2 Natural Products 2
  - 1.2.1 Alkaloids 3
  - 1.2.2 Terpenoids 3
  - 1.2.3 Flavonoids 4
- 1.3 Medicinal Plants as Source of Bioactive Natural Products 4
- 1.4 The Role of Plant-derived Natural products in Drug Discovery 6
- 1.5 Current plant-derived Natural Products in Therapeutic Use and Clinical 7
  - 1.5.1 Galantamine 7
  - 1.5.2 Artemisinine 7
  - 1.5.3 Paclitaxel 7
  - 1.5.4 Calanolide A 8
- 1.6 *Sarcotheca griffithii* (Hook F) Hallier F 8
- 1.7 *Piper retrofractum* 10
- 1.8 *Talinum triangulare* 12
- 1.9 *Amorpha fruticosa* 12
- 1.10 Aims and Scope of the Study 14

2 Publication 1 15
- 2.1 New flavones C-glycosides from leaves *Sarcotheca griffithii* (Hook F) Hallier F 15

3 Publication 2 50
- 3.1 New amides from the fruits of *Piper retrofractum* 50

4 Publication 3 80
- 4.1 New C-methylated flavonoids and α-pyrone derivative from roots of *Talinum triangulare* growing in Nigeria 80

5 Publication 4 86
- 5.1 Antibacterial and cytotoxic phenolic metabolites from fruits of *Amorpha fruticosa* 86

6 Discussion 207
- 6.1 Isolated Natural Products from *Sarcotheca griffithii* (Hook F) Hallier F 207
  - 6.1.1 Flavone C-glycosides 207
  - 6.1.2 Biological activity of Chrysin C-glycosides 208
- 6.2 Isolated Natural Product from *Piper retrofractum* 209
  - 6.2.1 Piperamides 209
  - 6.2.2 Biological activity of Piperamides 213
  - 6.2.2.1 Antifungal activity of Piperamides 213
  - 6.2.2.2 Cytotoxicity activity of Piperamides 214

Contents

6.3 Isolated Natural Product of *Talinum Triangulare* 215
6.3.1 C-Methylated Flavonoids 215
6.3.2 α-Pyrone 216
6.3.3 Lignanamides and Aurantiamides 217
6.4 Isolated Natural Products of *Amorpha fruticosa* 218
6.4.1 Amorfrutins 218
6.4.2 Rotenoids 219
7 Further Scientific Achievements 224
8 References 225
9 List of Abbreviations 237
10 Research Contribution 240
11 Curriculum Vitae 241

Introduction

1. Introduction

Plants are an attractive source of new therapeutic candidates since tremendous chemical diversity is found in thousands of species of flowering plants, conifers, bryophytes and ferns. Estimation of the amount of identified plant species is now around 374,000, including 295,383 species of flowering plants (Christenhusz, 2016). The highest diversity of plants occurs in the old world, particularly in the tropical rainforest region.

Throughout the millennia, terrestrial plants have been an important source of food and medicine for humans. Records of medicinal plant use to treat diseases can date back to the early years of human history thanks to the existence of sophisticated traditional systems from great civilizations, such as Mesopotamia, Egypt, China, India, Greeks and Romans. About 1,000 plant-derived medicines were recorded in the traditional medicine system of Mesopotamian in 2600 BC. More than 700 drugs, mainly of plant origin, were recorded in the Ebers-Papyrus of Egypt from 1550 BC. Traditional Chinese Medicine (TCM) has been preserved and is well documented over the millennia. The Indian Ayurveda system originates from the 1st millennium BC. The traditional medicine system in the western world was recognized through the compendia written by the Greek physician Dioscorides (1st century AD), the Romans Plyny the Elder (1st century AD) and Galen (2nd century AD) (Sneader *et al*, 2005). The knowledge of medicinal plants from the West (Greek-Roman) and from the East (China and India) were well preserved by the Arabs and advanced by employing their own medicinal expertise (Savoia *et al*, 2012). Use of plants as medicines in the Southeast Asia region, particularly in Java, Indonesia, is depicted on relics of the Borobudur temple, a Mahayana Budhist temple built in 9th century AD, depicting images of a physician, drink seller, and herbalist in ancient Java. The oldest preserved traditional medicine (Jamu) book dating ca. 1,700 from the Mataram kingdom contains 3,000 entries of Jamu recipes.

Currently, plants are still used for the treatment of diseases as medicines, particularly as alternative therapeutics, where commercial drugs are merely not affordable, especially in developing countries. For example, antibiotics for treating sprue, mouth freshener or eye drop cleaners are not easily affordable in rural regions and can be substituted by tonics from leaves of *Piper betle*. In Southeast Asia, *P. betle* leaves are easy to find and have been employed for treating sprue, bad mouth smell, eye irritation, and many other ailments for a long time. Experimental studies showed that *P. betle* exhibits diverse biological activities including antibacterial, antifungal, larvicidal, antiprotozoal, anti-inflammatory and antioxidant activities

(Fazal, F. *et al*., 2014).

1.1 Significance of This Study

Plants produce numerous secondary metabolites with considerable structural diversity, most of which are found to be biologically active. Due to the advanced technology of isolation, structure elucidation and bioassays in the last two decades, a great amount of new natural compounds were obtained with interesting structures and bioactivities. Even structurally known compounds also revealed new insights of their bioactivity.

Approximately 40% of all flowering plants have been investigated so far. However, most of them were not investigated thoroughly for their molecular biology and pharmacological activities (Rates *et al*, 2001; Phillipson, 2001; Atanasov *et al*, 2015). Hence, the exploitation of structural chemical databases or banks of compounds from single medicinal plant species are still necessary, in order to facilitate pharmacological evaluation and to discover new lead compounds.

1.2 Natural Products

Natural products are organic compounds produced by living organisms found in nature, including plants, animals, bacteria and fungi. There are two categories of natural products in a wide sense, primary and secondary metabolites. Primary metabolites are involved in the process of modifying and synthesizing carbohydrates, fats, proteins and nucleic acids, which are essential for living organisms. These processes are called primary metabolism that exists in all organisms. The pathways involved in primary metabolism are known as primary metabolic pathways. Oppositely, secondary metabolites (natural products in a strict sense) are more restricted to certain organisms, or groups of organisms, or even characteristic to individual species (Dewick, 2009). In phytochemistry, the definition of natural product is more restricted to secondary metabolites. Secondary metabolites (natural products) are produced by organisms not for crucial life processes, but for chemical interaction with other organisms or species, for adapting to the environment, and for chemical warfare against prey, predators and competing organisms. This chemical communication is principally a sign mediated interaction between species or organisms, which does not happen under all conditions. There are certain or sometimes extreme situations, where organisms purposely produce secondary metabolites. For example, deadly compounds will be produced when the species face attack from other species. Volatile compounds or coloring

agents will be created to attract or warn the same or other species. In another case, extreme climate or environmental conditions will trigger the species to release certain natural products (Dewick, 2009; Cseke *et al*, 2006). Some natural products inhibit or kill other species. Subsequently, most secondary metabolites are known to be pharmacologically active. However, the ecological roles of many secondary metabolites are not all that well known in many cases even today.

Natural products show a great diversity of structures. The most abundant classes of natural product in plants are alkaloids, terpenoids and flavonoids.

1.2.1 Alkaloids

The name - alkaloid is derived from the Latin words alkali (meaning ash) and -oid (like). Alkaloids are a group of nitrogen-containing compounds occurring mainly but not only in plants. Over 27,000 different alkaloids have been characterized so far, 21,000 of which are from plants. One or more nitrogen atoms in the form of primary, secondary or tertiary amines are present in the structures of alkaloids. These nitrogen atoms provide basic properties to alkaloids, and enable alkaloids to be present as water-soluble salts after reaction with acids. Alkaloids containing quaternary nitrogen atoms are also found in nature (Dewick, 2009). All alkaloids fall into four major groups: true alkaloids, protoalkaloids, polyamine alkaloids, peptide and cyclopeptide alkaloids and pseudoalkaloids. This might have some exceptions, such as galantamine which does not contain an isoquinoline building block, but is attributed to isoquinoline alkaloids. The remaining building blocks of alkaloids may be derived from the acetate or shikimate pathway. From a pharmaceutical view, alkaloids have been known for their wide spectra of biological activities.

1.2.2 Terpenoids

Terpenoids are a large and structurally diverse family of natural products, where at least 35,000 different compounds have been characterized up to date (Dewick, 2009). The carbon skeletons of terpenoids are constructed from C_5 isoprene units which are joined in a head to tail fashion, even though tail to tail junctions are found in nature as well. The combination of isoprene units can be modified by cyclisation reactions, though the isoprene unit is usually still easily recognizable. The classification of terpenoids is characterized by the number of isoprene

units in the carbon skeleton. Therefore, they are classified as hemiterpenes (C_5), monoterpenes (C_{10}), sesquiterpenes (C_{15}), diterpenes (C_{20}), sesterterpenes (C_{25}), triterpenes (C_{30}), and tetraterpenes (C_{40}). Biosynthetically, the main precursor to terpenoid synthesis is isopentenyl pyrophospate (IPP). IPP can be formed through two pathways, mevalonic acid (MVA) pathway which is present in the cytosol and the methylerythritol phosphate (MEP) way in plastids (Cseke *et al*. 2006).

1.2.3 Flavonoids

In the year 2000, 4,000 different flavonoids have been reported as naturally occurring compounds (Iwashina *et al*, 2000). Flavonoids are commonly found in green plants except the Anthocerotae (Markham *et al*, 2006). They are often present as glycosides in leaves, flowers, stems and roots. The basic building blocks of flavonoids consist of two benzene rings connected by three carbons as a propene unit (C_6-C_3-C_6), which is built from a cinnamoyl Co-A starting unit followed by chain extension using three molecules malonyl Co-A. Flavonoid classes are distinguished by additional oxygens present as substituents of the heterocyclic ring and by hydroxyl groups as well as by the positions of aryl moieties (C_6) (Harborne and Williams, 2000; Dewick, 2009). Thus, the flavonoid classes are chalcones, flavones, flavonols, flavanones, anthocyanins, and isoflavones. Due to presence of conjugated double bonds, flavonoids are often brightly colored (Harborne and Williams, 2000). This is especially true for anthocyanins.

1.3 Medicinal Plants as Sources of Bioactive Natural Products

Plant extracts and products have been contributing to human life as foodstuffs, flavoring agents and spices, perfumes and cosmetics as well as pharmaceutical and biological agents. The profound knowledge of traditional medicine systems has been guiding the search for pharmacologically active plant-derived natural products. Because of demography, climate and tradition influence, each civilization had their own traditional medicine systems describing specific plants as well as their usage and methods of application (Phillipson, 2001; Dewick, 2009; Gurib-Fakim *et al*, 2006). In the 19th century, the isolation of active constituents of medicinal plants began and the discovery of quinine as an active constituent in Cinchona trees became a turning point in the field of pharmacognosy (Phillipson, 2001). Since then, many plants used in traditional medicine were brought to the laboratory for the investigation of their active

constituents.

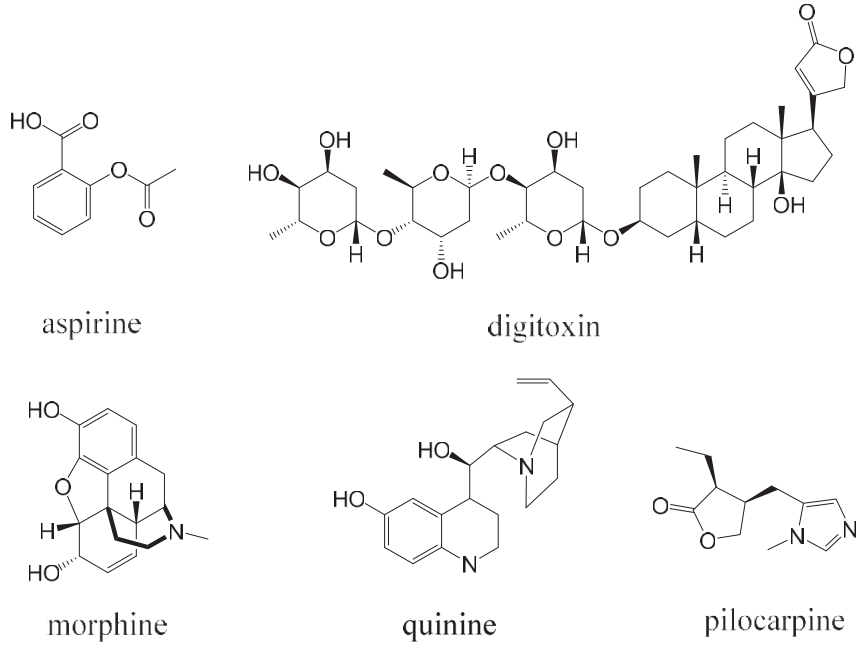

Figure 1.3. Several early plant-derived natural compounds and derivatives (aspirine) used as drugs.

Aspirin, a derivative of salicin from the bark of *Salix alba*, digitoxin from leaves of Digitalis, morphine from latex of opium poppy, quinine from bark of Cinchona, pilocarpine from leaves of Pilocarpus are well-known examples of plant-derived compounds from early medicines and still in clinical use today (Rates *et al*,2001) (Figure 1.3). Other examples of traditional medicinal plants providing significantly bioactive compounds include *Catharantus roseus* (Apocynaceae), *Rauwolfia serpentina* (Apocynaceae) and *Ephedra sinica* (Ephedraceae). *Catharantus roseus*, known as *Vinca rosea*, is an ornamental and medicinal plant from Madagascar. Folklore usage of the plant extract was for the treatment of diabetes, malaria, and lymphoma (Dewick, 2009, Warber*et al*, 2006). From the plant extract, 150 natural products had been characterized including vinblastine and vincristine, two bisindole alkaloids, which have been proven extremely valuable as drugs for treating lymphomas and childhood leukemia, respectively. Rhizome and roots of *Rauwolfia serpentina* (Apocynaceae) were recorded in traditional medicine of Africa and India as an antidote for snakebite, for treating fever, stomach pains, vomiting and headache due to the presence of reserpine and deserpidine exhibiting antihypertensive activity and as mild tranquillizers (Phillipson, 2001: Dewick, 2009; Warber *et*

al, 2006). *Ephedra sinica* (Ephedraceae), known as Ma Huang, has been long used in traditional Chinese medicine for treating common cold. The significantly active compound is ephedrine that acts to decongest the nose and relieve asthma. It is the lead compound for synthesis of the antiasthma agent salbutamol and salmetrol (Dewick, 2009; Newman and Cragg, 2013: Warber *et al*, 2006).

In 2001, one quarter of the drugs administered worldwide originated from plants. Moreover, 11% of 252 essential drugs listed by the World Health Organisation (WHO), were solely of plant origin and a considerable number of drugs were synthetics acquired from natural product lead compounds (Rates *et al*, 2001). Additionally, 80% of 122 plant-derived natural compounds were used for the same or related ethnomedical purposes and were derived from only 97 plant species (Newman and Cragg, 2013).

1.4 The Role of Plant-Derived Natural Products in Drug Discovery

Recent drug discovery attempts focus on lead compounds that are active towards target proteins. Even though recently pharmaceutical companies and funding organizations take interest in molecular modeling, combinatorial chemistry and synthetic chemistry, natural products, and specifically those of plant origin, persist as an important source of new drugs, new drug leads and new chemical entities (NCEs) (Balunas and Kinghorn, 2005; Newman and Cragg, 2016). A recent review regarding the role of natural products in drug discovery was published by Newman and Cragg in 2016. Approximately one quarter of 1,211 approved small molecular drugs are natural products or derived from natural products, indicating that natural products highly influence the process and development of drug discovery (Newman and Cragg, 2016).

There are two reasons why natural products are interesting in drug development. First, the structural diversity of natural products ranges from simple skeletons to highly complex molecules, often with multiple chiral centers, which can be challenging for total synthesis. Secondly, natural products possess highly selective and specific biological activities based on unique mechanisms of action. Due to the progress of the human genome sequencing techniques, thousands of new molecular targets have been recognized for various diseases (Balunas and Kinghorn, 2005). Hence, natural products, which are previously known to not be bioactive, now have a chance to be assayed against these newly identified targets (Craig and Newman, 2013).

1.5 Current Plant-Derived Natural Products in Therapeutic Use

1.5.1 Galantamine

Galantamine is an alkaloid isolated from *Galanthus woronowii* (Amaryllidaceae) by Losink in 1950s (Heinrich *et al*, 2010). It was approved to treat Alzheimer's disease by FDA in 2001 and is marketed under the trade name of Razadyne or Reminyl (Atanasov *et al*, 2015; Balunas and Kinghorn, 2005). The compound inhibits acetylcholinesterase (AChE) as well as modulates the nicotinic acetylcholine receptor (nAChR).

1.5.2 Artemisinin

Artemisinin is an antimalarial drug naturally occurring in *Artemisia annua*, which has been used in traditional Chinese medicine for the treatment of Malaria for at least 2,000 years. The discovery of this natural product back in 1972 by Tu Youyou, was distinguished by the Nobel Prize in Medicine which was awarded to her in 2015. Artemisinin is a sesquiterpene lactone containing an unusual peroxide bridge, which is believed to be important for the bioactivity. Clinical trials have proven that artemisinin can be employed to treat infections of multidrug resistant strains of *Plasmodium falciparum*, which cause human malignant cerebral malaria (Phillipson, 2001). Arteether (trade name Artemotil®), one of the semi-synthetic derivatives of artemisinin, was developed to overcome the poor bioavailability of artemisinin (Atanasov *et al*, 2015; Balunas and Kinghorn, 2005).

1.5.3 Paclitaxel

Paclitaxel (trade name Taxol®) was first isolated from *Taxus brevifolia*, the western yew, in late 1960s. It is a highly oxygenated tetracyclic diterpenoid. Two decades after its discovery, paclitaxel was found to be an antimitotic agent that acts by inhibiting the polymerization of tubulin to form microtubules. In 1990s, paclitaxel and its semi-synthetic derivative were shown to be clinically effective against breast and ovarian cancers. At present, paclitaxel is approved for the treatment of various cancers (Atanasov *et al*, 2015). Consequently, the demand of paclitaxel is extremely high. By contrast, the availability of paclitaxel from natural sources is limited and the total synthesis could not meet the market demands. To enhance the availability of paclitaxel in the market, several approaches were pursued. First, taxanes, such as bacchatin III and 10-deacetylbacchatin III, are used as starting material to produce paclitaxel, because those natural

products occur more abundantly in various yew plants. The second approach is based on cell cultures of *Taxus* plants. Furthermore, after the discovery of paclitaxel in endophytic fungi isolated from *Taxus* plants in 1993 (Stierle *et al*, 1993), endophytic fungi become another reservoir to produce paclitaxel (Heinig *et al*, 2013).

1.5.4 Calanolide A

Calanolide A is a dipyranocoumarin first isolated from *Calophyllum lanigerum* var. *austrocoriaceum* (Clusiaceae) (Balunas and Kinghorn, 2015). It is an anti-HIV drug that acts as a non-nucleoside reverse transcriptase inhibitor (NNRTi) of type-1 HIV and an inhibitor of AZT-resistant strains of HIV. Currently, it is under phase II clinical trial (Balunas and Kinghorn, 2015).

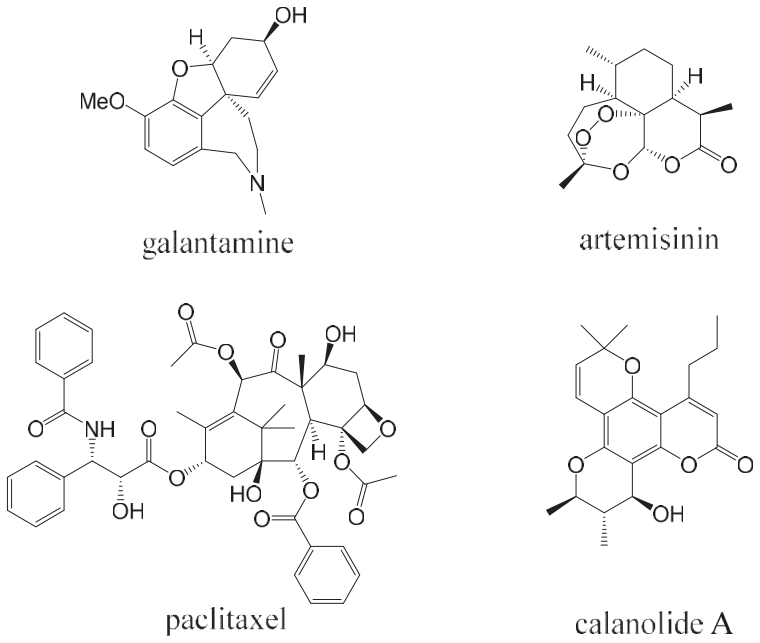

Figure 1.5. Several plant-derived natural products for therapeutic useor in clinical trials

1.6 *Sarcotheca griffithii* (Hook F) Hallier F

Sarcotheca griffithii (Hook F) Hallier F (Oxalidaceae) is an evergreen tree that is native to Sumatra and Peninsular Malaysia (Kubitzki *et al*, 2004; Veldkamp, 1967). In its original habitat (West Kalimantan, Indonesia), local people know it as Belimbing hutan. Traditionally, the plant is used for various purposes. For example, the fruits were reported to be applied as remedies for treating cough (Veldkamp, 1967), while the leaves are assumed to be a sensory agent because

they are sensitive to the touch (Veldkamp, 1967).

Oxalis triangularis :

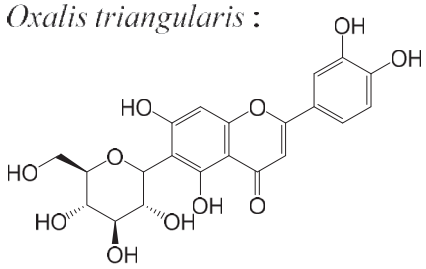

luteolin 6-C-β-D-glucoside

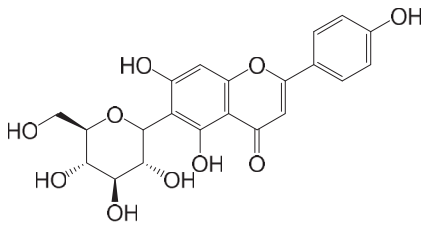

apigenin 6-C-β-D-glucoside

Averrhoa carambola :

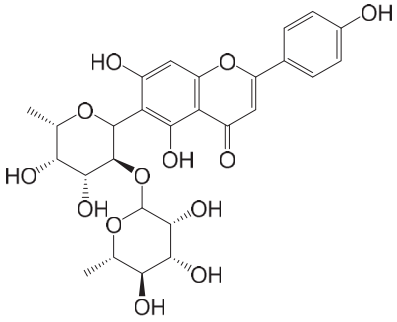

apigenin 6-C-β-(2"-O-α–L-rhamnopyranosyl)-β-L-fucopyranoside

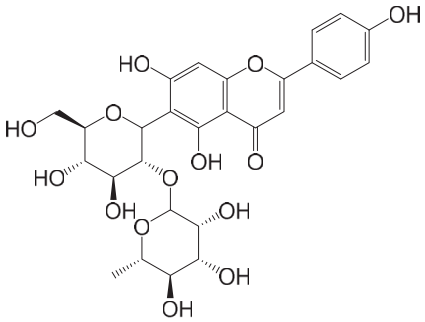

apigenin 6-C-β-(2"-O-α–L-rhamnopyranosyl)-β-D-glucopyranoside

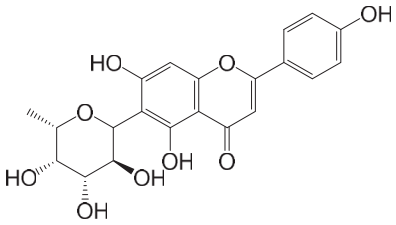

apigenin 6-C-β-L-fucopyranoside

Figure 1.6 Flavonoids reported from genera Averhoa and Oxalis (Morescoet *al*, 2012; Arahoet *al*, 2005; Mizokami *et al*, 2008)

Closely related genera are Averrhoa with several species known widely as exotic Star Fruits (*Averrhoa carambola*), and Oxalis, i.e. *Oxalis triangularis* which has been reported to contain flavonoids (figure 1.3.1.1). No chemical investigations have been reported for the genus *Sarcotheca*. Therefore, this study is important since *S. griffithii* is investigated here for the first time.

1.7 *Piper retrofractum*

The genus *Piper* is a large plant genus that consists of more than 1,000 species that are distributed pantropically (Gutierrez *et al*, 2013). In spite of this large number of species, only a limited number of species are used in traditional medicinal systems, such as Jamu (Indonesian folk medicine), traditional Chinese medicine, the Indian Ayurveda system, or folklore medicines of Latin America and of the West Indies (Limyati *et al*, 1998; Gutierrez *et al*, 2013). Since the first isolation of piperine from *Piper nigrum* in 1819 by Hans Christian Ørsted, the chemical investigation of Piper species has been widely conducted and lead to the isolation of diverse physiologically active compounds, including amide alkaloids, lignans, flavones, monoterpenes, sesquiterpenes, phenylpropanoids, propenylphenols and chalcones. Among them, amide alkaloids are characteristic secondary metabolites in the Piperaceae family. Amide alkaloids from Piperaceae are known as piperamides in order to differentiate them from those contained in other plant families (Gutierrez *et al*, 2013).

Up to now, more than 200 piperamides have been isolated (Gutierrez *et al*, 2013; Paula *et al*, 2012). The piperamides demonstrate diverse structures classified as open chain amide alkaloids, alkamides, aristolactams, dioxyaporhines, pyrrol amides, pyrrolidine amides, ceramides, methylenedioxyphenyl amides, cyclohexenamides and cyclobutanamides with pyrrolidine, dihydropyridone, piperidine or isobutyl amines as basic structural units (Figure 1.7) (Paula *et al*, 2012). Alkaline hydrolysis of these amides will result in the substituted basic and acidic structural subunits (Okwute *et al*, 2013). These acidic units have various origins such as long chain fatty acids, shikimic acid or a combination of these two. The basic units such as piperidines, pyrrolidines or isobutylamines originate biosynthetically from L-lysin, L-proline or L-valine, respectively (Dewick, 2009). As a result, the genus *Piper* is still a promising genus to provide novel and structurally interesting piperamides.

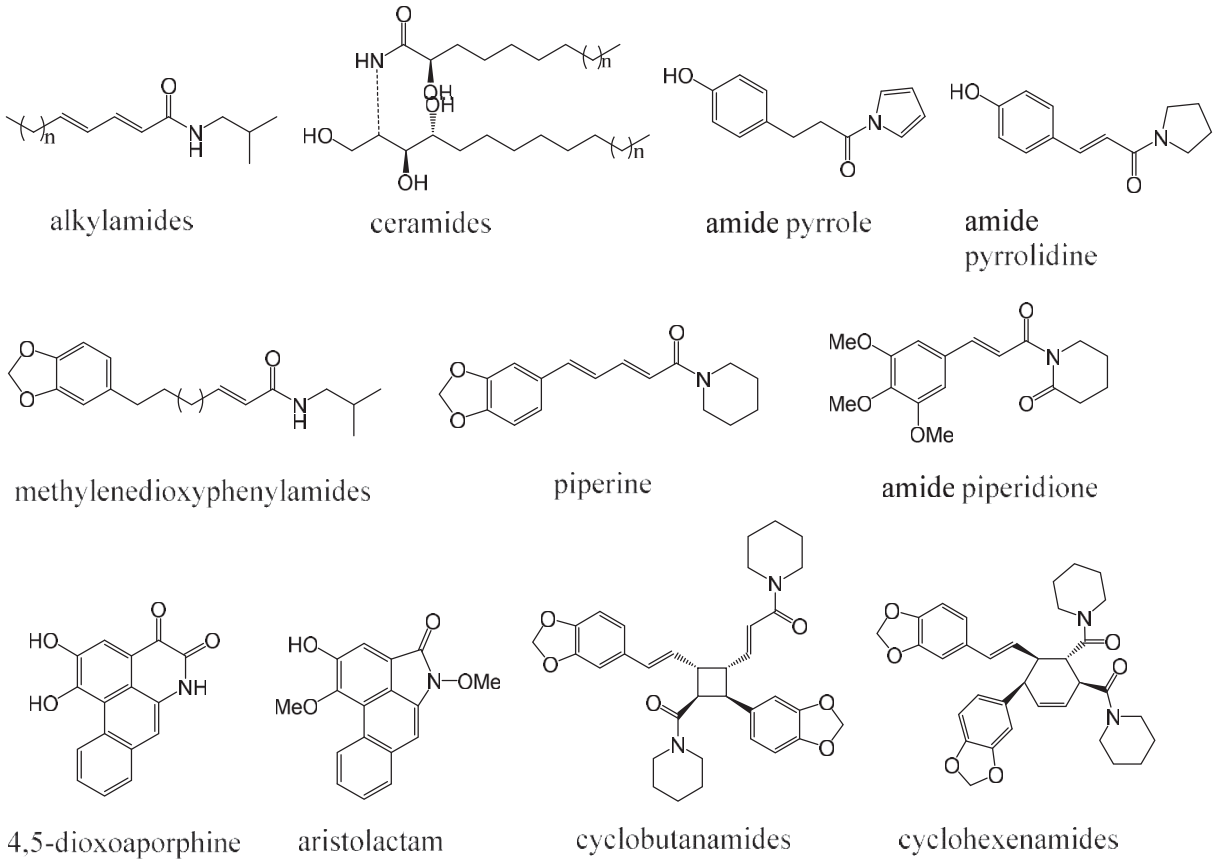

Figure 1.7 Classes of piperamides contained in the family Piperaceae

Piper retrofractum is a well-known medicinal Piper plant in the Southeast Asia region, and is used as a substituent for pepper. In Indonesia, *P. retrofractum* are cultivated in several regions, such as East Java and Central Java. As a medicinal plant, *P. retrofractum* serves for treating fever, hypotension, abdominal pain, beriberi, cholera, no perspiration and as an anthelmintic in Indonesia.

Despite the fact that *P. retrofractum* is already known as a medicinal plant, a chemical investigation of this species was done in 1985 by Banerji *et al*. Secondary metabolites, such as alkylglycosides, phenylpropanoids, and piperamides from the leaves and fruits have been reported (Banerji *et al*, 1985; Ahn *et al*, 1992; Kikuzaki *et al*, 1993; Kubo *et al*, 2013; Luyen, 2014; Muharini *et al*, 2015). Thus, knowledge of the structural diversity of piperamides gave an impetus reason for finding new interesting compounds, which was conducted in this study.

1.8 *Talinum triangulare*

Talinum triangulare (Portulaceae) is vegetable plant cultivated widely in Western Africa, Asia and South America. Besides being consumed as food, it is also used as a traditional medicine for treating cuts, wound, scabies and peptic ulcer (Lawal *et al*, 2009; Onwurah *et al*, 2013). The most frequently used parts of the plant are stems and leaves, while in Indonesia, a tonic is prepared from the fleshy roots. Numerous phytochemical and pharmaceutical studies of *T. triangulare* were performed. Isolation and structure elucidation of secondary metabolites from *T. triangulare* were firstly reported in 2014, during which acrylamides and phaeophytins were obtained from the stems and leaves (figure 1.8) (Amorim *et al*, 2014).However, no chemical investigation exists yet on natural products from roots of *T. triangulare*, which gave an impetus for discovering more compounds from this species.

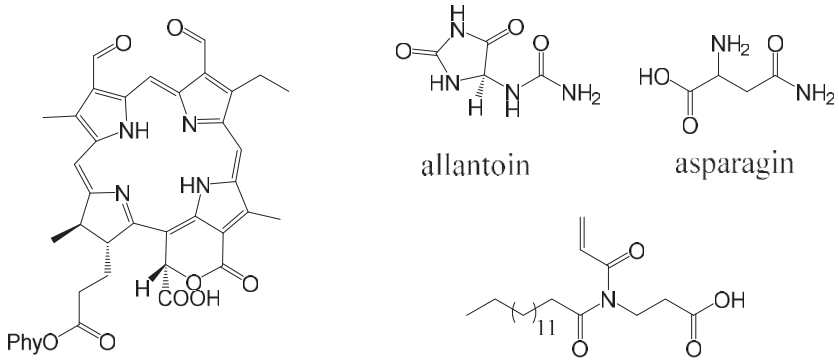

Figure 1.8 Previous reported secondary metabolites from *T. triangulare*.

1.9 *Amorpha fruticosa*

Amorpha fruticosa (Fabaceae), known as false indigo-bush, is a flowering plant that is native to Northern America. Crude extract from the fruits of *A. fruticosa* is known to possess antibacterial (Mitscher *et al*, 1981), insecticidal (Liang *et al*, 2015) and cytotoxic (Lee *et al*, 2006) activities. The first chemical investigation of *A. fruticosa* was reported in 1904 regarding the essential oil from dry fruits (Vittorio*et al*,1904). Since then, *A. fruticosa* was studied for its essential oil, which resulted in the isolation of monoterpenes and sesquiterpenes such as *α*-pinene, *α*-zingiberene, myrcene and *α*-cadinene and their antibacterial activity. In 1938, an apigenin glycoside was reported for the first time from leaves of *A. fruticosa* (Ryoho *et al*, 1938),

followed by the isolation of amorphin and its aglycone, amorphigenin, from seeds of this species (Acree *et al*., 1943).

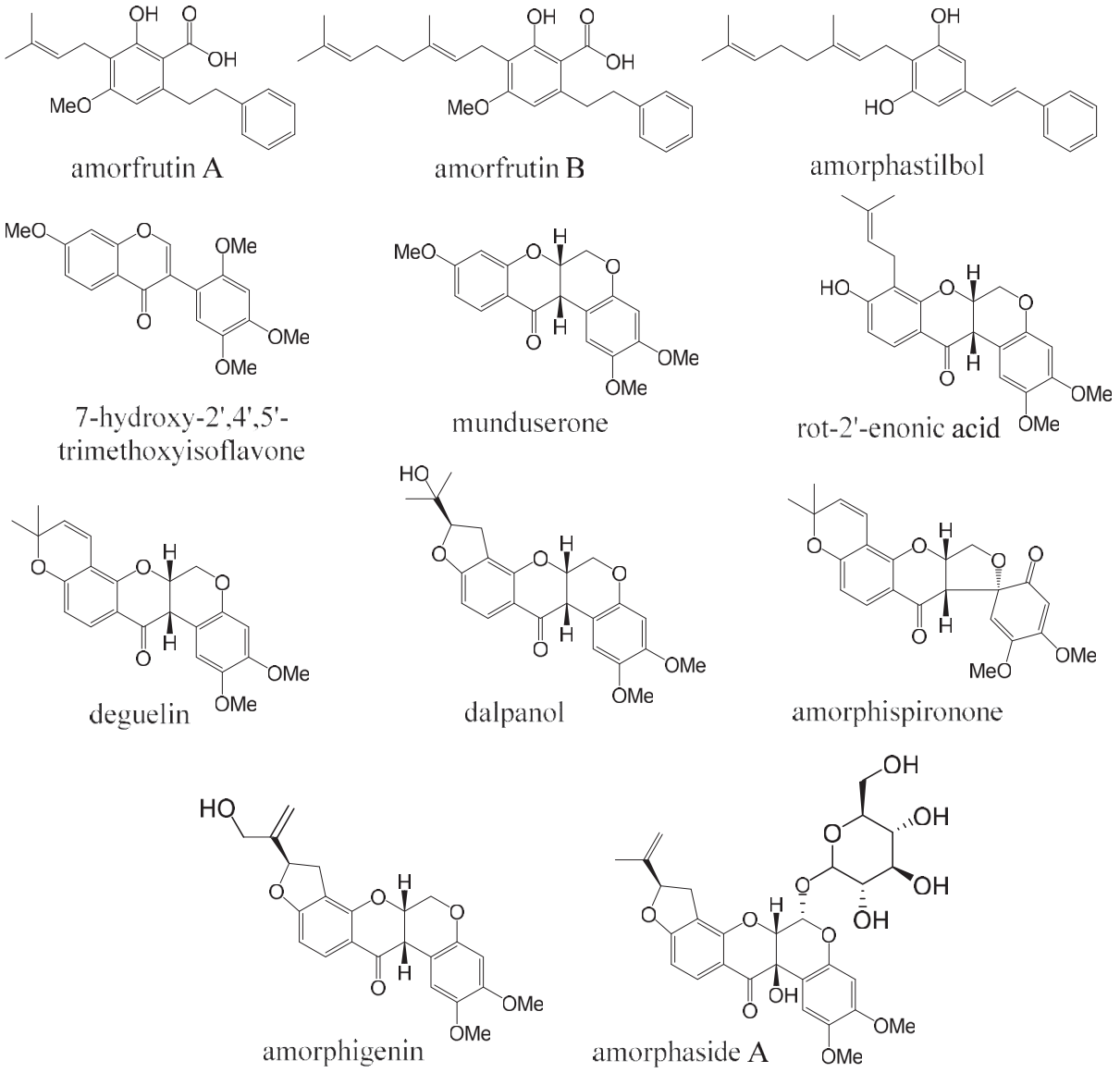

Figure. 1.9 Several secondary metabolites reported previously from *A. fruticosa*

As a species belonging to the legume plant family, *A. fruticosa* is rich in isoflavone derivatives originating from the shikimate and malonate pathways (Harborne and Williams, 2000; Veitch *et al*, 1993). Up to now, various geranylated bibenzyl and rotenoids have also been reported from *A. fruticosa* (Figure 1.9) (Acree *et al*, 1943; Terada *et al*, 1993; Dat *et al*, 2008; Wu *et al*, 2015). From the chromatographic profiles of the crude extract of *A. fruticosa*, signals

of new interesting compounds were observed as described in one of the publications from this thesis.

1.10 Aims and Scope of This Study

As previously mentioned, plants are rich and diverse in secondary metabolites. They have proven to be perfect natural laboratories for producing various molecules ranging from simple skeletons to highly complex chemical structures (Lahlou *et al*, 2013) and maintain an important source for providing physiologically active secondary metabolites. The aim of this study is to isolate and elucidate novel bioactive secondary metabolites from several medicinal plants as well as to evaluate their biological and pharmaceutical properties. Four medicinal plants, *Sarcotheca griffithy*, *Piper retrofractum, Tallinum triangulare* and *Amorpha fruticosa*, were investigated in this study.

Bioactive secondary metabolites were isolated through solvent extraction of medicinal plants followed by various open column chromatographic steps and reverse phase semi-preparative HPLC. The purity of the isolated compounds was analyzed by analytical HPLC, and their molecular weight and fragmentation patterns were recorded using LC-ESIMS. The structures of the isolated compounds were elucidated by state-of-the-art approaches including one- and two-dimensional nuclear magnetic resonance (NMR), mass spectrometric (MS) and circular dichroism (CD) analyses, as well as by comparison with literature data. The isolated compounds containing sugars were hydrolyzed and the sugars as well as the agylcones were analyzed for their absolute configuration. The absolute configurations of chiral compounds were determined by comparison of their optical rotation values with those reported in the literature, whereas ECD calculations were undertaken to establish the absolute configurations of selected chiral compounds where no published data of similar compounds were available.

All pure compounds were evaluated for their antifungal activities against *Cladosporium cladosporiodes*, for their antimicrobial activities against *Mycobacterium tuberculosis*, *Staphylococcus aureus*, *Enterococcus faecalis* and *Enterococcus faecium* as well as for their cytotoxicity against the mouse lymphoma L5178Y cell line, the human monocytic THP-1 cell line and the human lung fibroblast MRC-5 cell line.

2. Publication 1

2.1 New flavones C-glycosides from leaves *Sarcotheca griffithii* (Hook F) Hallier F

Published in "Phytochemistry Letters"

Impact factor: 1.542

The overall contribution to the paper: 60% of the first author. The first author involved to all laboratory works, structure elucidation, literature research and the manuscript writing.

Reprinted by permission from "Muharini, R., Wray, V., Lai, D., Proksch, P." (2014) New flavones C-glycosides from leaves *Sarcotheca griffithii* (Hook F) Hallier F. *Phytochemistry Letters* 9; 26 – 32.

Publication 1

Phytochemistry Letters 9 (2014) 26–32

Contents lists available at ScienceDirect

Phytochemistry Letters

journal homepage: www.elsevier.com/locate/phytol

New flavone C-glycosides from leaves of *Sarcotheca griffithii* (Hook F) Hallier F

Rini Muharini [a,b], Victor Wray [c], Daowan Lai [a,*], Peter Proksch [a,*]

[a] Institut für Pharmazeutische Biologie und Biotechnologie, Heinrich-Heine-Universität Düsseldorf, Universitätsstrasse 1, Geb.26.23, 40225 Düsseldorf, Germany
[b] Department of Chemistry Education, Faculty of Education, Tanjungpura University, Jl. Prof. Dr. H. Hadari Nawawi, 78124 Pontianak, Indonesia
[c] Helmholtz Centre for Infection Research, Inhoffenstraße 7, 38124 Braunschweig, Germany

ARTICLE INFO

Article history:
Received 23 January 2014
Received in revised form 12 March 2014
Accepted 7 April 2014
Available online 20 April 2014

Keywords:
Oxalidaceae
Sarcotheca griffithii
Flavonoids
Chrysin C-glycosides

ABSTRACT

Five new flavone C-glycosides, including chrysin 6-C-(2″-O-α-L-rhamnopyranosyl)-β-D-glucopyranoside (**1**), chrysin 6-C-(2″-O-α-L-rhamnopyranosyl)-β-D-glucopyranosyl-7-O-β-D-glucopyranoside (**2**), chrysin 6-C-(2″-O-α-L-rhamnopyranosyl)-6′-deoxy-*ribo*-hexos-3-uloside (**3**), chrysin 6-C-(2″-O-α-L-rhamnopyranosyl)-β-L-fucopyranoside (**4**), chrysin 6-C-β-boivinopyranosyl-7-O-β-L-glucopyranoside (**5**), together with one known compound, isovitexin 2″-O-α-L-rhamnopyranoside (**6**), were isolated from leaves of *Sarcotheca griffithii* (Hook F) Hallier F (Oxalidaceae). Their structures were elucidated by analysis of the 1D, 2D NMR, and MS data, as well as by comparison with the literature data. This is the first report of secondary metabolites from the genus *Sarcotheca*.

1. Introduction

The family Oxalidaceae comprises more than 900 species belonging to seven genera, namely, *Averrhoa*, *Dapania*, *Biophytum*, *Eichleria*, *Hypseocharis*, *Oxalis* and *Sarcotheca*. A few species in the family belonging to the genera *Averrhoa*, *Biophytum* and *Oxalis* have previously been analyzed with respect to their flavonoids (Moresco et al., 2012; Araho et al., 2005; Rayyan et al., 2005). The genus *Sarcotheca* contains 11 species and is distributed widely in Borneo, Sumatra, Peninsular Malaya, and Sulawesi. *Sarcotheca griffithii* (Hook F) Hallier F, known as Belimbing Hutan in Indonesia, is believed to be native to Sumatra and Peninsular Malaya (Kubitzki, 2004; Veldkamp, 1967). It is an evergreen tree and may be up to 42 m high growing wild in the first storey of primary tropical forest. The fruits of this species are edible and have a sour taste, which are used as ingredients for curries or sweets in local area. Traditionally, the fruits are also used as remedies to treat coughs (Veldkamp, 1967). The leaves are trifoliolate and irritable to the touch (Veldkamp, 1967).

The genus *Sarcotheca* has until now not been investigated for its natural products. In this study, five new chrysin C-glycosides were isolated from *S. griffithii* and identified using spectroscopic methods including UV, NMR, and mass spectra. The new compounds include chrysin 6-C-(2″-O-α-L-rhamnopyranosyl)-β-D-glucopyranoside (**1**), chrysin 6-C-(2″-O-α-L-rhamnopyranosyl)-β-D-glucopyranosyl-7-O-β-D-glucopyranoside (**2**), chrysin 6-C-(2″-O-α-L-rhamnopyranosyl)-6′-deoxy-*ribo*-hexos-3-uloside (**3**), chrysin 6-C-(2″-O-α-L-rhamnopyranosyl)-β-L-fucopyranoside (**4**), and chrysin 6-C-β-boivinopyranosyl-7-O-β-L-glucopyranoside (**5**) (Fig. 1). In addition, the known flavone glycoside isovitexin 2″-O-α-L-rhamnopyranoside (**6**) was likewise isolated (Nikolov et al., 1982).

2. Results and discussion

A methanol (MeOH) extract was obtained from the leaves (300 g) of *S. griffithii* and fractionated by column chromatography over silica gel with mixtures of *n*-hexane – ethyl acetate (EtOAc), dichloromethane (DCM) – MeOH in increasing polarity to give 18 fractions. Compound **1** was the main component of the extract and obtained as a yellowish powder. It appeared on thin layer chromatography (TLC) as a yellow spot after treatment with Naturstoff reagent A-PEG. The molecular formula $C_{27}H_{31}O_{13}$ was deduced for compound **1** from HRESIMS, which gave a pseudo-molecular peak at *m/z* 563.17611 $[M+H]^+$. In the LC/MS spectrum, a

* Corresponding authors. Tel.: +49 211 81 14163; fax: +49 211 81 11923.
E-mail addresses: laidaowan123@gmail.com (D. Lai), proksch@uni-duesseldorf.de (P. Proksch).

http://dx.doi.org/10.1016/j.phytol.2014.04.005
1874-3900/

Publication 1

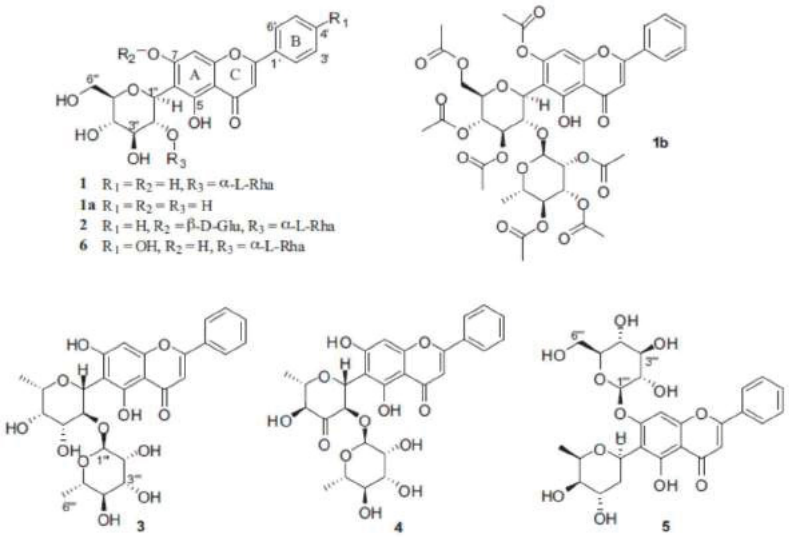

Fig. 1. Flavone C-glycosides isolated from *S. griffithii*.

signal at *m/z* 417 $[M+H-146]^+$ due to the loss of one deoxyhexosyl unit was observed. The UV spectrum of **1** showed absorption maxima at 213, 271.8, and 317.8 nm which were characteristic for a chrysin skeleton. This suggestion was supported by ^{1}H NMR data.

The ^{1}H NMR spectrum showed two aromatic protons at δ 8.08 (d, J = 7.3 Hz, H-2′, H-6′), two aromatic protons at δ 7.58 (t, J = 7.3 Hz, H-3′, H-5′), and a methine proton at δ 7.61 (d, J = 7.3 Hz, H-4′), indicating a mono-substituted benzene ring. Two further aromatic protons at δ 6.98 (1H, s) and δ 6.57 (1H, s) were assigned as H-3 and H-8, respectively, by HMQC and HMBC experiments. Furthermore, signals at δ 13.4 (1H, s) and δ 11.0 (1H, s) were assigned by HMBC as protons of OH-5 and OH-7, respectively. These ^{1}H NMR data were in agreement with chrysin that was substituted at C-6 (Miyaichi and Tomimori, 1994). Sugar proton signals appeared between δ 0.52–5.08 ppm (Agrawal, 1992). ^{13}C NMR spectra revealed 11 signals of oxygenated carbons and one signal of a methyl carbon, in addition to the signals characteristic for chrysin.

Acid hydrolysis of **1** yielded rhamnose and a chrysin monoglycoside (**1a**). The latter gave a pseudomolecular ion peak at *m/z* 417 $[M+H]^+$ in the ESIMS spectrum. The ^{1}H and ^{13}C NMR spectra of **1a** were identical with those reported for chrysin 6-C-β-D-glucopyranoside (Miyaichi and Tomimori, 1994). The linkage of β-D-glucose at C-6 of chrysin was corroborated by analysis of the HMBC spectrum, in which the anomeric proton (H-1″) showed correlations to C-6, C-5 and C-7. Thus, compound **1** was composed of one chrysin 6-β-D-glucosyl unit and one additional rhamnosyl unit.

Due to the broadening and the overlapping of sugar proton signals in the ^{1}H NMR spectrum of **1**, the sugar moieties were determined further following acetylation of **1**. The ^{1}H NMR spectrum of the acetylated product (**1b**) showed well-separated signals for the sugar protons that were used to determine the coupling constants. ^{1}H and ^{13}C NMR spectra of **1b** showed signals for seven acetate groups resonated at δ 1.84 (3H, s), 1.90 (3H, s), 1.98 (3H, s), 1.99 (6H, s), 2.03 (3H, s), and 2.29 (3H, s), and for seven carbonyl groups at δ 167.6, 169.3, 169.4, 169.4, 169.6, 169.7, and 170.0. This result suggested that six hydroxyl groups of the sugar moiety and one hydroxyl group attached to ring A of chrysin had been successfully acetylated. Two sets of sugar signals were identified by ^{1}H–^{1}H COSY, HSQC and HMBC experiments. The β-glucose moiety resonated at δ 5.19 (1H, d, J = 9.7 Hz, H-1″), 4.38 (1H, t, J = 9.7 Hz, H-2″), 5.39 (1H, t, J = 9.7 Hz, H-3″), 4.92 (1H, t, J = 9.7 Hz, H-4″), 4.08 (1H, d, J = 9.7 Hz, H-5″), 4.16 (1H, dd, J = 4.2, 12.3 Hz, H-6″a) and 3.86 (1H, d, J = 12.3 Hz, H-6″b). The second sugar moiety was identified as rhamnose from the signals at δ 4.86 (1H, br s, H-1‴), 4.85 (1H, d, J = 3.2 Hz, H-2‴), 4.77 (1H, dd, J = 3.2, 10.0 Hz, H-3‴), 4.62 (1H, t, J = 10.0 Hz, H-4‴), 2.55 (1H, br s, H-5‴) and 0.49 (3H, d, J = 6.1 Hz). The HMBC spectrum showed correlation between δ_H 4.86 (H-1‴) and δ_C 75.3 (C-2″) confirming that the rhamnosyl moiety was attached at C-2″ of the glucose. The relative configuration of the anomeric carbons was assigned as β for glucose and α for rhamnose, respectively, by analysis of the coupling pattern of the anomeric protons. The L-configuration of α-rhamnose was determined by TLC by comparison with an authentic standard. Based on these data, compound **1** was assigned as chrysin 6-C-(2″-O-α-L-rhamnopyranosyl)-β-D-glucopyranoside.

Compound **2** was obtained as a yellowish white powder and its UV spectrum indicated the presence of a chrysin moiety (λ_{max} 246, 270, 310 nm). Compound **2** exhibited a pseudomolecular ion peak in the HRESIMS at *m/z* 725.2284 $[M+H]^+$, which is consistent with the molecular formula $C_{33}H_{40}O_{18}$. This indicated that **2** is a chrysin triglycoside. The ESIMS spectrum showed fragment peaks at *m/z* 579.0 $[M+H-146]^+$ and 416.9 $[M+H-146-162]^+$, suggesting the presence of one deoxyhexosyl and one hexosyl unit in the molecule. The ^{1}H NMR spectrum of **2** showed similar resonances to those of **1**, which included signals for a monosubstituted benzene (B ring) at δ 8.11 (2H, dd, J = 1.5 Hz, 6.9 Hz, H-2′, H-6′), 7.61 (2H, t, J = 6.9 Hz, H-3′, H-5′), and 7.64 (1H, d, J = 6.9 Hz, H-4′), and signals assigned to H-8 at δ 6.97 (1H, s) and H-3 at δ 7.08 (1H, s), corroborating that chrysin was again the aglycone. The three sugar moieties of **2** were characterized by the presence of three anomeric protons which appeared at δ 4.73 (1H, d, J = 9.5 Hz, H-1″), 4.96 (1H, br s, H-1‴) and 4.95 (1H, br s, H-1⁗) and correlated, respectively, with ^{13}C resonances at δ 71.2 (C-1″), 100.6 (C-1‴) and 101.9 (C-1⁗) as detected from the HSQC spectrum. A combined analysis of the ^{13}C NMR, ^{1}H–^{1}H COSY and HMBC spectra and of the coupling constants permitted the identification of the sugars as two β-glucose and one α-rhamnose moiety. The loss of a hexose unit ($[M+H-162]^+$) and a deoxyhexose unit ($[M+H-146]^+$) during MS analysis of **2** suggested that β-glucose moiety was linked to chrysin via an C–O bond, whereas the rhamnose moiety was attached to the second β-glucose via an O-glycosidic bond. The

Publication 1

presence of a hydrogen bond between OH-5 (δ 13.3, 1H, s) and the carbonyl C-4 revealed that one sugar is bound to chrysin at C-7, whereas the remaining two sugars form a diglycoside that is attached to the flavones at C-6. The connectivity of the sugar moieties was analyzed by HMBC experiment. The C–C linkage of one β-glucose to C-6 of chrysin was confirmed by HMBC correlations from δ_H 4.73 (H-1″) to δ_C 159.3 (C-5), 110.8 (C-6) and 162.9 (C-7). The second β-glucose moiety was attached via an O-glycosidic bond to O-7 due to the correlation of δ_H 4.96 (H-1‴) to δ_C 162.9 (C-7). The (1→2) glycosidic bond of rhamnose to the first glucose was indicated by the cross peak of δ_H 4.95 (H-1‴) to δ_C 76.7 (C-2″). Thus, compound **2** was assigned as chrysin 6-C-(2″-O-α-L-rhamnopyranosyl)-β-D-glucopyranosyl-7-O-β-D-glucopyranoside.

Compound **3** was isolated as a yellowish powder and had the molecular formula $C_{27}H_{30}O_{12}$ (*m/z* 547.1811 $[M+H]^+$) as established by HRESIMS. The UV and ^{1}H NMR spectra of **3** showed signals similar to those of **2**, indicating **3** to be a chrysin derivative. In the LC/MS spectrum, an ion peak was observed at *m/z* 401.2 $[M+H-146]^+$ due to the loss of a deoxyhexosyl unit. The molecular mass difference between **3** and chrysin suggested that the former contained two deoxyhexosyl moieties. This suggestion was confirmed by the detection of two anomeric protons at δ 4.68 (1H, d, *J* = 9.3 Hz, H-1″) and δ 4.98 (1H, br s, H-1‴), respectively, as well as the signals of two methyl groups at δ 1.12 (3H, d, *J* = 6.5 Hz, H-6″) and δ 0.54 (3H, d, *J* = 6.1 Hz, H-6‴). Based on ^{1}H–^{1}H COSY and *J* value analysis, the sugars were recognized as β-fucose and α-rhamnose. The attachment of the sugar moieties to the aglycone was established by HMBC. The HMBC correlations between the anomeric proton of β-fucose at δ 4.68 (1H, d, *J* = 9.3 Hz, H-1″) and the ^{13}C resonance at δ 109.8 (C-6) and δ 159.0 (C-5) confirmed that the β-fucose was linked to C-6 of chrysin. The anomeric proton of α-rhamnose (δ 4.98, H-1‴) showed HMBC correlation to C-2″ (δ 74.1) of the fucopyranosyl moiety, and H-2″ (δ 4.26) correlated to C-1‴ of the α-rhamnose (δ 100.5), which confirmed that α-rhamnose was connected to β-fucose at C-2″. Previously, an apigenin-6-C-(2″-O-α-L-rhamnosyl)-β-L-fucopyranoside isolated from the leaves of *Averrhoa carambola* had been reported by Araho et al. (2005). The optical rotation of compound **3** agreed with that of the reported compound. Thus, compound **3** was elucidated as chrysin-6-C-(2″-O-α-L-rhamnosyl)-β-L-fucopyranoside.

Compound **4** was obtained as a yellowish powder and exhibited $UV_{\lambda max}$ at 250, 272, 318 nm indicating a chrysin moiety. The molecular formula was deduced as $C_{27}H_{28}O_{12}$ by HRESIMS (*m/z* 545.1651 $[M+H]^+$). In the LC–MS spectrum, the presence of an ion peak at *m/z* 399 $[M+H-146]^+$ was consistent with the loss of a rhamnose unit. The ^{1}H and ^{13}C NMR spectra showed the characteristic resonances of chrysin, which included signals at δ 8.08 (2H, d, *J* = 7.4 Hz, H-2′, H-6′), 7.58 (2H, t, *J* = 7.4 Hz, H-3′, H-5′) and 7.61 (1H, d, *J* = 7.4 Hz, H-4′) assigned to the B ring, and those at δ 6.98 (1H, s, H-3) and at 6.53 (1H, br s, H-8). The signal at δ 13.6 (1H, s) was assigned to OH-5. In the sugar proton region, two anomeric protons appeared at δ 4.86 (1H, d, *J* = 10.2 Hz, H-1″) and at δ 4.64 (1H, d, *J* = 3.9 Hz, H-1‴), which indicated the existence of two sugar moieties. One α-rhamnose moiety was confirmed by ^{1}H–^{1}H COSY and *J* values, as well as by acid hydrolysis of **4**, which gave α-L-rhamnose. The ^{1}H NMR, ^{13}C NMR, ^{1}H–^{1}H COSY and HSQC spectra revealed that the remaining sugar moiety lacks a proton at C-3″. The ^{13}C NMR of **4** showed two carbonyl resonances at δ 206.2 for one sugar and δ 182.0 for the chrysin moiety, assigned to C-3″ and C-4, respectively. Based on these data, the remaining sugar moiety of **4** was identified as 3-ketohexose. The HMBC spectrum indicated that the 3-ketohexose was attached to C-6 of chrysin, as confirmed by correlations from H-1″ to C-5 and C-6. The α-L-rhamnose moiety was linked to C-2″ of the 3-ketohexose via an O-glycosidic bond. The ^{1}H and ^{13}C NMR data for the sugar moieties of **4** were comparable with those of cassiaoccidentalin A, an apigenin-6-C-(2″-O-α-L-rhamnopyranoyl)-6′-deoxy-*ribo*-hexos-3-uloside isolated from *Cassia occidentalis* (Hatano et al., 1999). The specific optical rotation of **4** also agreed with that of cassiaoccidentalin A. Thus, compound **4** was assigned as chrysin-6-C-(2″-O-α-L-rhamnopyranoyl)-6′-deoxy-*ribo*-hexos-3-uloside.

Compound **5** was obtained as a yellowish powder, with the molecular formula $C_{27}H_{30}O_{12}$, as determined from the HRESIMS spectrum (*m/z* 547.1810, $[M+H]^+$). The UV spectrum revealed maximum absorptions at 246, 272, 310 nm, which was characteristic of chrysin. The typical resonances of the B ring of chrysin were observed at δ 8.09 (2H, d, *J* = 7.3 Hz, H-2′, H-6′), 7.59 (2H, t, *J* = 7.3 Hz, H-3′, H-5′) and 7.63 (1H, d, *J* = 7.3 Hz, H-4′), and at δ 126.5 (C-2′, C-6′), 129.2 (C-3′, C-5′) and 132.2 (C-4′). Additional signals were observed at δ 7.09 (1H, s, H-3) and at 7.01 (1H, s, H-8). Two anomeric protons were observed at δ 5.32 (1H, br d, *J* = 9.5 Hz, H-1″) and at δ 4.87 (1H, d, *J* = 8.0 Hz, H-1‴). The presence of an ion peak at *m/z* 385.2 $[M+H-162]^+$ in the ESI-MS of **5** suggested the loss of one hexosyl unit. The resonance for OH-5 appeared at δ 13.4 (1H, s, OH-5), indicating that one sugar moiety was attached to C-7 of chrysin. This was confirmed by the HMBC data, where a correlation was detected between H-1‴ (δ 4.87) and C-7 (δ 163.4). The hexosyl unit was assigned as β-D-glucose by analysis of ^{1}H–^{1}H COSY, *J* values and HSQC data. For the second sugar moiety, the ^{1}H NMR data revealed methylene protons at δ 2.88 (1H, dt, *J* = 2.6, 13.2 Hz, H-2″) and δ 1.25 (1H, d, *J* = 13.2 Hz, H-2″), and a methyl proton at δ 1.05 (3H, d, *J* = 6.7 Hz, H-6″), which, respectively, correlated with δ 29.9 (C-2″) and 17.2 (C-6″) in the HSQC spectrum. ^{1}H–^{1}H COSY and *J* values data revealed that the orientation of H-1″ (δ_H 5.32, br d, *J* = 9.5 Hz) and H-3″ (δ_H 3.86, br s) was axial and equatorial, respectively. In addition, H-4″ (δ_H 3.19, br d, *J* = 3.2 Hz) coupled with H-3″ with a small coupling constant, while H-4″ did not show coupling to H-5″ (δ_H 3.92, d, *J* = 6.7 Hz). These data indicated that H-4″ and H-5″ were equatorial and axial, respectively. Thus, the second sugar was assigned as a β-boivinose, a sugar found rarely in nature. The HMBC data showed a correlation between δ 5.32 (H-2″) and δ 113.2 (C-6), indicating that β-boivinose was attached to chrysin at C-6 via a C–C bond. The ^{1}H and ^{13}C NMR data of the sugar moieties of **5** resembled those of luteolin 6-C-β-boivinopyranosyl-7-O-β-D-glucopyranoside isolated from *Pogonetherum crinitum* (Zhu et al., 2010). Hence, compound **5** was assigned as chrysin 6-C-β-boivinopyranosyl-7-O-β-D-glucopyranoside.

A broadening or duplication of signals in the NMR spectra was detected for all isolated compounds. This phenomenon is due to the presence of rotamers resulting from hindered rotation around the C(sp3)–C(sp2) glucosyl-flavone linkage in flavone 6-C glucosides (Hatano et al., 1999; Rayyan et al., 2005; Andersen and Markham, 2006). The L-configuration of the rhamnose moiety of **1**–**4** was determined by acid hydrolysis followed by TLC analysis using an authentic standard (Araho et al., 2005; Zhu et al., 2010).

Flavonoids are generally known to possess antioxidant activity (Harbone and Williams, 2000). However, the lack of hydroxyl groups in the B ring of flavones and the increasing number of sugar residues are known to reduce the antioxidant activity (Mantoro et al., 2001; Yan et al., 2011a,b). Based on this, compounds **1**–**5** were not assayed for antioxidant activity. A methanolic extract of the leaves of *S. griffithii* was tested for its cytotoxicity using L5178Y mouse lymphoma cells but was found to be inactive.

3. Experimental

3.1. General experimental procedures

Melting point was measured on a Büchi Melting Point instrument B-540 (Switzerland). Optical rotation was measured with a JASCO P-2000 polarimeter. ^{1}H, ^{13}C and 2D NMR spectra were

Publication 1

recorded in deuterated DMSO on Bruker Avance ARX 500 or on Bruker Avance III 600 and 700 spectrometers. Chemical shifts were given in δ (ppm) with tetramethylsilane (TMS) as an internal standard. ESI/MS spectra were measured on a Finnigan LCQ Deca mass spectrometer (Thermo Finnigan) and high-resolution mass spectra (HRESIMS) were recorded on a UHR-QTOF maXis 4G (Bruker Daltonics, Bremen) mass spectrometer. HPLC analysis was performed with a Dionex P580 system coupled to a photodiode array detector (UVD340s). The UV detection was set at 235, 254, 280, and 340 nm. The separation column (125 mm × 4 mm, L × ID) was prefilled with Eurospher-10 C_{18} (Knauer, Germany). Semi-preparative RP-HPLC was used for purification of compounds and consisted of a Lachrom-Merck Hitachi HPLC system (Pump L7100 and UV detector L7400) and a Eurospher 100-10 C_{18} column (300 mm × 8 mm) (Knauer, Germany). The flow rates were 2, 3 or 5 mL/min. Column chromatography was performed using Merck MN Silica gel 60 M (0.04–0.063 mm) or Sephadex LH-20 (Sigma) as stationary phase. Thin layer chromatography (TLC) was performed on pre-coated Silica Gel 60 F_{254} plates (layer thickness 0.2 mm, E. Merck, Darmstadt, Germany) with detection under UV at 254 and 366 nm and after spraying with Naturstoff reagent. Solvents were distilled before use, and spectral grade solvents were used for spectroscopic measurements.

3.2. Plant material

The leaves of *S. griffithii* were collected in the Otong forest, Sambas district, Kalimantan Barat province, Indonesia in June 2012. A specimen has been deposited in Herbarium Bogoriense with specimen number 2519/IPH.1.02/If.8/X/2012, Cibinong, Indonesia.

3.3. Extraction and isolation

Leaves (300 g) of *S. griffithii* were shade dried, ground and extracted with methanol (MeOH) three times at room temperature. The methanolic solution was concentrated under vacuum to yield 40 g of extract. 10 g of the extract was subjected to vacuum liquid chromatography (VLC) on silica gel (0.04–0.063 mm) and eluted with *n*-hexane-ethyl acetate (EtOAc), EtOAc, dichloromethane (DCM), and DCM–MeOH gradients of increasing polarity to give 18 fractions (A1–A18). An aliquot of 1 g of fraction A15 (4.63 g, DCM–MeOH 30:70) was separated further by CC on Sephadex LH-20 (MeOH as mobile phase) to give 15 subfractions. Fraction A15-10 (67.2 mg) containing the major constituent was purified by semi-preparative HPLC using an Eurospher 100-10 (Knauer, Germany) (300 mm ×8 mm, L × ID) column and MeOH–H_2O (54:46) as eluent (flow rate 5 mL/min) to give compound **1** (12.2 mg). Fraction A15-12 (26.7 mg) was purified using semi-preparative RP-HPLC with MeOH–H_2O (gradient 43:57–50:50, flow rate 5 mL/min) as eluent to yield compound **6** (10.7 mg). Fraction A15-5 (189.5 mg) was subjected to column chromatography on silica gel (0.2–0.5 mm) and eluted with EtOAc–MeOH–H_2O (30:3:2) to give ten subfractions. Fraction A15-5-9 (60 mg) was purified repeatedly by RP-HPLC with MeOH–H_2O (gradient 43:57–46:54) as eluent, flow rate 3 mL/min to yield compound **2** (3.76 mg). Fraction A14 (3.182 g) was subjected to VLC on silica gel and eluted with mixtures of *n*-hexane-EtOAc, EtOAc, DCM, and DCM–MeOH of increasing polarity. Fraction A14-2 (1.2 g) was fractionated further on Sephadex LH-20 using MeOH as mobile phase to give subfractions A14-2-6-6 (20 mg) and A14-2-6-10 (64 mg). Purification of A14-2-6-6 was achieved using semi-preparative RP-HPLC with MeOH–H_2O (58:42, flow rate 4 mL/min) as mobile phase to yield compound **3** (2.5 mg). Fraction A14-2-6-10 (64 mg) was purified repeatedly using semi-preparative RP-HPLC with MeOH–H_2O (51:49, flow rate 4 mL/min) as eluent to give compound **4** (4.98 mg) and compound **5** (5.32 mg).

3.3.1. Chrysin 6-C-(2″-O-α-L-rhamnopyranosyl)-β-D-glucopyranoside (**1**)

Yellow powder; mp 198–200 °C; $UV_{\lambda_{max}}$ (PDA) 213, 271.8, 317.8 nm; $[\alpha]_D^{23}$ −29.3 (*c* 0.4, MeOH); ^1H and ^{13}C NMR see Table 1; ESIMS *m/z* (%) $[M+H]^+$ 562.9 (100), $[M+H-146]^+$ 417.1 (10); HRESIMS *m/z* 563.17611 $[M+H]^+$ (calcd for $C_{27}H_{31}O_{13}$ 563.17592).

3.3.2. Chrysin 6-C-(2″-O-α-L-rhamnopyranosyl)-β-D-glucopyranosyl-7-O-β-D-glucopyranoside (**2**)

Yellow powder; mp 219–221 °C; $UV_{\lambda_{max}}$ (PDA) 246, 270, 310 nm; $[\alpha]_D^{21}$ −28.5 (*c*. 1.134, MeOH); ^1H and ^{13}C NMR, see Tables 3 and 4; ESIMS *m/z* (%) 725.0 (100) $[M+H]^+$, 747.1 (10) $[M+Na]^+$; HRESIMS *m/z* 725.2284 $[M+H]^+$ (calcd for $C_{33}H_{41}O_{18}$ 725.2287).

3.3.3. Chrysin 6-C-(2″-O-α-L-rhamnosyl)-β-L-fucopyranoside (**3**)

Yellow powder; mp 196–198 °C; $UV_{\lambda_{max}}$ (PDA) 214, 272, 316 nm; $[\alpha]_D^{22}$ +10.8 (*c* 1.144, MeOH); ^1H and ^{13}C NMR see Tables 3 and 4; ESIMS *m/z* (%) 547.1 (100) $[M+H]^+$, 401.2 (5) $[M+H-146]^+$, 569.2 (15) $[M+Na]^+$; HRESIMS *m/z* 547.1811 $[M+H]^+$ (calcd for $C_{27}H_{31}O_{12}$ 547.1811).

3.3.4. Chrysin 6-C-(2″-O-α-L-rhamnopyranosyl)-6′-deoxy-ribo-hexos-3-uloside (**4**)

Yellow powder; mp 164–167 °C; $UV_{\lambda_{max}}$ (PDA) 250, 272, 318 nm; $[\alpha]_D^{21}$ −62.2 (*c* 0.485, MeOH); ^1H and ^{13}C NMR, see Tables 3 and 4; ESIMS *m/z* (%) 545.0 (100) $[M+H]^+$, 399.2 (10) $[M+H-146]^+$, 568.2 (15) $[M+Na]^+$; HRESIMS *m/z* 545.1651 $[M+H]^+$ (calcd for $C_{27}H_{29}O_{12}$ 545.1654).

3.3.5. Chrysin 6-C-β-boivinopyranosyl-7-O-β-D-glucopyranoside (**5**)

Yellow powder; mp 230–233 °C; $UV_{\lambda_{max}}$ (PDA) 246, 272, 310 nm; $[\alpha]_D^{22}$ -47.2 (*c*. 1.166, MeOH); ^1H and ^{13}C NMR see Tables 3 and 4; ESIMS *m/z* (%) 547.1 (100) $[M+H]^+$, 569.2 (10) $[M+Na]^+$, 385.2 (5) $[M+H-162]^+$; HRESIMS *m/z* 547.1810 $[M+H]^+$ (calcd for $C_{27}H_{31}O_{12}$ 547.1810).

3.3.6. Acetylation of **1**

4 mg of **1**, 1 mL pyridine and 5 mL acetic anhydride were mixed and kept at room temperature overnight. After addition of 2.5 mL water, the mixture was extracted with EtOAc (3 mL × 8 mL) to give a water layer and a EtOAc layer. The EtOAc layer was evaporated under vacuum and then purified using RP-HPLC and acetonitrile–water (45:55) as mobile phase. The flow rate was 4 ml/min. 6.72 mg of compound **1b** was obtained. ^1H and ^{13}C NMR data for **1b**, see Table 2.

3.3.7. Acid hydrolysis

5 mg of compound **1** and 2 mL HCl 2 N were kept at 90 °C for 4 h. The mixture was then partitioned against EtOAc (3 mL × 1 mL) to give a water phase and an EtOAc phase. The EtOAc phase containing the chrysin monoglycoside was evaporated under vacuum and dried under N_2 gas. Further, it was purified by performing RP-HPLC and gave compound **1a** (3.33 mg) as hydrolysis product. The water phase containing the sugar was then examined by TLC using L-rhamnose as an authentic standard (Sigma–Aldrich, Germany). The eluent system was DCM–MeOH–H_2O (6:4:1), or EtOAC–MeOH–H_2O (40:6:4) or DCM–MeOH–H_2O (10:3:0.5), and anisaldehyde was used as a spraying reagent.

Compounds **2**–**5** (each 1 mg) were separately hydrolyzed with 2 N HCl (2 mL) at 90 °C for 4 h, following by the same treatment as described for **1** to obtain the sugars. L-Rhamnose was detected in

Publication 1

Table 1
NMR spectral data for **1** and **1a** (DMSO-d_6, δ in ppm, J in Hz).[a]

Position	1		COSY	1a		HMBC (H→C)
	δ_H	δ_C		δ_H	δ_C	
2		162.5			162.8	
3	6.98, 1H, s	104.8		6.96, 1H, s	105.1	C-1′, C-2, C-4, C-10
4		181.8			181.9	
5		161.3			160.7	
OH-5	13.4, 1H, s			13.4, 1H, s		
6		109.2			109.2	
7		163.8			164.5	
OH-7	11.0, 1H, s			nd		
8	6.57, 1H, s	92.9		6.52, 1H, s	93.9	C-6, C-7, C-9, C-10
9		156.6			156.4	
10		103.9			103.4	
1′		130.6			130.7	
2′/6′	8.08, 2H, d (7.3)	126.2	H-3′/H-5′	8.07, 2H, d (7.2)	126.4	C-2, C-1′, C-3′/C-5′
3′/5′	7.58, 2H, t (7.3)	129.0	H-2′/H-6′, H-4′	7.58, 2H, t (7.2)	129.2	C-4′, C-2,/C-6′
4′	7.61,1H, d (7.3)	131.9	H-3′/H-5′	7.61, 1H, d (7.2)	132.0	C-2′/C-6′, C3′/C-5′
1″	4.68, 1H, d (9.6)	70.9	H-2″	4.60, 1H, d (9.4)	73.1	C-5, C-6, C-7, C-2″, C-3″
2″	4.19, 1H, t (9.6)	nd	H-1″, H-3″	4.06, 1H, t (9.4)	70.6	C-1″, C-3″
3″	3.38, 1H, m, overlapped	nd	H-2″, H-4′	3.17, 1H, m	78.9	C-2″, C-4″
4″	3.71, 1H, m, overlapped	nd	H-3″, H-5″	3.41, 1H, m	70.2	C-5″
5″	4.52, 1H, m, overlapped	75.4	H-4″, H-6″	3.20, 1H, m	81.6	
6″	3.16, 1H, m	nd	H-5″	3.14, 1H, m	61.5	
	3.10,1H, m			3.69, 1H, d (10.3)		
1‴	4.36, 1H, d (3.9)	95.9	H-2‴			
2‴	4.26, 1H, br s	74.3	H-1‴, H-3‴			
3‴	3.14,1H, t (5.3)	70.2	H-2‴, H-4‴			
4‴	2.92, 1H, m	71.3	H-3‴, H-5‴			
5‴	2.32, 1H, m	67.9	H-4‴, H-6‴			
6‴	0.61, 1H, d (5.7)	17.3	H-5‴			
	0.52, 2H, d (5.7)					

[a] Recorded at 600 MHz for ^{1}H, and 150 MHz for ^{13}C.

Table 2
NMR Spectral data for **1b** (DMSO-d_6, δ in ppm, J in Hz).[a]

Position	δ_H	δ_C	COSY	HMBC (H→C)
2		160.5		
3	6.96, 1H, br s	100.2		nd
4		174.9		
5		nd		
OH-5	11.8, 1H, s			
6		116.2		
7		149.9		
8	6.72, 1H, s	107.5		nd
9		nd		
10		nd		
1′		130.7		
2′/6′	8.02, 2H, d (7.2)	126.0	H-3′/H-5′	C-2, C-3′/5′, C-4′
3′/5′	7.56, 2H, t (7.2)	129.1	H-2′/H-6′, H-4′	C-1′
4′	7.58, 1H, d (7.2)	131.6	H-3′/H-5′	C-2′/4′
1″	5.19, 1H, d (9.7)	71.3	H-2″	C-2″, C-5, C-6
2″	4.38, 1H, t (9.7)	75.3	H-1″, H-3″	C-1″, C-3″ C-1‴, C-6
3″	5.39 1H, t (9.7)	75.9	H-2″, H-4″	C-2″, C-4″, CH_3CO (169.7)
4″	4.92, 1H, t (9.7)	68.3	H-3″, H-5″	C-3″, C-6″, CH_3CO (169.3)
5″	4.08, 1H, d (9.7)	74.5	H-4″, H-6″	
6″a	4.16, 1H, dd (4.2, 12.3)	61.9	H-5″	C-4″, C-5″, CH_3CO (170.0)
6″b	3.86, 1H, d (12.3)			
1‴	4.86, 1H, br s	97.1	H-2‴	C-2″, C-2‴, C-3‴, C-5‴
2‴	4.85, 1H, d (3.2)	69.1	H-1‴, H-3‴	C-4‴, CH_3CO (169.4)
3‴	4.77, 1H, dd (3.2, 10.0)	67.9	H-2‴, H-4‴	C-4‴, CH_3CO (169.4)
4‴	4.62, 1H, t (10.0)	69.6	H-3‴, H-5‴	C-3‴, C-5‴, CH_3CO (169.6)
5‴	2.55, 1H, brs	65.9	H-4‴, H-6‴	
6‴	0.49, 3H, d (6.1)	16.9	H-5‴	C-4‴, C-5‴
CH_3CO	2.29, 3H, s	21.0		CH_3CO (167.6)
	2.03, 3H, s	20.4		CH_3CO (169.6)
	1.99, 6H, s	20.5		CH_3CO (169.6, 170.0)
	1.98, 3H, s	20.5		CH_3CO (169.4)
	1.90, 3H, s	20.3		CH_3CO (169.4)
	1.84, 3H, s	20.2		CH_3CO (169.3)
CH_3CO		170.0, 169.7, 169.6, 169.4, 169.4, 169.3, 167.6		

[a] Recorded at 600 MHz for ^{1}H, and 150 MHz for ^{13}C.

Publication 1

Table 3
^{1}H NMR data of compounds **2–5** (DMSO-d_6, δ in ppm, J in Hz).

Position	2[a]	3[a]	4[b]	5[a]
3	7.08, 1H, s	6.87, 1H, s	6.98, 1H, s	7.09, 1H, s
8	6.97, 1H, s	6.39, 1H, s	6.53, 1H, br s	7.01,1H, s
OH-5	13.4, 1H, s	13.3, 1H, s	13.6, 1H, s	13.4, 1H, s
2′/6′	8.11, 2H, d (6.9)	8.05, 2H, d (7.4)	8.08, 2H, d (7.4)	8.09, 2H, d (7.3)
3′/5′	7.61, 2H, t (6.9)	7.57, 2H, t (7.4)	7.58, 2H, t (7.4)	7.59, 2H, t (7.3)
4′	7.64, 1H, d (6.9)	7.59, 1H, d (7.4)	7.61, 1H, d (7.4)	7.63, 1H, d (7.3)
1″	4.73, 1H, d (9.5)	4.68, 1H, d (9.3)	4.86, 1H, d (10.2)	5.32, 1H, brd (9.5)
2″	4.1, 1H, t (9.5)	4.26, 1H, d (9.3)	5.31, 1H, d (10.2)	2.88, 1H, dt (2.6, 13.2) 1.25, 1H, d (13.2)
3″	3.38, 1H, m, overlapped	3.58, 1H, d (9.3)	nd	3.86, 1H, br s
4″	3.37, 1H, m, overlapped	3.55, 1H, d (6.5)	3.90, 1H, m	3.19, 1H, br d (3.2)
5″	3.30, 1H, m, overlapped	3.66, 1H, q (6.5)	3.38, 1H, m	3.92, 1H, d (6.7)
6″	3.62, 2H, m	1.12, 3H, d (6.5)	1.30, 1H, d (6.0)	1.05, 3H, d (6.7)
1‴	4.95, 1H, br s	4.98, 1H, br s	4.64, 1H, d (3.9)	4.87, 1H, d (8.0)
2‴	3.61, H, m	4.36, 1H, d (4.9)	3.69, 1H, m	3.40, 1H, dd (3.5, 8.0)
3‴	3.16, 1H, m	3.24, 1H, m	3.04, 1H, m	4.98, 1H, d (3.5)
4‴	2.87, 1H, dt (4.4, 9.3)	2.92, 1H, dt (9.4, 3.5)	2.97, 1H, dt (3.9, 9.4)	3.21, 1H, d (3.5)
5‴	2.32, 1H, dt (6.2, 9.3)	2.36, 1H, m	2.42, 1H, overlapped	3.49, 1H, dd (1.5, 5.4)
6‴	0.59, 2H, d (6.2) 0.48, 1H, d (6.2)	0.54, 3H, d (6.1)	0.82, 1H, d (6.1) 0.69, 2H, d (6.1)	3.81, 1H, dd (5.4, 10.0) 3.51, 1H, d (5.4)
1⁗	4.96, 1H, br s			
2⁗	3.19, 1H, m			
3⁗	3.32, 1H, overlapped			
4⁗	3.51, 1H, m			
5⁗	3.25, 1H, m			
6⁗	3.79, 1H, dd (2.0, 6.1) 3.55, 1H, q (6.1)			

[a] Recorded at 500 MHz.
[b] At 700 MHz.

Table 4
^{13}C NMR data of compounds **2–5** (125 MHz, DMSO-d_6, δ_C in ppm).

Position	2	3	4	5
2	163.5	161.9	160.3	163.8
3	105.3	104.8	105.2	105.6
4	182.3	181.1	182.0	182.4
5	159.3	159.0	161.2	158.2
6	110.8	109.8	107.8	113.2
7	162.9	169.0	163.0	163.4
8	94.5	95.3	93.5	95.03
9	156.8	156.4	156.8	156.5
10	105.3	100.3	104.9	105.6
1′	130.5	130.6	130.6	130.5
2′	126.5	126.2	126.4	126.5
3′	129.3	129.1	129.2	129.2
4′	132.4	131.7	132.1	132.2
5′	129.3	129.1	129.2	129.2
6′	126.5	126.2	126.4	126.5
1″	71.2	71.1	73.3	64.7
2″	76.7	74.1	75.4	29.9
3″	73.8	76.2	206.2	67.2
4″	79.5	72.4	78.1	69.2
5″	69.6	73.7	78.1	69.8
6″	60.3	17.1	19.2	17.2
1‴	100.6	100.5	99.1	102.1
2‴	70.5	70.7	70.2	73.7
3‴	70.3	70.4	70.2	75.1
4‴	71.6	71.6	71.2	69.2
5‴	68.4	68.1	68.9	77.5
6‴	17.6	17.5	17.4	60.7
1⁗	101.9			
2⁗	80.9			
3⁗	75.9			
4⁗	77.3			
5⁗	69.7			
6⁗	60.9			

the hydrolysate of **2–4**, while D-glucose was found in that of **2** and **5** by TLC using the same protocol as mentioned for **1**.

3.4. Cell proliferation assay

Cytotoxicity was tested against the L5178Y mouse lymphoma cells line using MTT (3-(4,5-dimethylthiazol-2-yl)-2,5-diphenyl-2H-tetrazolium bromide) assay as described earlier (Kreuter et al., 1992; Pham et al., 2013).

Acknowledgments

R.M. wishes to thank DIKTI (Directorate General of Higher Education – Indonesia) for a scholarship. The financial support by a grant of BMBF (project No. 0315772) to P.P. is gratefully acknowledged. We are indebted to Prof. W.E.G. Müller (University of Mainz, Mainz, Germany) for cytotoxicity assays and Mrs. Christel Kakoschke (Institut für Biophysikalische Analytik, Helmholtz-Zentrum für Infektionsforschung GmBH, Braunschweig) for NMR measurements of compounds **2–5**.

References

Agrawal, P.K., 1992. NMR spectroscopy in the structural elucidation of oligosaccharides and glycosides. Phytochemistry 31, 3307–3330.
Andersen, Ø.M., Markham, K.R., 2006. Flavonoids: Chemistry, Biochemistry and Applications. CRC Press, Boca Raton.
Araho, D., Miyakoshi, M., Chou, W.Z., Kambara, T., Mizutani, K., Ikeda, T., 2005. A new flavone C-glycosides from the leaves of *Averrhoa carambola*. Nat. Med. 59, 113–116.
Harbone, J.B., Williams, C.A., 2000. Review: advances in flavonoid research since 1992. Phytochemistry 55, 481–504.
Hatano, T., Mizuta, S., Ito, H., Yoshida, T., 1999. C-glycosidic flavonoids from *Cassia occidentalis*. Phytochemistry 52, 1379–1383.
Kreuter, M.H., Robitzki, A., Chang, S., Steiffen, R., Michaelis, M., Kjajic, Z., Bachmann, M., Schroder, H.C., Müller, W.E.G., 1992. Production of cytotatic agent aeroplysinin by the sponge *Verongia aerophoba* in *in vitro* culture. Comp. Biochem. Physiol. 101C, 183–187.

Publication 1

Kubitzki, K., 2004. The Families and Genera of Vascular Plants. Flowering Plants Dicotyledons Celastrales, Oxalidales, Rosales, Cornales, Ericales, vol. VI. Springer-Verlag, Berlin, , pp. 287–288.

Mantoro, P., Carbone, V., Simone, F., Pizza, C., Tommasi, N., 2001. Studies on the constituents of *Cyclanthera pedata* Fruits: isolation and structure elucidation of new flavonoid glycosides and their antioxidant activity. J. Agric. Food Chem. 49, 5156–5160.

Miyaichi, Y., Tomimori, T., 1994. Studies on the constituents of *Scutellaria* species. XVI: On the phenol glycosides of the root of *Scutellaria baicalensis* Georgi. Nat. Med. 48, 215–218.

Moresco, H.H., Queiroz, G.S., Pizzolatti, M.G., Brighente, I.M., 2012. Chemical constituents and evaluation of the toxic and antioxidant activities of *Averrhoa carambola* leaves. Braz. J. Pharmacogn. 22, 319–324.

Nikolov, N., Seligmann, O., Wagner, H., Horowitz, R.M., Gentili, B., 1982. New flavonoid glycosides from *Crataegus monogyna* and *Crataegus pentagyna*. Planta Med. 44, 50–53.

Pham, C.D., Hartmmann, R., Bohler, P., Stork, B., Wesselborg, S., Lin, W., Lai, D., Proksch, P., 2013. Callyspongiolide, a cytotoxic macrolide from the marine sponge *Callyspongia* sp. Org. Lett. 16, 266–289.

Rayyan, S., Fossen, T., Andersen, Ø.M., 2005. Flavone C-glycosides from leaves of *Oxalis triangularis*. J. Agric. Food Chem. 53, 10057–10060.

Veldkamp, J.F., 1967. A revision of *Sarcotheca* Bl and *Dapania* Korth (Oxalidaceae). Blumea 15, 519–543.

Yan, C., Lin, L., Liu, H.J., Lin, Z.X., Chen, P.Y., Cai, C., Zhen, L.A., 2011a. The research of flavones type constituent from *Santalum album*. China J. Chinese Mater. Med. 36, 3130–3133.

Yan, R., Cao, Y., Chen, C., Dai, H., Yu, S., Wei, J., Hua, L., Yang, B., 2011b. Antioxidant flavonoids from the seed of *Oroxylum indicum*. Fitoterapia 82, 841–848.

Zhu, D., Yang, J., Lai, M.X., Wang, Q., 2010. A new C-glycosylflavone from *Pogonatherum crinitum*. Chinese J. Nat. Med. 8, 411–413.

2.2 Supporting Information

S1. UV spectrum of chrysin 6-C-(2″-O-α-L-rhamnopyranosyl)-*β*-D-glucopyranoside (**1**)

S1-1. HRESIMS of chrysin 6-C-(2″-O-α-L-rhamnopyranosyl)-*β*-D-glucopyranoside (**1**)

S1-2. ^{1}H NMR spectrum of chrysin 6-C-(2″-O-α-L-rhamnopyranosyl)-*β*-D-glucopyranoside (**1**) in DMSO-d_6 (600 MHz)

S1-3. ^{1}H-^{1}H COSY spectrum of chrysin 6-C-(2″-O-α-L-rhamnopyranosyl)-*β*-D-glucopyranoside (**1**) in DMSO-d_6 (600 MHz)

S1-4. HMBC spectrum of chrysin 6-C-(2″-O-α-L-rhamnopyranosyl)-*β*-D-glucopyranoside (**1**) in DMSO-d_6 (600 MHz, 150 MHz)

S1-5. HSQC spectrum of chrysin 6-C-(2″-O-α-L-rhamnopyranosyl)-*β*-D-glucopyranoside (**1**) in DMSO-d_6 (600 MHz, 150 MHz)

S1a. UV spectrum of hydrolyzed product of **1** (**1a**)

S1a-1. ^{1}H NMR spectrum of hydrolyzed product of **1** (**1a**) in DMSO-d_6 (600 MHz)

S1a-2. ^{1}H-^{1}H COSY spectrum of hydrolyzed product of **1** (**1a**) in DMSO-d_6 (600 MHz)

S1b. UV spectrum of acetylated product of **1** (**1b**)

S1b-1. ^{1}H NMR spectrum of acetylated product of **1** (**1b**) in DMSO-d_6 (600 MHz)

S1b-2. ^{1}H-^{1}H COSY spectrum of acetylated product of **1** (**1b**) in DMSO-d_6 (600 MHz)

S1b-3. HMBC spectrum of acetylated product of **1** (**1b**) in DMSO-d_6 (600 MHz, 150 MHz)

S1b-4. HSQC spectrum of acetylated product of **1** (**1b**) in DMSO-d_6 (600 MHz, 150 MHz)

S2. UV spectrum of chrysin 6-C-(2″-O-α-L-rhamnopyranosyl)-*β*-D-glucopyranosyl-7-O-*β*-D-glucopyranoside (**2**)

S2-1. HRESIMS of chrysin 6-C-(2″-O-α-L-rhamnopyranosyl)-*β*-D-glucopyranosyl-7-O-*β*-D-glucopyranoside (**2**)

S2-2. ^{1}H NMR spectrum of chrysin 6-C-(2″-O-α-L-rhamnopyranosyl)-*β*-D-glucopyranosyl-7-O-*β*-D-glucopyranoside (**2**) in DMSO-d_6 (600 MHz)

S2-3. ^{13}C NMR spectrum of chrysin 6-C-(2″-O-α-L-rhamnopyranosyl)-*β*-D-glucopyranosyl-7-O-*β*-D-glucopyranoside (**2**) in DMSO-d_6 (150 MHz)

S2-4. HMBC spectrum of chrysin 6-C-(2″-O-α-L-rhamnopyranosyl)-*β*-D-glucopyranosyl-7-O-*β*-D-glucopyranoside (**2**) in DMSO-d_6 (600 MHz, 150 MHz)

S2-5. HSQC spectrum of chrysin 6-C-(2″-O-α-L-rhamnopyranosyl)-*β*-D-glucopyranosyl-7-O-*β*-D-glucopyranoside (**2**) in DMSO-d_6 (600 MHz, 150 MHz)

S3. UV spectrum of chrysin 6-C-(2″-O-α-L-rhamnosyl)-*β*-L-fucopyranoside (**3**)

S3-1. HRESIMS of chrysin 6-C-(2″-O-α-L-rhamnosyl)-*β*-L-fucopyranoside (**3**)

S3-2. ^{1}H NMR spectrum of chrysin 6-C-(2″-O-α-L-rhamnosyl)-*β*-L-fucopyranoside (**3**) in DMSO-d_6 (600 MHz)

S3-3. ^{13}C NMR spectrum of chrysin 6-C-(2″-O-α-L-rhamnosyl)-*β*-L-fucopyranoside (**3**) in DMSO-d_6 (150 MHz)

S3-4. HMBC spectrum of chrysin 6-C-(2″-O-α-L-rhamnosyl)-*β*-L-fucopyranoside (**3**) in DMSO-d_6 (600 MHz, 150 MHz)

S3-5. HSQC spectrum of chrysin 6-C-(2″-O-α-L-rhamnosyl)-*β*-L-fucopyranoside (**3**) in DMSO-d_6 (600 MHz, 150 MHz)

S4. UV spectrum of chrysin 6-C-(2″-O-α-L-rhamnopyranosyl)-6′-deoxy-ribo-hexos-3-uloside (**4**)

S4-1. HRESIMS of chrysin 6-C-(2″-O-α-L-rhamnopyranosyl)-6′-deoxy-ribo-hexos-3-uloside (**4**)

S4-2. ^{1}H NMR spectrum of chrysin 6-C-(2″-O-α-L-rhamnopyranosyl)-6′-deoxy-ribo-hexos-3-uloside (**4**) in DMSO-d_6 (600 MHz)

S4-3. ^{13}C NMR spectrum of chrysin 6-C-(2″-O-α-L-rhamnopyranosyl)-6′-deoxy-ribo-hexos-3-uloside (**4**) in DMSO-d_6 (150 MHz)

S4-4. HMBC spectrum of chrysin 6-C-(2″-O-α-L-rhamnopyranosyl)-6′-deoxy-ribo-hexos-3-uloside (**4**) in DMSO-d_6 (600 MHz, 150 MHz)

S5. UV spectrum of chrysin 6-C-β-boivinopyranosyl-7-O-*β*-D-glucopyranoside (**5**)

S5-1. HRESIMS of chrysin 6-C-β-boivinopyranosyl-7-O-*β*-D-glucopyranoside (**5**)

S5-2. ^{1}H NMR spectrum of chrysin 6-C-β-boivinopyranosyl-7-O-*β*-D-glucopyranoside (**5**) in DMSO-d_6 (600 MHz)

S5-3. ^{13}C NMR spectrum of chrysin 6-C-β-boivinopyranosyl-7-O-*β*-D-glucopyranoside (**5**) in DMSO-d_6 (150 MHz)

S5-4. HMBC spectrum of chrysin 6-C-β-boivinopyranosyl-7-O-*β*-D-glucopyranoside (**5**) in DMSO-d_6 (600 MHz, 150 MHz)

S5-5. HSQC spectrum of chrysin 6-C-β-boivinopyranosyl-7-O-*β*-D-glucopyranoside (**5**) in DMSO-d_6 (600 MHz, 150 MHz)

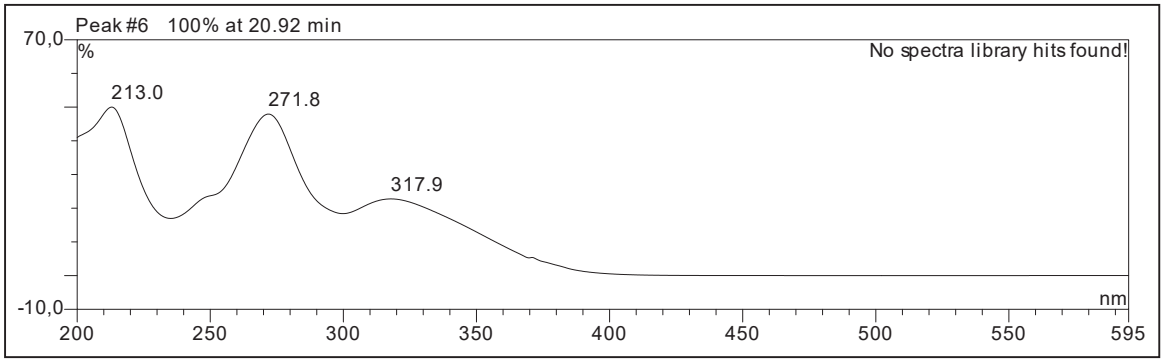

S1. UV spectrum of chrysin 6-C-(2″-O-α-L-rhamnopyranosyl)-*β*-D-glucopyranoside (**1**)

Mass Spectrum SmartFormula Report

Analysis Info

Analysis Name	D:\Data\HHU Service\Proksch13000024.d	Acquisition Date	3/26/2013 3:24:40 PM
Method	tune_low.m	Operator	Peter Tommes
Sample Name	R. Muharini A15-10-3 in CH3OH (CH3CN/H2O)	Instrument / Ser#	maXis 4G 20213
Comment			

Acquisition Parameter

Source Type	ESI	Ion Polarity	Positive	Set Nebulizer	0.3 Bar
Focus	Not active	Set Capillary	4000 V	Set Dry Heater	180 °C
Scan Begin	50 m/z	Set End Plate Offset	-500 V	Set Dry Gas	4.0 l/min
Scan End	1500 m/z	Set Collision Cell RF	600.0 Vpp	Set Divert Valve	Source

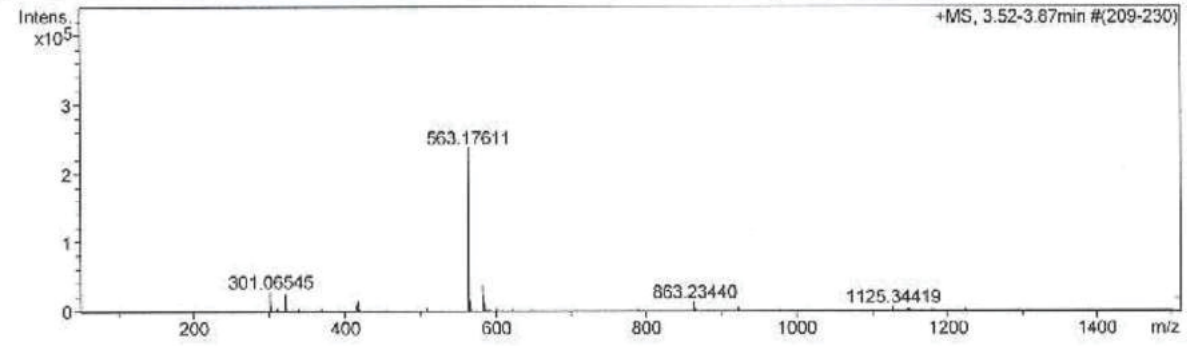

Meas. m/z	#	Formula	Score	m/z	err [mDa]	err [ppm]	mSigma	rdb	e⁻ Conf	N-Rule
563.17611	1	C 24 H 23 N 10 O 7	48.57	563.17457	-1.54	-2.74	8.8	18.5	even	ok
	2	C 27 H 31 O 13	100.00	563.17592	-0.19	-0.34	9.6	12.5	even	ok
	3	C 28 H 27 N 4 O 9	52.39	563.17725	1.14	2.03	17.8	17.5	even	ok
	4	C 25 H 19 N 14 O 3	74.85	563.17591	-0.20	-0.36	23.6	23.5	even	ok
	5	C 40 H 23 N 2 O 2	9.84	563.17540	-0.71	-1.25	80.8	30.5	even	ok

S1-1. HRESIMS of chrysin 6-C-(2″-O-α-L-rhamnopyranosyl)-*β*-D-glucopyranoside (**1**)

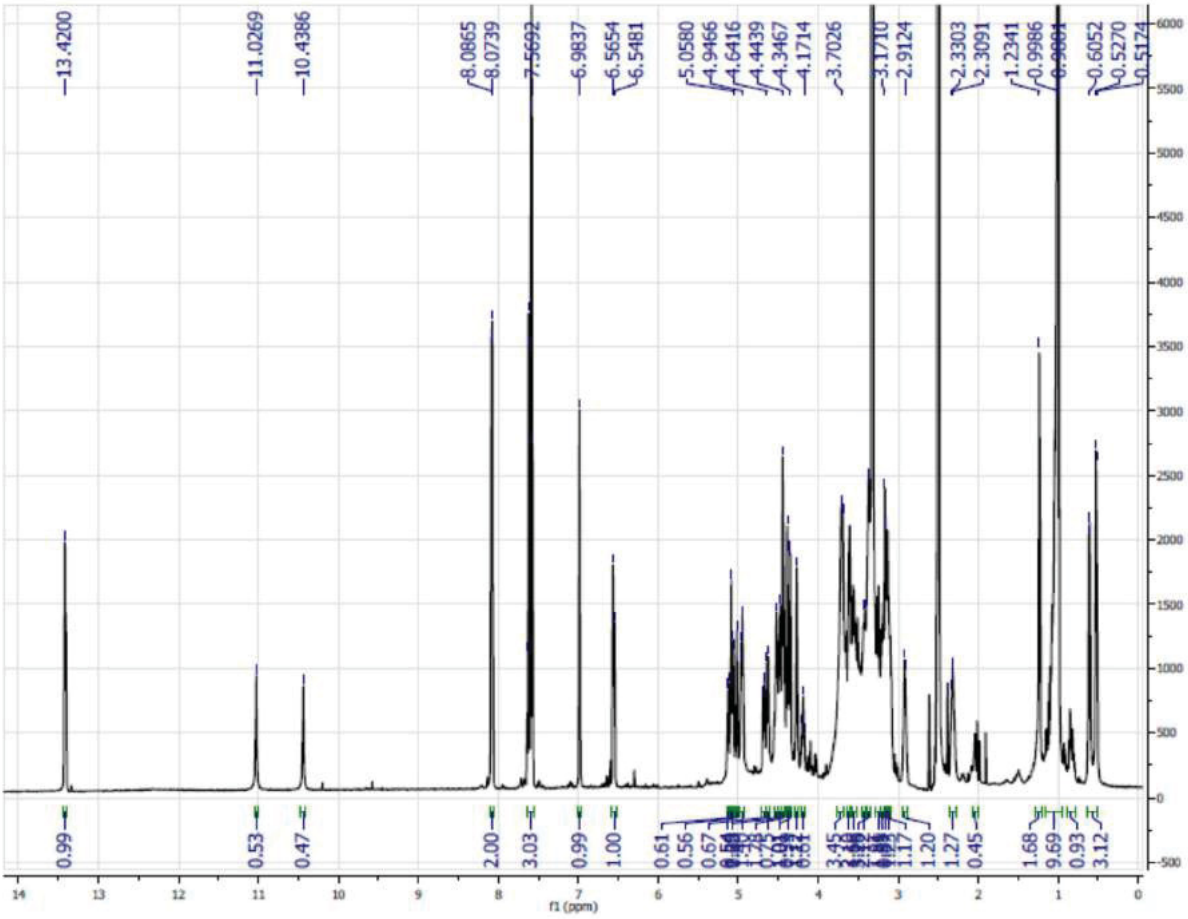

S1-2. [1]H NMR spectrum of chrysin 6-C-(2″-O-α-L-rhamnopyranosyl)-*β*-D-glucopyranoside (**1**) in DMSO-d_6 (600 MHz)

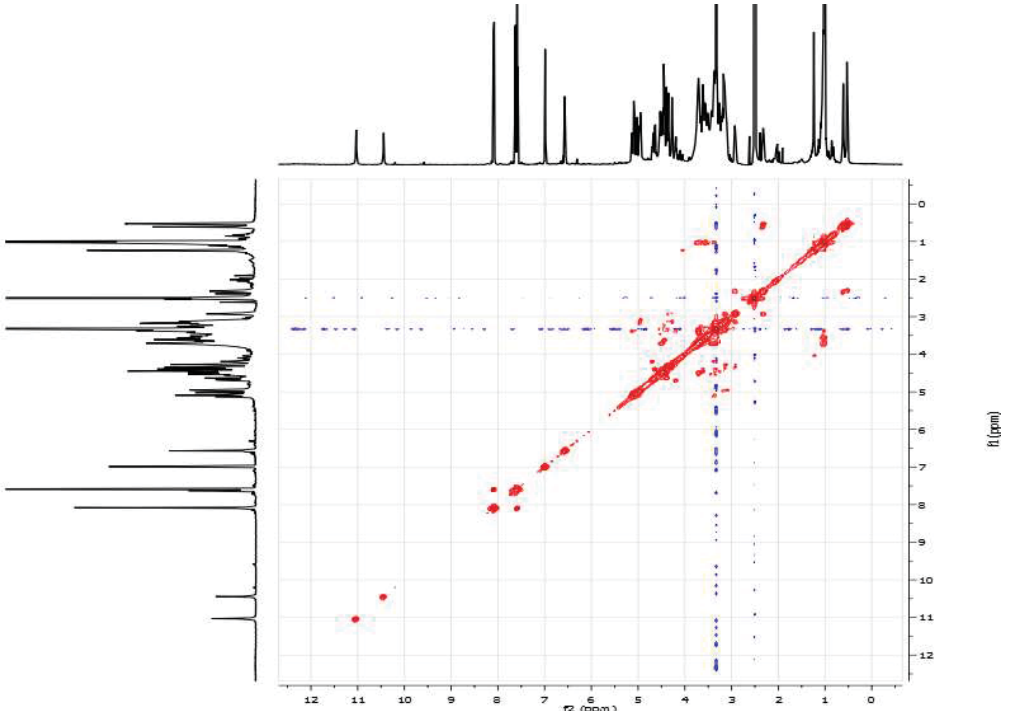

S1-3. ^{1}H-^{1}H COSY spectrum of chrysin 6-C-(2″-O-α-L-rhamnopyranosyl)-*β*-D-glucopyranoside (**1**) in DMSO-d_6 (600 MHz)

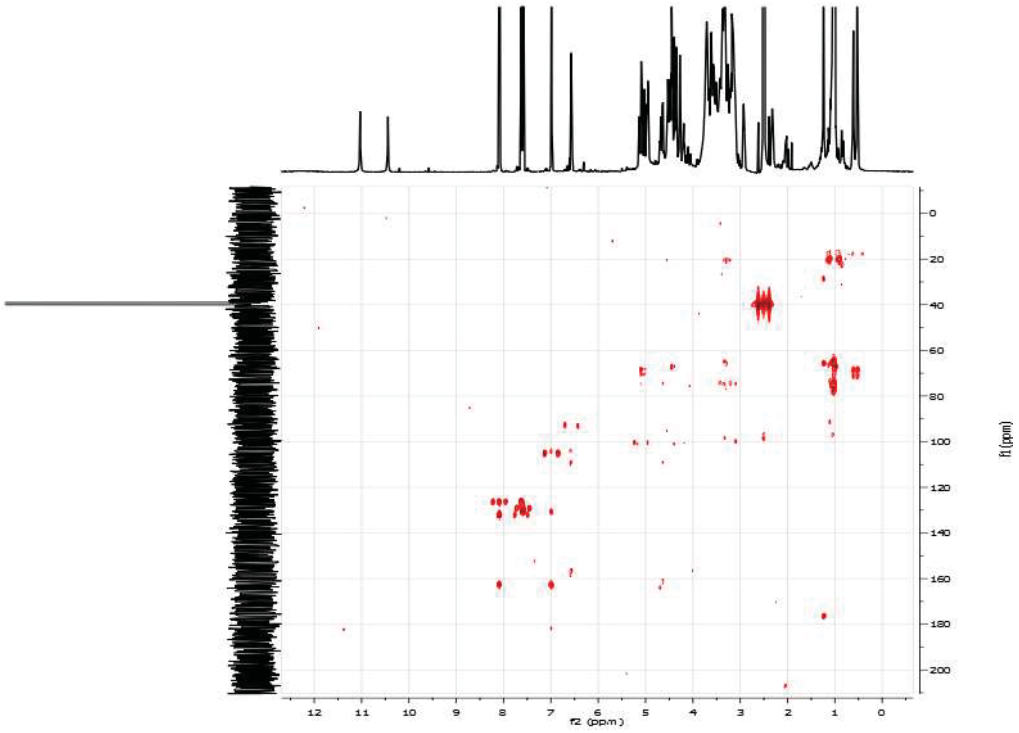

S1-4. HMBC spectrum of chrysin 6-C-(2″-O-α-L-rhamnopyranosyl)-*β*-D-glucopyranoside (**1**) in DMSO-d_6 (600 MHz)

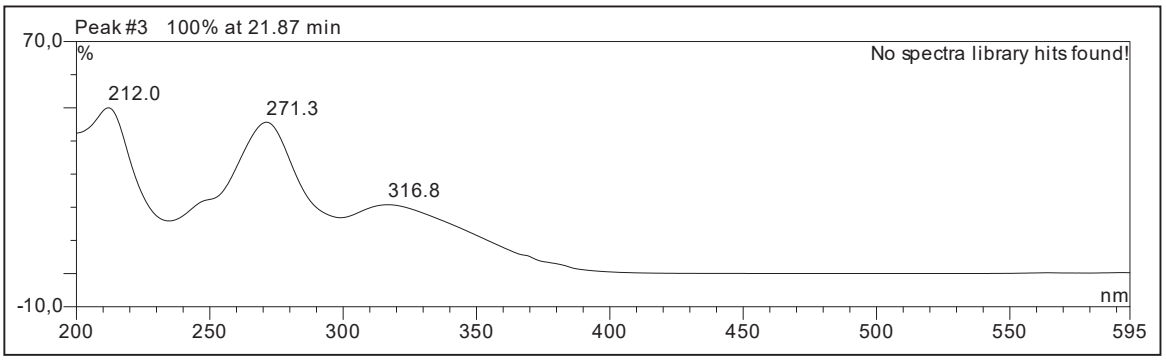

S1a. UV spectrum of hydrolyzed product of **1** (**1a**)

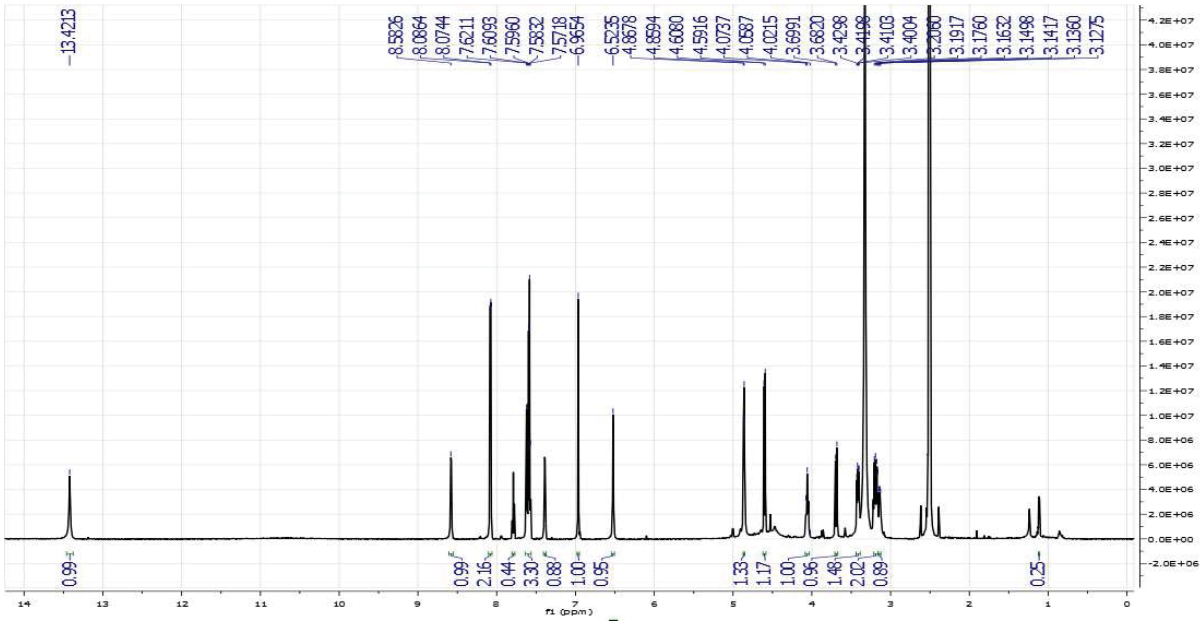

S1a-1. ^{1}H NMR spectrum of hydrolyzed product of **1** (**1a**) in DMSO-d_6 (600 MHz)

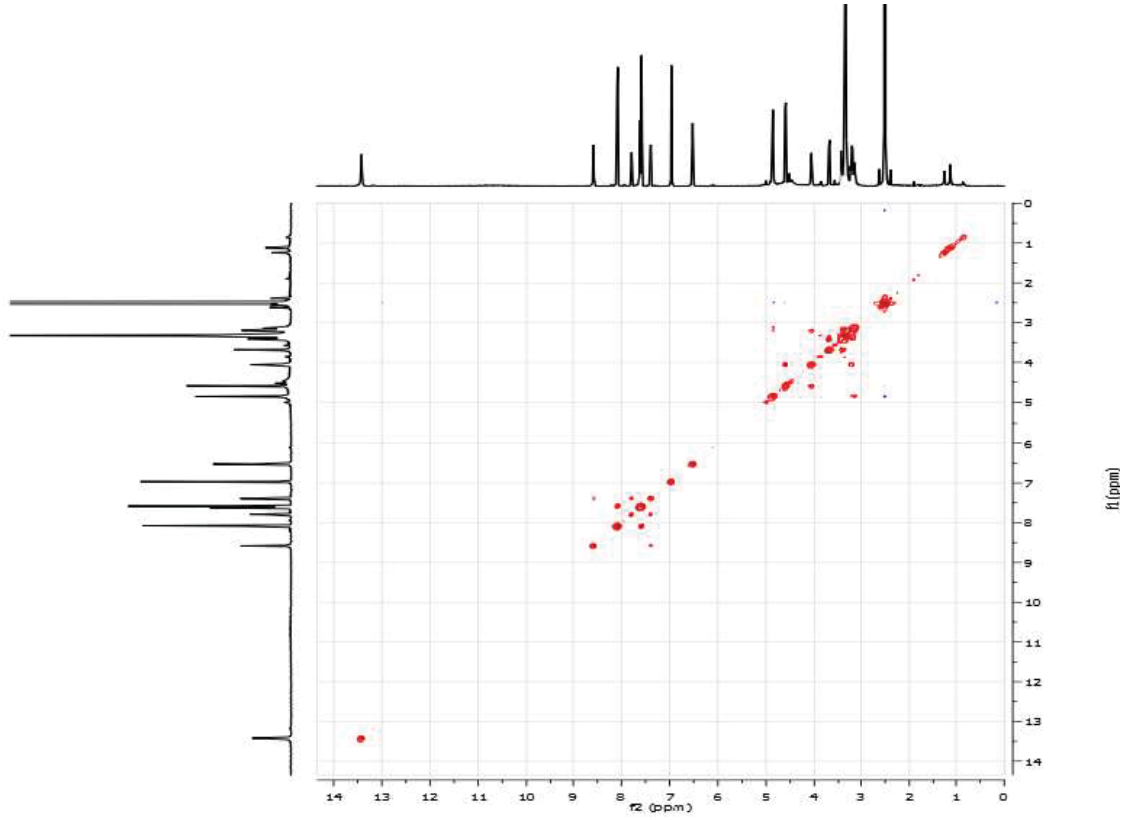

S1a-2. ^{1}H-^{1}H COSY spectrum of hydrolyzed product of **1** (**1a**) in DMSO-d_6 (600 MHz)

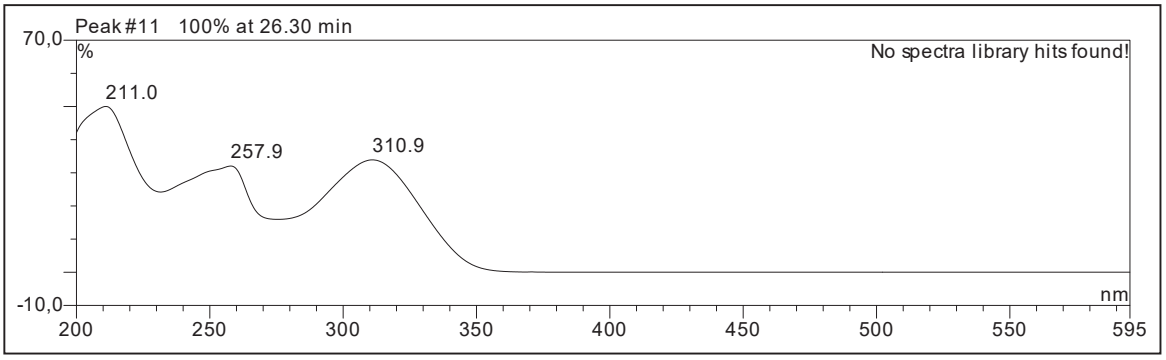

S1b. UV spectrum of acetylated product of **1** (**1b**)

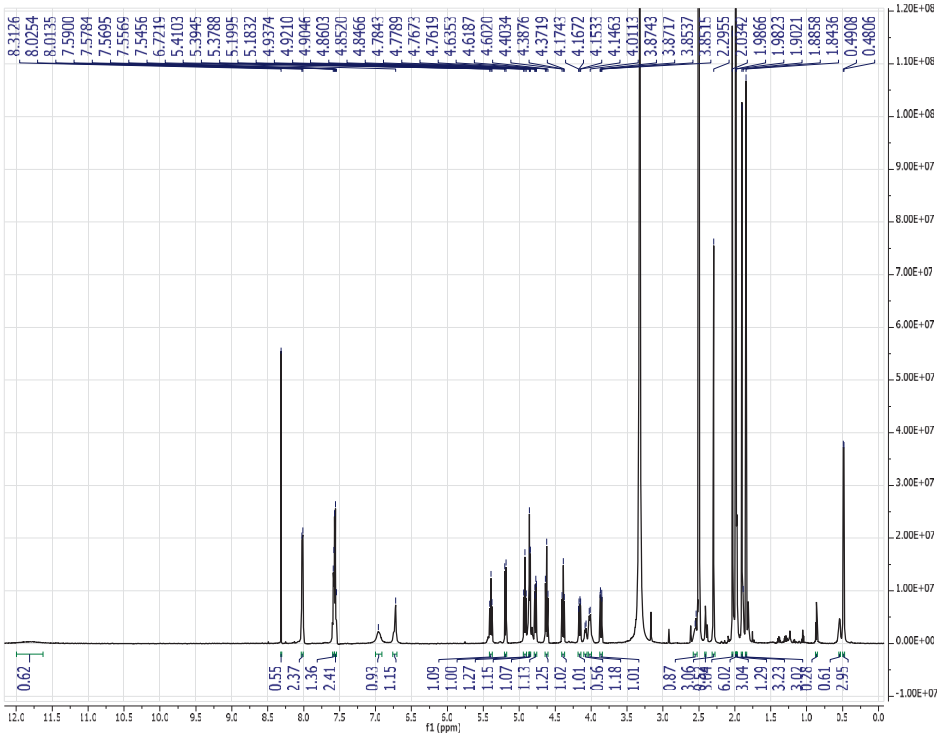

S1b-1. ^{1}H NMR spectrum of acetylated product of **1** (**1b**) in DMSO-d_6 (600 MHz)

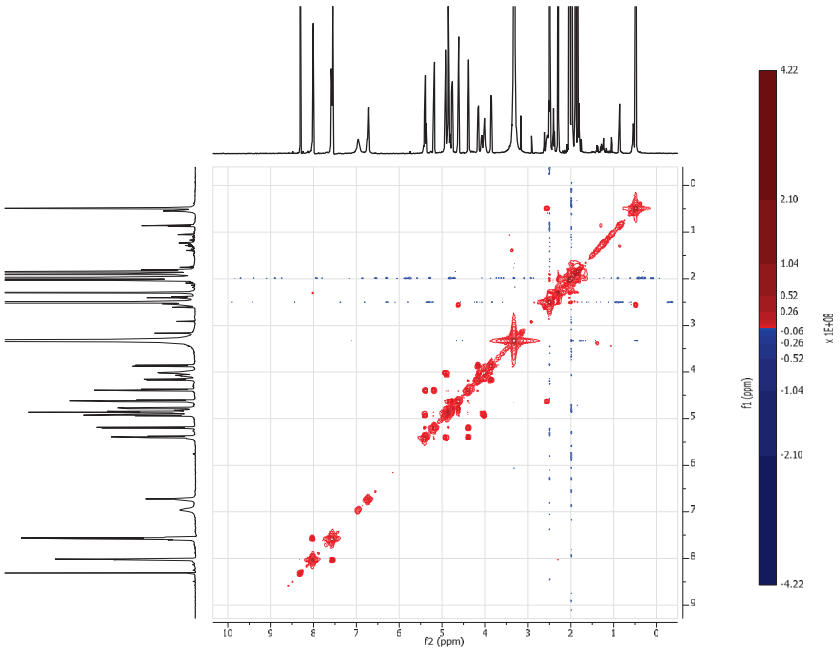

S1b-2. ^{1}H-1H COSY spectrum of acetylated product of **1** (**1b**) in DMSO-d_6 (600 MHz)

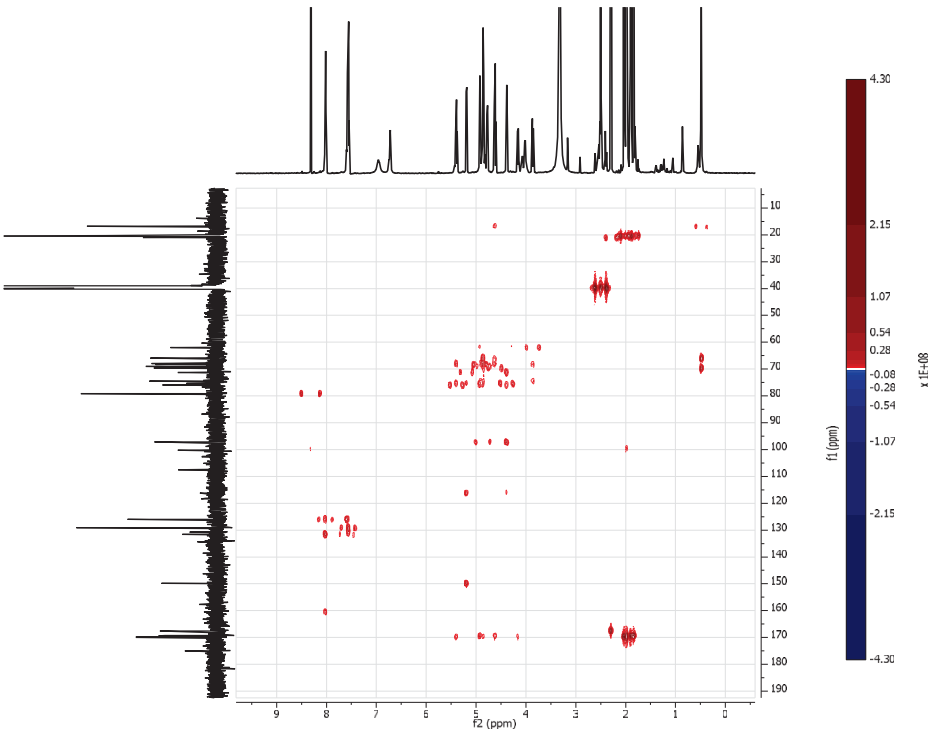

S1b-3. HMBC spectrum of acetylated product of **1** (**1b**) in DMSO-d_6 (600 MHz, 150 MHz)

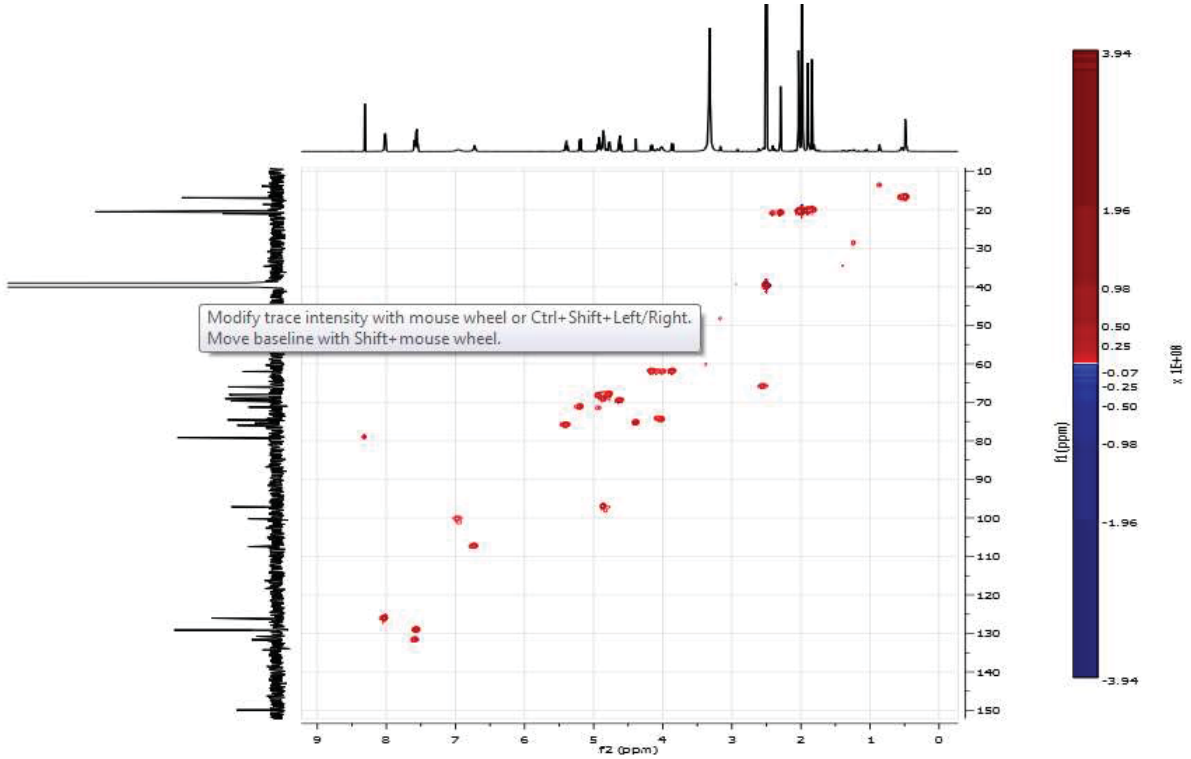

S1b-4. HCQC spectrum of acetylated product of **1** (**1b**) DMSO-d_6 (600 MHz, 150 MHz)

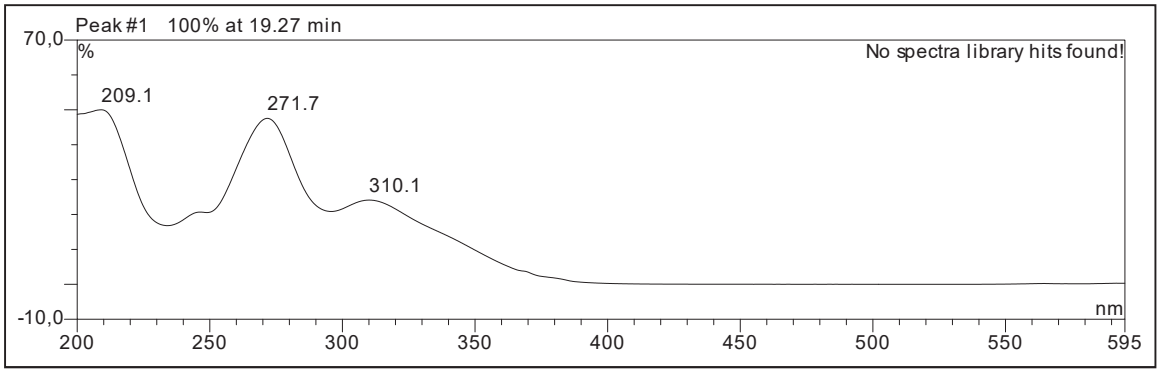

S2. UV spectrum of chrysin 6-C-(2″-O-α-L-rhamnopyranosyl)-*β*-D-glucopyranosyl-7-O-β-D-glucopyranoside (**2**)

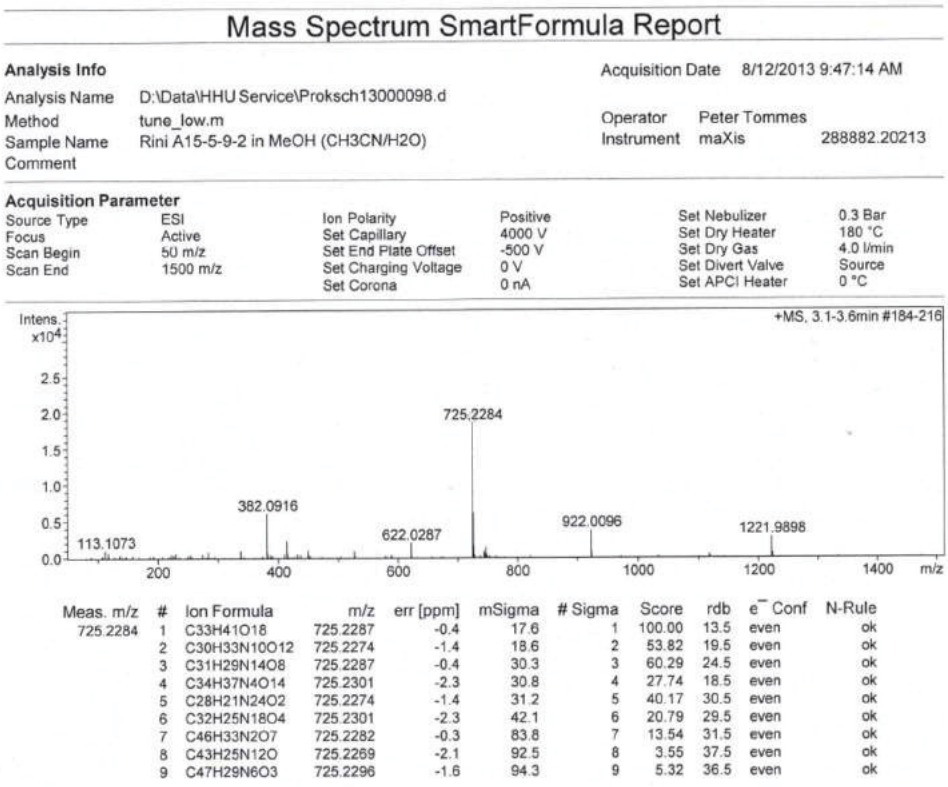

Mass Spectrum SmartFormula Report

Analysis Info

Analysis Name	D:\Data\HHU Service\Proksch13000098.d	Acquisition Date	8/12/2013 9:47:14 AM
Method	tune_low.m	Operator	Peter Tommes
Sample Name	Rini A15-5-9-2 in MeOH (CH3CN/H2O)	Instrument	maXis 288882.20213
Comment			

Acquisition Parameter

Source Type	ESI	Ion Polarity	Positive	Set Nebulizer	0.3 Bar
Focus	Active	Set Capillary	4000 V	Set Dry Heater	180 °C
Scan Begin	50 m/z	Set End Plate Offset	-500 V	Set Dry Gas	4.0 l/min
Scan End	1500 m/z	Set Charging Voltage	0 V	Set Divert Valve	Source
		Set Corona	0 nA	Set APCI Heater	0 °C

Meas. m/z	#	Ion Formula	m/z	err [ppm]	mSigma	# Sigma	Score	rdb	e⁻ Conf	N-Rule
725.2284	1	C33H41O18	725.2287	-0.4	17.6	1	100.00	13.5	even	ok
	2	C30H33N10O12	725.2274	-1.4	18.6	2	53.82	19.5	even	ok
	3	C31H29N14O8	725.2287	-0.4	30.3	3	60.29	24.5	even	ok
	4	C34H37N4O14	725.2301	-2.3	30.8	4	27.74	18.5	even	ok
	5	C28H21N24O2	725.2274	-1.4	31.2	5	40.17	30.5	even	ok
	6	C32H25N18O4	725.2301	-2.3	42.1	6	20.79	29.5	even	ok
	7	C46H33N2O7	725.2282	-0.3	83.8	7	13.54	31.5	even	ok
	8	C43H25N12O	725.2269	-2.1	92.5	8	3.55	37.5	even	ok
	9	C47H29N6O3	725.2296	-1.6	94.3	9	5.32	36.5	even	ok

S2-1. HRESIMS of chrysin 6-C-(2″-O-α-L-rhamnopyranosyl)-*β*-D-glucopyranosyl-7-O-β-D-glucopyranoside (**2**)

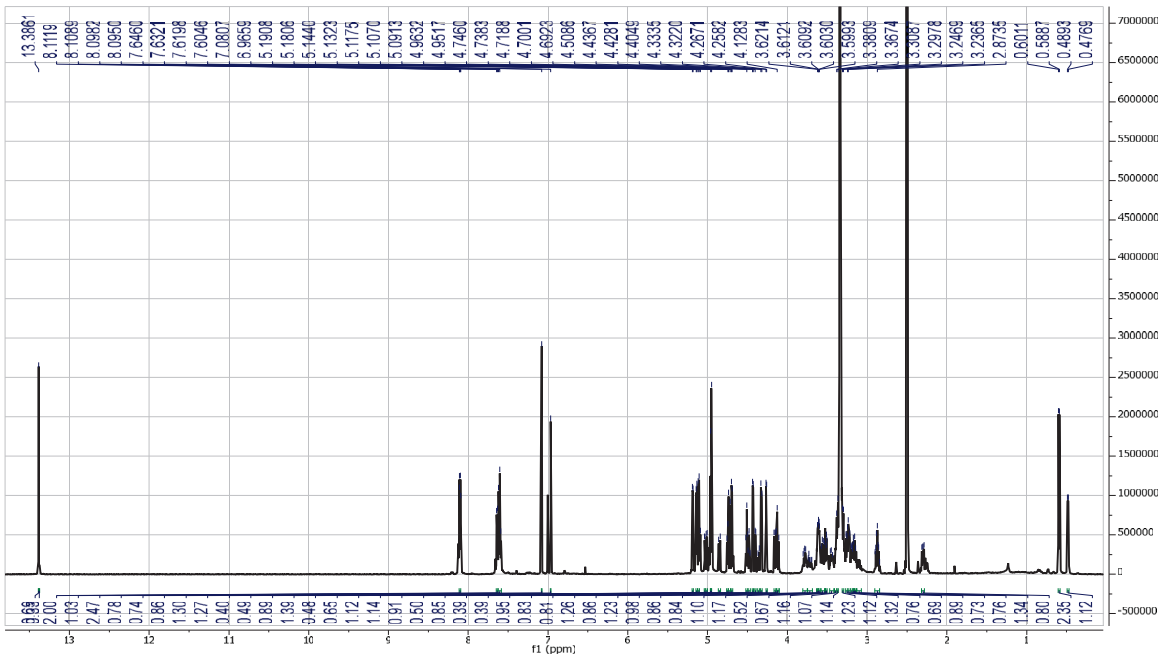

S2-2. [1]H NMR spectrum of chrysin 6-C-(2″-O-α-L-rhamnopyranosyl)-*β*-D-glucopyranosyl-7-O-*β*-D-glucopyranoside (**2**) in DMSO-d_6 (600 MHz)

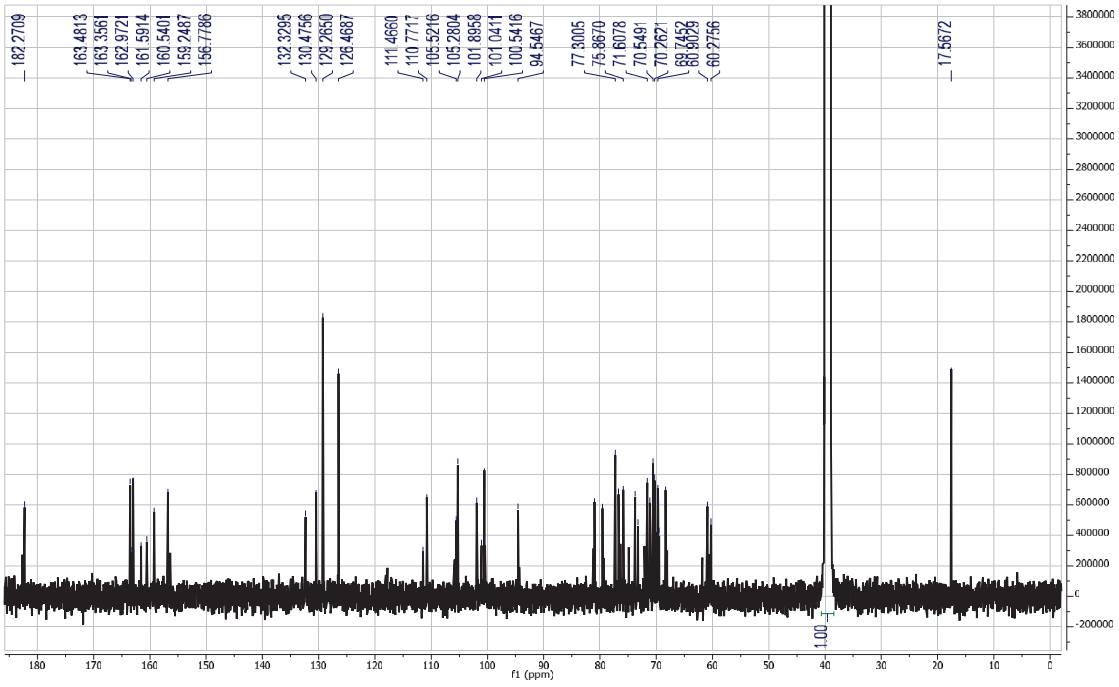

S2-3. [13]C NMR spectrum of chrysin 6-C-(2″-O-α-L-rhamnopyranosyl)-*β*-D-glucopyranosyl-7-O-*β*-D-glucopyranoside (**2**) in DMSO-d_6 (150 MHz)

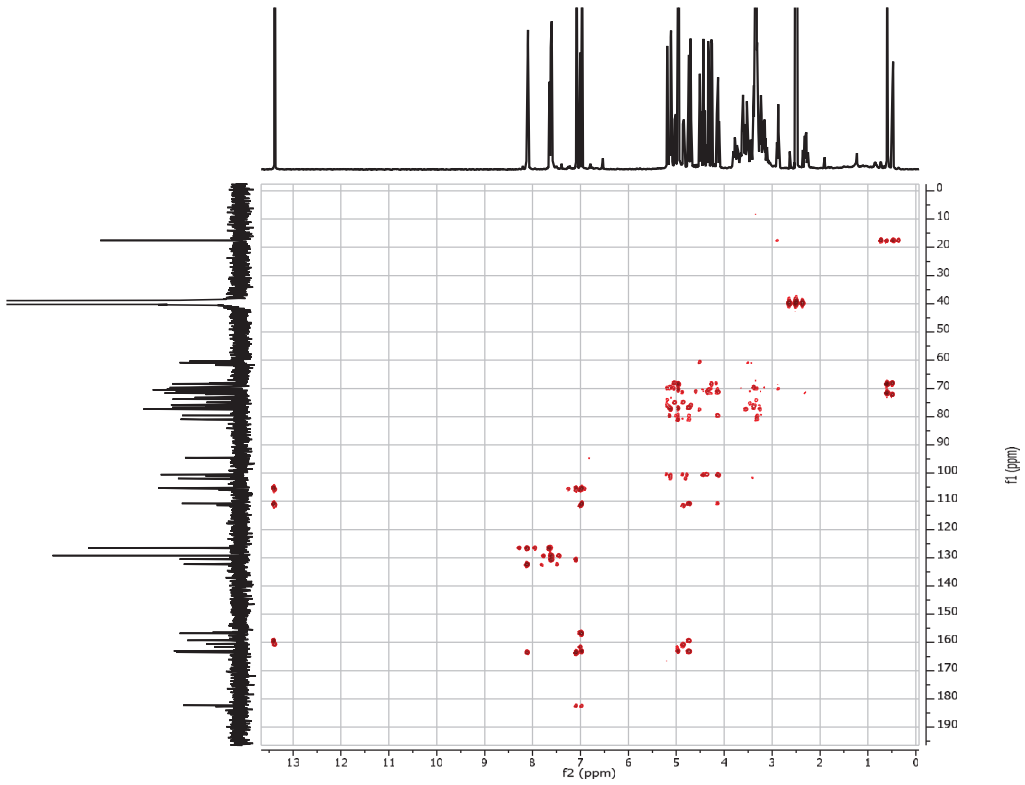

S2-4. HMBC spectrum of chrysin 6-C-(2″-O-α-L-rhamnopyranosyl)-*β*-D-glucopyranosyl-7-O-*β*-D-glucopyranoside (**2**) in DMSO-d_6 (600 MHz, 150 MHz)

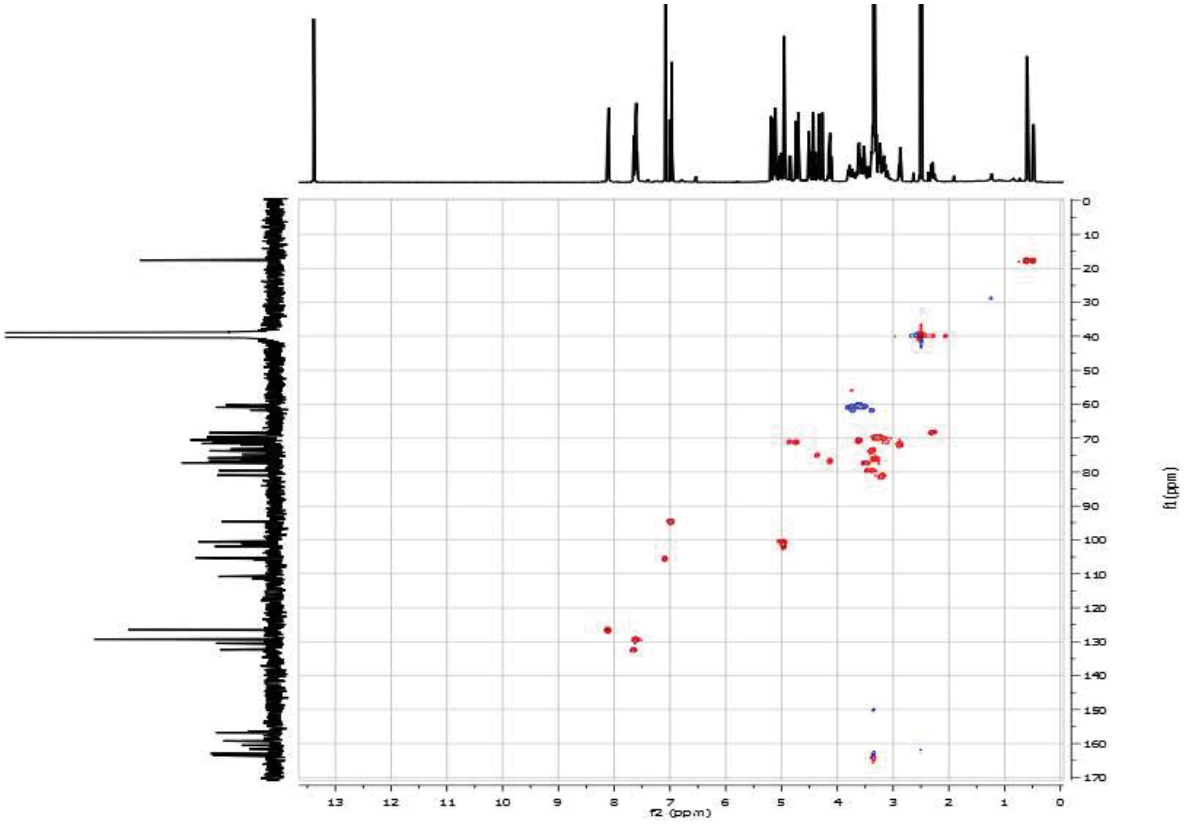

S2-4. HSQC spectrum of chrysin 6-C-(2″-O-α-L-rhamnopyranosyl)-*β*-D-glucopyranosyl-7-O-*β*-D-glucopyranoside (**2**) in DMSO-d_6 (600 MHz, 150 MHz)

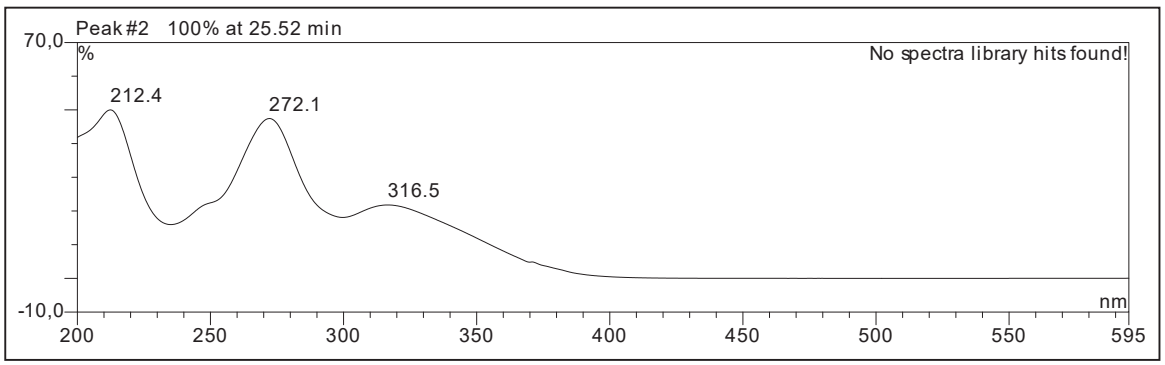

S3. UV spectrum of chrysin 6-C-(2″-O-α-L-rhamnosyl)-*β*-L-fucopyranoside (**3**)

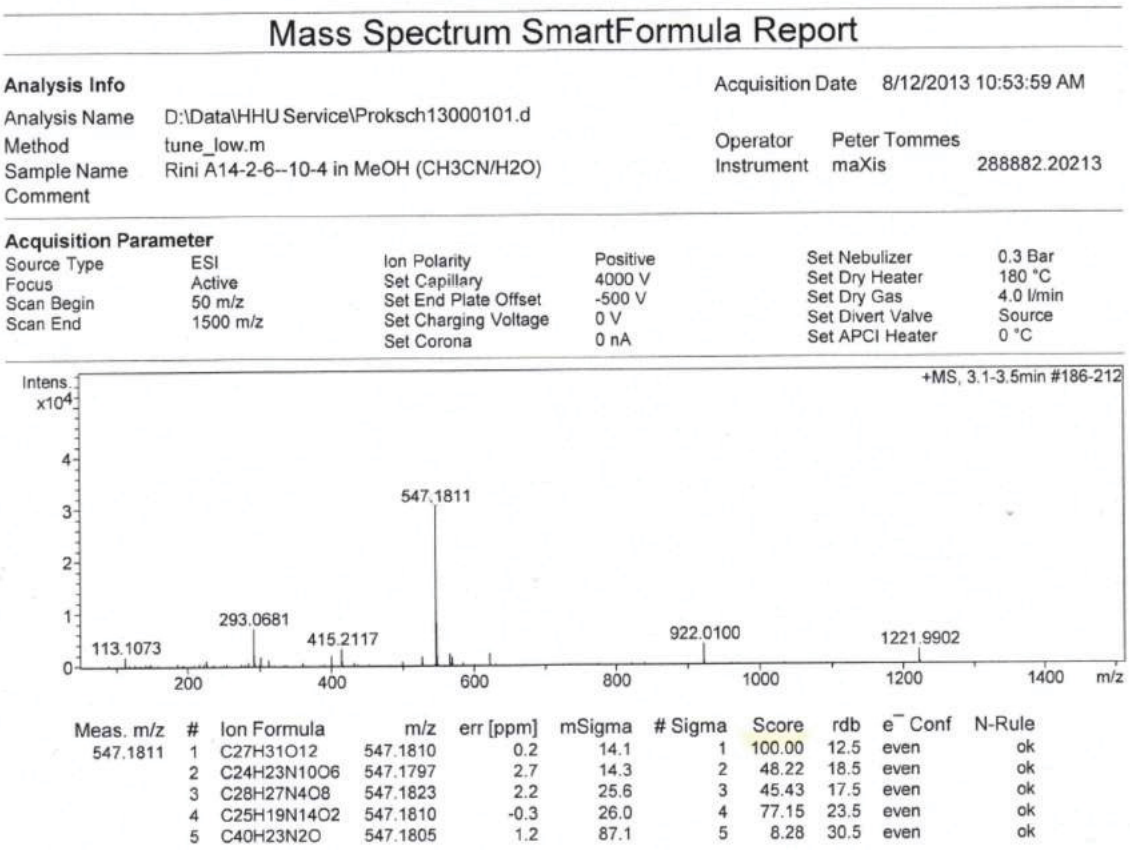

Mass Spectrum SmartFormula Report

Analysis Info

Analysis Name	D:\Data\HHU Service\Proksch13000101.d	Acquisition Date	8/12/2013 10:53:59 AM
Method	tune_low.m	Operator	Peter Tommes
Sample Name	Rini A14-2-6--10-4 in MeOH (CH3CN/H2O)	Instrument	maXis 288882.20213
Comment			

Acquisition Parameter

Source Type	ESI	Ion Polarity	Positive	Set Nebulizer	0.3 Bar
Focus	Active	Set Capillary	4000 V	Set Dry Heater	180 °C
Scan Begin	50 m/z	Set End Plate Offset	-500 V	Set Dry Gas	4.0 l/min
Scan End	1500 m/z	Set Charging Voltage	0 V	Set Divert Valve	Source
		Set Corona	0 nA	Set APCI Heater	0 °C

Meas. m/z	#	Ion Formula	m/z	err [ppm]	mSigma	# Sigma	Score	rdb	e⁻ Conf	N-Rule
547.1811	1	C27H31O12	547.1810	0.2	14.1	1	100.00	12.5	even	ok
	2	C24H23N10O6	547.1797	2.7	14.3	2	48.22	18.5	even	ok
	3	C28H27N4O8	547.1823	2.2	25.6	3	45.43	17.5	even	ok
	4	C25H19N14O2	547.1810	-0.3	26.0	4	77.15	23.5	even	ok
	5	C40H23N2O	547.1805	1.2	87.1	5	8.28	30.5	even	ok

S3-1. HRESIMS of chrysin 6-C-(2″-O-α-L-rhamnosyl)-*β*-L-fucopyranoside (**3**)

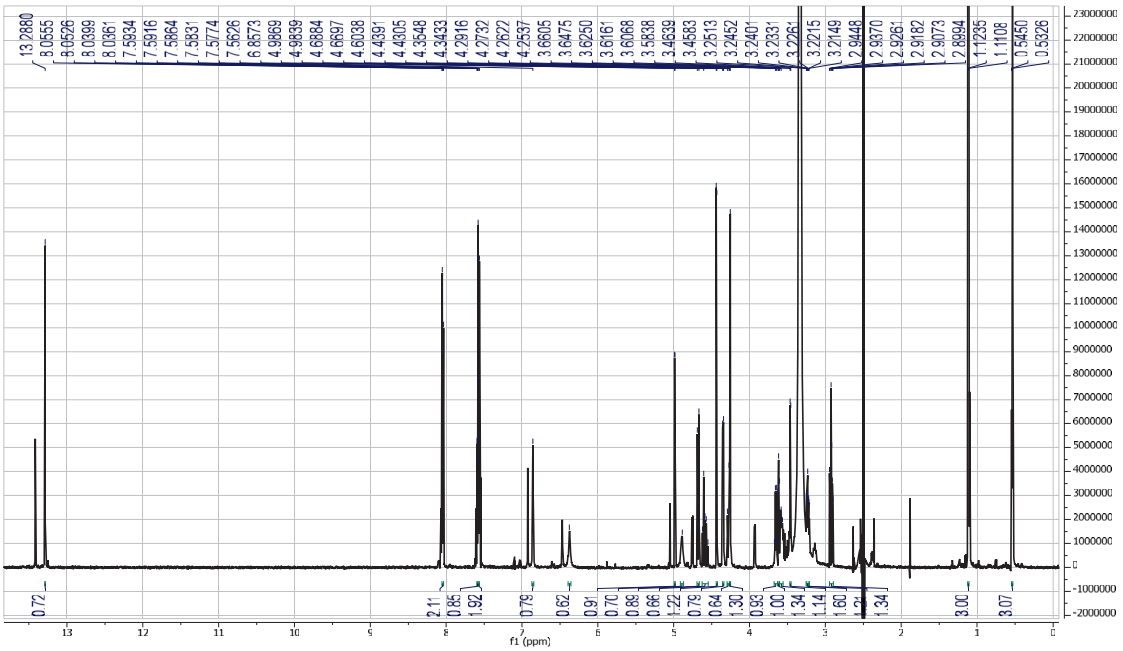

S3-2 ^{1}H NMR spectrum of chrysin 6-C-(2″-O-α-L-rhamnosyl)-*β*-L-fucopyranoside (**3**) in DMSO-*d*$_6$ (600 MHz)

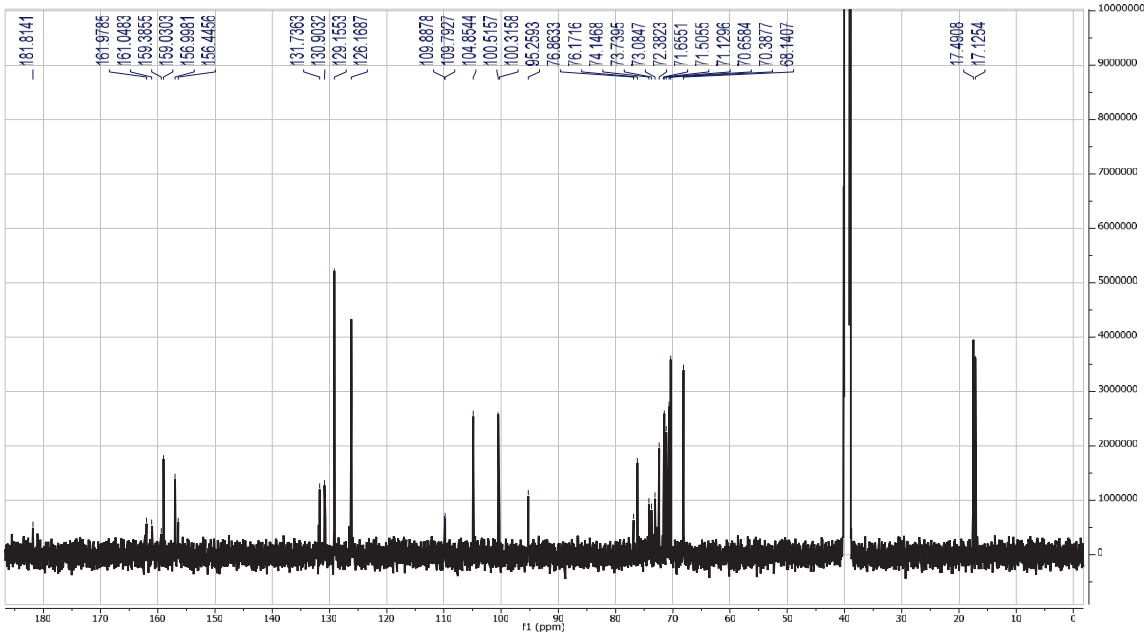

S3-3. ^{13}C NMR spectrum of chrysin 6-C-(2″-O-α-L-rhamnosyl)-*β*-L-fucopyranoside (**3**) in DMSO-*d*$_6$ (150 MHz)

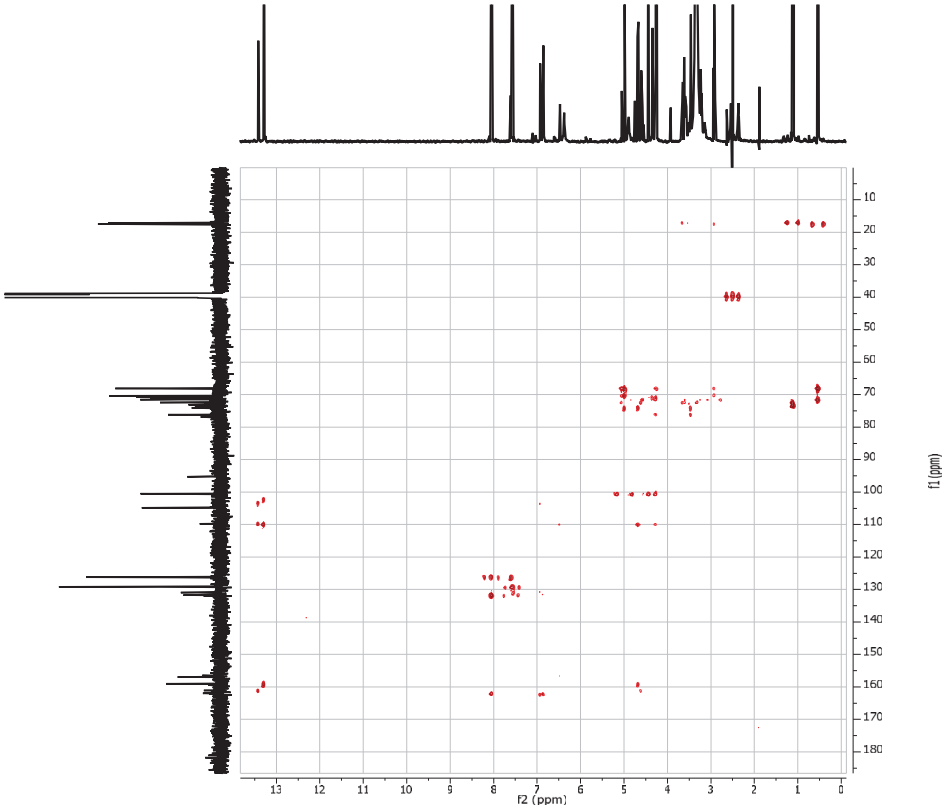

S3-4. HMBC spectrum of chrysin 6-C-(2″-O-α-L-rhamnosyl)-*β*-L-fucopyranoside (**3**) in DMSO-d_6 (600 MHz, 150 MHz)

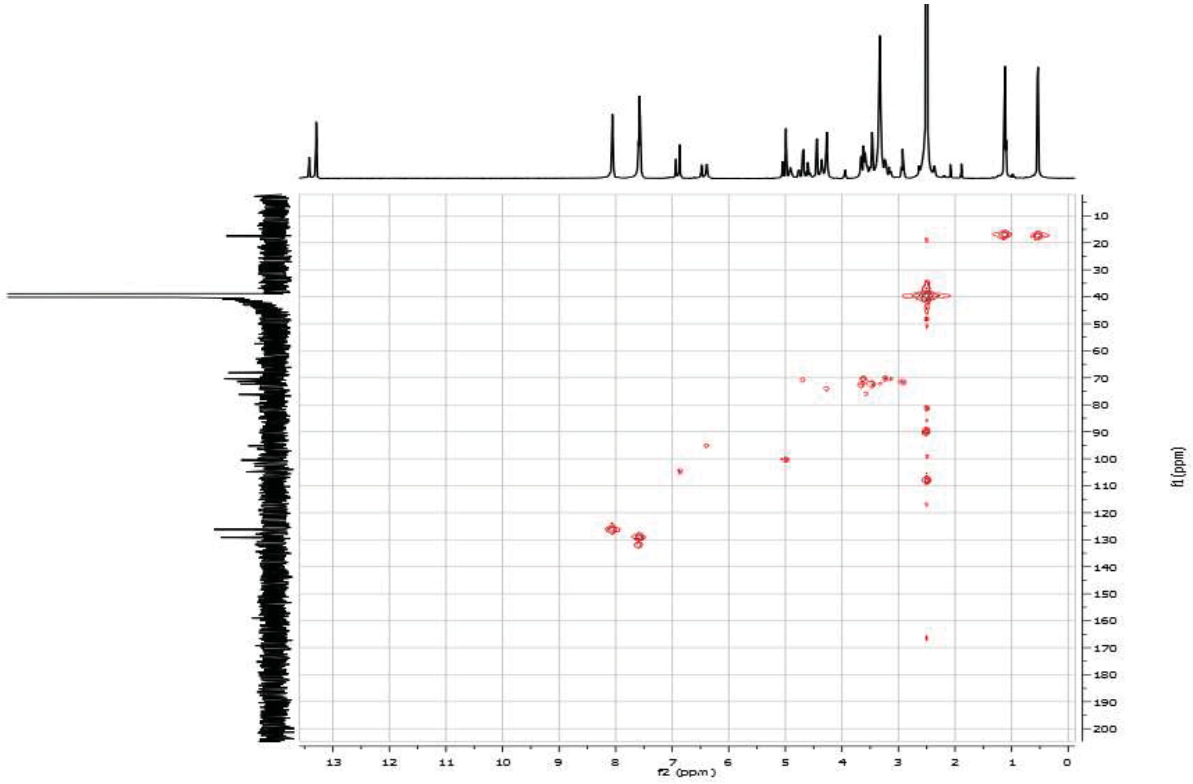

S3-5. HSQC spectrum of chrysin 6-C-(2″-O-α-L-rhamnosyl)-*β*-L-fucopyranoside (**3**) in DMSO-d_6 (600 MHz, 150 MHz)

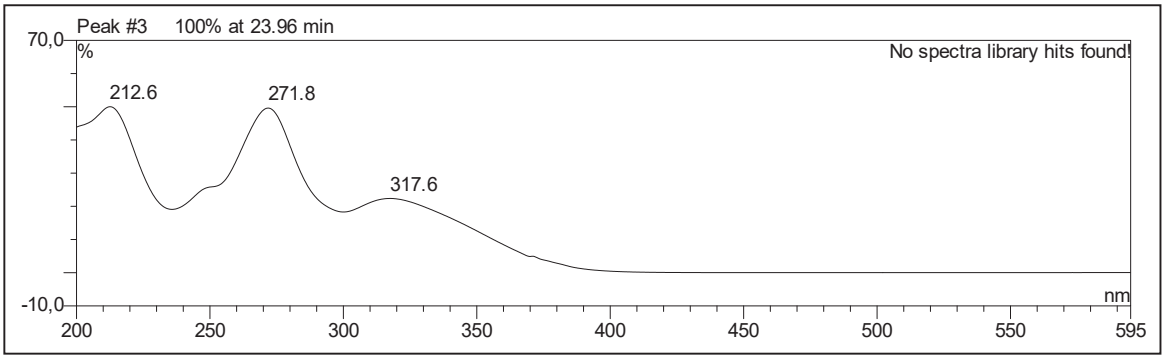

S4. UV spectrum of chrysin 6-C-(2″-O-α-L-rhamnopyranosyl)-6′-deoxy-ribo-hexos-3-uloside (**4**)

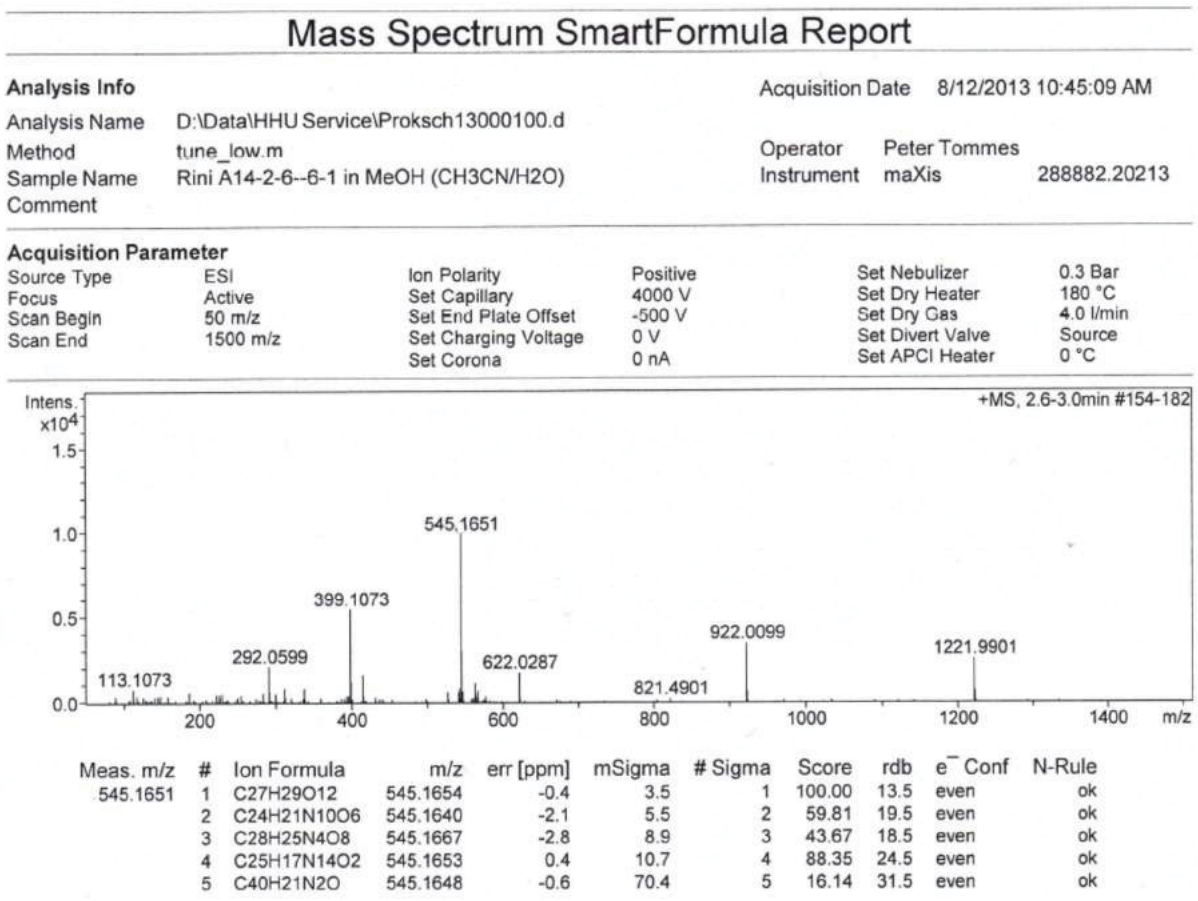

Mass Spectrum SmartFormula Report

Analysis Info

Acquisition Date 8/12/2013 10:45:09 AM

Analysis Name D:\Data\HHU Service\Proksch13000100.d
Method tune_low.m
Sample Name Rini A14-2-6--6-1 in MeOH (CH3CN/H2O)
Comment

Operator Peter Tommes
Instrument maXis 288882.20213

Acquisition Parameter

Source Type	ESI	Ion Polarity	Positive	Set Nebulizer	0.3 Bar
Focus	Active	Set Capillary	4000 V	Set Dry Heater	180 °C
Scan Begin	50 m/z	Set End Plate Offset	-500 V	Set Dry Gas	4.0 l/min
Scan End	1500 m/z	Set Charging Voltage	0 V	Set Divert Valve	Source
		Set Corona	0 nA	Set APCI Heater	0 °C

Meas. m/z	#	Ion Formula	m/z	err [ppm]	mSigma	# Sigma	Score	rdb	e¯ Conf	N-Rule
545.1651	1	C27H29O12	545.1654	-0.4	3.5	1	100.00	13.5	even	ok
	2	C24H21N10O6	545.1640	-2.1	5.5	2	59.81	19.5	even	ok
	3	C28H25N4O8	545.1667	-2.8	8.9	3	43.67	18.5	even	ok
	4	C25H17N14O2	545.1653	0.4	10.7	4	88.35	24.5	even	ok
	5	C40H21N2O	545.1648	-0.6	70.4	5	16.14	31.5	even	ok

S4-1. HRESIMS of chrysin 6-C-(2″-O-α-L-rhamnopyranosyl)-6′-deoxy-ribo-hexos-3-uloside (**4**)

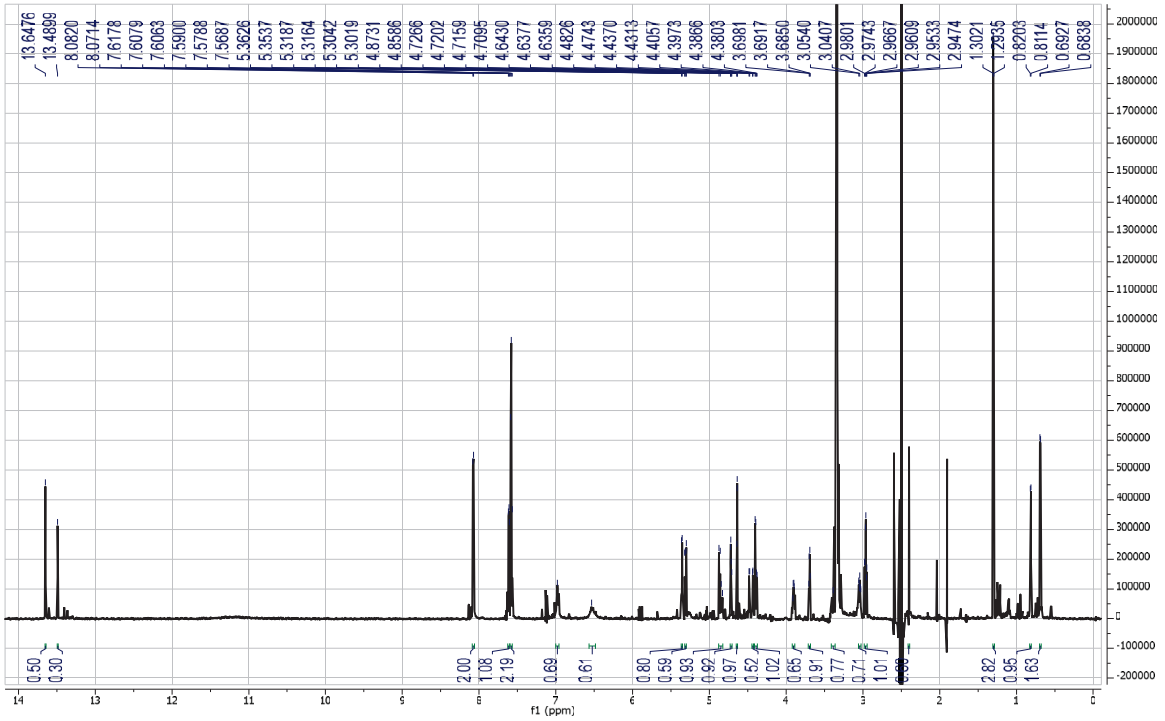

S4-2. ^{1}H NMR spectrum of chrysin 6-C-(2″-O-α-L-rhamnopyranosyl)-6′-deoxy-ribo-hexos-3-uloside (**4**) in DMSO-d_6 (600 MHz)

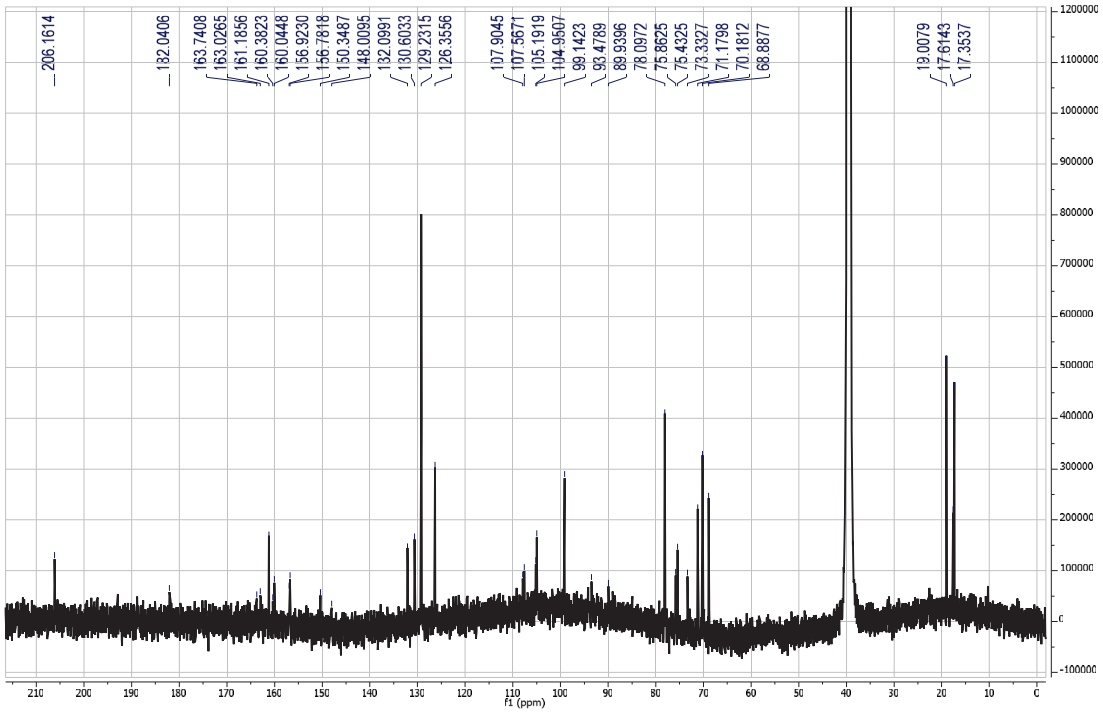

S4-3. ^{13}C NMR spectrum of chrysin 6-C-(2″-O-α-L-rhamnopyranosyl)-6′-deoxy-ribo-hexos-3-uloside (**4**) in DMSO-d_6 (150 MHz)

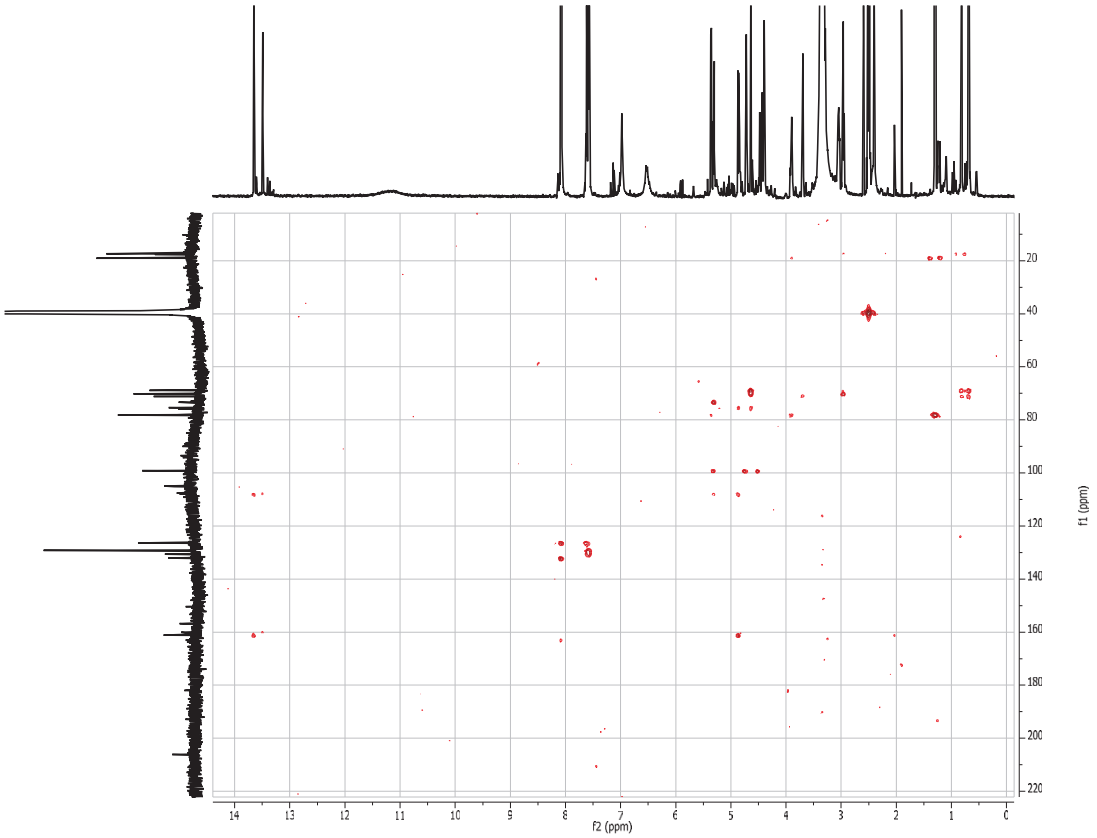

S4-4. HMBC spectrum of chrysin 6-C-(2″-O-α-L-rhamnopyranosyl)-6′-deoxy-ribo-hexos-3-uloside (**4**) in DMSO-d_6 (600 MHz, 150 MHz)

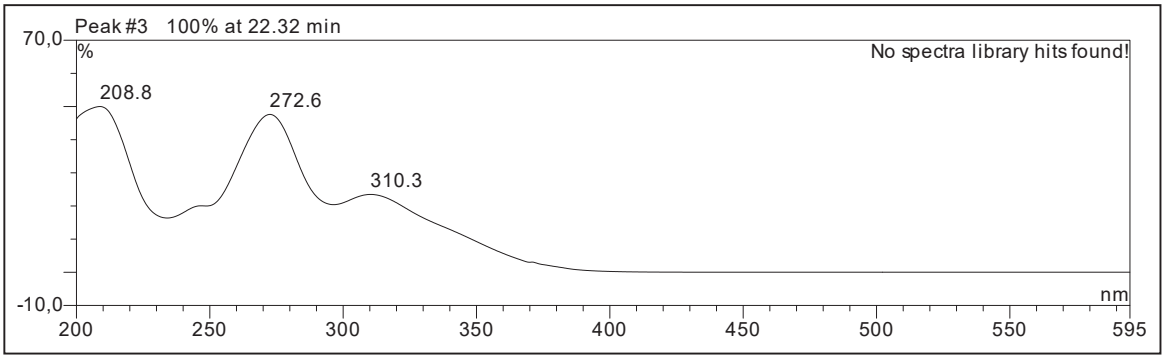

S5. UV spectrum of chrysin 6-C-β-boivinopyranosyl-7-O-β-D-glucopyranoside (**5**)

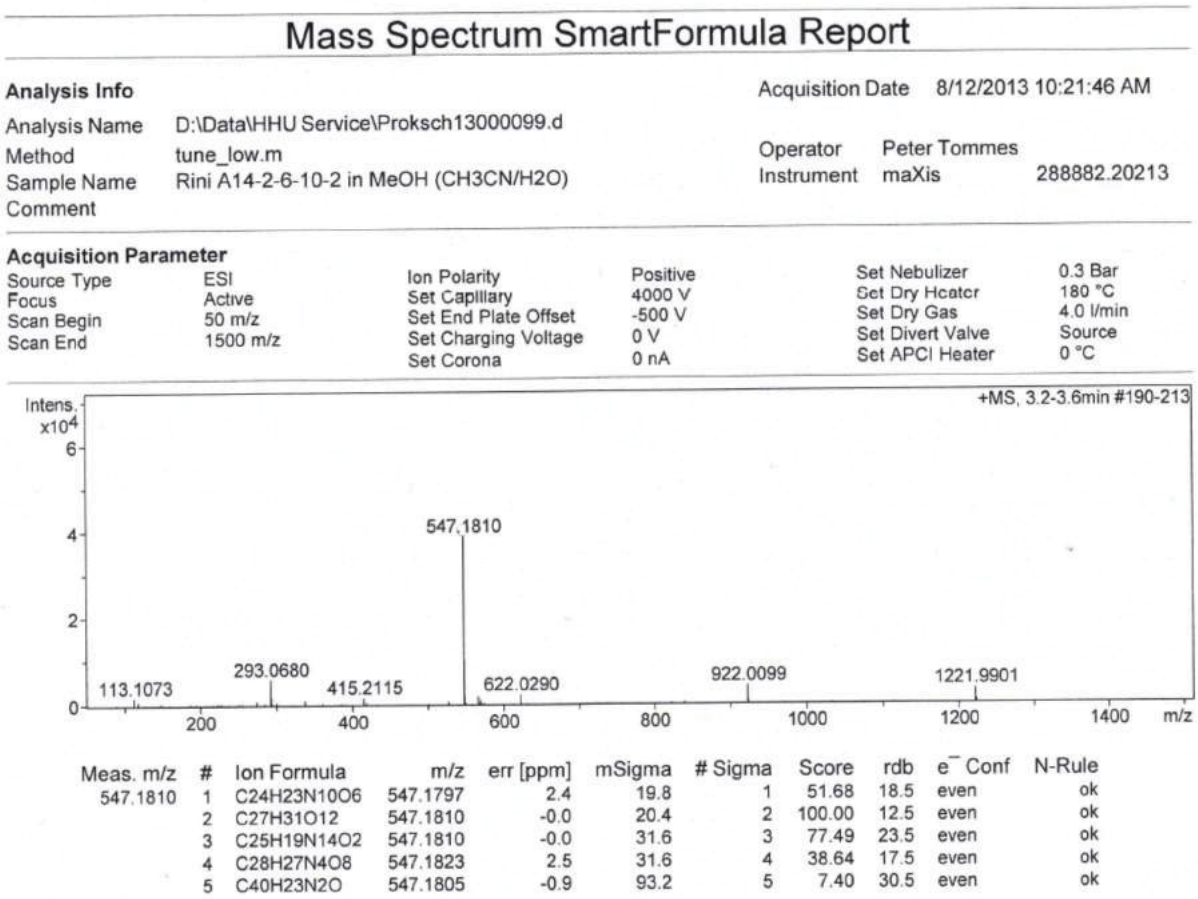

Mass Spectrum SmartFormula Report

Analysis Info

Acquisition Date 8/12/2013 10:21:46 AM

Analysis Name D:\Data\HHU Service\Proksch13000099.d
Method tune_low.m
Sample Name Rini A14-2-6-10-2 in MeOH (CH3CN/H2O)
Comment

Operator Peter Tommes
Instrument maXis 288882.20213

Acquisition Parameter

Source Type	ESI	Ion Polarity	Positive	Set Nebulizer	0.3 Bar
Focus	Active	Set Capillary	4000 V	Set Dry Heater	180 °C
Scan Begin	50 m/z	Set End Plate Offset	-500 V	Set Dry Gas	4.0 l/min
Scan End	1500 m/z	Set Charging Voltage	0 V	Set Divert Valve	Source
		Set Corona	0 nA	Set APCI Heater	0 °C

Meas. m/z	#	Ion Formula	m/z	err [ppm]	mSigma	# Sigma	Score	rdb	e⁻ Conf	N-Rule
547.1810	1	C24H23N10O6	547.1797	2.4	19.8	1	51.68	18.5	even	ok
	2	C27H31O12	547.1810	-0.0	20.4	2	100.00	12.5	even	ok
	3	C25H19N14O2	547.1810	-0.0	31.6	3	77.49	23.5	even	ok
	4	C28H27N4O8	547.1823	2.5	31.6	4	38.64	17.5	even	ok
	5	C40H23N2O	547.1805	-0.9	93.2	5	7.40	30.5	even	ok

S5-1. HRESIMS of chrysin 6-C-*β*-boivinopyranosyl-7-O-*β*-D-glucopyranoside (**5**)

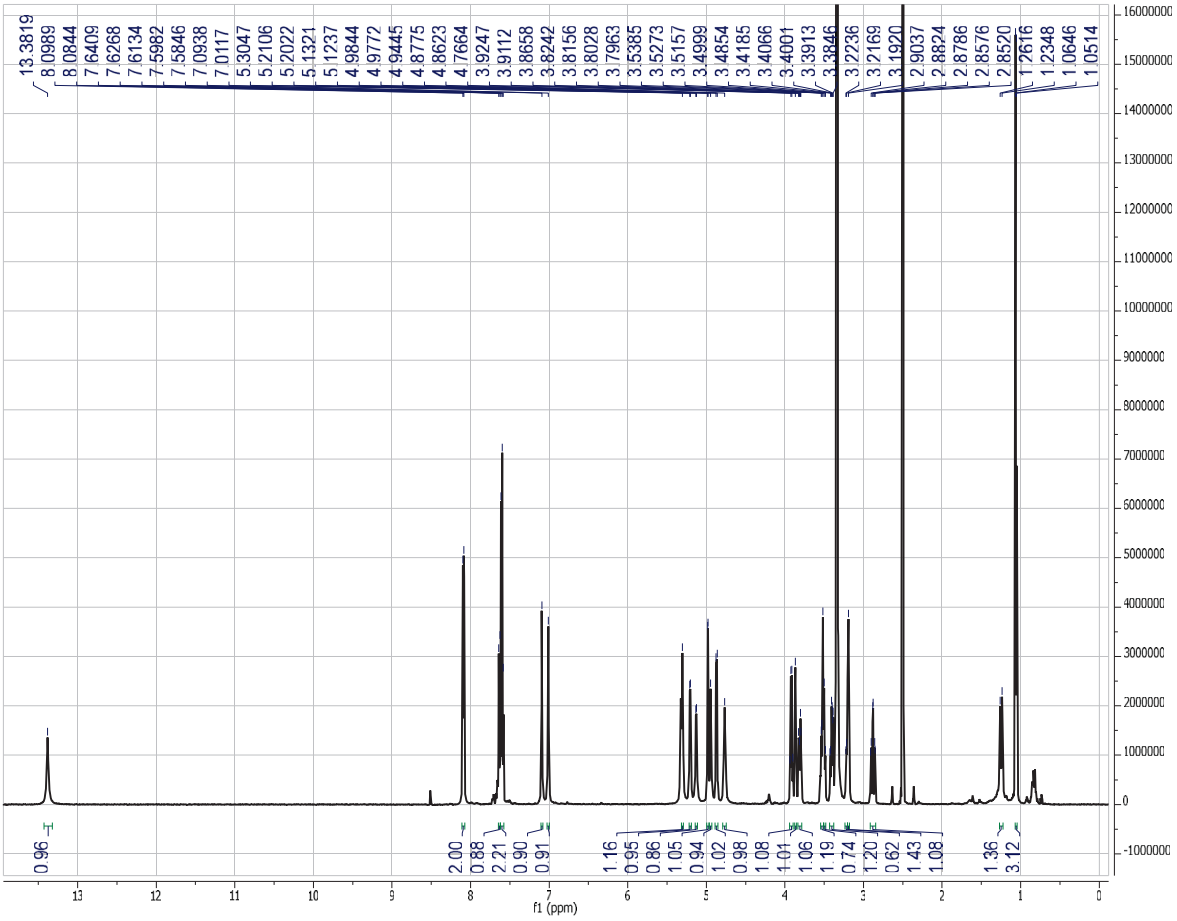

S5-2. ^{1}H NMR spectrum of chrysin 6-C-*β*-boivinopyranosyl-7-O-*β*-D-glucopyranoside (**5**) in DMSO-d_6 (600 MHz)

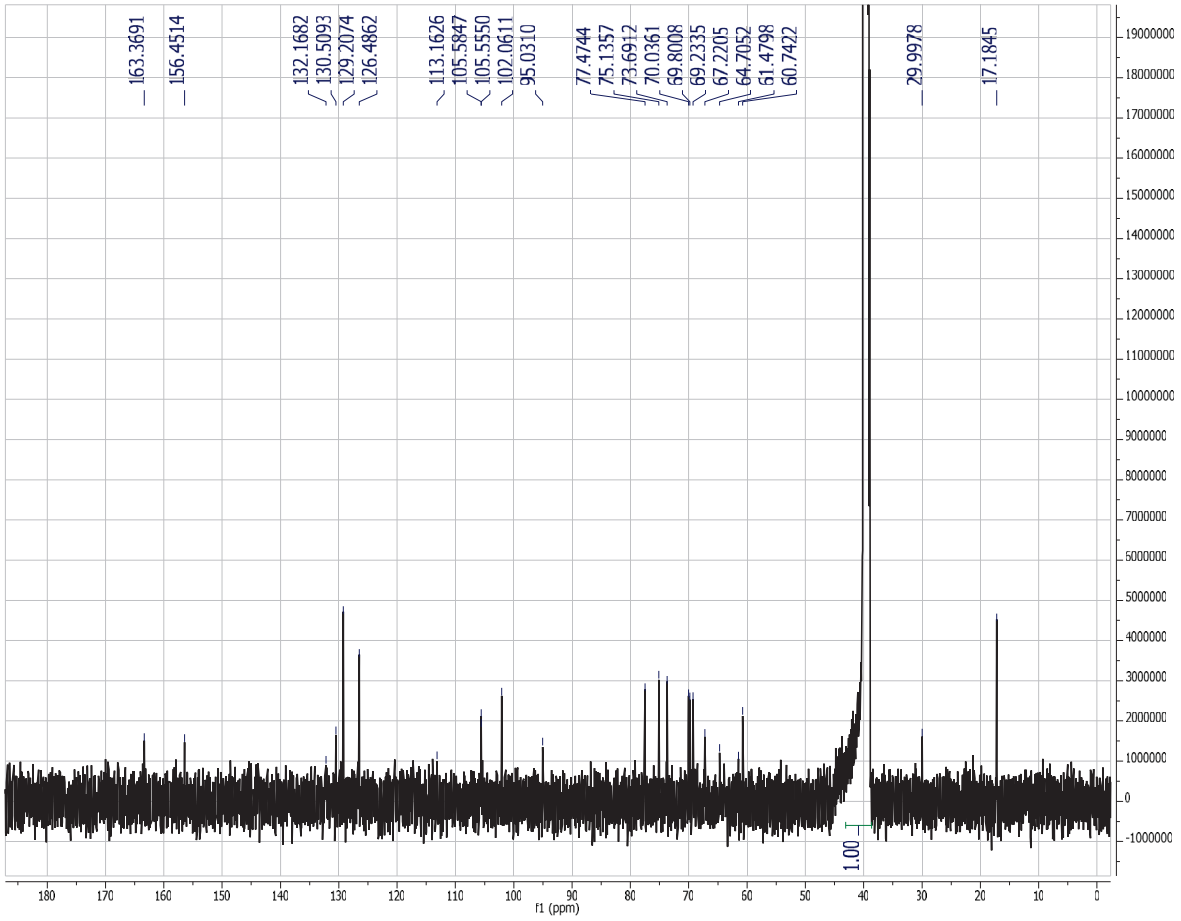

S5-3. ^{13}C NMR spectrum of chrysin 6-C-*β*-boivinopyranosyl-7-O-*β*-D-glucopyranoside (**5**) in DMSO-d_6 (150 MHz)

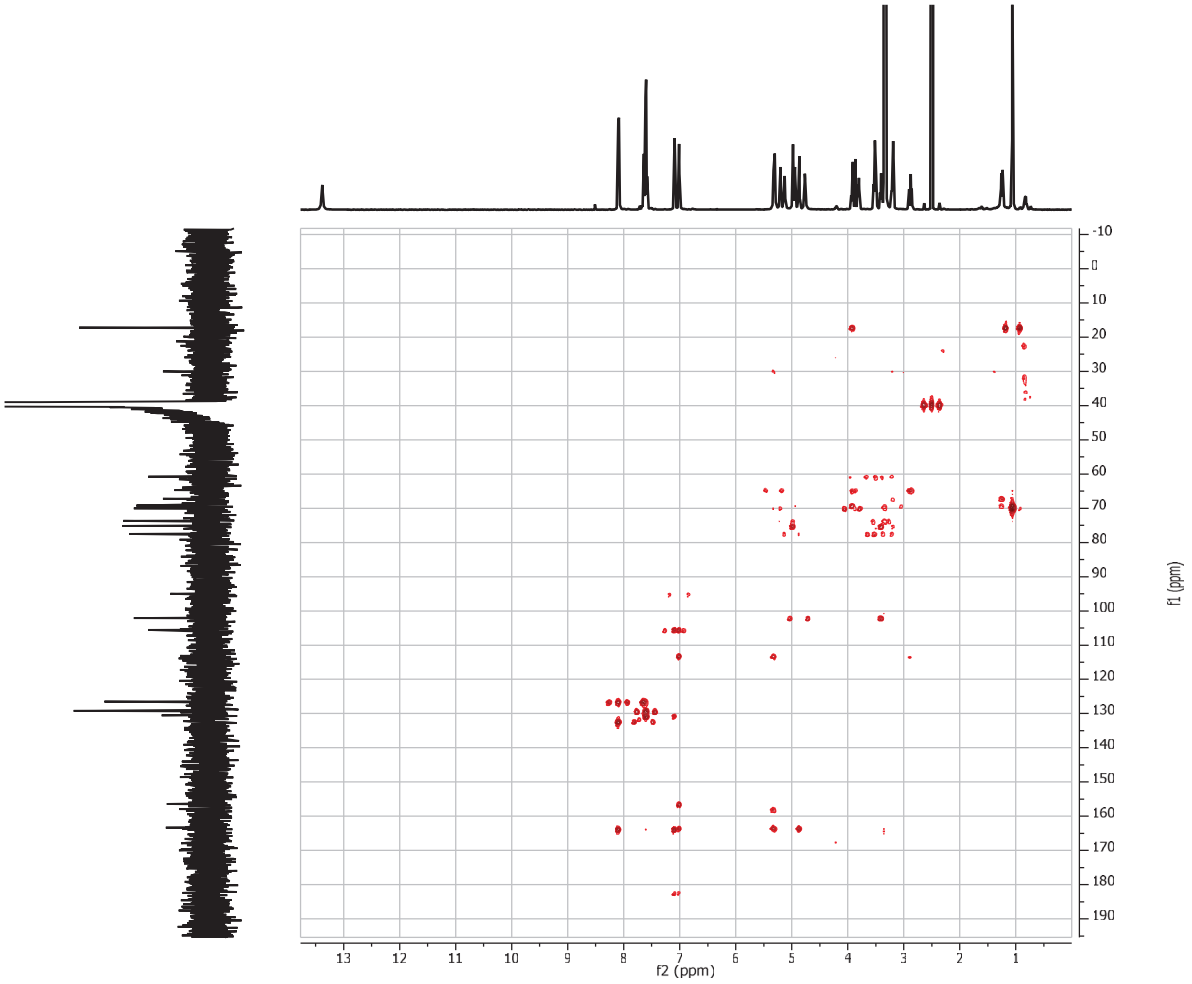

S5-4. HMBC spectrum of chrysin 6-C-*β*-boivinopyranosyl-7-O-*β*-D-glucopyranoside (**5**) in DMSO-d_6 (600 MHz, 150 MHz)

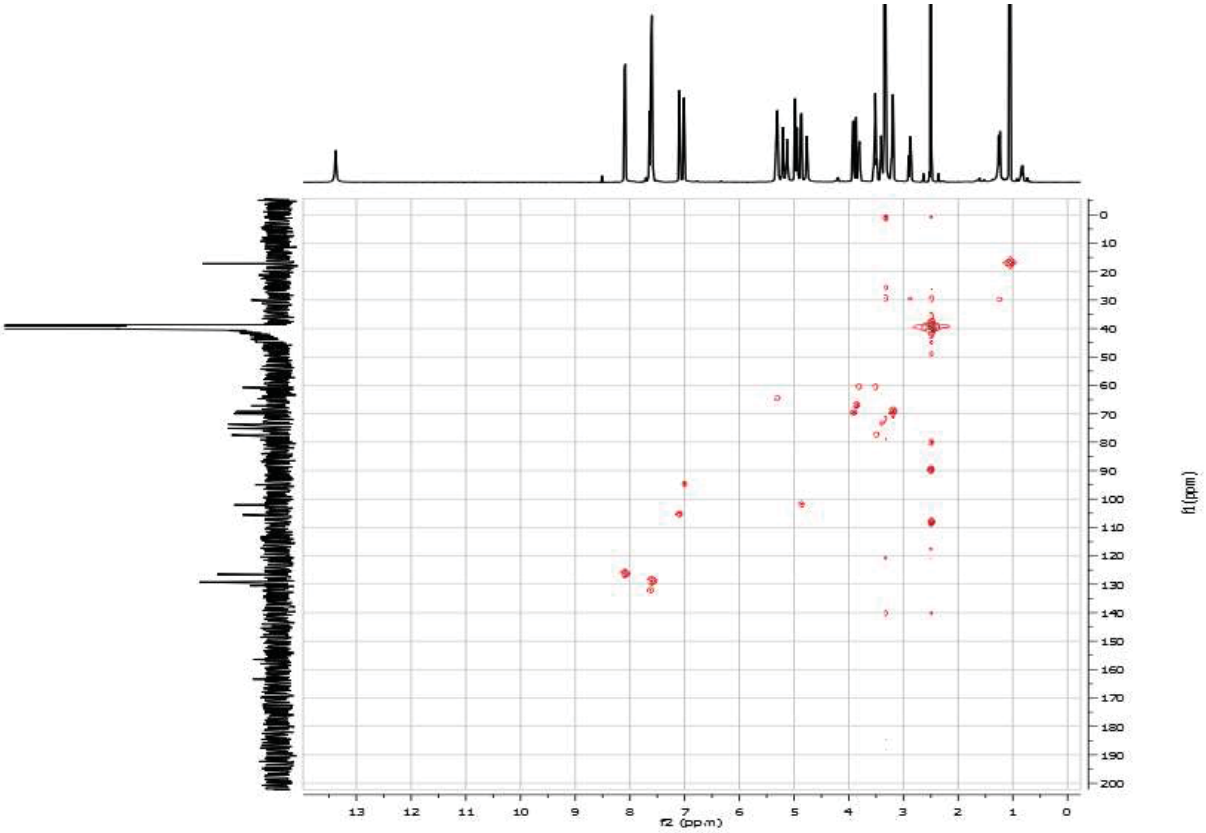

S5-4. HSQC spectrum of chrysin 6-C-*β*-boivinopyranosyl-7-O-*β*-D-glucopyranoside (**5**) in DMSO-d_6 (600 MHz, 150 MHz)

3. Publication 2

3.1 New Amides from the fruit of *Piper retrofractum*

Published in “Tetrahedron Letters”

Impact factor: 2.391

The overall contribution to the paper: 60% of the first author. The first author involved to all laboratory works, structure elucidations, literature research and manuscript writing.

Reprinted by permission from “Muharini, R., Liu, Z., Lin, W., Proksch, P.” (**2015**) New Amides from the fruits of Piper retrofractum. *Tetradedron Letters* 56; 2521 – 2525.

Publication 2

Tetrahedron Letters 56 (2015) 2521–2525

Contents lists available at ScienceDirect

Tetrahedron Letters

journal homepage: www.elsevier.com/locate/tetlet

New amides from the fruits of *Piper retrofractum*

Rini Muharini [a,b], Zhen Liu [a,*], Wenhan Lin [c], Peter Proksch [a,*]

[a] Institut für Pharmazeutische Biologie und Biotechnologie, Heinrich-Heine-Universität Düsseldorf, Universitätsstrasse 1, Geb.26.23, 40225 Düsseldorf, Germany
[b] Department of Chemistry Education, Faculty of Education, Tanjungpura University, Jl. Prof. Dr. H. Hadari Nawawi, 78124 Pontianak, Indonesia
[c] State Key Laboratory of Natural and Biomimetic Drugs, Peking University, 100191 Beijing, PR China

ARTICLE INFO

Article history:
Received 27 January 2015
Revised 23 March 2015
Accepted 25 March 2015
Available online 31 March 2015

Keywords:
Piper retrofractum
Amides
Antifungal activity
Cytotoxicity

ABSTRACT

Three new amides, (2*E*,14*Z*)-*N*-isobutyleicosa-2,14-dienamide (**1**), dipiperamides F and G (**2** and **3**), together with 30 known compounds were isolated from the fruits of *Piper retrofractum*. Their structures were elucidated by extensive spectroscopic analyses including 1D and 2D NMR as well as MS, and by comparison with the literature. A plausible biosynthetic pathway leading to the amides isolated in this study is discussed. All isolated compounds were screened for their antifungal and cytotoxic activities. Piperanine (**9**) showed growth inhibition against the fungus *Cladosporium cladosporioides*, while dipiperamides F and G (**2** and **3**), chabamide (**30**), nigramide R (**31**), dehydropipernonaline (**24**), pipernonaline (**25**), guineensine (**22**), brachystamide B (**23**), retrofractamide C (**20**), pellitorine (**13**), and pipericine (**14**) exhibited considerable cytotoxicity against L5178Y mouse lymphoma cells with IC_{50} values of 10.0, 13.9, 11.6, 9.3, 8.9, 17.0, 17.0, 16.4, 13.4, 28.3, and 24.2 μM, respectively.

Introduction

The genus *Piper* (Piperaceae) consists of approximately 1000 species and has been known as a commercially, economically, and medicinally important genus. *Piper retrofractum* Vahl, known as *cabe jawa* in Indonesia, is native to Southeast Asia and mostly cultivated in Indonesia and Thailand.[1] Traditionally, the fruits of *P. retrofractum* are used in Indonesian folk medicine (*Jamu*) as a tonic against a variety of digestive, stimulant, carminative, intestinal disorders, and for treating postpartum women.[1,2] The fruit extract has been reported to possess various bioactivities such as antifungal, insecticidal, antibacterial, antidiabetic, antiobesity, and cytotoxic activity.[1,2] Amides are the major constituents of the genus *Piper*. So far close to 300 different amides have been reported from this genus.[3,4] Several amides from the genus *Piper* exhibit significant biological activities, such as insecticidal,[5] antifungal,[6,7] antituberculosis,[8] antiobesity,[9] neurotropic,[10] hepatoprotective,[11] cytotoxic,[12] gastroprotective,[13] CYP3A4 inhibitory,[14] and CYP2D6 inhibitory activity.[15] In our study the crude extract of the fruits of *P. retrofractum* and several subfractions after VLC showed growth inhibition against *Cladosporium cladosporioides*, which is a common plant pathogenic fungus to be used in antifungal tests. Further investigation of secondary metabolites yielded 33 different amides including the new compounds (2*E*,14*Z*)-*N*-isobutyleicos-2,14-dienamide (**1**) and dipiperamides F and G (**2** and **3**) (Fig. 1). Herein, we describe the structure elucidation of the new compounds, and the biological activities of the new and of the known compounds with focus on their antifungal and cytotoxic activities. In addition, a plausible biosynthetic pathway leading to the amides isolated in this study is presented.

Results and discussion

(2*E*,14*Z*)-*N*-Isobutyleicosa-2,14-dienamide (**1**) was isolated as a white amorphous powder. Its HRESIMS spectrum exhibited a quasimolecular ion peak at *m*/*z* 364.3578 $[M+H]^+$, consistent with the molecular formula $C_{24}H_{45}NO$ and three degrees of unsaturation. The ^1H NMR spectrum displayed four olefinic proton signals at δ_H 6.83 (dt, *J* = 15.2, 7.0 Hz, H-3), 5.75 (d, *J* = 15.2 Hz, H-2), and 5.35 (m, H-14 and H-15), and three methyl groups at δ_H 0.93 (d, *J* = 6.7 Hz, Me-3′ and Me-4′), and 0.90 (t, *J* = 7.0 Hz, Me-20). The ^{13}C NMR spectrum showed the presence of a carbonyl carbon at δ_C 166.6 (C-1), and four olefinic carbons at δ_C 144.9 (C-3), 129.9 (C-14 and C-15), and 123.5 (C-2). The NMR data of **1** (Table 1) were similar to those of (2*E*,4*E*,14*Z*)-*N*-isobutyleicosa-2,4,14-trienamide (**17**). Both compounds differ with regard to C-4/C-5, where the olefinic double bond in the structure of **17** is replaced by two methylene groups in the structure of **1** as evident from the COSY correlations between H-3/H_2-4 (δ_H 2.17 q, *J* = 7.0 Hz) and H_2-4/H_2-5 (δ_H 1.44 qui, *J* = 7.0 Hz). The shielded carbon signals of C-13

* Corresponding authors. Tel.: +49 211 81 14163; fax: +49 211 81 11923.
E-mail addresses: zhenfeizi0@sina.com (Z. Liu), proksch@uni-duesseldorf.de (P. Proksch).

http://dx.doi.org/10.1016/j.tetlet.2015.03.116
0040-4039/

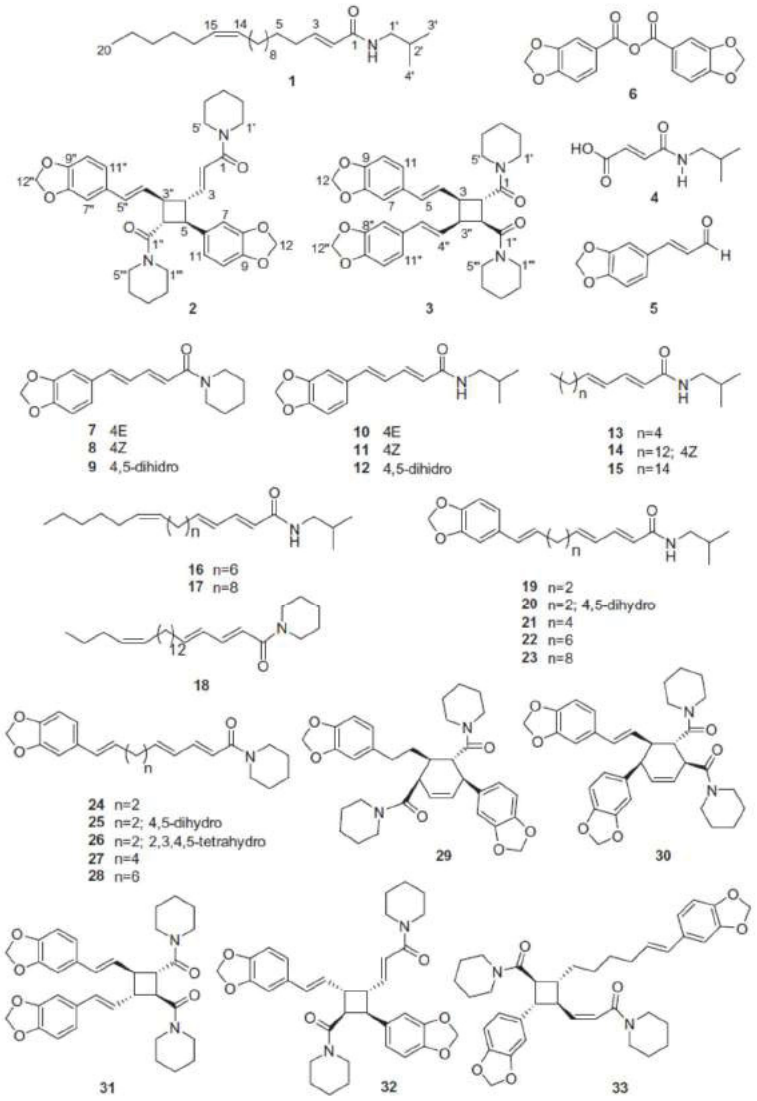

Figure 1. Structures of compounds **1**–**33** from *Piper retrofractum*.

and C-16 (δ_C 26.9 and 27.2) suggested the geometry of the isolated double bond at C-14/C-15 to be *Z*.[16] Thus, compound **1** was deduced as the new (2*E*,14*Z*)-*N*-isobutyleicosa-2,14-dienamide.

Dipiperamide F (**2**) was obtained as a yellow powder and gave absorption maxima at 209.6, and 267.6 nm in the UV spectrum. The molecular formula of **2** was established as $C_{34}H_{38}N_2O_6$ by the HRESIMS data (*m*/*z* 571.2804 $[M+H]^+$). Analyses of the ^{1}H NMR and COSY spectra indicated the presence of a cyclobutane ring, two methylenedioxyphenyl groups, two *E* configured olefinic double bonds and two piperidine groups (Table 2). Taking these structural elements into consideration, compound **2** was suggested to be an asymmetric bisamide. The presence of carbonyl groups at C-1 and C-1″ was implied by the HMBC cross peaks from H-2 (δ_H 6.29) and H-3 (δ_H 6.94) to C-1 (δ_C 165.1), and from H-3″ (δ_H 3.12) and H-5 (δ_H 3.59) to C-1″ (δ_C 169.9). In addition, the HMBC spectrum showed correlations from H-7 (δ_H 6.78) to C-5 (δ_C 45.2), and from H-7″ (δ_H 6.89) to C-5″ (δ_C 130.8), implying that two methylenedioxyphenyl moieties were present at C-5 and at C-5″. Detailed analysis of the 2D NMR spectra revealed **2** to possess the same gross structure as dipiperamide E (**32**) isolated previously from *P. nigrum*.[14] The different chemical shifts of the protons H-4, H-5, H-2″, and H-3″ observed for **2** and **32** suggested that the stereochemistry of the cyclobutane ring in **2** differed from that of **32**. The NOE relationships from H-3 to H-5 and H-3″ of compound **2** ascertained the same orientation for H-5 and H-3″, whereas the NOE interactions between H-7/H-4 (δ_H 2.94), H-7/H-2″ (δ_H 3.09), H-4/H-4″ (δ_H 6.09), and H-2″/H-4″ indicated H-4 and H-2″ to be present on the opposite face of the cyclobutane ring relative to H-5. Therefore, the relative configuration of the cyclobutane ring of **2** as shown in Figure 2 differs from that of **32**.

Dipiperamide G (**3**), which was isolated as a yellow powder, possessed the same molecular formula as **2** on the basis of the

Table 1
NMR data for compound **1** ($CDCl_3$, δ in ppm, J in Hz)[a]

Position	δ_H	δ_C	COSY	HMBC
1		166.1		
2	5.75, d (15.2)	123.5	H-3	C-1, C-4
3	6.83, dt (15.2, 7.0)	144.9	H-2, H-4	C-1, C-4, C-5
4	2.17, q (7.0)	32.0	H-3, H-5	C-2, C-3
5	1.44, qui (7.0)	28.3	H-4, H-6	C-3
6–12	1.26, m	29.2–29.8	H-5, H-13	
13	2.01, q (7.0)	26.9	H-12, H-14	C-14, C-15
14	5.35, m	129.9	H-13	C-13, C-16
15	5.35, m	129.9	H-16	C-13, C-16
16	2.01, q (7.0)	27.2	H-15, H-17	C-14, C-15
17	1.32, m	29.3	H-16	
18	1.32, m	32.0		
19	1.32, m	22.3	H-20	
20	0.90, t (7.0)	14.0	H-19	C-18, C-19
1′	3.15, t (6.4)	46.8	H-2′, NH	C-1, C-2′, C-3′, C-4′
2′	1.80, m	28.6	H-1′, H-3′, H-4′	C-1′, C-3′, C-4′
3′, 4′	0.93, d (6.7)	20.1	H-2′	C-1′, C-2′
NH	5.42, br s		H-1′	

[a] Recorded at 600 MHz for ^1H and 150 MHz for ^{13}C.

Table 2
NMR data for dipiperamide F (**2**) ($CDCl_3$, δ in ppm, J in Hz)[a]

Position	δ_H	δ_C	COSY	HMBC
1		165.1		
2	6.29, d (15.1)	120.0	H-3	C-1, C-4
3	6.94, dd (15.1, 6.6)	144.3	H-2, H-4	C-1
4	2.94, q (8.3)	47.3	H-3, H-5, H-3″	C-2, C-3
5	3.59, m	45.2	H-4, H-2″	C-1″, C-7, C-11
6		135.0		
7	6.78, d (1.3)	106.9	H-11	C-5, C-11
8		147.6		
9		147.0		
10	6.72, d (8.2)	108.0	H-11	C-8
11	6.75, dd (8.2, 1.3)	120.6	H-10, H-7	C-5, C-7, C-9
12	5.93, s	100.9		C-8, C-9
1′	3.54, m	42.7		
2′	1.50, m	25.9		
3′	1.60, m	24.7		
4′	1.50, m	25.9		
5′	3.40, m	46.3		
1″		169.9		
2″	3.09, m	44.3	H-5, H-3″	
3″	3.12, m	44.8	H-4, H-2″, H-4″	C-1″
4″	6.09, dd (15.7, 7.6)	127.8	H-3″, H-5″	C-2″
5″	6.40, d (15.7)	130.8	H-4″	C-3″, C-7″, C-11″
6″		131.4		
7″	6.89, d (1.3)	105.0	H-11″	C-5″, C-9″
8″		147.6		
9″		146.6		
10″	6.72, d (8.9)	107.9	H-11″	C-8″
11″	6.75, dd (8.9, 1.3)	119.9	H-7″, H-10″	C-5″, C-9″
12″	5.91, s	100.9		C-8″, C-9″
1‴	3.60, m	43.1		
	3.43, m			
2‴	1.50, m	25.2		
3‴	1.50, m	24.5		
4‴	1.23, m	25.2		
5‴	3.22, m	46.8		
	3.12, m			

[a] Recorded at 600 MHz for ^1H and 150 MHz for ^{13}C.

HRESIMS data (m/z 571.2807, $[M+H]^+$). Interpretation of the 2D NMR data (Table 3) indicated **3** to be a stereoisomer of the previously reported compound nigramide R (**31**).[17] The relative stereochemistry of the cyclobutane ring of **3** was deduced by interpretation of the ROESY spectrum. NOE correlations (Fig. 3) from H-2 (δ_H 4.18) to H-4 (δ_H 6.04) and H-4″ (δ_H 6.20), and between H-2″ (δ_H 3.88)/H_2-1′ (δ_H 3.30 and 3.24) were observed. Thus, H-3, H-2″, and H-3″ were oriented on the opposite face of the cyclobutane ring relative to H-2.

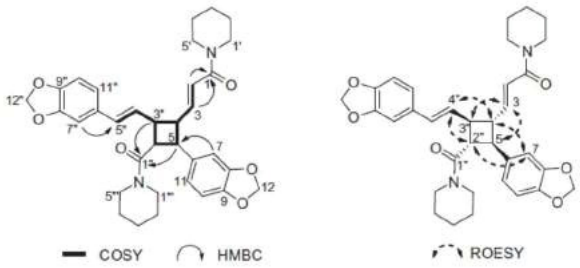

Figure 2. Key COSY, HMBC, and ROESY correlations of compound **2**.

Table 3
NMR data for dipiperamide G (**3**) ($CDCl_3$, δ in ppm, J in Hz)[a]

Position	δ_H	δ_C	COSY	HMBC
1		171.1		
2	4.18, t (8.7)	40.7	H-2″, H-3	C-4, C-1″
3	3.44, m	43.4	H-2, H-3″	
4	6.04, q (15.5, 8.5)	126.9	H-3, H-5	C-6
5	6.31, d (15.5)	131.0	H-4	C-7, C-11
6		131.7		
7	6.81, br s	105.4	H-10, H-11	C-9, C-11
8		146.9		
9		147.3		
10	6.68, overlapped	108.0		
11	6.72, overlapped	120.6		
12	5.93, m	101.0		C-8, C-9
1′	3.30, 3.24m	45.7	H-2′	
2′	1.46, m	26.4	H-1′, H-3′	
3′	1.54, m	24.4	H-2′	
4′	1.46, m	25.6	H-5′	
5′	3.68, 3.37, m	43.1	H-4′	
1″		168.8		
2″	3.88, t (8.7)	41.2	H-2, H-3″	C-4″, C-1
3″	3.46, m	44.4	H-2″, H-3	
4″	6.20, dd (15.5, 10.1)	124.7	H-3″, H-5″	C-6″
5″	6.29, d (15.5)	133.0	H-4″	C-7″, C-11″
6″		131.4		
7″	6.88, d (1.3)	105.6	H-10″, H-11″	C-9″, C-11″
8″		146.9		
9″		147.3		
10″	6.68, overlapped	108.0	H-7″, H-11″	
11″	6.72, overlapped	120.6	H-7″, H-10″	
12″	5.89, m	101.0		C-8″, C-9″
1‴	3.42, m	43.0	H-2‴	
2‴	1.46, m	26.4	H-1‴, H-3‴	
3‴	1.62, m	24.7	H-2‴	
4‴	1.54, m	25.6	H-5‴	
5‴	3.62, 3.48, m	46.6	H-4‴	

[a] Recorded at 600 MHz for ^1H and 150 MHz for ^{13}C.

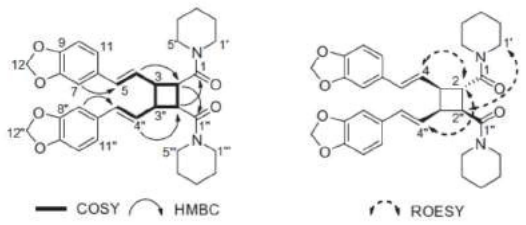

Figure 3. Key ^1H–^1H COSY, HMBC, and ROESY correlations for **3**.

The alpha D values of compounds **2** and **3** were close to zero indicating that both compounds are present as racemic mixtures. This is in concordance with previous studies on cyclobutane

amides from the genus Piper that were likewise shown to be present as racemates.[11,14,17]

The remaining known compounds were identified as (*E*)-4-(isobutylamino)-4-oxo-2-butenoic acid (**4**),[3,4,15] 3,4-methylenedioxy cinnamaldehyde (**5**),[3,4,20] piperonyl anhydride (**6**)[21] piperine (**7**),[3,4,19] isochavicine (**8**),[3,4,11] piperanine (**9**),[3,4,22] piperlonguminine (**10**),[3,4,19] scutifoliamide A (**11**),[3,4,23] dihydropiperlonguminine (**12**),[3,4] pellitorine (**13**),[3,4,24] pipericine (**14**),[3,4,25] (2*E*,4*E*)-*N*-isobutyleicosa-2,4-dienamide (**15**),[3,4,26] (2*E*,4*E*,12*Z*)-*N*-isobutyloctadec-2,4,12-trienamide (**16**),[3,4,16] (2*E*,4*E*,14*Z*)-*N*-isobutyleicosa-2,4,14-eicosatrienamide (**17**),[3,4,16] pipereicosalidine (**18**),[3,4,27] retrofractamide A (**19**),[3,4,18] retrofractamide C (**20**),[3,4,18] retrofractamide B (**21**),[3,4,8] guineensine (**22**),[3,4,19] brachystamide B (**23**),[3,4,11] dehydropipernonaline (**24**),[28] pipernonaline (**25**),[29] piperolein B (**26**),[3,4,11] piperundecaline (**27**),[3,4] piperchabamide C (**28**),[13] nigramide F (**29**),[3,4,17] chabamide (**30**),[4,5,30] nigramide R (**31**),[4,5,17] dipiperamide E (**32**),[4,5,14] and piperchabamide H (**33**).[3,4,11] Their structures were established based on spectroscopic evidence, which was in a good agreement with data reported in the literature.

The amides reported from *P. retrofractum* in this study include long chain alkylamides (**1**, **4**, **13**–**18**), methylenedioxyphenyl amides (**7**–**12**, **19**–**28**), cyclobutanamides (**2**, **3**, **21**–**33**), and cyclohexenamides (**29**, **30**). The basic structural unit of the amides from *P. retrofractum* is a piperidyl or isobutyl amino moiety, which is biogenetically derived from L-lysine or L-valine, respectively. Additionally, methylenedioxyphenyl amides are known to be derived from piperoyl-CoA through the shikimic acid pathway, with ferulic acid as a starter molecule.[31,32] The presence of **5** in our study gave another evidence to support this hypothesis. The methylenedioxy-bridge formation has been reported to occur in a number of plant natural products from the phenylpropanoid pathway by oxidative cyclization of an *ortho*-hydroxymethoxy-substituted aromatic ring involving a cytochrome P450 (CYP450)-dependent monooxygenase.[32,33]

The dimeric amide alkaloids isolated from *P. retrofractum* in this study add to the chemical diversity of amides known from this species. Within the family Piperaceae, dimeric amides were previously obtained from *P. nigrum* and *P. chaba*.[3,4,12,14,17,30,34] The formation of dimeric amides has been suggested to be due to photodimerization through an intermolecular Diels–Alder reaction, which may involve [4+2] or [2+2] cycloaddition reactions, starting from the same or from different monomeric amides.[35–37] In order to confirm the dimeric amides were natural compounds, co-chromatography was performed for isolated dimeric amides and fresh crude extract prepared in the dark. Fortunately, all dimeric amides were presented in HPLC spectra and they were checked by ESIMS data. Thus, all isolated compounds may be not artifacts but natural products.

Table 4
Cytotoxicity of the isolated compounds (**2**, **3**, **13**, **14**, **20**, **22**–**25**, **30**, **31**) against the mouse lymphoma cell line L5178Y

Compound	IC_{50} (μM)
Pellitorine (**13**)	28.3
Pipericine (**14**)	24.2
Dehydropipernonaline (**24**)	8.9
Pipernonaline (**25**)	17.0
Guineensine (**22**)	17.0
Brachystamide B (**23**)	16.4
Retrofractamide C (**20**)	13.4
Dipiperamides F (**2**)	10.0
Dipiperamides G (**3**)	13.9
Chabamide (**30**)	11.6
Nigramide R (**31**)	9.3

Kahalalide F used as positive control, IC_{50} 4.3 μM.

All compounds isolated in this study were tested for antifungal activity toward *Cladosporium cladosporioides*. Only piperanine (**9**) (0.5 μmol, diameter of inhibition zone 15.0 mm) showed potent activity compared to the positive control nystatin (0.5 μmol, diameter of inhibition zone 29.6 mm). In addition, cytotoxicity of the isolated compounds was evaluated against the L5178Y mouse lymphoma cell line using the MTT method (Table 4). Dehydropipernonaline (**24**) proved to be the most active compound, followed by nigramide R (**31**) with IC_{50} values 8.9 μM and 9.3 μM, respectively. Alkylamides such as pellitorine (**13**) and pipericine (**14**) displayed moderate cytotoxicity. The presence of methylenedioxyphenyl moieties in retrofractamide C (**20**), guineensine (**22**), brachystamide B (**23**), dehydropipernonaline (**24**), and pipernonaline (**25**) was found to increase the cytotoxic activities of the respective derivatives. Moreover, dimeric amides including dipiperamides F and G (**2** and **3**), chabamide (**30**), and nigramide R (**31**) showed pronounced cytotoxicity (IC_{50} 9.3–13.9 μM), in comparison with the positive control kahalalide F (IC_{50} 4.3 μM).

Acknowledgements

Financial support by a Grant of BMBF to P.P. and by MOST to W.H.L. is gratefully acknowledged. R.M wishes to thank the DIKTI (Directorate General of Higher Education—Indonesia) for a scholarship. We are indebted to Prof. W. E. G Müller (University of Mainz, Mainz, Germany) for cytotoxicity assays.

Supplementary data

Supplementary data (experimental, UV, MS, and NMR spectroscopic data of compounds **1**, **2**, and **3**) associated with this article can be found, in the online version, at http://dx.doi.org/10.1016/j.tetlet.2015.03.116.

References and notes

1. Lim, T. K. In *Edible Medicinal and Non-medicinal Plants* In ; Springer Science & Business: Netherlands, 2012; Vol. 4, p 351.
2. Luyen, B. T. T.; Tai, B. H.; Thao, N. P.; Yang, S. Y.; Cuong, N. M.; Kwon, I. Y.; Jang, H. D.; Kim, Y. H. *Bioorg. Med. Chem. Lett.* **2014**, *24*, 4120–4124.
3. Gutierrez, R. M. P.; Gonzales, A. M. N.; Hoyo-Vadillo, C. *Mini-Rev. Med. Chem.* **2013**, *13*, 163–193.
4. Paula, J. C. N. V. F.; David, J. M.; David, J. P. *Quim. Nova* **2012**, *35*, 2288–2311.
5. Siddiqui, B. S.; Gulzar, T.; Begum, S.; Rasheed, M.; Sattar, F. A.; Afshan, F. *Helv. Chim. Acta* **2003**, *86*, 2760–2767.
6. Marques, J. V.; de Oliveira, A.; Raggi, L.; Young, M. C. M.; Kato, M. J. *J. Braz. Chem. Soc.* **2010**, *21*, 1807–1813.
7. Navickiene, H. M. D.; Alecio, A. L.; Kato, M. J.; Bolzani, V. S.; Young, M. C. M.; Cavalheiro, A. J.; Furlan, M. *Phytochemistry* **2000**, *55*, 621–626.
8. Rukachaisirikul, T.; Siriwattanakit, P.; Sukcharoenphol, K.; Wongvein, C.; Ruttanaweang, P.; Wongwattanavuch, P.; Suksamrarn, A. *J. Ethnopharmacol.* **2004**, *93*, 173–176.
9. Kim, K. J.; Lee, M. S.; Jo, K.; Hwang, J. K. *Biochem. Biophys. Res. Commun.* **2011**, *411*, 219–225.
10. Kubo, M.; Ishii, R.; Ishino, Y.; Harada, K.; Matsui, N.; Akagi, M.; Kato, E.; Hosoda, S.; Fukuyama, Y. *J. Nat. Prod.* **2013**, *76*, 769–773.
11. Matsuda, H.; Ninomiya, K.; Morikawa, T.; Daisuke, Y.; Yamaguchi, I.; Yoshikawa, M. *Bioorg. Med. Chem.* **2009**, *17*, 7313–7323.
12. Rao, V. R. S.; Suresh, G.; Babu, K. S.; Raju, S. S.; Vardhan, M. V. P. S. V.; Ramakrishna, S.; Rao, J. M. *Tetrahedron* **2011**, *67*, 1885–1892.
13. Morikawa, T.; Matsuda, H.; Yamaguchi, I.; Pongpiriyadacha, Y.; Yoshikawa, M. *Planta Med.* **2004**, *70*, 152–159.
14. Tsukamoto, S.; Tomise, K.; Miyakawa, K.; Cha, B. C.; Abe, T.; Hamada, T.; Hirota, H.; Ohta, T. *Bioorg. Med. Chem.* **2002**, *10*, 2981–2985.
15. Subehan, U. T.; Kadota, S.; Tezuka, Y. *Planta Med.* **2006**, *72*, 527–532.
16. Kikuzaki, H.; Kawabata, M.; Ishida, E.; Akazawa, Y.; Takei, Y.; Nakatani, N. *Biosci., Biotechnol., Biochem.* **1993**, *57*, 1329–1333.
17. Wei, K.; Li, W.; Koike, K.; Chen, Y.; Nikaido, T. *J. Org. Chem.* **2004**, *70*, 1164–1176.
18. Banerji, A.; Bandyopadhyay, D.; Sarkar, M.; Siddhanta, A. K.; Pal, S. C.; Somnath, G.; Abraham, K.; Shoolery, J. N. *Phytochemistry* **1985**, *24*, 279–284.
19. Narui, T.; Takeuchi, M.; Ishii, R.; Ishida, T.; Okuyama, T. *Nat. Med.* **1995**, *49*, 438–441.

Publication 2

20. Vijay, G.; Sayed, S. H. *J. Pharm. Res.* **2011**, *4*, 4265–4267.
21. Chonajka, M. W.; Lough, A. J.; Wylie, R. S.; Gossage, R. A. *J. Mol. Struct.* **2011**, *991*, 158–161.
22. Addae-Mensah, I.; Torto, F. G.; Dimonyeka, C. I.; Baxter, I.; Sanders, J. K. M. *Phytochemistry* **1977**, *16*, 757–759.
23. Marques, J. V.; Kitamura, R. O. S.; Lago, J. H. G.; Young, M. C. M.; Guimaraes, E. F.; Kato, M. J. *J. Nat. Prod.* **2007**, *21*, 1807–1813.
24. Nakatani, N.; Inatani, R. *Agric. Biol. Chem.* **1981**, *45*, 1473–1476.
25. Siddiqui, B. S.; Begum, S.; Gulzar, T.; Farhat; Noor, F. *Phytochemistry* **1997**, *45*, 1617–1619.
26. Raina, M.; Dhar, K.; Atal, C. K. *Planta Med.* **1976**, *30*, 198–200.
27. Ahn, J. W.; Ahn, M. J.; Zee, O. P.; Kim, E. J.; Lee, G. S.; Kim, H. J.; Kubo, I. *Phytochemistry* **1992**, *31*, 3609–3612.
28. Shoji, N.; Umeyama, A.; Saito, N.; Takemoto, T.; Kajiwara, A.; Ohizumi, Y. *J. Pharm. Sci.* **1986**, *75*, 1188–1189.
29. Tabuneng, W.; Bando, H.; Amiya, T. *Chem. Pharm. Bull.* **1983**, *31*, 3562–3565.
30. Rukachaisirikul, T.; Prabpai, S.; Champung, P.; Suksamrarn, A. *Planta Med.* **2002**, *68*, 853–855.
31. Okwute, S. K.; Egharevba, H. O. *Int. J. Chem.* **2013**, *5*, 99–122.
32. Dewick, P. M. In *Medicinal Natural Product: A Biosynthetic Approach*; John Wiley and Sons: West Sussex, 2012.
33. Bauer, W.; Zenk, M. H. *Phytochemistry* **1991**, *30*, 2953–2961.
34. Fujiwara, Y.; Naithou, K.; Miyazaki, T.; Hashimoto, K.; Mori, K.; Yamamoto, Y. *Tetrahedron Lett.* **2001**, *42*, 2497–2499.
35. Ulrich, H.; Rao, D. V.; Stuber, F. A.; Sayigh, A. A. *J. Org. Chem.* **1970**, *35*, 1121–1125.
36. Liu, R.; Zhang, M.; Wyche, T. P.; Winston-McPherson, G. N.; Bugni, T. S.; Tang, W. *Angew. Chem., Int. Ed.* **2012**, *124*, 7621–7624.
37. Gutekunst, W. R.; Baran, P. S. *J. Org. Chem.* **2014**, *79*, 2430–2452.

3.2 Supporting information

Supplementary Data

New amides from the fruits of *Piper retrofractum*

Rini Muharini[a,b], Zhen Liu[a,*], Wenhan Lin[c], Peter Proksch[a,*]

[a]*Institut für Pharmazeutische Biologie und Biotechnologie, Heinrich-Heine-Universität Düsseldorf, Universitätsstrasse 1, Geb.26.23, 40225 Düsseldorf, Germany*

[b]*Departement of Chemistry Education, Faculty of Education, Tanjungpura University, Jl. Prof. Dr. H. Hadari Nawawi, 78124, Pontianak, Indonesia*

[c]*State Key Laboratory of Natural and Biomimetic Drugs, Peking University, 100191 Beijing, PR China*

*Corresponding authors.

Tel.: +49 211 81 14163; fax: +49 211 81 11923.

E-mail address: zhenfeizi0@sina.com (Z. Liu)

proksch@uni-duesseldorf.de (P. Proksch)

Table of Contents

	Page
Experimental	3
S1. UV spectrum of compound **1**.	7
S2. HRESIMS spectrum of compound **1.**	7
S3. ^{1}H NMR (600 MHz, $CDCl_3$) spectrum of compound **1**.	8
S4. ^{1}H-^{1}H COSY (600 MHz, $CDCl_3$) spectrum of compound **1**.	9
S5. ^{13}C NMR (150 MHz, $CDCl_3$) spectrum of compound **1**.	10
S6. HSQC (600 and 150 MHz, $CDCl_3$) spectrum of compound **1**.	11
S7. HMBC (600 and 150 MHz, $CDCl_3$) spectrum of compound **1**.	12
S8. UV spectrum of compound **2**.	13
S9. HRESIMS spectrum of compound **2.**	13
S10. ^{1}H NMR (600 MHz, $CDCl_3$) spectrum of compound **2**.	14
S11. ^{1}H-^{1}H COSY (600 MHz, $CDCl_3$) spectrum of compound **2**.	15
S12. HSQC (600 and 150 MHz, $CDCl_3$) spectrum of compound **2**.	16
S13. HMBC (600 and 150 MHz, $CDCl_3$) spectrum of compound **2**.	17
S14. ROESY (600 MHz, $CDCl_3$) spectrum of compound **2**.	18
S15. UV spectrum of compound **3**.	19
S16. HRESIMS spectrum of compound **3**.	19
S17. ^{1}H NMR (600 MHz, $CDCl_3$) spectrum of compound **3**.	20
S18. 1H-1H COSY (600 MHz, $CDCl_3$) spectrum of compound **3**.	21
S19. HSQC (600 and 150 MHz, $CDCl_3$) spectrum of compound **3**.	22
S20. HMBC (600 and 150 MHz, $CDCl_3$) spectrum of compound **3**.	23
S21. ROESY (600 MHz, $CDCl_3$) spectrum of compound **3**.	24

Experimental

General Experimental Procedure

NMR experiments were performed on a Bruker Avance ARX 500 or Bruker Avance III 600 spectrometer, while chemical shifts were given in δ (ppm) referring to the solvent peaks at δ_H 7.26 and δ_C 77.0 for $CDCl_3$. Mass spectra were obtained on a LC-MS HP1100 Agilent Finnigan LCQ Deca XP Thermoquestman spectrometer and HRESIMS spectra were recorded on a UHR-QTOF maXis 4G (Bruker Daltonics) mass spectrometer. Optical rotations were measured with a JASCO P-1020 polarimeter. HPLC analysis was performed using a Dionex P580 system coupled to a photodiode array detector (UVD340s). The separation column (125 ×4 mm, L × ID) was prefilled with Eurospher 10 C_{18} (Knauer, Germany). Semi-preparative RP-HPLC was used for purification of compounds and consisted of a HPLC Lachrom-Merck Hitachi system (Pump L7100 and UV detector L7400) and a Eurospher 100-10 C18 (300 × 8 mm) column (Knauer, Germany). Column chromatography was conducted using Merck MN Silica gel 60 M (0.04-0.063 mm) or Sephadex LH-20 as stationary phase. Thin Layer Chromatography (TLC) was performed on pre-coated Silica Gel 60 F_{254} plates (layer thickness 0.2 mm, E. Merck, Darmstadt, Germany) with detection under UV at 254 and 365 nm. Solvents were distilled before use, and spectral grade solvents were used for spectroscopic measurements.

Plant Material

The dried fruits of *P. retrofractum* used in this study were supplied from *Indopharma PT* (Jakarta, Indonesia) in 2000, and kept from light and high humidity. A voucher specimen was deposited at the Institute of Pharmaceutical Biology and Biotechnology, Heinrich-Heine University Duesseldorf, Germany.

Extraction and Isolation

The dried fruits of *P. retrofractum* (100 g) were powdered and extracted with methanol (MeOH) at room temperature to give 7 g of pale yellow extract. The crude extract was subjected initially to silica gel vacuum liquid chromatography (VLC), eluting with *n*-hexane (*n*-hex), ethyl acetate (EtOAc), dichloromethane (DCM) and MeOH by increasing the polarity to afford 13 fractions. Fraction A (1.19g) was fractionated with silica gel CC eluted with *n*-hex-EtOAC (9:1) to give 9 subfractions. Subfraction A-6 (397.54 mg) was subjected to Sephadex LH-20 CC, eluting with DCM-MeOH (3:7), and followed by semi-preparative RP-HPLC (MeOH-H_2O, gradient 90:10 to 100:0, flow rate 2 mL/min) to give **4** (6.6 mg), **14** (4.1 mg) and **15** (1.6 mg). Subfraction A-7 (119.7 mg) was subjected to silica gel CC, eluting with *n*-hex–EtOAc (8:2), and was further purified using RP-HPLC with MeOH-H_2O (gradient 90:10 to 100:0, flow rate 2 mL/min) to give **1** (2.04 mg), **16** (2.6 mg) and **17** (3.4 mg). Subfraction A-8 (298.2 mg) was subjected to silica CC, eluting with *n*-hex-EtOAc (8:2), and yielded 8 subfractions. Subfractions A-8-4 (35.8 mg) and A-8-5 (12.2 mg) were purified using RP-HPLC with MeOH-H_2O (gradient 90:10 to 100:0) as eluent, to yield **13** (2.6 mg) and **18** (1.7 mg), respectively. Fraction B (1.1 g) was separated using silica gel CC, eluting with *n*-hex-EtOAc (gradient 80:20 to 100:0) to give 9 subfractions. Subfraction B-5 (97.2 mg) was fractionated using Sephadex LH-20 CC with MeOH as mobile phase, followed by semi-preparative RP-HPLC with MeOH-H_2O (gradient 80:20 to 100:0, flow rate 5 mL/min) to give **20** (1.45 mg), **22** (7.84 mg), **25** (5 mg), **26** (1.1 mg), **27** (0.7 mg) and **28** (0.7 mg). Subfraction B-7 (399.9 mg) was subjected to Sephadex LH-20 CC, eluting with MeOH to give 5 subfractions. Separation of subfraction B-7-3 (276.9 mg) was performed using silica gel CC with MeOH as eluent, followed by purification by RP-HPLC with MeOH-H_2O (gradient 70:30 to 100:0, flow rate 4 mL/min) to yield **19** (0.9 mg), **21** (2.9 mg) and **33**

(1.17 mg). Subfraction B-7-4 (54.4 mg) yielded **7** (4.87 mg), **8** (3.3 mg), **11** (3.4 mg) and **24** (0.92 mg) following purification by RP-HPLC (gradient MeOH-H_2O (70:30) to 100% MeOH, flow rate 2 mL/min). Repeated purification of subfraction B-9 (511.2 mg) by performing Sephadex LH-20 CC (MeOH as mobile phase) and silica gel CC with *n*-hex-EtOAc (8:2) as eluent followed by RP-HPLC with MeOH-H_2O (90:10, flow rate 5 mL/min) as mobile phase gave **22** (14.6 mg) and **23** (6.9 mg). Fraction C (1.5 g) was subjected to silica gel CC, eluting with *n*-hex-EtOAc (1:1) and gave 10 subfractions. Purification of C-4 (18.8 mg) was achieved using reverse-phase HPLC (gradient MeOH-H_2O (70:30) to 100% MeOH, flow rate 4 mL/min) to yield **11** (2.79 mg), **12** (1.37 mg), **25** (4.62 mg) and **29** (4.56 mg). Subfractions C-6 (1.04 g) was subjected to silica gel CC with *n*-hex-EtOAc (7:3) as eluent to give 6 subfractions. C-6-5 (374.9 mg) was fractionated by performing silica gel CC, eluting with *n*-hex-EtOAc (7:3) to give 10 subfractions. Subfraction C-6-5-1 (2.89 mg) was purified using RP-HPLC (isocratic gradient MeOH-H_2O (90:10), flow rate 5 mL/min) to give **5** (1.43 mg). Compound **9** (49.4 mg) was found to be a major substance, together with **7** (20.0 mg) and **8** (20.1 mg) after purification of subfraction C-6-5-3 (154.2 mg) using semi-preparative RP-HPLC (isocratic gradient MeOH-H_2O (90:10), flow rate 5 mL/min). Purification of subfraction C-6-5-7 using RP-HPLC with MeOH-H_2O (90:10, flow rate 5 mL/min) as mobile phase gave **31** (1.73 mg), while purification of subfraction C-6-5-8 (15.4 mg) using RP-HPLC (MeOH-H_2O 90:10, flow rate 5 mL/min) yielded **2** (1.77 mg) and **3** (0.95 mg). After performing silica gel CC, followed by Sephadex LH-20 CC and RP-HPLC with subfraction C-9 (91.2 mg), **6** (0.81 mg) was obtained. Fraction D (159.6 mg) was subjected to silica gel CC, eluting with *n*-hex-EtOAc (7:3), and gave 10 subfractions. Subfraction D-4 (17.9 mg) was purified by RP-HPLC with MeOH-H_2O (gradient 70:30 to 100:0,

flow rate 4 mL/min) as eluent, to give **32** (1.1 mg). Purification of subfraction D-5 (34.2 mg) using semi-preparative RP-HPLC (MeOH-H_2O 80:20, flow rate 5 mL/min) gave **30** (13.4 mg).

*(2E,14Z)-N-isobutyleicosa-2,14-dienamide (**1**).* White amorphous powder; $UV_{\lambda max}$ (PDA) 208.9 nm; ^1H and ^{13}C NMR see Table 1; ESIMS *m/z* 364 $[M+H]^+$, 386 $[M+Na]^+$; HRESIMS *m/z* 364.3578 $[M+H]^+$ (calcd for $C_{24}H_{46}NO$ 364.3574).

*Dipiperamide F (**2**).* Yellow powder; $UV_{\lambda max}$ (PDA) 209.6, 267.6 nm; $[\alpha]_D^{23}$ -0.614 (*c* 0.54, MeOH); ^1H and ^{13}C NMR see Table 2; ESIMS *m/z* 571 $[M+H]^+$, 593 $[M+Na]^+$; HRESIMS *m/z* 571.2804 $[M+H]^+$ (calcd for $C_{34}H_{39}N_2O_6$ 571.2803).

*Dipiperamide G (**3**).* Yellow powder; $UV_{\lambda max}$ (PDA) 208.4, 268.0, 305.2 nm; $[\alpha]_D^{23}$ -0.531 (*c* 0.62, MeOH); ^1H and ^{13}C NMR see Table 3; ESIMS *m/z* 571 $[M+H]^+$, 593 $[M+Na]^+$; HRESIMS *m/z* 571.2807 $[M+H]^+$ (calcd for $C_{34}H_{39}N_2O_6$ 571.2803).

Antifungal assay

The antifungal assay was performed using the agar diffusion method as described before (Kirby-Bauer) and nystatin was used as a positive control.

Cell proliferation assay

Cytotoxicity was evaluated using the L5178Y mouse lymphoma cell line employing the MTT (3-(4,5-dimethylthiazol-2-yl)-2,5-diphenyl-2H-tetrazolium bromide) assay as described earlier.[1] All experiment were carried out in triplicate and repeated three times. As negative control, media with 0.1% DMSO was included in the experiments. Kahalalide F was used as a positive control.

References

1. Pham, C. D.; Hartmmann, R.; Bohler, P.; Stork, B.; Wesselborg, S.; Lin, W.; Lai, D.; Proksch, P. *Org. Lett.* **2013**, *16*, 266-289.

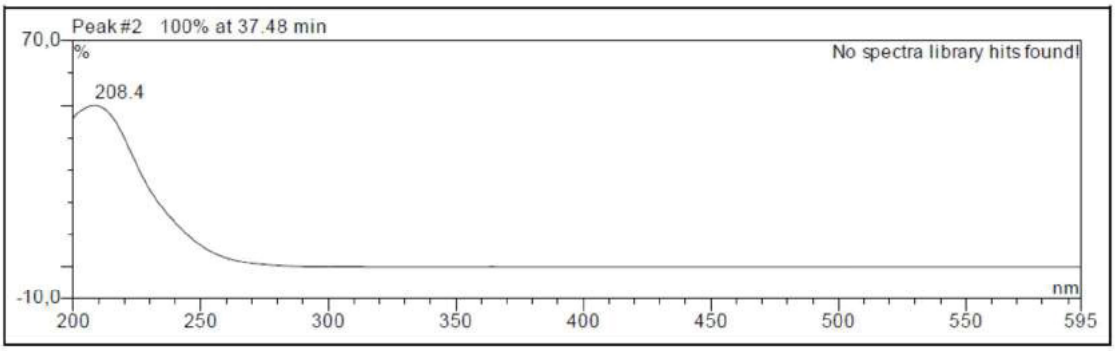

S1. UV spectrum of compound **1**.

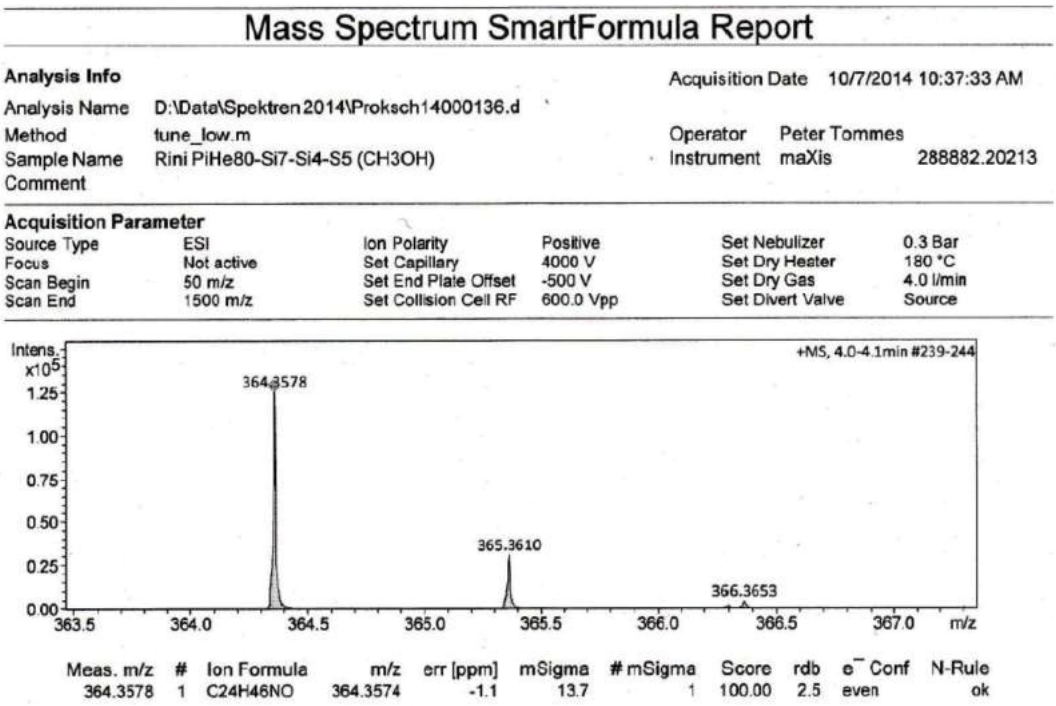

S2. HRESIMS spectrum of compound **1**.

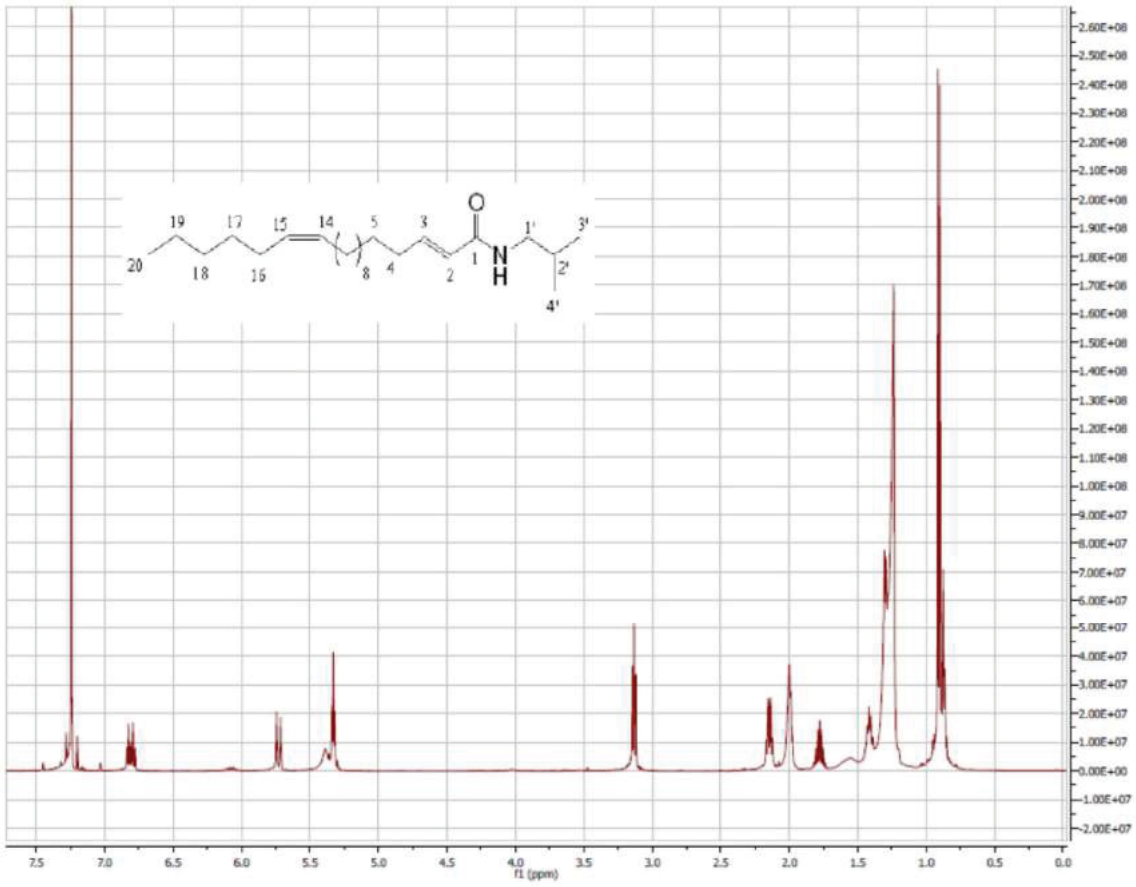

S3.^{1}H NMR (600 MHz, $CDCl_3$) spectrum compound **1**.

8

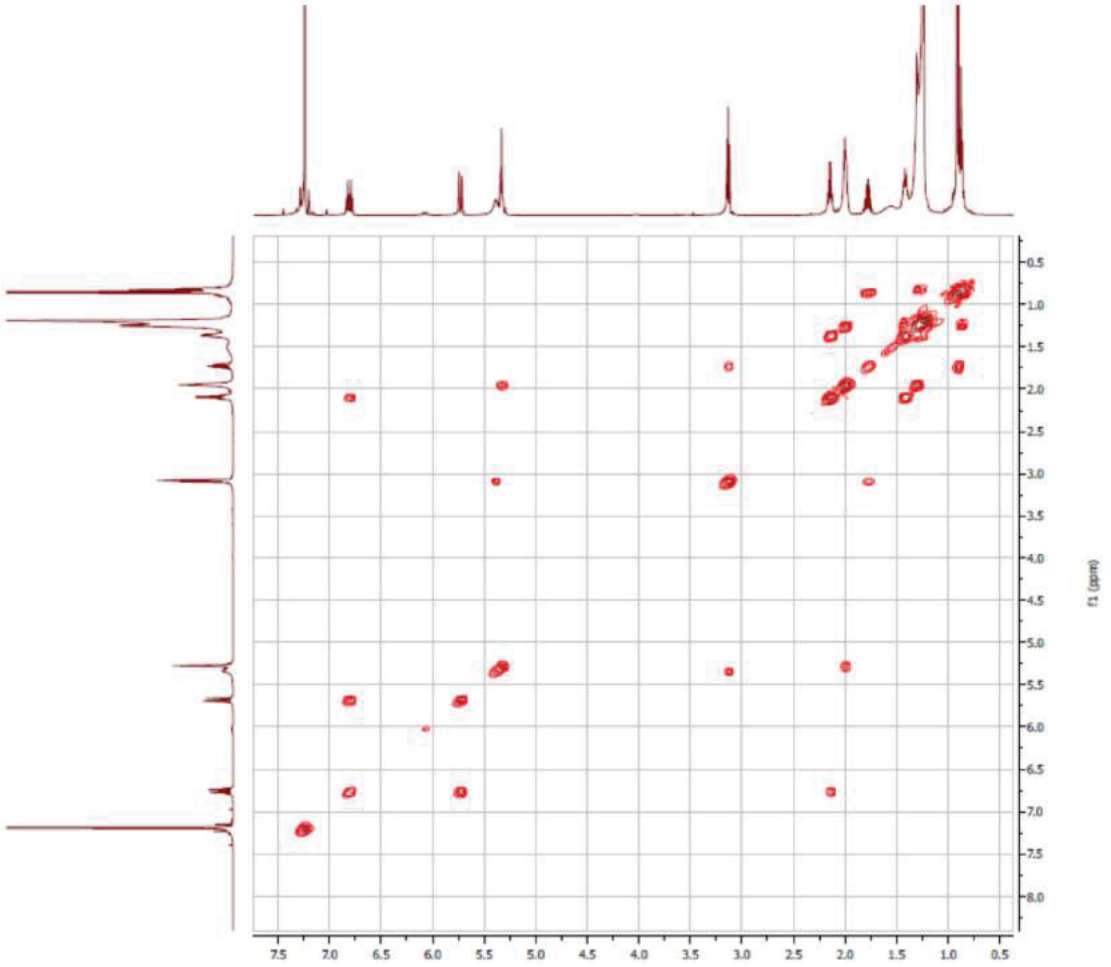

S4. ^{1}H-^{1}H COSY (600 MHz, $CDCl_3$) spectrum of compound**1**.

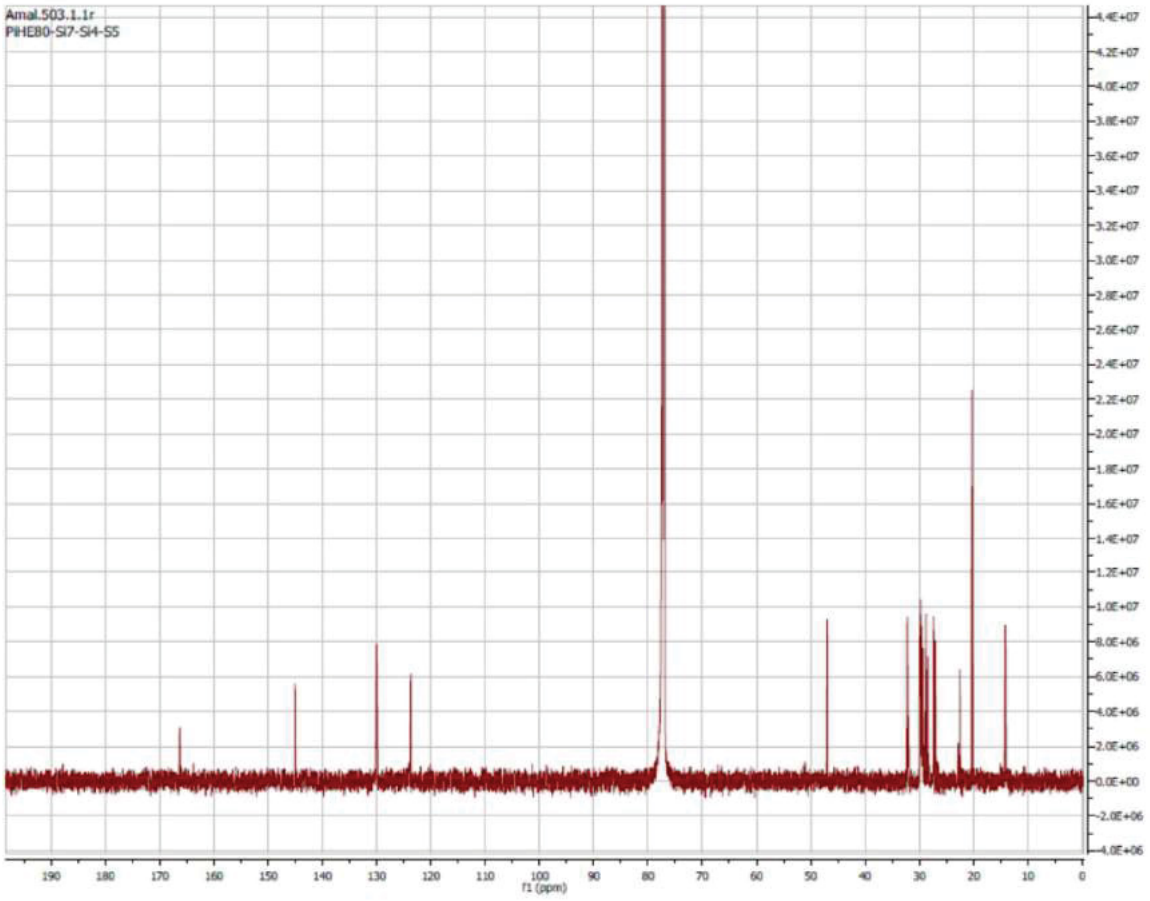

S5. ^{13}C NMR (150 MHz, $CDCl_3$) spectrum of compound**1**.

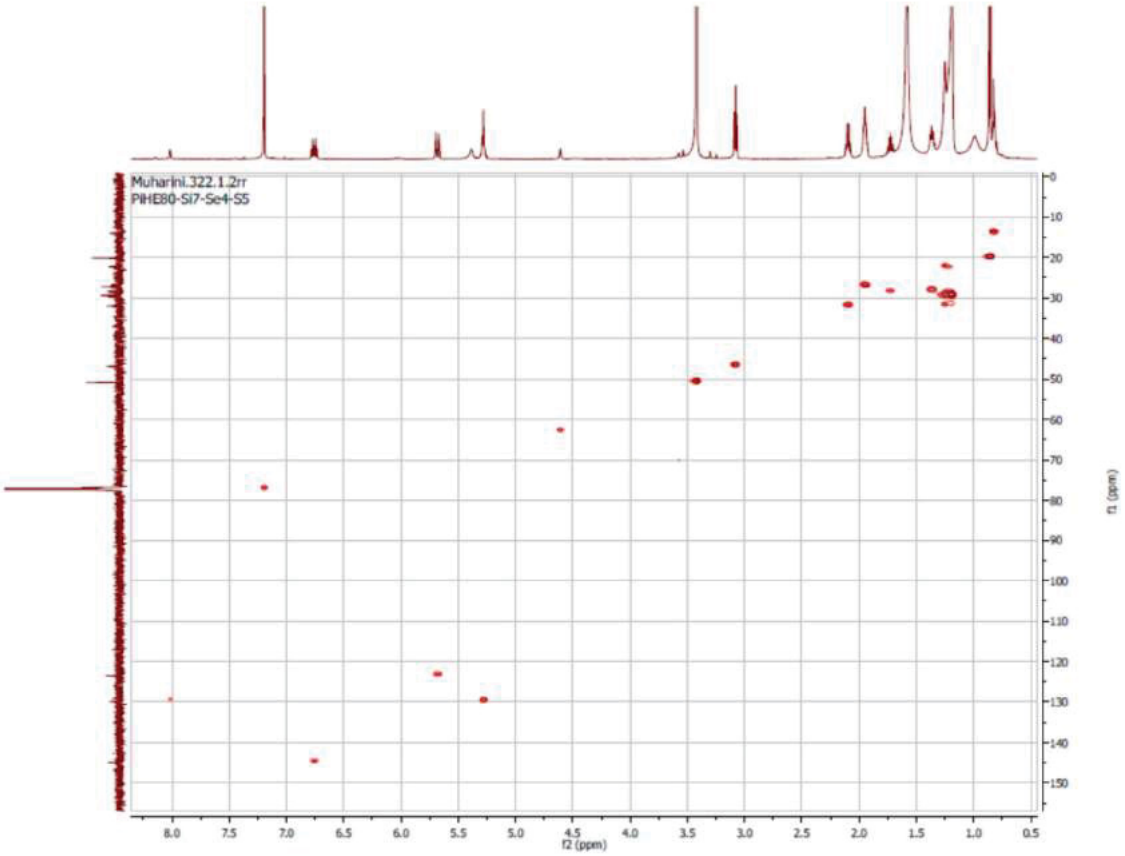

S6. HSQC (600 and 150 MHz, $CDCl_3$) spectrum of compound**1**.

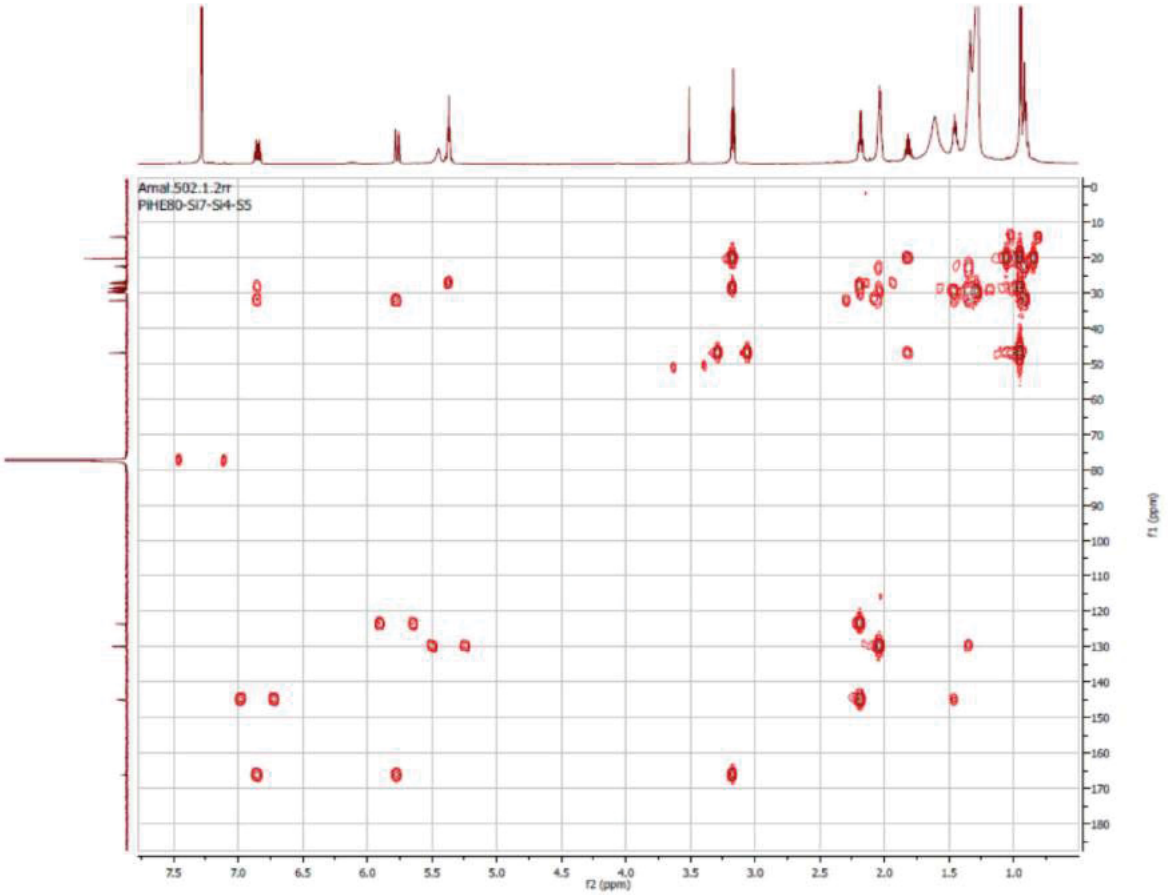

S7. HMBC (600 and 150 MHz, $CDCl_3$) spectrum of compound**1**.

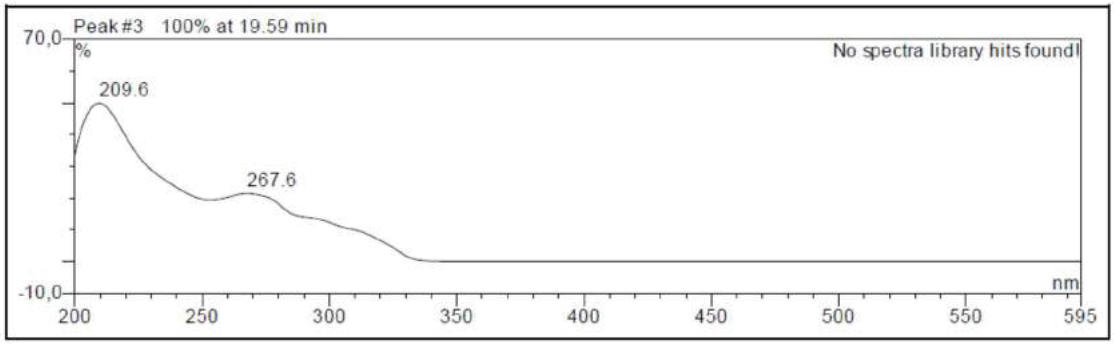

S8. UV spectrum of compound **2**.

Mass Spectrum SmartFormula Report

Analysis Info

Analysis Name	D:\Data\Spektren 2014\Prokseh14000131.d	Acquisition Date	9/22/2014 4:08:41 PM
Method	tune_low.m	Operator	Peter Tommes
Sample Name	Rini PiHE40-Si6-Si5-Si8-S7 (CH3OH)	Instrument	maXis 288882.20213
Comment			

Acquisition Parameter

Source Type	ESI	Ion Polarity	Positive	Set Nebulizer	0.3 Bar
Focus	Not active	Set Capillary	4000 V	Set Dry Heater	180 °C
Scan Begin	50 m/z	Set End Plate Offset	-500 V	Set Dry Gas	4.0 l/min
Scan End	1500 m/z	Set Collision Cell RF	600.0 Vpp	Set Divert Valve	Source

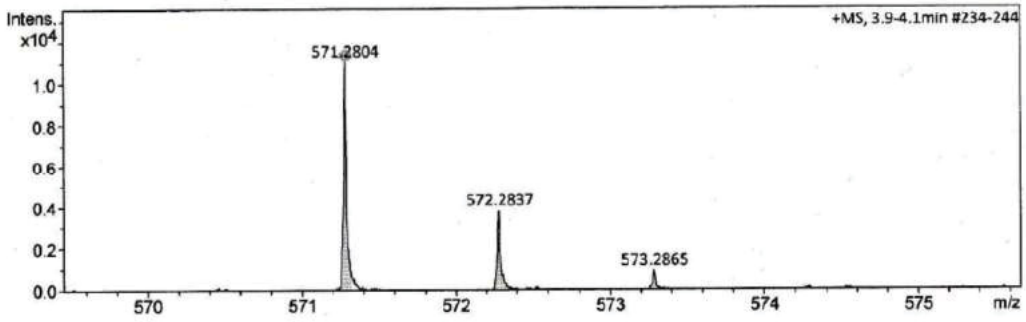

Meas. m/z	#	Ion Formula	m/z	err [ppm]	mSigma	# mSigma	Score	rdb	e⁻ Conf	N-Rule
571.2804	1	C34H39N2O6	571.2803	-0.2	17.0	1	100.00	16.5	even	ok
	2	C31H31N12	571.2789	-2.6	18.4	2	47.23	22.5	even	ok
	3	C35H35N6O2	571.2816	2.1	28.8	3	43.97	21.5	even	ok

S9. HRESIMS spectrum of compound **2**.

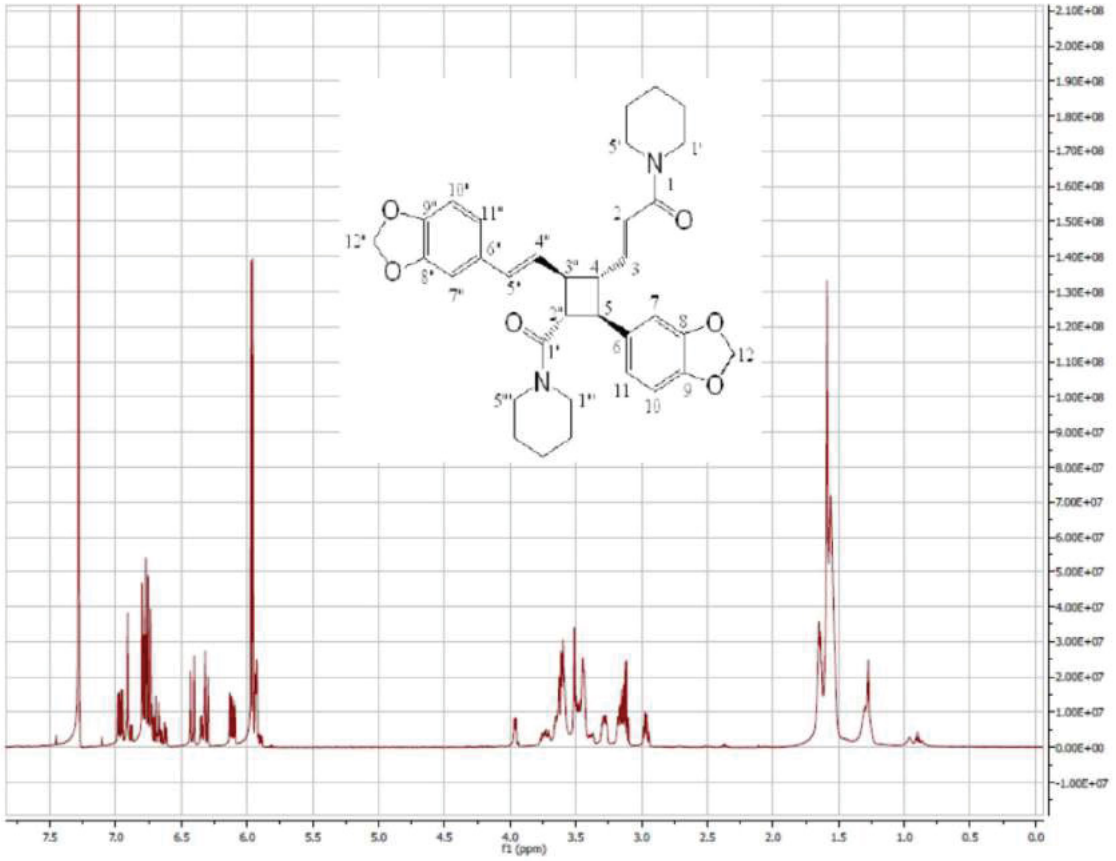

S10. ^{1}H NMR (600 MHz, $CDCl_3$) spectrum of compound **2**.

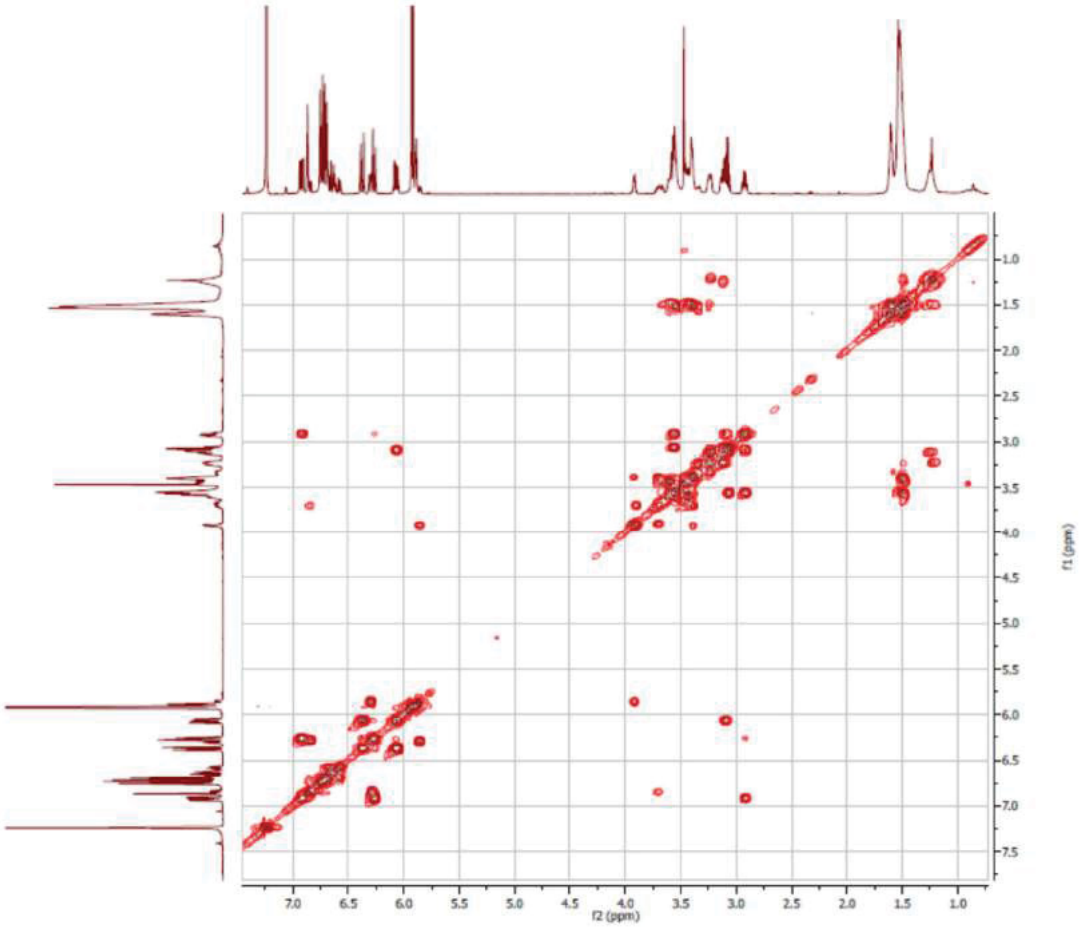

S11. ^{1}H-^{1}H COSY (600 MHz, $CDCl_3$) spectrum of compound **2**.

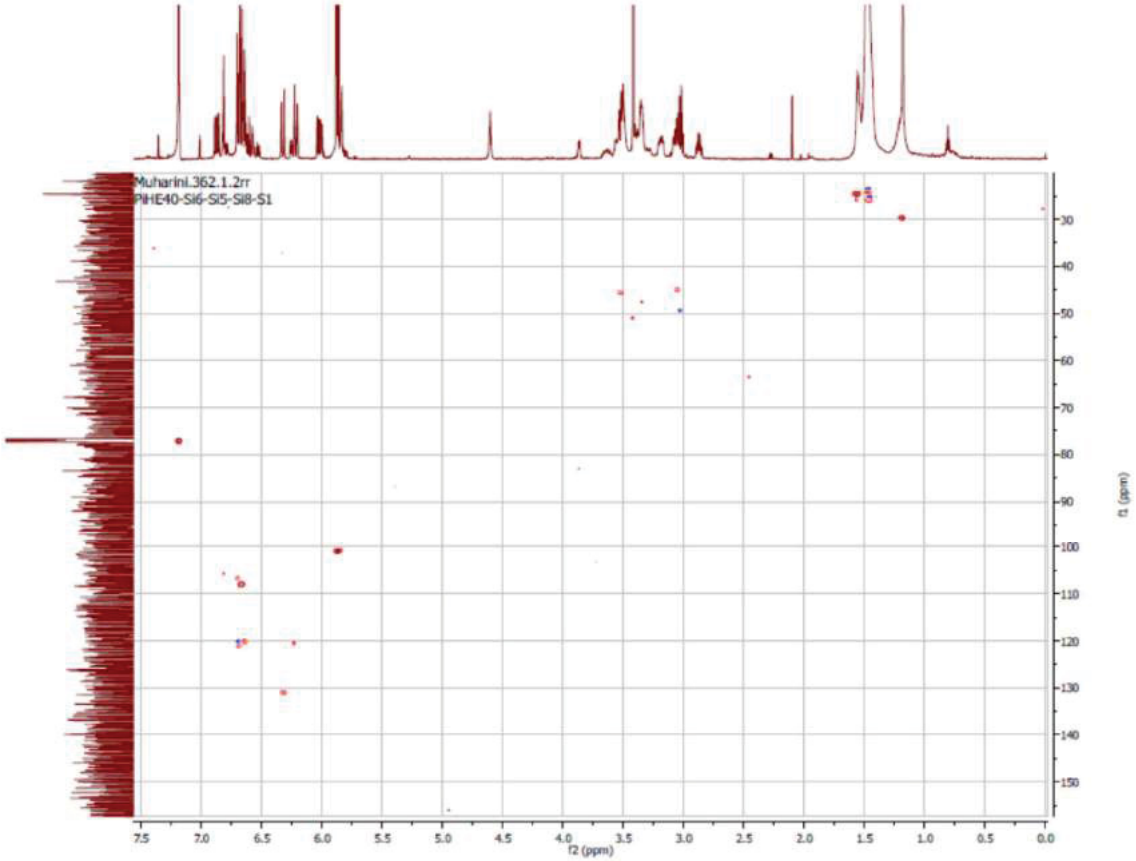

S12. HSQC (600 and 150 MHz, $CDCl_3$) spectrum of compound **2**.

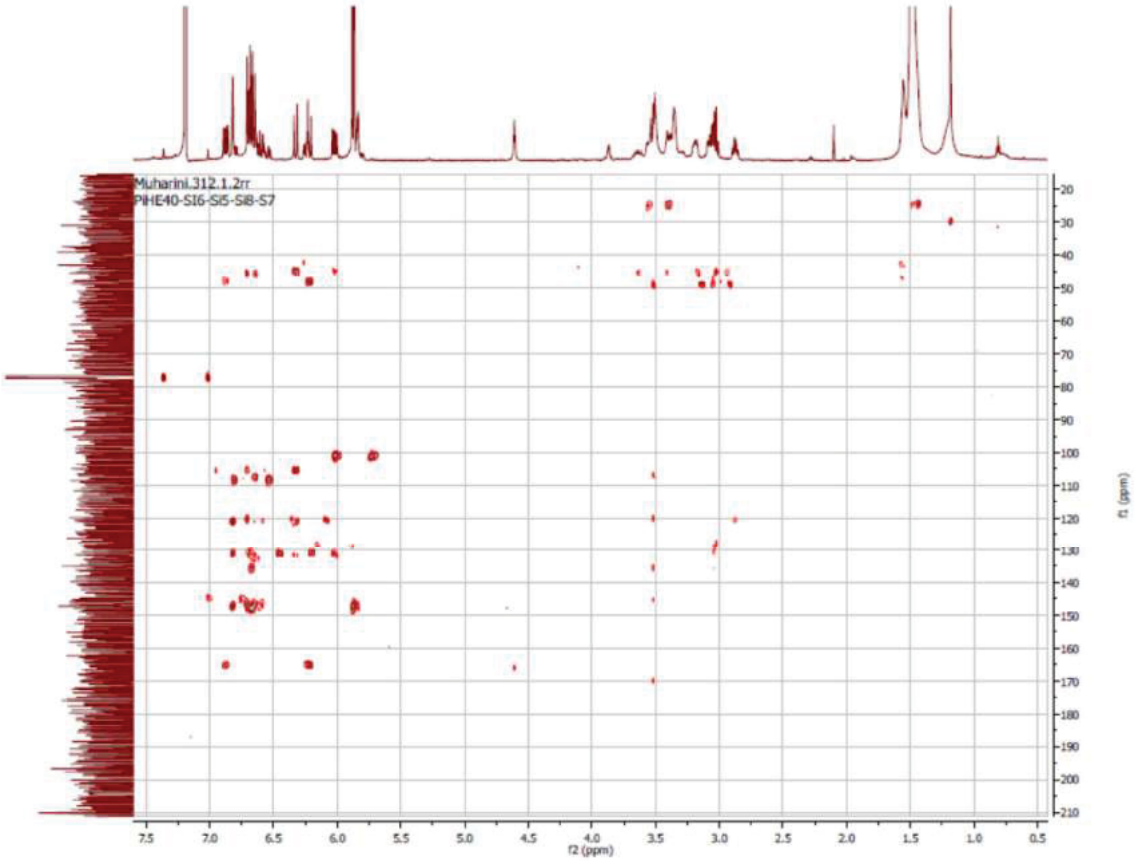

S13. HMBC (600 and 150 MHz, $CDCl_3$) spectrum of compound **2**.

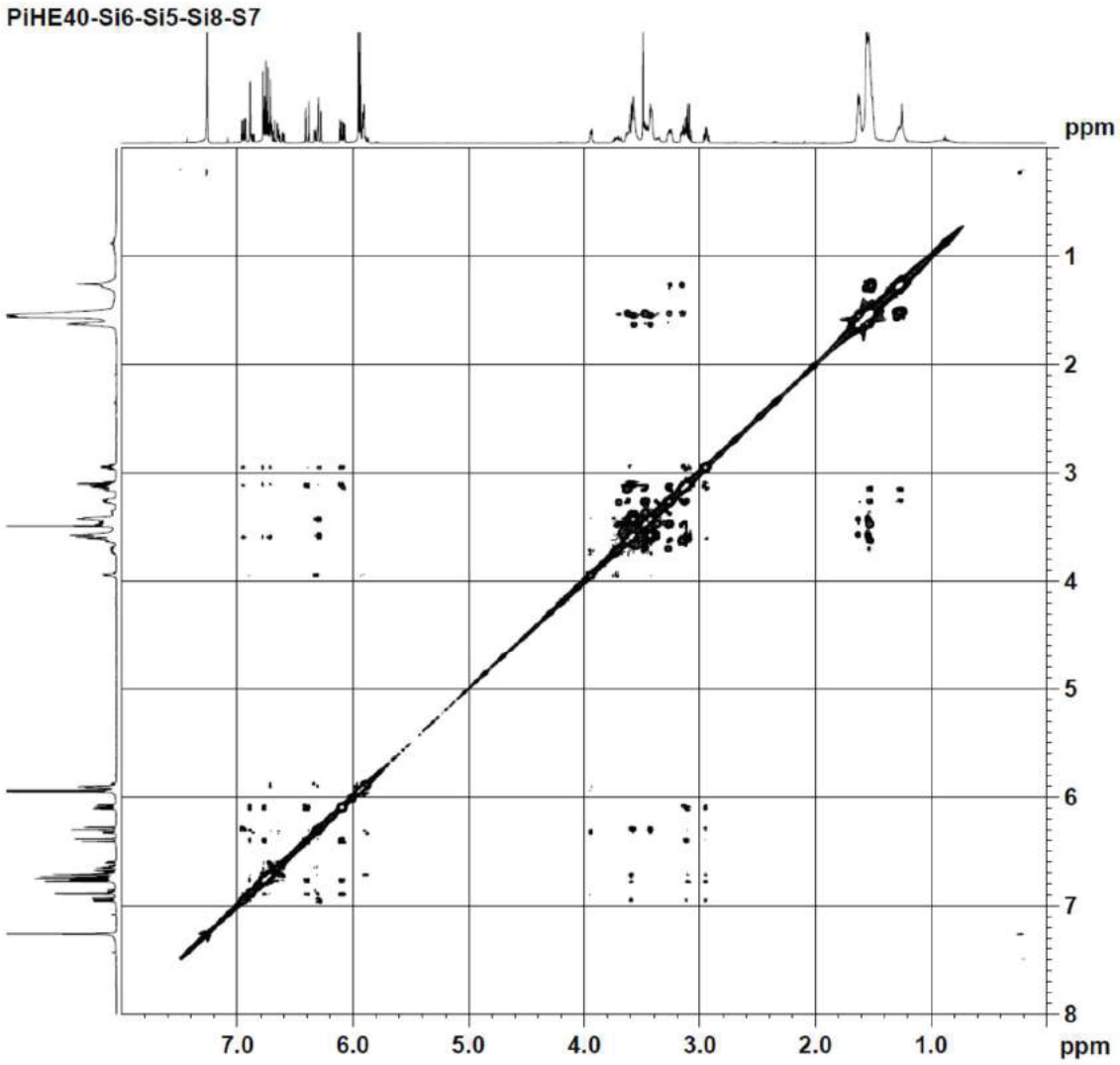

S14. ROESY (600 MHz, $CDCl_3$) spectrum of compound **2**.

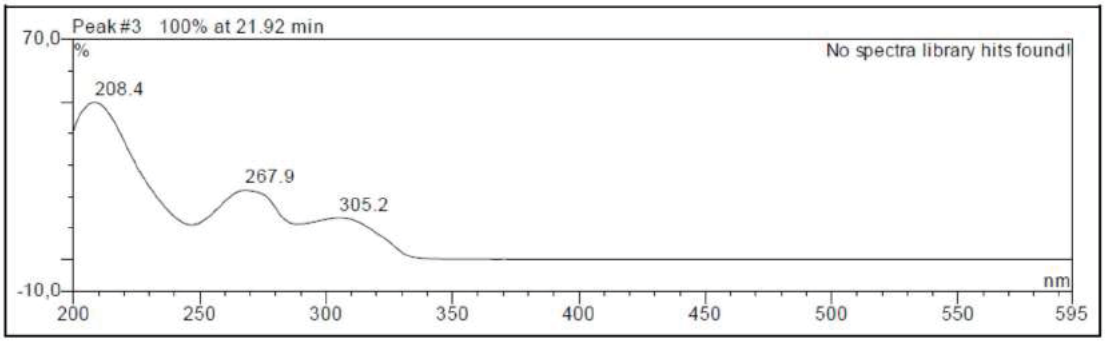

S15. UV spectrum of compound **3**.

Mass Spectrum SmartFormula Report

Analysis Info

Analysis Name	D:\Data\Spektren2014\Proksch14000132.d	Acquisition Date	9/23/2014 8:32:49 AM
Method	tune_low.m	Operator	Peter Tommes
Sample Name	Rini PiHE40-Si6-Si5-Si8-S8 (CH3OH)	Instrument	maXis 288882.20213
Comment			

Acquisition Parameter

Source Type	ESI	Ion Polarity	Positive	Set Nebulizer	0.3 Bar
Focus	Not active	Set Capillary	4000 V	Set Dry Heater	180 °C
Scan Begin	50 m/z	Set End Plate Offset	-500 V	Set Dry Gas	4.0 l/min
Scan End	1500 m/z	Set Collision Cell RF	600.0 Vpp	Set Divert Valve	Source

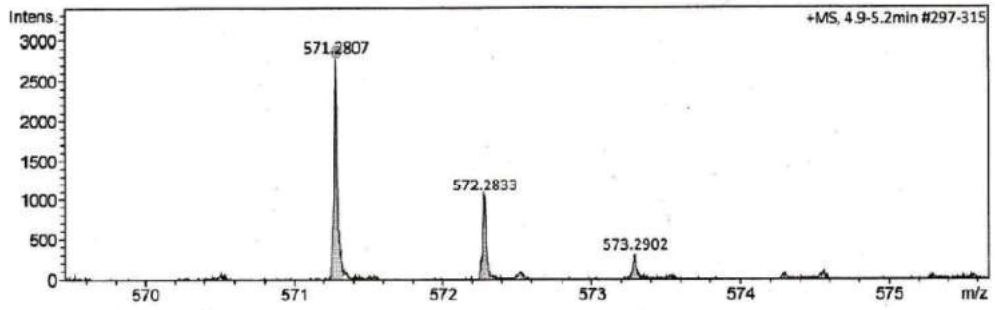

Meas. m/z	#	Ion Formula	m/z	err [ppm]	mSigma	# mSigma	Score	rdb	e⁻ Conf	N-Rule
571.2807	1	C34H39N2O6	571.2803	-0.7	14.3	1	100.00	16.5	even	ok
	2	C35H35N6O2	571.2816	1.6	17.6	2	71.89	21.5	even	ok
	3	C31H31N12	571.2789	-3.1	19.1	3	41.05	22.5	even	ok

S16. HRESIMS spectrum of compound **3**.

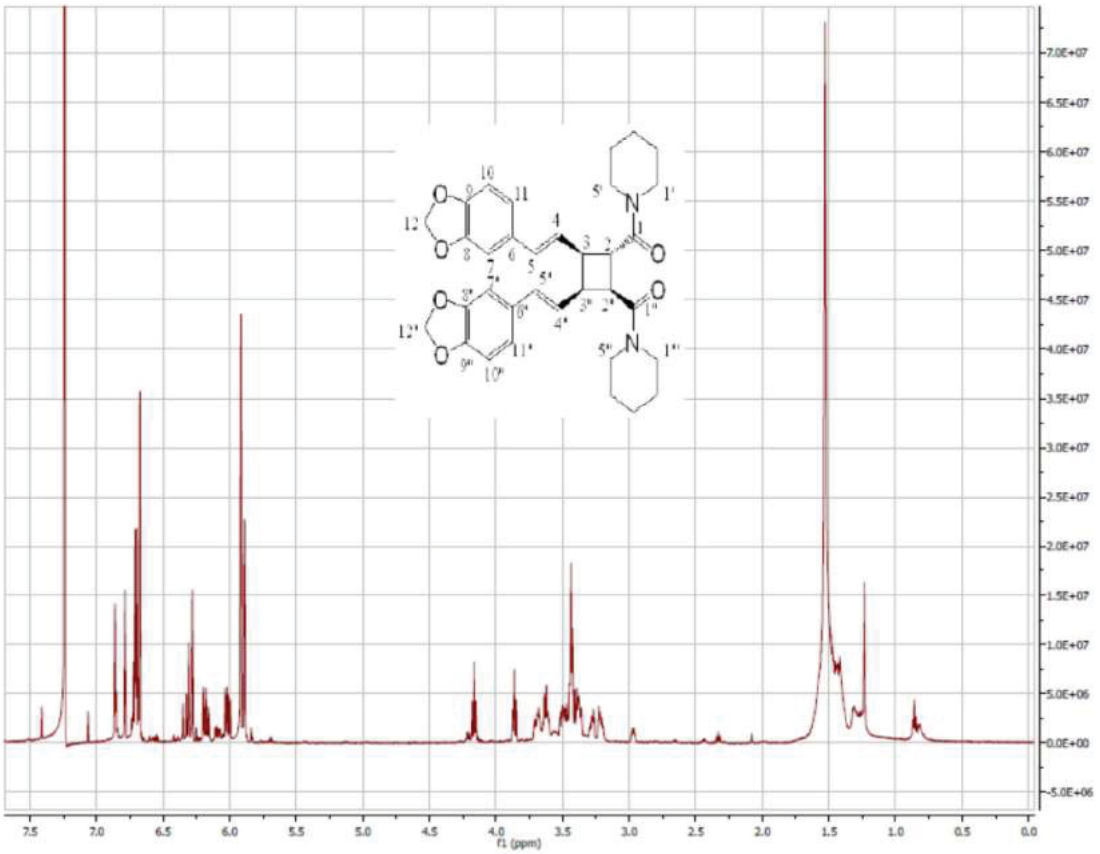

S17. ^{1}H NMR (600 MHz, $CDCl_3$) spectrum of compound **3**.

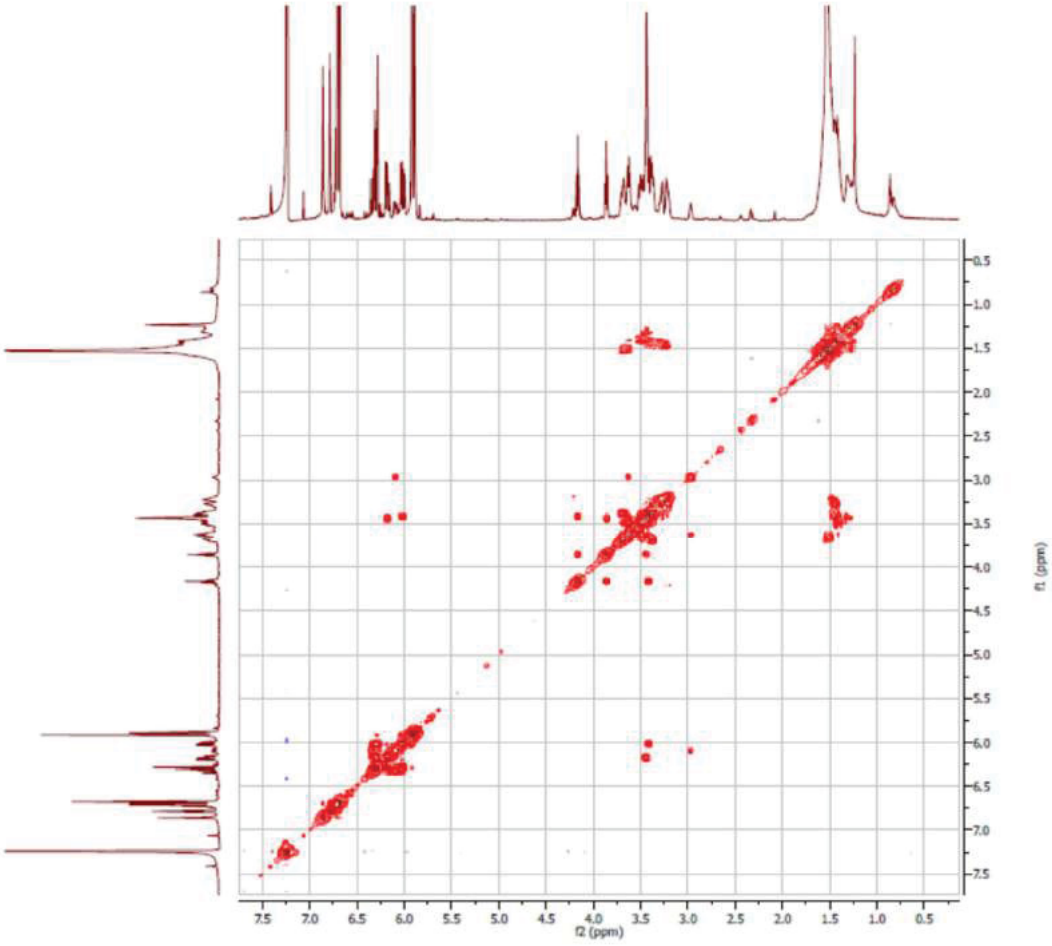

S18. ^{1}H-^{1}H COSY (600 MHz, $CDCl_3$) spectrum of compound**3**.

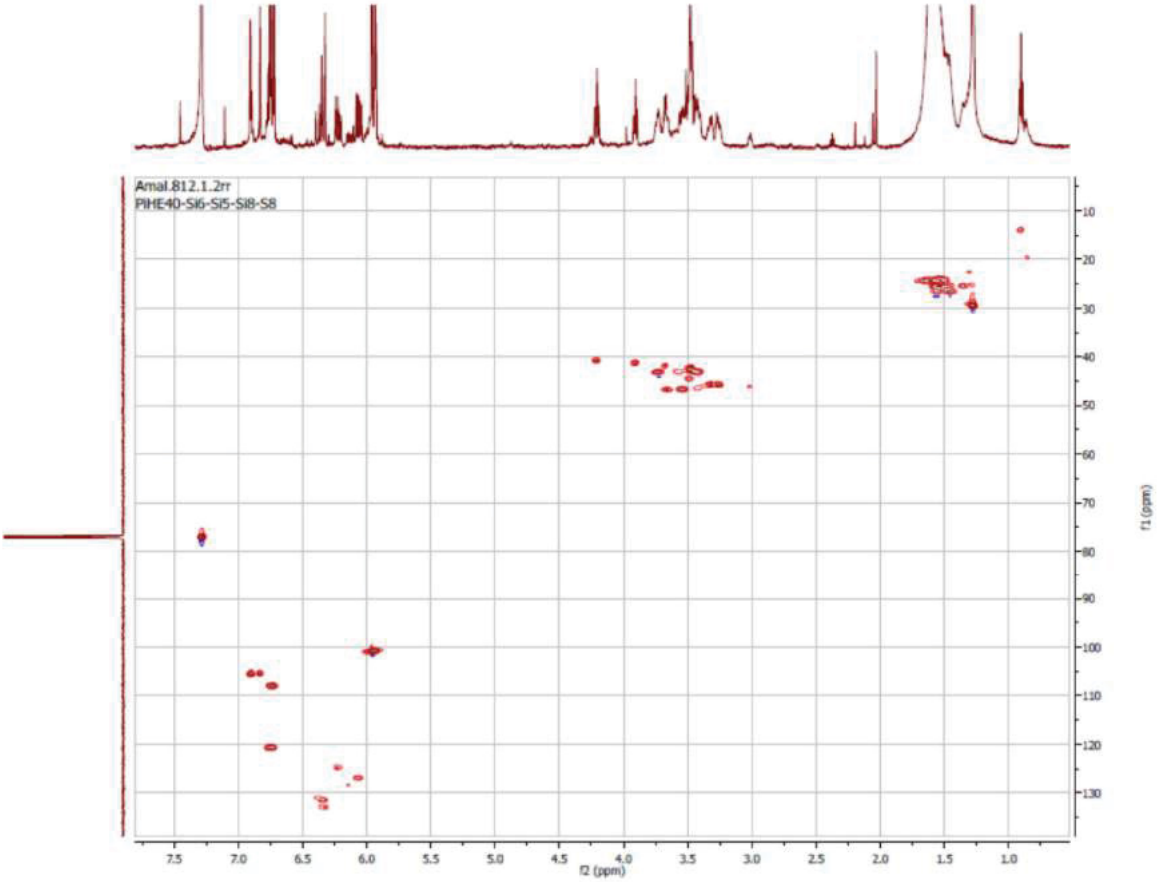

S19. HSQC (600 and 150 MHz, $CDCl_3$) spectrum of compound**3**.

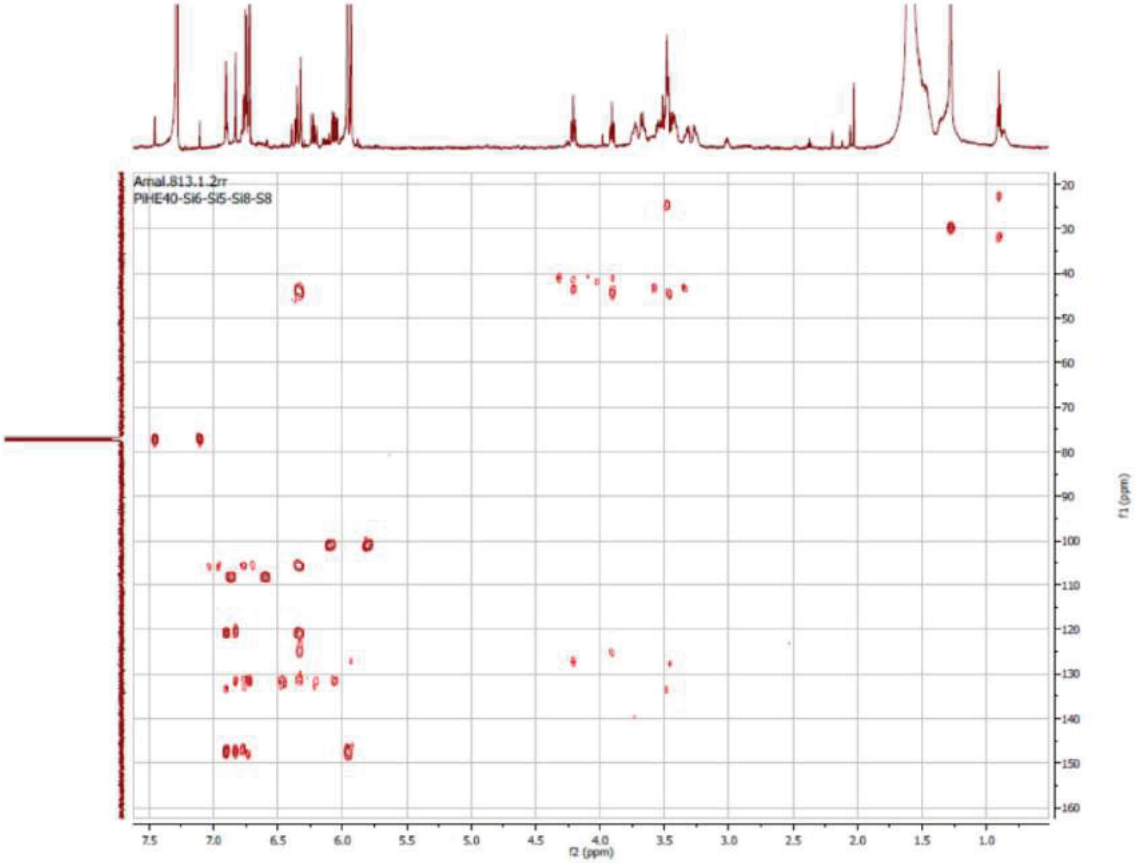

S20. HMBC (600 and 150 MHz, $CDCl_3$) spectrum of compound **3**.

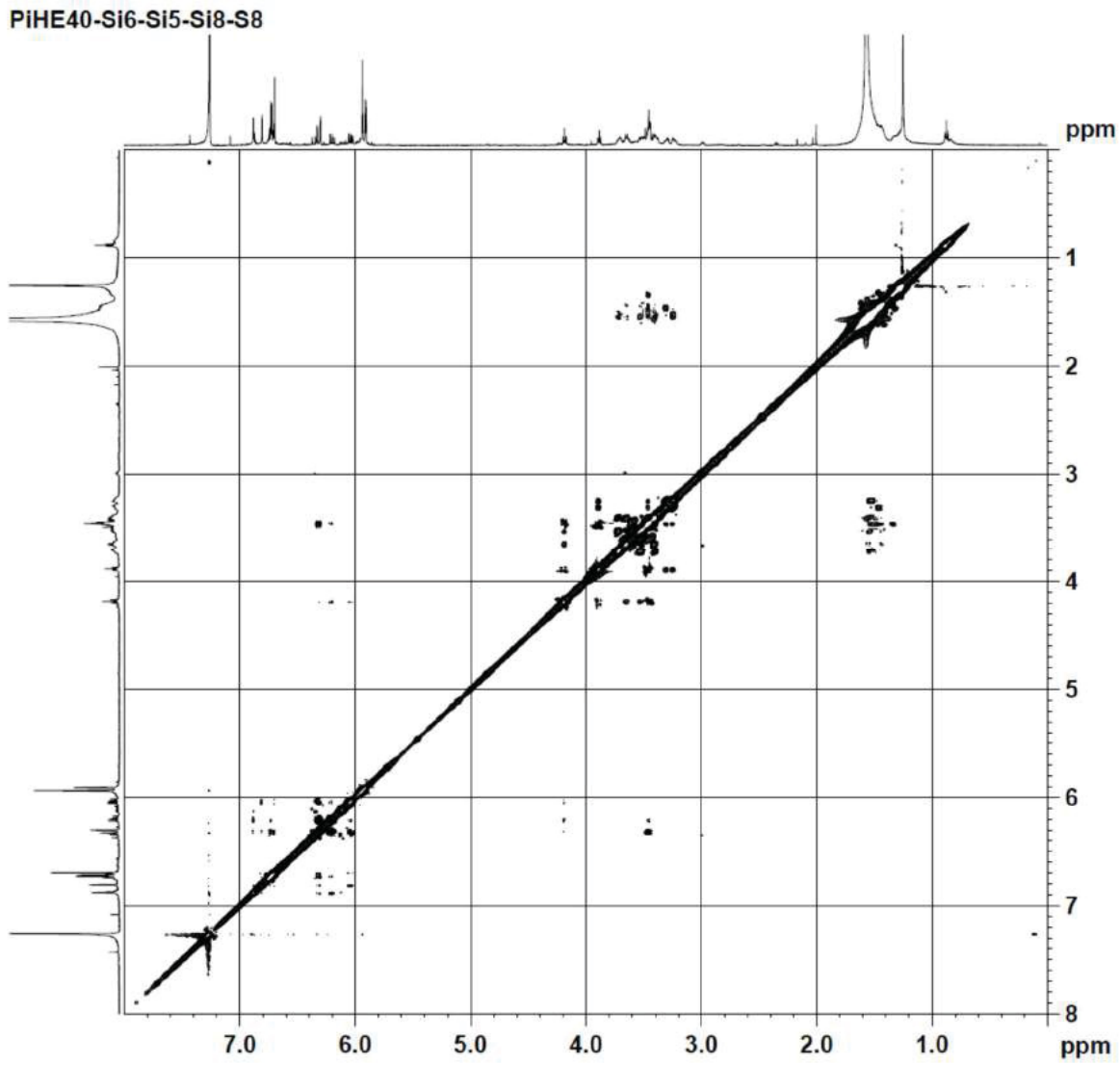

S21. ROESY (600 MHz, $CDCl_3$) spectrum of compound **3**.

4. Publication 3

4.1 New C-methylated flavonoids and α-pyrone derivative from roots of *Talinum triangulare* growing in Nigeria

Published in: “Fitoterapia”

Impact factor: 2.345

The overall contribution to the paper: 20%, conducting three sets of experiments (HPLC and LCMS analysis of fractions in isolation process, measuring alpha D values of isolated compounds and performing antifungal assays), and preparing samples for cytotoxicity assay.

Reprinted with permission from “Omeokoli, B.O., Muharini, R., Okoye, F.B., Ajiwe, V.I., Akpuaka, M.I.U., Lin, W., Liu, Z., Proksch, P., (2016) New C-methylated flavonoids and α-pyrone derivative from roots of Talinum triangualare growing in Nigeria. Fitoterapia 109: 169 – 173.”

Publication 3

Fitoterapia 109 (2016) 169–173

Contents lists available at ScienceDirect

Fitoterapia

journal homepage: www.elsevier.com/locate/fitote

New *C*-methylated flavonoids and α-pyrone derivative from roots of *Talinum triangulare* growing in Nigeria

Blessing O. Umeokoli [a,b], Rini Muharini [a], Festus B. Okoye [b], Vincent I. Ajiwe [c], Mabel U. Akpuaka [c], Wenhan Lin [d], Zhen Liu [a,*], Peter Proksch [a,*]

[a] Institute of Pharmaceutical Biology and Biotechnology, Heinrich-Heine-Universität Düsseldorf, Universitätsstrasse 1, 40225 Düsseldorf, Germany
[b] Department of Pharmaceutical and Medicinal Chemistry, Nnamdi Azikiwe University, Awka, Nigeria
[c] Department of Pure and Industrial Chemistry, Nnamdi Azikiwe University, Awka, Nigeria
[d] State Key Laboratory of Natural and Biomimetic Drugs, Peking University, 100191 Beijing, China

ARTICLE INFO

Article history:
Received 11 November 2015
Received in revised form 30 December 2015
Accepted 4 January 2016
Available online 7 January 2016

Keywords:
Talinum triangulare
C-methylated flavonoids
α-pyrone
Amides

ABSTRACT

The first chemical examination of roots of the traditionally used medicinal plant *Talinum triangulare* (Portulacaceae) from Nigeria led to the isolation of two new *C*-methylated flavonoids, 5,6-dimethoxy-7-hydroxy-8-methyl-flavone (**1**), 5,6-dimethoxy-8-methyl-2-phenyl-7*H*-1-benzopyran-7-one (**2**), and one new α-pyrone derivative, 4-methoxy-6-(2-hydroxy-4-phenylbutyl)-2*H*-pyran-2-one (**3**), along with thirteen known compounds, including nine amides (**4–12**), indole-3-carboxylic acid (**13**), *p*-hydroxy benzoic acid (**14**), and two steroids (**15–16**). Their structures were elucidated by extensive spectroscopic measurements including 1D, 2D NMR, MS, and by comparison with the literature. All isolated compounds were screened for their cytotoxic and antifungal activities. However, none of them showed significant activity.

1. Introduction

Talinum triangulare (Portulacaceae) is probably native to tropical America but has been introduced to Nigeria and other tropical regions in Africa as a leaf vegetable. Now it becomes one of the most important vegetables in Nigeria and known as "waterleaf" [1]. The ethnobotanical use of leaves from this plant in Nigeria includes the treatment of peptic ulcer in different parts of Nigeria [2]. Macerated leaves of *T. triangulare* are also applied locally for the treatment of cuts, wounds and scabies in Ovia North East Edo state in Nigeria [3], whereas a decoction of roots from *T. triangulare* is taken three times daily for 7 days in the treatment of hypertension in Iregun area of Ogun state in Nigeria [4–5]. Phytochemical studies of this plant are rare with one exception that is reported frequently encountered metabolites such as steroids and allantoin among others from stems and leaves [6]. No phytochemical studies exist yet on natural products from the roots of *T. triangulare*. Our present study on metabolites from the roots of *T. triangulare* yielded 16 compounds including three new compounds 5,6-dimethoxy-7-hydroxy-8-methyl-flavone (**1**), 5,6-dimethoxy-8-methyl-2-phenyl-7*H*-1-benzopyran-7-one (**2**), and 4-methoxy-6-(2-hydroxy-4-phenylbutyl)-2*H*-pyran-2-one (**3**) (Fig. 1). Herein, we describe the structure elucidation of the new compounds, and screening results on the biological activities of all isolated metabolites.

2. Results and discussions

Compound **1** was isolated as an orange sticky solid. Its UV spectrum showed absorption maxima at 213, 267, and 314 nm, which agreed with a flavonoid skeleton. The molecular formula of **1** was determined as $C_{18}H_{16}O_5$ based on HRESIMS data, indicating 11 degrees of unsaturation. The ^{1}H NMR spectrum (Table 1) showed two aromatic protons at δ_H 7.90 (dd, J = 7.7, 2.0 Hz, H-2′ and H-6′), one aromatic proton at δ_H 7.53 (m, H-4′), and two aromatic protons at δ_H 7.52 (m, H-3′ and H-5′), suggesting the presence of a monosubstituted benzene ring *B*, which was further confirmed by the HMBC correlations (Fig. 2) from H-2′ and H-6′ to C-4′ (δ_C 131.4), from H-3′ and H-5′ to C-1′ (δ_C 131.8), and from H-4′ to C-2′ and C-6′ (δ_C 126.0). On the basis of the HMBC correlations from H-3 (δ_H 6.73, s) to C-2 (δ_C 161.3), C-4 (δ_C 178.0), C-10 (δ_C 112.1), and C-1′, and from H-2′ and H-6′ to C-2, the nature of ring *C* was established and ring *B* was deduced to be substituted at C-2. Furthermore, key HMBC correlations from H_3-11 (δ_H 2.44, s) to C-7 (δ_C 152.0), C-8 (δ_C 108.2), and C-9 (δ_C 152.7), from 5-OMe (δ_H 3.96, s) to C-5 (δ_C 148.6), and from both 6-OMe (δ_H 4.05, s) and H-3 to C-6 (δ_C 137.7) confirmed the nature of ring *A* and the attachments of methyl, hydroxy, methoxy and methoxy groups at C-8, 7, 6 and 5 positions, respectively. Thus, compound **1** was elucidated as 5,6-dimethoxy-7-hydroxy-8-methyl-flavone.

* Corresponding authors.
E-mail addresses: zhenfeizi0@sina.com (Z. Liu), proksch@uni-duesseldorf.de (P. Proksch).

http://dx.doi.org/10.1016/j.fitote.2016.01.002
0367-326X/

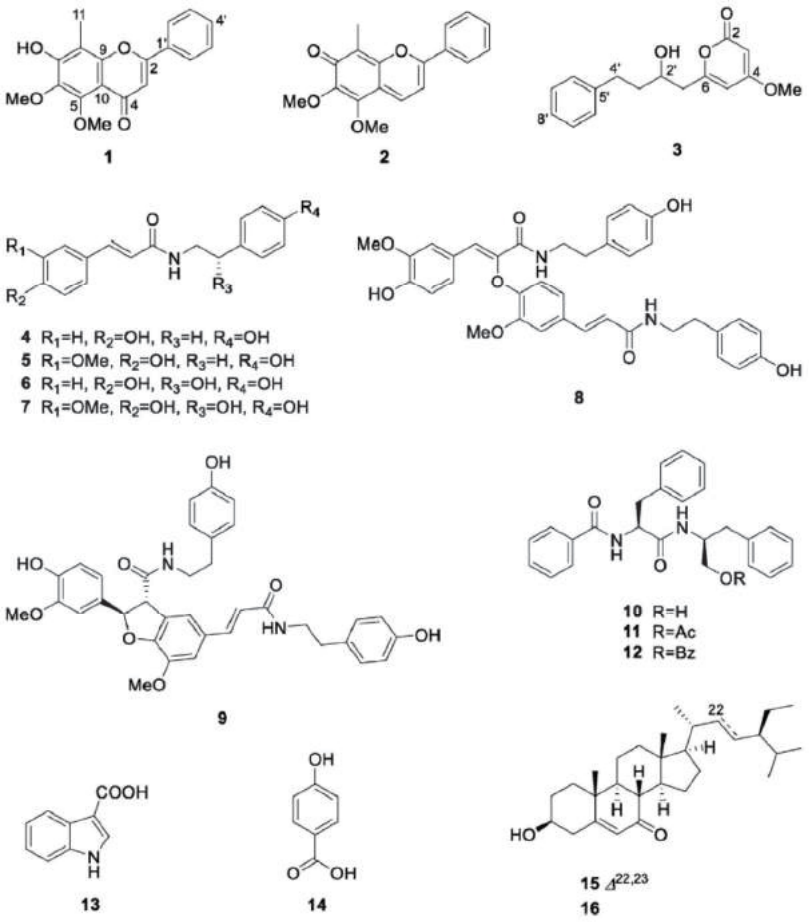

Fig. 1. Structures of compounds **1–16** from *Talinum triangulare*.

Compound **2** was obtained as a red solid. It exhibited a pseudomolecular ion peak at *m/z* 297.1122 $[M + H]^+$, which was consistent with the molecular formula of $C_{18}H_{16}O_4$. The ^1H NMR spectrum of **2** (Table 1) showed similar resonances to those of **1**, which included signals for a monosubstituted benzene ring *B* at δ_H 8.07 (dd, J = 7.6, 2.1 Hz, H-2′ and H-6′), 7.59 (m, H-4′), and 7.58 (m, H-3′ and H-5′), a signal for a methyl substituent at δ_H 2.25 (s, H_3-11), and signals for two methoxy groups at δ_H 4.08 (s, 5-OMe) and 3.92 (s, 6-OMe). However, two doublet olefinic protons at δ_H 7.34 (d, J = 7.6 Hz, H-3) and 8.15 (d, J = 7.6 Hz, H-4) were observed in ^1H NMR spectrum of **2** instead of a singlet olefinic proton (H-3) in that of **1**. The COSY correlation between H-3 and H-4, together with the HMBC correlations from H-3 to C-2 (δ_C 161.5), C-10 (δ_C 119.7), and C-1′ (δ_C 132.5), and from H-4 to C-2, C-5 (δ_C 147.5), and C-9 (δ_C 154.6), indicated the presence of two double bonds at C-2/C-3 and C-4/C-10 in ring *C* of **2** (Fig. 2). In

Table 1
^{13}C and ^1H NMR data of compounds **1** and **2**.

Position	1[a]		2[b]	
	δ_C	δ_H (J in Hz)	δ_C	δ_H (J in Hz)
2	161.3, C		161.5, C	
3	107.7, CH	6.73, s	104.7, CH	7.34, d (7.6)
4	178.0, C		137.1, CH	8.15, d (7.6)
5	148.6, C		147.5, C	
6	137.7, C		145.0, C	
7	152.0, C		181.2, C	
8	108.2, C		111.0, C	
9	152.7, C		154.6, C	
10	112.1, C		119.7, C	
11	8.5, CH_3	2.44, s	8.0, CH_3	2.25, s
1′	131.8, C		132.5, C	
2′, 6′	126.0, CH	7.90, dd (7.7, 2.0)	127.2, CH	8.07, dd (7.6, 2.1)
3′, 5′	129.1, CH	7.52, m	130.5, CH	7.58, m
4′	131.4, CH	7.53, m	133.1, CH	7.59, m
5-OMe	62.1, CH_3	3.96, s	62.1, CH_3	4.08, s
6-OMe	61.8, CH_3	4.05, s	60.9, CH_3	3.92, s

[a] Recorded at 600 MHz for ^1H and 150 MHz for ^{13}C in $CDCl_3$.
[b] Recorded at 600 MHz for ^1H and 150 MHz for ^{13}C in CD_3OD.

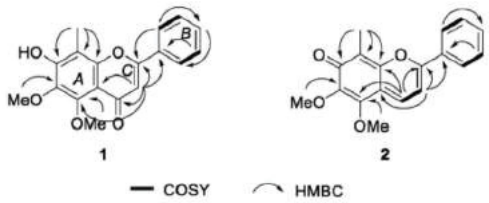

Fig. 2. Key COSY and HMBC correlations of compounds **1** and **2**.

addition, H_3-11 showed correlations to C-7 (δ_C 181.2), C-8 (δ_C 111.0), and C-9, confirming a ketone group to be located at the C-7 position. Thus, compound **2** was determined to be 5,6-dimethoxy-8-methyl-2-phenyl-7*H*-1-benzopyran-7-one. The quinonoidal structure of compound **2** was further supported by comparison of its NMR data with that of carajurin, whose structure was confirmed by X-ray crystallographic analysis [7]. Compound **2** could be regarded as a natural 3-deoxyanthocyanidin, which is more stable than anthocyanins and anthocyanidins because there is neither a glucose group nor a hydroxyl group at C-3 position of 3-deoxyanthocyanidins [8–9]. It has been reported that anthocyanidins exist in four different pH-dependent structural isoforms in aqueous solution, namely quinoid base, flavylium cation, hemiacetal and chalcone [10–11]. The thermodynamically more stable red quinoid base is the major species for compound **2** probably due to the presence of *O*-substituted group at C-5 position and not in C-3 position [11].

Compound **3** was isolated as a white solid. It has a molecular formula of $C_{16}H_{18}O_4$ which was evident from the appearance of a pseudomolecular peak at *m/z* 275.1279 $[M + H]^+$, implying 8 degrees of unsaturation. A monosubstituted benzene ring *B* (Fig. 3) was recognized from the signals at 7.25 (t, $J = 7.4$ Hz, H-7′ and H-9′), 7.20 (d, $J = 7.4$ Hz, H-6′ and H-10′), and 7.15 (t, $J = 7.4$ Hz, H-8′) (Table 2). This was further confirmed by the COSY correlations between H-6′ (10′)/H-7′ (9′) and H-7′ (9′)/H-8′, and the HMBC correlations from H-6′ (10′) to C-8′ (δ_C 126.7), from H-7′ (9′) to C-5′ (δ_C 143.3), and from H-8′ to C-6′ (10′) (δ_C 129.4). A 2-hydroxybutyl partial structure was established based on the COSY correlations between H_2-1′ (δ_H 2.68 and 2.56)/H-2′ (δ_H 3.93), H-2′/H_2-3′ (δ_H 1.82 and 1.77), and H_2-3′/H_2-4′ (δ_H 2.81 and 2.69). Besides, the HMBC correlations from H_2-3′ to C-5′, from H_2-4′ to C-5′ and C-6′ (10′), and from H-6′ (10′) to C-4′ indicated benzene ring *B* to be located at C-4′. Apart from these signals, two doublet olefinic protons at δ_H 5.54 (d, $J = 2.2$ Hz, H-3) and 6.05 (d, $J = 2.2$ Hz, H-5) were observed in ^{1}H NMR. In the HMBC spectrum, H-3 showed correlations to C-2 (δ_C 164.5), C-4 (δ_C 173.8), and C-5 (δ_C 103.2), while H-5 exhibited correlations to C-3 (δ_C 88.4) and C-6 (δ_C 164.7). Combined with its molecular formula, these data indicated the presence of an α-pyrone ring *A* in **3**. Furthermore, key HMBC correlations from 4-OMe (δ_H 3.85, *s*) to C-4 and from H_2-1′ to C-5 and C-6 confirmed the attachments of methoxy and butyl groups at C-4 and 6 in ring *A*, respectively. Thus, compound **3** was identified as 4-methoxy-6-(2- hydroxy-4-phenylbutyl)-2*H*-pyran-2-one. An attempt to determine the absolute configuration at C-2′ of **3** using Mosher's method was unsuccessful due to its limited amount.

The thirteen known compounds were identified as *N-trans*-*p*-coumaroyltyramine (**4**) [12], *N-trans*-feruloyltyramine (**5**) [12], (*S*)-*N-trans*-*p*-coumaroyloctopamine (**6**) [13], (*S*)-*N-trans*-feruloyloctopamine (**7**) [14], cannabisin F (**8**) [15], grossamide (**9**) [16], aurantiamide (**10**) [17], aurantiamide acetate (**11**) [18], aurantiamide benzoate (**12**) [19], indole-3-carboxylic acid (**13**) [20], *p*-hydroxy benzoic acid (**14**) [21],

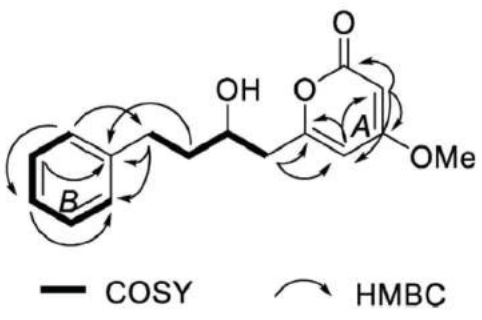

Fig. 3. Key COSY and HMBC correlations of compound **3**.

Table 2
^{13}C and ^{1}H NMR data of compound **3**.

Position	3[a]	
	δ_C	δ_H (*J* in Hz)
2	164.5, C	
3	88.4, CH	5.54, d (2.2)
4	173.8, C	
5	103.2, CH	6.05, d (2.2)
6	164.7, C	
1′	42.6, CH_2	2.68, m
		2.56, dd (14.5, 8.6)
2′	69.2, CH	3.93, m
3′	40.2, CH_2	1.82, m
		1.77, m
4′	32.9, CH_2	2.81, ddd (13.6, 9.7, 5.5)
		2.69, m
5′	143.3, C	
6′, 10′	129.4, CH	7.20, d (7.4)
7′, 9′	129.5, CH	7.25, t (7.4)
8′	126.7, CH	7.15, t (7.4)
4-OMe	56.9, CH_3	3.85, s

[a] Recorded at 600 MHz for ^{1}H and 150 MHz for ^{13}C in CD_3OD.

3β-hydroxystigmast-5,22-dien-7-one (**15**) [22], 3β-hydroxystigmast-5-en-7-one (**16**) [23].

All isolated compounds were tested for their cytotoxic activity against the mouse lymphoma cell line (L5178Y) using the MTT assay. However, none of them showed significant inhibitory activity at the concentration of 10.0 μg/mL. Also, all tested compounds failed to exhibit antifungal activity against *Cladosporium cladosporioides* when tested at a dose of 50 μg.

This is the first phytochemical study on roots of *T. triangulare* in which we describe the presence of two new *C*-methylated flavonoids (**1–2**), one new α-pyrone derivative (**3**), four lignanamides (**4–7**) and dimers (**8–9**), three aurantiamide derivatives (**10–12**), indole-3-carboxylic acid (**13**), *p*-hydroxy benzoic acid (**14**), and two steroids (**15–16**). These metabolites are structurally very different from those reported from stems and leaves of *T. triangulare*, which may be responsible for their different traditional medicinal use. Compounds **1** and **2** belong to a novel class of *C*-methylated flavonoids, most of which are obtained from families Myrtaceae and Ericaceae [24]. Compound **2** could also be regarded as a natural 3-deoxyanthocyanidin, which is rarely found in plants. *Sorghum* (Poaceae) contains high levels of these rare 3-deoxyanthocyanidin pigments [25,26]. They have also been found from *Dracaena draco* (Dracaenaceae) [11,27] and *Arrabidaea chica* (Bignoniaceae) [28]. To the best of our knowledge, this is the first report on *C*-methylated flavonoids and 3-deoxyanthocyanidins from Portulacaceae. Unusual α-pyrone derivative **3** is assumed to be biosynthesized through polyketide synthase (PKS) pathway. Its analogs have been synthesized in a recent report by 4-coumarate CoA ligase (4CL) and chalcone synthase (CHS), the two pivotal enzymes involved in the biosynthesis of flavonoids [29].

3. Experimental section

3.1. General experimental procedures

1D and 2D NMR spectra were recorded on a Bruker DMX 600 NMR spectrometer. LC–MS spectra were obtained on a Thermofinnigan LCQ Deca XP Thermoquest coupled to an Agilent 1100 HPLC system and HRESIMS spectra were measured on a FTHRMS-Orbitrap (Thermo Finnigan) mass spectrometer. HPLC analysis was performed with a Dionex Ultimate 3000 LC system coupled with a photodiode array detector (UVD340S). TLC was performed on TLC plates pre-coated with silica gel (Merck, Germany). Semi-preparative HPLC was performed on a HPLC system (Merck, Darmstadt, Germany) coupled with a UV detector L7400. The separation column (8 × 250 mm) was pre-packed with Eurosphere C_{18} (Germany) and MEOH/H_2O containing 0.1% TFA was

Publication 3

used as solvent system at a flow rate of 5 mL/min. All solvents were distilled before use and spectroscopic measurements were performed with spectral grade solvents.

3.2. Plant material

The roots of *Talinum triangulare* were collected in July 2014 in Nawfia town, Anambra state, Nigeria. This plant was identified by Dr. V. I. Mbaekwe of Botany Department, Nnamdi Azikiwe University, Awka, Nigeria. A voucher specimen was deposited at the Department of Pharmacognosy, Faculty of Pharmaceutical Sciences, Nnamdi Azikiwe University, Awka, Nigeria.

3.3. Extraction and isolation

The air dried roots of *Talinum triangulare* (900 g) were pulverized into coarse powder and extracted with MeOH for 3 days on a shaker with successive replacement of solvent. The filtrate was then concentrated in vacuo at 40 °C to give a reddish residue (40 g), which was fractionated by vacuum liquid chromatography (VLC) on silica gel using a gradient elution of n-hexane/EtOAc (9:1, 8:2, 4:6, 2:8, 0:10, each 1000 mL) and of dichloromethane (DCM)/methanol (10:0, 7:3, 5:5, 2:8, 0:10, each 1000 mL) to afford 10 fractions (V1-10). Fraction V3 (288.0 mg) was chromatographed on sephadex LH-20 with DCM-MeOH (1:1) as solvent, followed by further purification with semi-preparative RP-HPLC to give compounds **11** (3.4 mg), **12** (2.5 mg), **15** (4.0 mg), and **16** (1.0 mg). Fraction V4 fraction (1.09 g) was subjected to VLC with the same gradient as above to give 10 fractions (V4A-J). Subfraction V4D (177.0 mg) was further purified by semi-preparative RP-HPLC to yield compounds **2** (4.2 mg) and **3** (1.0 mg). Fraction V5 (273.4 mg) was chromatographed over sephadex LH-20 using 100% MeOH, and then purified by semi-preparative RP-HPLC to afford compounds **6** (1.2 mg), **8** (5.0 mg), and **9** (4.0 mg). Fraction V8 (1.7 g) was fractionated by VLC using a gradient of *n*-hexane/EtOAc (100:0 to 0:100, gradient in 10% each step) and DCM/MeOH (100:0 to 0:100, gradient in 10% each step) to give 22 subfractions (V8A-V). Subfraction V8D (33.6 mg) was purified by semi-preparative RP-HPLC to yield compound **1** (6.3 mg), **10** (1.0 mg), **13** (1.0 mg) and **14** (1.3 mg). Following the same procedures, Subfraction V9C (47.6 mg) was obtained from fraction V9 and subsequently purified by semi-preparative HPLC to afford compounds **4** (1.2 mg), **5** (6.0 mg), and **7** (2.0 mg).

3.3.1. 5,6-dimethoxy-7-hydroxy-8-methyl-flavone (*1*)

Yellow solid; UV (MeOH) λ_{max}: 213, 267 and 314 nm; ^{1}H and ^{13}C NMR data see Table 1; HRESIMS $[M + H]^+$ *m/z* 313.1078 (calcd. for $C_{18}H_{17}O_5$, 313.1076).

3.3.2. 5,6-dimethoxy-8-methyl-2-phenyl-7H-1-benzopyran-7-one (*2*)

Red solid; UV (MeOH) λ_{max}: 275, 320 and 485 nm; ^{1}H and ^{13}C NMR data see Table 1; HRESIMS $[M + H]^+$ *m/z* 297.1122 (calcd. for $C_{18}H_{17}O_4$, 297.1127).

3.3.3. 4-methoxy-6-(2-hydroxy-4-phenylbutyl)-2H-pyran-2-one (*3*)

White solid; −4.4° (*c* 0.2, MeOH); UV (MeOH) λ_{max}: 207 and 283 nm; ^{1}H and ^{13}C NMR data see Table 2; HRESIMS $[M + H]^+$ *m/z* 275.1279 (calcd. for $C_{16}H_{19}O_4$, 275.1278).

3.4. Cytotoxicity assay

Cytotoxicity was tested against L5178Y mouse lymphoma cell line using MTT's method as described before [30]. Kahalalide F was used as positive control and a media with 0.1% DMSO were incorporated as negative control.

3.5. Antifungal assay

The antifungal assay was performed using Kirby-Bauer agar diffusion method and nystatin was used as a positive control.

Acknowledgment

This research was supported by a grant from Dr. Willmar Schwabe Research Scholarship for Young Scientists by the Society for Medicinal Plant and Natural Product Research (GA).

References

[1] O.B. Afolabi, O.J. Oloyede, T. Oladimeji, Effect of extract of *Talinum triangulare* (water leaf) in lead-induced chromosomal aberration, J. Phytopharmacol. 3 (2014) 238–241.

[2] N.N. Onwurah, I.G. Eke, A.O. Anaga, Antiulcer properties of aqueous extract of *Talinum triangulare* leaves in experimentally induced gastric ulceration in mice, Asian J. Phar. Biol. Res. 3 (2013) 4–7.

[3] R.K.A. Egharevba, M.I. Ikhatua, Ethno-medical uses of plants in the treatment of various skin diseases in Ovia North East, Edo State, Nigeria, Res. J. Agric. Biol. Sci. 4 (2008) 58–64.

[4] I.O. Lawal, N.E. Uzokwe, D.O. Ladipo, I.O. Asinwa, A.B.I. Igboanugo, Ethnophytotherapeutic information for the treatment of high blood pressure among the people of Ilugun, Ilugun area of Ogun State, south-west Nigeria, Afr. J. Pharm. Pharmacol. 3 (2009) 222–226.

[5] J.K. Mensah, R.I. Okoli, A.A. Turay, E.A. Ogie-Odia, Phytochemical analysis of medicinal plants used for the management of hypertention by Esan people of Edo State, Nigeria, Ethnobotanical Leaflets 13 (2009) 1273–1287.

[6] A.P. de Oliveira Amorim, A.R. de Carvalho Jr, N.P. Lopes, R.N. Castro, M.C.C. de Oliveira, M.G. de Cavalho, Chemical compounds isolated from *Talinum triangulare* (Portulacaceae), Food Chem. 160 (2014) 204–208.

[7] B. Devia, G. Llabres, J. Wouters, L. Dupont, M.T. Escribano-Bailon, S. de Pascual-Teresa, L. Angenot, M. Tits, New 3-deoxyanthocyanidins from leaves of *Arrabidaea chica*, Phytochem. Anal. 13 (2002) 114–120.

[8] L. Yang, L. Dykes, J.M. Awika, Thermal stability of 3-deoxyanthocyanidin pigments, Food Chem. 160 (2014) 246–254.

[9] A. Sousa, P. Araujo, J. Azevedo, L. Cruz, I. Fernandes, N. Mateus, V. de Freitas, Antioxidant and antiproliferative properties of 3-deoxyanthocyanidins, Food Chem. 192 (2016) 142–148.

[10] G. Woodward, P. Kroon, A. Cassidy, C. Kay, Anthocyanin stability and recovery: implications for the analysis of clinical and experimental samples, J. Agric. Food Chem. 57 (2009) 5271–5278.

[11] M.J. Melo, M. Sousa, A.J. Parola, J.S.S. de Melo, F. Catarino, J. Marcalo, F. Pina, Identification of 7,4′-dihydroxy-5-methoxyflavylium in "dragon's blood": to be or not to be an anthocyanin, Chem. Eur. J. 13 (2007) 1417–1422.

[12] J.C. Holzbach, L.M.X. Lopes, Aristolactams and alkaamides of *Aristolochia giganteam*, Molecules 15 (2010) 9462–9472.

[13] F. Matsuda, H. Miyagawa, T. Ueno, Absolute structure of *N*-*p*-coumaroyloctopamine in elicitor-treated potato tuber tissue, Biosci. Biotechnol. Biochem. 64 (2000) 625–627.

[14] M. DellaGreca, L. Previtera, R. Purcaro, A. Zarrelli, Cinnamic acid amides and lignanamides from *Aptenia cordifolia*, Tetrahedron 62 (2006) 2877–2882.

[15] I. Sakakibara, Y. Ikeya, K. Hayashi, M. Okada, M. Maruno, Three acyclic *bis*-phenylpropane lignanamides from fruits of *Cannabis sativa*, Phytochemistry 38 (1995) 1003–1007.

[16] A.M.L. Seca, A.M.S. Silva, A.J.D. Silvestre, J.A.S. Cavaleiro, F.M.J. Domingues, C. Pascoal-Neto, Lignanamides and other phenolic constituents from the bark of kenaf (*Hibiscus cannabinus*), Phytochemistry 58 (2001) 1219–1223.

[17] B. Xu, Z. Huang, C. Liu, Z. Cai, W. Pan, P. Cao, X. Hao, G. Liang, Synthesis and anti-hepatitis B virus activities of Matijing-Su derivatives, Bioorg. Med. Chem. 17 (2009) 3118–3125.

[18] J. Tang, T. Supinya, Z. Wang, Z. Tu, Aurantiamide acetate from stems of *Zanthoxylum dissitum* hemsley, J. Chin. Pharm. Sci. 12 (2003) 231–233.

[19] M. Faccione, D.T. Ferreira, R. Braz-Filho, A.M. Pomini, Rev. Latinoam. Quim. 32 (2004) 7–14.

[20] Y. Wang, A. Hämäläinen, J. Tois, R. Franzen, Preparation of indole-phosphine oxazoline (IndPHOX) ligands and their application in allylic alkylation, Tetrahedron Asymmetry 21 (2010) 2376–2384.

[21] S. Sivakumar, M.L.P. Reddy, A.H. Cowley, K.V. Vasudevan, Synthesis and crystal structures of lanthanide 4-benzyloxy benzoates: influence of electron-withdrawing and electron-donating groups on luminescent properties, Dalton Trans. 39 (2010) 776–786.

[22] H. Choi, M.P. Doyle, Optimal TBHP allylic oxidation of Δ^5-steroids catalyzed by dirhodium caprolactamate, Org. Lett. 9 (2007) 5349–5352.

[23] X. Zhang, P. Geoffroy, M. Miesch, D. Julien-David, F. Raul, D. Aoude-Werner, E. Marchioni, Gram-scale chromatographic purification of β-sitosterol synthesis and characterization of β-sitosterol oxides, Steroids 70 (2005) 886–895.

[24] B.A. Bohm, Introduction to flavonoids, Harwood Academic Publishers, Amsterdam, The Netherlands, 1998 26.

[25] B. Geera, L.O. Ojwang, J.M. Awika, New highly stable dimeric 3-deoxyanthocyanidin pigments from *Sorghum bicolour* leaf sheath, J. Food Sci. 77 (2012) 566–572.

Publication 3

[26] A.R. Massey, L. Reddivari, J. Vanamala, The dermal layer of sweet sorghum (*Sorghum bicolor*) stalk, a byproduct of biofuel production and source of unique 3-deoxyanthocyanidins, has more antiproliferative and proapoptotic activity than the pith in p53 variants of HCT116 and colon cancer stem cells, J. Agric. Food Chem. 62 (2014) 3150–3159.
[27] M.M. Sousa, M.J. Melo, A.J. Parola, J.S.S. de Melo, F. Catarino, F. Pina, F.E.M. Cook, M.S.J. Simmonds, J.A. Lopes, Flavylium chomophores as species markers for dragon's blood resins from *Dracaena* and *Daemonorops* trees, J. Chromatogr. A 1209 (2008) 153–161.
[28] B. Zorn, A.J. Garcia-Pineres, V. Castro, R. Murillo, G. Mora, I. Merfort, 3-Desoxyanthocyanidins from *Arrabidaea chica*, Phytochemistry 56 (2001) 831–835.
[29] T. Mo, J. Wang, B. Gao, L. Zhang, X. Liu, X. Wang, P. Tu, S. Shi, Combinatorial synthesis of flavonoids and 4-hydroxy-ö-lactones by plant-originated enzymes, Chin. J. Org. Chem. 35 (2015) 1052–1059.
[30] M. Ashour, R. Edrada, R. Ebel, V. Wray, W. Watjen, K. Padmakumar, W.E.G. Müller, W.H. Lin, P. Proksch, J. Nat. Prod. 69 (2006) 1547–1553.

5. Publication 4

5.1 Antibacterial and Cytotoxic Phenolic Metabolites from fruits of *Amorpha fruticosa*

Submitted at “Journal of Natural Products”

Impact factor: 3.798

The overall contribution to the paper: 50% of the first author. The first author involved to all laboratory works, structure elucidations, literature research and manuscript writing.

Publication 4

Antibacterial and Cytotoxic Phenolic Metabolites from Fruits of *Amorpha fruticosa*

Rini Muharini,[†,‡] Adriana Díaz,[†] Weaam Ebrahim,[†,§] Attila Mándi,[⊥] Tibor Kurtán,[⊥] Nidja Rehberg,[†] Rainer Kalscheuer,[†] Rudolf Hartmann,[#] Raha S. Orfali,[‖] Wenhan Lin,[▽] Zhen Liu,*[,†] Peter Proksch,*[,†]

[†]Institute of Pharmaceutical Biology and Biotechnology, Heinrich-Heine-Universität Düsseldorf, Universitätsstrasse 1, Geb.26.23, 40225 Düsseldorf, Germany

[‡]Department of Chemistry Education, Faculty of Education, Tanjungpura University, Jl. Prof. Dr. H. Hadari Nawawi, 78124, Pontianak, Indonesia

[§]Department of Pharmacognosy, Faculty of Pharmacy, Mansoura University, Mansoura 35516, Egypt

[⊥] Department of Organic Chemistry, University of Debrecen, Egyetem tér 1, Debrecen 4032, Hungary

[#]Institute of Complex Systems: Strukturbiochemie, Forschungszentrum Juelich, Wilhelm-Johnen-Straße, 52428 Juelich, Germany

[‖]Department of Pharmacognosy, Faculty of Pharmacy, King Saud University, Riyadh, Saudi Arabia

[▽]State Key Laboratory of Natural and Biomimetic Drugs, Peking University, Beijing 100191, China

Publication 4

ABSTRACT:

Fourteen new natural products, including 2-[(*Z*)-styryl]-5-geranyl-resorcin-1-carboxylic acid (**1**), amorfrutin D (**2**), 4-demethylamorfrutin D (**3**), 8-geranyl-3,5,7-trihydroxyflavanone (**13**), 8-geranyl-3′,5,7-trihydroxy-4′-methoxyisoflavone (**14**), 6-geranyl-3′,5,7-trihydroxy-4′-methoxyisoflavone (**15**), 8-geranyl-3′,7-dihydroxy-4′-methoxyisoflavone (**16**), 3-demethyldalbinol (**42**), 6a,12a-dehydro-3-demethylamorphigenin (**43**), (6a*R*,12a*R*,5′*R*)-amorphigenin (**44**), amorphispironone B−C (**45**−**46**), resokaempferol 3-*O*-*β*-D-glucopyranosyl-(1→2)-*β*-D-glucopyranoside-7-*O*-*α*-L-rhamnopyranoside (**51**), daidzein 7-*O*-*β*-D-glucopyranosyl-(1→2)-*β*-D-glucopyranoside (**52**), together with 40 known compounds, were isolated from fruits of *Amorpha fruticosa*. Their structures were elucidated by 1D and 2D NMR spectroscopic analyses as well as by mass data. CD calculation was performed to determine the absolute configuration of **11** and **45**. Compounds **1**, **4**−**8**, **12**−**15** showed potent to moderate antibacterial activities against several gram-positive bacteria with MIC values ranging from 3.1 to 100 μM. In addition, compounds **25**, **27**, **30**, **32**, **34**, **35**, **37**, **41**, **45**, **48** and **53** possessed significant cytotoxicity against the L5178Y mouse lymphoma cell line and exhibited IC_{50} values from 0.2 to 10.2 μM.

Publication 4

Amorpha fruticosa (Fabaceae) is a deciduous shrub, which is native to North America and has been introduced to Europe and West Asia as an ornamental plant.[1,2] Since the beginning of 20th century, this plant has attracted phytochemists. The essential oil from its dry fruits was shown to consist of monoterpenes and sesquiterpenes such as *α*-pinene and *δ*-cadinene as major constituents.[3] The crude extract of dry fruits of *A. fruticosa* was demonstrated to possess antibacterial,[4] insecticidal,[5] and cytotoxic[2] activities. Amorfrutins A and B, two bibenzyl metabolites, were reported to exhibit promising antimicrobial,[4] antidiabetic[6] and antiinflammatory[7,8] activities. Other phenolic compounds classified as flavonoids and rotenoids were also discovered in previous studies on *A. fruticosa*.[9–12] Some of the latter compounds showed antibacterial,[11] antiviral[13,14] and cytotoxic[15,16] activities.

In this study, screening of fractions derived from a dichloromethane (DCM)-methanol (MeOH) extract of dry fruits of *A. fruticosa* revealed promising antibacterial or cytotoxic activities. Detailed investigation of the secondary metabolites contained in these bioactive fractions afforded 54 phenolic compounds including 14 new natural compounds, which included three new bibenzyl compounds, 2-[(*Z*)-styryl]-5-geranyl-resorcin-1-carboxylic acid (**1**), amorfrutin D (**2**) and 4-demethylamorfrutin D (**3**), a new geranylated flavonoid, 8-geranyl-3,5,7-trihydroxyflavanone (**13**), three new geranylated isoflavonoids, 8-geranyl-3′,5,7-trihydroxy-4′-methoxyisoflavone (**14**), 6-geranyl-3′,5,7-trihydroxy-4′-methoxyisoflavone (**15**) and 8-geranyl-3′,7-dihydroxy-4′-methoxyisoflavone (**16**), five new rotenoids, 3-demethyldalbinol (**42**), 6a,12a-dehydro-3-demethylamorphigenin (**43**), (6a*R*,12a*R*,5′*R*)-amorphigenin (**44**), amorphispironones B and C (**45** and **46**), a new flavonoid glycoside, resokaempferol 3-*O*-*β*-D-glucopyranosyl-(1→2)-*β*-D-glucopyranoside-7-*O*-*α*-L-rhamnopyranoside (**51**) and a new isoflavonoid glycoside, daidzein 7-*O*-*β*-D-glucopyranosyl-(1→2)-*β*-D-glucopyranoside (**52**).

Publication 4

The structures of the new compounds were elucidated by extensive NMR spectroscopic methods and mass spectrometric analysis. The absolute configurations of **11**, **42**, **44** and **45** were determined employing CD calculation or by comparison with literature data. The sugars were characterized following acid hydrolysis of the respective glycosides, derivatization, and HPLC analysis with comparison to known standards. In this paper, we describe the isolation, structure elucidation as well as antibacterial and cytotoxic activities of the isolated compounds.

Publication 4

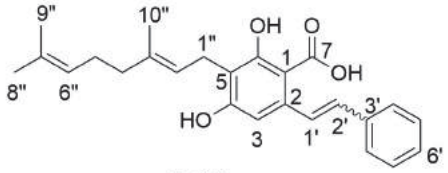

1 1'Z
4 1'*E*

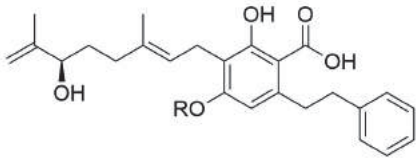

2 R = Me
3 R = H

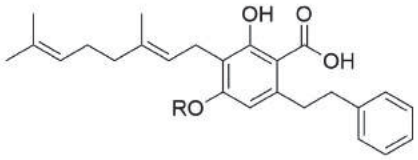

5 R = Me
6 R = H

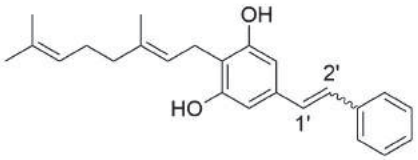

7 1'Z
8 1'*E*
9 1',2'-dihydro

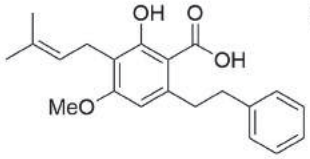

10

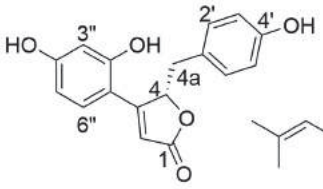

11

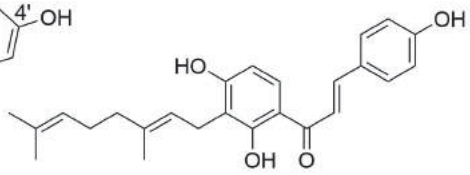

12

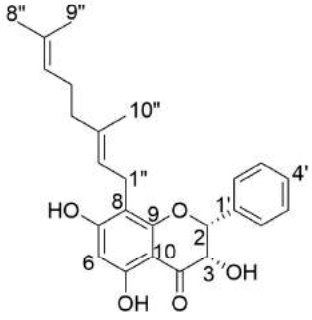

13

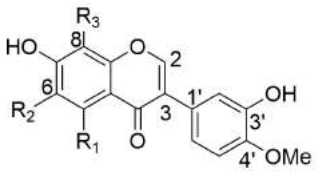

14 R_1=OH,R_2=H,R_3=geranyl
15 R_1=OH,R_2=geranyl,R_3=H
16 R_1=R_2=H,R_3=geranyl

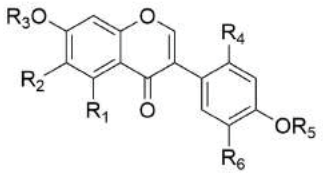

17 R_1=R_2=R_3=R_4=R_5=R_6=H
18 R_1=OH,R_2=R_3=R_4=R_6=H,R_5=Me
19 R_1=OH,R_2=R_4=R_6=H,R_3=R_5=Me
20 R_1=R_3=R_4=R_6=H,R_2=OMe,R_5=Me
21 R_1=R_2=R_3=H,R_4=R_6=OMe,R_5=Me
22 R_1=R_2=H,R_3=R_5=Me,R_4=R_6=OMe

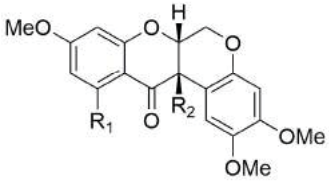

23 R_1=R_2=H
24 R_1=H,R_2=OH
25 R_1=OH,R_2=H
26 R_1=R_2=OH

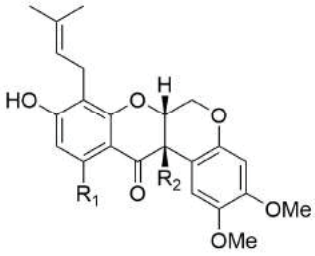

27 R_1=R_2=H
28 R_1=H,R_2=OH
29 R_1=OH,R_2=H

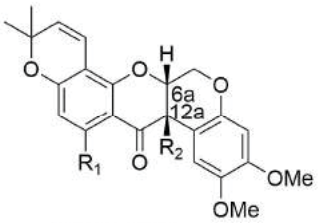

30 R_1=R_2=H
31 R_1=H,R_2=OH
32 R_1=OH,R_2=H
33 R_1=R_2=OH
34 R_1=H,6a,12a-dehydro

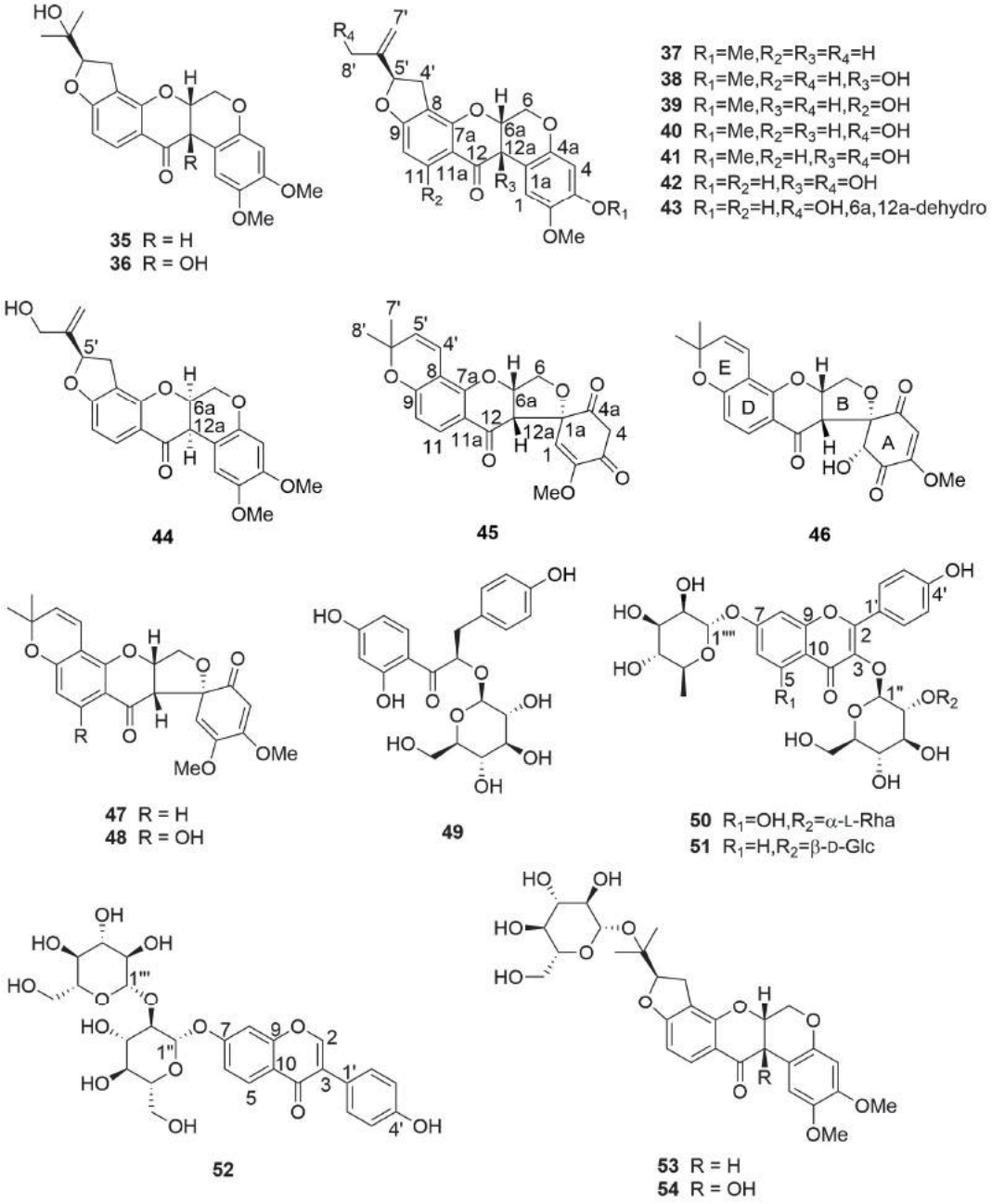

RESULTS AND DISSCUSSION

Chromatographic fractionation of the DCM-MeOH (1:1) extract of air dried fruits of *A. fruticosa* using vacuum liquid chromatography (VLC) gave 25 fractions. All fractions were tested for their antibacterial activity. Further fractionation and purification of the bioactive fractions yielded 54 phenolic natural products, of which fourteen are new.

Publication 4

Compound **1** was obtained as an amorphous solid. Its molecular formula was established as $C_{25}H_{28}O_4$ by HRESIMS data, indicating twelve degrees of unsaturation. The ^{1}H NMR spectrum of **1** (Table 1) showed a chelated hydroxy signal at δ_H 11.93 (s, 6-OH), signals of a monosubstituted benzene ring around δ_H 7.13−7.17 (5H, H-4′−8′), two olefinic protons at δ_H 6.86 (d, H-1′) and 6.58 (d, H-2′), an aromatic proton at δ_H 6.20 (s, H-3), and characteristic signals of a geranyl side chain. The above data were almost identical to those of the known 2-[(*E*)-styryl]-5-geranyl-resorcin-1-carboxylic acid (**4**).[17] However, the smaller $^3J_{1',2'}$ value of **1** (12.0 Hz) compared to that of **4** (16.0 Hz) indicated a *Z* double bond at C-1′/C-2′ in **1**. Except the configuration of double bond, **1** shared the same gross structure as **4** as confirmed by 2D NMR analysis. Thus, **1** was elucidated as 2-[(*Z*)-styryl]-5-geranyl-resorcin-1-carboxylic acid. Since compound **1** was already detected in the crude extract of fruits of *A. fruticosa*, it is assumed to be a true natural product and not to arise from the *E* isomer of this compound by light induced isomerization during the isolation procedure.

The HRESIMS spectrum of **2** exhibited a $[M+H]^+$ peak at *m/z* 425.2319, corresponding to the molecular formula $C_{26}H_{32}O_5$. Its UV spectrum gave maximum absorbance at wavelength 222, 269 and 309 nm, which are similar to those of amorfrutin B (**5**).[4] The NMR data of **2** (Table 1) were very similar to those of **5** except for the detection of a terminal olefinic methylene (δ_C 110.6, δ_H 4.89 and 4.80, CH_2-8″) and an oxygenated methine (δ_C 75.6, δ_H 4.03, CH-6″) in **2**. The HMBC correlations from Me-9″ (δ_H 1.70) to C-6, C-7″ (δ_C 147.0), and C-8″, and the COSY correlations between H-6″/H_2-5″ (δ_H 1.65) and H_2-5″/H_2-4″ (δ_H 2.03) indicated a terminal olefinic double bond located at C-7″/C-8″ and a hydroxy group attached at C-6″ in **2**. Thus, **2** was identified as a new amorfrutin derivative as shown in Figure 1, for which the trivial name amorfrutin D is proposed. By comparison its optical rotation value (-24) with those of two

related known compounds (*R*)- and (*S*)-2′-(6-hydroxy-3,7-dimethyl-2,7-octadien-1-yl)-3′-methoxy-5′,6-dihydroxy-2-arylbenzofuran (-6.6 and +6.6, respectively),[18] the absolute configuration of **2** is suggested to be *R*.

Table 1. ^{1}H and ^{13}C NMR data for compounds **1**−**3**.

Position	**1**[a]		**2**[a]		**3**[a]	
	δ_C, type	δ_H (*J* in Hz)	δ_C, type	δ_H (*J* in Hz)	δ_C, type	δ_H (*J* in Hz)
1	102.4, C		103.2, C		103.1, C	
2	n.d.[b]		145.4, C		145.8, C	
3	110.5, CH	6.20, s	105.9, CH	6.20, s	110.5, CH	6.24, s
4	160.7, C		161.7, C		159.8, C	
5	112.9, C		114.7, C		112.5, C	
6	163.4, C		162.5, C		161.8, C	
7	n.d.[b]		174.2, C		n.d.[b]	
1′	130.7, CH	6.86, d (12.0)	39.0, CH_2	3.25, m	38.8, CH_2	3.18, m
2′	129.3, CH	6.58, d (12.0)	37.8, CH_2	2.92, m	37.6, CH_2	2.88, m
3′	n.d.[b]		141.7, C		142.2, C	
4′, 8′	128.0, CH	7.17, m	128.5, CH	7.20, m	128.4, CH	7.20, m
5′, 7′	129.1, CH	7.13, m	128.3, CH	7.29, m	128.3, CH	7.29, m
6′	126.9, CH	7.15, m	125.7, CH	7.20, m	126.0, CH	7.20, m
1″	21.8, CH_2	3.45, d (7.2)	21.7, CH_2	3.36, d (7.0)	22.1, CH_2	3.43, d (7.0)
2″	120.8, CH	5.27, t (7.2)	122.7, CH	5.25, t (7.0)	122.1, CH	5.32, t (7.0)
3″	139.3, C		134.5, C		138.0, C	
4″	39.5, CH_2	2.06, m	35.6, CH_2	2.03, m	35.8, CH_2	2.11, m
5″	26.1, CH_2	2.08, m	32.6, CH2	1.65, m	32.7, CH_2	1.69, m
6″	123.5, CH	5.04, t (6.3)	75.6, CH	4.03, t (6.2)	76.1, CH	4.06, t (6.1)
7″	132.0, C		147.0, C		147.4, C	
8″	25.5, CH_3	1.64, s	110.6, CH_2	4.89, s	111.2, CH_2	4.91, s
				4.80, s		4.82, s
9″	17.5, CH_3	1.58, s	17.3, CH_3	1.70, s	17.7, CH_3	1.71, s
10″	16.0, CH_3	1.79, s	15.8, CH_3	1.80, s	16.6, CH_3	1.84, s
4-OMe			55.2, CH_3	3.78, s		
6-OH		11.93, s		11.67, s		11.97, s

[a]Recorded at 300 MHz for ^{1}H and 75 MHz for ^{13}C in $CDCl_3$. [b]n.d. = not detected.

The UV spectrum of **3** was similar to that of **2**. Its molecular formula was determined as $C_{25}H_{30}O_5$ by analysis of its HRESIMS spectrum, lacking a CH_2 unit compared to **2**. Based on the disappearance of the methoxy signal in **3** and the similarity of the remaining NMR data between

2 and **3** (Table 1), compound **3** was determined to be a 4-demethyl derivative of **2**, which was further confirmed by detailed analysis of the 2D NMR spectra of **3**.

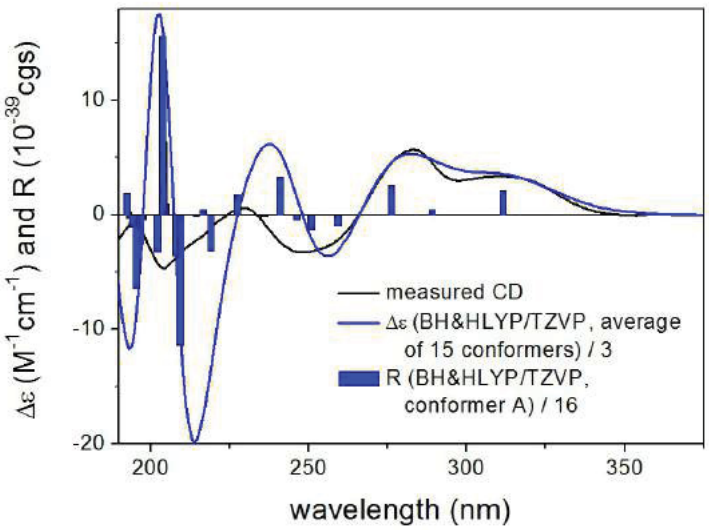

Figure 1. Experimental ECD spectrum of **11** in MeCN compared with the Boltzmann-weighted BH&HLYP/TZVP PCM/MeCN ECD spectrum of (*S*)-**11** computed for the B97D/TZVP PCM/MeCN conformers. Bars represent the rotational strength of the lowest-energy conformer.

The NMR data and optical rotation value of **11** were in agreement with those of (+)-puerol A,[19,20] whose absolute configuration had not been reported yet. In order to determine the absolute configuration of **11**, Merk Molecular Force Field (MMFF) conformational search, DFT optimizations and ECD calculations were performed on the arbitrarily chosen (*S*) enantiomer.[21] Reoptimization of the initial 48 MMFF conformers resulted in 11 and 15 low-energy (≥ 2%) conformers at B3LYP/6-31G(d) *in vacuo* and B97D/TZVP[22,23] PCM/MeCN levels, respectively. Both gas-phase and solvent model calculations reproduced well the main features of the experimental ECD spectrum with BH&HLYP/TZVP (PCM/MeCN) ECD calculation of the B97D/TZVP (PCM/MeCN) conformers giving the best agreement (Figure 1). In the low-energy conformers, the two benzene rings adopted a folded orientation, in which the 2″-OH oriented

above the plane of the other benzene ring assuming a bonding interaction. The low-energy conformers showed similar ECD spectra and there was a good overall agreement between the experimental and Boltzmann-weighted computed ECD spectra at all the applied levels, and thus the absolute configuration of (+)-**11** could be unambiguously assigned as *S*.

Compound **13** was obtained as a yellow amorphous solid. Its molecular formula was determined to be $C_{25}H_{28}O_5$ on the basis of the HRESIMS spectrum. The NMR data of **13** (Table 2 and 3) resembled those of 6-geranyl-3,5,7-trihydroxyflavanone.[24] However, the HMBC correlations from H-1″ (δ_H 3.41) to C-7 (δ_C 162.6), C-8 (δ_C 113.6), and C-9 (δ_C 154.9) indicated the geranyl moiety to be attached at the C-8 position in **13**. Thus, **13** was characterized as 8-geranyl-3,5,7-trihydroxyflavanone. The small $^3J_{2,3}$ value (4.6 Hz) indicated the *cis* configuration between H-2 and H-3.[21]

Compound **14** had the molecular formula $C_{26}H_{28}O_6$ as established by HRESIMS, containing an additional oxygen atom compared to olibergin B (8-geranyl-5,7-dihydroxy-4′-methoxyisoflavone).[25] The NMR data of **14** (Table 2 and 3) were also closely related to those of olibergin B. The singlets at δ_H 12.86, 7.91 and 6.33 were assigned as the chelated hydroxy group 5-OH, and as H-2 and H-6, respectively. A series of proton resonances at δ_H 3.51 (d, H-1″), 5.25 (d, H-2″), 2.07 (m, H_2-4″), 2.11 (m, H_2-5″), 5.05 (t, H-6″), 1.67 (s, Me-8″), 1.59 (s, Me-9″), 1.83 (s, Me-10″) due to the presence of a geranyl moiety were also observed, with the latter being linked to C-8 based on the HMBC correlations from H-1″ to C-7 (δ_C 160.9), C-8 (δ_C 104.9) and C-9 (δ_C 154.9). The *E*-configurated double bond at C-2″/C-3″ was deduced from the cross peaks between H-2″/H_2-4″ and H-1″/Me-10″ in the ROESY spectrum. However, instead of *ortho*-coupled A_2B_2-type protons in olibergin B, an ABX aromatic spin system of the B-ring at δ_H 7.09 (d, J = 2.0 Hz, H-2′), 6.93 (d, J = 8.3 Hz, H-5′) and 7.07 (dd, J = 8.3, 2.0 Hz, H-6′) was observed

in **14**. The HMBC correlations from H-2′, H-6′, and the methoxy group (δ_H 3.93, s) to C-4′ (δ_C 146.8), and from H-5′ to C-3′ (δ_C 145.7), as well as the NOE relationship between H-5′ and the methoxy group, indicated a hydroxy group and a methoxy group to be attached at C-3′ and C-4′, respectively. Thus, **14** was elucidated as 8-geranyl-3′,5,7-trihydroxy-4′-methoxyisoflavone.

Table 2. ^{13}C NMR data for compounds **13**−**16**.

Position	**13**[a]	**14**[b]	**15**[b]	**16**[a]
2	84.1, CH	152.7, CH	152.6, CH	152.2, CH
3	73.5, CH	123.3, C	123.2, C	124.2, C
4	189.0, C	181.1, C	180.6, C	175.9, C
5	162.0, C	160.8, C	159.6, C	125.5, CH
6	103.2, CH	99.8, CH	109.6,C	114.5,CH
7	162.6, C	160.9, C	161.4, C	158.8, C
8	113.6, C	104.9, C	94.0, CH	113.9, C
9	154.9, C	154.9, C	155.8, C	155.0, C
10	104.9, C	106.3, C	105.6, C	118.4, C
1′	137.6, C	123.9, C	123.7, C	125.0, C
2′	126.6, CH	115.1, CH	114.9, CH	114.8, CH
3′	128.4, CH	145.7, C	145.7, C	145.4, C
4′	128.2, CH	146.8, C	146.5, C	146.4, C
5′	128.4, CH	110.7, CH	110.4, CH	110.4, CH
6′	126.6, CH	121.0, CH	121.3, CH	120.8, CH
1″	21.3, CH_2	21.6, CH_2	21.2, CH_2	22.0, CH_2
2″	120.0, CH	120.9, CH	120.8, CH	120.0, CH
3″	140.2, C	139.3, C	140.0, C	139.6, C
4″	39.4, CH_2	39.7, CH_2	39.5, CH_2	39.5, CH_2
5″	26.1, CH_2	26.3, CH_2	26.1, CH_2	26.0, CH_2
6″	123.4, CH	123.6, CH	123.4, CH	123.5, CH
7″	132.3, C	132.1, C	132.0, C	132.0, C
8″	25.8, CH_3	25.7, CH_3	25.6, CH_3	25.5, CH_3
9″	17.6, CH_3	17.7, CH_3	17.6, CH_3	17.5, CH_3
10″	16.0, CH_3	16.2, CH_3	16.1, CH_3	16.2, CH_3
4′-OMe		56.0, CH_3	55.8, CH_3	55.7, CH_3

[a]Recorded at 175 MHz in $CDCl_3$. [b]Recorded at 150 MHz in $CDCl_3$.

Compound **15** had the same molecular formula as **14**. Both compounds also had almost identical ^{1}H and ^{13}C NMR data (Table 2 and 3). Interpretation of the 2D NMR spectra of **15** revealed that it shared the same 3′,5,7-trihydroxy-4′-methoxyisoflavone substructure with **14**.

However, H-1″ (δ_H 3.48, d) of the geranyl side chain in **15** showed HMBC correlations to C-5 (δ_C 159.6), C-6 (δ_C 109.6 and C-7 (δ_C 161.4), indicating that the geranyl side chain was attached at the C-6 position in **15**. Thus, **15** was identified as 6-geranyl-3′,5,7-trihydroxy-4′-methoxyisoflavone, an isomer of **14**.

Table 3. ^{1}H NMR data for compounds **13**−**16**.

Position	**13**[a]	**14**[b]	**15**[b]	**16**[a]
2	5.56, d (4.6)	7.91, s	7.84, s	7.97, s
3	5.19, d (4.6)			
5				8.10, d (8.7)
6	5.90, s	6.33, s		6.91, d (8.7)
8			6.39, s	
2′	7.40, m	7.09, d (2.0)	7.08, d (2.1)	7.12, d (2.2)
3′	7.38, m			
4′	7.38, m			
5′	7.38, m	6.93, d (8.3)	6.92, d (8.3)	6.92, d (7.8)
6′	7.40, m	7.07, dd (8.3, 2.0)	7.05, dd (8.3, 2.1)	7.12, dd (7.8, 2.2)
1″	3.41, d (7.2)	3.51, d (7.1)	3.48, d (7.1)	3.64, d (6.9)
2″	5.21, t (7.2)	5.25, d (7.1)	5.28, d (7.1)	5.29, t (6.9)
4″	2.06, m	2.07, m	2.09, m	2.09, m
5″	2.10, m	2.11, m	2.12, m	2.12, m
6″	5.03, t (6.6)	5.05, t (6.8)	5.05, t (6.6)	5.05, t (6.7)
8″	1.67, s	1.67, s	1.68, s	1.67, s
9″	1.58, s	1.59, s	1.60, s	1.59, s
10″	1.80, s	1.83, s	1.83, s	1.86, s
5-OH	12.02, s	12.86, s	13.28, s	
4′-OMe		3.93, s	3.93, s	3.92, s

[a]Recorded at 700 MHz in $CDCl_3$. [b]Recorded at 600 MHz in $CDCl_3$.

The molecular formula of **16** was deduced as $C_{26}H_{28}O_5$ by the pseudomolecular ion peak at *m/z* 421.2010 $[M+H]^+$ in the HRESIMS spectrum, missing one oxygen atom compared to **14**. The ^{1}H NMR data of **16** (Table 2) were comparable to those of **14** except for the replacement of the chelated hydroxy signal by an additional aromatic proton (δ_H 8.10, d, H-5), which exhibited COSY correlation with H-6 (δ_H 6.91, d) and HMBC correlations to C-4 (δ_C 175.9), C-7 (δ_C 158.8) and C-9 (δ_C 155.0). Taking these data into consideration, **16** was identified as the new 8-geranyl-

3′,7-dihydroxy-4′-methoxyisoflavone.

Compound **42** was obtained as a yellow amorphous solid. Based on the HRESIMS data, its molecular formula was determined to be $C_{22}H_{20}O_8$, missing one CH_2 unit compared to that of dalbinol (**41**).[26] Its UV spectrum showed typical absorption maxima of rotenoids at 212, 242 and 296 nm.[26] The NMR data of **42** (Table 4 and 5) were similar to those of **41** except for the presence of only one methoxy group (δ_C 56.9 and δ_H 3.64, respectively) in **42** rather than two methoxy groups in **41**. The proton at δ_H 6.63 showing HMBC correlation to C-12a (δ_C 68.6) was assigned to H-1, while the proton at δ_H 6.39 showing HMBC correlation to C-1a (δ_C 109.6) was assigned to H-4. In the ROESY spectrum of **42**, the methoxy protons exhibited NOE correlation with H-1, indicating the methoxy group to be attached at C-2 and subsequently a hydroxy group to be attached at C-3 in consideration of its molecular formula. Thus, **42** was elucidated as 3-demethyldalbinol. The relative configuration of **42** was suggested to be the same as that of **41** on the basis of their similar coupling constants and NOE correlations. Furthermore, on the basis of the very similar ECD spectra of **41** and **42**, the absolute configuration of **42** was determined to be identical to that of **41**.

The molecular formula of **43** was determined to be $C_{22}H_{18}O_7$ by its HRESIMS data, missing a H_2O unit compared to that of **42**. The oxygenated methylene CH_2-6 in **43** showed two doublet proton signals at δ_H 4.99 and 4.97 in contrast to two dd proton signals in **42**, suggesting C-6a to be a quaternary carbon. In addition, in the HMBC spectrum of **43**, H_2-6 exhibited correlations to C-4a (δ_C 146.6), C-6a (δ_C 156.0), and C-12a (δ_C 111.7), indicating a new double bond at C-6a/C-12a in **43**. Analysis of the 2D NMR spectra revealed that **43** shared the same substructure as **42** except for this C-6a/C-12a double bond. Considering the structural relationship between **43** and amorphigenin (**40**),[15] **43** was named 6a,12a-dehydro-3-demethylamorphigenin. Its absolute

configuration at C-5′ is suggested to be identical to that of **40**−**42** due to their close biosynthetic relationships.

Table 4. ^{13}C NMR data for compounds **42**−**46**.

Position	**42**[a]	**43**[b]	**44**[b]	**45**[c]	**46**[a]
1	111.8, CH	109.1, CH	110.2, CH	113.1, CH	75.3, CH
1a	109.6, C	110.2, C	104.5, C	86.7, C	94.6, C
2	143.1, C	141.6, C	143.7, C	152.4, C	192.1, C
3	149.3, C	145.7, C	149.3, C	186.5, C	164.1, C
4	104.7, CH	102.6, CH	100.8, CH	53.0, CH_2	110.2, CH
4a	149.9, C	146.8, C	147.2, C	198.5, C	190.6, C
6	64.5,CH_2	64.2, CH_2	66.1, CH_2	75.6, CH_2	74.3, CH_2
6a	77.1, CH	156.0, C	72.3, CH	81.7, CH	82.2, CH
7a	158.4, C	152.1, C	157.8, C	156.3, C	157.7, C
8	114.0, C	112.7, C	112.7, C	109.3, C	110.2, C
9	168.0, C	164.2, C	166.7, C	160.8, C	159.9, C
10	105.4, CH	108.2, CH	104.8, CH	112.2, CH	111.0, CH
11	130.2, CH	127.3, CH	129.9, CH	127.9, CH	127.6, CH
11a	113.6, C	112.7, C	113.4, C	113.7, C	116.8, C
12	191.6, C	174.2, C	188.7, C	185.9, C	189.5, C
12a	68.6, C	111.7, C	44.5, CH	56.2, CH	48.6, CH
4′	32.3, CH_2	31.3, CH_2	31.6, CH_2	115.3, CH	116.2, CH
5′	86.2, CH	85.0, CH	85.4, CH	129.5, CH	129.5, CH
6′	149.1, C	146.2, C	146.4, C	78.1, C	78.0, C
7′	110.5, CH_2	112.6, CH_2	112.5, CH_2	28.3, CH_3	28.4, CH_3
8′	62.3, CH_2	62.5, CH_2	62.8, CH_2	28.1, CH_3	28.1, CH_3
2-OMe	56.9, CH_3	55.9, CH_3	56.2, CH_3	55.3, CH_3	
3-OMe			55.7, CH_3		57.1, CH_3

[a]Recorded at 150 MHz in CD_3COCD_3. [b]Recorded at 175 MHz in $CDCl_3$. [c]Recorded at 75 MHz in $CDCl_3$.

Compound **44** shared the same gross structure as (6a*S*,12a*S*,5′*R*)-amorphigenin[15] (**40**) as confirmed by analysis of the HRESIMS and the 2D NMR data. Both compounds also had the same *cis*-configuration for H-6a and H-12a on the basis of the small value of $^3J_{6a,12a}$ (4.1 Hz). However, **44** exhibited almost a mirror image ECD spectrum compared to that of **40**.[27] Considering that the CD curves are mainly governed by the chirality of C-6a and C-12a, it is assumed that compounds **40** and **44** differ by their opposite absolute configurations at these positions. Thus, **44** was determined to be (6a*R*,12a*R*,5′*R*)-amorphigenin.

Table 5. ^{1}H NMR data for compounds **42**−**46**.

Position	**42**[a]	**43**[b]	**44**[b]	**45**[c]	**46**[a]
1	6.63, s	8.45, s	6.78, s	5.49, s	4.75, s
4	6.39, s	6.59, s	6.45, s	4.25, d (17.7)	6.21, s
				3.63, d (17.7)	
6	4.55, dd (12.2,	4.99, d (14.8)	4.61, dd (12.1,	4.67, d (10.6)	4.39, d (10.8)
	2.5)	4.97, d (14.8)	3.1)	4.30, dd (10.6,	3.82, dd (10.8,
	4.45, dd (12.2,		4.18, dd (12.1,	2.5)	3.2)
	1.1)		1.0)		
6a	4.68, dd (2.5,		4.94, ddd (4.1,	5.26, dd (4.5,	5.31, dd (6.4,
	1.1)		3.1, 1.0)	2.5)	3.2)
10	6.54, d (8.5)	6.94, d (8.6)	6.52, d (8.5)	6.52, d (8.7)	6.43, d (8.6)
11	7.77, d (8.5)	8.14, d (8.6)	7.85, d (8.5)	7.66, d (8.7)	7.57, d (8.6)
12a			3.86, d (4.1)	3.34, d (4.5)	4.31, d (6.4)
4′	3.31, dd (15.7,	3.60, dd (15.6,	3.37, dd (15.7,	6.66, d (10.1)	6.63, d (10.1)
	9.9)	9.9)	9.9)		
	3.04, dd (15.7,	3.34, dd (15.6,	3.09, dd (15.7,		
	8.3)	8.3)	8.3)		
5′	5.45, dd (9.9,	5.58, dd (9.9,	5.46, dd (9.9,	5.66, d (10.1)	5.72, d (10.1)
	8.3)	8.3)	8.3)		
7′	5.23, s	5.33, s	5.25, s	1.48, s	1.44, s
	5.17, s	5.32, s	5.23, s		
8′	4.21, d (14.6)	4.33, d (13.6)	4.25, d (13.6)	1.45, s	1.42, s
	4.17, d (14.6)	4.30, d (13.6)	4.21, d (13.6)		
2-OMe	3.64, s	3.96, s	3.77, s	3.27, s	
3-OMe			3.81, s		3.90, s

[a]Recorded at 600 MHz in CD_3COCD_3. [b]Recorded at 700 MHz in $CDCl_3$. [c]Recorded at 300 MHz in $CDCl_3$

Compound **45** was obtained as a yellow amorphous solid. Its HRESIMS spectrum revealed a pseudomolecular ion peak at *m/z* 397.1281 $[M+H]^+$ corresponding to the molecular formula $C_{22}H_{20}O_7$. The NMR data of **45** (Table 4 and 5) resembled those of amorphispironone[9] (**47**) except for the disappearance of a double bond and a methoxy group and the presence of additional methylene (δ_C 53.0, δ_H 4.25 and 3.63, CH_2-4) and carbonyl group (δ_C 186.5, C-3) instead in **45**. The HMBC correlations from H-12a (δ_H 3.34) to C-1 (δ_C 113.1) and C-4a (δ_C 198.5) of **45** indicated an aromatic methine and a carbonyl group at C-1 and C-4a, respectively.

The presence of the C-1/C-2 double bond and a methoxy group attached at C-2 position were confirmed by the HMBC correlation from the protons of the methoxy group (δ_H 3.27) to C-2 (δ_C 152.4) as well as by the NOE relationship between the protons of the methoxy group and H-1 (δ_H 5.49). Furthermore, the HMBC correlations from H-1 to C-3, and from H_2-4 to C-1 and C-3 indicated that the additional methylene and carbonyl group of **45** were present at C-4 and C-3 positions, respectively. Detailed analysis of the 2D NMR spectra revealed that **45** shared the same substructure with **47** regarding to rings B−E. Thus, **45** was identified as a new amorphispironone derivative, and was given the name amorphispironone B. Based on the similar coupling constants and NOE relationships, compound **45** is expected to share the same relative configuration with **47**. For the configurational assignment of **45**, the same solution TDDFT-ECD calculation protocol (Figure 2) was carried out on (1a*R*,6a*S*,12a*R*)-**45** as on **11**. Reoptimization of the initial 12 MMFF conformers yielded 5 and 1 low-energy conformers at B3LYP/6-31G(d) *in vacuo* and B97D/TZVP (PCM/MeCN) level, respectively. While solvent model calculations usually result in similar or a larger number of low-energy conformers than the gas-phase ones,[23,28,29] **45** represented an interesting counter-example where all minor conformers had negligible contributions in the solvent model calculation. Although solvent model ECD spectra computed for the single B97D/TZVP (PCM/MeCN) conformer also allowed the assignment of the absolute configuration as (1a*R*,6a*S*,12a*R*), the *in vacuo* ECD calculations computed for the B3LYP/6-31G(d) *in vacuo* conformers gave a far better overall agreement indicating that the minor conformers were better estimated and they cannot be neglected. The ECD study of **11** and **45** supports the idea that there is no superior single method for ECD calculations and the experimental ECD spectra could be reproduced best by different functionals, basis sets and solvent models as also indicated previously in the literature.[23,30]

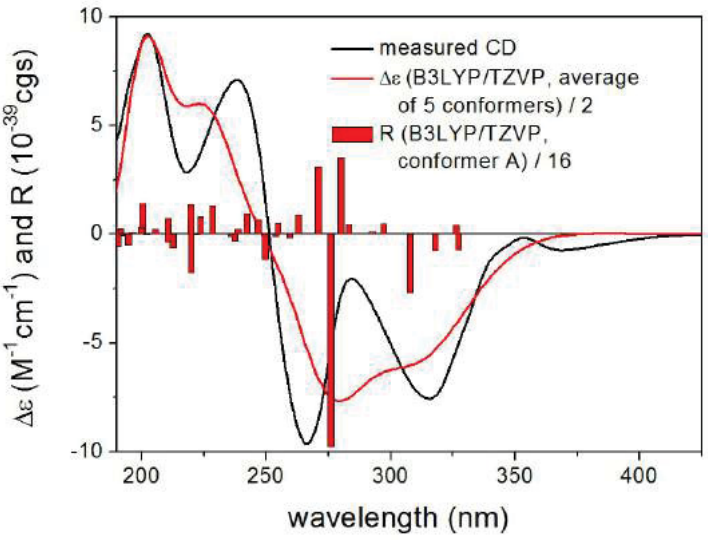

Figure 2. Experimental ECD spectrum of **45** in MeCN compared with the Boltzmann-weighted B3LYP/TZVP ECD spectrum of (1a*R*,6a*S*,12a*R*)-**45** computed for the B3LYP/6-31G(d) *in vacuo* conformers. Bars represent the rotational strength of the lowest-energy conformer.

The molecular formula of amorphispironone C (**46**) was established as $C_{22}H_{20}O_8$, containing an additional oxygen atom compared to **45**. Comparison of their NMR data (Table 4 and 5) indicated that the methylene group (CH_2-4) in **45** was replaced by an oxygenated methine (δ_C 75.3, δ_H 4.75, CH-1) in **46**. Analysis of the 2D NMR spectra of **46** disclosed that it shared the same amorphispironone substructure with **45** except for the substituent in ring A. In the HMBC spectrum of **46**, H-12a (δ_H 4.31) exhibited correlations to C-1 and C-4a (δ_C 190.6), suggesting a hydroxy and a carbonyl group to be located at C-1 and C-4a positions, respectively. The HMBC correlations from the singlet olefinic proton at δ_H 6.21 (H-4) to C-1a (δ_C 94.6) and C-3 (δ_C 164.1), and from protons of the methoxy group at δ_H 3.90 to C-3 as well as the NOE relationship between H-4 and protons of the methoxy group indicated a double bond at C-3/C-4 with a methoxy group linked to C-3. In addition, both H-1 and H-4 showed HMBC correlations to C-2 (δ_C 192.1), revealing the presence of an additinal carbonyl group at the C-2 position. The

absolute configuration at C-1a, C-6a, and C-12a of **46** was proposed to be the same as **45** considering their similar coupling constants and NOE correlations as well as their close biogenetic relationship. Thus, the NOE cross peak between H-1 and H-12a of **46** suggested the 1*R* configuration and the structure of amorphispironone C (**46**) was elucidated as shown. The ECD spectra of **45**–**48** showed similar pattern, two intense negative Cotton effects (CEs) above 270 nm and a positive CE around 240 nm, which suggested that they have identical absolute configuration at C-6a, C-12a and C-1a.

Compound **51** was obtained as a yellow amorphous solid and its UV spectrum suggested it to be a kaempferol derivative with maximum absorbances at 266 and 348 nm.[31] The HRESIMS spectrum exhibited a pseudomolecular ion peak at *m/z* 741.2237 $[M+H]^+$ which established the molecular formula $C_{33}H_{40}O_{19}$. Further analysis of ESIMS spectrum displayed fragment peaks at *m/z* 579 $[M+H-162]^+$, 417 $[M+H-162-162]^+$ and 271 $[M+H-162-162-146]^+$, suggesting the presence of two hexoses and one deoxyhexose residues in the molecule. The ^1H NMR spectrum (Table 6) showed signals for a 1,4-disubstituted benzene ring at δ_H 8.10 (d, J = 8.8 Hz, H-2′ and 6′) and 6.93 (d, J = 8.8 Hz, H-3′ and 5′), a 1,2,4-trisubstituted benzene ring at δ_H 8.10 (d, J = 8.8 Hz, H-5), 7.16 (dd, J = 8.8, 2.1 Hz, H-6) and 7.33 (d, J = 2.1 Hz, H-8), three anomeric protons at δ_H 5.64 (d, J = 1.8 Hz, H-1‴), 5.47 (d, J = 7.6 Hz, H-1″) and 4.76 (d, J = 7.8 Hz, H-1‴), indicating the presence of resokaempferol as aglycone and three sugar residues. Combining the TOCSY and HSQC spectra, three sugar units were recognized and their chemical shifts and coupling constants were in good agreement with two units of glucopyranose and one unit of rhamnopyranose, which was confirmed by HPLC analysis of the acid hydrolysis products of **51** in comparison to known standards. The J values of the anomeric protons of the glucopyranose (7.6 or 7.8 Hz) and rhamnopyranose (1.8 Hz) were in accordance with those of *β*-D-

glucopyranose and *α*-L-rhamnopyranose, respectively. The HMBC correlations from anomeric proton H-1″ to C-3 (δ_C 136.6), and from H-1‴ to C-2″ (δ_C 82.3) confirmed that a *β*-D-glucopyranosyl-(1→2)-*β*-D-glucopyranosidic fragment was linked to the 3-hydroxy group of resokaempferol. In addition, the anomeric proton H-1⁗ showed HMBC correlation to C-7 (δ_C 162.0), indicating the *α*-L-rhamnopyranose to be linked to the 7-hydroxy group of resokaempferol. Thus, the structure of **51** was identified as resokaempferol 3-*O*-*β*-D-glucopyranosyl-(1→2)-*β*-D-glucopyranoside-7-*O*-*α*-L-rhamnopyranoside.

The UV spectrum of compound **52** exhibited almost identical absorbances to the isoflavone daidzein (**17**).[32] Its molecular formula was determined as $C_{27}H_{30}O_{14}$ based on the HRESIMS data. The positive and negative ESIMS spectra displayed fragment peaks at *m/z* 255 $[M+H-324]^+$ and 253 $[M-H-324]^-$, respectively, corresponding to the loss of two hexoses. The ^{1}H NMR spectrum showed signals characteristic for daidzein including an *ortho*-coupled A_2B_2 aromatic spin system at δ_H 7.39 (d, J = 8.6 Hz, H-2′ and 6′) and 6.85 (d, J = 8.6 Hz, H-3′ and 5′), an ABX aromatic spin system at δ_H 8.15 (d, J = 8.9 Hz, H-5), 7.24 (dd, J =8.9, 2.3 Hz, H-6) and 7.27 (d, J = 2.3 Hz, H-8), and an olefinic proton at δ_H 8.21 (s, H-2). In addition, two anomeric protons at δ_H 5.31 (d, J = 7.4 Hz, H-1″) and 4.69 (d, J = 7.9 Hz, H-1‴) as well as twelve additional protons between δ_H 3 and 4 were observed due to the presence of two hexose units, which were further identified as two glucoses by HPLC analysis of the acid hydrolysis products of **52**. The coupling constants of the anomeric protons of the glucoses were in accordance with that of the *β*-D anomer. In the HMBC spectrum, the two anomeric protons H-1″ and H-1‴ showed correlations to C-7 (δ_C 163.0) and C-2″ (δ_C 83.3), respectively, indicating that the inner *β*-D-glucopyranosyl moiety was attached to C-7 of the daidzein aglycone and that the second *β*-D-glucopyranosyl residue and the inner one were 1,2-linked. Taking these data into consideration, **52** was elucidated as daidzein 7-

O-*β*-D-glucopyranosyl-(1→2)-*β*-D-glucopyranoside.

Table 6. ^{1}H and ^{13}C NMR data for compounds **51** and **52**.

Position	**51**[a]		**52**[b]	
	δ_C, type	δ_H (*J* in Hz)	δ_C, type	δ_H (*J* in Hz)
2	158.9, C		154.8, C	8.21, s
3	136.6, C		126.0, C	
4	175.8, C		177.8, C	
5	127.6, CH	8.10, d (8.8)	128.0, CH	8.15, d (8.9)
6	116.4, CH	7.16, dd (8.8, 2.1)	116.7, CH	7.24, dd (8.9, 2.3)
7	162.0, C		163.0,C	
8	104.1, CH	7.33, d (2.1)	104.7, CH	7.27, d (2.3)
9	157.8, C		158.8, C	
10	119.3, C		119.9, C	
1′	122.7, C		123.7, C	
2′, 6′	132.2, CH	8.10, d (8.8)	131.2, CH	7.39, d (8.6)
3′, 5′	116.0, CH	6.93, d (8.8)	116.0, CH	6.85, d (8.6)
4′	161.2, CH		158.5, CH	
1″	100.7, CH	5.47, d (7.6)	100.1, CH	5.31, d (7.4)
2″	82.3, CH	3.76, dd (9.0, 7.6)	83.3, CH	3.77, dd (9.0, 7.4)
3″	77.7, CH	3.60, dd (9.0, 8.7)	77.3, CH	3.72, dd (9.0, 8.8)
4″	71.0, CH	3.36, m	70.7, CH	3.47, dd (9.8, 8.8)
5″	78.0, CH	3.17, m	78.0, CH	3.56, ddd (9.8, 5.8, 2.3)
6″	62.1, CH_2	3.66, m	61.9, CH	3.93, dd (12.2, 2.3)
		3.48, m		3.72, dd (12.2, 5.8)
1‴	104.5, CH	4.76, d (7.8)	105.3, CH	4.69, d (7.9)
2‴	75.3, CH	3.35, m	75.8, CH	3.24, dd (9.0, 7.9)
3‴	77.6, CH	3.39, dd (9.1, 7.6)	77.5, CH	3.41, t (9.0)
4‴	71.0, CH	3.36, m	70.9, CH	3.35, dd (9.6, 9.0)
5‴	77.9, CH	3.29, m	77.7, CH	3.27, ddd (9.6, 4.5, 2.4)
6‴	62.5, CH_2	3.78, dd (11.9, 2.7)	61.7, CH_2	3.61, dd (11.8, 4.5)
		3.68, dd (11.9, 5.0)		3.52, dd (11.8, 2.4)
1⁗	99.7, CH	5.64, d (1.8)		
2⁗	71.4, CH	4.06, dd (3.3, 1.8)		
3⁗	71.9, CH	3.86, dd (9.3, 3.3)		
4⁗	73.3, CH	3.50, t (9.3)		
5⁗	71.0, CH	3.60, dq (9.3, 6.2)		
6⁗	17.8, CH_3	1.25, d (6.2)		

[a]Recorded at 700 MHz for ^{1}H and 175 MHz for ^{13}C in CD_3OD.
[b]Recorded at 600 MHz for ^{1}H and 150 MHz for ^{13}C in CD_3OD.

The remaining known compounds were identified as 2-[(*E*)-styryl]-5-geranyl-resorcin-1-

carboxylic acid (**4**),[17] amorfrutin B (**5**),[4] 2-carboxy-3,5-dihydroxy-4-geranylbibenzyl (**6**),[1] 2-geranyl-5-[(*Z*)-styryl]-resorcin (**7**),[33] amorphastilbol (**8**),[34] 2-geranyl-5-(2-phenylethyl)-resorcin (**9**),[35] amorfrutin A (**10**),[4] xanthoangelol (**12**),[36] daidzein (**17**),[32] 5,7-dihydroxy-4'-methoxyisoflavone (**18**),[37] 5-hydroxy-4',7-dimethoxyisoflavone (**19**),[38] afrormorsin (**20**),[39] 7-hydroxy-2',4',5'-trimethoxyisoflavone (**21**),[40] 7,2',4',5'-tetramethoxyisoflavone (**22**),[41] munduserone (**23**),[42] *cis*-12a-hydroxymunduserone (**24**),[42] sermundone (**25**),[43] 6-deoxyclitoriacetal (**26**),[44] rot-2'-enonic acid (**27**),[45] *cis*-12a-hydroxyrot-2'-enonic acid (**28**),[45] sumatrolic acid (**29**),[46] deguelin (**30**),[42] tephrosin (**31**),[47] α-toxicarol (**32**),[47] 11-hydroxytephrosin (**33**),[47] 6a,12a-dehydrodeguelin (**34**),[48] dalpanol (**35**),[49] 12a-hydroxydalpanol (**36**),[15] rotenone (**37**),[50] rotenolone (**38**),[51] 11-hydroxyrotenone (**39**),[52] amorphigenin (**40**),[15] dalbinol (**41**),[26] amorphispironone (**47**),[9] 11-hydroxyamorphispironone (**48**),[1] licoagroside F (**49**),[53] kaempferol 3-*O*-α-L-rhamnopyranosyl-(1→2)-β-D-glucopyranoside-7-*O*-α-L-rhamnopyranoside (**50**),[31] 6'-*O*-β-D-glucopyranosyldalpanol (**53**),[15] and 6'-*O*-β-D-glucopyranosyl-12a-hydroxydalpanol (**54**)[2] by comparison with the literature data.

All isolated compounds were evaluated for their antimicrobial activity against a set of humanpathogenic gram-positive bacteria. Among them, the geranylated bibenzyl derivatives **4**, **5**, **8**, **9** and the likewise geranylated chalcone **12** showed significant antibacterial activity with MIC values ranging from 3.1 to 25 μM, while compounds **1**, **6**, **7**, **10**, **13**–**15** displayed moderate activity with MIC values ranging from 25 to 100 μM (Table 7). Compounds **5**, **8**–**10** and **12** were previously reported for their antibacterial activity against *S. aureus* ATCC13709[4,54] and ATCC25923,[55] two standard laboratory strains of *S. aureus*. However, their antibacterial activity against the methycilin-resistant strain *S. aureus* ATCC700699, vancomycin-resistant strains *E. faecalis* ATCC51299 and *E. faecium* ATCC700221 as well as against two standard laboratory

strains *E. faecalis* ATCC29212 and *E. faecium* ATCC35667 are reported for the first time in this study. Compound **5** (MIC value of 6.3 μM against vancomycin-resistant strain *E. faecium* ATCC700221), **8** (MIC values of 3.1 and 6.3 μM against methicillin-resistant *S. aureus* strain ATCC700699 and vancomycin-resistant *E. faecium* strain ATCC700221, respectively) and **12** (MIC values of 3.1 against both methicillin-resistant *S. aureus* strain ATCC700699 and vancomycin-resistant *E. faecium* strain ATCC700221) were similar with regard to their antibiotic activity to the positive control moxifloxacin. However, none of the isolated compounds exhibited activity against *Mycobacterium tuberculosis* or against the gram-negative bacterium *Acinetobacter baumannii* ATCCBAA1605 (MIC > 50 μM).

Table 7. Antimicrobial (MIC, μM) and cytotoxic activities (IC_{50}, μM).

compound	*S. aureus*		*E. faecalis*		*E. faecium*		MRC-5	THP-1
	ATCC 25923	ATCC 700699	ATCC 29212	ATCC 51299	ATCC 35667	ATCC 700221		
1	50	100	50	100	50	100	100	100
4	12.5	12.5	25	25	25	25	100	100
5	12.5	12.5	6.3	6.3	6.3	6.3	100	100
6	100	100	100	100	100	100	100	100
7	100	100	100	100	100	100	100	100
8	6.3	3.1	12.5	6.3	6.3	6.3	50	25
8a[a]	>100	>100	>100	>100	100	>100	100	100
9	25	6.3	25	12.5	12.5	12.5	-	50
10	50	6.3	100	25	50	25	-	50
12	25	3.1	12.5	6.3	12.5	3.1	25	25
13	100	100	50	100	100	100	100	100
14	100	100	50	100	25	25	50	50
15	100	100	25	50	25	12.5	50	50
Moxifloxacin[b]	<0.9	3.8	0.9	0.9	1.9	7.8	-	-

[a] **8a** was dimethoxy product of **8**. [b] positive control.

All antibacterially active compounds (Table 7) were further tested for their cytotoxicity against eukaryotic cells using the human lung fibroblast MRC-5 cell line and the human monocytic THP-1 cell line as models. The IC_{50} values of **4** and **5** were 100 μM against MRC-5 and THP-1 cells for both compounds indicating a high degree of selectivity for the antibacterial vs. cytotoxic activity which makes these two compounds interesting candidates for further

studies on the molecular targets and models of action underlying the antibiotic activity. For compounds **8** and **12**, the IC_{50} values against the two eukaryotic cell lines varied from 25 to 50 μM.

A preliminary structure-activity relationship for the antibacterial activity of the geranylated bibenzyl derivatives is proposed. The chain length of the isoprenoid derived side chain seems to be important for antibacterial activity against *E. faecalis* and *E. faecium* strains since compound **10**, which differs from **5** only by an isoprene vs. a geranyl side chain was largely inactive whereas **5** showed strong antibiotic activity. Presence of a double bond at the C-1/C-2 position of the analyzed bibenzyl derivatives is not essential as indicated by the strong antibiotic activity of the hydrogenated compound **5** and **9**. Compounds with an *E*-configurated double bond at the C-1/C-2 position such as **4** and **8** are more active than the corresponding Z isomers as exemplified by comparison of **1** and **7**. Addition of an oxo function to the central chain linking the aromatic rings of bibenzyl derivatives as present in compound **12** has no significant effect on the antibiotic activity in comparison to **8**. Presence of a carboxylic group at C-1 of one of the aromatic rings is not required for activity as shown by comparison of **4** vs. **8**, which is corroborating earlier results by Mitscher *et al.*[4] Methylation of phenolic OH groups like for compound **5** increases its antibiotic activity compared to the demethylated derivative **6**.

In addition to studying the antibiotic activity, all compounds isolated in this study were subjected to a MTT assay using the mouse lymphoma cell line L5178Y as a model for evaluating cytotoxicity (Table 8).[56–57] As expected from the results of the cytotoxicity counter screen carried out for the bibenzyl derivatives (**1**−**10**), none of these latter metabolites showed activity against the mouse lymphoma cell thus corroborating the results obtained with the MRC-5 and THP-1 cell lines. From all compounds analyzed only rotenoid derivatives were active against the

L5178Y cell line, which is in agreement with previous reports on the cytotoxicity of rotenoids against human cell lines such as MDB-MB-231[58] and MCF-7[12] human breast cancer cell lines, HCT-116 human colon cancer cell line[12] and HEL299 human lung normal cell lines.[2]

Table 8. Cytotoxicity against the mouse lymphoma cell line L5178Y.

compound	IC_{50} (μM)
25	0.2
27	0.6
30	0.2
32	0.2
34	10.2
35	0.7
37	0.3
41	0.2
45	7.6
48	1.3
53	1.7
Kahalalide F[a]	4.3

[a] positive control.

The strongest cytotoxic activity was observed in this study for compounds **25**, **27**, **30**, **32**, **35**, **37**, **41**, **48** and **53** which exhibited IC_{50} values ranging from 0.2 to 1.7 μM, respectively. These compounds were more potent than the positive control kahalalide F. 12a-H substituted rotenoids seem to be more active than corresponding 12a-OH substituted derivatives by comparison of **25** vs **26**, **27** vs **28**, **30** vs **31**, **32** vs **33**, **35** vs **36**, **37** vs **38**, and **53** vs **54**. The presence of a double bond at the C-6a/C-12a (**34** vs **30**) decreased activity while the loss of methoxy group (**42** vs **41**) led to total loss of cytotoxicity. Spirorotenoid compounds **47** and **48** were less active compared to their corresponding biosynthetic precursors **30** and **32**. In addition, the rotenoid glycoside **53** was less cytotoxic compared to its aglycone **35**.

In summary, bioactivity-guided isolation of fruits of *A. fruticosa* gave 54 phenolic metabolites including eleven bibenzyl compounds (**1**–**11**), two chalcone derivatives (**12** and **49**), three flavonoids (**13**, **50**–**51**), ten isoflavonoids (**14**–**22**, **52**) and twenty-eight rotenoids (**23**–**48**,

53–**54**), of which fourteen were new compounds. Several geranylated bibenzyl compounds, especially **4**, **5**, **8**, **9** and **12** exhibited significant antibacterial activity. Rotenoids and their derivatives, being present as dominant substances in the crude extract of fruits from *A. fruticosa*, displayed significant cytotoxicity against the L5178Y mouse lymphoma cell line. This study revealed the presence of numerous additional new and known phenolic metabolites in fruits of *A. fruticosa* compared to previous reports and provided several potential antibacterial and cytotoxic substances.

EXPERIMENTAL SECTION

General Experimental Procedures

NMR experiments were carried out on a Bruker 300, Bruker Avance III 600 or Bruker Biospin 700 spectrometers, while chemical shifts were given in δ (ppm) referring to the solvent peaks at δ_H 7.26 and δ_C 77.0 for $CDCl_3$, δ_H 3.31 and δ_C 49.0 for CD_3OD, δ_H 2.05 and δ_C 29.8 for CD_3COCD_3. ESI mass spectra were acquired from a LC-MS HP1100 Agilent Finnigan LCQ Deca XP Thermoquestman spectrometer and HRESIMS spectra were recorded on a UHR-QTOF maXis mass 4G spectrometer. ECD spectroscopy was conducted using JASCO J-810 CD spectropolarimeter. JASCO P-2000 polarimeter was used for measuring optical rotations. UV/Vis Spectrofometer (Perkin Elmer Instruments) was utilized to obtain UV absorbance spectra. HPLC analysis was carried out using a Dionex P580 system connected to a photodiode array detector (UVD340s) and the separation column (125 ×4 mm) was prefilled with Eurospher 10 C_{18} (Knauer, Germany). Semi-preparative RP-HPLC purification was achieved by a HPLC Lachrom-Merck Hitachi system (Pump L7100 and UV detector L7400) with an Eurospher 100-10 C_{18} (300 × 8 mm) column. Open column chromatography was applied for fractionation using Merck MN Silica gel 60 M (0.04-0.063 mm), Sephadex LH-20 (Sigma-Aldrich), Diaon HP-20

(Merck), or LiChroprep Diol (40-63 μm, Merck) as stationary phase. Thin Layer Chromatography (TLC) was used for monitoring and accomplished on pre-coated silica gel 60 F_{254} plates (Macherey-Nagel GmBH, Germany) with detection at 254 and 365 nm. Distillated solvents were used during isolation and spectral grade solvents were employed for spectroscopic measurements.

Plant Material

Air dried fruits of *A. fruticosa* used in this study were purchased from Friedrich Nature Discovery Company, Euskirchen, Germany. A voucher specimen was deposited at the Institute of Pharmaceutical Biology and Biotechnology, Heinrich-Heine University Duesseldorf, Germany.

Extraction and Isolation

The dry fruits of *A. fruticosa* (500 g) were powdered and extracted three times with dichloromethane (DCM) – methanol (MeOH) (1:1) at room temperature for 24 h each. The solution was dried in vacuo to yield 72.5 g of pale yellow crude extract, 55 g of which was subjected initially to silica gel vacuum liquid chromatography (VLC), eluting with *n*-hexane, ethyl acetate (EtOAc), DCM, and MeOH in order of polarity to afford 25 fractions. All fractions were tested for their anti-tuberculosis and antibacterial activity. A growth inhibition against gram-positive bacteria was exhibited by fractions 11, 12, and 14-19 whereas none of the analyzed fractions showed growth inhibition towards *M. tuberculosis* or against gram-negative *A. baumannii* ATCCBAA1605.

Fraction 11 (1.8 g) was fractionated using a Sephadex LH-20 column with MeOH as eluent to give nine subfractions (11-1 to 11-9). Subfractions 11-3 (96 mg) and 11-8 (74 mg) were further subjected to a Sephadex LH-20 column using acetone as mobile phase followed by

purification using semi-preparative HPLC (gradient MeOH-H_20, 50:50 to 100:0) to yield **19** (2.0 mg) and **3** (2.8 mg), respectively.

Fraction 12 (1.3 g) was subjected to a Sephadex LH-20 column using MeOH as mobile phase to afford eight subfractions (12-1 to 12-8). Subfraction 12-2 (21.8 mg) was purified by semi-preparative HPLC (gradient MeOH-H_2O, 50:50 to 100:0) to give **2** (0.3 mg).

Fraction 13 (370 mg) was subjected to a LiChroprep Diol column eluting with DCM to afford four subfractions (13-1 to 13-4). Subfraction 13-1 (194.0 mg) was fractionated over a Sephadex LH-20 column using DCM-MeOH (1:1) as eluent, followed by purification with semi-preparative HPLC to yield **25** (1.0 mg), **30** (2.0 mg), and **32** (3.0 mg). Following the similar procedures, **10** (3.0 mg), **29** (0.5 mg) and **28** (1.0 mg) were obtained from subfraction 13-2, while **5** (21.0 mg), **9** (0.5 mg), **14** (2.0 mg) and **18** (1.0 mg) were isolated from subfraction 13-3 (41 mg).

Fraction 14 (330 mg) was chromatographed over a LiChroprep Diol column using DCM to yield nine subfractions (14-1 to 14-9). Subfraction 14-2 (59 mg) was purified by semi-preparative HPLC to yield **34** (0.5 mg), **37** (2.0 mg), and **39** (0.8 mg). Further purification of subfraction 14-**7** (24.0 mg) with semi-preparative HPLC gave **5** (14.0 mg), **15** (2.0 mg), and **27** (0.5 mg).

Fraction 15 (600 mg) was subjected to a Sephadex LH-20 column eluting with DCM-MeOH (1:1) to give nine subfractions (15-1 to 15-9). Subfraction 15-4 (95.6 mg) was further separated by a silica gel column with DCM-MeOH (99:1) as mobile phase, followed by purification using semi-preparative HPLC (gradient MeOH-H_2O, 50:50 to 100:0) to afford **26** (0.7 mg), **24** (0.9 mg), **23** (1.3 mg), **38** (3.1 mg), **31** (10.4 mg), and **33** (4.8 mg). Separation of subfraction 15-6 (142.5 mg) by a Sephadex LH-20 column using DCM-MeOH (1:1), followed

by a silica gel column using *n*-hexane-EtOAc (6:4) gave **12** (42.5 mg) and **6** (4.8 mg).

Fraction 17 (800 mg) was separated by a Sephadex LH-20 column using acetone as eluent to afford sixteen subfractions (17-1 to 17-16), among which subfraction 17-13 was a pure compound **17** (1.0 mg). Subfraction 17-4 (112.9 mg) was further purified by a Sephadex LH-20 column with acetone to give **48** (41.0 mg). Subfraction 17-8 (35.4 mg) was purified with semi-preparative HPLC (gradient MeOH-H_2O, 60:40 to 100:0) to yield **16** (0.5 mg) and **4** (11.4 mg).

Fraction 18 and 19 (3 g) were combined and chromatographed by silica vacuum liquid chromatography (VLC) using *n*-hexane, EtOAc, DCM, and MeOH by increasing the polarity of eluting solvents, to afford seventeen subfractions (18-1 to 18-17). After purification by semi-preparative HPLC with a gradient of MeOH-H_2O (50:50 to 100:0) as eluent system, **7** (0.6 mg) and **8** (17.0 mg) were obtained from subfraction 18-3 (32.8 mg), while **13** (0.6 mg), **1** (2.7 mg), and **4** (17.3 mg) were isolated from subfraction 18-4 (53.8 mg). Subfraction 18-6 (559 mg) was subjected to a LiChroprep Diol column using *n*-hexane-acetone (80:20, 60:40, 20:80, 0:100), followed by purification with semi-preparative HPLC (gradient MeOH-H_2O 50:50 to 100:0) to give **20** (0.6 mg) and **35** (14.6 mg). Subfraction 18-7 (1.3 g) was separated by a silica gel column using a gradient of *n*-hexane-acetone (6:1 to 0:100), followed by purification with semi-preparative HPLC using MeOH-H_2O (40:60 to 100:0) to afford **36** (1.9 mg), **40** (1.0 mg), and **11** (3.4 mg). Subfraction 18-8 (251 mg) was fractionated by a Sephadex LH-20 column with acetone to give 12 subfractions (18-8-1 to 18-8-12). Semi-preparative HPLC using MeOH-H_2O (50:50 to 100:0) was applied for further purification. **47** (0.6 mg), **45** (24.6 mg), and **22** (0.5 mg) were obtained from subfraction 18-8-6 (36.9 mg); **46** (0.6 mg) was purified from subfraction 18-8-8 (28.8 mg); **41** (4.9 mg) and **44** (0.6 mg) were isolated form subfraction 18-8-10 (31.9 mg); **42** (1.1 mg), **21** (0.4 mg) and **43** (2.4 mg) were obtained from subfraction 1819-8-12 (17 mg).

Fraction 24 (6 g) was fractionated by a Diaion HP-20 column using a gradient of MeOH-H_2O (0:100, 20:80, 40:60, 80:20, 100:0) to give 12 subfractions (24-1 to 24-12). Subfraction 24-7 (425.6 mg) was subjected to a Sephadex LH-20 column with MeOH to give 9 subfractions (24-7-1 to 24-7-9). Subfraction 24-7-4 (27.0 mg) was purified by semi-preparative HPLC using MeOH-H_2O (gradient 30:70 to 100:0) to yield **51** (1.2 mg) and **50** (11.6 mg), while subfraction 24-7-7 (24.1 mg) was purified by semi-preparative HPLC with MeOH-H_2O (gradient 40:60 to 100:0) to afford **52** (2.8 mg) and **49** (2.0 mg). Subfraction 24-11 (23.3 mg) was purified by semi-preparative HPLC using MeOH-H_2O (gradient 40:60 to 100:0) to give **54** (2.9 mg) and **53** (1.3 mg).

2-[(*Z*)-Styryl]-5-geranyl-resorcin-1-carboxylic acid (1): yellow amorphous solid; UV (MeOH) λ_{max} (log ε) 224 (2.89), 301 (2.46) nm; ^{1}H and ^{13}C NMR, see Table 1; HRESIMS *m/z* 393.2059 $[M+H]^+$ (calc. for $C_{25}H_{29}O_4$, 393.2060).

Amorfrutin D (2): white amorphous solid; UV (MeOH) λ_{max} (log ε) 222 (3.34), 269 (2.94), 309 (1.96) nm; $[\alpha]_D^{22}$ –24 (*c* 0.10, MeOH); ^{1}H and ^{13}C NMR, see Table 1; HRESIMS *m/z* 425.2319 $[M+H]^+$ (calc. for $C_{26}H_{33}O_5$, 425.2323).

Demethoxyamorfrutin D (3): white amorphous solid; UV (MeOH) λ_{max} (log ε) 230 (3.34), 266 (2.94), 304 (1.96) nm; $[\alpha]_D^{22}$ –16 (*c* 0.14, MeOH); ^{1}H and ^{13}C NMR, see Table 1; HRESIMS *m/z* 411.2164 $[M+H]^+$ (calc. for $C_{25}H_{31}O_5$, 411.2166).

(+)-Puerol A (11): white amorphous solid; UV (MeOH)) λ_{max} (log ε) 287 (2.74), 326 (2.84) nm; $[\alpha]_D^{21}$ +32 (*c* 0.18, MeOH); ECD {MeCN, λ [nm] (Δε), $c = 2.52\times10^{-4}$ M}: 312 (3.75), 283 (6.14), 248 (–3.27), 230 (1.30), 202 (–4.34); ^{1}H and ^{13}C NMR were identical with those previously published[19,20]; ESIMS *m/z* 299 $[M+H]^+$.

8-Geranyl-3,5,7-trihydroxyflavanone (13): yellow amorphous solid; UV (MeOH) λ_{max}

(log ε) 219 (4.53), 263 (4.05), 293 (3.73) nm; $[\alpha]_D^{21}$ –5 (*c* 0.18, MeOH); ^{1}H and ^{13}C NMR, see Table 2 and 3; HRESIMS *m/z* 409.2011 $[M+H]^+$ (calc. for $C_{25}H_{29}O_5$, 409.2010).

8-Geranyl-3′,5,7-trihydroxy-4′-methoxyisoflavone (14): yellow amorphous solid; UV (MeOH) λ_{max} (log ε) 213 (3.69), 268 (3.53) nm; ^{1}H and ^{13}C NMR, see Table 2 and 3; HRESIMS *m/z* 437.1961 $[M+H]^+$ (calcd. for $C_{26}H_{29}O_6$, 437.1959).

6-Geranyl-3′,5,7-trihydroxy-4′-methoxyisoflavone (15): yellow amorphous solid; UV (MeOH) λ_{max} (log ε) 206 (3.67), 267 (3.58) nm; ^{1}H and ^{13}C NMR, see Table 2 and 3; HRESIMS *m/z* 437.1966 $[M+H]^+$ (calc. for $C_{26}H_{29}O_6$, 437. 1959).

8-Geranyl-3′,7-dihydroxy-4′-methoxyisoflavone (16): yellow amorphous solid; UV (MeOH) λ_{max} (log ε) 251 (3.73), 292 (3.35) nm; ^{1}H and ^{13}C NMR, see Table 2 and 3; HRESIMS *m/z* 421.2010 $[M+H]^+$ (calc. for $C_{26}H_{29}O_5$, 421.2010).

3-Demethyldalbinol (42): yellow amorphous solid; UV (MeOH) λ_{max} (log ε) 212 (2.86), 242 (2.74), 296 (2.65) nm; $[\alpha]_D^{20}$ –105 (*c* 0.11, MeOH); ECD {MeCN, λ [nm] (Δε), *c* = 1.82×10^{-4} M}: 324 (–4.48), 277 (–2.62), 243 (5.36), 221sh (–8.27), 205 (–15.70), negative below 198 nm; ^{1}H and ^{13}C NMR, see Table 4 and 5; HRESIMS *m/z* 413.1227 $[M+H]^+$ (calc. for $C_{22}H_{21}O_8$, 413.1231).

6a,12a-Dehydro-3-demethylamorphigenin (43): yellow amorphous solid; UV (MeOH) λ_{max} (log ε) 232 (3.86), 280 (3.74), 341 (3.65) nm; $[\alpha]_D^{21}$ –17 (*c* 0.19, MeOH); ECD {MeCN, λ [nm] (Δε), *c* = 1.90×10^{-4} M}: 302sh (–0.82), 279 (–1.26), 249 (0.06), 235 (–0.71), 215 (0.28), 197 (–1.60); ^{1}H and ^{13}C NMR, see Table 4 and 5; HRESIMS *m/z* 395.1128 $[M+H]^+$ (calc. for $C_{22}H_{19}O_7$, 395.1125).

(6a*R*,12a*R*,5′*R*)-Amorphigenin (44): yellow amorphous solid; UV (MeOH) λ_{max} (log ε) 204 (2.99), 236 (2.99), 295 (2.59) nm; $[\alpha]_D^{22}$ –4 (*c* 0.11, MeOH); ^{1}H and ^{13}C NMR, see Table 4

and 5; HRESIMS *m/z* 411.1437 $[M+H]^+$ (calc. for $C_{23}H_{23}O_7$, 411.1438).

Amorphispironone B (45): yellow amorphous solid; UV (MeOH) λ_{max} (log ε) 256 (4.05), 265 (4.05), 319 (3.66) nm; $[\alpha]_D^{21}$ –175 (*c* 0.49, MeOH); ECD {MeCN, λ [nm] (Δε), *c* = 1.89×10^{-4} M}: 369 (–0.74), 344sh (–0.74), 316 (–7.63), 267 (–9.77), 239 (7.33), 203 (9.84); ^{1}H and ^{13}C NMR, see Table 4 and 5; HRESIMS *m/z* 397.1281 $[M+H]^+$ (calc. for $C_{22}H_{21}O_7$, 397.1282).

Amorphispironone C (46): yellow amorphous solid; UV (MeOH) λ_{max} (log ε) 257 (3.44), 265 (3.57), 320 (2.84) nm ; $[\alpha]_D^{21}$ –92 (c 0.37, MeOH); ECD {MeCN, λ [nm] (Δε), *c* = 1.82×10^{-4} M}: 359sh (–1.16), 312 (–6.78), 274 (–9.18), 255 (6.52), 235 (–3.30), 203 (13.77); ^{1}H and ^{13}C NMR, see Table 4 and 5; HRESIMS *m/z* 413.1231 $[M+H]^+$ (calc. for $C_{22}H_{21}O_8$, 413.1231).

Resokaempferol 3-*O*-*β*-D-glucopyranosyl-(1→2)-*β*-D-glucopyranoside-7-*O*-*α*-L-rhamnopyranoside (51): yellow amorphous powder; UV (MeOH) λ_{max} (log ε) 266 (4.38), 348 (4.11) nm; $[\alpha]_D^{19}$ –51 (*c* 0.10, MeOH); ^{1}H and ^{13}C NMR, see Table 6; HRESIMS *m/z* 741.2237 $[M+H]^+$ (calcd for $C_{33}H_{41}O_{19}$, 741.2237).

Daidzein 7-*O*-*β*-D-glucopyranosyl-(1→2)-*β*-D-glucopyranoside (52): yellow amorphous solid; UV (MeOH) λ_{max} (log ε) 251 (4.11), 294 (3.65) nm; $[\alpha]_D^{21}$ –34 (*c* 0.56, MeOH); ^{1}H and ^{13}C NMR, see Table 6; HRESIMS *m/z* 579.1706 $[M+H]^+$ (calcd for $C_{27}H_{31}O_{14}$, 579.1708).

Acid Hydrolysis and HPLC Analysis of Compounds 51 and 52

Compounds **51** and **52** were separately hydrolyzed with 2 N HCl (0.1 mL) at 80°C for 4 h. After drying in vacuo, the residue was dissolved in pyridine (0.1 mL) containing L-cysteine methyl ester hydrochloride (0.5 mg) and heated at 60 °C for 1 h. A solution of *p*-tolylisothicyanate (0.5 mg) in pyridine (0.1 mL) was added to the mixture, which was heated at

60 °C for 1h. After the solvent was removed, the residue was dissolved in MeOH and analysed by HPLC (MeOH–H_2O, 1 mL/min). The peaks at 24.580 min and 25.587 min were identical to the derivatives of pure standard β-D-glucose and α-L-rhamnose that had been prepared using the same method as described for compounds **51** and **52**.[59]

Methylation of Compound 8

A mixture of potassium carbonate (254 mg) and dry methyliodide (0.12 mL) were added to an acetone solution (2 mL) of **8** (3.0 mg). After stirring at room temperature for 10 h, the remaining acetone was evaporated in vacuo. The residue was then dissolved in 15 mL ethyl acetate and 5 mL water was added. The organic layer was separated and dried over anhydrous magnesium sulphate. The dried organic layer was filtered and concentrated to afford 3.8 mg of a brown amorphous solid.

Antimicrobial Assay

The antibacterial activity of isolated compounds were evaluated by calculating their minimal inhibitory concentration (MIC) against *M. tuberculosis*, *S. aureus* ATCC25923, *S. aureus* ATCC700699, *E. faecalis* ATCC29212, *E. faecalis* ATCC 51299, *E. faecium* ATCC35667, *E. faecium* ATCC700221 and *A. baumannii* ATCCBAA1605. MIC for each strain was determined by the broth micro dilution method according to the recommendation of the Clinical and Laboratory Standards Institute (CLSI).[60] Moxifloxacin and DMSO were used as positive and negative control, respectively.

Cell Proliferation Assay

All isolated compounds were evaluated for their cytotoxicity against mouse lymphoma cell line L5178Y using MTT method as described before.[61] Experiment were accomplished in three times with kahalalide F and 0.1% DMSO in media as positive and negative control, respectively.

Cytotoxicity test against the human lung fibroblast MRC-5 cell line (American Type Culture Collection) and the human monocytic THP-1 cell line (German Collection of Microorganisms and Cell Cultures) were conducted by employing the protocol that has been described previously.[62]

Computational Section

Mixed torsional/low-frequency mode conformational searches were carried out by means of the Macromodel 9.9.223 software using the Merck Molecular Force Field (MMFF) with an implicit solvent model for $CHCl_3$.[63] Geometry reoptimizations were carried out at the B3LYP/6-31G(d) level *in vacuo* and B97D/TZVP[22,23] level with the PCM solvent model for MeCN. TDDFT ECD calculations were run with various functionals (B3LYP, BH&HLYP, PBE0) and the TZVP basis set as implemented in the Gaussian 09 package with the same or no solvent model as in the preceding DFT optimization step.[64] ECD spectra were generated as sums of Gaussians with 2400 to 3000 cm^{-1} widths at half-height (corresponding to ca. 14 to 17 nm at 240 nm, respectively), using dipole-velocity-computed rotational strength values.[65] Boltzmann distributions were estimated from the ZPVE-corrected B3LYP/6-31G(d) energies in the gas-phase calculations and from the B97D/TZVP energies in the solvated ones. The MOLEKEL software package was used for visualization of the results.[66]

ASSOCIATED CONTENT

Supporting Information

UV, HRESIMS and NMR spectra of all the new compounds, and structure and population of the low-energy conformers (≥2%) of compounds **11** and **45** as well as dose-response curves of antibacterial active compounds **4**, **5**, **8** and **12**. The Supporting Information is available free of charge on the ACS Publications website at DOI:

AUTHOR INFORMATION

Corresponding Authors

*Tel: +49 211 81 15979; Fax: +49 211 81 11923; E-mail: zhenfeizi0@sina.com. (Z.L.)

*Tel: +49 211 81 14163; Fax: +49 211 81 11923; E-mail: proksch@uni-duesseldorf.de. (P.P.)

ACKNOWLEDGMENTS

P.P. wants to thank BMBF (project BALIPEND) for support. R.M. wishes to thank DIKTI (Directorate General Higher Education) Indonesia for scholarship. T.K. and A.M. thank the Hungarian National Research Foundation (OTKA K105871) for financial support and the National Information Infrastructure Development Institute (NIIFI 10038) for CPU time.

REFERENCES

1) Dat, N. T.; Lee, J. H.; Lee, K.; Hong, Y. S.; Kim, Y. H.; Lee, J. J. *J. Nat. Prod.* **2008**, *71*, 1696–1700.

2) Lee, H. J.; Kang, H. Y.; Kim, C. H.; Kim, H. S.; Kwon, M. C.; Kim, S. M.; Shin, I. S.; Lee, H. Y. *Cytotechnology* **2006**, *52*, 219–226.

3) Lis, A.; Jozef, G. *J. Essent. Oil Res*. **2001**, *13*, 340–342.

4) Mitscher, L. A.; Park, Y. H.; Al-Shamma, A.; Hudson, P. B.; Haas, T. *Phytochemistry* **1981**, *20*, 781–785.

5) Liang, Y.; Li, X.; Gu, Z.; Qin, P.; Ji, M. *Molecules* **2015**, 20, 3238–3254.

6) Sauer, S. *ChemBioChem* **2014**, *15*, 1231–1238.

7) Shi, H.; Ma, J.; Mi, C.; Li, J.; Wang, F.; Lee, J. J.; Jin, X. *Int. Immunopharmacol*. **2014**, *21*, 56–62.

8) Fuhr, L.; Rousseau, M.; Plauth, A.; Schroeder, F. C.; Sauer, S. *J. Nat. Prod*. **2014**, *78*, 1160–1164.

9) Terada, H.; Kokumai, M.; Konoshima, T.; Kozuka, M.; Haruna, M.; Ito, K.; Estes, J. R.; Li,

L.; Wang, H. K.; Lee, K. H. *Chem. Pharm. Bull*. **1993**, *41*, 187–190.

10) Konoshima, T.; Terada, H.; Kokumai, M.; Kozuka, M. *J. Nat. Prod*. **1993**, *56*, 843–848.

11) Kim, Y. S.; Ryu, Y. B.; Curtis-Long, M. J; Yuk, H. J.; Cho, J. K.; Kim, J. Y.; Kim, K. D.; Lee, W. S.; Park, K. H. *Food Chem. Toxicol*. **2011**, *49*, 1849–1856.

12) Wu, X.; Liao H. B.; Li, G. Q.; Liu, Y.; Cui, L.; Wu, K. F.;, Zhu, X. H.; Zeng, X. B. *Fitoterapia* **2015**, *100*, 75-80.

13) Takastsuki, A.; Nakatani, N.; Morimoto, M.; Tamura, G.; Matsui, M.; Arima, K.; Yamaguchi, I.; Misato, T. *Appl. Microbiol*. **1969**, *18*, 660–667.

14) Pancheva, S.; Manolova, N.; Gagov, I.; Maksimova, V. *Acta Microbiol. Bulg*. **1982**, *10*, 1–14.

15) Li, L.; Wang, H. K.; Chang, J.; McPhail. A. T.; McPhail, D. R.; Terada, H. Konoshia, T.; Kokumai, M.; Kozuka, M.; Estes, J. R.; Lee, K. H. *J. Nat. Prod*. **1993**, *56*, 690–698.

16) Weidner, C.; Rousseau, M.; Micikas, R. J.; Fischer, C.; Plauth, A.; Wowro, S. J.; Siems, K.; Hetterling, G.; Kliem, M.; Schroeder, F. C.; Sauer, S. *J. Nat. Prod*. **2015**, *79*, 2–12.

17) Bohlmann, F.; Hoffmann, E. *Phytochemistry* **1979**, *18*, 1371-1374.

18) Zhang, Y. L.; Luo, J. G.; Wan, C. X.; Zhou, Z. B.; Kong, L. Y. *Fitoterapia* **2014**, *92*, 116–126.

19) Bezuidenhoudt, B. C. B.; Swanepoel, A.; Brandt, E. V.; Ferreira, D. *J. Chem. Soc. Perkin Trans. 1* **1990**, 2599–2602.

20) Ghribi, L.; Waffo-Téguo, P.; Cluzet, S.; Marchal, A.; Marques, J.; Mérillon, J. M.; Jannet, H. B. *Bioorg. Med. Chem. Lett*. **2015**, *25*, 3825–3830.

21) Mándi, A.; Mudianta, I. W.; Kurtán, T.; Garson, M. J. *J. Nat. Prod.* **2015**, *78*, 2051−2056.

22) Grimme, S. *J. Comput. Chem.* **2006**, *27*, 1787–1799.

23) Sun, P.; Xu, D. X.; Mándi, A.; Kurtán, T.; Li, T. J.; Schulz, B.; Zhang, W. *J. Org. Chem.* **2013**, *78*, 7030–7047.

24) Bohlmann, F.; Zdero, C. *Phytochemistry* **1983**, *22*, 2877–2878.

25) Ito, C.; Itoigawa, M.; Kanematsu, T.; Ruangrungsi, N.; Mukainaka, T.; Tokuda, H.; Nishino, H.; Furukawa, H. *Phytochemistry* **2003**, *64*, 1265–1268.

26) Abe, F.; Donnelly, D. M. X.; Moretti, C.; Polonsky, J. *Phytochemistry* **1985**, *24*, 1071–1076.

27) Kostova, I.; Ognyanov, I. *Z. Naturforsch., B: Anorg. Chem., Org. Chem.* **1983**, *38*, 761–763.

28) Mándi, A.; Swamy, M. M. M.; Taniguchi, T.; Anetai, M.; Monde, K. *Chirality* **2016**, *28*, 453–459.

29) Zhang, P.; Meng, L. H.; Mándi, A.; Kurtán, T.; Li, X. M.; Liu, Y.; Li, X.; Li, C. S.; Wang, B. G. *Eur. J. Org. Chem.* **2014**, 4029–4036.

30) Pescitelli, G.; Bruhn, T. *Chirality*, **2016**, *28*, 466–474.

31) Fiorentino, A.; Ricci, A.; Abrosea, B.; Golino, A.; Izzo, A.; Pasearella, M. T.; Piccolella, S.; Esposito, A. *Chem. Biodiversity* **2009**, *6*, 204–217.

32) Kim, H. J.; Lee, D. H.; Hwang, Y. Y.; Lee, K. S.; Lee, J. S. *J. Agric. Food Chem.* **2005**, *53*, 5882–5888.

33) Ham, J. Y.; Ahn, H. Y.; Park, Y. H.; Kim, S. N.; Lee, U. J.; Yang, H. O.; Kwon, H. C. *Repub. Korea* **2009**, KR 894832 B1 20090424.

34) Kemal, M.; Khalil, S. K. W.; Rao, N. G. S. *J. Nat. Prod.* **1979**, *42*, 463–468.

35) Crombie, L. W.; Crombie, W. M. L.; Firth, D. F. *J. Chem. Soc. Perkin Trans. 1* **1988**, 1263–1270.

36) Jayasinghe, L.; Balasooriya, B. A. I. S.; Padmini, W. C.; Hara, N.; Fujimoto, Y. *Phytochemistry* **2004**, *65*, 1287–1290.

37) Pelter, A.; Ward, R. S.; Bass, R. J. *J. Chem. Soc. Perkin Trans. 1* **1978**, 666–668.

38) Wang, S. F.; Jiang, Q.; Ye, Y. H.; Li, Y.; Tan, R. X. *Bioorg. Med. Chem.* **2005**, *13*, 4880–4890.

39) Yuk, H. J.; Lee, J. H.; Curtis-Long, M. J.; Lee, J. W.; Kim, Y. S.; Ryu, H. W.; Park, C. G.; Jeong, T. S.; Park, K. H. *Food Chem.* **2011**, *126*, 1057–1063.

40) Burns, D. T.; Dalgarno, B. G.; Gargan, P. E.; Grimshaw, J. *Phytochemistry* **1984**, *23*, 167–169.

41) Ognyanov, I.; Somleva, T. *Planta Med.* **1980**, *38*, 279–280.

42) Dagne, E.; Yenesew, A.; Waterman, P. G. *Phytochemistry* **1989**, *28*, 3207–3210.

43) Nakatani, N.; Ohta, H.; Matsui, M. *Agr. Biol. Chem.* **1972**, *36*, 2433–2439.

44) Lin, L. J.; Ruangrungsi, N.; Cordell, G. A.; Shieh, H. L.; You, M.; Pezzuto, J. M. *Phytochemistry* **1992**, *31*, 4329–4331.

45) Singhal, A. K.; Sharma, R. P.; Baruah, J. N.; Govindan, S. V.; Herz, W. *Phytochemistry* **1982**, *21*, 949–951.

46) Crombie, L.; Rossiter, J. T.; Bruggen, N. V.; Whiting, D. A. *Phytochemistry* **1992**, *31*, 451–461.

47) Andrei, C. C.; Vieira, P. C.; Fernandes, J. B.; da Silva, M. F. das G. F.; Rodrigues Fo, E. *Phytochemistry* **1997**, *46*, 1081–1085.

48) Ye, H.; Chen, L.; Li, Y.; Peng, A.; Fu, A.; Song, H.; Tang, M.; Luo, H.; Luo, Y.; Xu, Y.; Shi, J.; Wei, Y. *J. Chromatogr. A* **2008**, *1178*, 101–107.

49) Nakatani, N.; Matsui, M. *Agr. Biol. Chem.* **1977**, *41*, 601–602.

50) Fang, N.; Casida, J. E. *J. Org. Chem.* **1997**, *62*, 350–353.

51) Magalhaes, A. F.; Tozzi, A. M. G. A.; Sales, B. H. L. N.; Magalhaes, E. G. *Phytochemistry*

1996, *42*, 1459–1471.

52) Carlson, D. G.; Weisleder, D.; Tallent, W. H. *Tetrahedron* **1973**, *29*, 2731–2741.

53) Li, W.; Koike, K.; Asada, Y.; Hirotani, M.; Rui, H.; Yoshikawa, T.; Nikaido, T. *Phytochemistry* **2002**, *60*, 351–355.

54) Mitscher, L. A.; Gollapudi, S. R.; Drake, S.; Oburn, D. S. *Phytochemistry* **1985**, *24*, 1481–1483.

55) Ávila, H. P.; De Fátima Albino Smânia, E., Monache, F. D; Júnior, A. S. *Bioorg. Med. Chem*. **2008**, *16*, 9790–9794.

56) Daletos, G.; De Voogd, N. J.; Müller, W. E. G.; Wray, V.; Lin, W.; Feger, D.; Kubbutat, M.; Aly, A. H.; Proksch, P. *J. Nat. Prod*. **2014**, *77*, 218–226.

57) Ebrahim, W.; El-Neketi, M.; Lewald, L.; Orfali, R. S.; Lin, W.; Rehberg, N.; Kalscheuer, R.; Daletos, G.; Proksch, P. *J. Nat. Prod*. **2016**, *79*, 914–922.

58) Deyou, T.; Gumula, I.; Pang, F.; Gruhonjic, A.; Mumo, M.; Holleran, J.; Duffy, S.; Fitzpatrick, P. A.; Heydenreich, M.; Landberg, G.; Derese, S.; Avery, V.; Rissanen, K.; Erdelyi, M.; Yenesew, A. *J. Nat. Prod*. **2015**, *78*, 2932–2939.

59) Tanaka, T.; Nakashima, T.; Ueda, T.; Tomii, K.; Kouno, I. *Chem. Pharm. Bull*. **2007**, *55*, 899-901.

60) CLSI. Methods for Dilution Antimicrobial Susceptibility Tests for Bacteria That Grow Aerobically; Approved Standart–Ninth Edition**.** Clinical and Laboratory Standarts Institute, **2012**.

61) Ashour, M.; Edrada, R.; Ebel, R.; Wray, V.; Wätjen, W.; Padmakumar, K.; Müller, W. E. G.; Lin, W. H.; Proksch, P. *J. Nat. Prod.* **2006**, *69,* 1547−1553.

62) Daletos, G.; Kalscheuer, R.; Koliwer-Brandl, H.; Hartmann, R.; de Voogd, N. J.; Wray, V.;

Lin, W.; Proksch, P. *J. Nat. Prod*. **2015**, *78*, 1910–1925.

63) MacroModel; Schrödinger, LLC, 2012, http://www.schrodinger.com/MacroModel.

64) Frisch, M. J.; Trucks, G. W.; Schlegel, H. B.; Scuseria, G. E.; Robb, M. A.; Cheeseman, J. R.; Scalmani, G.; Barone, V.; Mennucci, B.; Petersson, G. A.; Nakatsuji, H.; Caricato, M.; Li, X.; Hratchian, H. P.; Izmaylov, A. F.; Bloino, J.; Zheng, G.; Sonnenberg, J. L.; Hada, M.; Ehara, M.; Toyota, K.; Fukuda, R.; Hasegawa, J.; Ishida, M.; Nakajima, T.; Honda, Y.; Kitao, O.; Nakai, H.; Vreven, T.; Montgomery, J. A. Jr.; Peralta, J. E.; Ogliaro, F.; Bearpark, M.; Heyd, J. J.; Brothers, E.; Kudin, K. N.; Staroverov, V. N.; Kobayashi, R.; Normand, J.; Raghavachari, K.; Rendell, A.; Burant, J. C.; Iyengar, S. S.; Tomasi, J.; Cossi, M.; Rega, N.; Millam, J. M.; Klene, M.; Knox, J. E.; Cross, J. B.; Bakken, V.; Adamo, C.; Jaramillo, J.; Gomperts, R.; Stratmann, R. E.; Yazyev, O.; Austin, A. J.; Cammi, R.; Pomelli, C.; Ochterski, J. W.; Martin, R. L.; Morokuma, K.; Zakrzewski, V. G.; Voth, G. A.; Salvador, P.; Dannenberg, J. J.; Dapprich, S.; Daniels, A. D.; Farkas, O.; Foresman, J. B.; Ortiz, J. V.; Cioslowski, J.; Fox, D. J. *Gaussian 09*, revision B.01; Gaussian, Inc.: Wallingford, CT, 2010.

65) Stephens, P. J.; Harada, N. *Chirality* **2010**, *22*, 229–233.

66) Varetto, U. *MOLEKEL*, v. 5.4; Swiss National Supercomputing Centre: Manno, Switzerland, 2009.

Publication 4

Supporting Information

Antibacterial and Cytotoxic Phenolic Metabolites from Fruits of *Amorpha fruticosa*

Rini Muharini,[†,‡] Adriana Díaz,[†] Weaam Ebrahim,[†,§] Attila Mándi,[⊥] Tibor Kurtán,[⊥] Nidja Rehberg,[†] Rainer Kalscheuer,[†] Rudolf Hartmann,[#] Raha S. Orfali,[‖] Wenhan Lin,[▽] Zhen Liu,*[,†] Peter Proksch,*[,†]

[†]Institute of Pharmaceutical Biology and Biotechnology, Heinrich-Heine-Universität Düsseldorf, Universitätsstrasse 1, Geb.26.23, 40225 Düsseldorf, Germany

[‡]Department of Chemistry Education, Faculty of Education, Tanjungpura University, Jl. Prof. Dr. H. Hadari Nawawi, 78124, Pontianak, Indonesia

[§]Department of Pharmacognosy, Faculty of Pharmacy, Mansoura University, Mansoura 35516, Egypt

[⊥]Department of Organic Chemistry, University of Debrecen, Egyetem tér 1, Debrecen 4032, Hungary

[#]Institute of Complex Systems: Strukturbiochemie, Forschungszentrum Juelich, Wilhelm-Johnen-Straße, 52428 Juelich, Germany

[‖]Department of Pharmacognosy, Faculty of Pharmacy, King Saud University, Riyadh, Saudi Arabia

[▽]State Key Laboratory of Natural and Biomimetic Drugs, Peking University, Beijing 100191, China

Publication 4

Table of Contents

Page

Figure S1. UV spectrum of the new compound **1**……... 6

Figure S2. HRESIMS of the new compound **1**……... 6

Figure S3. ^{1}H NMR (600 MHz, $CDCl_3$) spectrum of the new compound **1**……... 7

Figure S4. ^{1}H-^{1}H COSY (600 MHz, $CDCl_3$) spectrum of the new compound **1**..... 7

Figure S5. HSQC (600 MHz, 150 MHz, $CDCl_3$) spectrum of the new compound **1**……. 8

Figure S6. HMBC (600 MHz, 150 MHz, $CDCl_3$) spectrum of the new compound **1**…… 8

Figure S7. UV spectrum of the new compound **2**……... 9

Figure S8. HRESIMS of the new compound **2**…….. 9

Figure S9. ^{1}H NMR (600 MHz, $CDCl_3$) spectrum of the new compound **2**…….. 10

Figure S10. ^{1}H-^{1}H COSY (600 MHz, $CDCl_3$) spectrum of the new compound **2**……. 10

Figure S11. HSQC (600 MHz, 150 MHz, $CDCl_3$) spectrum of the new compound **2**…….. 11

Figure S12. HMBC (600 MHz, 150 MHz, $CDCl_3$) spectrum of the new compound **2**…….. 12

Figure S13. UV spectrum of the new compound **3**……. 12

Figure S14. HRESIMS of the new compound **3**……. 13

Figure S15. ^{1}H NMR (300 MHz, $CDCl_3$) spectrum of the new compound **3**……. 13

Figure S16. ^{1}H-^{1}H COSY (300 MHz, $CDCl_3$) spectrum of the new compound **3**……. 14

Figure S17. HMBC (300 MHz, 75 MHz, $CDCl_3$) spectrum of the new compound **3**…… 14

Figure S18. UV spectrum of compound **11**…… 15

Figure S19. ESIMS of compound **11**……. 15

Figure S20. ^{1}H NMR (600 MHz, $CDCl_3$) spectrum of compound **11**…… 16

Figure S21. HMBC (300 MHz, 75 MHz, $CDCl_3$) spectrum of compound **11**……... 17

Figure S22. CD spectrum of compound **11**…… 18

Figure S23. UV spectrum of the new compound **13**…….. 18

Figure S24. HRESIMS of the new compound **13**…….. 19

Figure S25. ^{1}H NMR (600 MHz, $CDCl_3$) spectrum of the new compound **13**…….. 20

Figure S26. ^{1}H-^{1}H COSY (600 MHz, $CDCl_3$) spectrum of the new compound **13**……... 21

Figure S27. HSQC (600 MHz, 150 MHz, $CDCl_3$) spectrum of the new compound **13**…….. 22

Figure S28. HMBC (600 MHz, 150 MHz, $CDCl_3$) spectrum of the new compound **13**…… 23

Figure S29. CD spectrum of the new compound **13**……... 23
Figure S30. UV spectrum of the new compound **14**……... 24
Figure S31. HRESIMS of the new compound **14**……... 24
Figure S32. ^{1}H NMR (600 MHz, $CDCl_3$) spectrum of the new compound **14**…….. 25
Figure S33. ^{1}H-^{1}H COSY (600 MHz, $CDCl_3$) spectrum of the new compound **14**……... 25
Figure S34. HSQC (600 MHz, 150 MHz, $CDCl_3$) spectrum of the new compound **14**……. 26
Figure S35. HMBC (600 MHz, 150 MHz, $CDCl_3$) spectrum of the new compound **14**…… 26
Figure S36. ROESY (600 MHz, $CDCl_3$) spectrum of the new compound **14**…… 27
Figure S37. UV spectrum of the new compound **15**……... 27
Figure S38. HRESIMS of the new compound **15**……... 28
Figure S39. ^{1}H NMR (600 MHz, $CDCl_3$) spectrum of the new compound **15**…….. 28
Figure S40. ^{13}C NMR (150 MHz, $CDCl_3$) spectrum of the new compound **15**……. 29
Figure S41. HMBC (600 MHz, 150 MHz, $CDCl_3$) spectrum of the new compound **15**…… 29
Figure S42. ROESY (600 MHz, $CDCl_3$) spectrum of the new compound **15**…… 30
Figure S43. UV spectrum of the new compound **16**…….. 30
Figure S44. HRESIMS of the new compound **16**…….. 31
Figure S45. ^{1}H NMR (600 MHz, $CDCl_3$) spectrum of the new compound **16**…….. 32
Figure S46. ^{1}H-^{1}H COSY (600 MHz, $CDCl_3$) spectrum of the new compound **16**……... 33
Figure S47. HMBC (600 MHz, 150 MHz, $CDCl_3$) spectrum of the new compound **16**…… 34
Figure S48. ROESY (600 MHz, $CDCl_3$) spectrum of the new compound **16**…… 35
Figure S49. UV spectrum of the new compound **42**…….. 36
Figure S50. HRESIMS of the new compound **42**……... 36
Figure S51. ^{1}H NMR (600 MHz, $(CD_3)_2CO$) spectrum of the new compound **42**…… 37
Figure S52. ^{1}H-^{1}H COSY (600 MHz, $(CD_3)_2CO$) spectrum of the new compound **42**…….. 38
Figure S53. ^{13}C NMR (150 MHz, $(CD_3)_2CO$) spectrum of the new compound **42**…… 39
Figure S54. HSQC (600 MHz, 150 MHz, $(CD_3)_2CO$) spectrum of the new compound **42**... 40
Figure S55. HMBC (600 MHz, 150 MHz, $(CD_3)_2CO$) spectrum of the new compound **42**.. 41
Figure S56. ROESY (600 MHz, $(CD_3)_2CO$) spectrum of the new compounds **42**…… 42
Figure S57. UV spectrum of the new compound **43**…….. 42
Figure S58. HRESIMS of the new compound **43**……... 43
Figure S59. ^{1}H NMR (700 MHz, $CDCl_3$) spectrum of the new compound **43**…….. 44

Figure S60. ^{1}H-^{1}H COSY (700 MHz, $CDCl_3$) spectrum of the new compound **43**……... 45
Figure S61. HSQC (700 MHz, 175 MHz, $CDCl_3$) spectrum of the new compound **43**……. 46
Figure S62. HMBC (700 MHz, 175 MHz, $CDCl_3$) spectrum of the new compound **43**…… 47
Figure S63. ROESY (700 MHz, $CDCl_3$) spectrum of the new compound **43**…… 48
Figure S64. UV spectrum of the new compound **44**…….. 49
Figure S65. HRESIMS of the new compound **44**……... 49
Figure S66. ^{1}H NMR (600 MHz, $CDCl_3$) spectrum of the new compound **44**…….. 50
Figure S67. ^{1}H-^{1}H COSY (700 MHz, $CDCl_3$) spectrum of the new compound **44**……... 51
Figure S68. HSQC (700 MHz, 175 MHz, $CDCl_3$) spectrum of the new compound **44**……. 52
Figure S69. HMBC (700 MHz, 175 MHz, $CDCl_3$) spectrum of the new compound **44**…… 53
Figure S70. ROESY (700 MHz, $CDCl_3$) spectrum of the new compound **44**…… 54
Figure S71. CD spectrum of the new compound **44**……... 54
Figure S72. UV spectrum of the new compound **45**……... 55
Figure S73. HRESIMS of the new compound **45**……... 55
Figure S74. ^{1}H NMR (300 MHz, $CDCl_3$) spectrum of the new compound **45**……... 56
Figure S75. ^{1}H-^{1}H COSY (300 MHz, $CDCl_3$) spectrum of the new compound **45**……... 57
Figure S76. ^{13}C NMR (75 MHz, $CDCl_3$) spectrum of the new compound **45**……... 58
Figure S77. HSQC (300 MHz, 75 MHz, $CDCl_3$) spectrum of the new compound **45**……... 59
Figure S78. HMBC (300 MHz, 75 MHz, $CDCl_3$) spectrum of the new compound **45**…….. 60
Figure S79. ROESY (600 MHz, $CDCl_3$) spectrum of the new compound **45**…… 61
Figure S80. CD spectrum of the new compound **45**……... 61
Figure S81. UV spectrum of the new compound **46**……... 62
Figure S82. HRESIMS of the new compound **46**……... 62
Figure S83. ^{1}H NMR (600 MHz, $(CD_3)_2CO$) spectrum of the new compound **46**……. 63
Figure S84. ^{1}H-^{1}H COSY (600 MHz, $(CD_3)_2CO$) spectrum of the new compound **46**…….. 64
Figure S85. HSQC (600 MHz, 150 MHz, $(CD_3)_2CO$) spectrum of the new compound **46**... 65
Figure S86. HMBC (600 MHz, 150 MHz, $(CD_3)_2CO$) spectrum of the new compound **46**.. 66
Figure S87. ROESY (600 MHz, $(CD_3)_2CO$) spectrum of the new compound **46**…….. 67
Figure S88. CD spectrum of the new compound **46**……... 67
Figure S89. UV spectrum of the new compound **51**……... 68
Figure S90. HRESIMS of the new compound **51**……... 68

Figure S91. ^{1}H NMR (700 MHz, CD_3OD) spectrum of the new compound **51**……. 69
Figure S92. ^{1}H-^{1}H COSY (600 MHz, CD_3OD) spectrum of the new compound **51**……. 70
Figure S93. TOCSY (700 MHz, CD_3OD) spectrum of the new compound **51**……. 71
Figure S94. HSQC (700 MHz, 175 MHz, CD_3OD) spectrum of the new compound **51**….. 72
Figure S95. HMBC (700 MHz, 175 MHz, CD_3OD) spectrum of the new compound **51**….. 73
Figure S96. ROESY (700 MHz, CD_3OD) spectrum of the new compound **51**…….. 74
Figure S97. UV spectrum of the new compound **52**……... 75
Figure S98. HRESIMS of the new compound **52**…….. 75
Figure S99. ^{1}H NMR (600 MHz, CD_3OD) spectrum of the new compound **52**……. 76
Figure S100. ^{1}H-^{1}H COSY (600 MHz, CD_3OD) spectrum of the new compound **52**…….. 77
Figure S101. HSQC (600 MHz, 150 MHz, CD_3OD) spectrum of the new compound **52**…. 78
Figure S102. HMBC (600 MHz, 150 MHz, CD_3OD) spectrum of the new compound **52**… 79
Figure S103. Structure and population of the low-energy B97D/TZVP PCM/MeCN conformers (≥ 2%) of (*S*)-**11**…… 79
Figure S104. Structure and population of the low-energy B3LYP/6-31G(d) *in vacuo* conformers (≥ 2%) of (1a*R*,6a*S*,12a*R*)-**45**…… 80
Figure S105. Experimental ECD spectrum of **45** in MeCN compared with the B3LYP/TZVP calculated ECD spectrum of (1a*R*,6a*S*,12a*R*)-**45** computed for the single major B97D/TZVP (PCM/MeCN) conformer…….. 80
Figure S106. Dose-response curves of compounds **4**, **5**, **8** and **12** against MRSA, *E. faecalis* ATCC 51299, *E. faecium* ATCC 700221 and the human cell lines THP-1 and MRC-5…….. 81

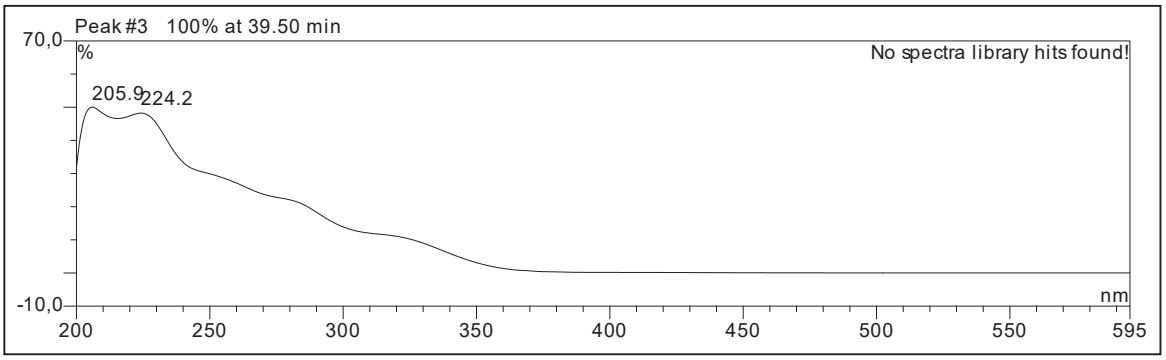

S1. UV Spectrum of the new compound **1**

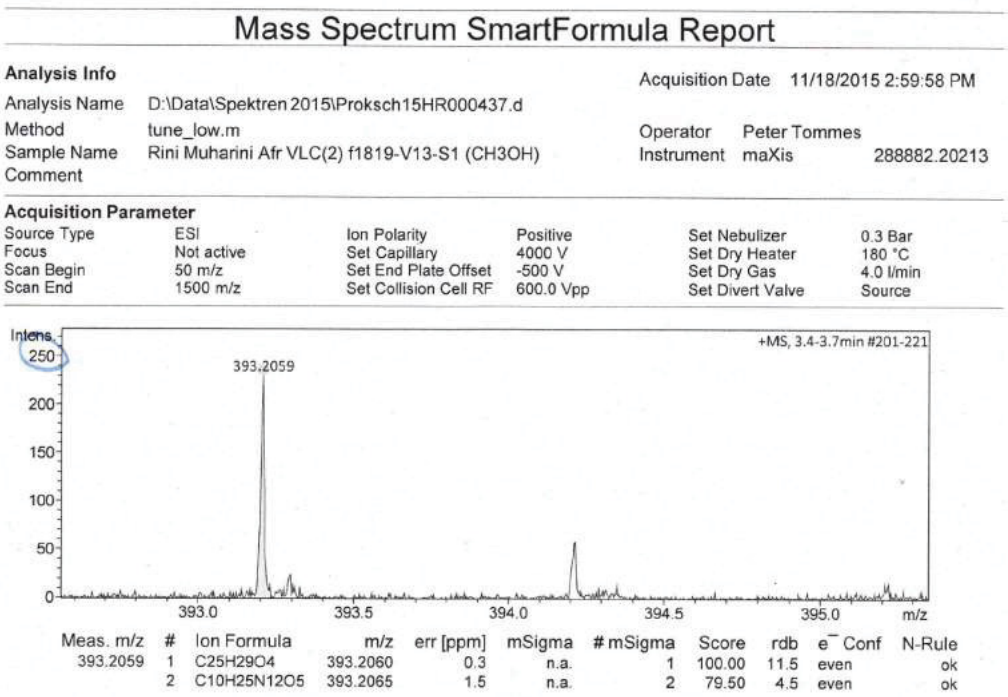

S2. HRESIMS of the new compound **1**

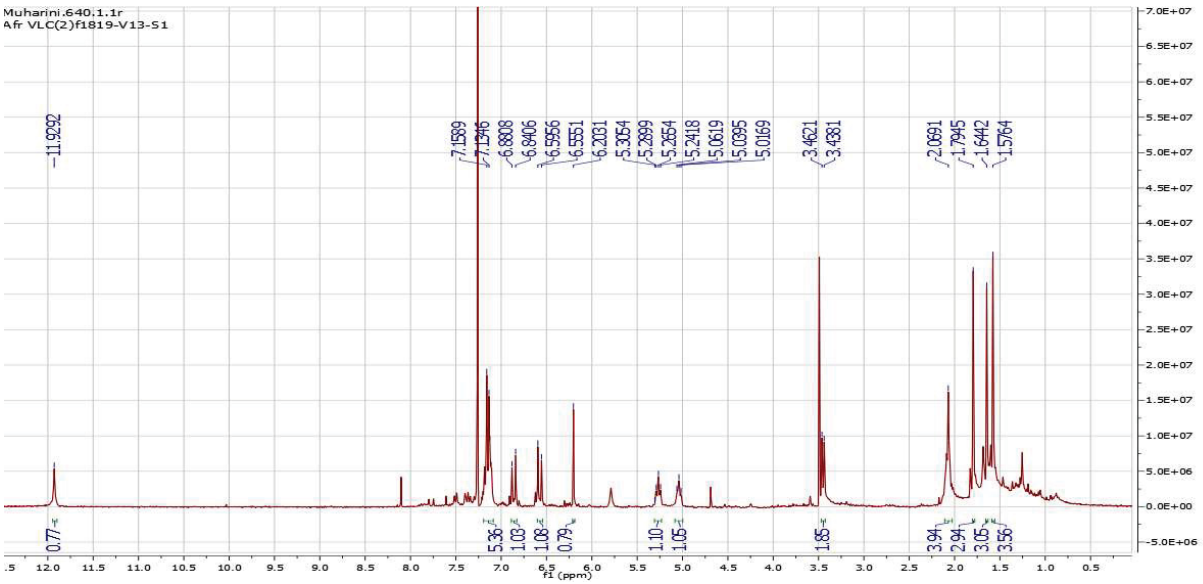

S3. ^{1}H NMR (300 MHz, $CDCl_3$) of the new compound **1**

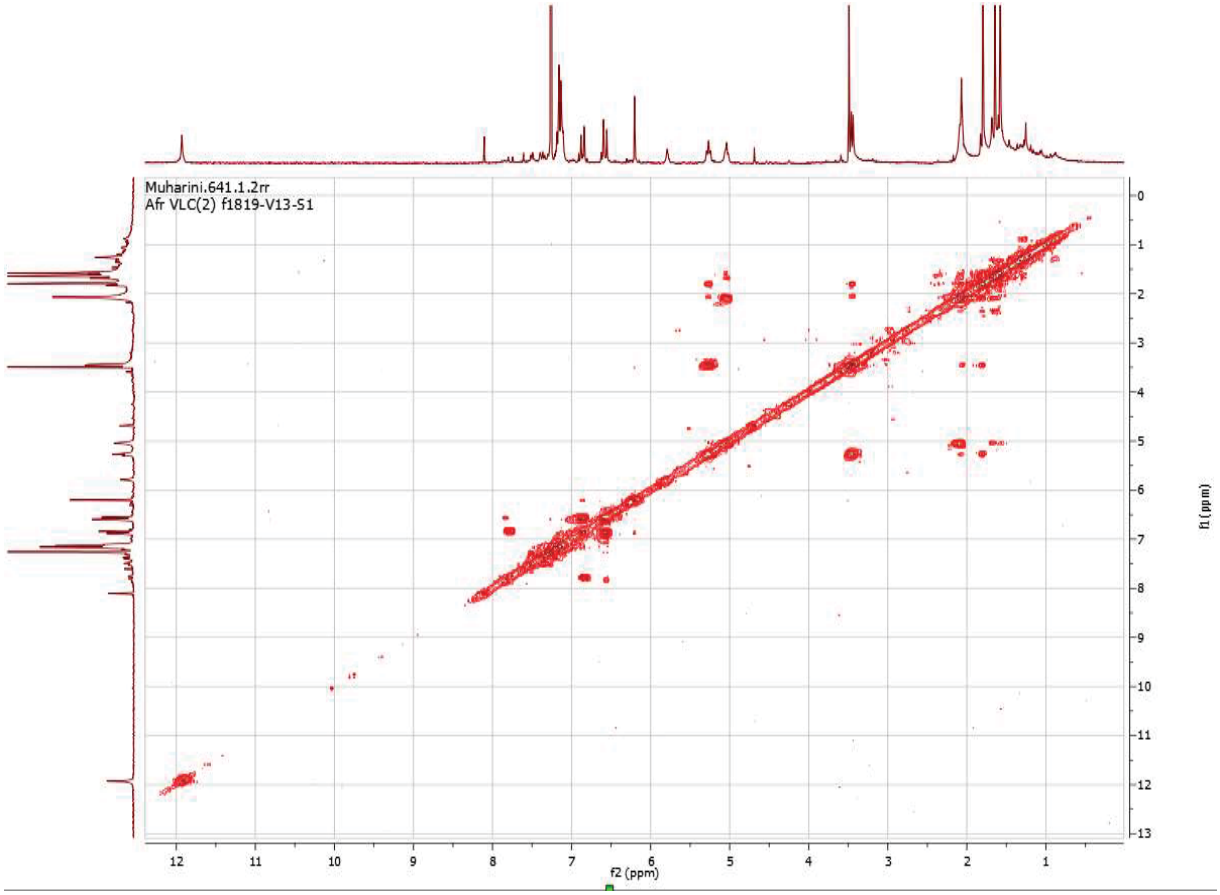

S4. ^{1}H-^{1}H COSY (300 MHz, $CDCl_3$) of the new compound **1**

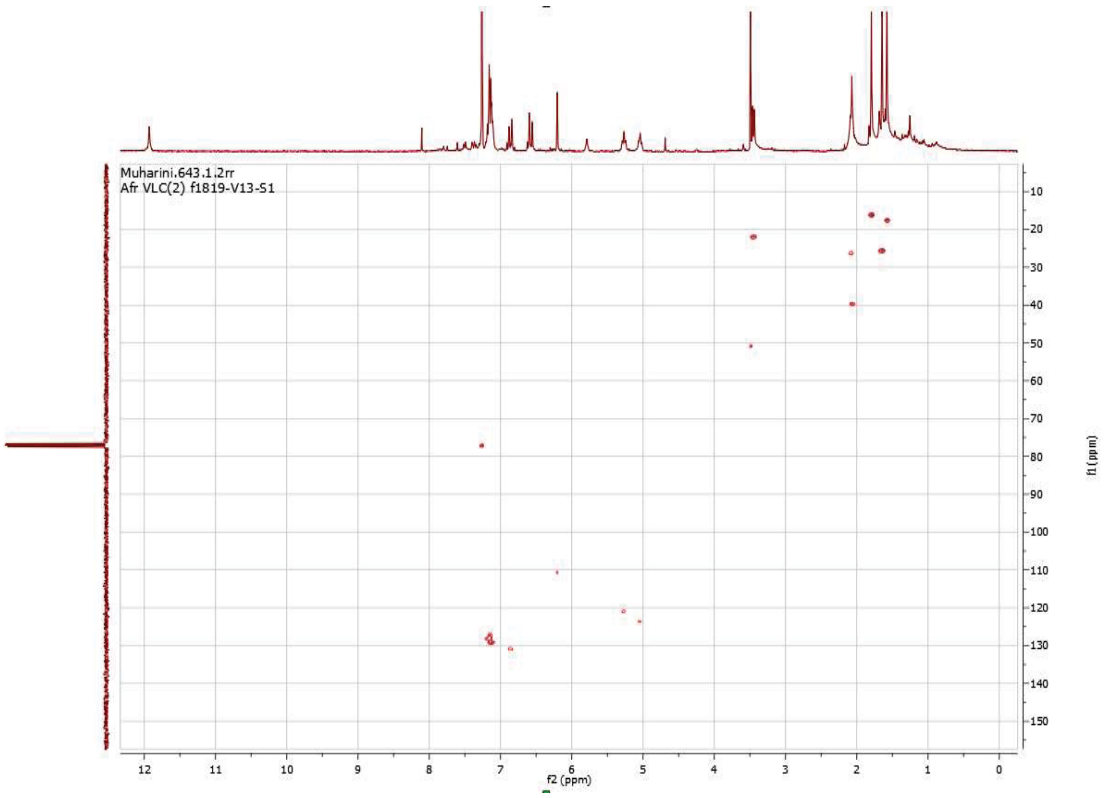

S5. HSQC (300 MHz, 75 MHz, $CDCl_3$) of the new compound **1**

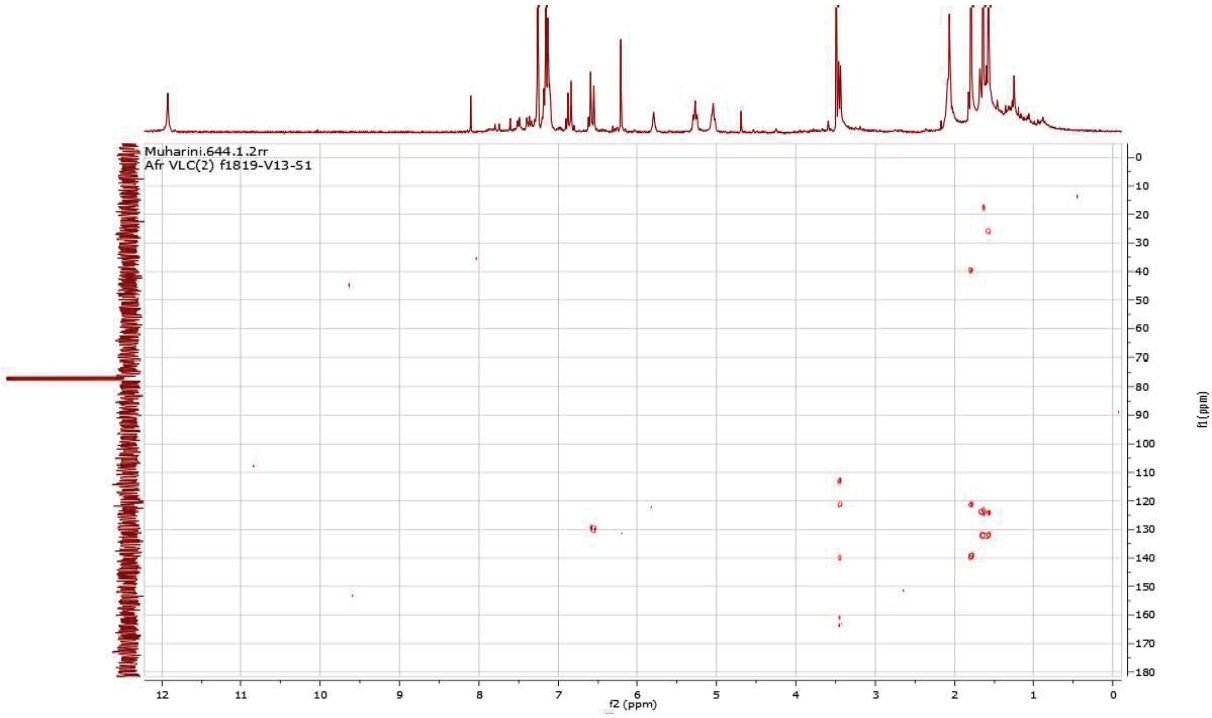

S6. HMBC (300 MHz, 75 MHz $CDCl_3$) of the new compound **1**

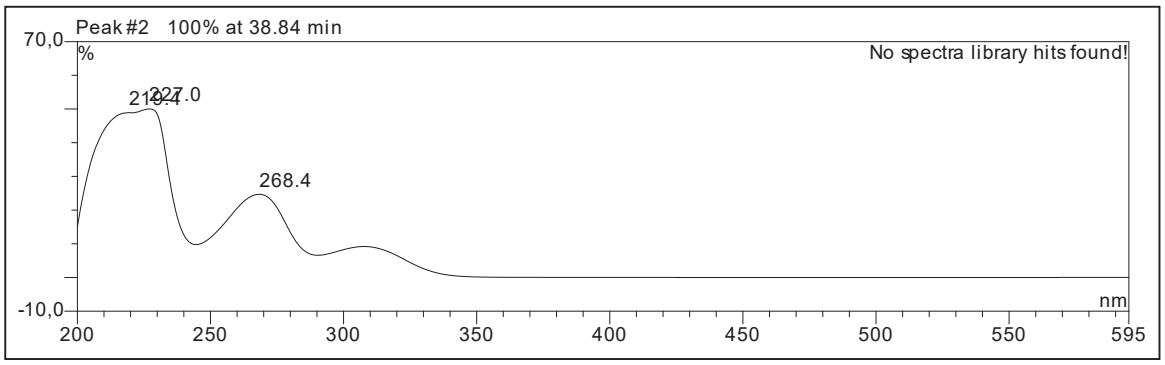

S7. UV spectrum of the new compound **2**

Mass Spectrum SmartFormula Report

Analysis Info

Analysis Name	D:\Data\Spektren 2015\Proksch15HR000266.d	Acquisition Date	8/19/2015 10:07:11 AM
Method	tune_low.m	Operator	Peter Tommes
Sample Name	Rini Muharini Afr VLC(2) f12-Se(2)Fr.57-62 S.prep Fr.1	Instrument	maXis 288882.20213
Comment			

Acquisition Parameter

Source Type	ESI	Ion Polarity	Positive	Set Nebulizer	0.3 Bar
Focus	Not active	Set Capillary	4000 V	Set Dry Heater	180 °C
Scan Begin	50 m/z	Set End Plate Offset	-500 V	Set Dry Gas	4.0 l/min
Scan End	1500 m/z	Set Collision Cell RF	600.0 Vpp	Set Divert Valve	Source

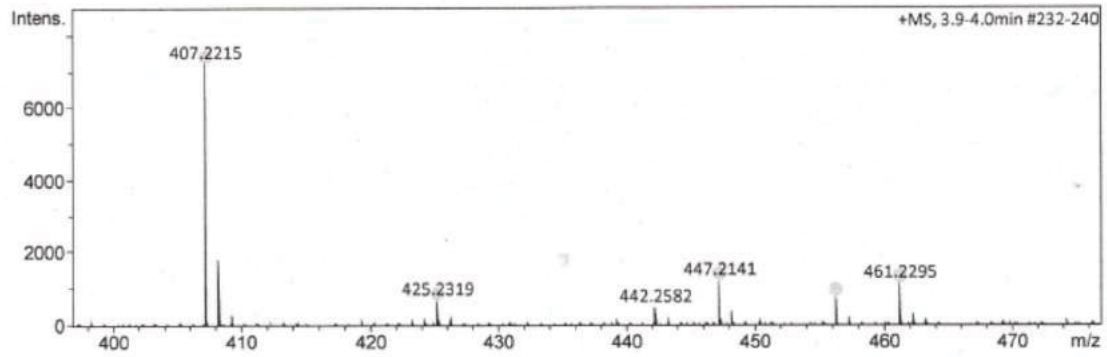

Meas. m/z	#	Ion Formula	m/z	err [ppm]	mSigma	# mSigma	Score	rdb	e⁻ Conf	N-Rule
407.2215	1	C26H31O4	407.2217	0.5	22.4	1	100.00	11.5	even	ok
425.2319	1	C26H33O5	425.2323	0.9	30.5	1	100.00	10.5	even	ok
447.2141	1	C26H32NaO5	447.2142	0.2	34.1	1	100.00	10.5	even	ok
456.2747	1	C27H38NO5	456.2744	-0.6	30.0	1	100.00	9.5	even	ok
461.2295	1	C27H34NaO5	461.2298	0.7	28.8	1	100.00	10.5	even	ok
	2	C25H29N6O3	461.2296	0.1	30.4	2	81.18	14.5	even	ok

S8. HRESIMS of the new compound **2**

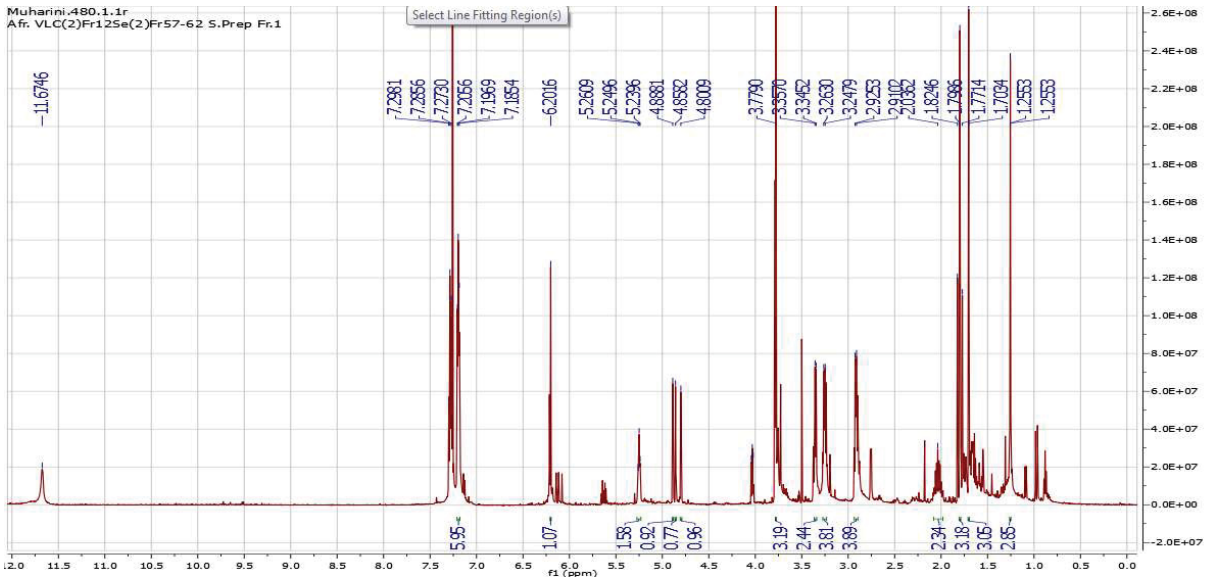

S9. ^{1}H NMR (600 MHz, $CDCl_3$) spectrum of the new compound **2**

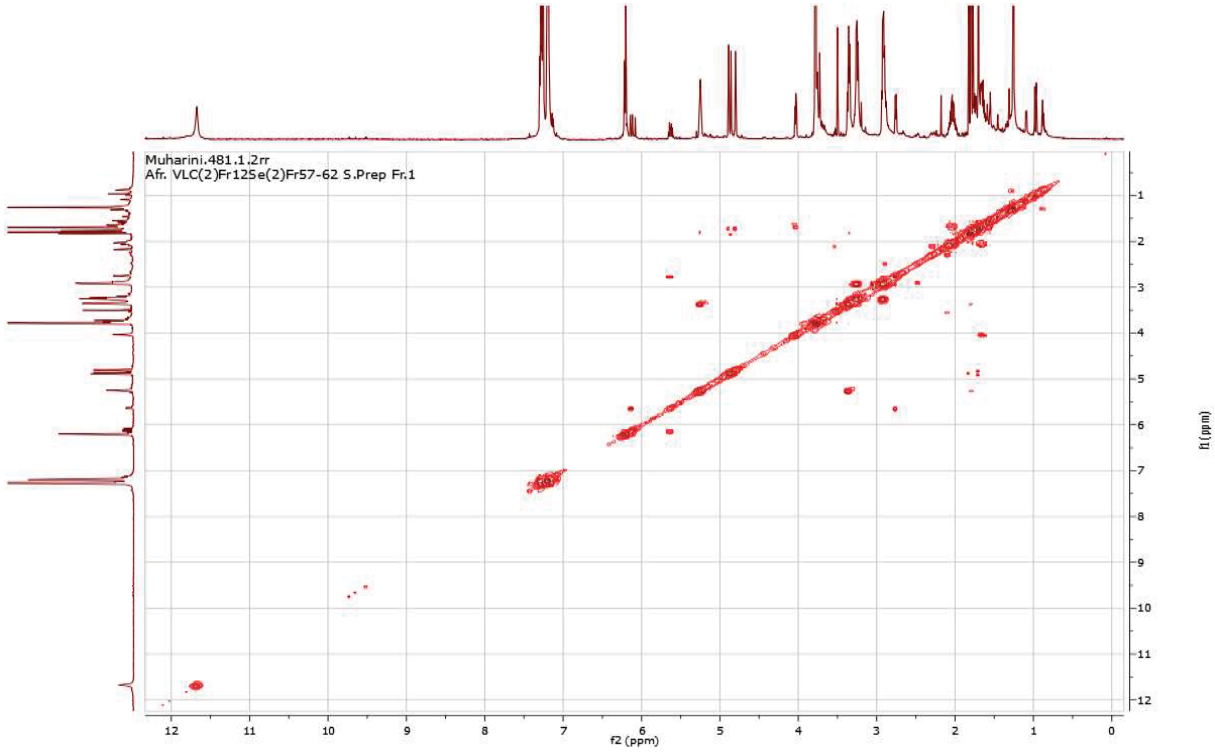

S10. ^{1}H-^{1}H COSY (600 MHz, $CDCl_3$) spectrum of the new compound **2**

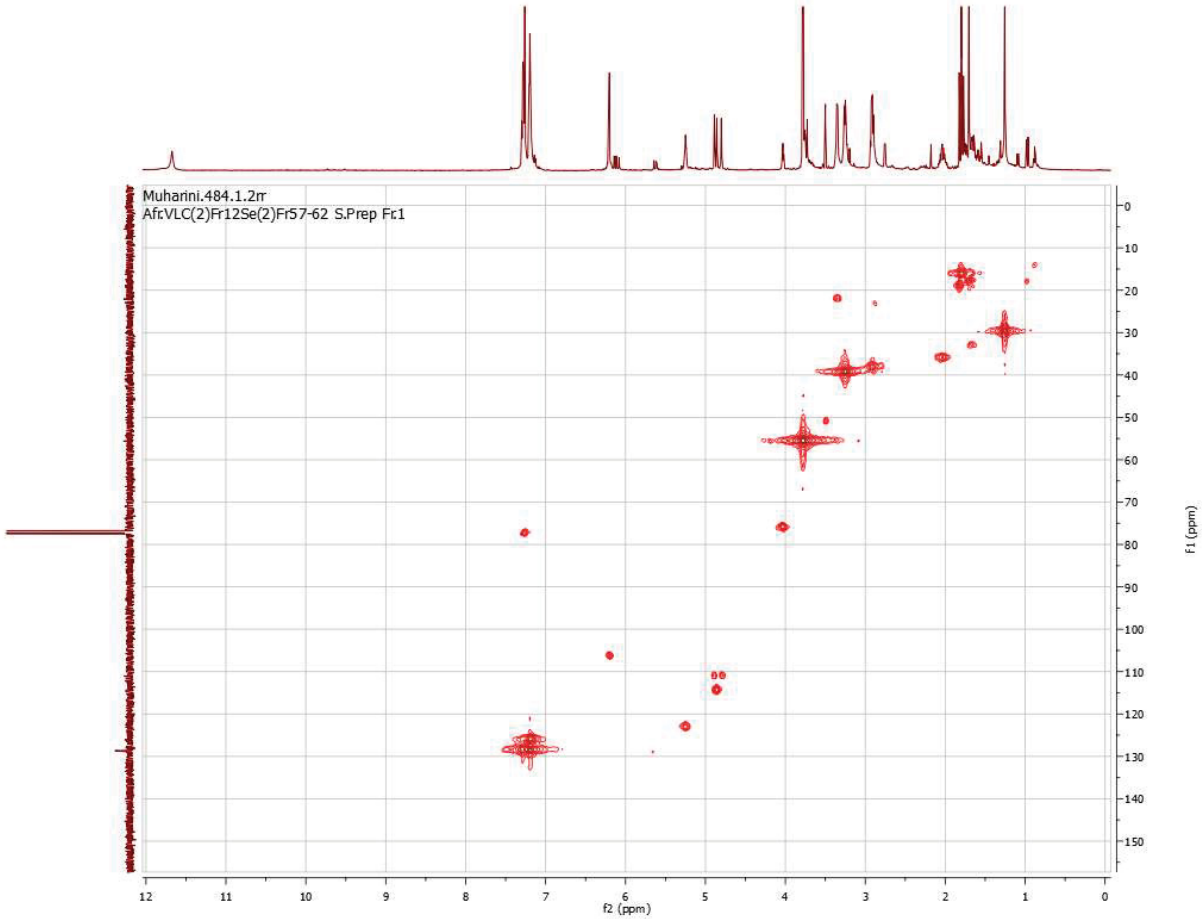

S11. HSQC (600 and 150 MHz $CDCl_3$) spectrum of the new compound **2**

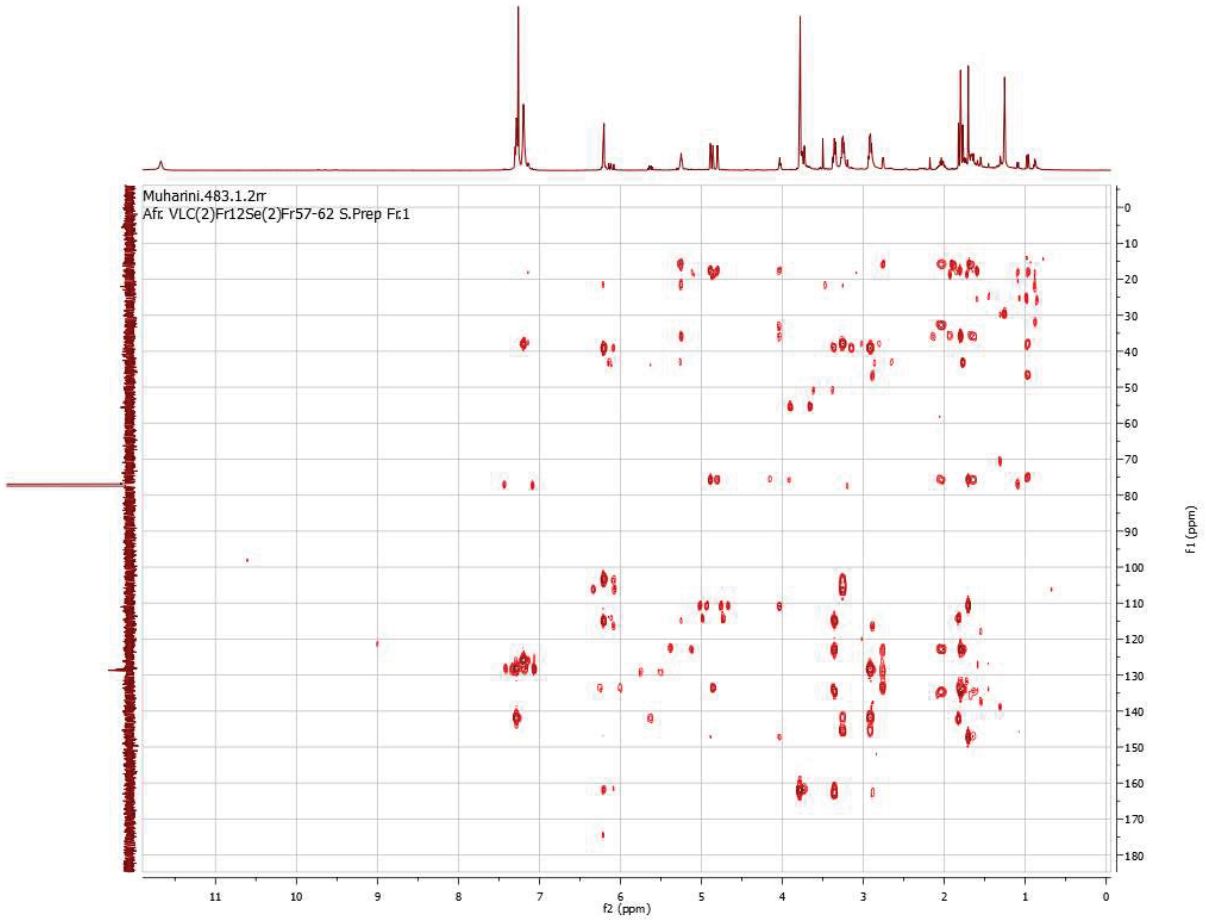

S12. HMBC (600 and 150 MHz, $CDCl_3$) spectrum of the new compound **2**

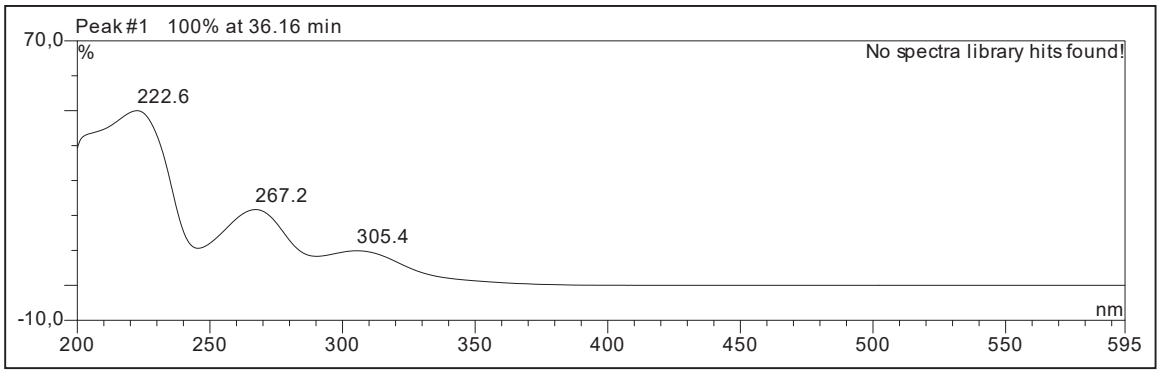

S13. UV Spectrum of the new compound **3**

Mass Spectrum SmartFormula Report

Analysis Info

Analysis Name	D:\Data\Spektren 2015\Proksch15HR000267.d	Acquisition Date	8/19/2015 10:45:12 AM
Method	tune_low.m	Operator	Peter Tommes
Sample Name	Rini Muharini Afr VLC(2) f11Se(1)Fr.105Se(2)Fr.168-183	Instrument	maXis 288882.20213
Comment			

Acquisition Parameter

Source Type	ESI	Ion Polarity	Positive	Set Nebulizer	0.3 Bar
Focus	Not active	Set Capillary	4000 V	Set Dry Heater	180 °C
Scan Begin	50 m/z	Set End Plate Offset	-500 V	Set Dry Gas	4.0 l/min
Scan End	1500 m/z	Set Collision Cell RF	600.0 Vpp	Set Divert Valve	Source

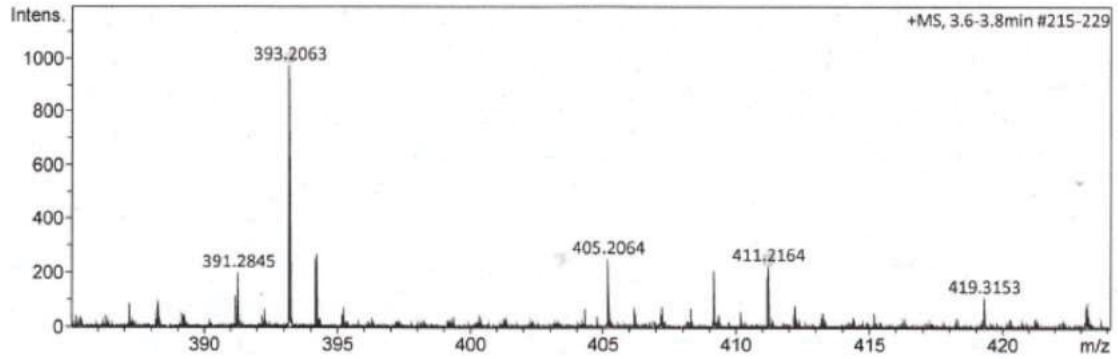

Meas. m/z	#	Ion Formula	m/z	err [ppm]	mSigma	# mSigma	Score	rdb	e¯ Conf	N-Rule
393.2063	1	C25H29O4	393.2060	-0.7	25.8	1	100.00	11.5	even	ok
411.2164	1	C25H31O5	411.2166	0.4	n.a.	1	100.00	10.5	even	ok
	2	C10H27N12O6	411.2171	1.6	n.a.	2	79.09	3.5	even	ok
	3	C7H19N22	411.2158	-1.7	n.a.	3	78.15	9.5	even	ok

S14. HRESIMS of the new compound **3**

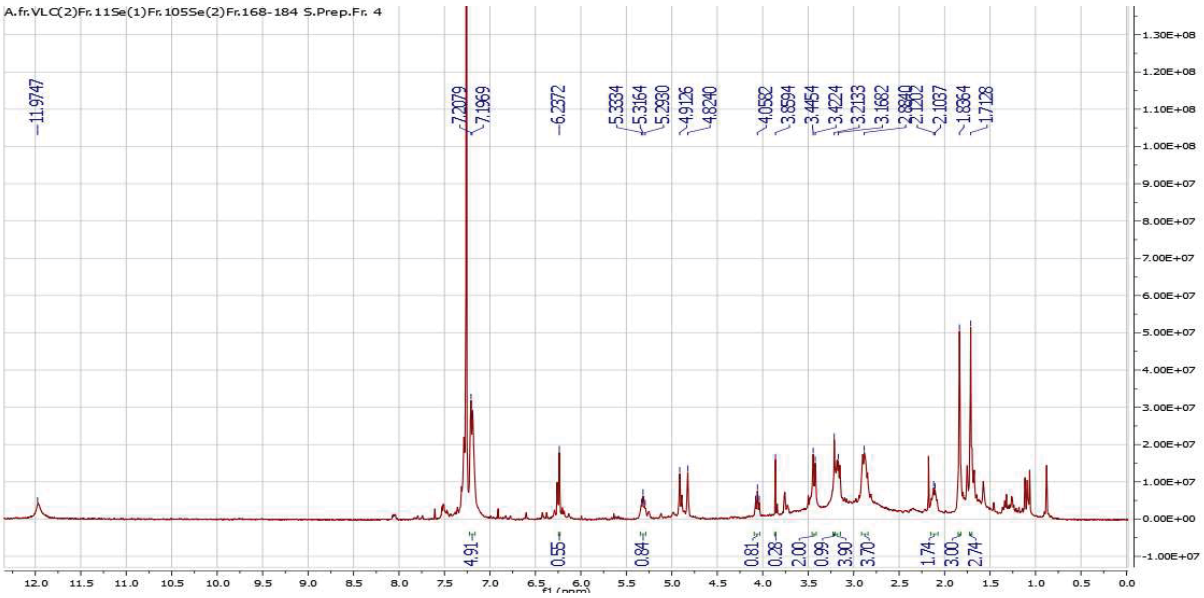

S15. ^{1}H NMR (600 MHz, $CDCl_3$) of the new compound **3**

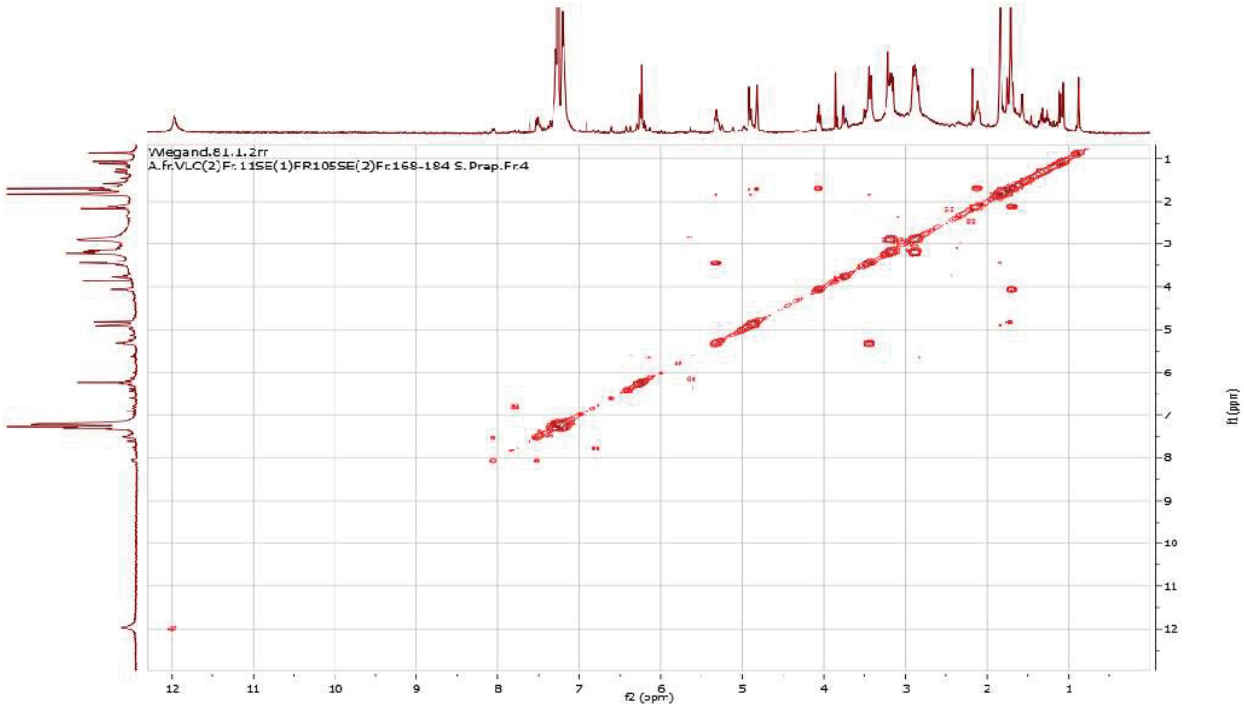

S16. ^{1}H-^{1}H COSY (600 MHz, $CDCl_3$) of the new compound **3**

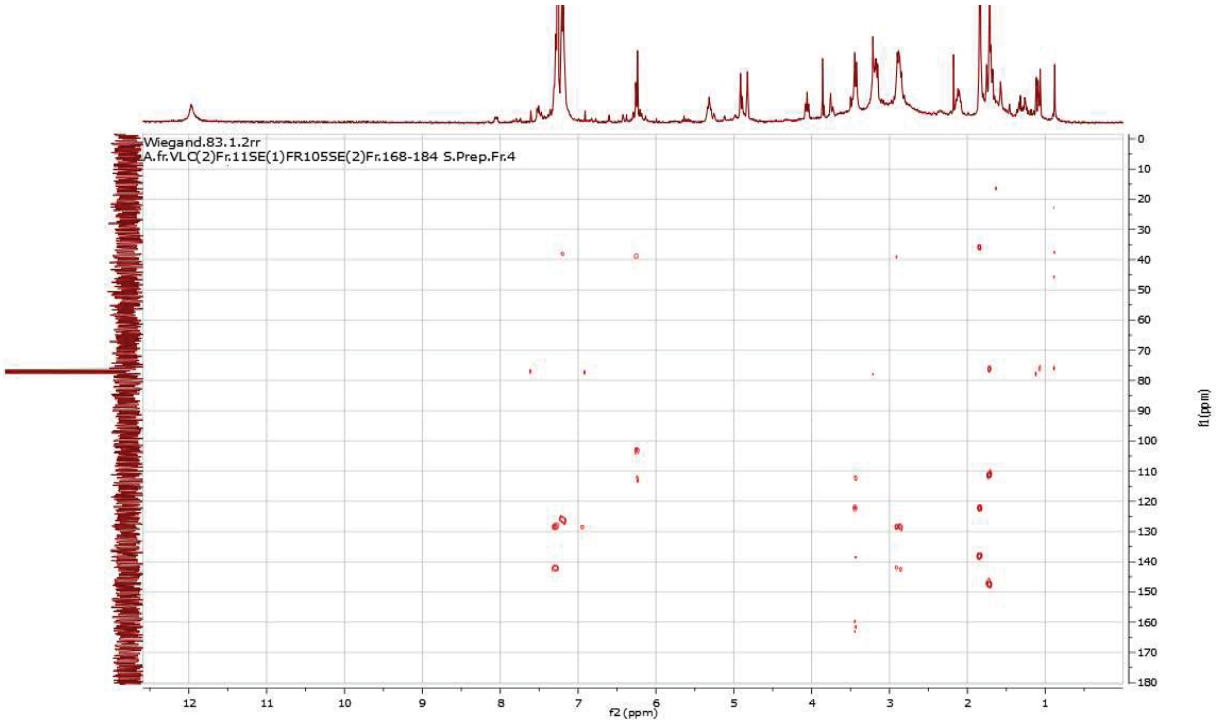

S17. HMBC (300 MHz, 75 MHz $CDCl_3$) of the new compound **3**

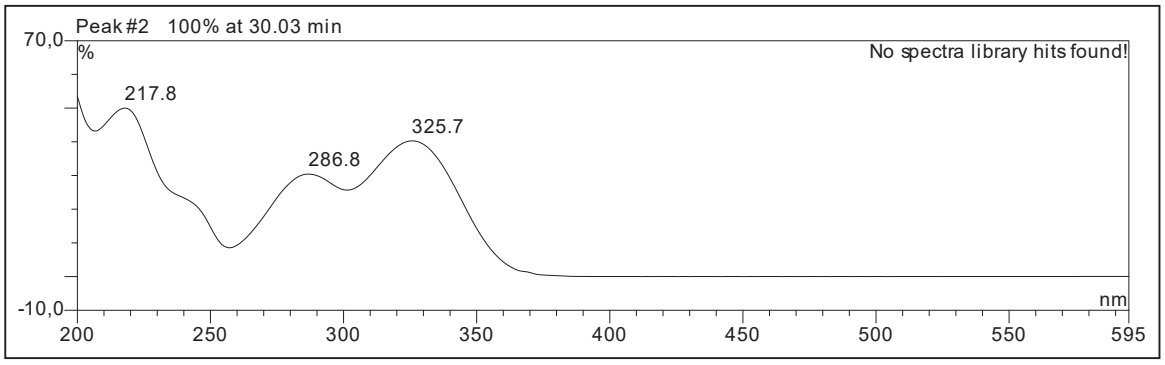

S18. UV spectrum of compound **11**

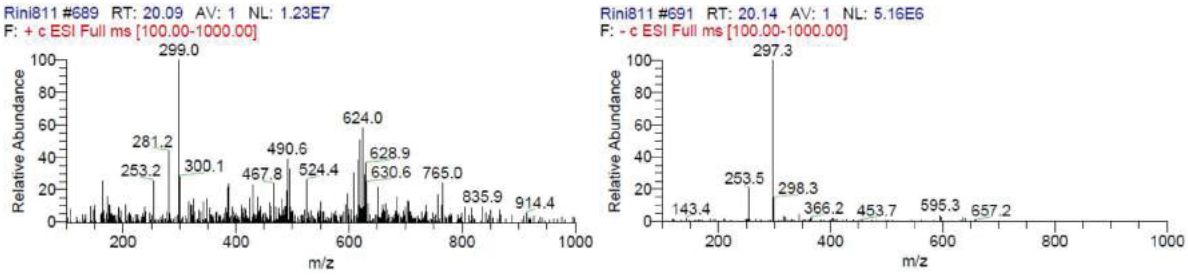

S19. ESIMS of compound **11**

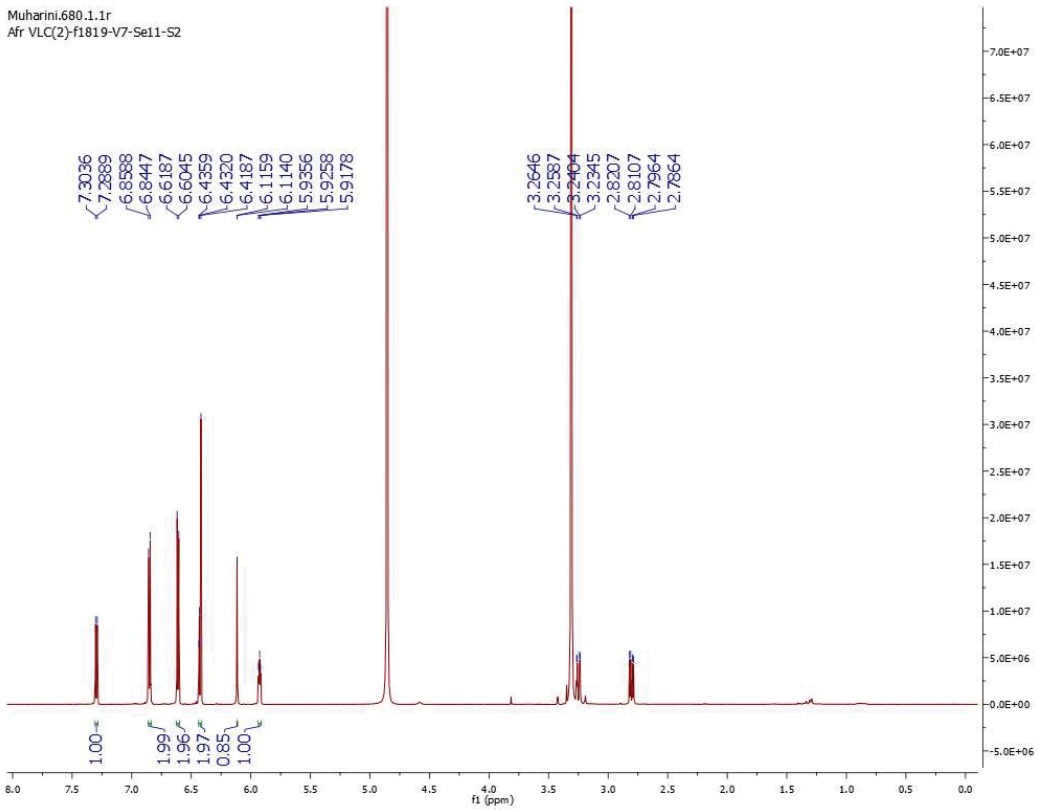

S20.^{1}H NMR (600 MHz, $CDCl_3$) spectrum of compound **11**

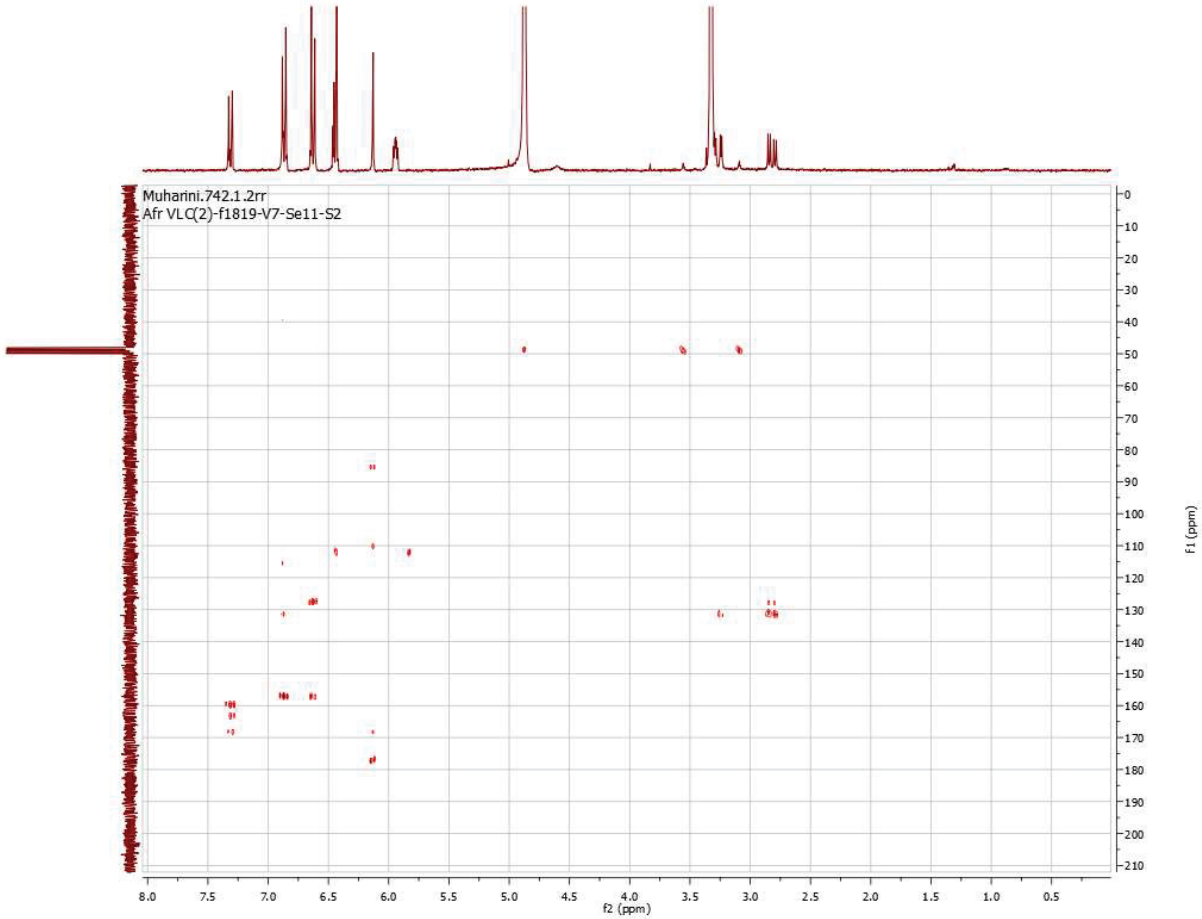

S21. HMBC (300 MHz, 75 MHz $CDCl_3$) spectrum of compound **11**

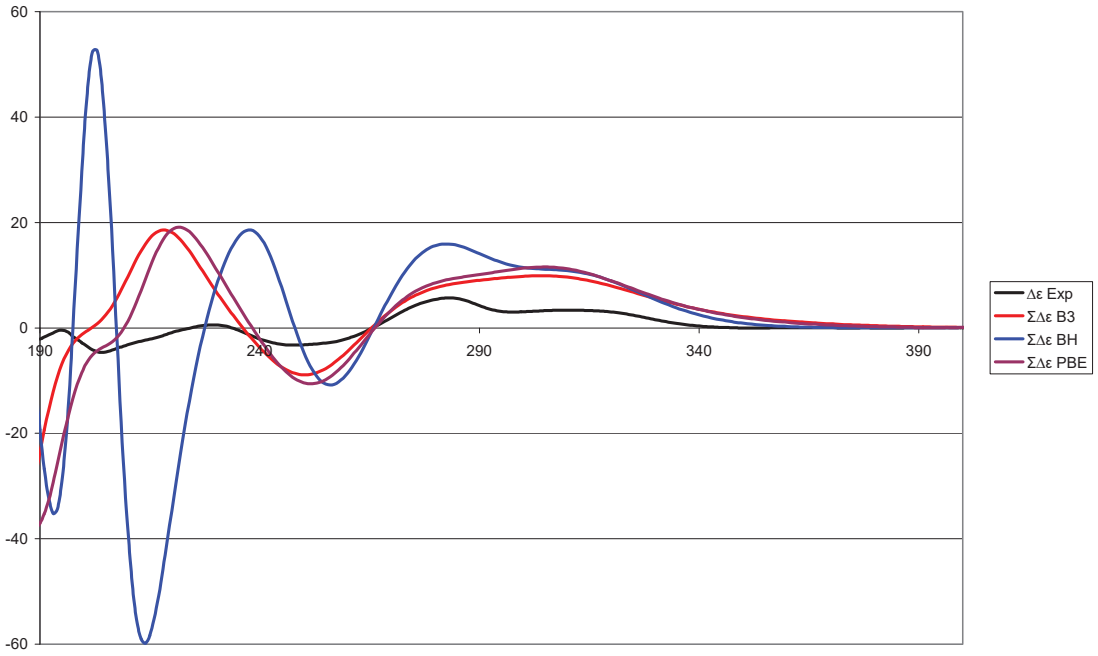

S22. CD spectrum of compound **11**

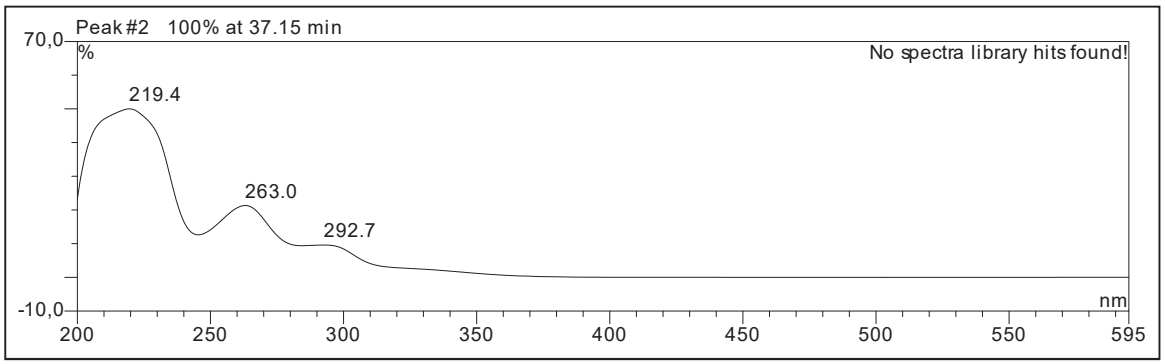

S23. UV spectrum of the new compound **13**

Mass Spectrum SmartFormula Report

Analysis Info

Analysis Name	D:\Data\Spektren 2015\Proksch15HR000242.d	Acquisition Date	7/21/2015 1:18:38 PM
Method	tune_low.m	Operator	Peter Tommes
Sample Name	Rini Afr VLC(2) f1819-V4-S2 (CH3OH)	Instrument	maXis 288882.20213
Comment	1 ul in 500 ul		

Acquisition Parameter

Source Type	ESI	Ion Polarity	Positive	Set Nebulizer	0.3 Bar
Focus	Not active	Set Capillary	4000 V	Set Dry Heater	180 °C
Scan Begin	50 m/z	Set End Plate Offset	-500 V	Set Dry Gas	4.0 l/min
Scan End	1500 m/z	Set Collision Cell RF	600.0 Vpp	Set Divert Valve	Source

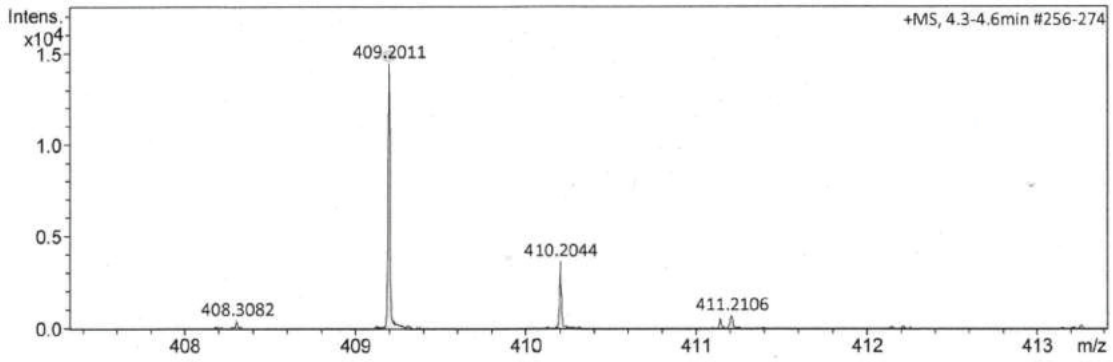

Meas. m/z	#	Ion Formula	m/z	err [ppm]	mSigma	# mSigma	Score	rdb	e⁻ Conf	N-Rule
409.2011	1	C25H29O5	409.2010	-0.4	13.9	1	100.00	11.5	even	ok

S24. HRESIMS of the new compound **13**

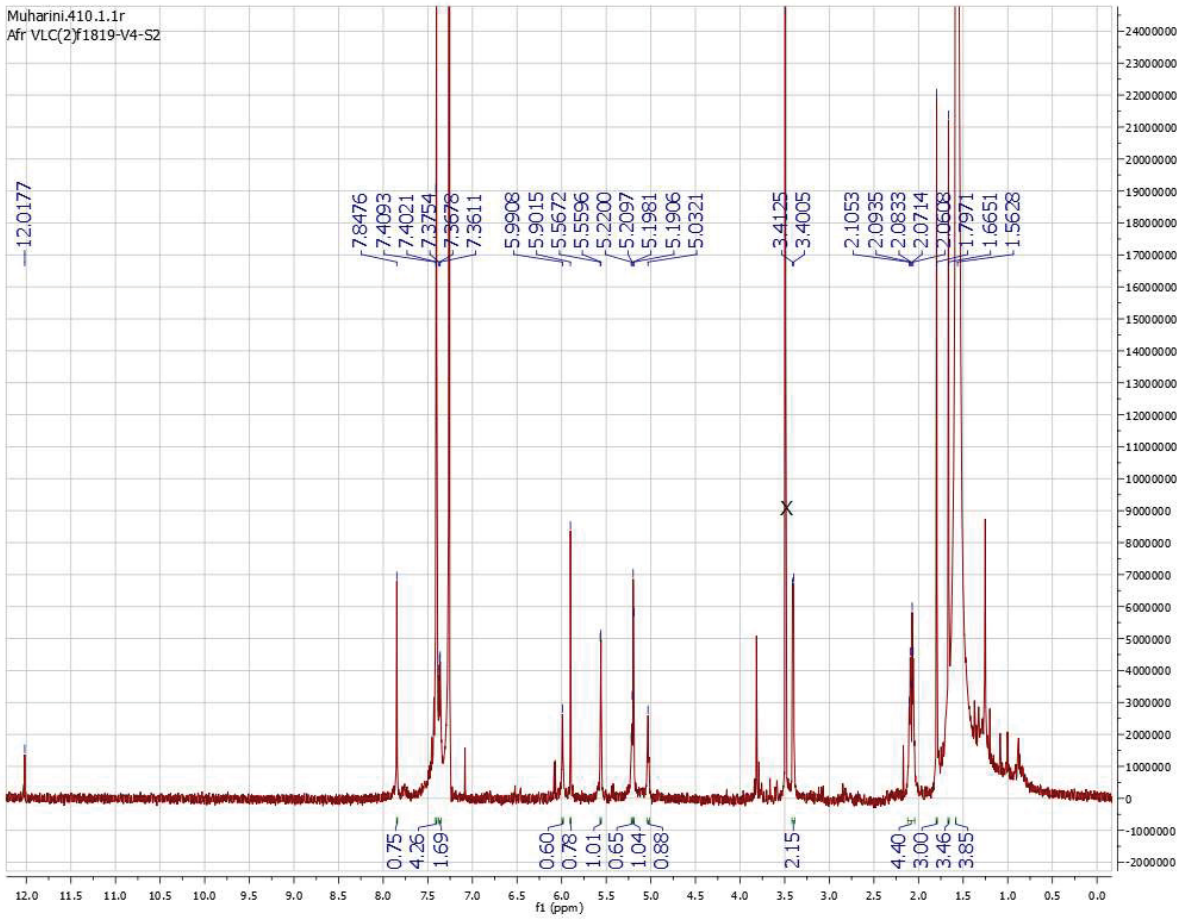

S25. ^{1}H NMR (600 MHz, $CDCl_3$) spectrum of the new compound **13**

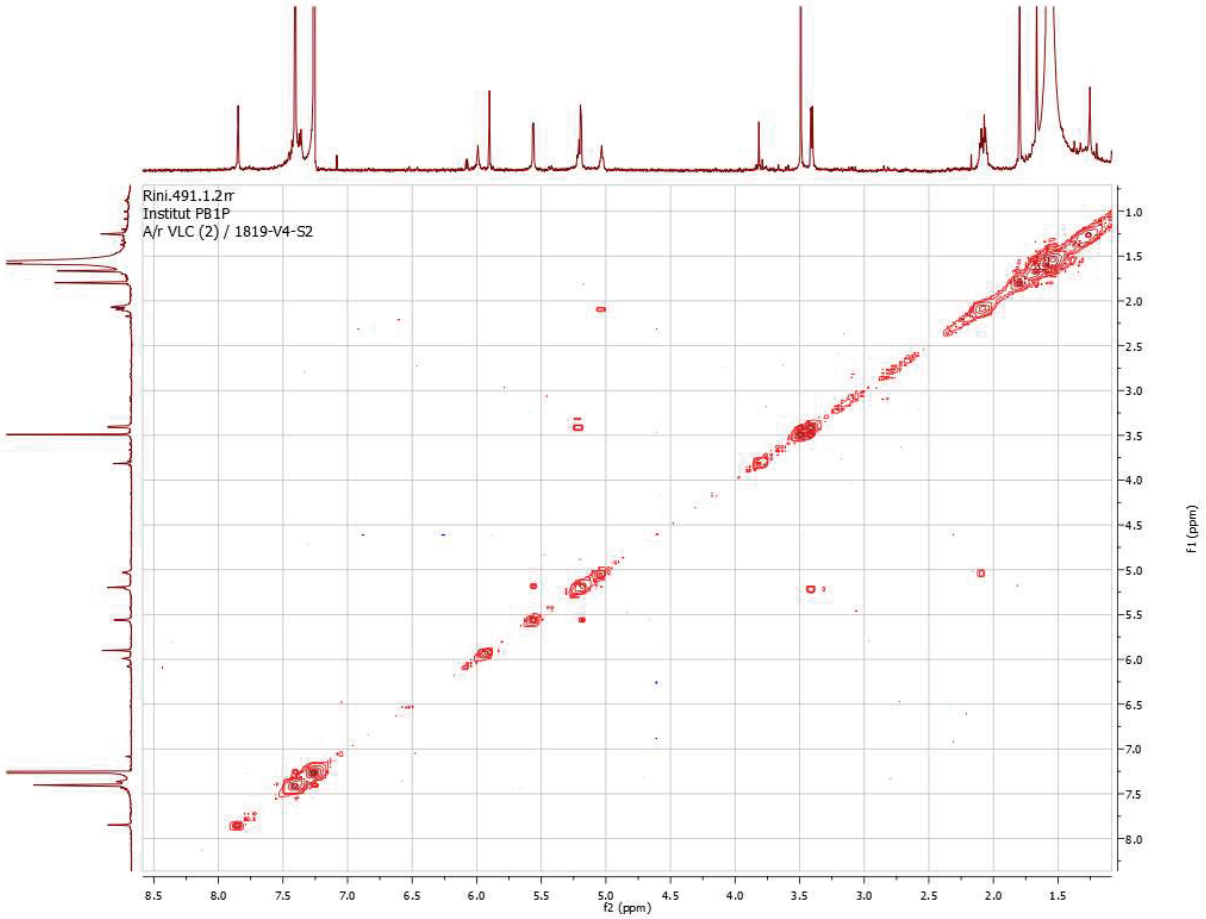

S26. ^{1}H-^{1}H COSY (500 MHz, $CDCl_3$) spectrum of the new compound **13**

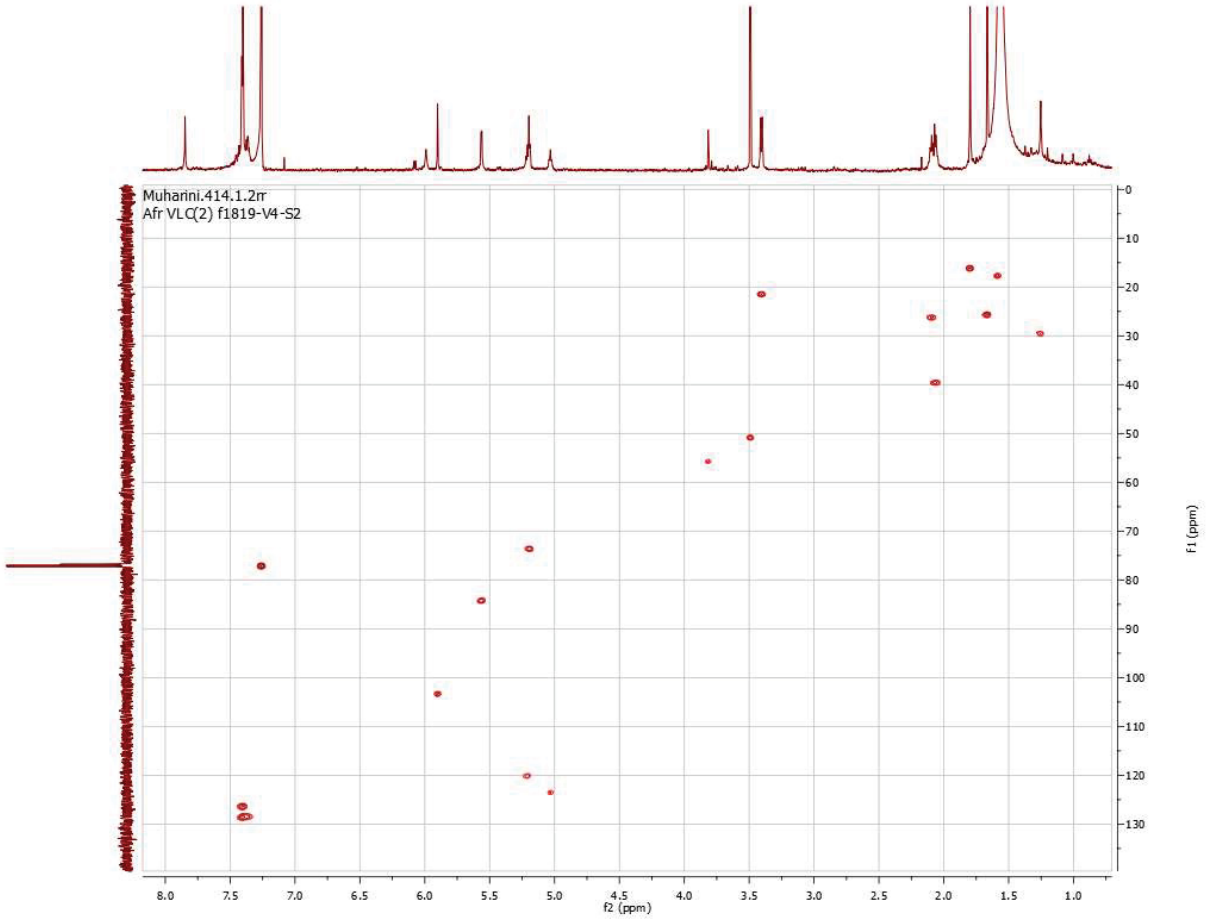

S27. HSQC (600 MHz, 150 MHz, $CDCl_3$) spectrum of the new compound **13**

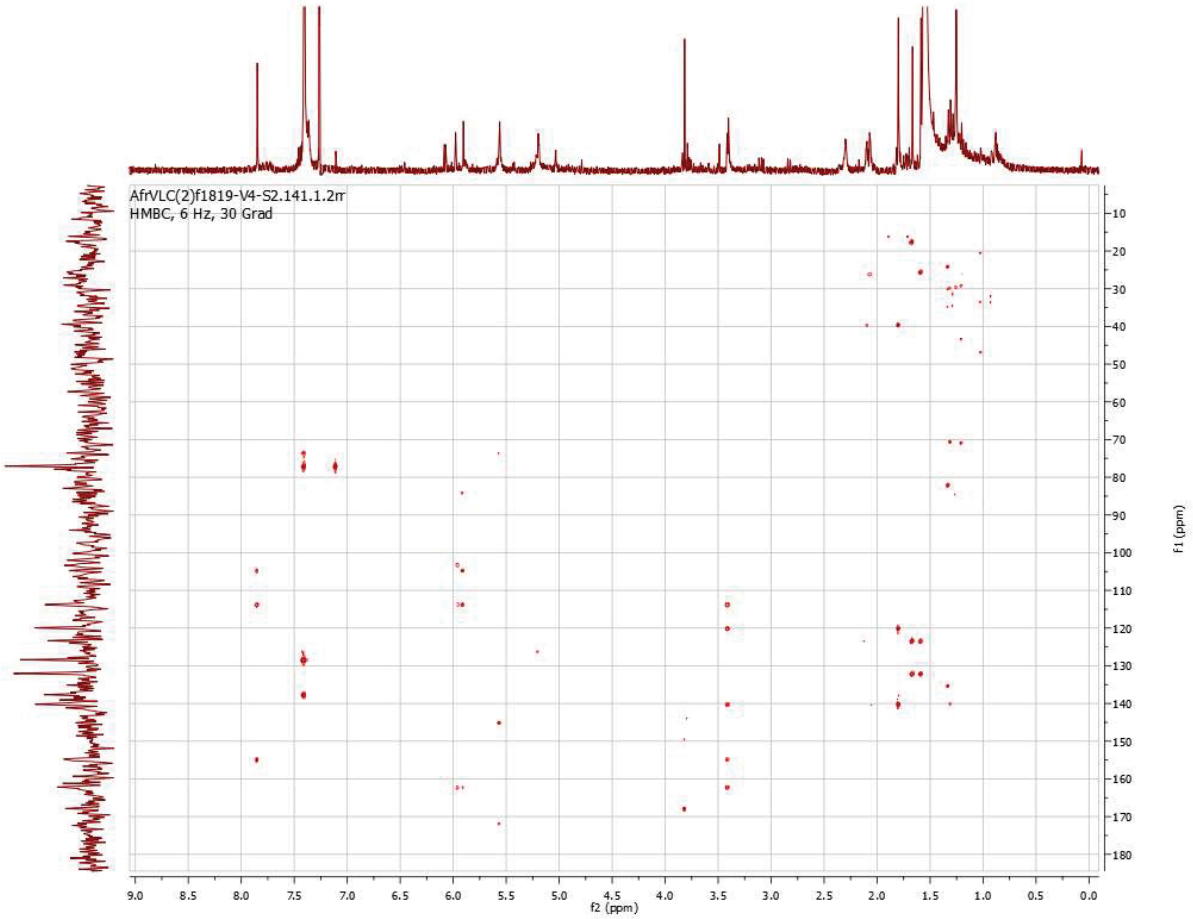

S28. HMBC (700 MHz, 175 MHz, $CDCl_3$) spectrum of the new compound **13**

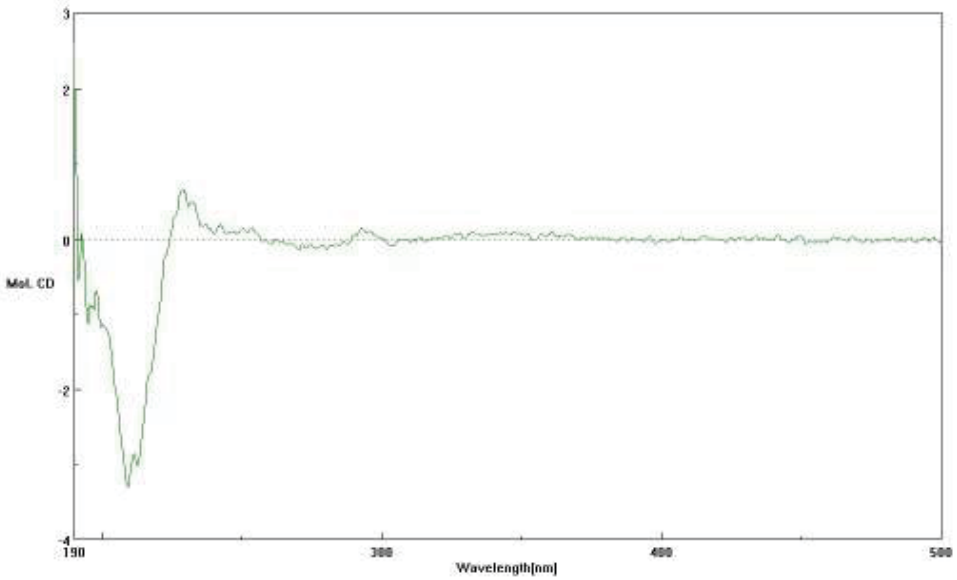

S29. CD spectrum of the new compound **13**

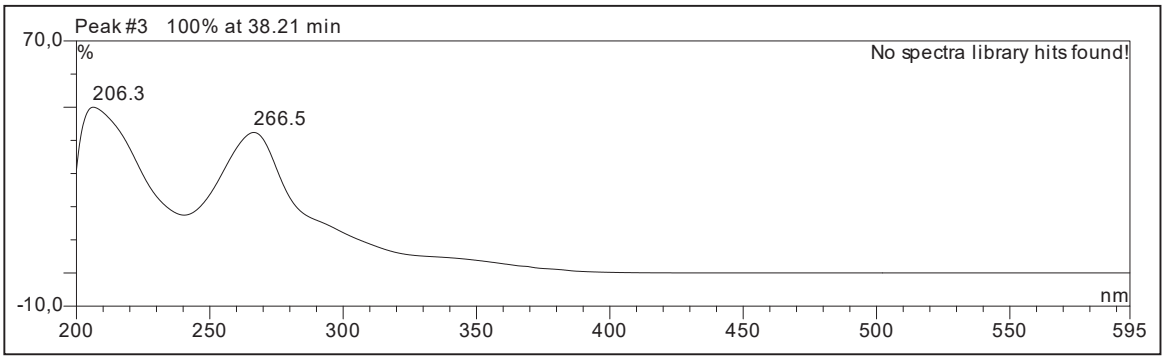

S30. UV spectrum of the new compound **14**

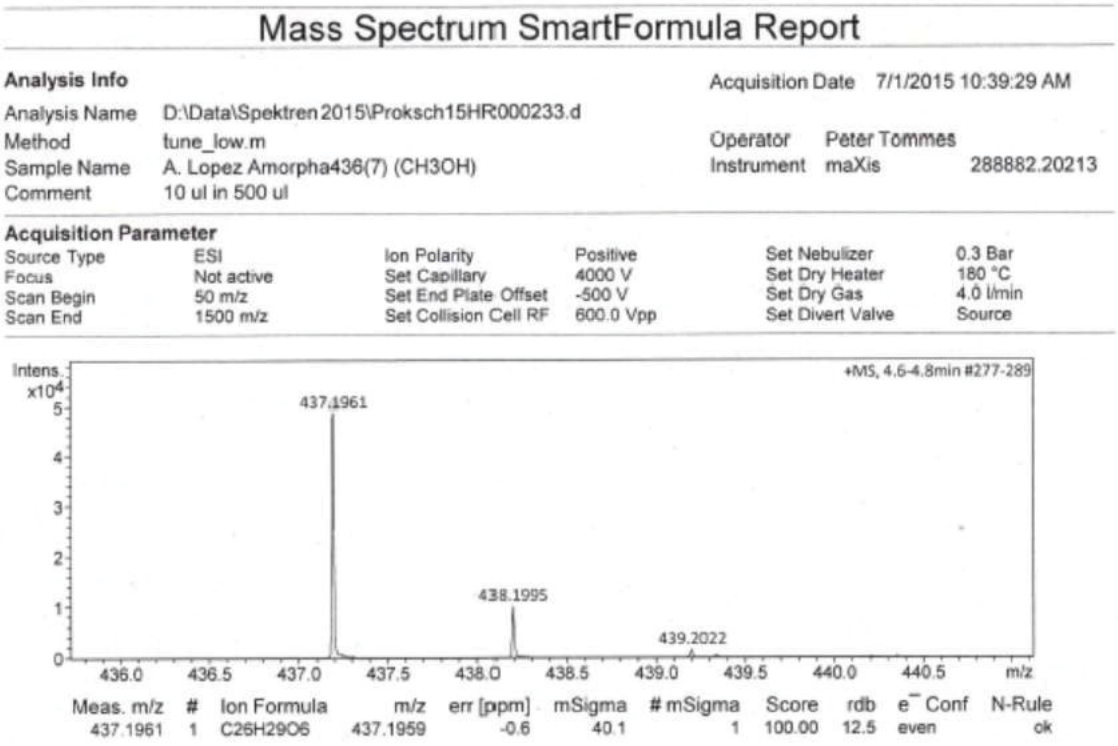

S31. HRESIMS of the new compound **14**

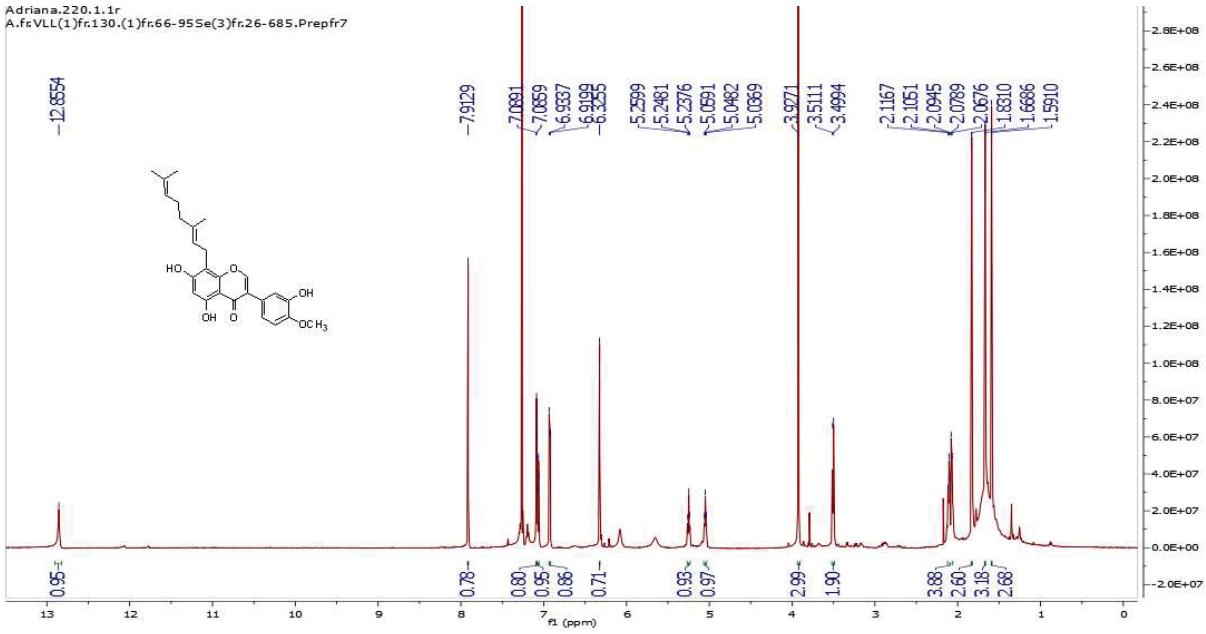

S32. ^{1}H NMR (600 MHz, $CDCl_3$) spectrum of the new compound **14**

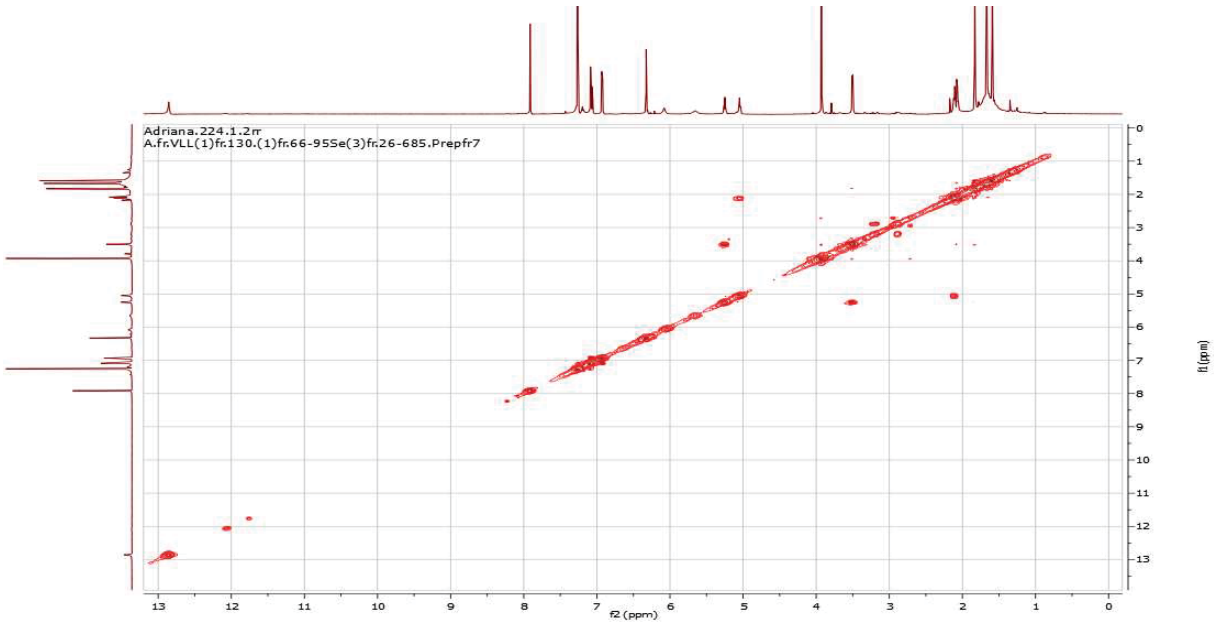

S33. ^{1}H-^{1}H COSY (600 MHz, $CDCl_3$) spectrum of the new compound **14**

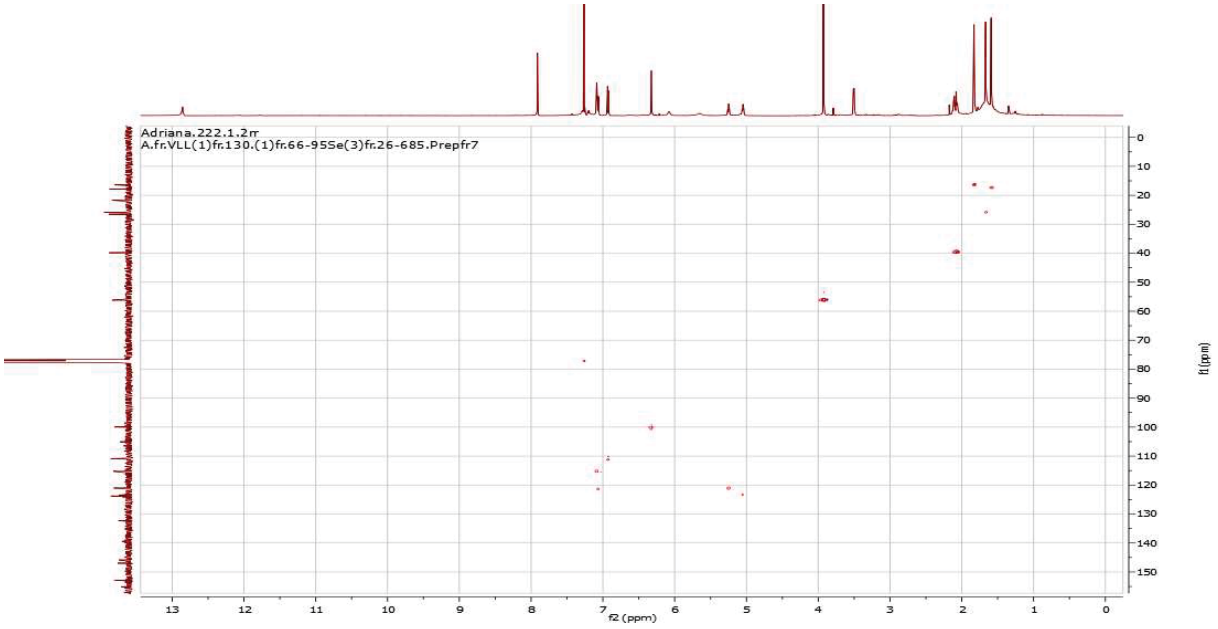

S34. HSQC (600 MHz, 150MHz, $CDCl_3$) spectrum of the new compound **14**

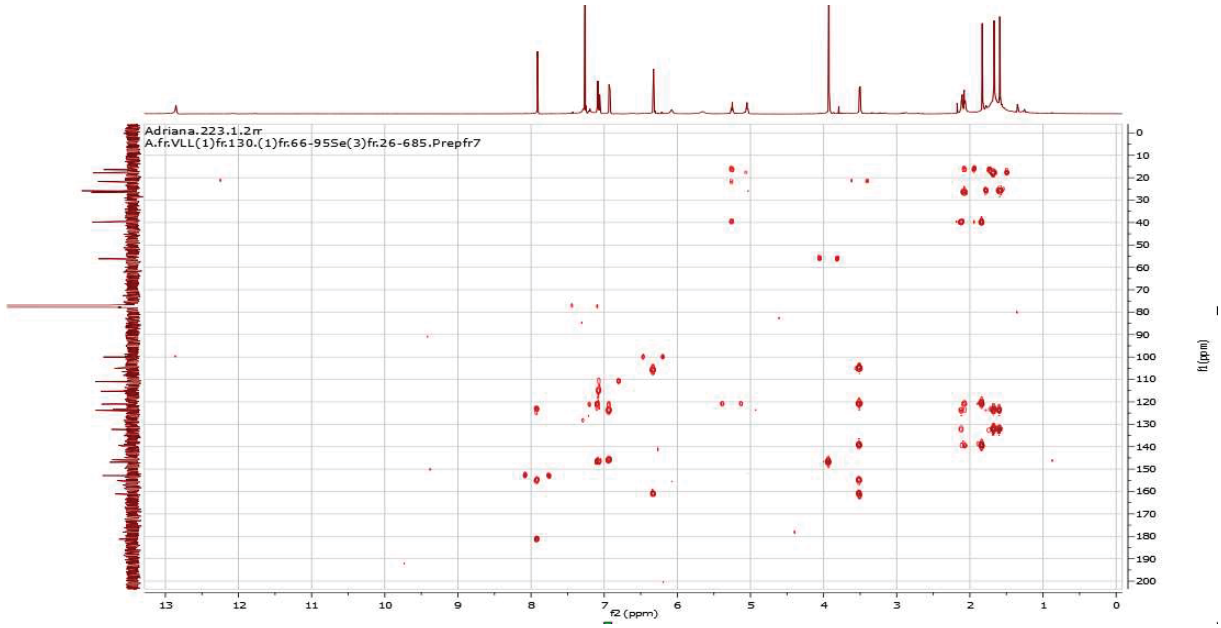

S35. HMBC (600 MHz, 150 MHz, $CDCl_3$) spectrum of the new compound **14**

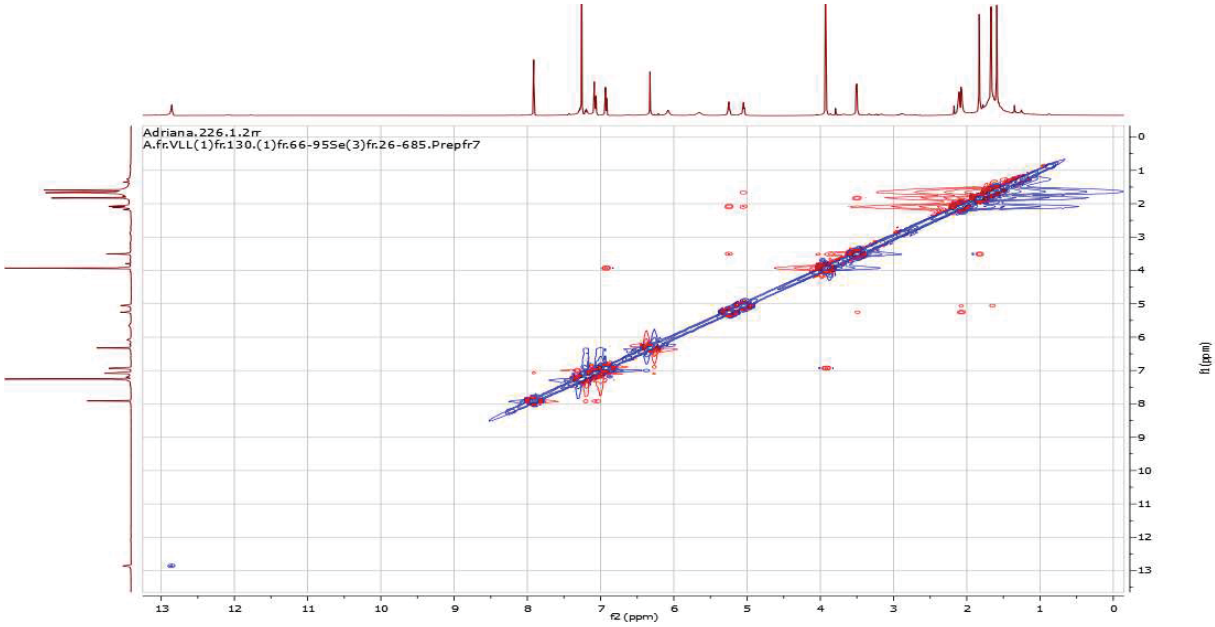

S36. ROESY (600 MHz, $CDCl_3$) spectrum of the new compound **14**

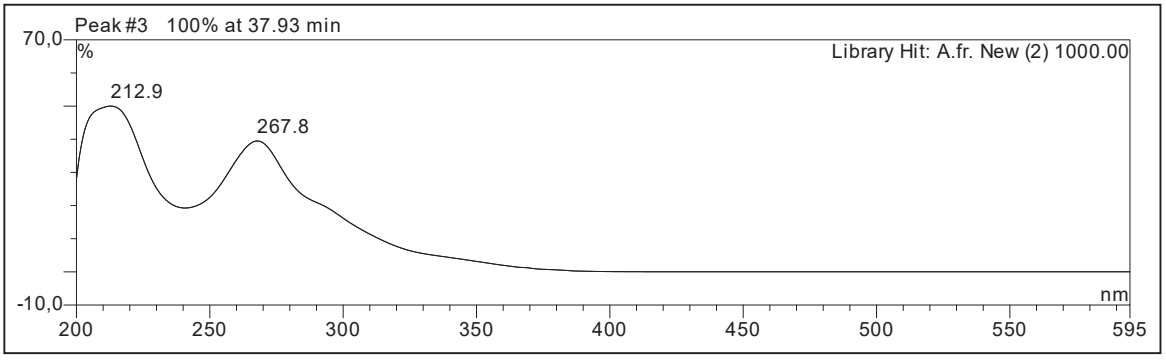

S37. UV spectrum of the new compound **15**

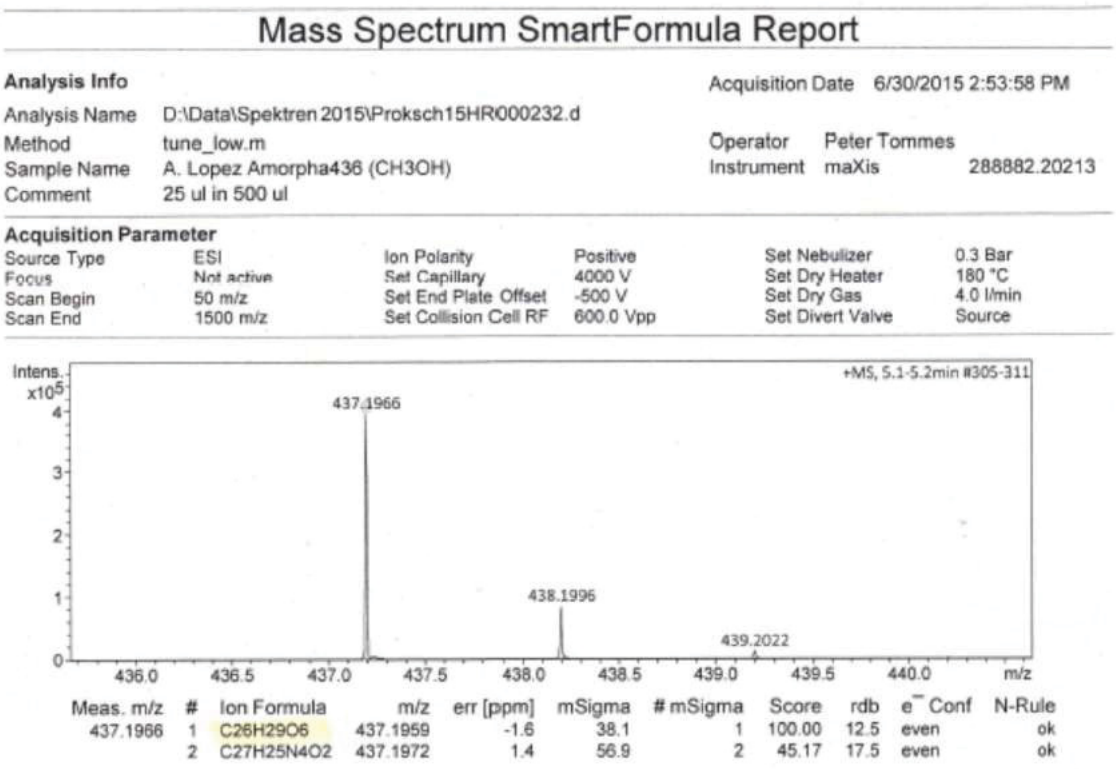

Mass Spectrum SmartFormula Report

Analysis Info

Analysis Name	D:\Data\Spektren 2015\Proksch15HR000232.d	Acquisition Date	6/30/2015 2:53:58 PM
Method	tune_low.m	Operator	Peter Tommes
Sample Name	A. Lopez Amorpha436 (CH3OH)	Instrument	maXis 288882.20213
Comment	25 ul in 500 ul		

Acquisition Parameter

Source Type	ESI	Ion Polarity	Positive	Set Nebulizer	0.3 Bar
Focus	Not active	Set Capillary	4000 V	Set Dry Heater	180 °C
Scan Begin	50 m/z	Set End Plate Offset	-500 V	Set Dry Gas	4.0 l/min
Scan End	1500 m/z	Set Collision Cell RF	600.0 Vpp	Set Divert Valve	Source

Meas. m/z	#	Ion Formula	m/z	err [ppm]	mSigma	# mSigma	Score	rdb	e⁻ Conf	N-Rule
437.1966	1	C26H29O6	437.1959	-1.6	38.1	1	100.00	12.5	even	ok
	2	C27H25N4O2	437.1972	1.4	56.9	2	45.17	17.5	even	ok

S38. HRESIMS of the new compound **15**

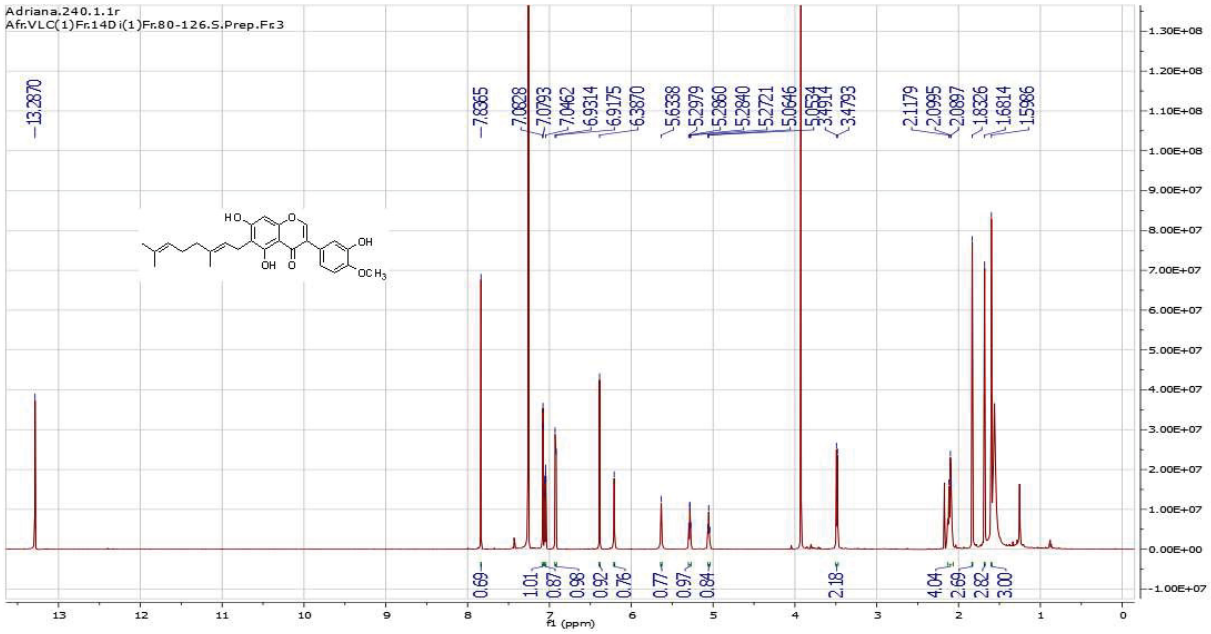

S39. ^{1}H NMR (600 MHz, $CDCl_3$) spectrum of the new compound **15**

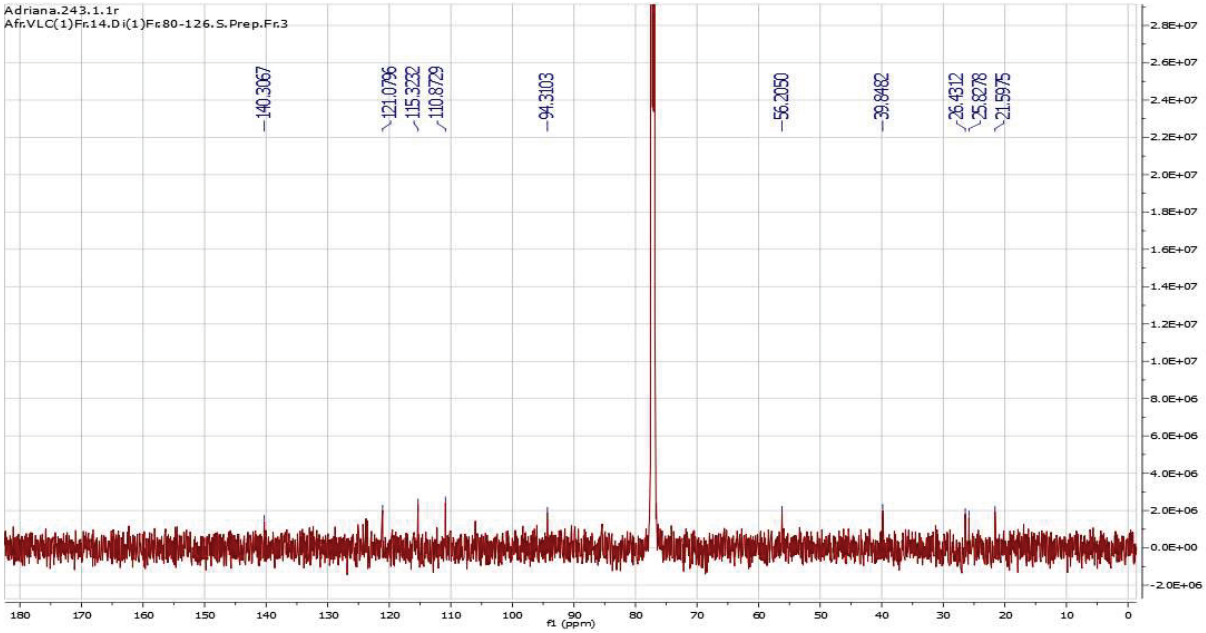

S40. ^{13}C NMR (150 MHz, $CDCl_3$) spectrum of the new compound **15**

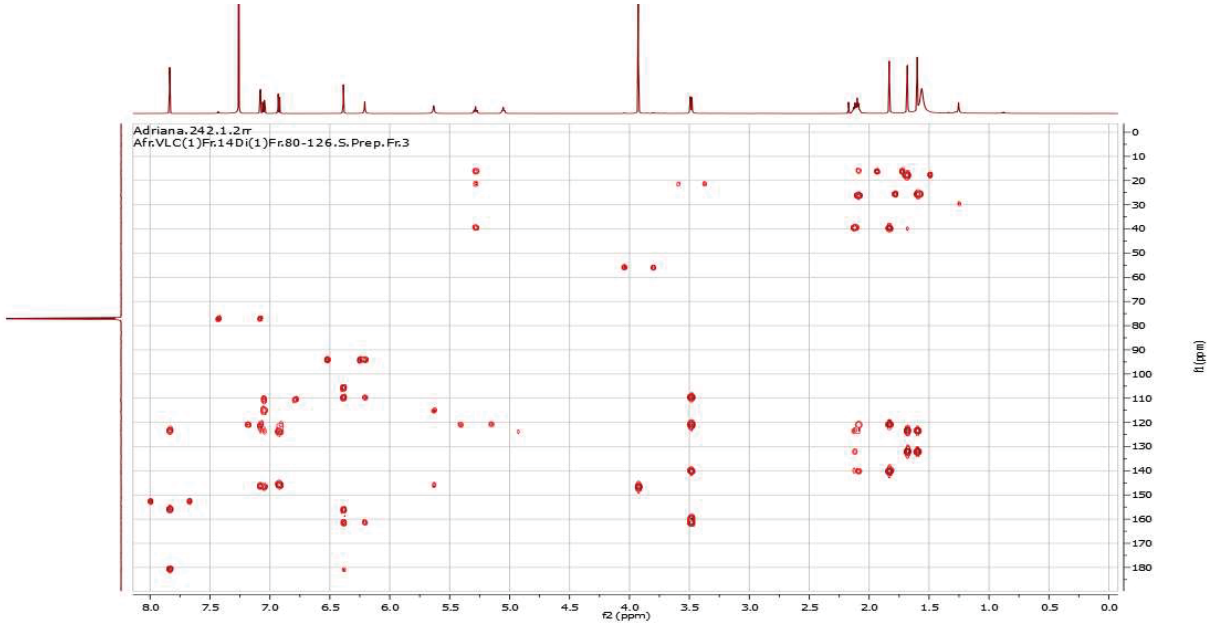

S41. HMBC (600 MHz, 150 MHz, $CDCl_3$) spectrum of the new compound **15**

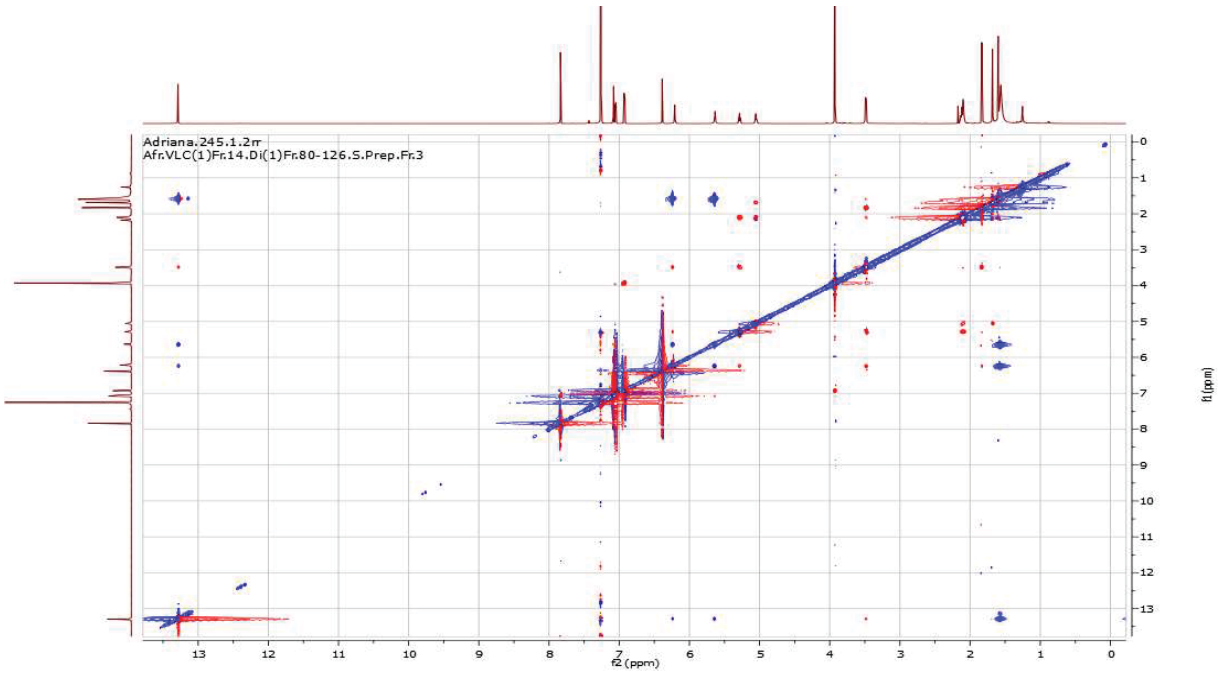

S42. ROESY (600 MHz, $CDCl_3$) spectrum of the new compound **15**

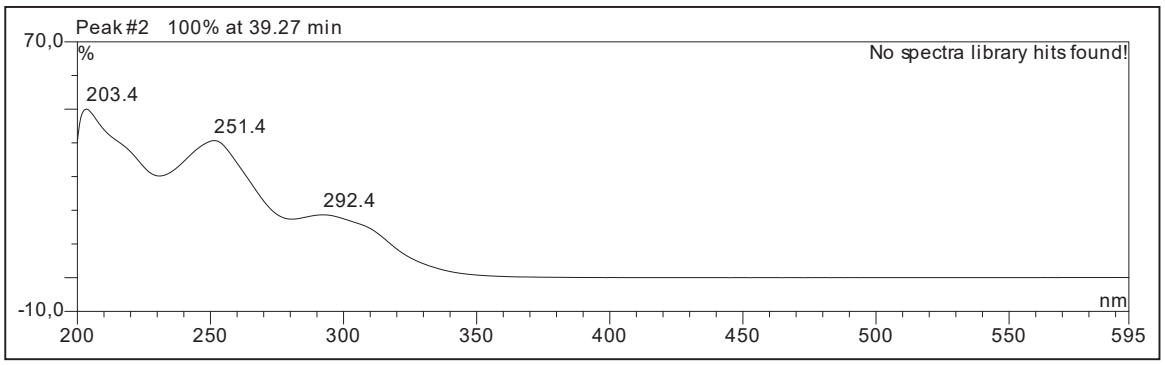

S43. UV spectrum of the new compound **16**

Mass Spectrum SmartFormula Report

Analysis Info

Analysis Name	D:\Data\Spektren 2015\Proksch15HR000375.d	Acquisition Date	10/21/2015 12:57:38 PM
Method	tune_low.m	Operator	Peter Tommes
Sample Name	R. Muharini Afr VLC(2) f17-Se8-S3 (CH3OH)	Instrument	maXis 288882.20213
Comment	2,5 ul in 1000 ul		

Acquisition Parameter

Source Type	ESI	Ion Polarity	Positive	Set Nebulizer	0.3 Bar
Focus	Not active	Set Capillary	4000 V	Set Dry Heater	180 °C
Scan Begin	50 m/z	Set End Plate Offset	-500 V	Set Dry Gas	4.0 l/min
Scan End	1500 m/z	Set Collision Cell RF	600.0 Vpp	Set Divert Valve	Source

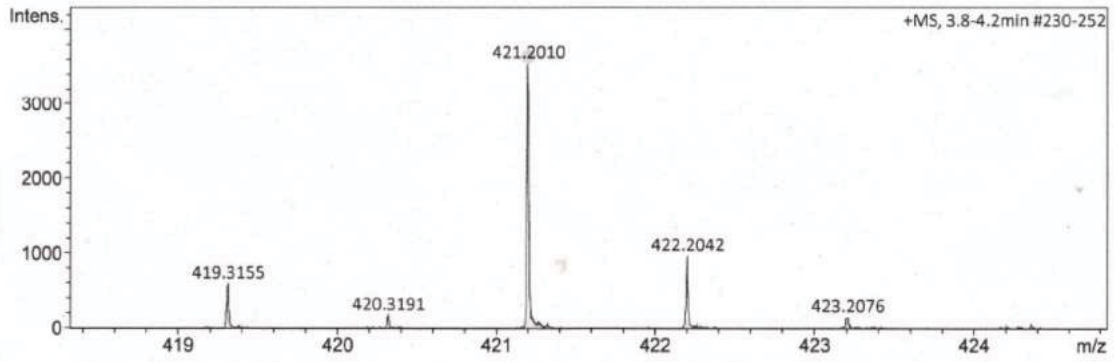

Meas. m/z	#	Ion Formula	m/z	err [ppm]	mSigma	# mSigma	Score	rdb	e⁻ Conf	N-Rule
421.2010	1	C26H29O5	421.2010	-0.1	10.0	1	100.00	12.5	even	ok

S44. HRESIMS of the new compound **16**

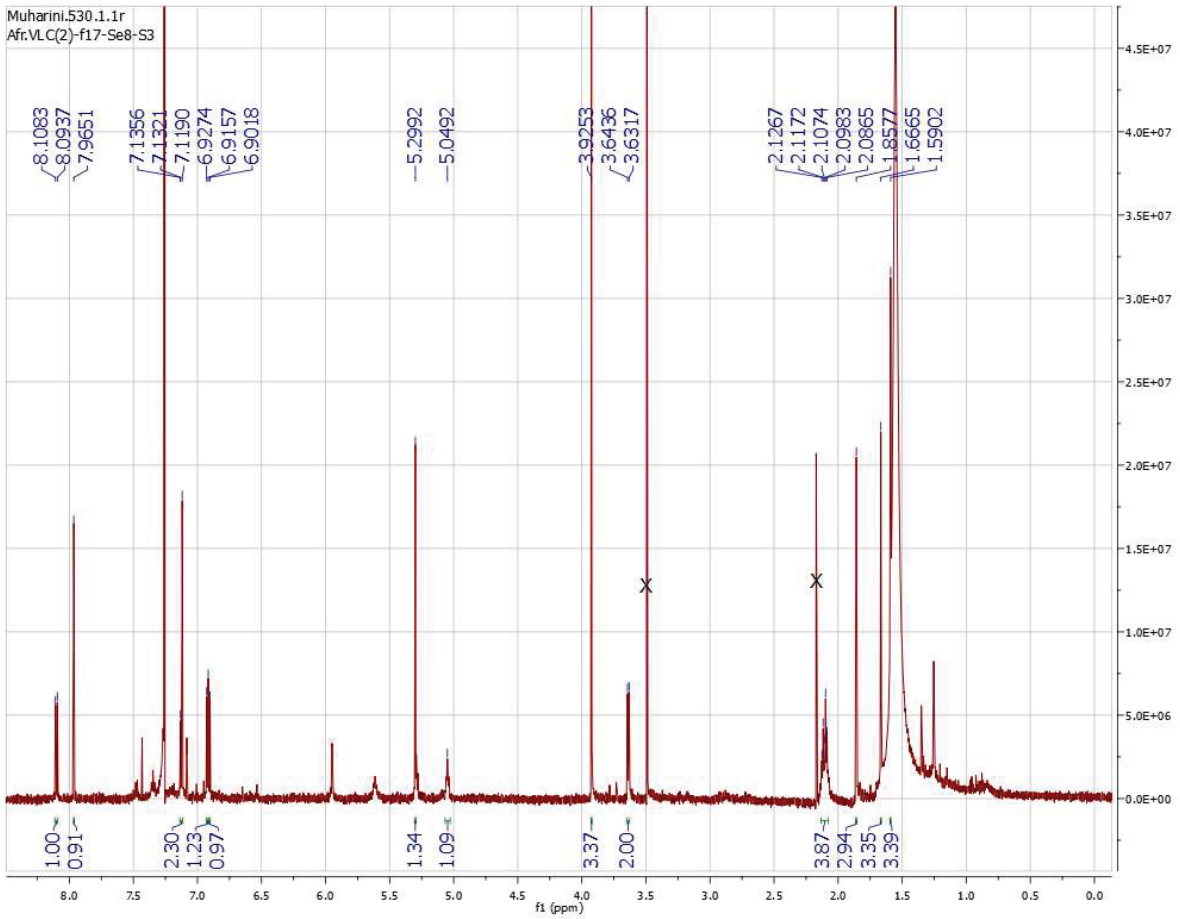

S45. ^{1}H NMR (600 MHz, $CDCl_3$) spectrum of the new compound **16**

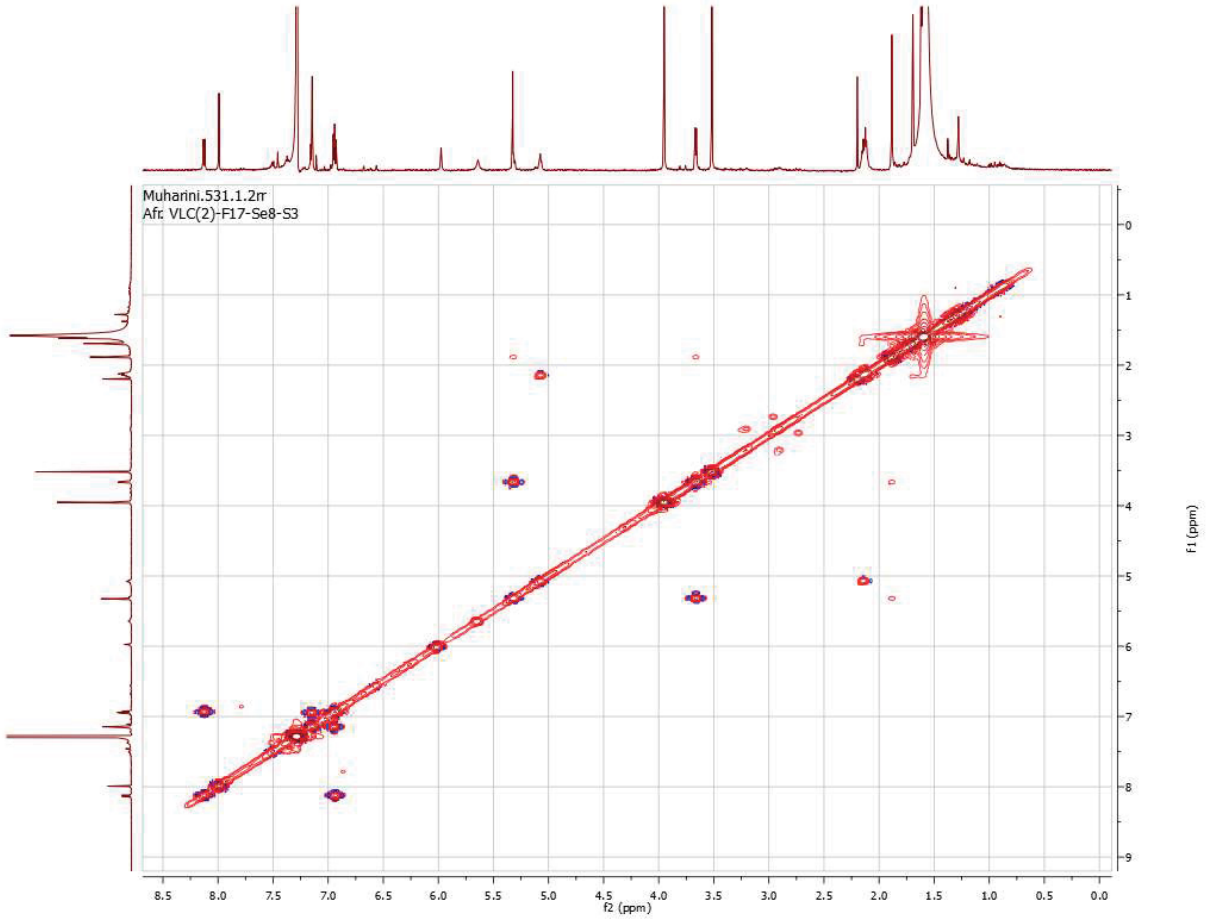

S46. ^{1}H-^{1}H COSY (600 MHz, $CDCl_3$) spectrum of the new compound **16**

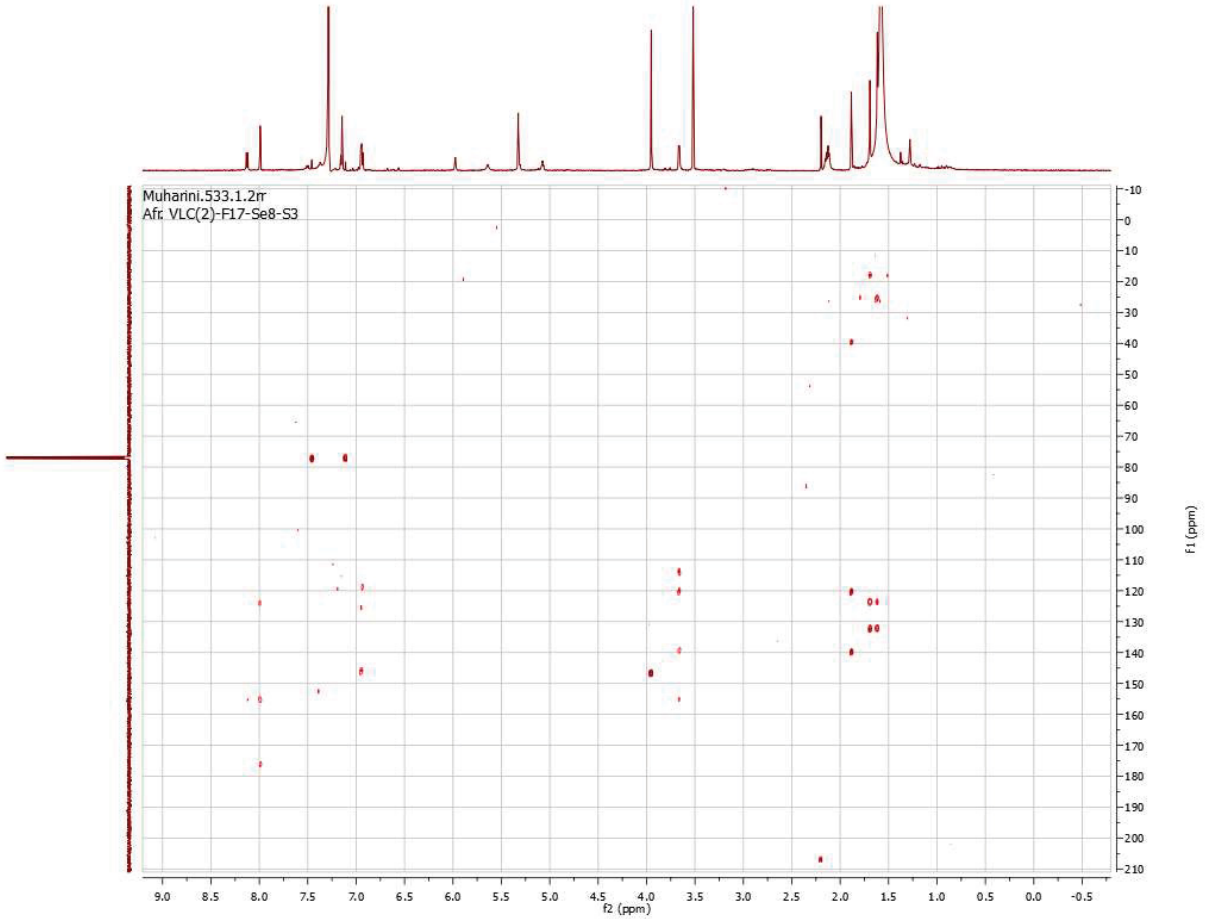

S47. HMBC (600 MHz, 150 MHz, $CDCl_3$) spectrum of the new compound **16**

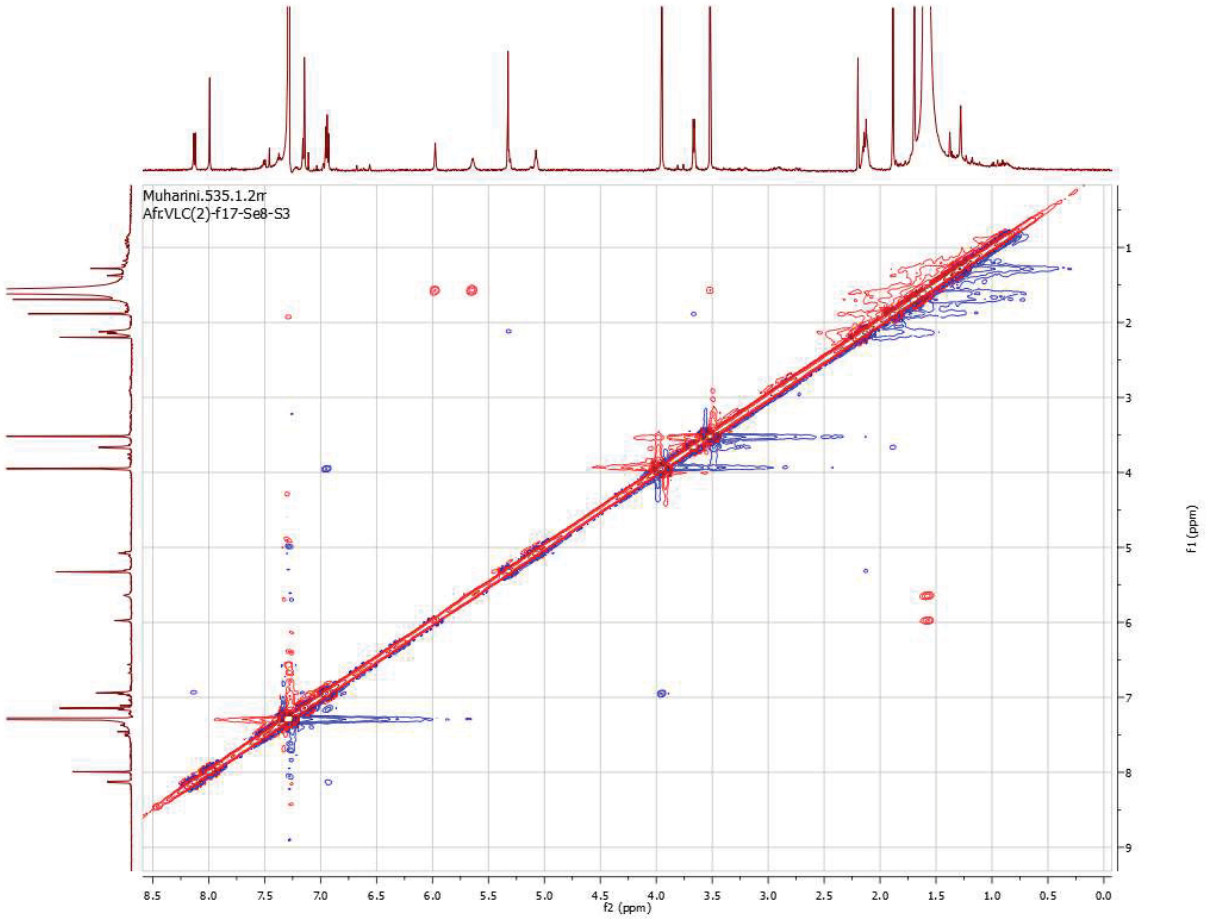

S48. ROESY (600 MHz, $CDCl_3$) spectrum of the new compound **16**

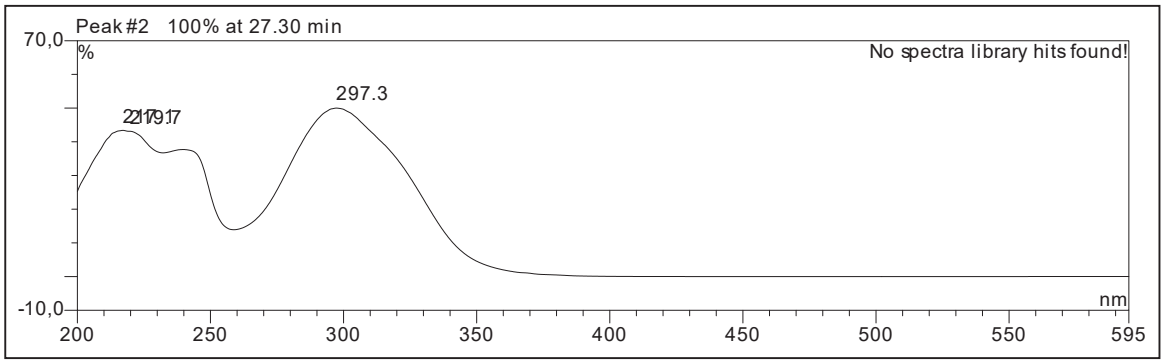

S49. UV spectrum of the new compound **42**

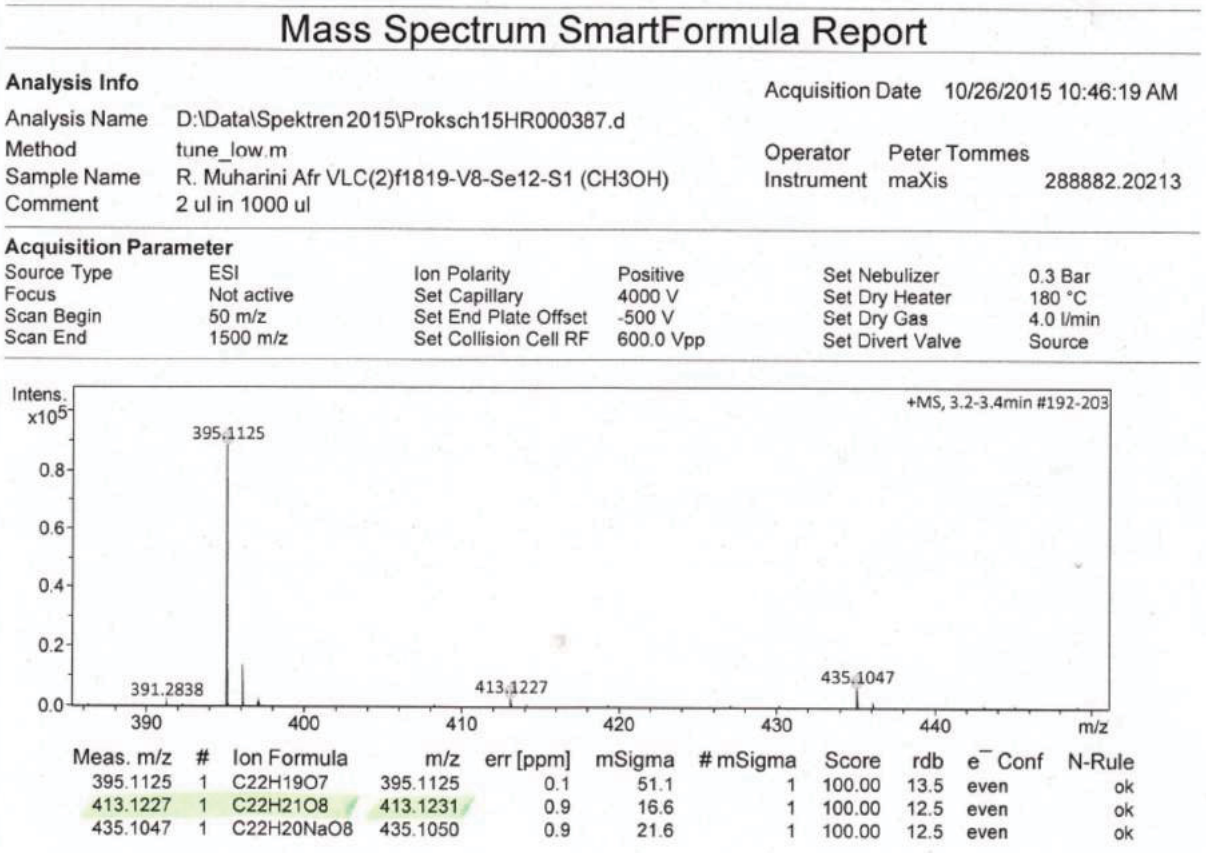

S50. HRESIMS of the new compound **42**

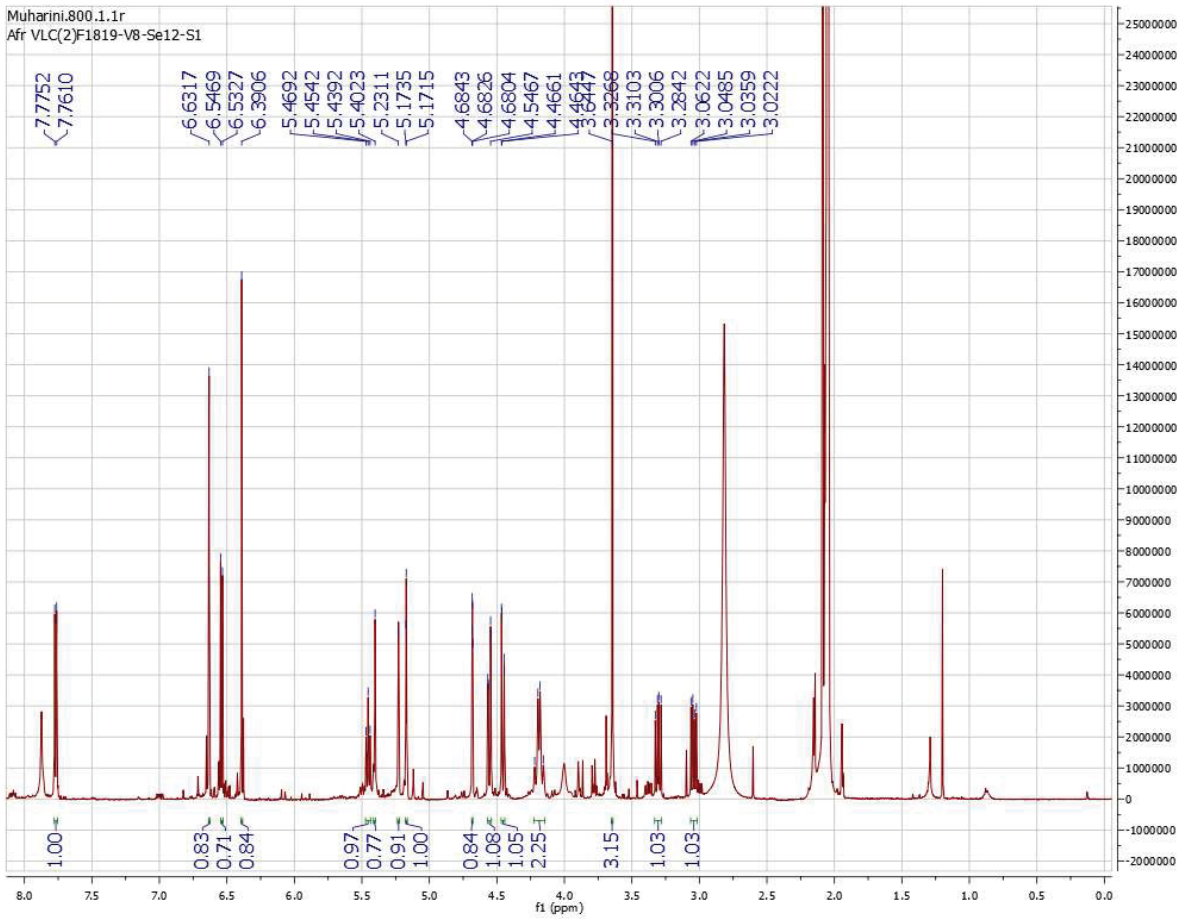

S51. ^{1}H NMR (600 MHz, $(CD_3)_2CO$) spectrum of the new compound **42**

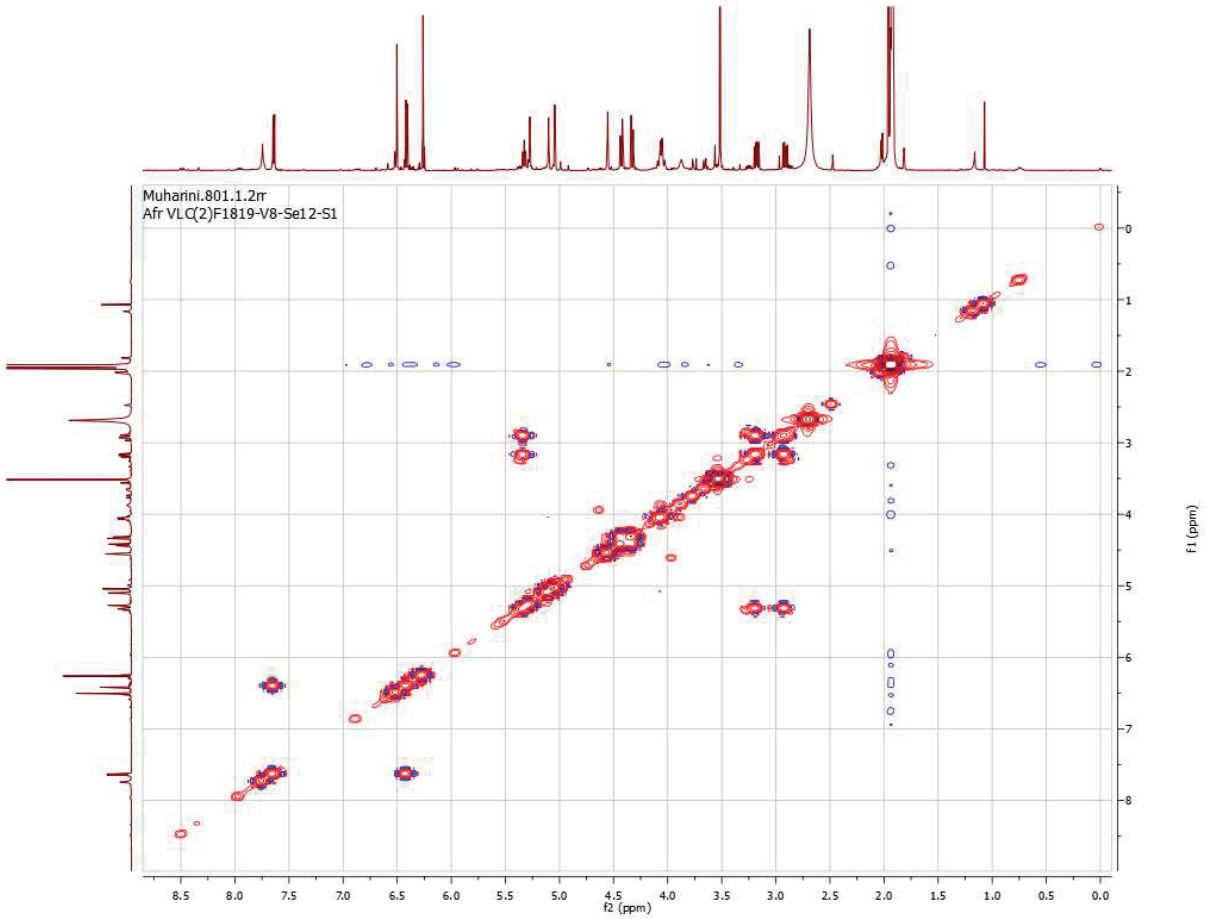

S52. ^{1}H-^{1}H COSY (600 MHz, $(CD_3)_2CO$) spectrum of the new compound **42**

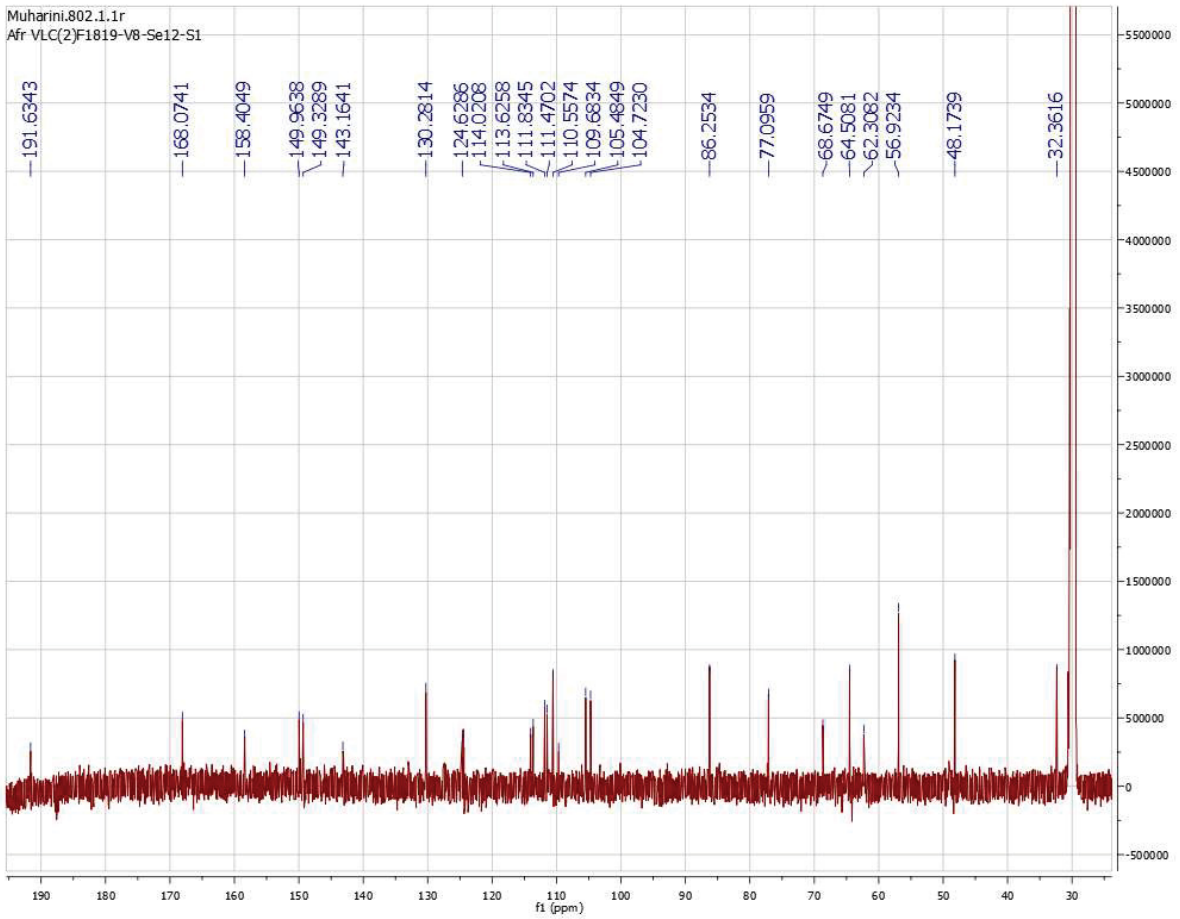

S53. ^{13}C NMR (150 MHz, $(CD_3)_2CO$) spectrum of the new compound **42**

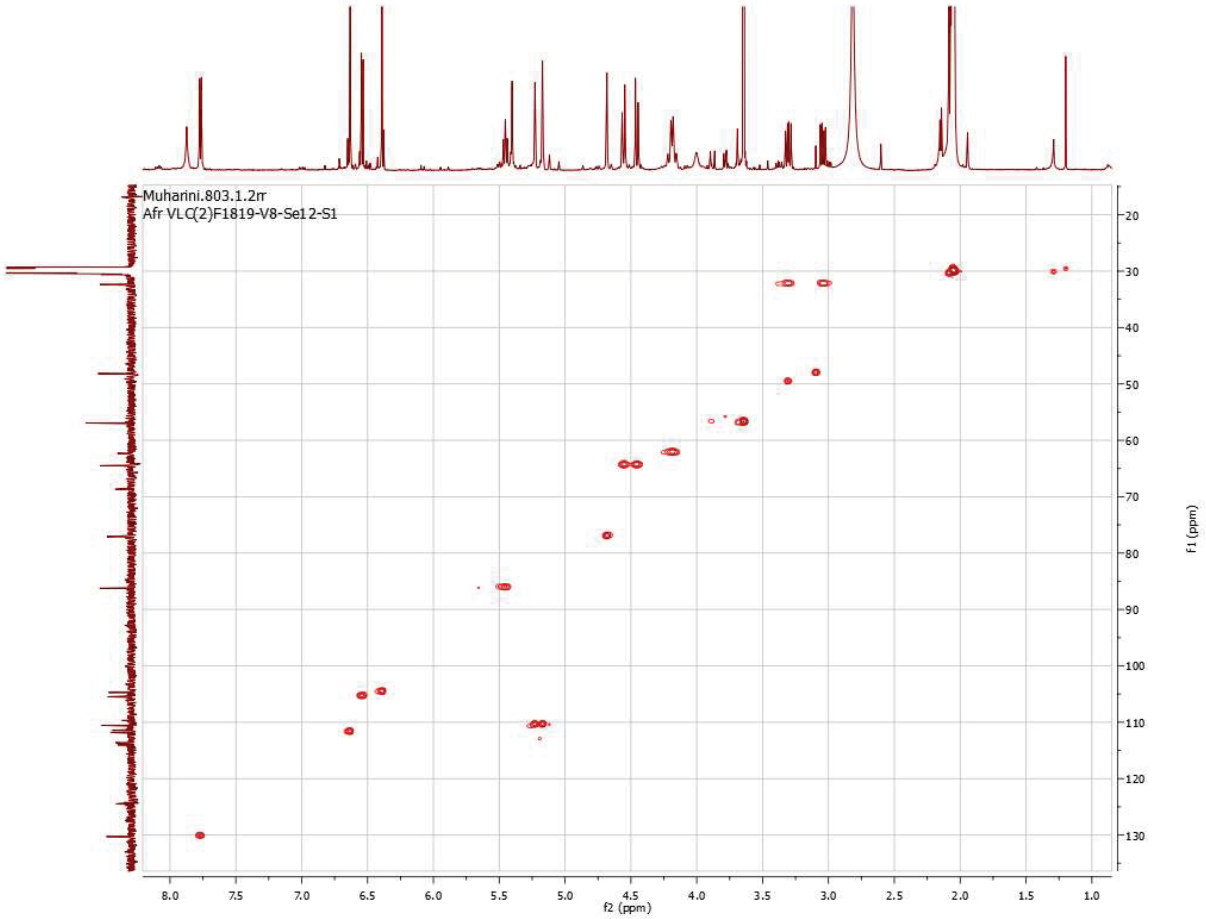

S54. HSQC (600 MHz, 150 MHz, $(CD_3)_2CO$) spectrum of the new compound **42**

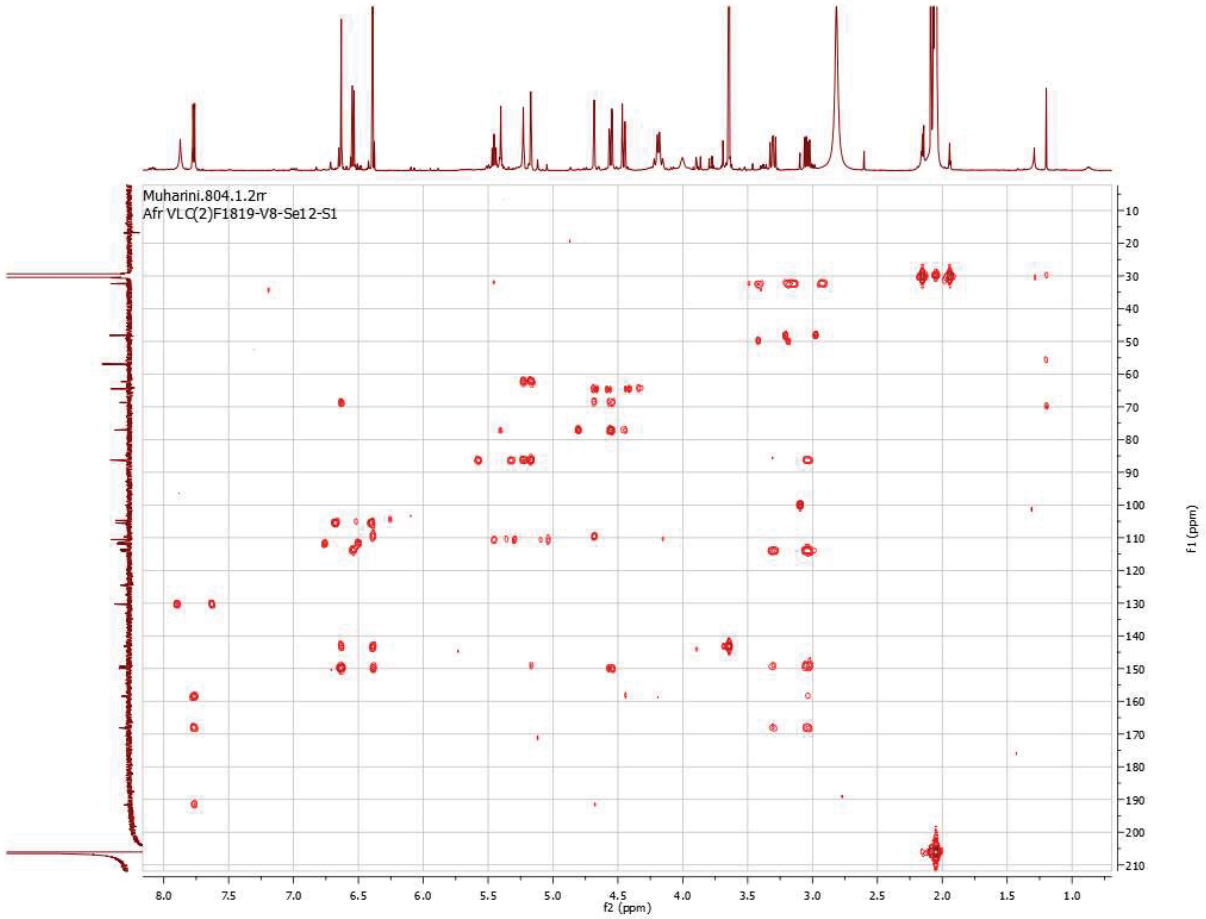

S55. HMBC (600 MHz, 150 MHz, $(CD_3)_2CO$) spectrum of the new compound **42**

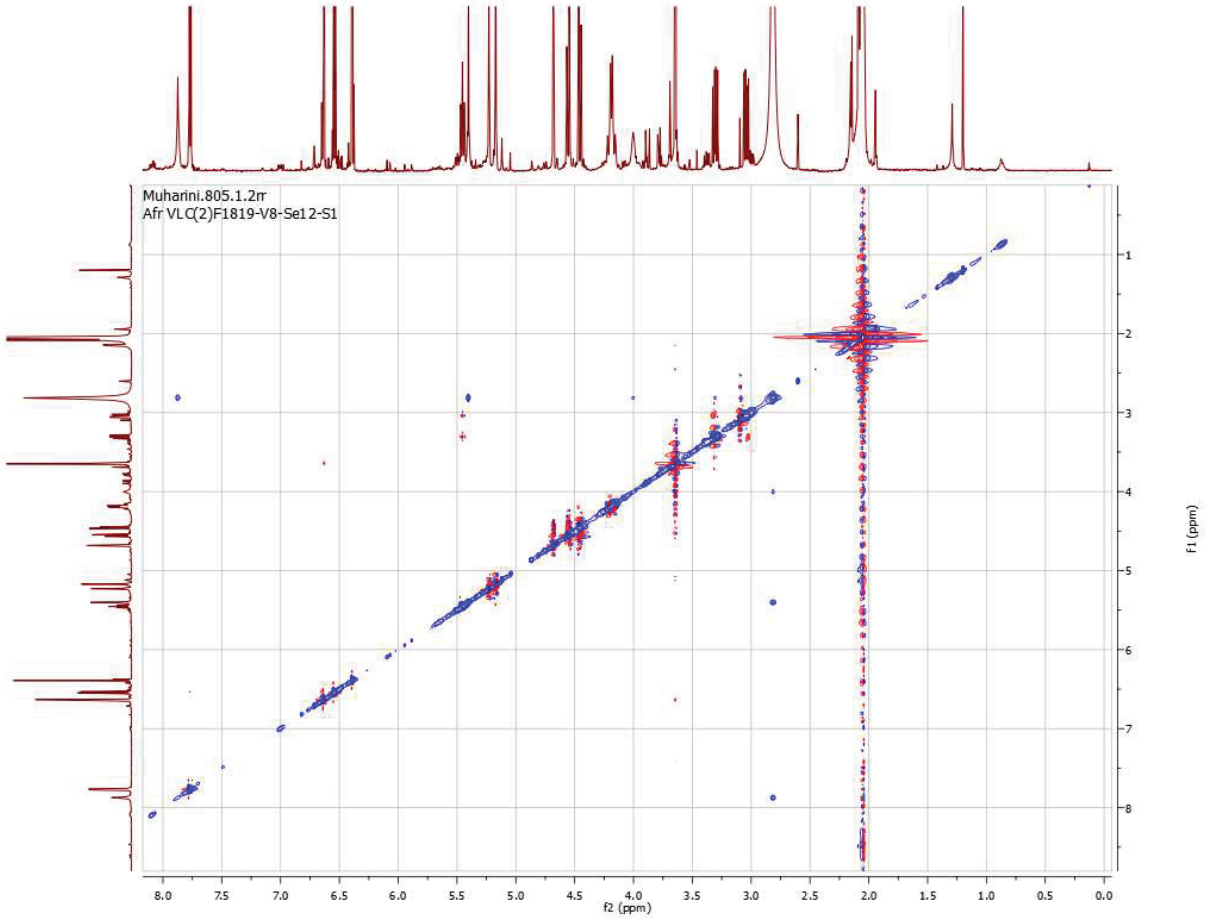

S56. ROESY (600 MHz, $(CD_3)_2CO$) spectrum of the new compound **42**

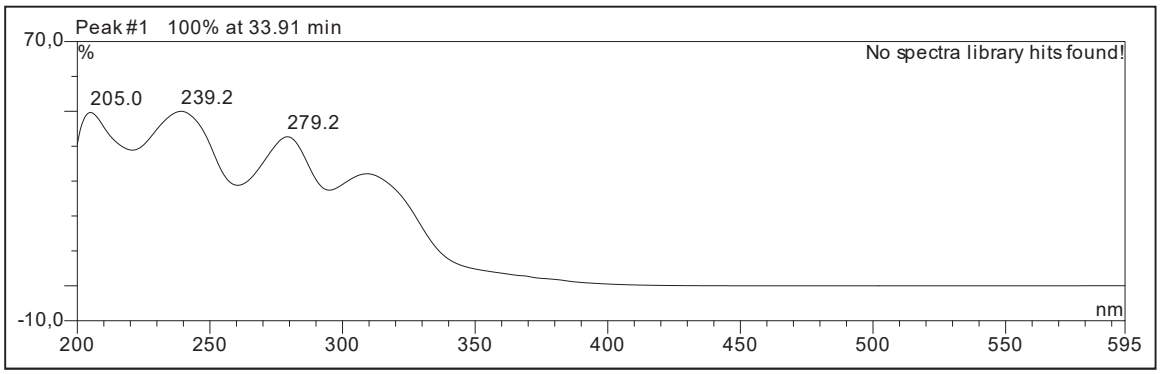

S57. UV spectrum of the new compound **43**

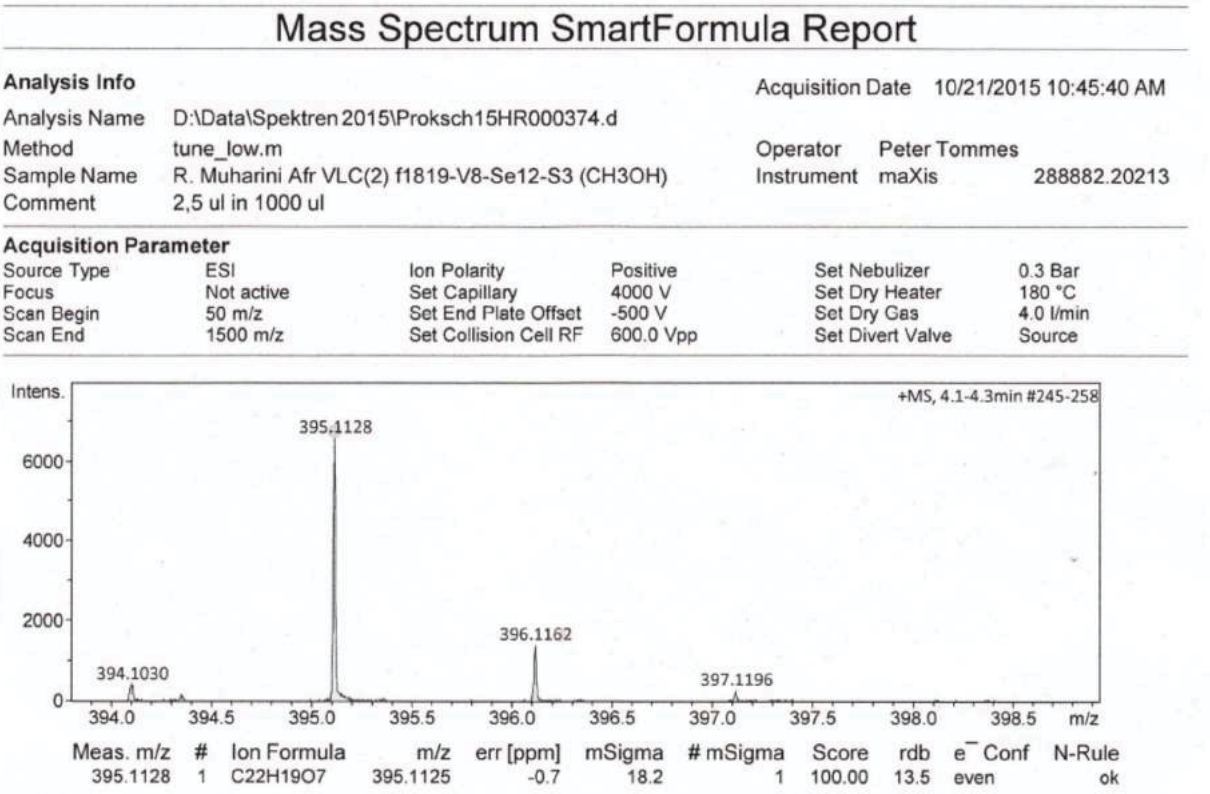

Mass Spectrum SmartFormula Report

Analysis Info

Analysis Name	D:\Data\Spektren 2015\Proksch15HR000374.d	Acquisition Date	10/21/2015 10:45:40 AM
Method	tune_low.m	Operator	Peter Tommes
Sample Name	R. Muharini Afr VLC(2) f1819-V8-Se12-S3 (CH3OH)	Instrument	maXis 288882.20213
Comment	2,5 ul in 1000 ul		

Acquisition Parameter

Source Type	ESI	Ion Polarity	Positive	Set Nebulizer	0.3 Bar
Focus	Not active	Set Capillary	4000 V	Set Dry Heater	180 °C
Scan Begin	50 m/z	Set End Plate Offset	-500 V	Set Dry Gas	4.0 l/min
Scan End	1500 m/z	Set Collision Cell RF	600.0 Vpp	Set Divert Valve	Source

Meas. m/z	#	Ion Formula	m/z	err [ppm]	mSigma	# mSigma	Score	rdb	e⁻ Conf	N-Rule
395.1128	1	C22H19O7	395.1125	-0.7	18.2	1	100.00	13.5	even	ok

S58. HRESIMS of the new compound **43**

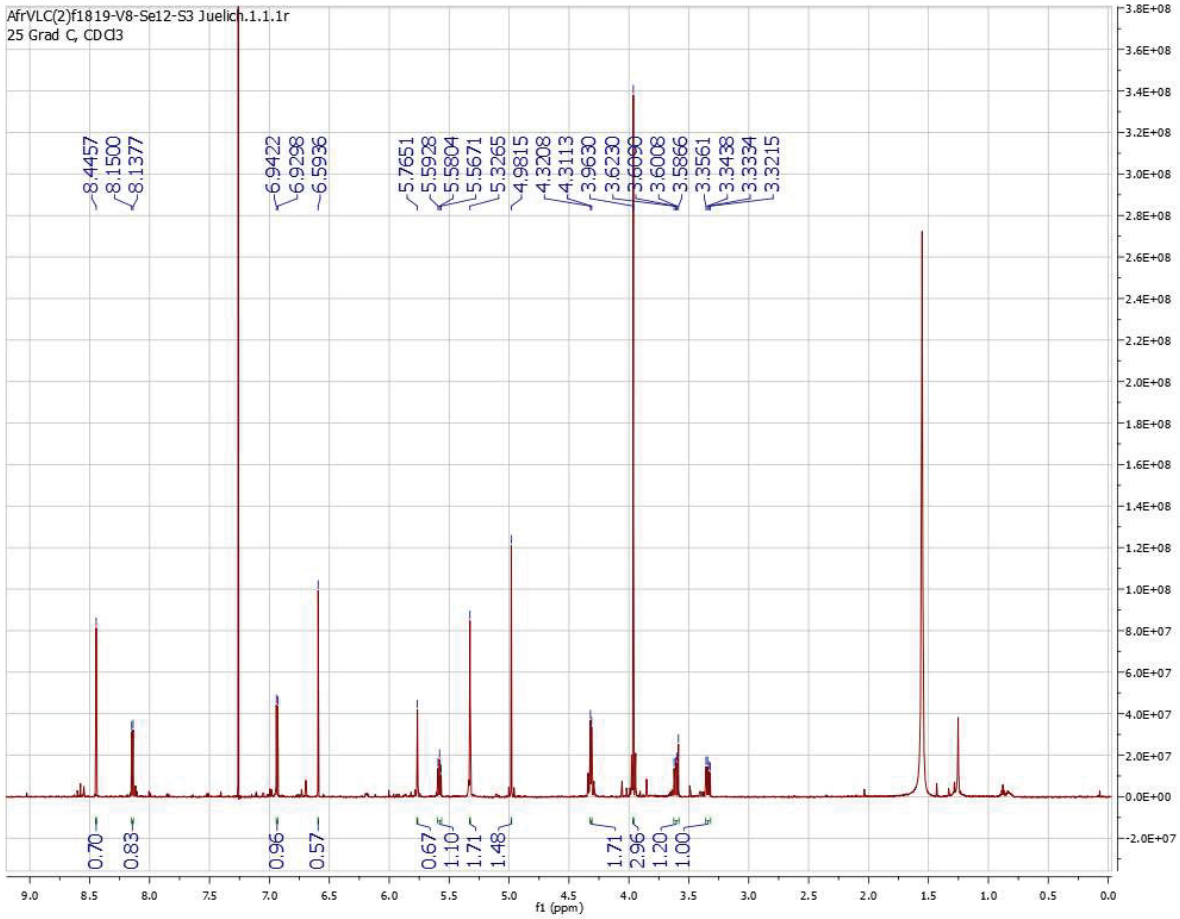

S59. ^{1}H NMR (700 MHz, $CDCl_3$) spectrum of the new compound **43**

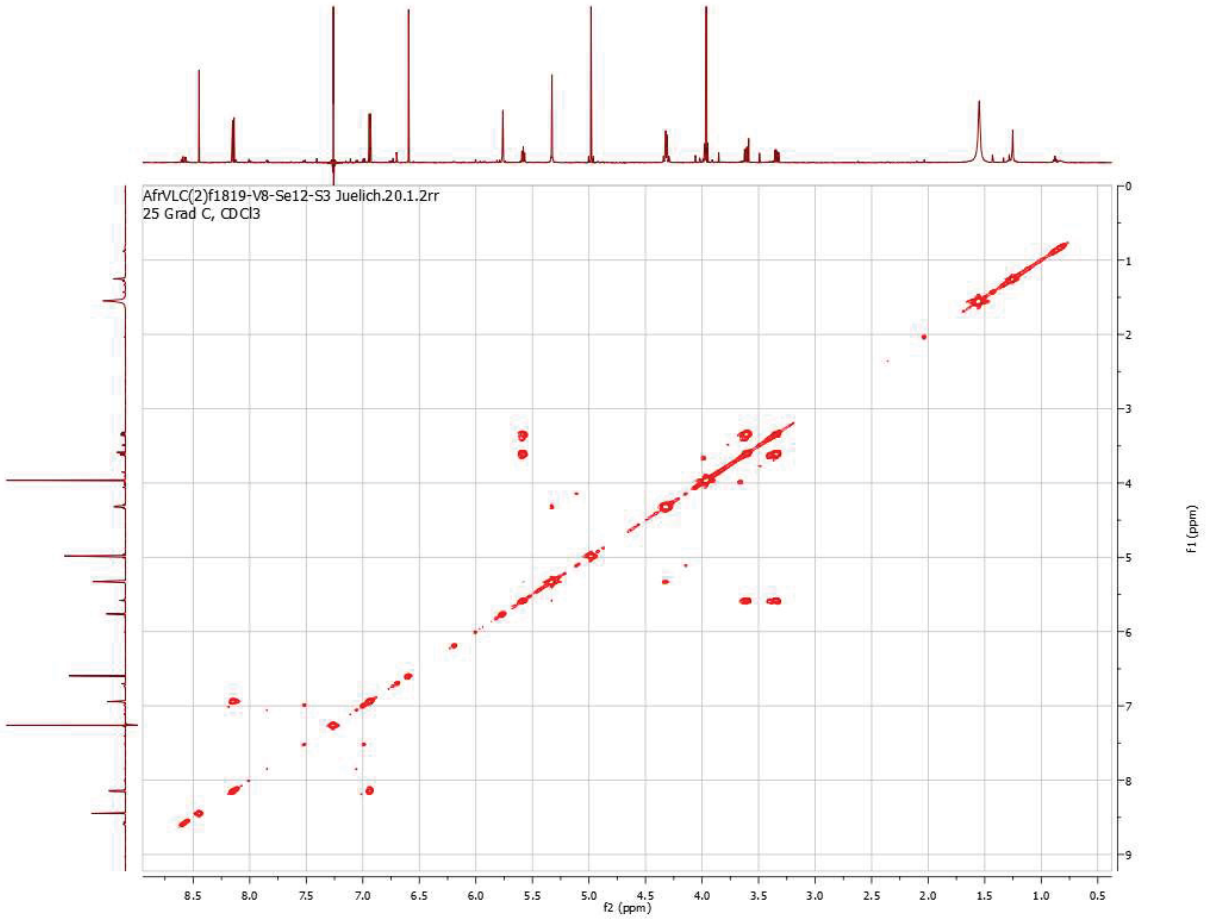

S60. ^{1}H-^{1}H COSY (700 MHz, $CDCl_3$) spectrum of the new compound **43**

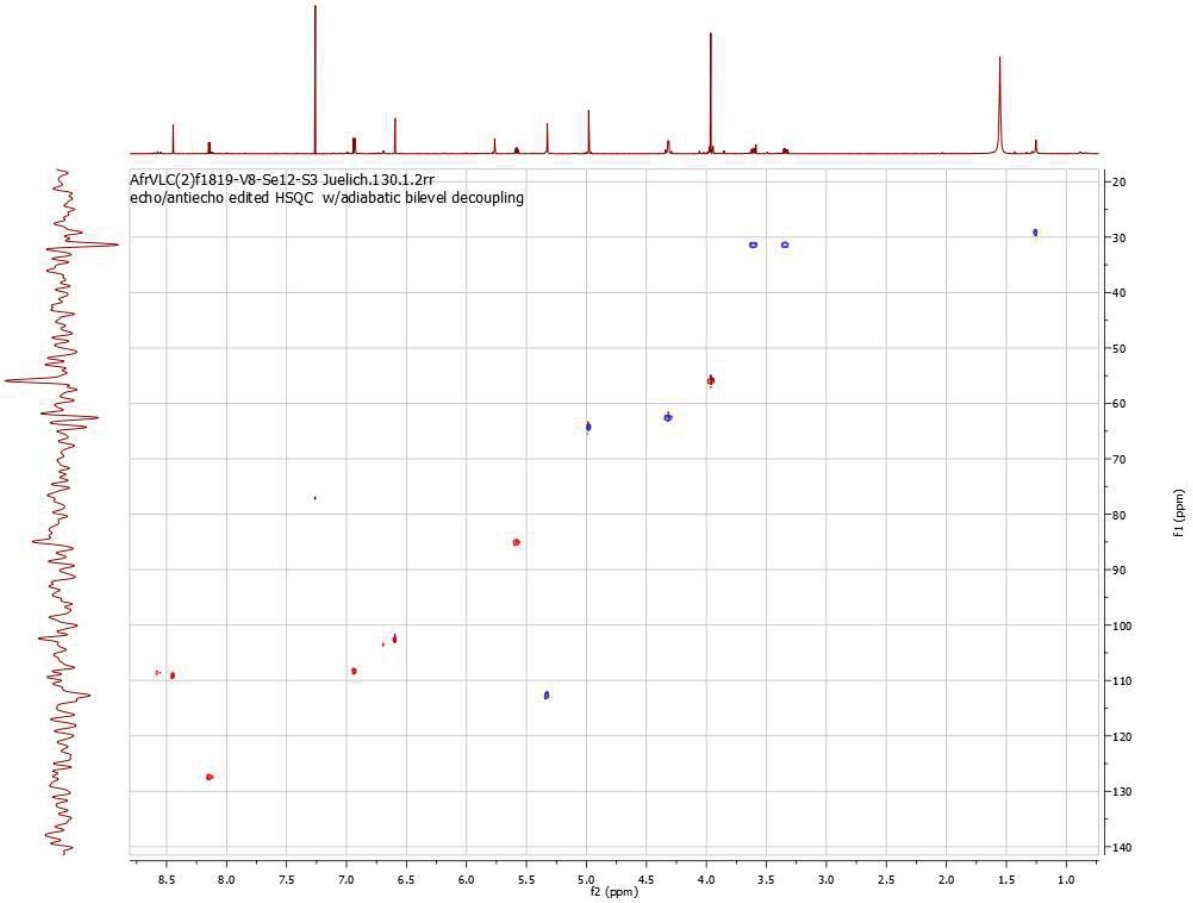

S61. HSQC (700 MHz, 175 MHz, $CDCl_3$) spectrum of the new compound **43**

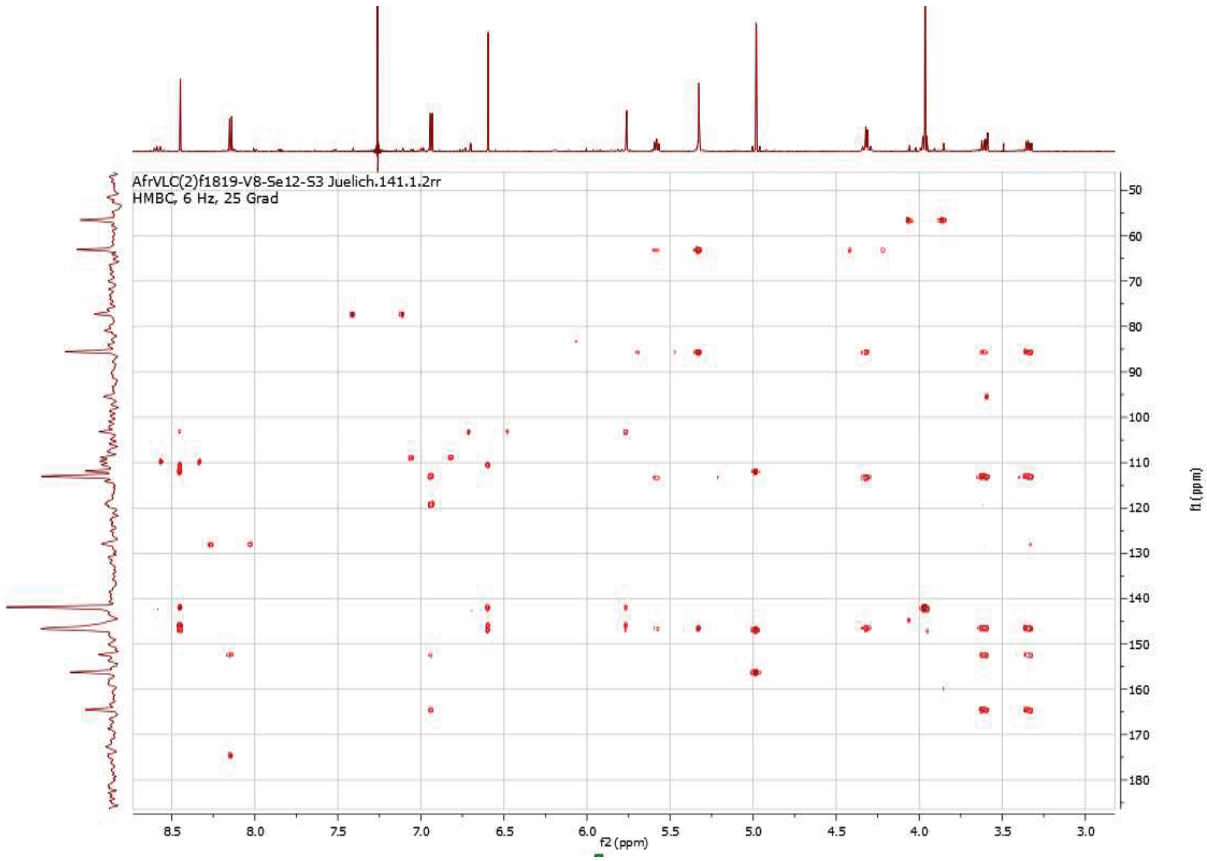

S62. HMBC (700 MHz, 175 MHz, $CDCl_3$) spectrum of the new compound **43**

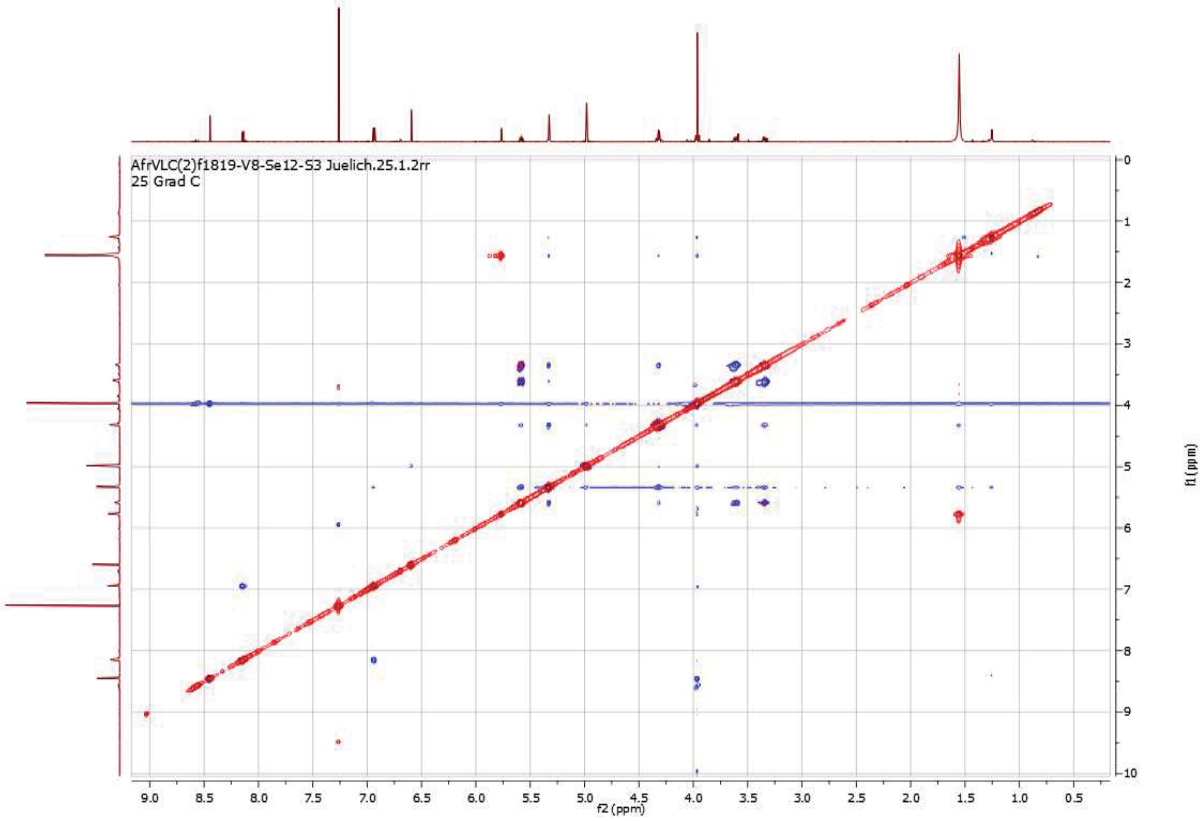

S63. ROESY (700 MHz, $CDCl_3$) spectrum of the new compound **43**

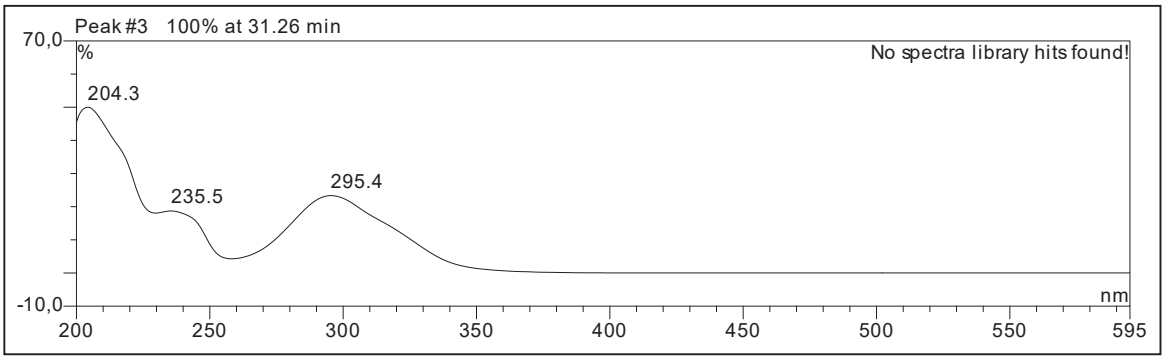

S64. UV spectrum of the new compound **44**

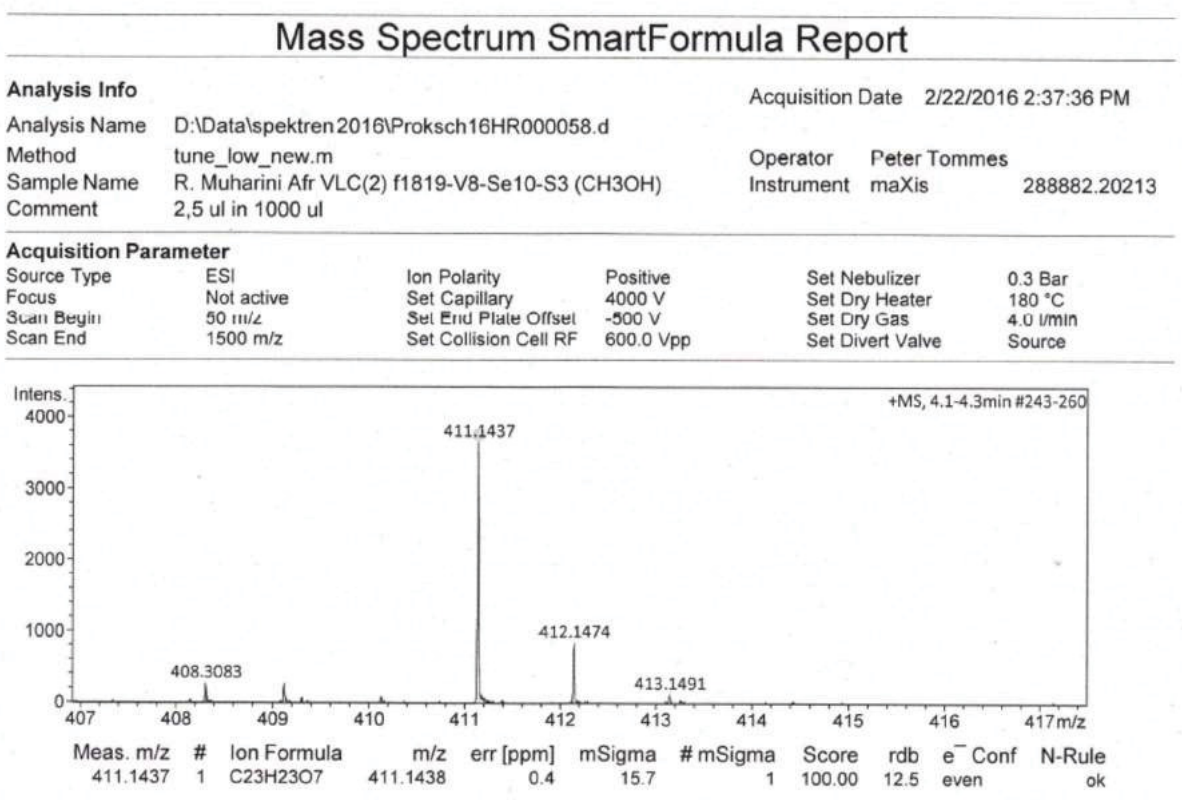

S65. HRESIMS of the new compound **44**

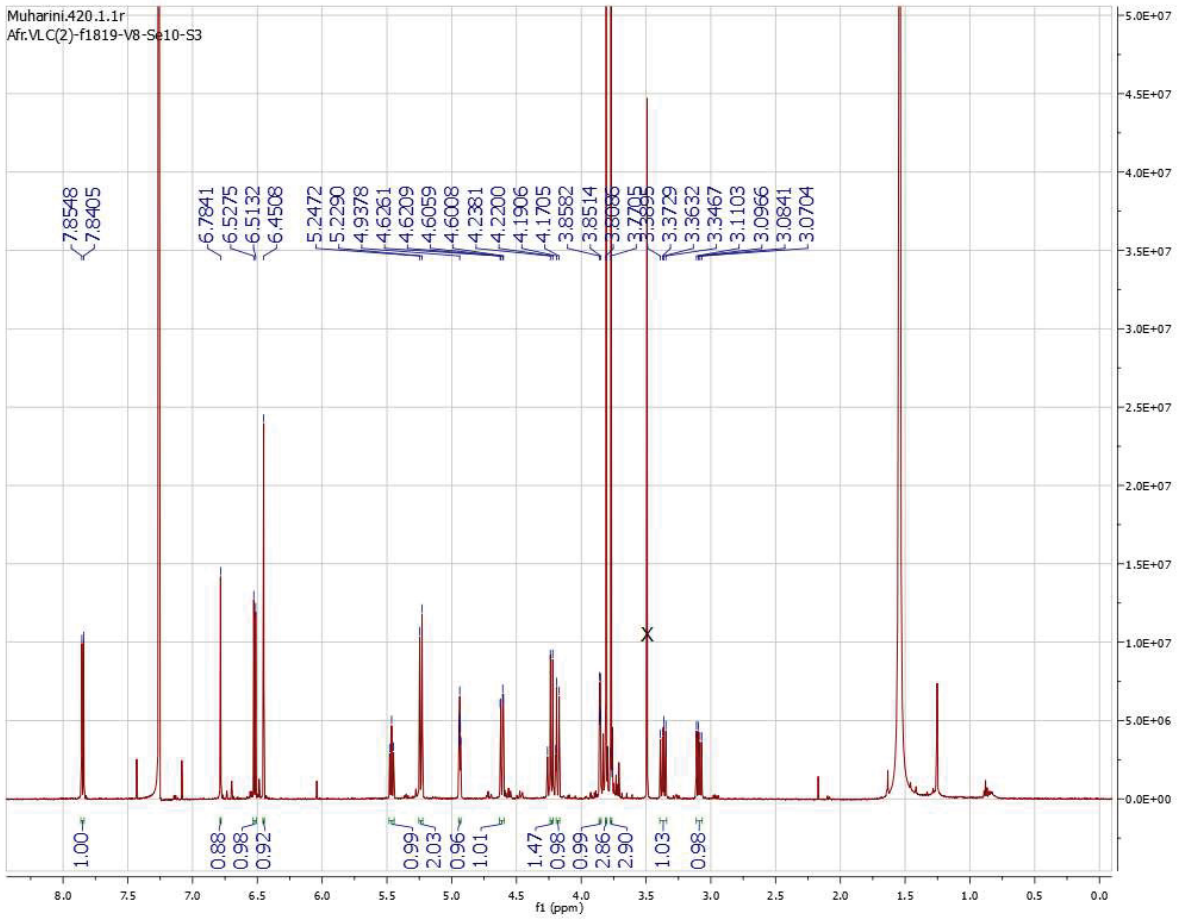

S66. ^{1}H NMR (600 MHz, $CDCl_3$) spectrum of the new compound **44**

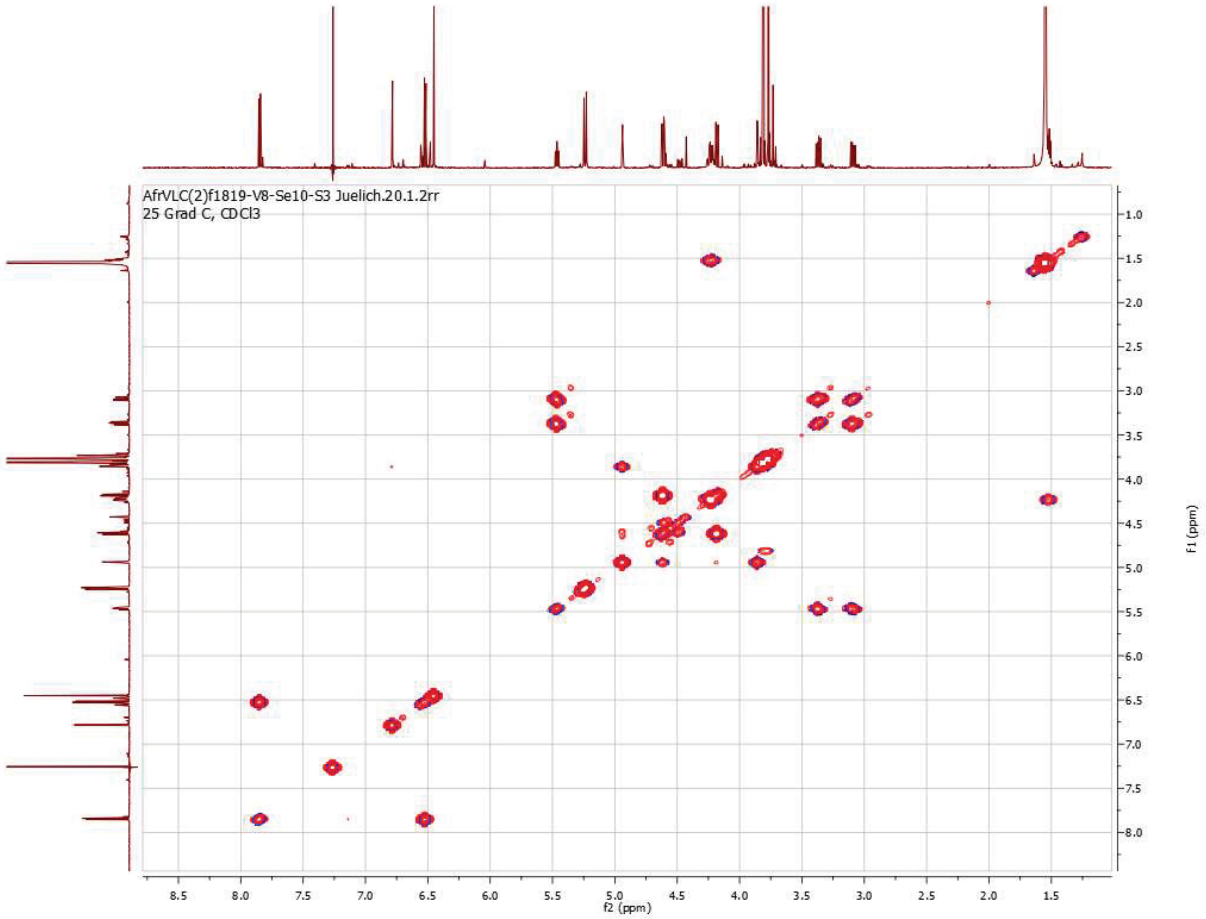

S67. ^{1}H-^{1}H COSY (700 MHz, $CDCl_3$) spectrum of the new compound **44**

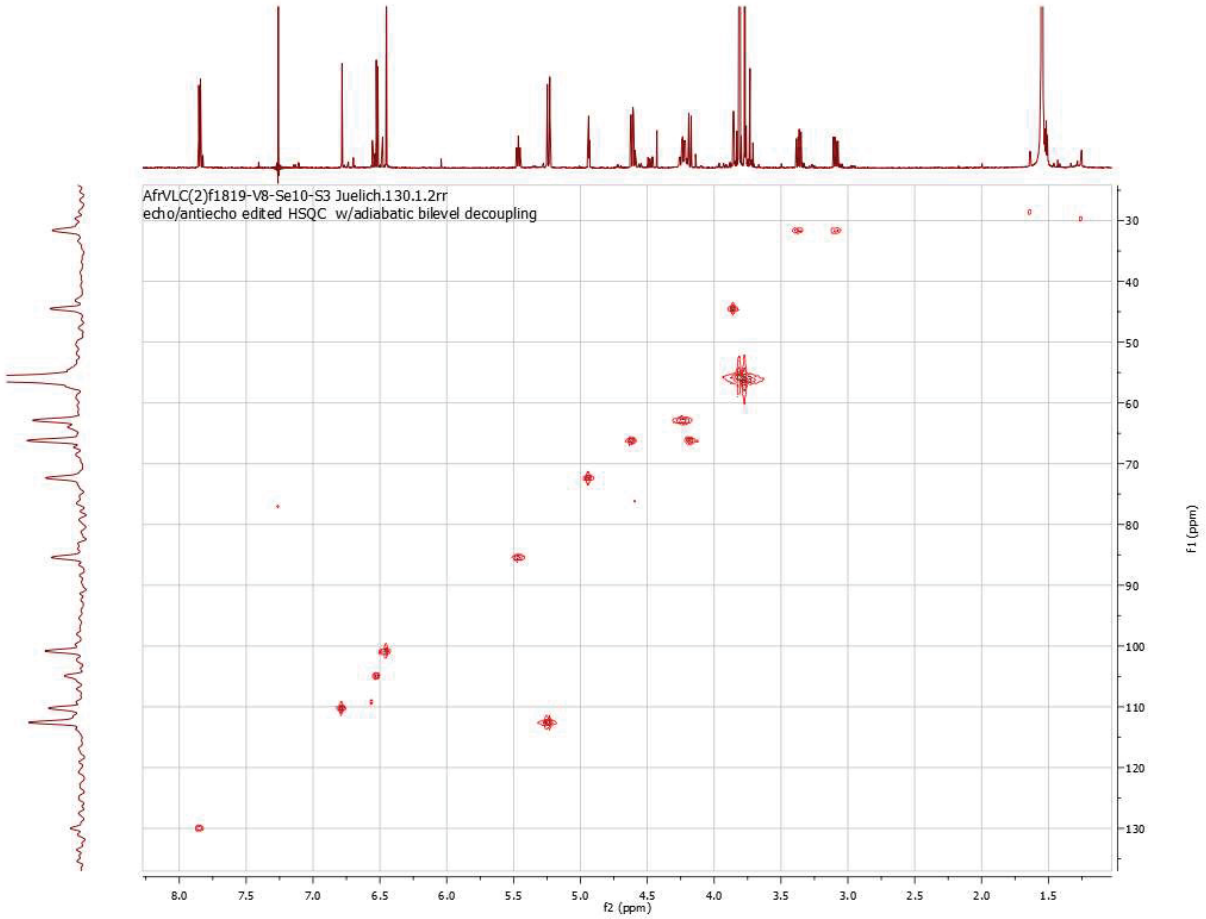

S68. HSQC (700 MHz, 175 MHz, $CDCl_3$) spectrum of the new compound **44**

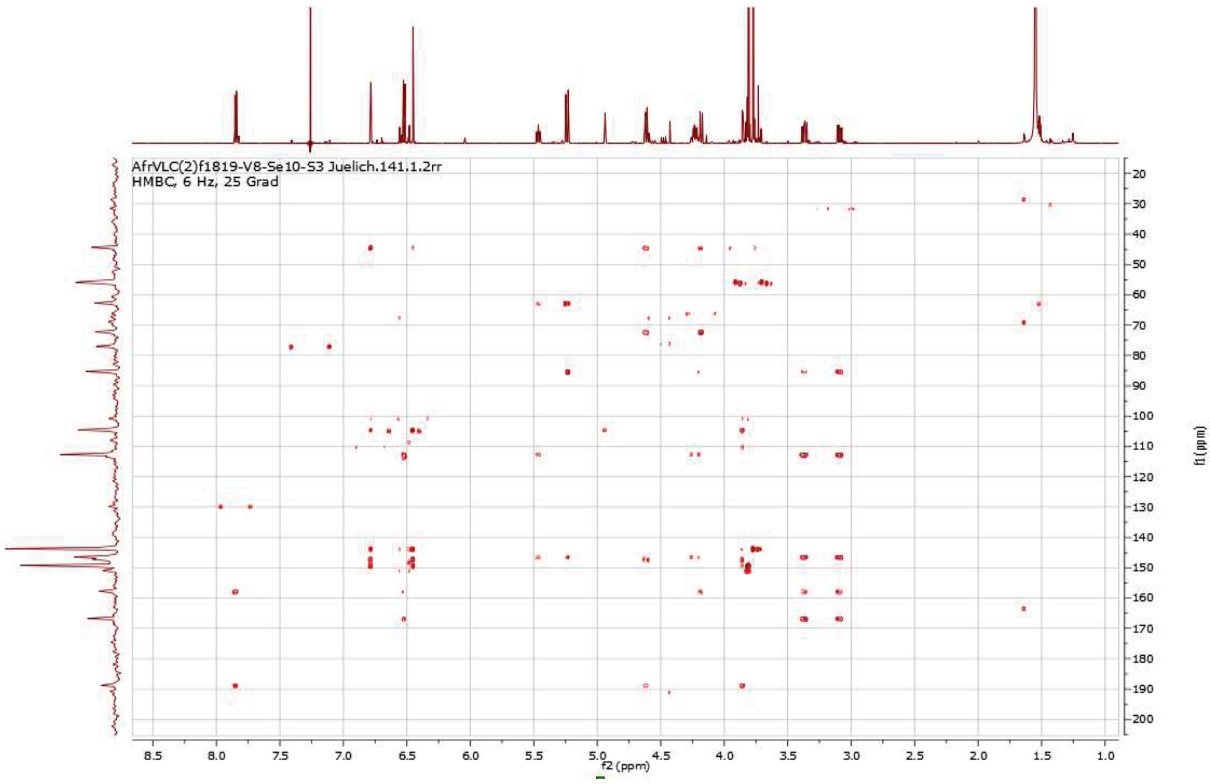

S69. HMBC (700 MHz, 175 MHz, $CDCl_3$) spectrum of the new compound **44**

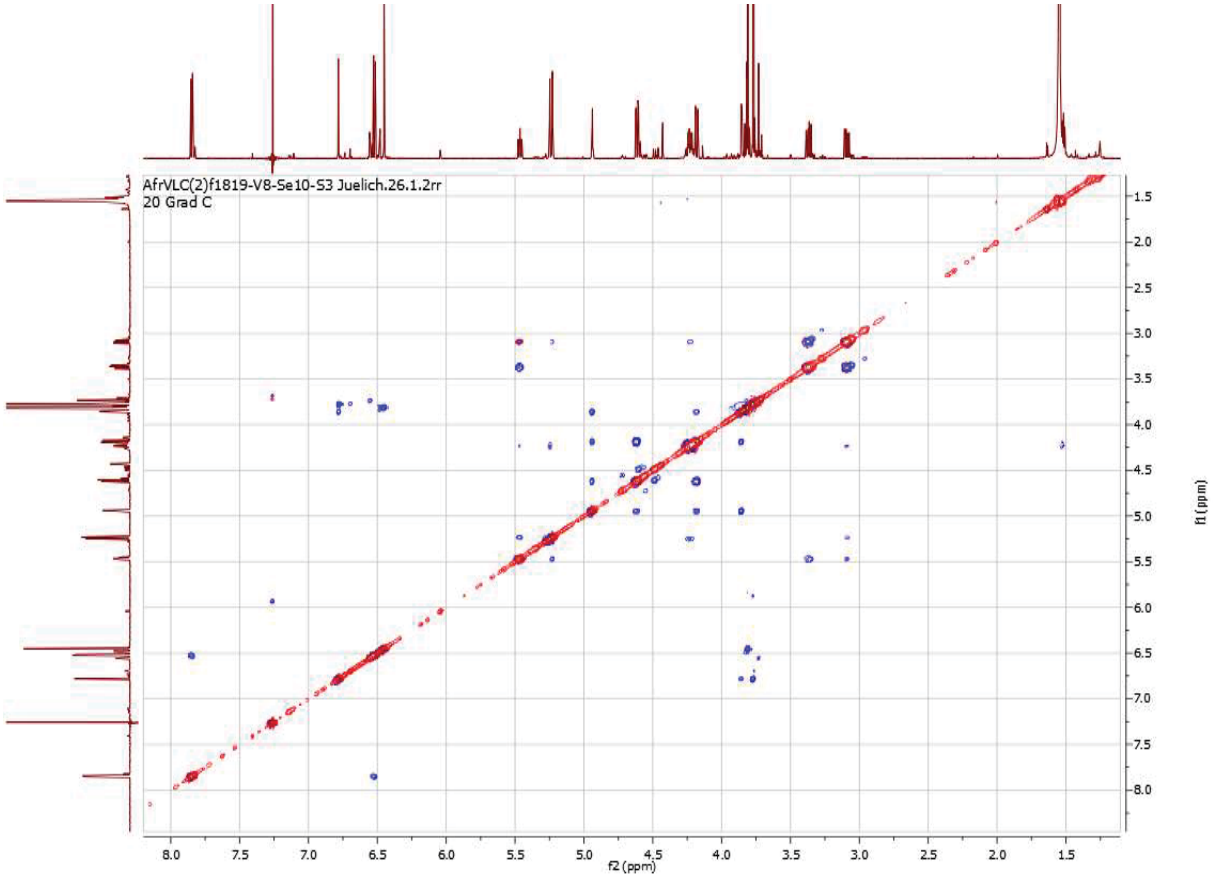

S70. ROESY (700 MHz, $CDCl_3$) spectrum of the new compound **44**

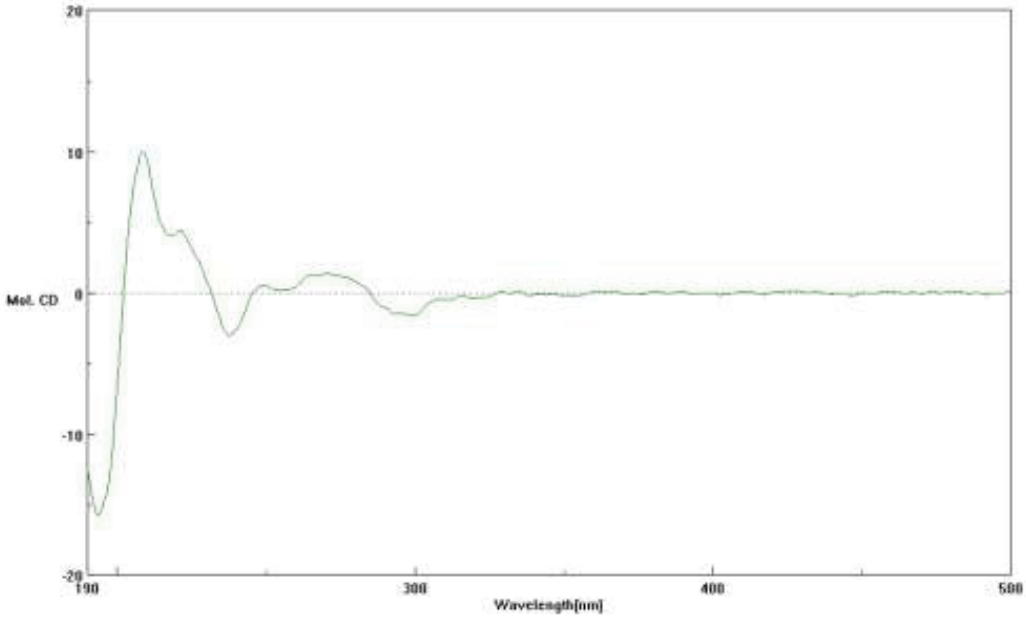

S71. CD spectrum of the new compound **44**

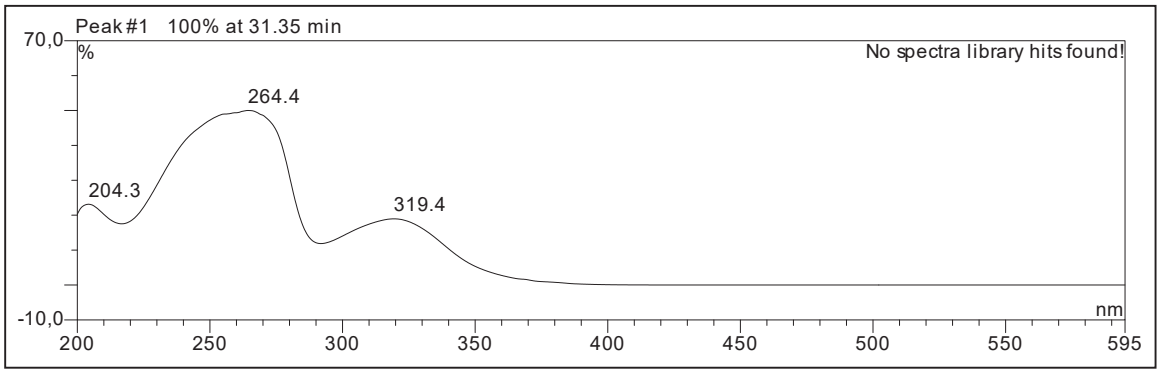

S72. UV spectrum of the new compound **45**

Mass Spectrum SmartFormula Report

Analysis Info

Analysis Name	D:\Data\Spektren 2015\Proksch15HR000228.d	Acquisition Date	6/29/2015 3:25:14 PM
Method	tune_low.m	Operator	Peter Tommes
Sample Name	Rini Muharini Afr VLC(2) f1819-V8-Se6-S2 (CH3OH)	Instrument	maXis 288882.20213
Comment			

Acquisition Parameter

Source Type	ESI	Ion Polarity	Positive	Set Nebulizer	0.3 Bar
Focus	Not active	Set Capillary	4000 V	Set Dry Heater	180 °C
Scan Begin	50 m/z	Set End Plate Offset	-500 V	Set Dry Gas	4.0 l/min
Scan End	1500 m/z	Set Collision Cell RF	600.0 Vpp	Set Divert Valve	Source

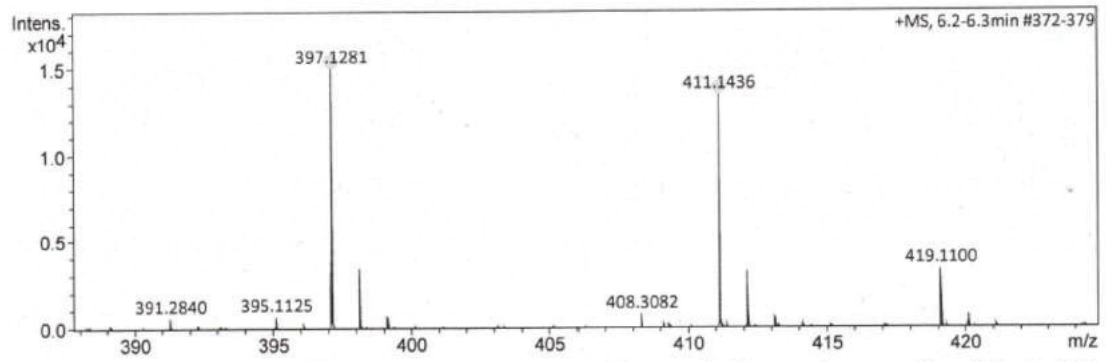

Meas. m/z	#	Ion Formula	m/z	err [ppm]	mSigma	# mSigma	Score	rdb	e⁻ Conf	N-Rule
397.1281	1	C22H21O7	397.1282	0.3	6.3	1	100.00	12.5	even	ok
	2	C19H13N10O	397.1268	-3.1	9.7	2	53.05	18.5	even	ok
	3	C23H17N4O3	397.1295	3.7	19.9	3	37.63	17.5	even	ok
411.1436	1	C23H23O7	411.1438	0.4	7.4	1	100.00	12.5	even	ok
	2	C20H15N10O	411.1425	-2.8	10.2	2	57.36	18.5	even	ok
	3	C24H19N4O3	411.1452	3.7	20.9	3	36.92	17.5	even	ok

S73. HRESIMS of the new compound **45**

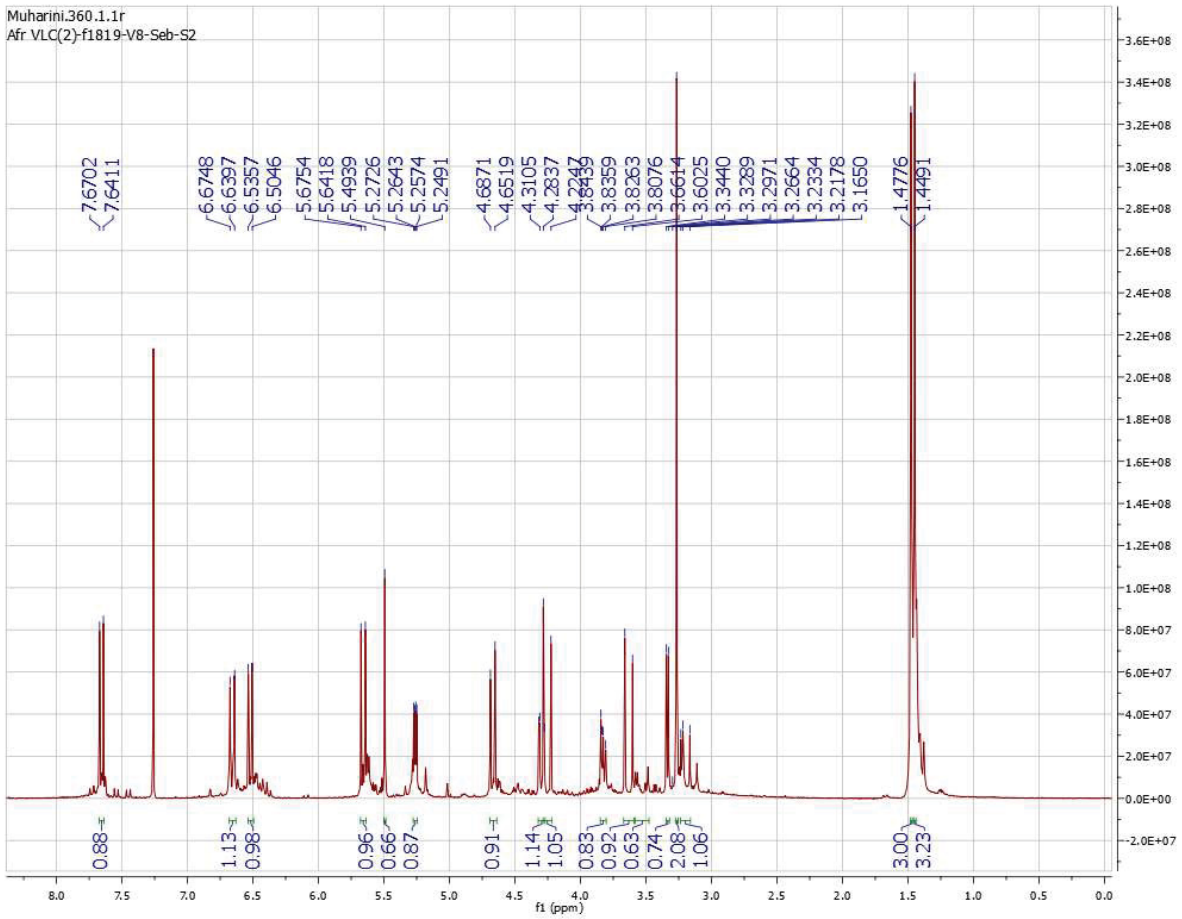

S74. ^{1}H NMR (300 MHz, $CDCl_3$) spectrum of the new compound **45**

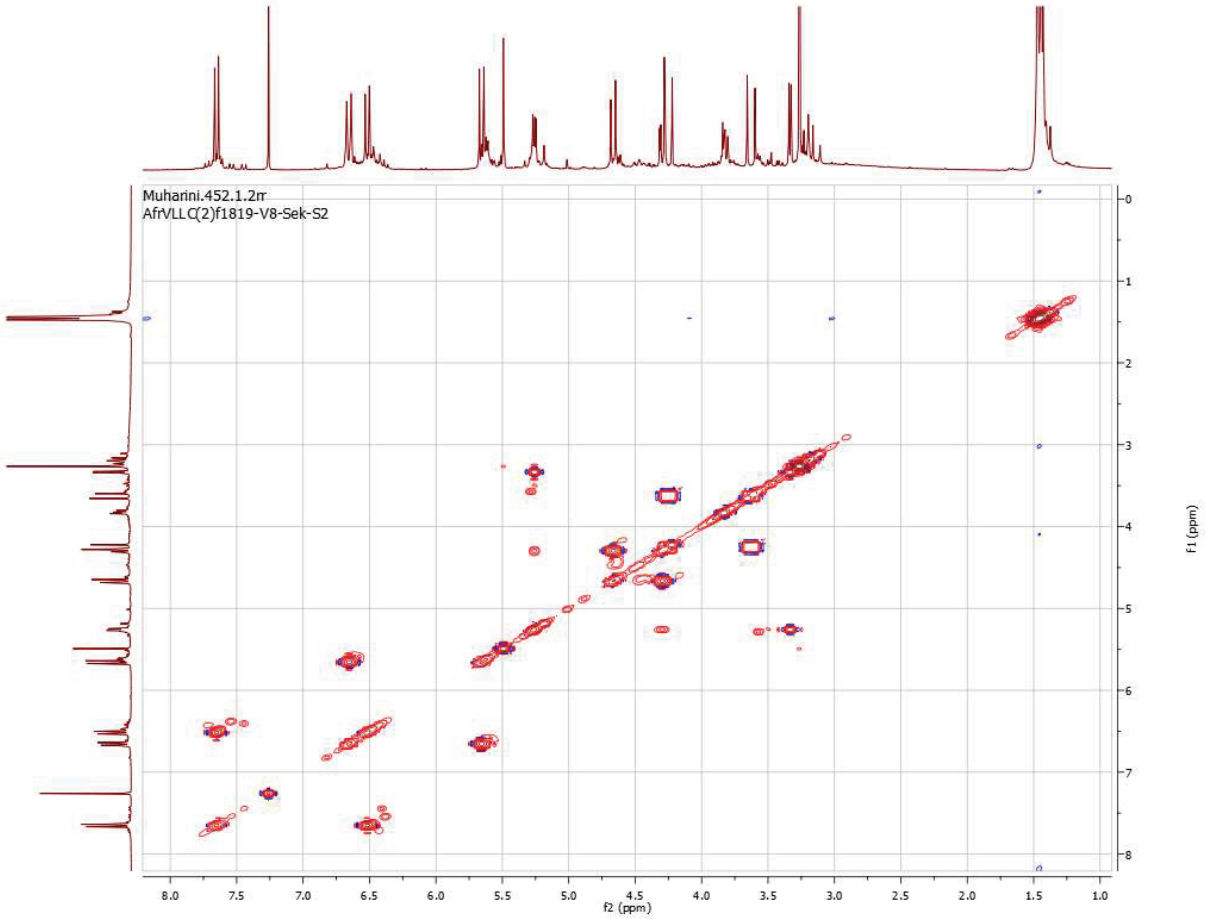

S75. ^{1}H-^{1}H COSY (300 MHz, $CDCl_3$) spectrum of the new compound **45**

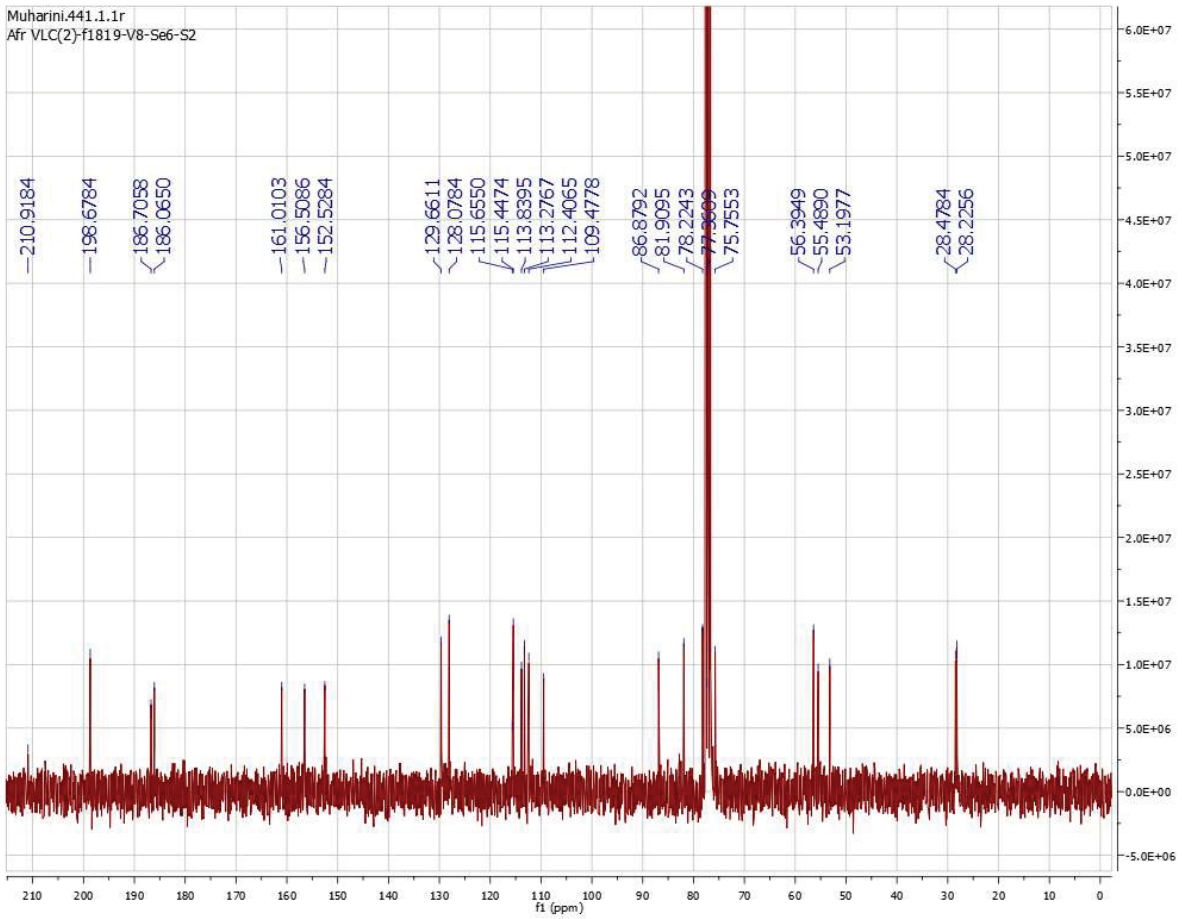

S76. ^{13}C NMR (75 MHz, $CDCl_3$) spectrum of the new compound **45**

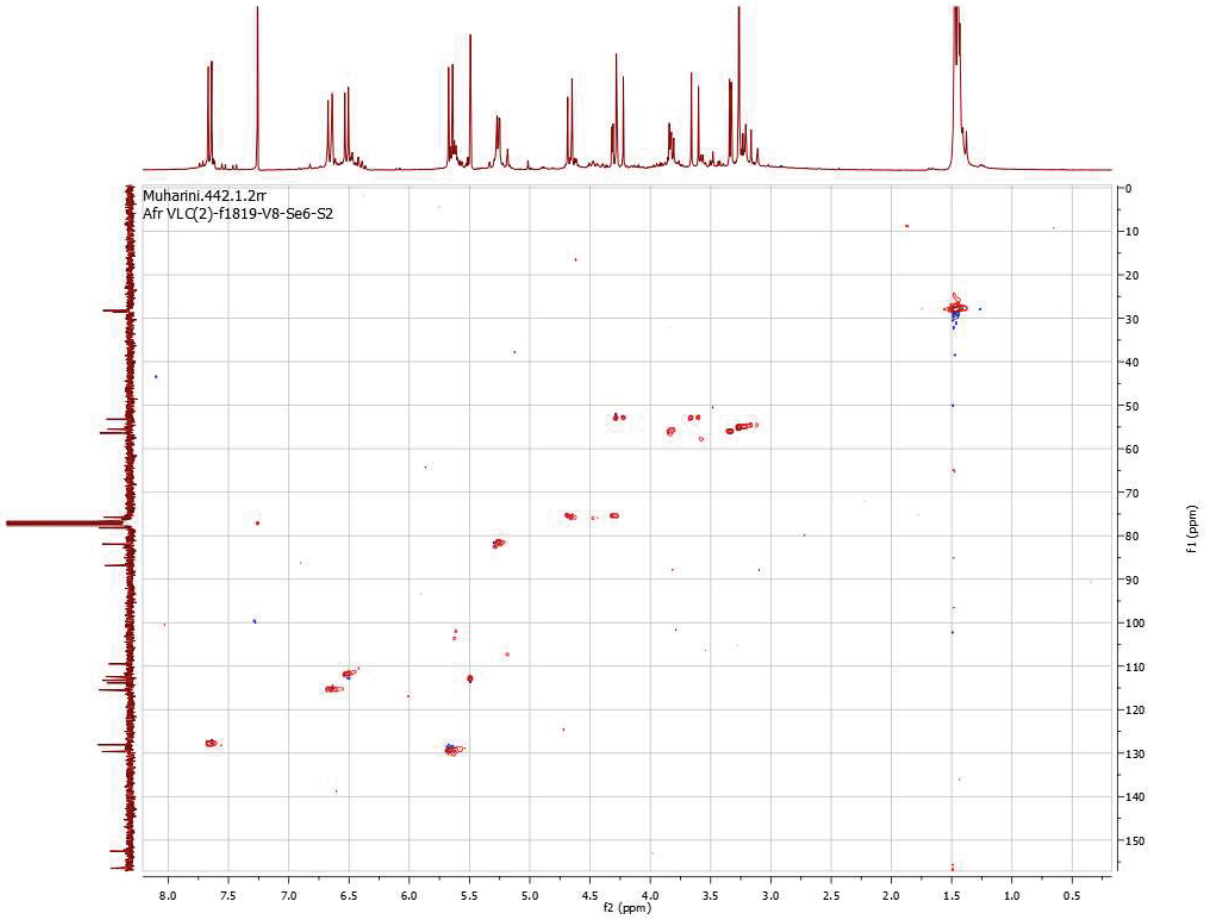

S77. HSQC (300 MHz, 75 MHz $CDCl_3$) spectrum of the new compound **45**

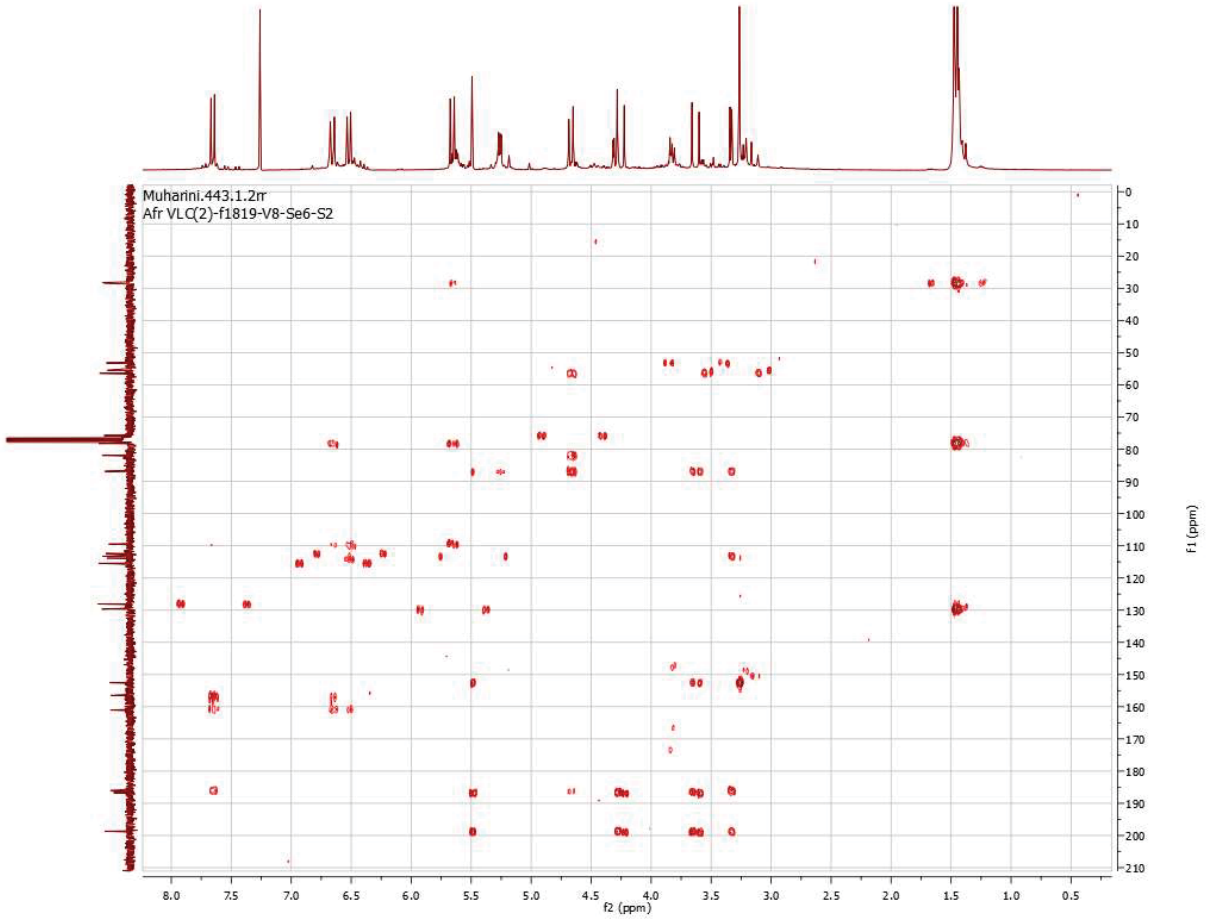

S78. HMBC (300 MHz, 75 MHz $CDCl_3$) spectrum of the new compound **45**

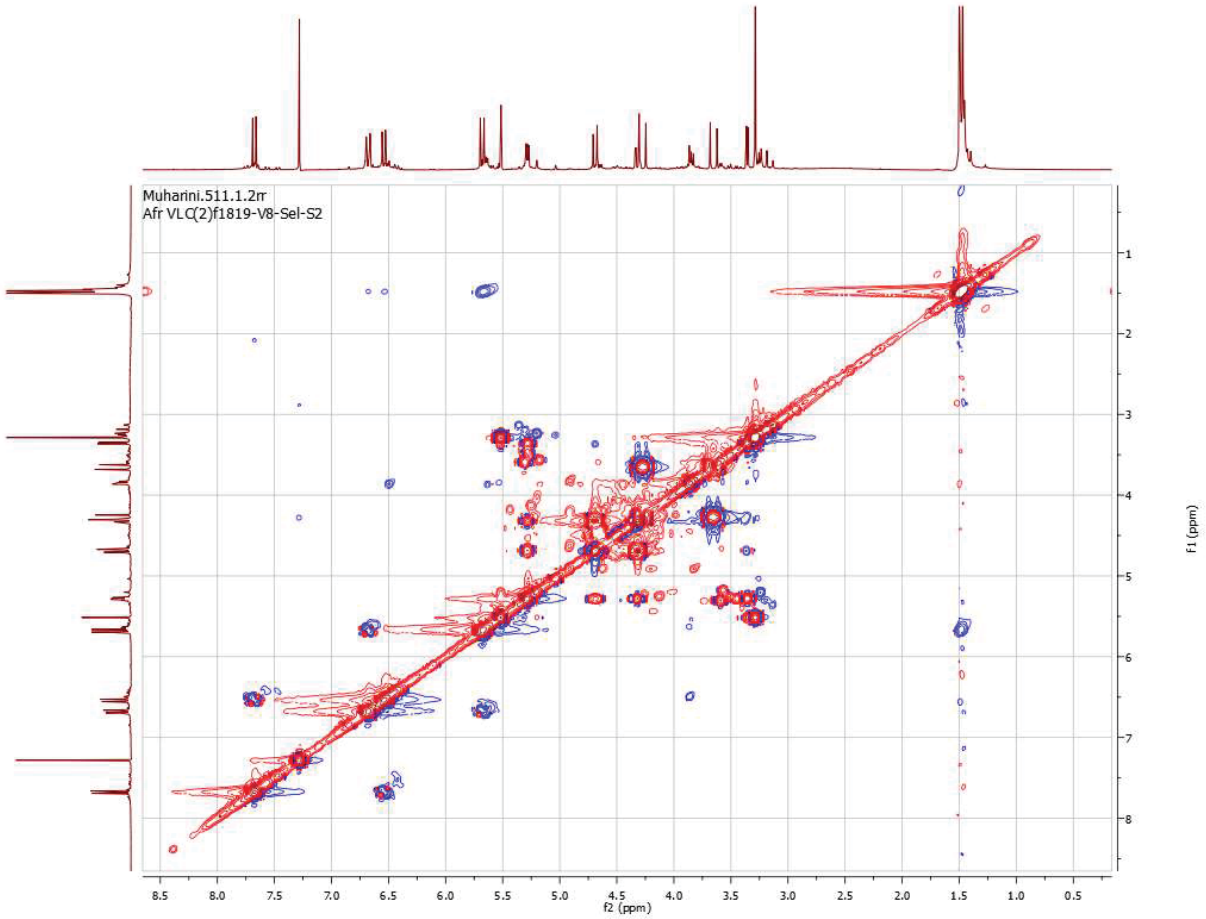

S79. ROESY (300 MHz, $CDCl_3$) spectrum of the new compound **45**

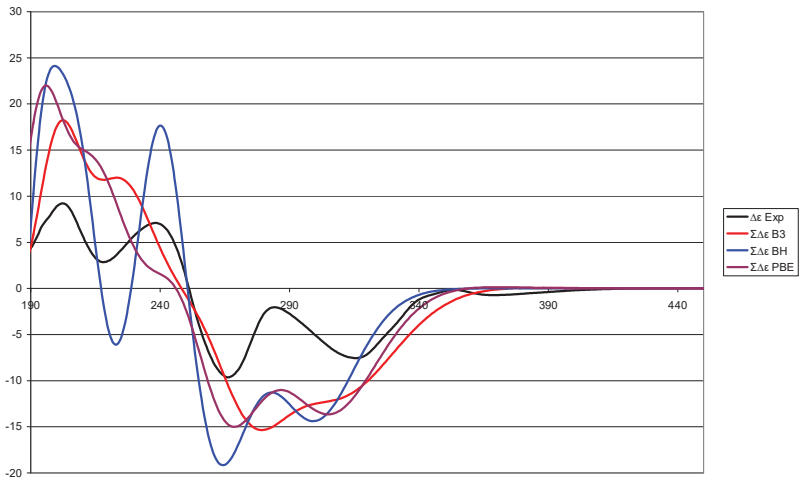

S80.CD spectrum of the new compound **45**

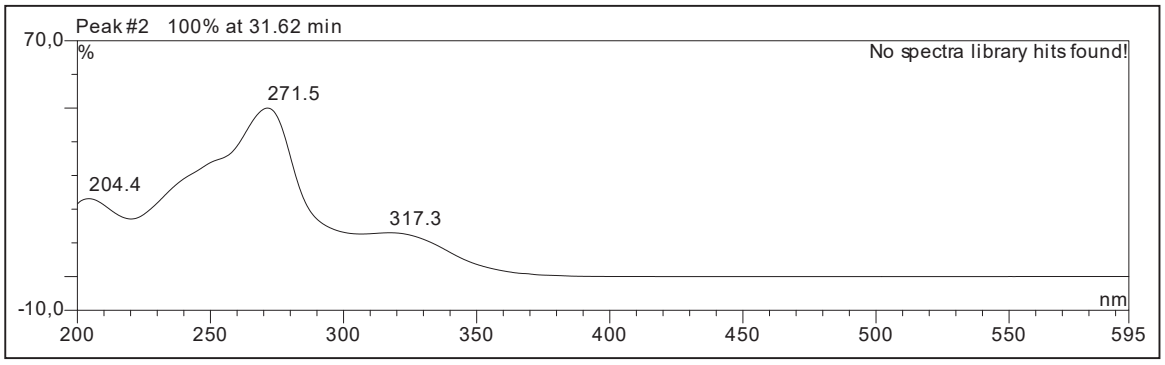

S81. UV spectrum of the new compound **46**

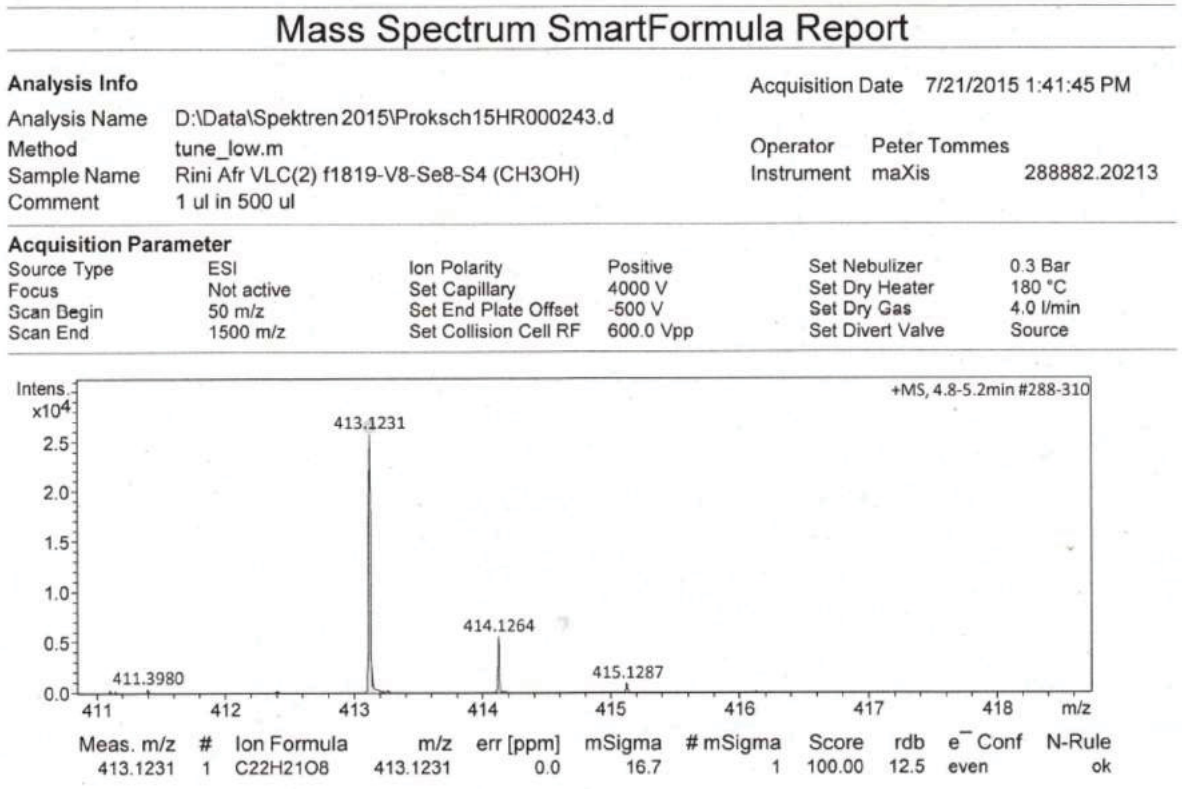

S82. HRESIMS of the new compound **46**

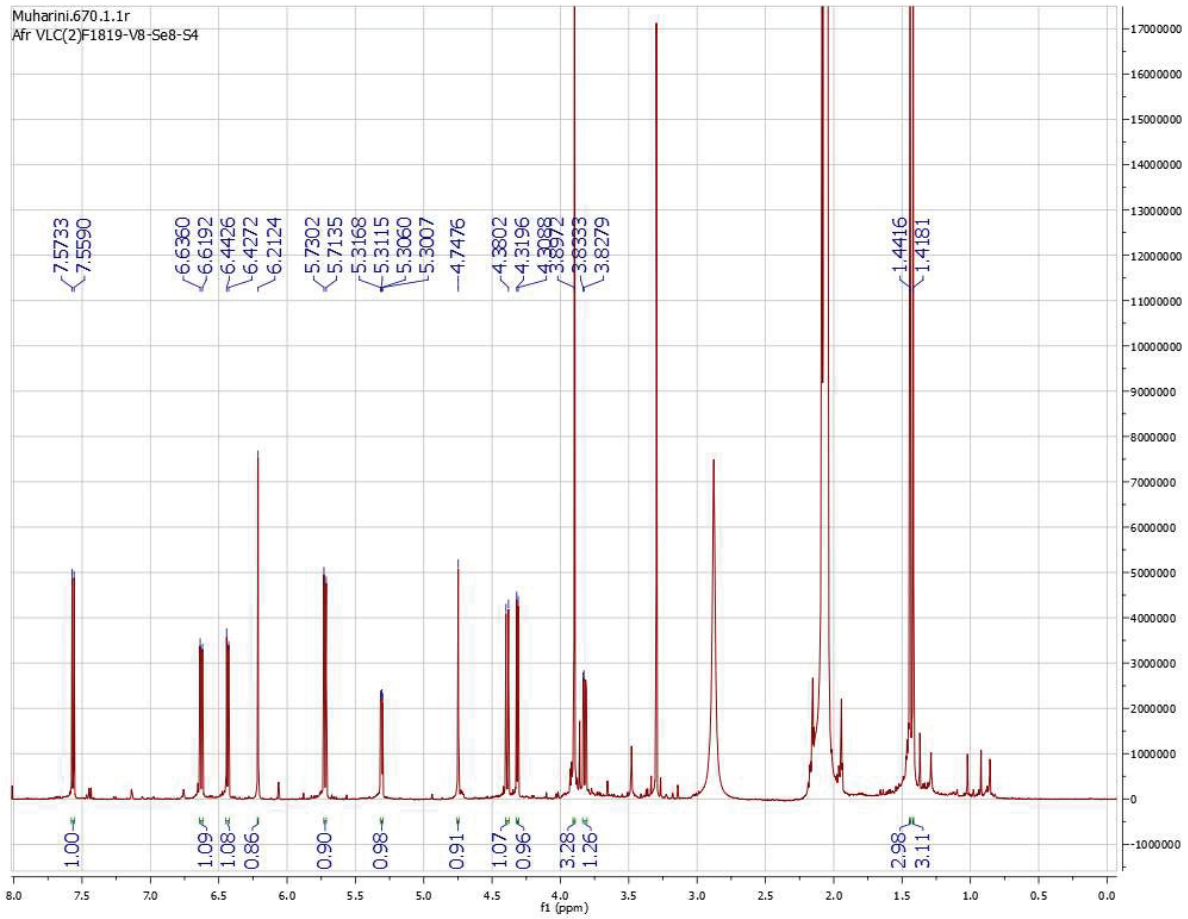

S83. ^{1}H NMR (600 MHz, $(CD_3)_2CO$) spectrum of the new compound **46**

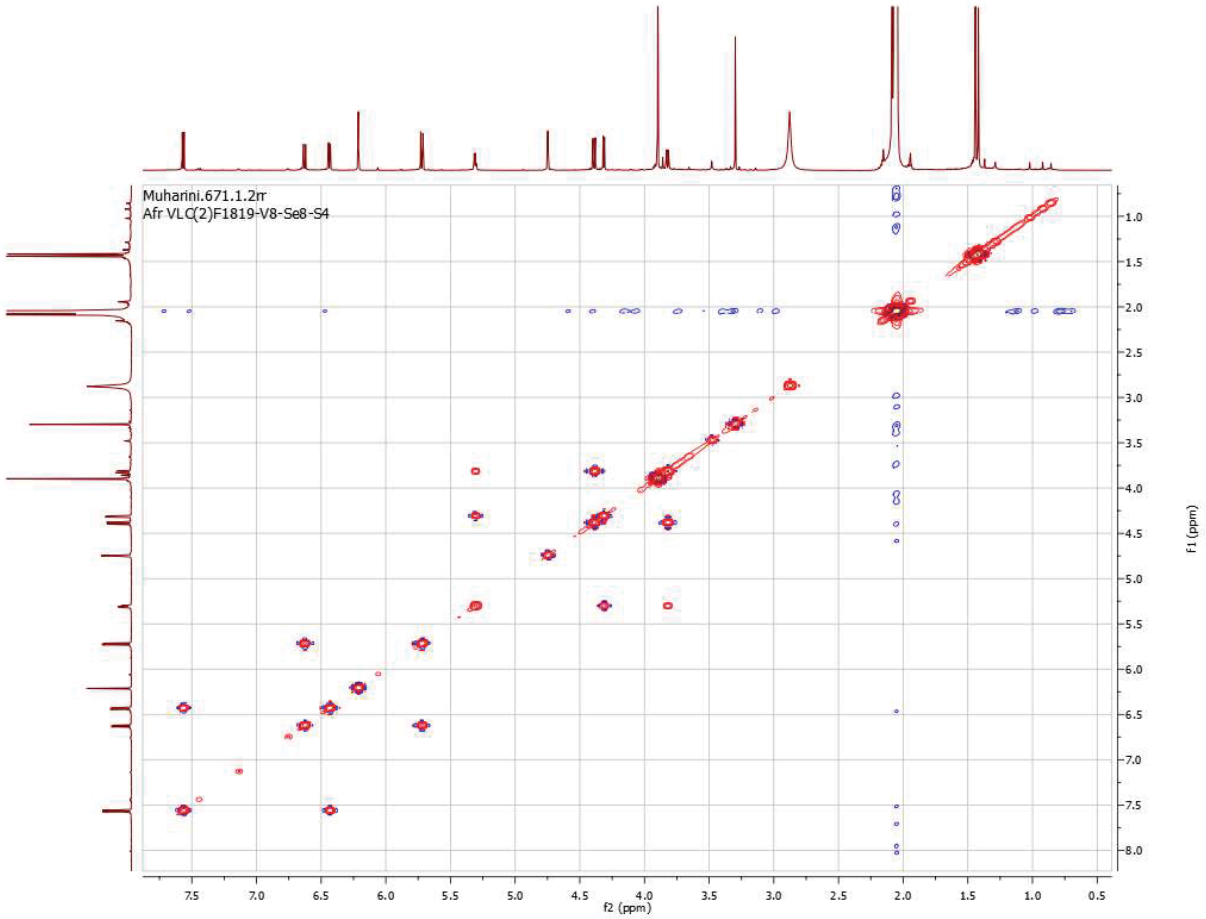

S84. ^{1}H-^{1}H COSY (600 MHz, $(CD_3)_2CO$) spectrum of the new compound **46**

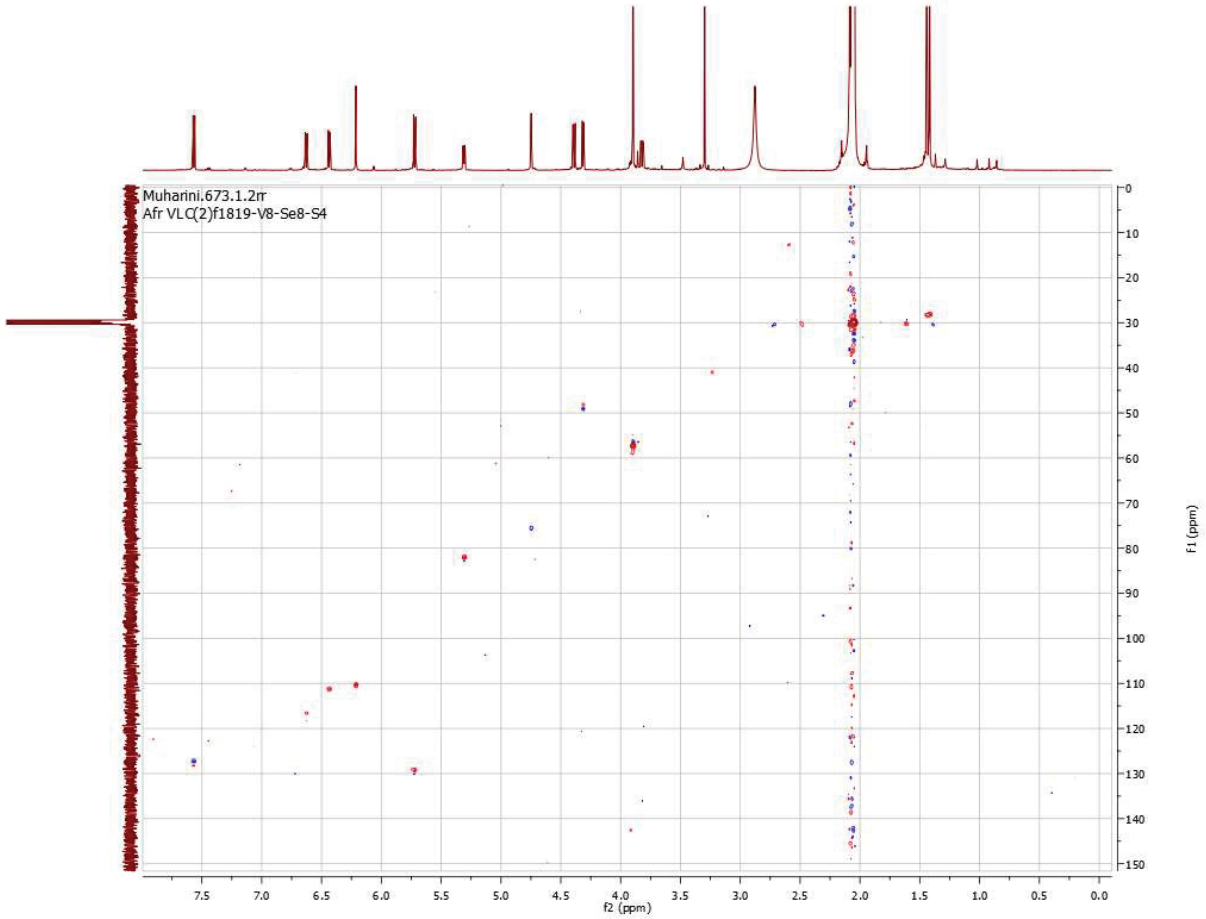

S85. HSQC (600 MHz, 150 MHz, $(CD_3)_2CO$) spectrum of the new compound **46**

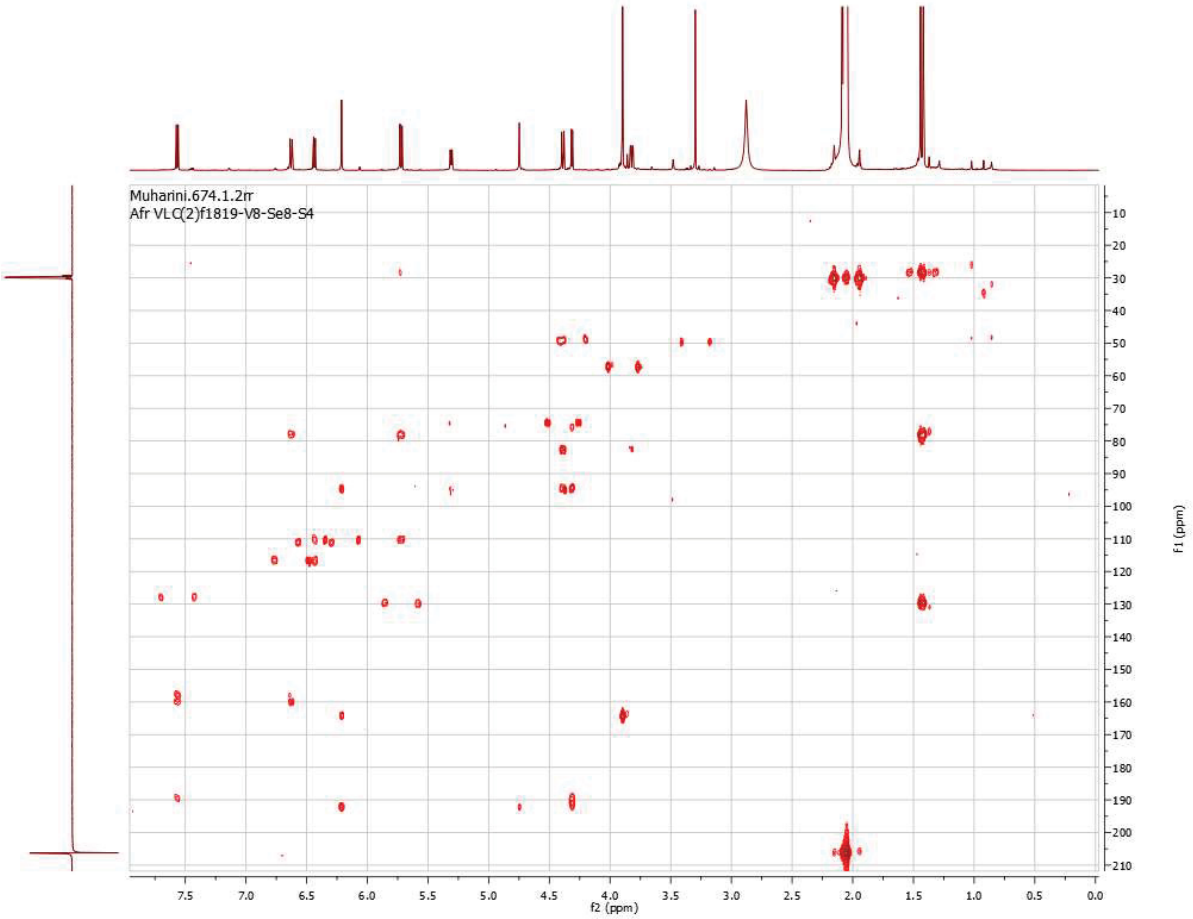

S86. HMBC (600 MHz, 150 MHz, $(CD_3)_2CO$) spectrum of the new compound **46**

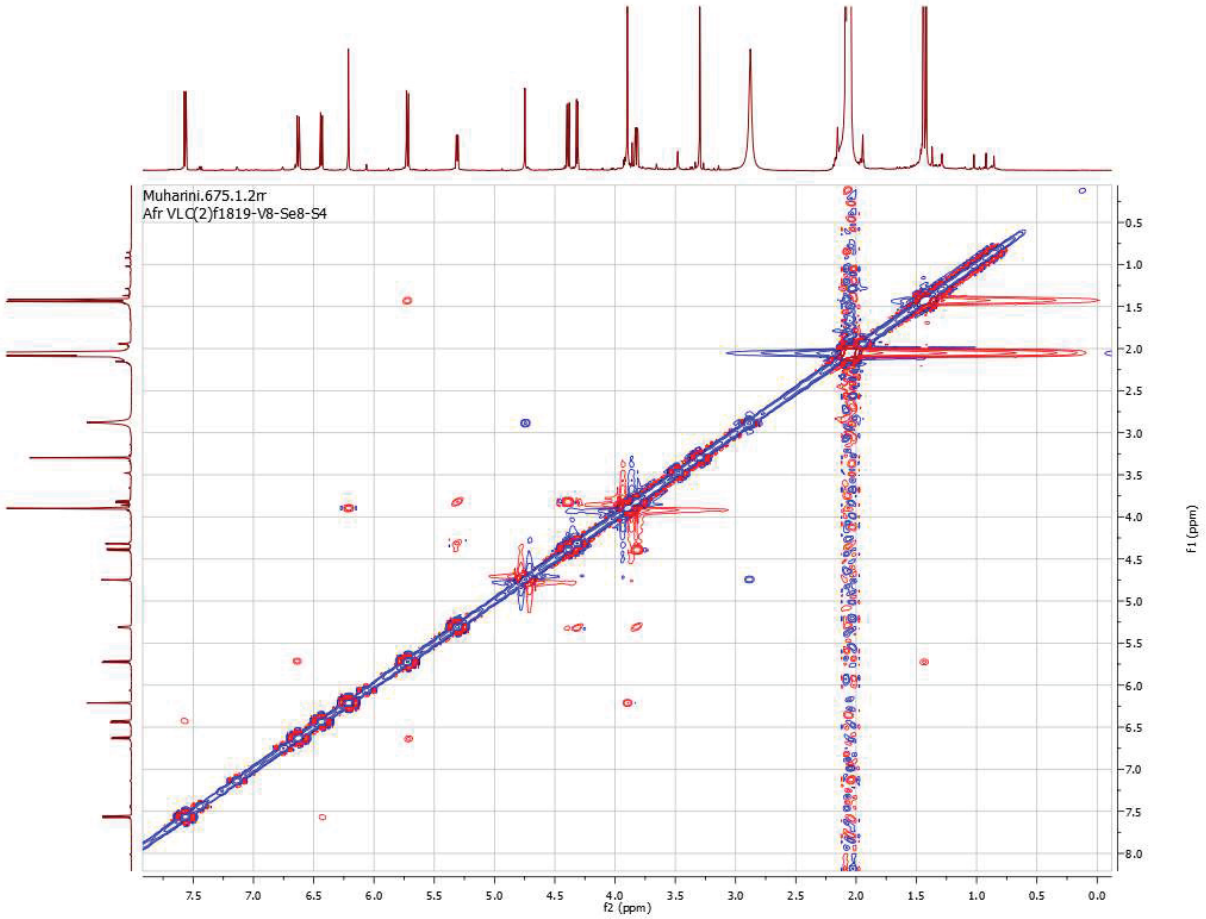

S87. ROESY (600 MHz, $(CD_3)_2CO$) spectrum of the new compound **46**

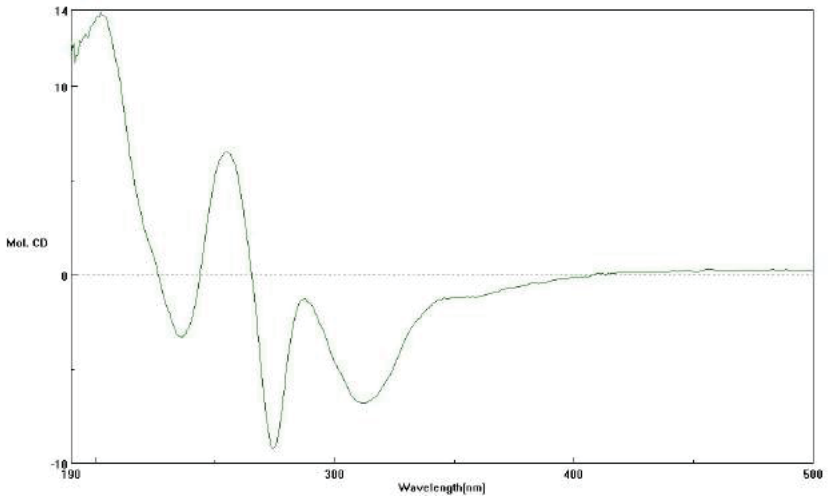

S88. CD measurement spectrum of the new compound **46**

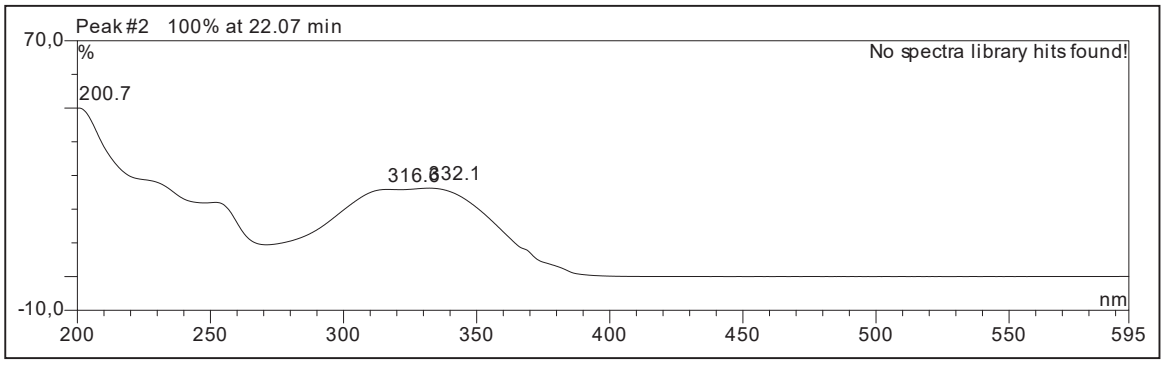

S89. UV spectrum of the new compound **51**

Mass Spectrum SmartFormula Report

Analysis Info

Analysis Name	D:\Data\Spektren 2015\Proksch15HR000373.d	Acquisition Date	10/21/2015 10:27:35 AM
Method	tune_low.m	Operator	Peter Tommes
Sample Name	R. Muharini Afr VLC(2) f124-H7-Se4-S1 (CH3OH)	Instrument	maXis 288882.20213
Comment	2 ul in 1000 ul		

Acquisition Parameter

Source Type	ESI	Ion Polarity	Positive	Set Nebulizer	0.3 Bar
Focus	Not active	Set Capillary	4000 V	Set Dry Heater	180 °C
Scan Begin	50 m/z	Set End Plate Offset	-500 V	Set Dry Gas	4.0 l/min
Scan End	1500 m/z	Set Collision Cell RF	600.0 Vpp	Set Divert Valve	Source

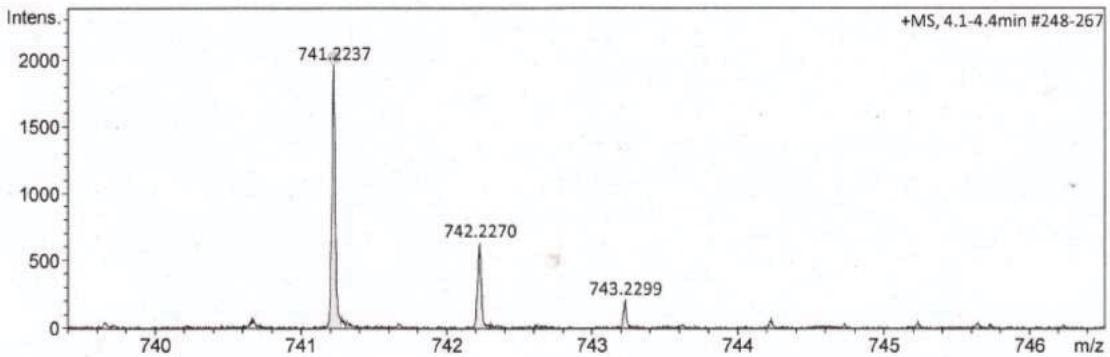

Meas. m/z	#	Ion Formula	m/z	err [ppm]	mSigma	# mSigma	Score	rdb	e⁻ Conf	N-Rule
741.2237	1	C33H41O19	741.2237	-0.0	25.7	1	100.00	13.5	even	ok
	2	C31H29N14O9	741.2236	-0.0	36.8	2	75.69	24.5	even	ok
	3	C46H33N2O8	741.2231	-0.7	97.8	3	6.63	31.5	even	ok
	4	C47H29N6O4	741.2245	1.1	109.5	4	3.27	36.5	even	ok

S90. HRESIMS of the new compound **51**

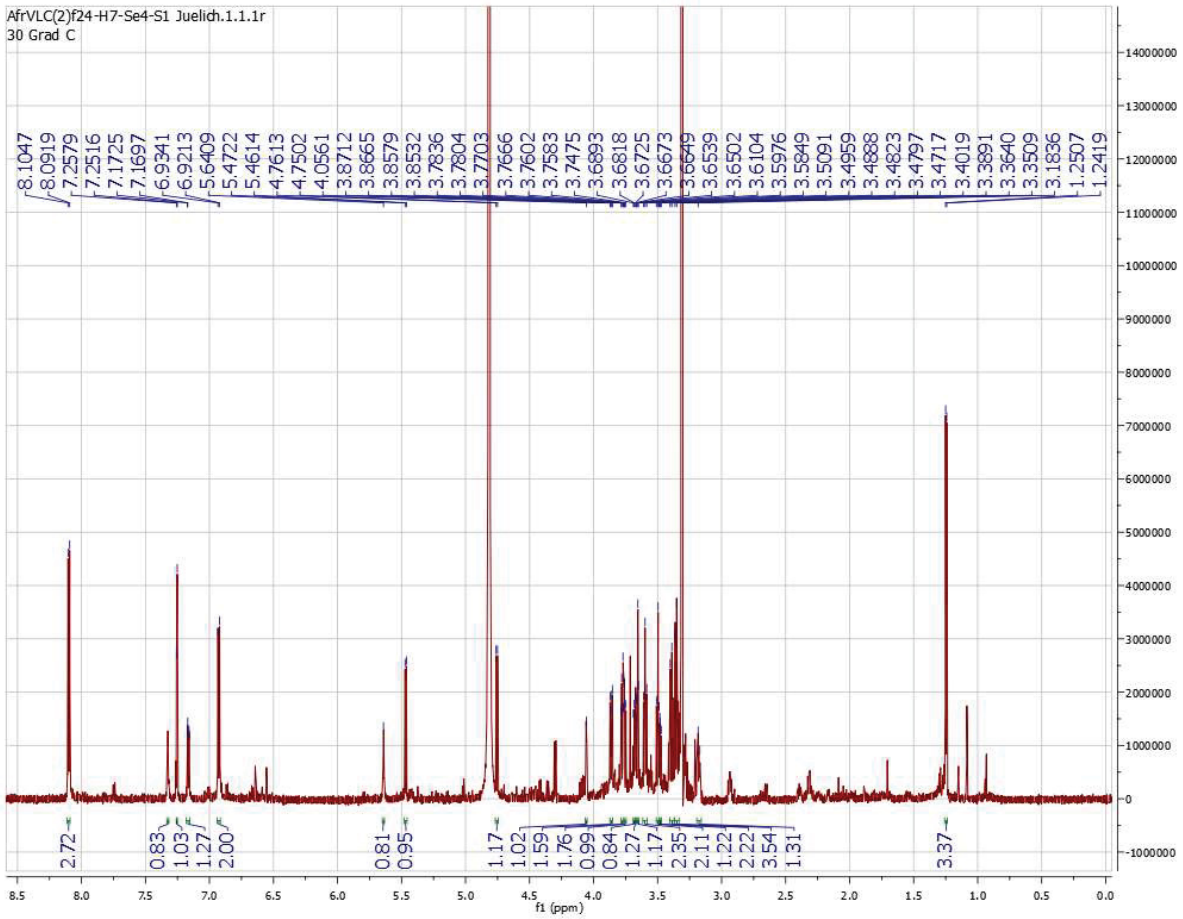

S91. ^{1}H NMR (700 MHz, CD_3OD) spectrum of the new compound **51**

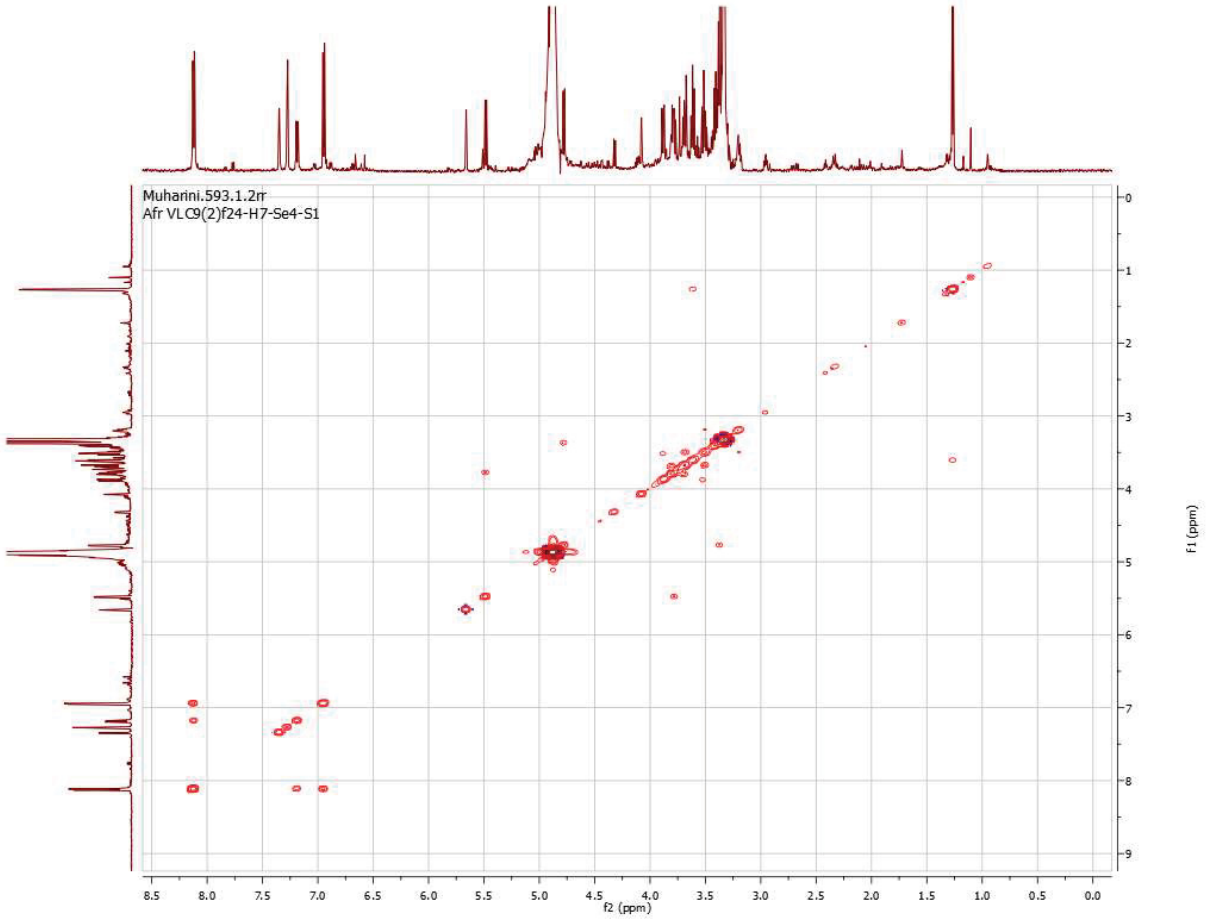

S92. ^{1}H-^{1}H COSY (600 MHz, CD_3OD) spectrum of the new compound **51**

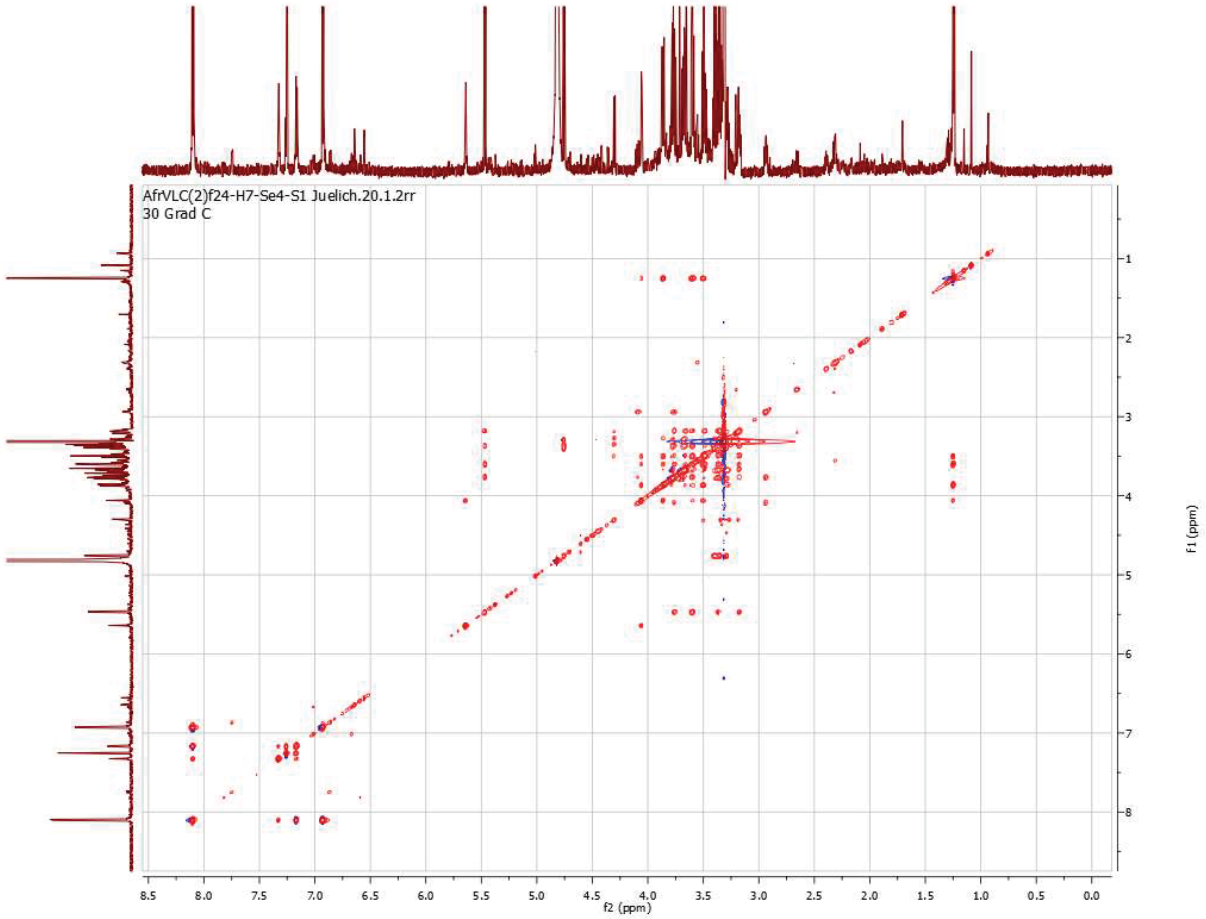

S93. TOCSY (700 MHz, CD_3OD) spectrum of the new compound **51**

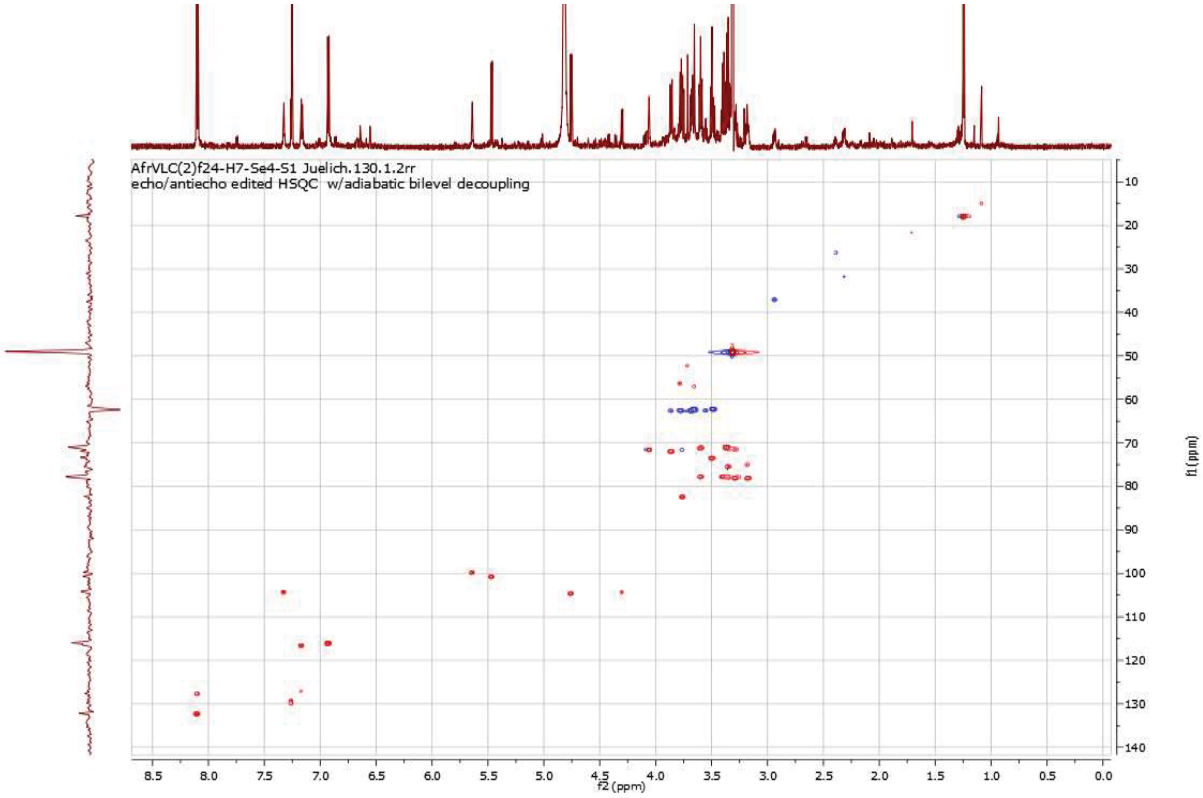

S94. HSQC (700 MHz, 175 MHz, CD_3OD) spectrum of the new compound **51**

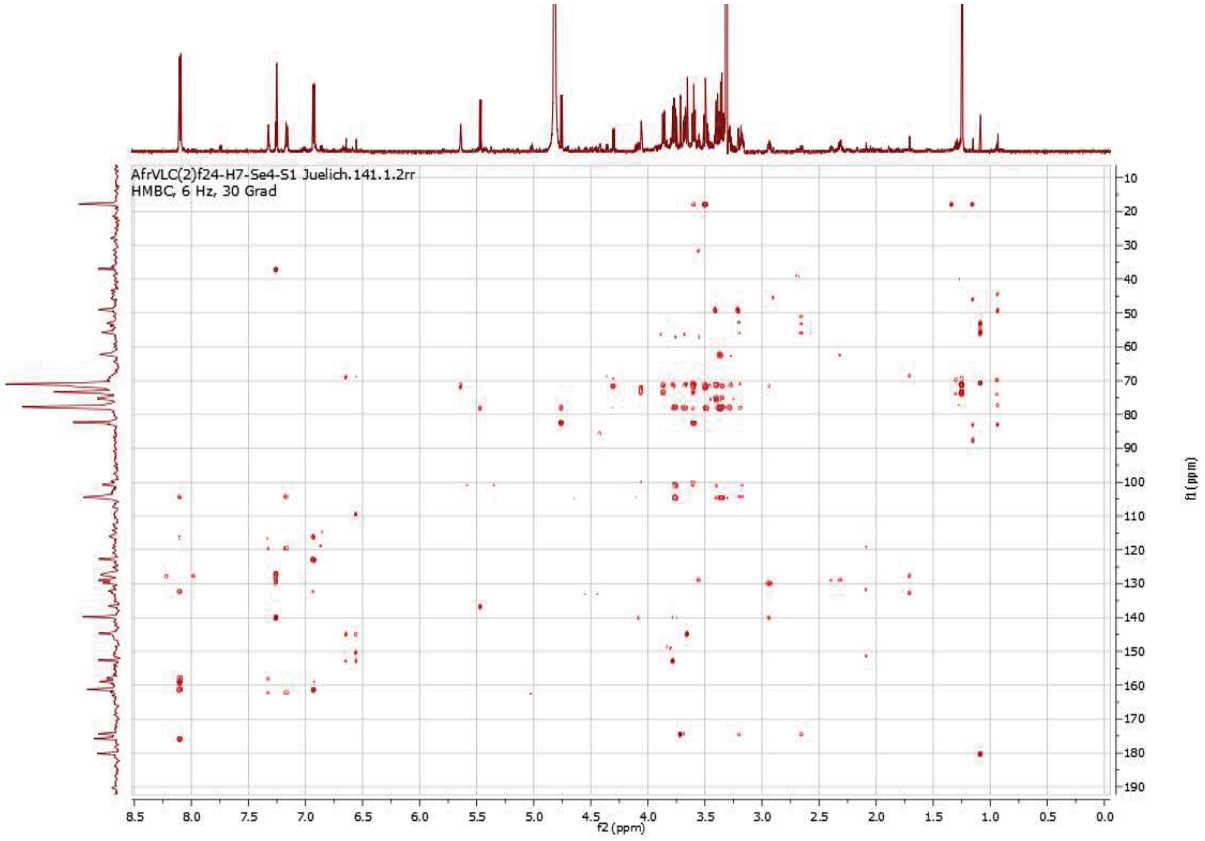

S95. HMBC (700 MHz, 175 MHz, CD_3OD) spectrum of the new compound **51**

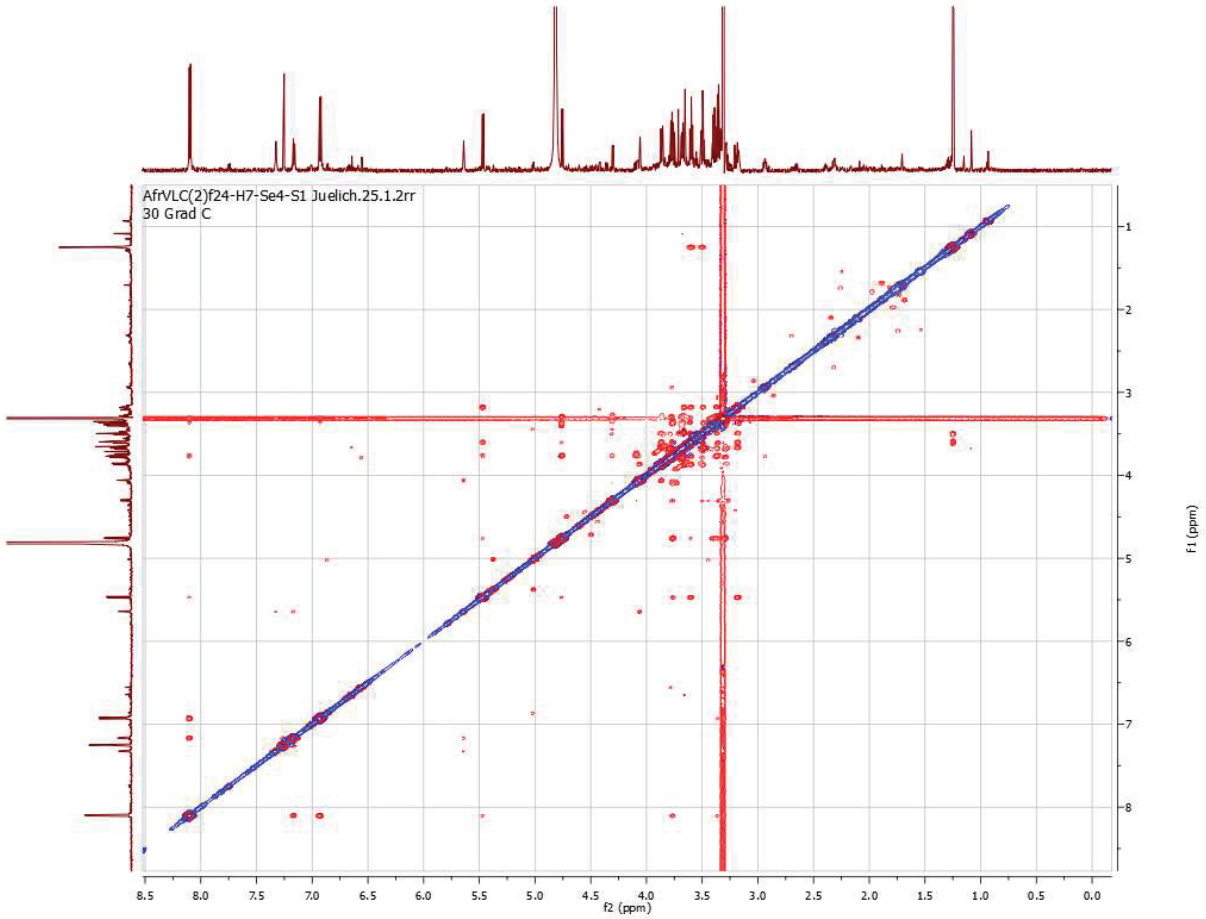

S96. ROESY (700 MHz, CD_3OD) spectrum of the new compound **51**

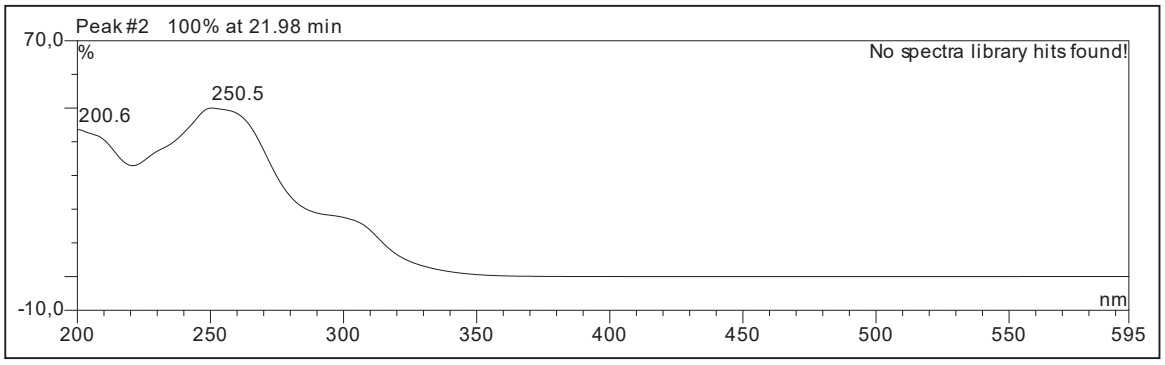

S97. UV spectrum of the new compound **52**

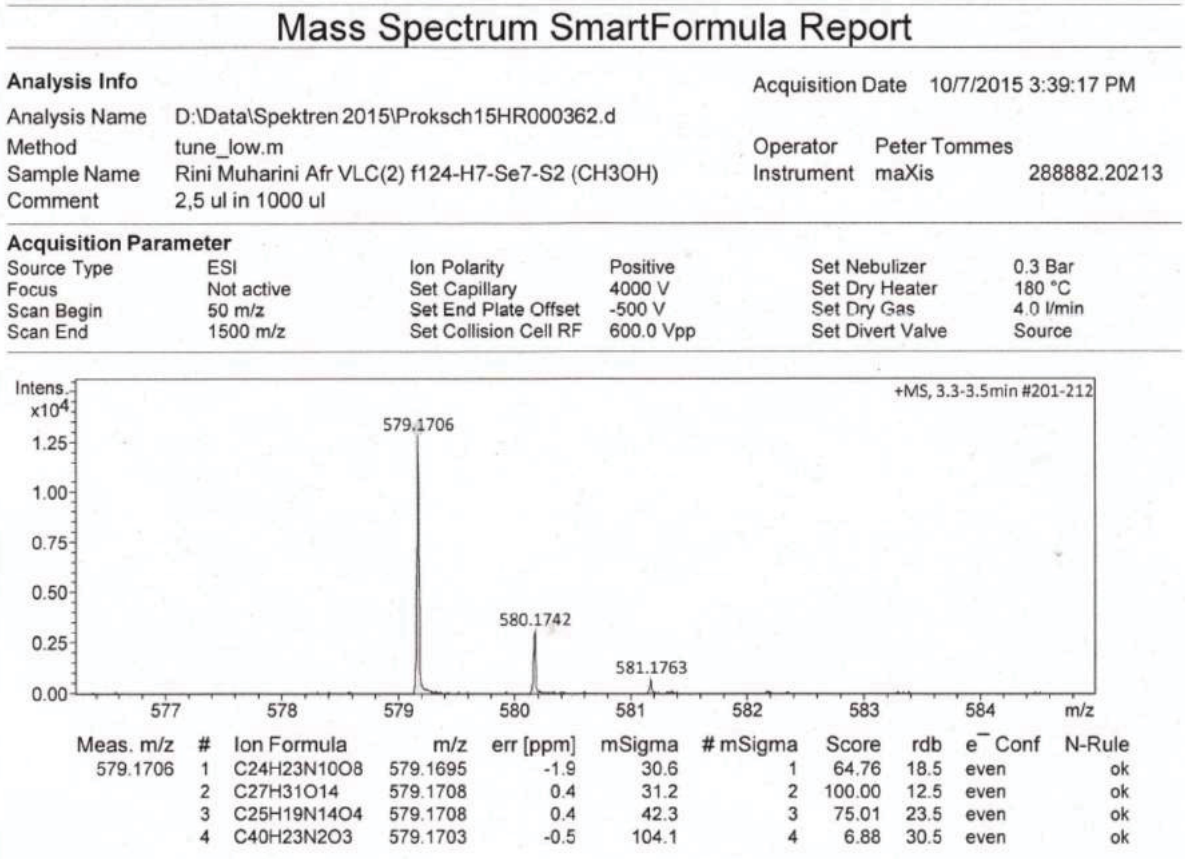

S98. HRESIMS of the new compound **52**

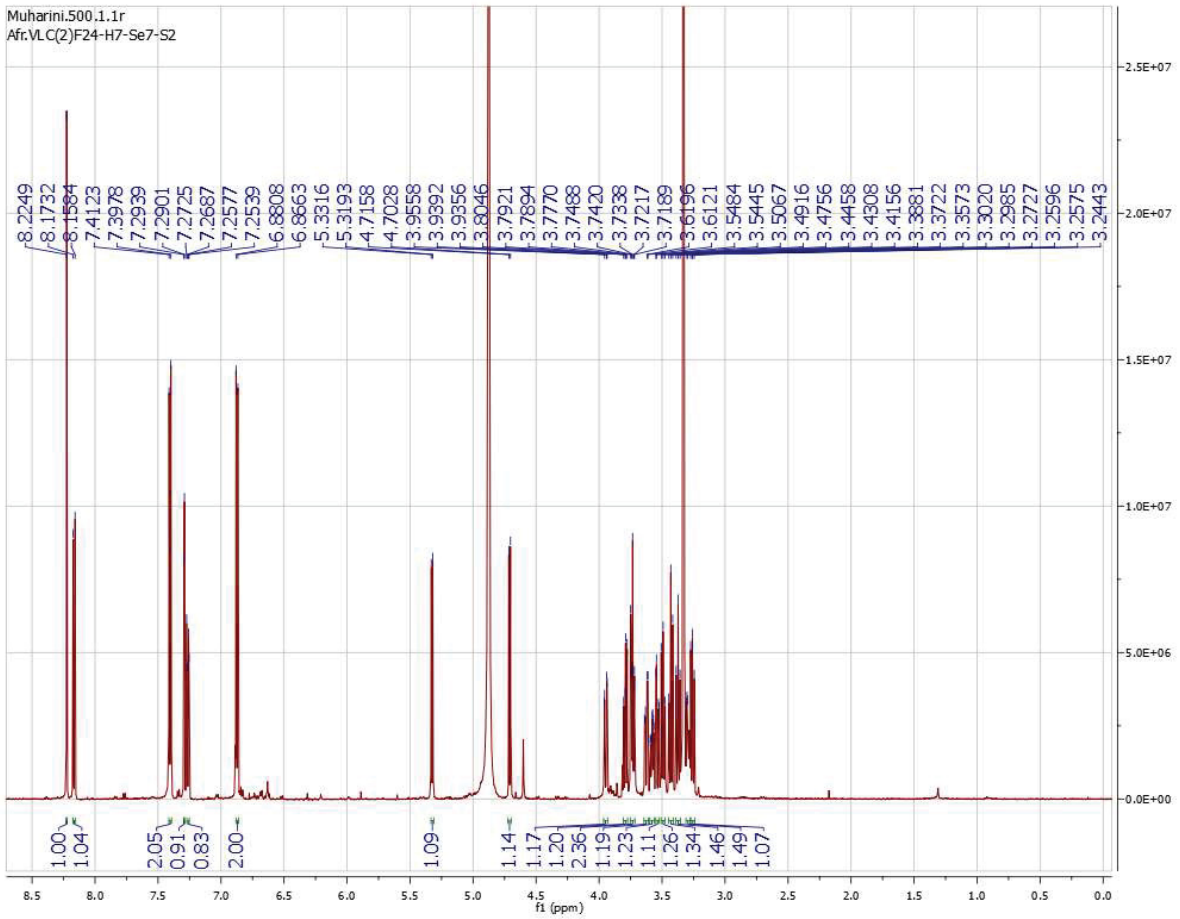

S99. ^{1}H NMR (600 MHz, CD_3OD) spectrum of the new compound **52**

S100. ^{1}H-^{1}H COSY (600 MHz, CD_3OD) spectrum of the new compound **52**

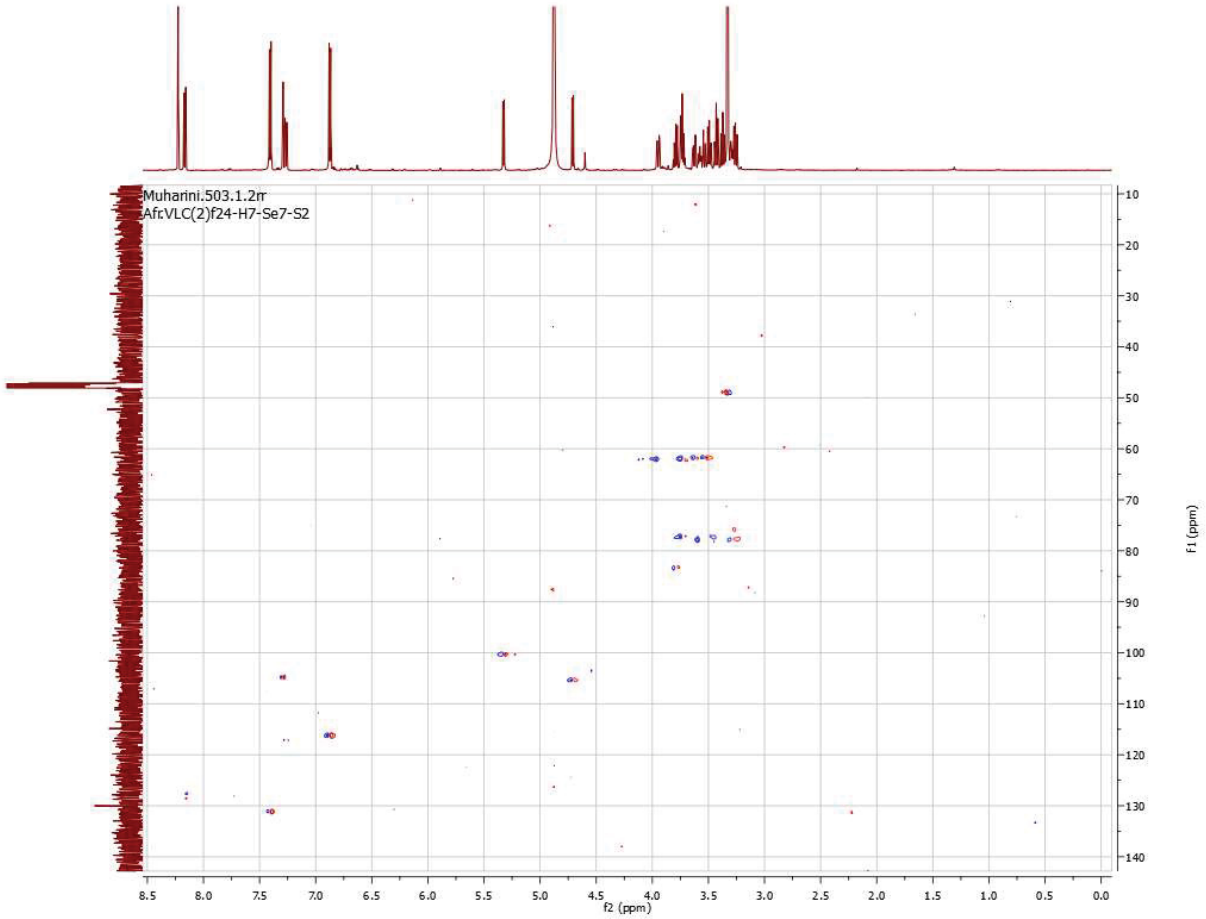

S101. HSQC (600 MHz, 150 MHz, CD_3OD) spectrum of the new compound **52**

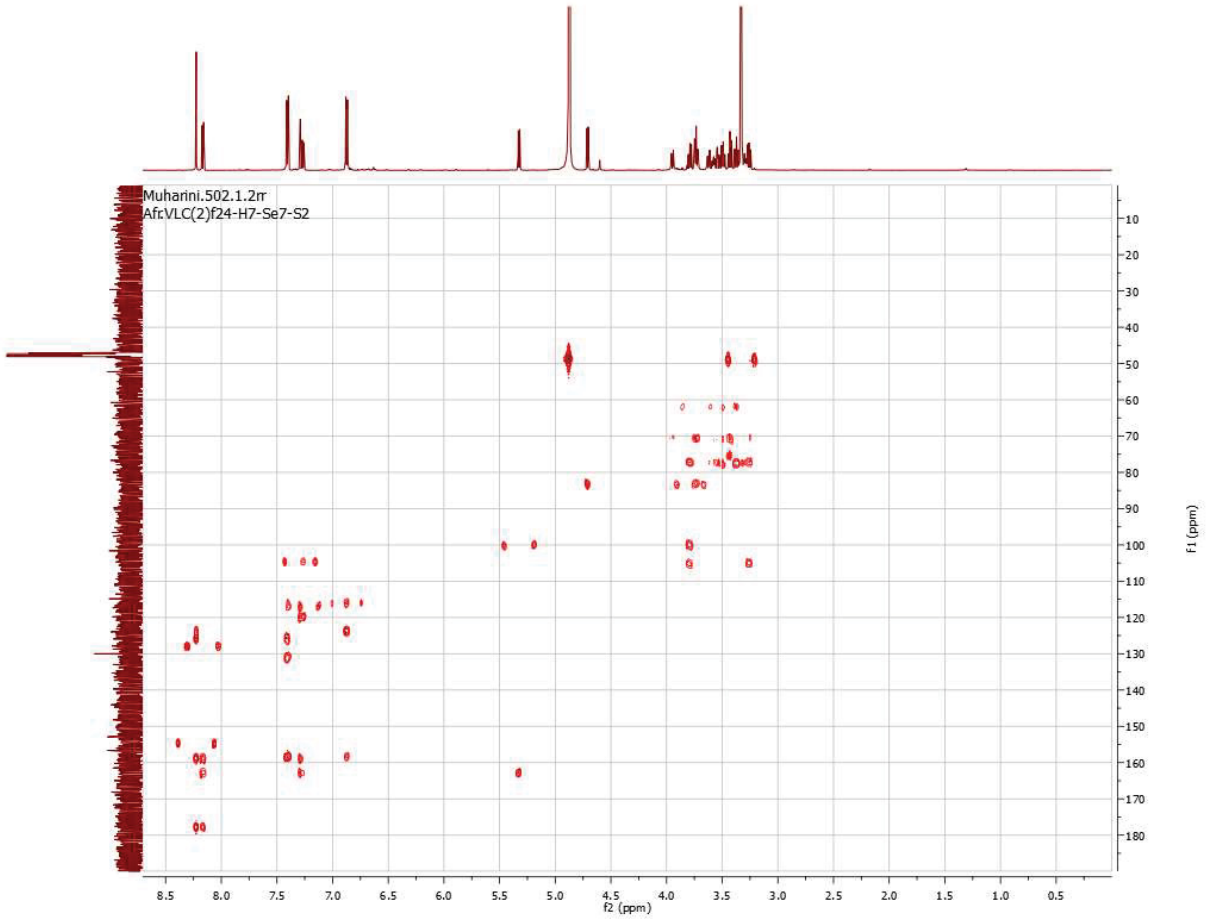

S102. HMBC (600 MHz, 150 MHz, CD_3OD) spectrum of the new compound **52**

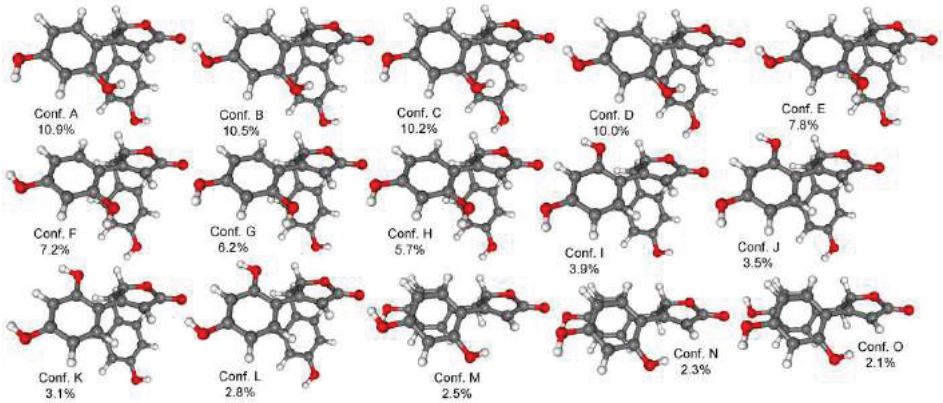

S103. Structure and population of the low-energy B97D/TZVP PCM/MeCN conformers (≥ 2%) of (*S*)-**11**.

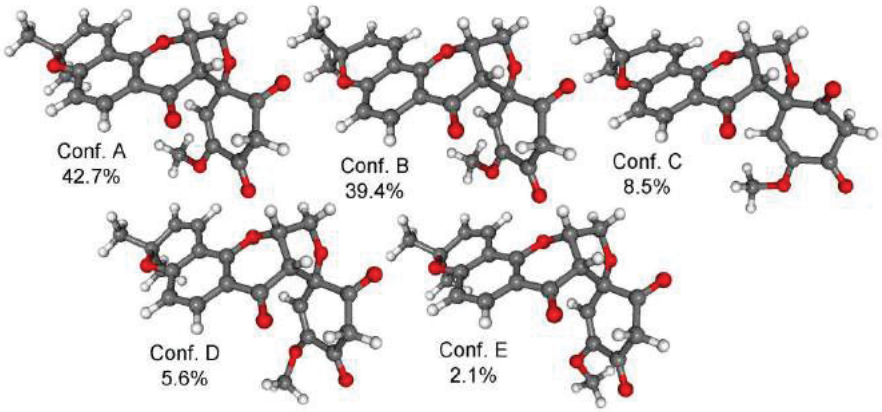

S104. Structure and population of the low-energy B3LYP/6-31G(d) *in vacuo* conformers (≥ 2%) of (1a*R*,6a*S*,12a*R*)-**45**.

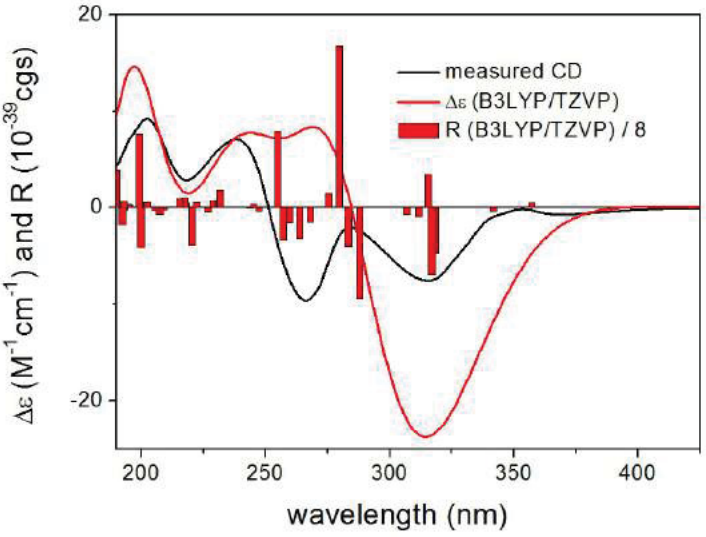

S105. Experimental ECD spectrum of **45** in MeCN compared with the B3LYP/TZVP calculated ECD spectrum of (1a*R*,6a*S*,12a*R*)-**45** computed for the single major B97D/TZVP (PCM/MeCN) conformer (99.1%). Bars represent the rotational strength of the single major conformer.

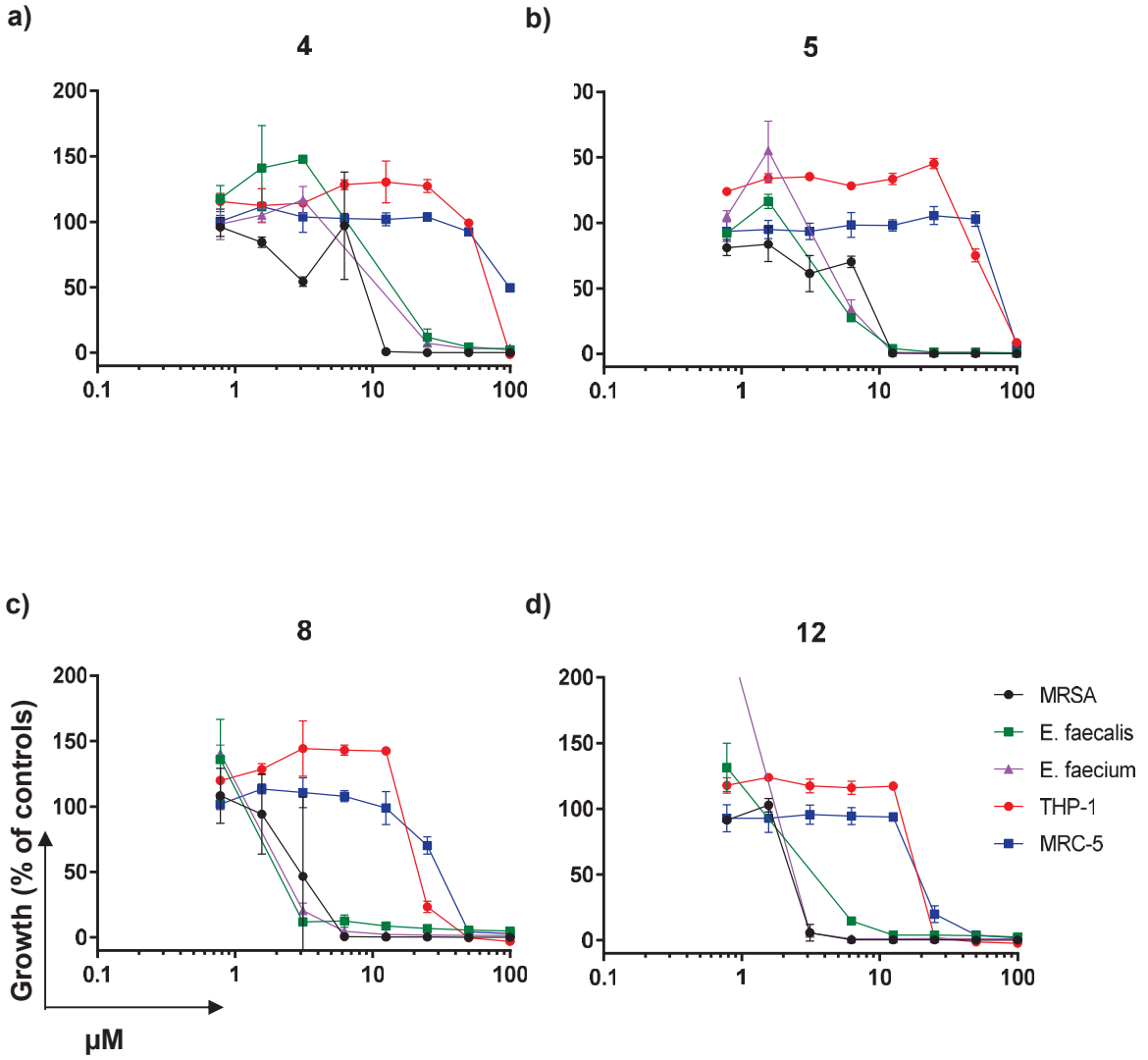

S106. Dose-response curves of compounds **4** (a), **5** (b), **8** (c) and **12** (d) against MRSA (●), *E. faecalis* ATCC 51299 (■), *E. faecium* (▲) ATCC 700221 and the human cell lines THP-1 (●) and MRC-5 (■).

6. Discussion

6.1 Isolated Natural Products from *Sarcotheca griffithii*

6.1.1 Flavone *C*-Glycosides

Chrysin is a 5,7-dihydroxyflavone which can be found in many plants. Biosynthetically, it is produced from a cinnamoyl starter unit, with chain extension using three molecules of malonyl CoA (Dewick, 2009). The glycosylation of chrysin takes place mainly at C-6, C-8 and/or O-7 of the core structure (Andersen *et al*, 2006).

The leaves of *S. griffithii* yielded five new chrysin 6-*C*-glycosides, namely chrysin 6-*C*-(2″-*O*-*α*-L-rhamnopyranosyl)-*β*-D-glucopyranoside (**1**), chrysin 6-*C*-(2″-*O*-*α*-L-rhamnopyranosyl)-*β*-D-glucopyranosyl-7-*O*-*β*-D-glucopyranoside (**2**), chrysin 6-*C*-(2″-*O*-*α*-L-rhamnopyranosyl)-*β*-L-fucopyranoside (**3**), chrysin 6-*C*-(2″-*O*-*α*-L-rhamnopyranosyl)-6′-deoxy-*ribo*-hexos-3-uloside (**4**), and chrysin 6-*C*-*β*-boivinopyranosyl-7-*O*-*β*-L-glucopyranoside (**5**), together with one known compound, isovitexin 2″-*O*-*α*-L-rhamnopyranoside (**6**). Further analysis of the HPLC, UV and MS data of the crude extract showed that most of the minor peaks were suggested to be additional chrysin *C*-glycosides. Considering this, it can be assumed that natural products produced by *S. griffithii* are mainly chrysin *C*-glycosides.

Chrysin derivatives with sugar residues attached at C-6 are considered typical flavonoid glycosides of *S. griffithii*, which have not been recorded from other genera in the family Oxalidaceae until now. Instead, they were reported to be produced by plants of genus *Scutellaria* in the family Lamiaceae (Andersen *et al*, 2006; Miyaichi *et al*, 1994; Takagi *et al*, 1981). Subsequently, it can be assumed that chrysin 6-*C*-glycosides, particularly the new compound chrysin 6-*C*-(2″-*O*-*α*-L-rhamnopyranosyl)-*β*-D-glucopyranoside (**1**), are chemotaxonomic markers for this species and probably for the whole genus *Sarcotheca* as well.

β-Boivinopyranose and 6′-deoxy-*ribo*-hexos-3-ulose sugar moieties obtained in this study are rarely found in nature. They were reported as glycosides in several species of higher plants (Seigler *et al*, 1998). *β*-Boivinopyranose is a 2,6-dideoxysugar produced through reduction at C-2 and C-6 of hexose. 6′-Deoxy-*ribo*-hexos-3-ulose possesses a keto group at C-3 by reduction of 6-deoxyglucose by NADH (Lombó *et al*, 2009) (Figure 6.1.1.1).

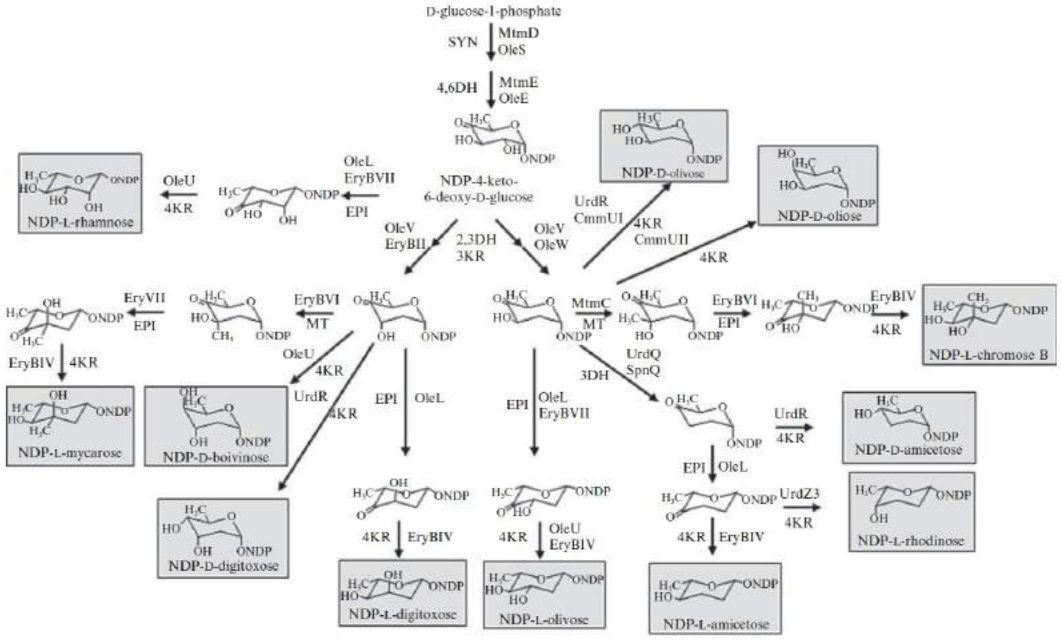

Figure 6.1.1.1. Biosynthesis of *β*-boivinopyranose and 6′-deoxy-*ribo*-hexos-3-ulose

6.1.2 Biological Activity of Chrysin *C*-Glycosides

The antioxidant properties of flavonoids are suggested to be dependent on the presence of a catechol moiety in ring B, a 3-hydroxyl and a carbonyl group at C-4, and a double bond at C-2/C-3 (Harborn and William, 2000). Thus, it was assumed that chrysin displays antioxidant activity as previously reported (Pushwalli *et al*, 2010). Despite this fact, another study reported that the lack of hydroxyl groups in the ring B of flavones and the increasing number of sugar residues will lessen the antioxidant activity (Mantoro *et al*, 2001; Yan *et al*, 2011), suggesting that the chrysin C-glycosides will not show antioxidant activity.

Chrysin had been known to demonstrate cell toxicity, inhibition of DNA synthesis at very low concentrations in a normal trout liver cell line, and to induce apoptosis in human cancer cell lines (Tsuji *et al*, 2009; Khoo *et al*, 2010). In this study, the crude extract that mainly contained chrysin 6 *C*-glycosides was evaluated for cytotoxicity against the mouse lymphoma L5178Y cell line and it was found to be not active. Cytotoxicity of chrysin *C*-glycosides has not been reported yet. It is likely that the sugar moieties at C-6 abolish the cytotoxicity of chrysin *C*-glycosides. Hence, the roles of chrysin 6-*C*-glycosides in leaves of *S. griffithii* are still unknown.

6.2 Isolated Natural Products from *Piper retrofractum*

6.2.1 Piperamides

The formation of cyclobutanamides and cyclohexenamides was suggested to originate from monomeric amides, such as piperines, by intermolecular Diels-alder reaction through [2+2] or [4+2] cycloaddition (Figure 6.2.1.1 and 6.2.1.2). This type of reaction can easily occur through non-enzymatic catalysis, such as photo-oxidation or catalyzed by a Lewis acid. Some chemical studies reported that piperines could be transformed to cyclohexenamides as a mixture of piperamide dimers by Diels-Alder cycloaddition reaction (Wei *et al*, 2005; Rao *et al*, 2011) (Figure 6.2.1.3).

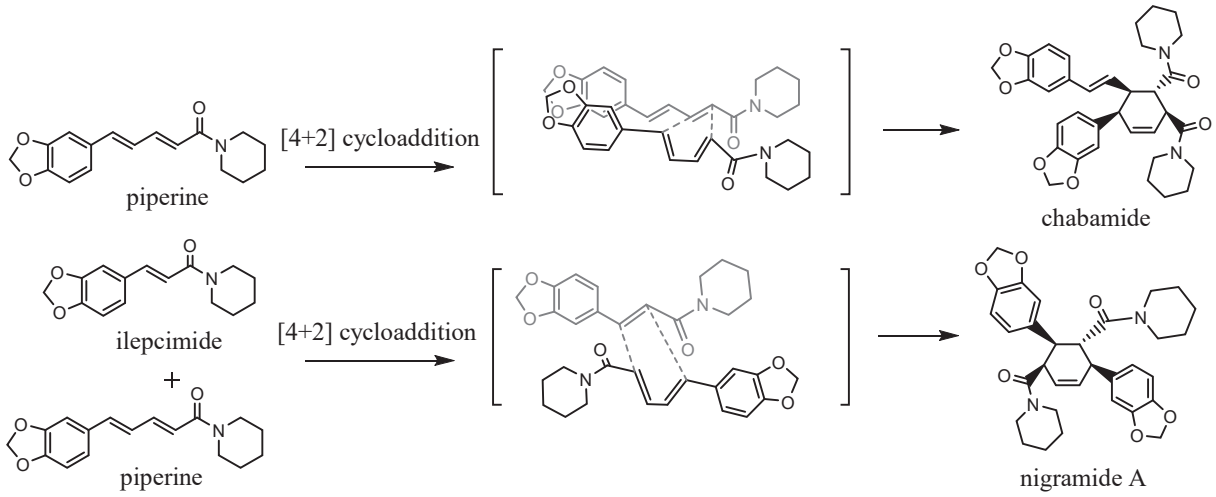

Figure 6.2.1.1. Plausible biosynthetic pathways of dimeric amides bearing cyclohexenamides isolated from *P. retrofractum* by an intermolecular Diels-Alder reaction.

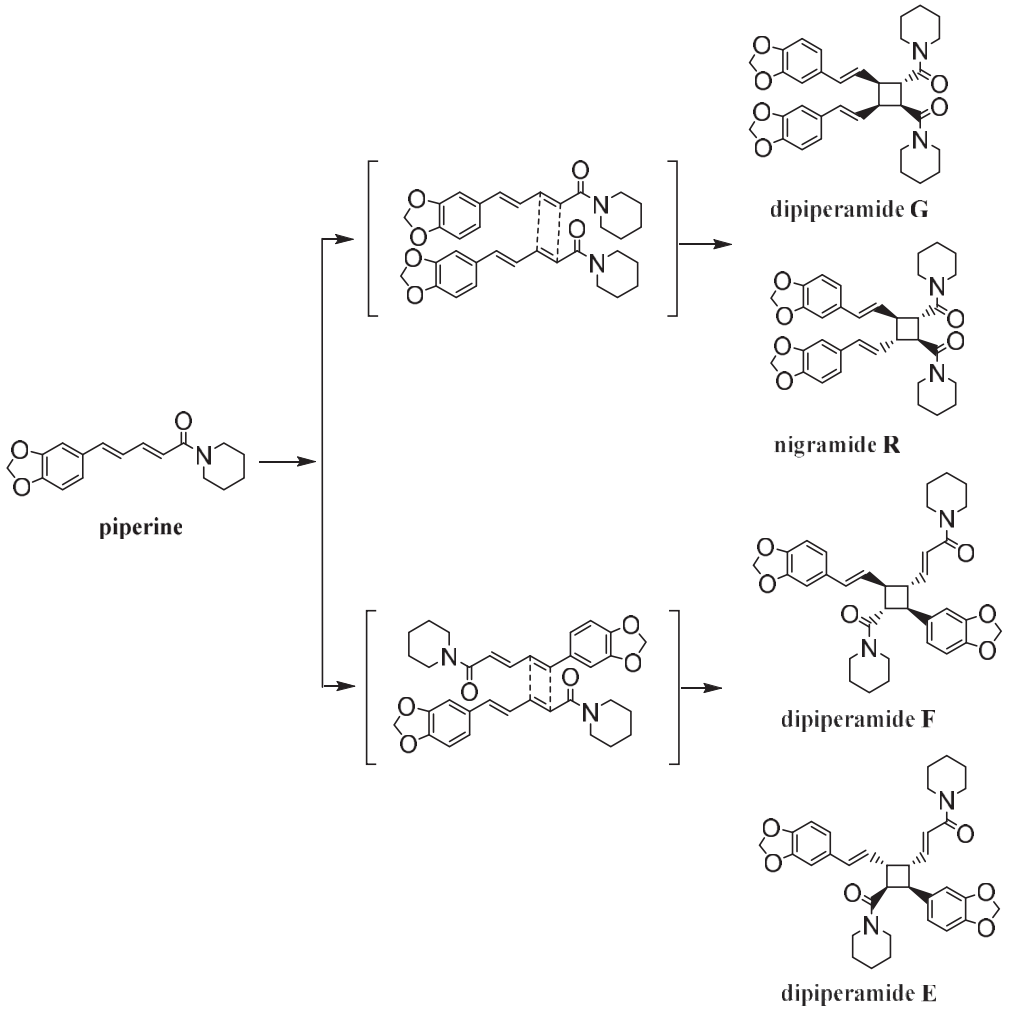

Figure 6.2.1.2. Plausible biosynthetic pathways of dimeric amides bearing cyclobutane rings isolated from *P. retrofractum* by an intermolecular Diels-Alder reaction.

Furthermore, a wide diversity of natural product adducts formed through [2+2] cycloaddition is found in nature. For example, piperarborenine B from *Piper arborescens* (Piperaceae) (Lee *et al*, 2004), tadehaginoside D from *Tadehagi triquetrum* (Fabaceae) (Zhang *et al*, 2016) and crotoeurin A from *Croton euryphyllus* (Euphorbiaceae) (Pan *et al*, 2015) (Figure 6.1.2.4) are cyclobutane-containing natural products formed by [2+2] cycloaddition reactions. The monomer of those natural products possesses one diene as reactive substrate to form a cyclobutane moiety. It was proposed that the [2+2] cycloaddition reaction originated due to ultra violet radiation, which was experimentally supported (Filho *et al*, 1981; Desiraju *et al*, 1984).

The genus *Piper*, particularly *P. retrofractum*, shows a high diversity of natural products due to the production of four membered ring-containing cyclobutanamides as shown in figure 6.1.2.2. Uniquely, the monomers of cyclobutanamides from *P. retrofratum* are mostly piperines with conjugated dienes. Meanwhile, previous experiments on the cycloaddition of piperine gave mainly cyclohexenamides, whereas theoretically both cyclohexenamides and cyclobutanamides were to be expected. Considering this evidence, it is suggested that the formation of cyclobutanamides in *P. retrofractum* occurs under the effect of other factors such as enzymatic catalysis rather than by ultra violet radiation.

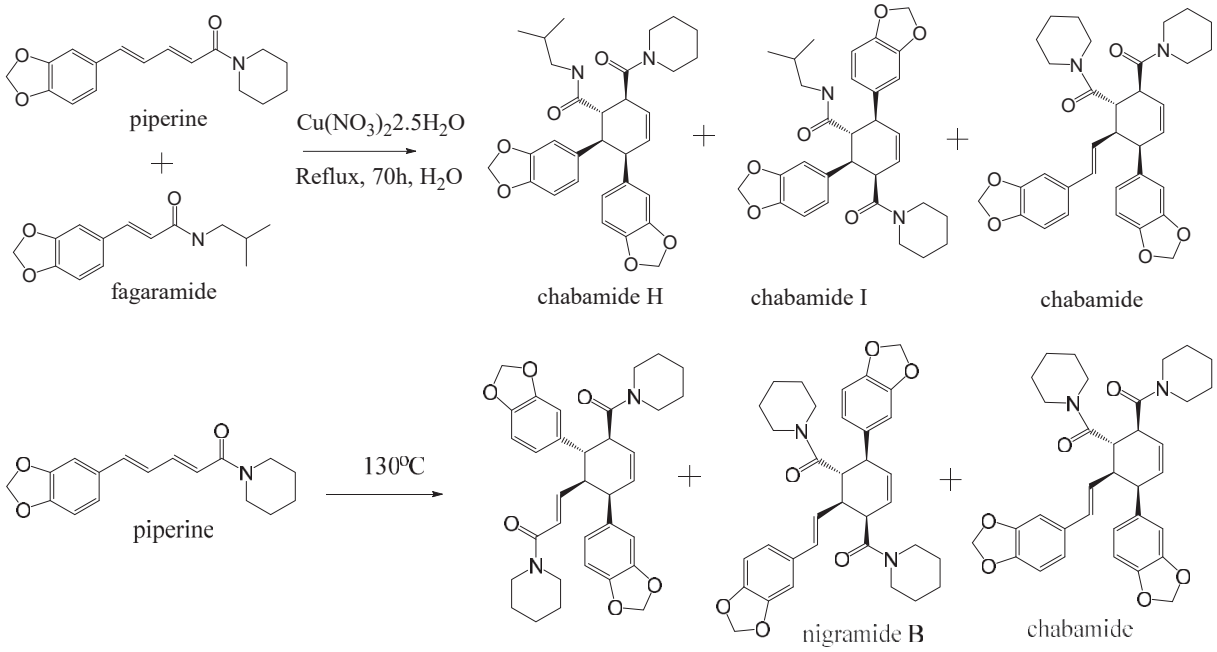

Figure 6.2.1.3 Formation of piperamide dimers from amide monomers by cycloaddition reaction

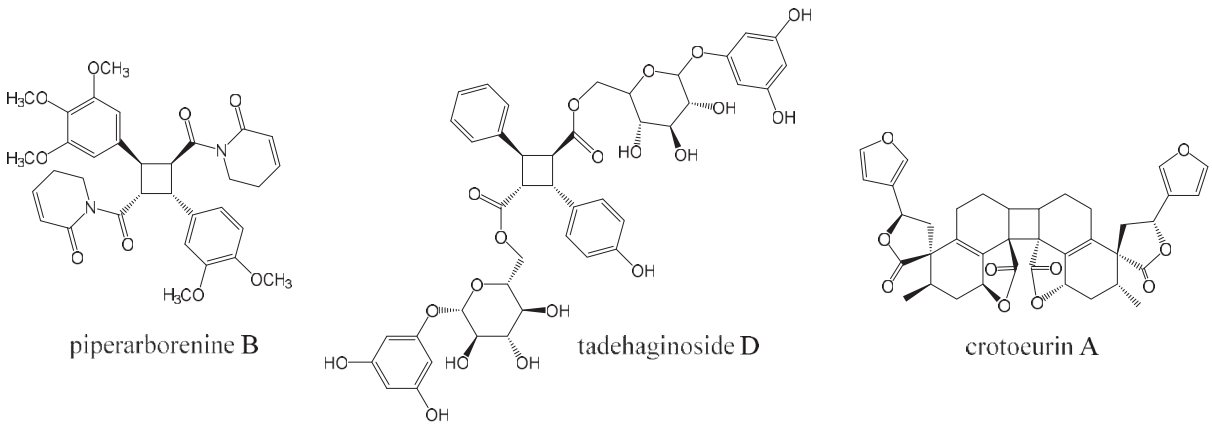

Figure 6.1.2.4. Structures of several cyclobutane-containing natural products

Discussion

The Diels-Alderase has been investigated for two decades in order to understand the mechanism of [4+2] or [2+2] cycloaddition reactions (Klas *et al*, 2015). Recently, SpnF was proposed to be a natural Diels-Alderase that catalyzes a [4+2] cycloaddition in the biosynthesis of spinosyn A (Kim *et al*, 2011; Fage *et al*, 2015). LNKS, lovastatin nonaketide synthase, chorismate mutase and solanopyrone synthase are some other enzymes representing the first naturally occurring Diels-Alderase enzymes that could be purified (Klas *et al*, 2015; Townsend *et al*, 2011). These enzymes are still under investigation regarding whether and how they catalyze the described reaction (Klas *et al*, 2015). As enzymes catalyzing the formation of six membered rings through [4+2] cycloaddition have been discovered, it is suspected that enzymes responsible for catalyzing [2+2] cycloaddition should also exist. In spite of that, up to now there is no literature study regarding the involvement of Diels-Alderase for [2+2] cycloaddition reactions. Taking this into consideration, plants of the genus *Piper*, particularly *P. retrofractum*, might possess similar Diels-Alderase enzymes, which are able to perform an intermolecular Diels-Alder reaction involving [4+2] and/or [2+2] cycloadditions. However, this field has not been studied so far.

Nevertheless, this result provoked the question whether dimeric amides that were isolated are truly natural products or rather artefacts formed during isolation. In order to prove that dimeric amides are not artificial compounds, crude extract of *P. retrofractum* was prepared avoiding presence of light, followed by HPLC and ESIMS analysis. All previously isolated dimeric amides that were present in extracts exposed to light were detectable proving that the isolated dimeric amides are in fact true natural products.

The basic structure units of the amides in *P. retrofractum* feature piperidyl or isobutyl amino moieties (Muharini *et al*, 2015; Banerji *et al*, 1985; Ahn *et al*, 1992; Kubo *et al*, 2013), whereas piperamides with pyrrolidyl moieties have not been discovered from this investigated species so far. It seems that the enzymes responsible for amide formation using pyrrolidyls do not exist in *P. retrofractum*.

6.2.2 Biological Activity of Piperamides

6.2.2.1 Antifungal Activity of Piperamides

Antifungal assays against phytopathogenic fungus, *Cladosporium cladosporioides* revealed three active fractions from *P. retrofractum*, including fractions PiHE60, PiHE40 and PiHE20. Fraction PiHE60 and PiHE40 were more active than PiHE20 (Table 6.2.2.1), suggesting that these two fractions contained the major active substances. Chromatographic work up of the latter fraction yielded four active compounds inhibiting the growth of *C. cladosporioides*. Piperanine displayed good inhibition compared to the positive control nystatine (Table 6.2.2.1), while piperine, isochavicine and piperlonguminine showed weak inhibition.

Table 6.2.2.1. Inhibition zone of fractions and compounds isolated from *P .retrofractum* against *C. cladosporioides*.

No.	Fractions (100 µg) / Compounds (0.5 µmol)	Zone of Inhibition (d, mm)
1.	PiHE60	12
2.	PiHE40	13
3.	PiHE20	7.5
4.	Piperanine	15.0
5	Piperine	8.0
6.	Isochavicine	7.0
7.	Piperlonguminine	6.5
8.	Nystatine (positive control)	29.6
Diameter of paper disk (d) = 6 mm		

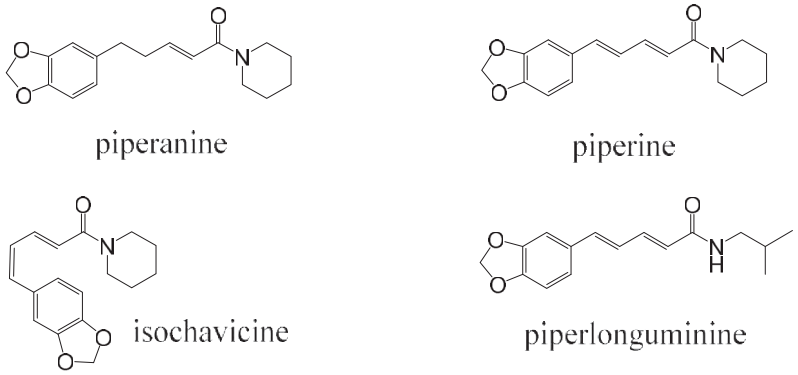

Figure 6.2.2.1 Structures of piperanine, piperine, isochavicine and piperlonguminine.

Isochavicine was reported for the first time in this study to inhibit the growth of *C. cladosporioides* while piperine, piperanine, and piperlonguminine had been reported previously to possess antifungal activity against *C. sphaerospermum* (Marques *et al*, 2007; Navickiene *et al*, 2000). The structural similarity of piperanine, piperine, isochavicine and piperlonguminine lies in the presence of methylenedioxyphenyl moieties and in the number of aliphatic carbons between the methylenedioxyphenyl moiety and the basic moiety (Figure 6.2.2.1), which is supposed to be a key factor for their antifungal activities against *C. cladosporioides*. Moreover, the loss of one double bond in piperanine might lead to its stronger activity compared to piperine and isochavicine. Meanwhile, the isobutyl amine moiety in piperlonguminine was found to decrease the antifungal activity.

6.2.2.2 Cytotoxicity of Piperamides

Piperamides are known for their cytotoxicity against several cancer cell lines (Okwute *et al*, 2013; Gutierrez *et al*, 2013). A cytotoxicity assay of the isolated compounds against the mouse lymphoma L5178Y cell line showed that dehydropipernonaline, a methylene dioxyphenyamide, and nigramide R, a cyclobutanamide, displayed good cytotoxicity by comparison with the positive control kahalalide F. Moreover, among the isolated alkylamides, pipericine and pellitorine exhibited moderate cytotoxicity against the mouse lymphoma L5178Y cell line. The presence of methylenedioxyphenyl moieties in retrofractamide C, guineensine, brachystamide B, dehydropipernonaline and pipernonaline apparently increased the cytotoxic activity (Publication 2).

Table 6.2.2.2 Cytotoxicity of isolated compounds from *P. retrofractum* against the mouse lymphoma L5178Y cell line.

No.	Compound	IC_{50} (μM)
1.	Pellitorine	28.3
2.	Pipericine	24.2
3.	Dehydropipernonaline	8.9
4.	Pipernonaline	17.0
5.	Guineensine	17.0
6.	Brachystamide B	16.4
7.	Retrofractamide C	13.4
8.	Dipiperamides F	10.0
9.	Dipiperamides G	13.9
10.	Chabamide	11.6
11.	Nigramide R	9.3
12.	Kahalalide F (positive control)	4.3

Piperanine, piperine, isochavicine, and piperlonguminine did not display cytotoxicity against the mouse lymphoma L5178Y cell line in this study. However, a previous report indicated that piperine was toxic towards Dalton's lymphoma ascites cell and Ehrlich ascites (Sunila *et al*, 2004). The group of Maleck *et al* described that piperlonguminine exhibited cytotoxicity against *Aedes aegypti* with 100% larval mortality at a dose of 30 μg/ml within 24h (Maleck *et al*, 2014).

6.3 Isolated Natural Products from *Talinum triangulare*

6.3.1 *C*-Methylated Flavonoids

C-methylated flavonoids are mostly obtained from the families Myrtaceae and Ericaceae (Bohm *et al*, 1998). *C*-methylated flavonoids are also present in *Piper carniconnectivum* roots (Piperaceae) (Facundo *et al*, 2004), *Pisonia grandis* roots (Nyctaginaceae) (Sutthivaiyakit *et al*, 2013), *Tripterygium wilfordii* roots (Celastraceae) (Zeng *et al*, 2010), and *Pinus densiflora* needles (Pinaceae) (Jung *et al*, 2001). In this study, two new *C*-methylated flavonoids, 5,6-dimethoxy-7-hydroxy-8-methyl-flavone (**1**) and 5,6-dimethoxy-8-methyl-2-phenyl-7H-1-benzopyran-7-one (**2**) were isolated. Compound **2** could also be classified as 3-deoxy-anthocyanidin. The isolation of **1** and **2** gave more evidence to suggest that *C*-methylation of flavonoids occur at C-6 and/or C-8 (Sutthivaiyakit *et al*, 2013; Dao *et al*, 2010; Jung *et al*, 2001; Wollenweber *et al*, 2000; Facundo *et al*, 2004; Harborne *et al*, 1993), and at C-3, which was supported by the isolation of two 3-C-methylflavone glycosides from *Eugenia kurzii* (Myrtaceae) (Painuly and Tandon, 1983).

It is suggested that the *C*-methylation of flavonoids takes place during the condensation of a three malonyl CoA units, in which A-ring is built (Bohm, 1998). This condensation forms alpha methylene carbon, which is adjacent to the carbonyl carbon. The alpha-methylene carbon is an active center for methylation.

The mechanisms of *O*-methyltransferases, which activate methylation by donating methyl moieties to a specific hydroxyl group of acceptor compound, are well studied (Dewick, 2009; Koirala *et al*, 2016). However, there is no report on the characterization of the C-methyltransferase so far (Dewick, 2009; Koirala *et al*, 2016).

The *O*- and *C*-methylation of flavonoids will increase the lipophilicity of the flavonoids. The increase of compound lipophylicity will enhance the membrane absorption, which is likely to increase the pharmaceutical effect of the compounds as well (Koirala *et al*, 2016). Currently, the bioactivities of *C*-methylated flavonoids have been investigated for antioxidant, antimicrobial (Sutthivaiyakit *et al*, 2013), anti-inflammatory (Zeng *et al*, 2010), and neuraminidase inhibitor for novel influenza H1N1 activities (Dao *et al*, 2010). In this study, compound **1** and **2** were screened for antioxidant activity using a TLC method with DPPH reagent, cytotoxicity against the mouse lymphoma L5178Y cell line, and antifungal against *C.cladosporioides*. However, they were found to be inactive in the above mentioned assays.

6.3.2 *α*-Pyrone

A new *α*-pyrone derivative (**3**), 4-methoxy-6-(2-hydroxy-4-phenylbutyl)-2*H*-pyran-2-one, was isolated in this study, which is formed from a cinnamoyl CoA and three malonyl-CoA extender units. As mentioned in publication 3, this new α-pyrone is suggested to be biosynthetically produced through the poliketyde synthase (PKS) pathway, in which cinnamate CoA ligase (CNL) and chalcone synthase (CHS) are presumably involved in the biosynthesis of the new *α*-pyrone derivatives (figure 6.3.2.1) (Dewick, 2009; Abe *et al*, 2004; Akiyama *et al*, 1999; Ting *et al*, 2015). The structure of **3** is similar to *p*-coumaroyltriacetic acid lactone (figure 6.3.2.2), which was synthesized in a recent report by 4-coumarate CoA ligase (4CL) and chalcone synthase (CHS) (Ting *et al*, 2015). Previously, *p*-coumaroyltriacetic acid lactone was considered a by-product of the biosynthesis of flavonoids (Abe *et al*, 2004; Akiyama *et al*, 1999).

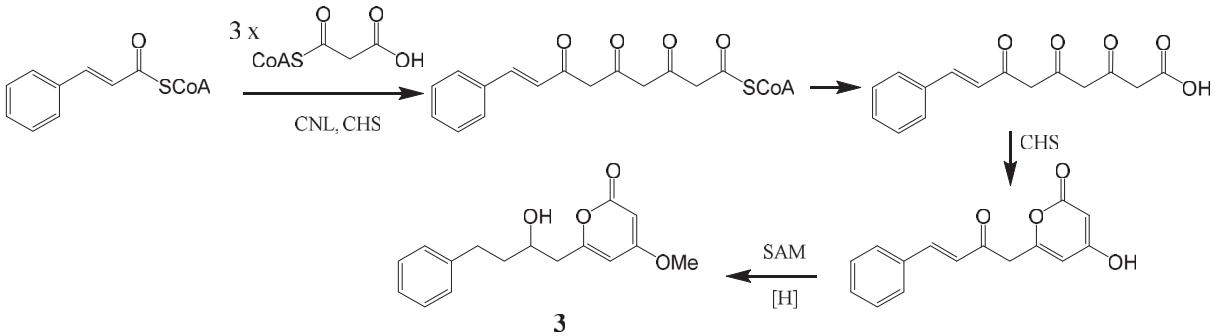

Figure 6.3.2.1. Plausible biosynthetic pathway of α-pyrone derivative (**3**)

Till now, no literature mentioned the bioactivity of *p*-coumaroyltriacetic acid lactone. Meanwhile, yangonin (figure 6.3.2.2), which was obtained from *Piper methysticum* (Piperaceae), demonstrated cytotoxicity by inducing apoptosis in human hepatocyte HepG2 cell line (Tang *et al*, 2011). Based on this information, the new α-pyrone derivative **3** was expected to have cytotoxicity against the mouse lymphoma L5178Y cell, which was conducted in this study. However, the new α-pyrone derivative **3** was found to be inactive.

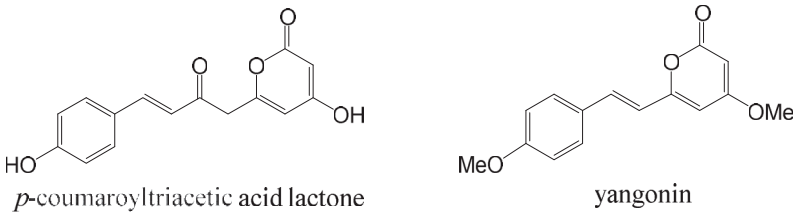

p-coumaroyltriacetic acid lactone yangonin

Figure 6.3.2.2. Structures of *p*-coumaroyltriacetic acid lactone and yangonin

6.3.3 Lignanamides and Aurantiamides

Literature study revealed that lignanamides are found mostly in the families Cannabinaceae and Solanaceae. The structures of lignanamides are built by phenylpropanoids (ferulic acid or 4-coumaric acid in this study), and by amino acid, particularly L-tyrosine, through mannich reactions. Based on the chromatogram analysis of the MeOH crude extracts, it is suggested that lignanamides are major secondary metabolites from roots of *T. triangulare*. Even though the lignanamides isolated in this study (compound **4-9**) are known compounds, this is the first report on lignanamides from family Portulacaceae.

Lignanamides displayed interesting bioactivities such as anti-inflammatory (Sun *et al*, 2014; Al-Taweel *et al*, 2012), antioxidant (Al-Taweel *et al*, 2012; Yan *et al*, 2015; Zhang et al, 2013), acetylcholinesterase inhibiting (Yan *et al*, 2015) and hepatoprotective activity (Li *et al*, 1998). By contrast, the cytotoxicity evaluation of all isolated lignanamides in this study (compounds **4-9**) against the mouse lymphoma L5178Y cell line revealed that compounds **4-9** were inactive. In addition, none of compounds **4-9** showed antifungal activity against *C. cladosporioides*.

Aurantiamides are dipeptide derivatives. Three aurantiamides isolated in this study are known compounds, aurantiamide (**10**), aurantiamide acetate (**11**) and aurantiamide benzoate (**12**).

Aurantiamide and aurantiamide acetate were firstly obtained from seeds of *Piper aurantiacum* (Piperaceae) (Banerji *et al*, 1981). Bioactivities of aurantiamides were evaluated by conducting the same assays mentioned previously in this study. All aurantiamides showed neither cytotoxic nor antifungal activities. Recently, aurantiamide acetate was reported for supressing the growth of maglinant glioma U87 and U251 cells, *in vitro* and *in vivo* by inhibiting autophagic flux (Yang *et al*, 2015).

6.4 Isolated Natural Products from *Amorpha fruticosa*

6.4.1 Amorfrutins

Amorfrutins were isolated for the first time from *A. fruticosa, A. nana* and *A. canescens* by the group of Kemal *et al* (Kemal *et al*, 1979). *Helichrysum umbraculigerum* (Bohlman, F. 1979) and *Glycyrrhiza acanthocarpa* (Ghisalberti *et al*, 1981) were reported to produce the same compounds. Recently, a new amorfrutin, amorfrutin C, was isolated from *Glycyrrhiza foetida* (Weidner *et al*, 2015). This class of compounds includes 2-hydroxybenzoic acids exhibiting hydroxyl or methoxyl groups at C-4 as well as isoprenyl/geranyl and styryl/aryl substituents as side chains (Sauer *et al*, 2014). Based on the structure relationships, it is likely that amorfrutins isolated from *A. fruticosa* originate biosynthetically from stilbenes (publication 4), where isoprenyl or geranyl moieties were introduced at a later stage of the pathway.

Among the isolated amorfrutins, amorfrutin B (**5**), amorphastilbol (**8**) and 2-(1′*E*-styryl)-5-geranyl-resorcin-1-carboxylic acid (**4**) were found to be promising antibacterial compounds, since both compounds showed good inhibitory activity, not only against laboratory gram-positive bacteria strains but also against methicilin-resistant *S. aureus* (MRSA ATCC700699) and vancomycin-resistant *E. faecium* (ATCC700221) (publication 4). The presence of a double bound in the styryl side chain is believed to be important for the antibacterial activities of amorfrutins. Moreover, a *trans*-configurated double bond rendered the resulting derivatives more active than the presence of a *cis*-configurated double bond, as shown for 2-(1′*Z*-styryl)-5-geranyl-resorcin-1-carboxylic acid (**1**) and 2-(1′*E*-styryl)-5-geranyl-resorcin-1-carboxylic acid (**4**)**.** The loss of the double bond in the styryl side chain seems to give no influence for the antibacterial activity (**5** and **9**). In addition, the presence of hydroxyl group at C-6" of the new compound **3** abolishes the antibacterial activity. Hence, although new compound **2** was not tested

for antibacterial activities due to the lack of sufficient amounts, it is suspected to be inactive. In order to investigate the role of the phenolic hydroxyl groups in the resorcinol moiety for the antibacterial activity, amorphastilbol was methylated and evaluated for antibacterial activity. The methylated amorphastilbol was found to be inactive, suggesting the importance of the phenolic hydroxyl groups for the antibacterial activity.

Interestingly, amorphastilbol (**8**) and 2-(1′*E*-styryl)-5-geranyl-resorcin-1-carboxylic acid (**4**) displayed weak cytotoxicity against the L5178Y, THP-1 and MRC-5 cell lines when compared to their much stronger antibacterial activity. For these latter compounds a sufficiently wide therapeutic window exists that makes further studies on the molecular targets and modes of action worthwhile.

6.4.2 Rotenoids

Rotenoids are a naturally occurring subclass of isoflavonoids found in the families Leguminaceae/Fabaceae, Iridaceae and Nyctaginaceae (Crombie *et al*, 1998). In the family Fabaceae, this group of compounds is reported not only to occur in the genus *Amorpha,* but also in the genera *Deguelia, Derris* and *Milletia* (Crombie *et al*, 1998). The rotenoids originate from rotenone, the first rotenoid that had been isolated from the genus *Derris* (Dewick *et al*, 2009; Crombie *et al*, 1998). Rotenoids feature a tetracyclic ring system with a *cis*-fused 6a,12a-dihydrochomeno[3,4-b]chromone nucleus (Figure 6.4.2.1).

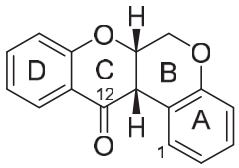

Figure 6.4.2.1 The core structure of rotenoids.

The first reported rotenoids from *A. fruticosa* were amorphigenin (**40**) and its glycoside, amorphin (Acree *et al*, 1943). Rotenoids share similar biosynthetic pathways with isoflavonoids with isoprenoid substituents to be introduced at later stage of their biosynthesis. Methylation of the hydroxyl group at C-2′ of the isoflavonoid core structure, followed by cyclization, causes the formation of the pyran ring B of rotenoids (Figure 6.4.2.2). A recent study reported that cyclization in the formation of ring B involved a free-radical pathway rather than a cationic

pathway (Kirckpatrik *et al*, 2016). The introduction of isoprenyl groups at C-8 of the isoflavonoid yields rotenonic acid (**27**). The isoprenyl moiety of rotenonic acid will cyclize to form ring E as a pyran or furan ring, thereby yielding deguelin or rotenone, respectively (Dewick, 2009). In nature, most reported rotenoids show a junction of rings B/C with a *cis*-configuration.

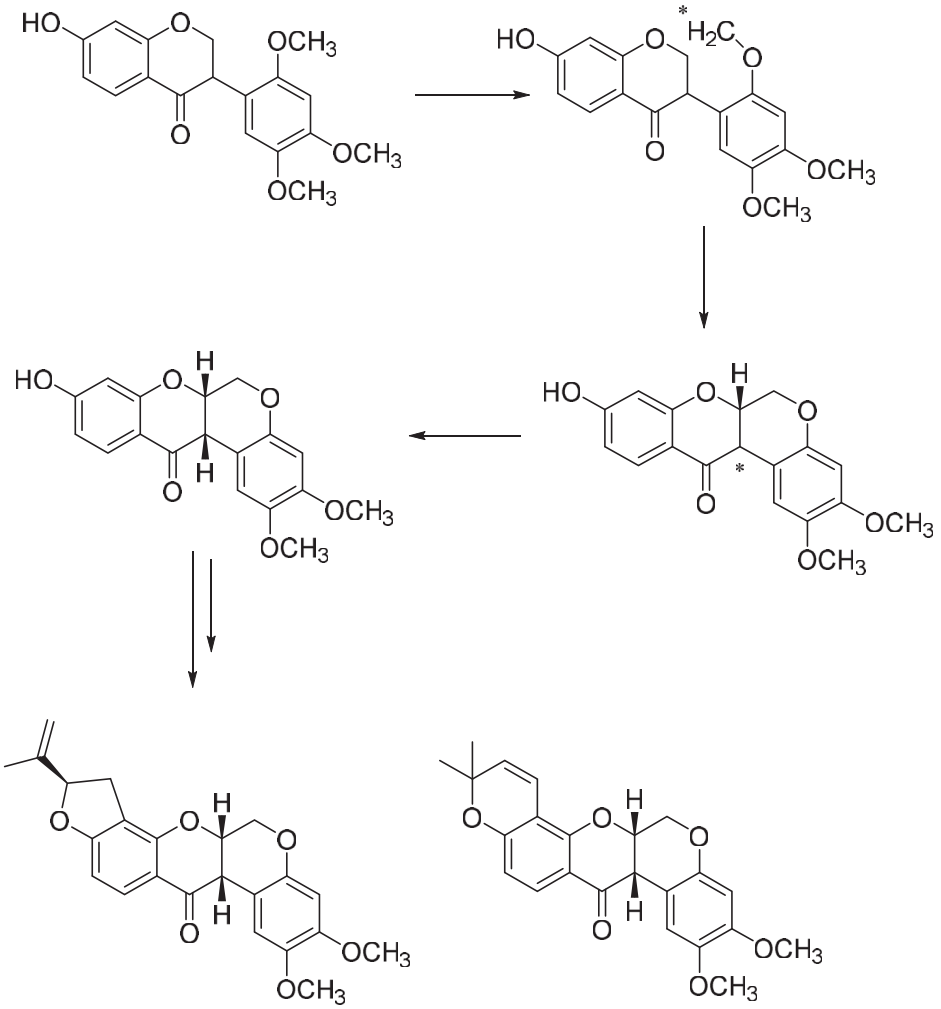

Figure 6.4.2.2. Construction of ring B in rotenoids from an isoflavonoid by oxidation of a methoxy group in the radical pathway.

A. fruticosa produces unusual rotenoids, namely spirorotenoids, which are characterized by the presence of a spiro ring (Li *et al*, 1991; Terada *et al*, 1992). The first isolated spirorotenoid from *A. fruticosa* was amorphispironone (**47**) (Li *et al*, 1991). Other types of spirorotenoids occur in the genera *Tephrosia* and *Derris*, which also belong to the family Fabaceae (Andrei *et al*,

2002; Yenesew *et al*, 2006) (Figure 6.4.2.3). Up to now, there is no report on the isolation of amorphispironone and its derivatives from the latter genera, suggesting that amorphispironone is a characteristic spirorotenoid for the genus *Amorpha*.

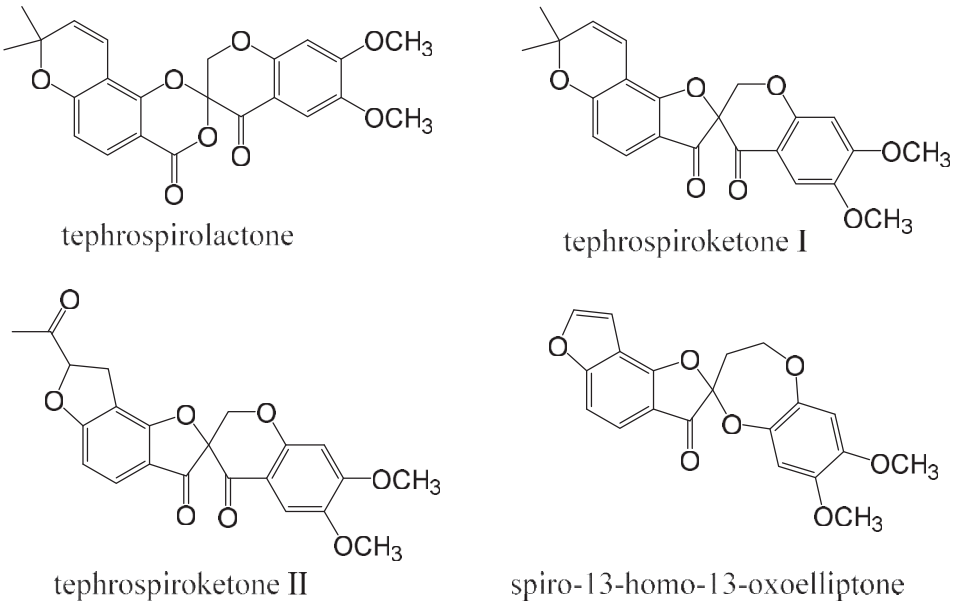

Figure 6.4.2.3 Spirorotenoids from the genera *Tephrosia* and *Derris*

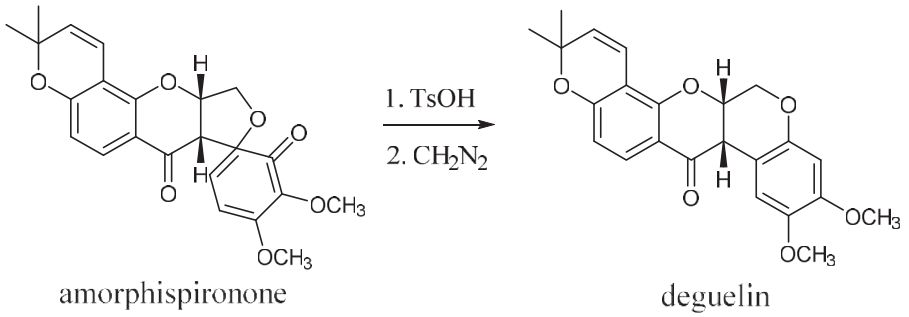

Figure 6.4.2.4 Reduction of amorphispironone produces deguelin

Biosynthetically, the spirorotenoid amorphispironone was assumed to be derived from deguelin (**30**) (Li *et al*, 1991; Terada *et al*, 1993; Crowbie *et al*, 1998) which was corroborated through chemical conversion experiments using *p*-toluenesulfonic acid and amorphisipironone followed by methylation with diazomethane (Terada *et al*, 1993) (Figure 6.3.2.4). Crowbie reported that amorphispironone was constructed from degeulin through an enzymatically

catalyzed oxidation in plants (1998). In this study, the isolation of new compounds, amorphispironones B (**45**) and C (**46**) from *A. fruticosa* would extend the plausible biosynthetic pathway for this type of compounds. Amorphispironone B (**45**) was derived from amorphispironone by demethylation. After alpha-oxidation, amorphispironone (**47**) can be formed.

Because of the cyclizations of rings B and E as well as spiro formation, stereogenic centers occur in the structures of rotenoids usually at C-5′, C-6a, C-12a and C-1a. The relative configuration of C-6a and C-12a of rotenoids can be determined easily by analysis of their ^{3}J values and by analysis of the chemical shift of H-1 (Kostova *et al*, 1986). In contrast, the determination of the relative configuration of C-5′ is challenging, but can be predicted using a biosynthetic approach (Crombie *et al*, 1998). As rotenone is the first isolated rotenoid, the absolute configuration and conformation of this compound were thoroughly studied and previously determined as 6a*S*, 12a*S* and 5′*R* by chemical and NMR spectroscopic studies (Büchi *et al*, 1961). In 1975, the absolute configuration of rotenone was confirmed by X-ray crystallography (Begley *et al*, 1975). Hence, rotenone became a model compound for determination of the absolute configuration of all other rotenoids. Since then, alpha D and CD measurements have become useful techniques. Kostova compiled CD spectra and NMR data of several rotenoids and found that the chemical shifts of *α*-oriented H-5′ were more downfield than the *β*-oriented ones, when H-6a and H-12a were *β*-oriented. In this study, by combining CD data and analysis of ROESY spectra, the absolute configuration of H-5′ could be assigned. However, the absolute configuration of compound **43** was complicated to be determined unambiguously due to the lack of data of comparably rotenoids in the literature. Instead, a biosynthetic approach was used in this case to solve the stereochemistry of this compound.

Rotenoids can be substituted by hydroxyl groups at C-6′, C-7′, C-11 or C-12a and dehydrogenated at C-6a and C-12 or C-6′ and C-7′. Cyclization, oxidation, methylation and dehydrogenation reactions as well as spiro formation of rotenoids from *A. fruticosa* lead to the diversity of rotenoids structures detected in this study. 6a*R*,12a*R*,5′*R*-Amorphigenin (**44**), 3-demethyldalbinol (**42**), 6a,12a-dehydro-3-demethylamorphigenin (**43**), amorphispironone B (**45**) and amorphispironone C (**46**) are new natural rotenoids described for the first time in this study (Publication 4).

Discussion

Rotenoids have been reported previously to show cytotoxicity against various human cell lines, i.e. MDB-MB-231 human breast cancer line (Li *et al*, 1993), MCF-7, HCT-116 (Wu *et al*, 2015) and HEL299 human lung cell line (Lee *et al*, 2006). In this study, these compounds exhibited significant cytotoxicity against the mouse lymphoma L5178Y cell line (publication 4). For instance, dalpanol (**35**), dalbinol (**41**), 11-hydroxyamorphispironone (**48**), amorphispironone B (**45**) and 6'-O-β-D-glucopyranosyldalpanol (**53**) displayed significant cytotoxicity with IC_{50} values of 0.7, 0.2, 1.3, 7.6 and 1.7 μM, respectively. In a previous report, amorphigenin and dalbinol showed cytotoxicity against the human lung carcinoma cell line Lu1 (Chin *et al*, 2006), while dalpanol was shown to be cytotoxic towards the neoplastic cell A-549, HC-8, TE671 and KB lines (Li *et al*, 1993). 11-Hydroxyamorphispironone (**48**), was shown to block the DNA binding activity of NF-κB in MCF-7 cells induced by TNF-α (Dat *et al*, 2008). Taking these data altogether, it is more likely that most rotenoids and spirorotenoids exhibit a wide spectrum of cytotoxicity, not only in animal cell lines, but also in human cell lines. Based on structure-activity relationship studies, it seems that glycosylation of rotenoids weakens or abolishes their cytotoxicity as shown by comparison of dalpanol (**35**) and its glycoside (**53**). Moreover, Wu *et al*. proposed that the positions of sugar substituents influenced the cytotoxicity of rotenoid glycosides (Wu *et al*, 2015). In contrast to their potent cytotoxicity, none of the isolated rotenoids obtained in this study showed antibacterial activities towards gram-positive and negative bacteria strains.

7. Further Scientific Achievement

The following poster was presented on the International Congress and Annual Meeting of the Society for Medicinal Plant and Natural Product Research, in Budapest, Hungary, on 23 -27 August 2015.

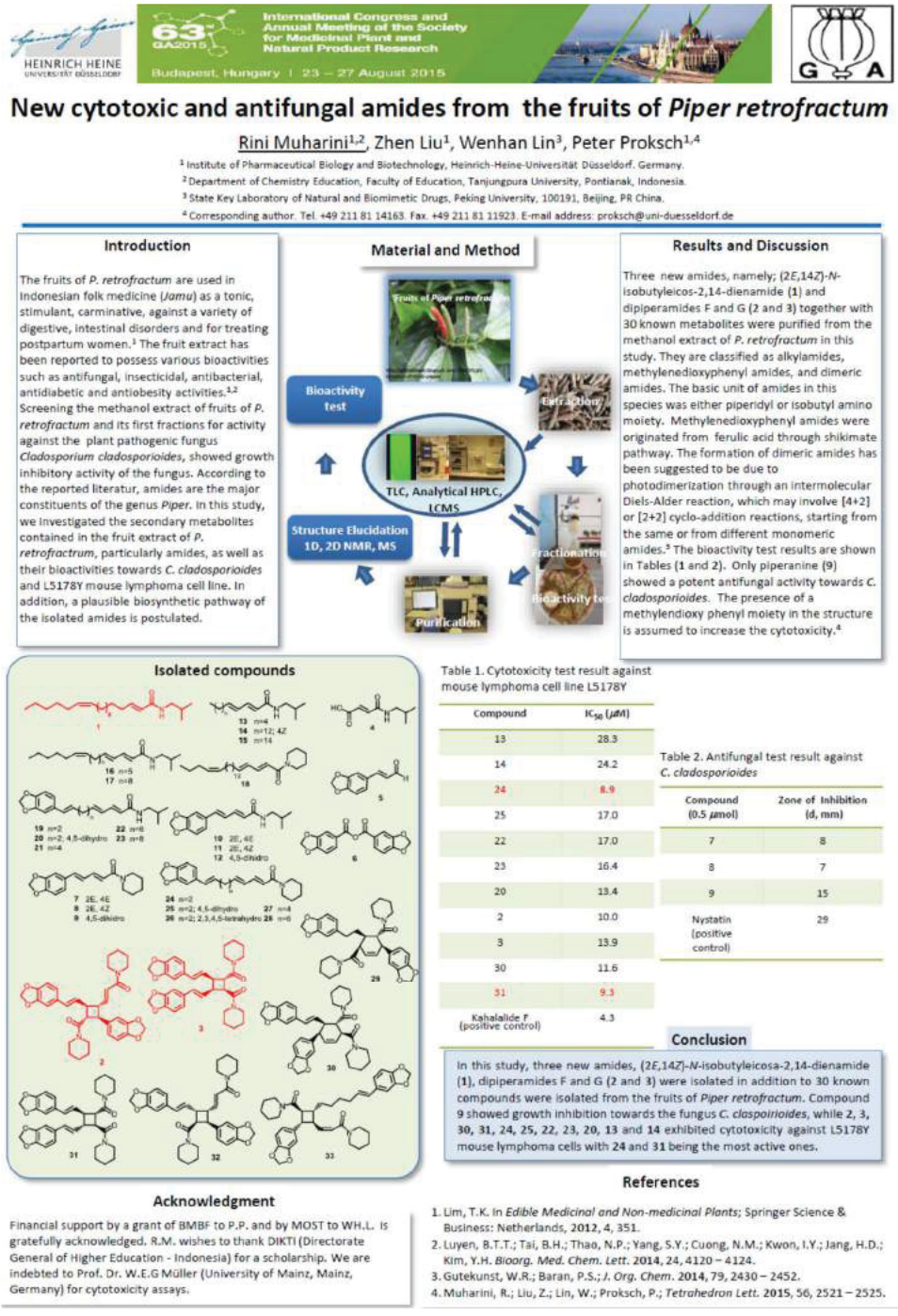

63rd GA2015 International Congress and Annual Meeting of the Society for Medicinal Plant and Natural Product Research
Budapest, Hungary | 23 – 27 August 2015

New cytotoxic and antifungal amides from the fruits of *Piper retrofractum*

Rini Muharini[1,2], Zhen Liu[1], Wenhan Lin[3], Peter Proksch[1,4]

[1] Institute of Pharmaceutical Biology and Biotechnology, Heinrich-Heine-Universität Düsseldorf. Germany.
[2] Department of Chemistry Education, Faculty of Education, Tanjungpura University, Pontianak, Indonesia.
[3] State Key Laboratory of Natural and Biomimetic Drugs, Peking University, 100191, Beijing, PR China.
[4] Corresponding author. Tel. +49 211 81 14163. Fax. +49 211 81 11923. E-mail address: proksch@uni-duesseldorf.de

Introduction

The fruits of *P. retrofractum* are used in Indonesian folk medicine (*Jamu*) as a tonic, stimulant, carminative, against a variety of digestive, intestinal disorders and for treating postpartum women.[1] The fruit extract has been reported to possess various bioactivities such as antifungal, insecticidal, antibacterial, antidiabetic and antiobesity activities.[1,2] Screening the methanol extract of fruits of *P. retrofractum* and its first fractions for activity against the plant pathogenic fungus *Cladosporium cladosporioides*, showed growth inhibitory activity of the fungus. According to the reported literatur, amides are the major constituents of the genus *Piper*. In this study, we investigated the secondary metabolites contained in the fruit extract of *P. retrofractrum*, particularly amides, as well as their bioactivities towards *C. cladosporioides* and L5178Y mouse lymphoma cell line. In addition, a plausible biosynthetic pathway of the isolated amides is postulated.

Material and Method

Results and Discussion

Three new amides, namely; (2*E*,14*Z*)-*N*-isobutyleicos-2,14-dienamide (**1**) and dipiperamides F and G (**2** and **3**) together with 30 known metabolites were purified from the methanol extract of *P. retrofractum* in this study. They are classified as alkylamides, methylenedioxyphenyl amides, and dimeric amides. The basic unit of amides in this species was either piperidyl or isobutyl amino moiety. Methylenedioxyphenyl amides were originated from ferulic acid through shikimate pathway. The formation of dimeric amides has been suggested to be due to photodimerization through an intermolecular Diels-Alder reaction, which may involve [4+2] or [2+2] cyclo-addition reactions, starting from the same or from different monomeric amides.[3] The bioactivity test results are shown in Tables (**1** and **2**). Only piperanine (**9**) showed a potent antifungal activity towards *C. cladosporioides*. The presence of a methylendioxy phenyl moiety in the structure is assumed to increase the cytotoxicity.[4]

Isolated compounds

Table 1. Cytotoxicity test result against mouse lymphoma cell line L5178Y

Compound	IC_{50} (μM)
13	28.3
14	24.2
24	8.9
25	17.0
22	17.0
23	16.4
20	13.4
2	10.0
3	13.9
30	11.6
31	9.3
Kahalalide F (positive control)	4.3

Table 2. Antifungal test result against *C. cladosporioides*

Compound (0.5 μmol)	Zone of Inhibition (d, mm)
7	8
8	7
9	15
Nystatin (positive control)	29

Conclusion

In this study, three new amides, (2*E*,14*Z*)-*N*-isobutyleicosa-2,14-dienamide (**1**), dipiperamides F and G (**2** and **3**) were isolated in addition to 30 known compounds were isolated from the fruits of *Piper retrofractum*. Compound **9** showed growth inhibition towards the fungus *C. claspoirioides*, while **2**, **3**, **30**, **31**, **24**, **25**, **22**, **23**, **20**, **13** and **14** exhibited cytotoxicity against L5178Y mouse lymphoma cells with **24** and **31** being the most active ones.

Acknowledgment

Financial support by a grant of BMBF to P.P. and by MOST to WH.L. is gratefully acknowledged. R.M. wishes to thank DIKTI (Directorate General of Higher Education - Indonesia) for a scholarship. We are indebted to Prof. Dr. W.E.G Müller (University of Mainz, Mainz, Germany) for cytotoxicity assays.

References

1. Lim, T.K. In *Edible Medicinal and Non-medicinal Plants*; Springer Science & Business: Netherlands, **2012**, 4, 351.
2. Luyen, B.T.T.; Tai, B.H.; Thao, N.P.; Yang, S.Y.; Cuong, N.M.; Kwon, I.Y.; Jang, H.D.; Kim, Y.H. *Bioorg. Med. Chem. Lett.* **2014**, 24, 4120 – 4124.
3. Gutekunst, W.R.; Baran, P.S.; *J. Org. Chem.* **2014**, 79, 2430 – 2452.
4. Muharini, R.; Liu, Z.; Lin, W.; Proksch, P.; *Tetrahedron Lett.* **2015**, 56, 2521 – 2525.

8. References

1. Abe, F., Donnelly, D. M. X., Moretti, C., Polonsky, J. Isoflavonoid constituents from *Dalbergia monetaria*. *Phytochemistry* **1985**, *24*, 1071–1076.
2. Abe, I., Watanabe, T., Noguchi, H. Enzumatic formation of long-chain polyketide pyrones by plant type III polyketide synthases. *Phytochemistry* **2004**, *65*, 2447 – 2453.
3. Acree, F. Jr., Jacobson, M., Haller, H. L. Amorphin, a glycoside in *Amorpha fruticosa*. *J. Org. Chem*. **1943**, *8*, 572–574.
4. Addae-Mensah, I., Torto, F. G., Dimonyeka, C. I., Baxter, I., Sanders, J. K. M. Alkaloids of Ghanaian medicinal plants. Part 6. Novel amide alkaloids from the roots of *Piper guineensis*. *Phytochemistry* **1977**, *16*, 757–759.
5. Agrawal, P. K. NMR spectroscopy in the structural elucidation of oligosaccharides and glycosides. *Phytochemistry* **1992,** *31*, 3307-3330.
6. Ahn, J. W., Ahn, M. J., Zee, O. P., Kim, E. J., Lee, G. S., Kim, H. J., Kubo, I. Piperidine alkaloids from *Piper retrofractum* fruits. *Phytochemistry* **1992**, *31*, 3609 – 3612.
7. Akiyama, T., Shibuya, M., Liu, H.M., Ebizuka, Y. p-Coumaryltriacetic acid synthase, a new homologue of chalcone synthase, drom *Hydrangea macrophylla* var. *thunbergii*. *Eur. J. Biochem.* **1999**, *263*, 834 – 839.
8. Al-Taweel, A.M., Perveen, S., El-Shafae, Fawzy, G.A., Malik, A., Afza., Iqbal, L., Latif, M. Bioactive phenolic amides from Celtis Africana. *Molecules* **2012**, *17*, 2675 – 2682.
9. Andersen, Ø. M., Markham, K. R. Flavonoids: Chemistry, Biochemistry and Applications. CRC Press. Taylor & Francis group. **2006**, 858 – 875.
10. Andrei, C. C., Vieira, P. C., Fernandes, J. B., da Silva, M. F. das G. F., Rodrigues Fo, E. Dimethylchromene from *Tephrosia candida*. *Phytochemistry* **1997**, *46*, 1081–1085.
11. Andrei, C. C., Vieira, P. C., Fernandes, J. B., Fátima das G.F da Silva, M., Fo, E.R. New spirorotenoids from *Tephrosia candida*. *Z. Naturforsch*. *C*. **2002**, *57c*, 418 – 422.
12. Appendino, G., Gibbons, S., Giana, A., Pagani, A., Grassi, G., Stavri, M., Smith, E., Rahman, M. M. Antibacterial cannabinoids from *Cannabis sativa*: a structure-activity study. *J. Nat. Prod*. **2008**, *71*, 8.
13. Araho, D., Miyakoshi, M., Chou, W. Z., Kambara, T., Mizutani, K., Ikeda, T. A new flavone C-glycosides from the leaves of *Averrhoa carambola. Nat. Med*. **2005,** *59*, 113-116.
14. Ashour, M., Edrada, R., Ebel, R., Wray, V., Wätjen, W., Padmakumar, K., Müller, W. E. G., Lin, W. H., Proksch, P. Kahalalide derivatives from the Indian Sacoglossan mollusk *Elysiagrandifolia*. *J. Nat. Prod.* **2006**, *69,* 1547−1553.
15. Atanasov, A. G., Waltenberger, B., Pferschy-Wenzig, E. M., Linder, T., Wawrosch, C., Uhrin, P., Temml., Wang, L., Scwaiger, S., Heiss, E.H., Rollinger, J.M., Schuster, D., Breuss, J. M., Bochkov, V., Mihovolovic, M. D., Kopp, B., Bauer, R., Dirsch, V. M., Stuppner, H. Discovery and resupply of pharcologically active plant-derived natural products: a review. *Biotechnology advances* **2015**, 1582 – 1614.

16. Ávila, H.P., De Fátima Albino Smânia, E., Monache, F.D, Júnior, A.S. Structure-activity relationship of antibacterial chalcones. *Bioorg. Med. Chem*. **2008**, *16*, 9790 – 9794.
17. Balunas, M. J., Kinghorn, A. D., Drug discovery from medicinal plants. *Life Sci*. **2005**, *78*, 431 – 441.
18. Banerji, A., Ray, R. Aurantiamides: a new class of modified dipeptides from *Piper aurantiacum*. *Phytochemistry* **1981**, *20*, 2217 – 2220.
19. Banerji, A., Bandyopadhyay, D., Sarkar, M., Siddhanta, A. K., Pal, S. C., Somnath, G., Abraham, K., Shoolery, J. N. Structural and synthetic studies on the retrofractamides – amide constituents of *Piper retrofractum*. *Phytochemistry* **1985**, *24*, 279 – 284.
20. Bezuidenhoudt, B. C. B., Swanepoel, A., Brandt, E. V., Ferreira, D. Structure and synthesis of the first flavonoid- and stilbene-related but-2-enolides. *J. Chem. Soc. Perkin Trans. 1* **1990**, 2599–2602.
21. Biron, K. K. *Antiviral. Res*. **2006**, 154 – 163.
22. Bohlmann, F., Hoffmann, E. Naturally occuring terpene derivaties Part 208. Cannabigerol-like compounds from *Helichrysum umbraculigerum*. *Phytochemistry* **1979**, *18*, 1371 – 1374.
23. Bohlmann, F., Zdero, C. Flavanones from *Helichrysum thapsus*. *Phytochemistry* **1983**, *22*, 2877-2878.
24. Bohm, B.A. Introduction to flavonoids, Harwood Academic Publishers, Amsterdam, The Netherlands, **1998**, 26.
25. Brielman, H. L., Setzer, W. N., Kaufman, P. B., Kirakosyan, A., Cseke, L. J. Phytochemicals: The chemical components of plants, in Natural products from plants 2nd. Taylor & Francis Group, Boca Raton. **2006**, 22 – 25.
26. Büchi, G., Crombie, L., Godin, P. J., Kaltenbronn, J. S., Siddalingaiah, K. S., Whiting, D. A. The absolute configuration of rotenone. *J. Chem. Soc*. **1961**, 2843 – 2840.
27. Burns, D. T., Dalgarno, B. G., Gargan, P. E., Grimshaw, J. An isoflavone and a coumestan from Eysenhardtia polystachya–Robert Boyle's fluorescent acid–base indicator. *Phytochemistry* **1984**, *23*, 167–169.
28. Carlson, D. G., Weisleder, D., Tallent, W. H. NMR Investigation of rotenoids. *Tetrahedron* **1973**, *29*, 2731–2741.
29. Chin, Y. W., Mdee, L. K., Mbwambo, Z. H., Mi, Q., Chai, H. H., Cragg, G. M., Swanson, S. M., Kinghorn, A. D. Prenylated flavonoids from the root bark of *Berchemia discolor*, a Tanzanian medicinal plant. *J. Nat. Prod*. **2006**, *69*, 1649 – 1652.
30. Christenhusz, M. J. M., Byng, J. W. The number of known plants species in the world and its annual increases. *Phytotaxa*. **2016**, *261*, 201 – 217.
31. Chonajka, M. W., Lough, A. J., Wylie, R. S., Gossage, R. A. Piperonylic anhydride: isolation and conformational analysis by X-ray crystallography and density functional theory calculations. *J. Mol. Struc*. **2011**, *991*, 158 – 161.
32. Chong, Y., Li, L., Hong Ju, L., Xin, Z.L.,Yu, P.C., Cong, C., An, L.Z. The research of flavones type constituent from *Santalum album*. *China J. Chinese Mat. Med*. **2011,** *36*, 3130 – 3133.

References

33. CLSI. Methods for Dilution Antimicrobial Susceptibility Tests for Bacteria That Grow Aerobically; Approved Standart – Ninth Edition. CLSI document M07-A9. Wayne, PA: Clinical and Laboratory Standarts Institute; **2012.**
34. Crombie, L., Lown, J. W. Determination of the geometry of the B/C fusion of rotenoids by means of long-range asymmetric magnetic shielding of the carbonyl group. *Proc. Chem. Soc*. London **1961**, 299 – 300.
35. Crombie, L., Whiting, D. A. Biosynthesis in the rotenoids group of natural products application of isotope methodology. *Phytochemistry* **1998**, *49* (6), 1479 – 1507.
36. Cseke, L. J., Lu, C. R., Kornfeld, A., Kaufman, P. B., Kirakosyan, A. How and why these compounds are synthesizes in plants, in Natural products from plants 2nd. CRC Taylor & Francis Group LLc, Boca Raton. **2006**, 51 – 98.
37. Dagne, E., Yenesew, A., Waterman, P. G. Flavonoids and isoflavonoids from *Tephrosia fulvinervis* and *Tephrosia pentaphylla*. *Phytochemistry* **1989**, *28*, 3207–3210.
38. Dat, N. T., Lee, J. H., Lee, K., Hong, Y. S., Kim, Y. H., Lee, J. J. Phenolic constituent of amorpha fruticosa that inhibit NF-*κ*B activation and related gene expression. *J. Nat. Prod.* **2008**, *71*, 1696 – 1700.
39. Desiraju, G. R., Kamala, R., Kumari, B. H., Sarma, J. A. R. P. Crystal engineering via nonbonded interactions involving oxygen. X-ray crystal structures of 3,4-methylenedioxycinnamic acid and 3,4-dimethoxy cinnamic acid. *J. Chem. Soc. Perkin Trans 2*. **1984**, 181 – 189.
40. Dewick, P. M. Medicinal natural product, a biosynthetic approach, 3rd edition. John Wiley and Sons: West Sussex, **2009**.
41. Deyou, T., Gumula, I., Pang, F., Gru, J., Jhonjic, A., Mumo, M., Holleran, J., Duffy, S., Fitzpatrick, P. A., Heydenreich, M., Landberg, G., Derese, S., Avery, V., Rissanen, K., Erdélyi, M., Yenesew, A. Rotenoids, flavonoids, and chalcones from the root bark of *Milletia usaramensis*. *J. Nat. Prod*. **2015**, *78*, 2932 – 2939.
42. Di, Z., Jie, Y., Mao-xiang, L., Qiang, W. A new C-glycosylflavone from *Pogonatherum crinitum. Chinese J. Nat. Med*. **2010,** *8*, 411-413.
43. Elliger, C. A., Chan, B. G., Anthony C. W. Jr., Lundin, R. E., Haddon, W. F., C-glycosylflavones from *Zea mays* that inhibit insect development. *Phytochemistry* **1980**, *19*, 293-297.
44. Ebrahim, W., El-Neketi, M., Lewald, L. I., Orfali, R. S., Lin, W., Rehberg, N., Kalscheuer, R., Daletos, G., Proksch, P. Metabolites from the fungal endophyte *Aspergillus austroafriacanus* in axenic culture and in fungal-bacterial mixed cultures. *J. Nat. Prod*. **2016**, *79*, 914 – 922.
45. Fage, C. D., Isiorho, E. A., Liu, Y., Wagner, D. T., Liu, H. W., Clay, A. T. K. The structure of SpnF, a standalone enzyme that catalyses [4+2] cycloaddition. *Nature Chemical Biology*. **2015,** *11*, 256 – 260.
46. Fang, N., Casida, J. E. Novel bioactive cubé insecticide constituents: Isolation and preparation of 13-hono-13-oxa-6a,12a-dehydrorotenoids. *J. Org. Chem.* **1997**, *62*, 350–353.

References

47. Filho, R ,B., De Souza, M. P., Mattos, M. E. O. Piplartine-dimer A, a new alkaloid from *Piper tuberculatum*. *Phytochemistry* **1981**, *20*, 345 – 346.
48. Fiorentino, A., Ricci, A., Abrosea, B., Golino, A., Izzo, A., Pasearella, M. T., Piccolella, S., Esposito, A. Kaempferol glycosides from *Lobularia maritime* and their potential role in plant interations. *Chem. Biodiversity* **2009**, *6*, 204–217.
49. Fuhr, L., Rousseau, M., Plauth, A., Schroeder, F. C., Sauer, S. Amorfrutins are natural PPARγ agonist with potent anti-inflammatory properties. *J. Nat. Prod*. **2014**, *78*, 1160 – 1164.
50. Fujiwara, Y., Naithou, K., Miyazaki, T., Hashimoto, K., Mori, K., Yamamoto, Y. Two new alkaloids, pipercyclobutanamides A and B, from *Piper nigrum*. *Tetrahedron Lett*. **2001**, *42*, 2497 – 2499.
51. Ghisalberti, E. L., Jefferies, P. R., McAdam, D. Isoprenylated resorcinol derivatives from *Glycyrrhiza acanthocarpa*. *Phytochemistry* **1981**, *20*, 1959 – 1961.
52. Ghribi, L., Waffo-Téguo, P., Cluzet, S., Marchal, A., Marques, J., Mérillon, J. M., Jannet, H. B. Isolation and structure elucidation of bioactive compounds from the roots of the Tunisian *Ononis angustissima* L. *Bio.Med.Chem.Lett*. **2015**, *25*, 3825 – 3830.
53. Gurib-Fakim, A. Medicinal plants: Tradition of yesterday and drugs of tomorrow. *Mol. Aspects Med*. **2006**, *27*, 1 – 93.
54. Gutekunst, W. R., Baran, P. S., Applications of C-H functionalization logic to cyclobutane synthesis. *J. Org. Chem*. **2014**, *79*, 2430 – 2452.
55. Ham, J. Y., Ahn, H. Y., Park, Y. H., Kim, S. N., Lee, U. J., Yang, H. O., Kwon, H. C. *Repub. Korea* **2009**, KR 894832 B1 20090424.
56. Harborne, J.B., Greenham, J., Williams, C.A., Eagles, J., Markham, K.R. Ten isoprenylated and C-methylated flavonoids from the leaves of three *Vellozia* species. *Phytochemistry Lett*. **1993**, *34*, 219 – 226.
57. Harborne, J. B., Williams, C. A. Advances Research in Flavonoids since 1992. *Phytochemistry* **2000**, *55*, 481-504.
58. Hatano, T., Mizuta, S., Ito, H., Yoshida, T. C-glycosidic flavonoids from *Cassia occidentalis*. *Phytochemistry* **1999**, *52*, 1379-1383.
59. Heinig, U., Scholz, S., Jenewein, S. Getting to the bottom of taxol biosynthesis by fungi. *Fungal diversity* **2013**, *60*, 1, 161 – 170.
60. Heinrich, M., Galanthamine from Galanthus and other Amaryllidaceae – Chemistry and biology based on traditional use, in The Alkaloids: Chemistry and Biology. **2010**, *68*, 157 – 165.
61. Ito, C., Itoigawa, M., Kanematsu, T., Ruangrungsi, N., Mukainaka, T., Tokuda, H., Nishino, H., Furukawa, H. Isoflavonoids from *Dalbergia olivari*. *Phytochemistry* **2003**, *64*, 1265–1268.
62. Iwashina, T. The structure and distribution of the flavonoids in plants. *J. Plant Res*. **2000**, *113*, 287 – 299.

63. Jayasinghe, L., Balasooriya, B. A. I. S., Padmini, W. C., Hara, N., Fujimoto, Y. Geranyl chalcone derivatives with antifungal and radical scavenging properties from the leaves of *Artocarpus nobilis*. *Phytochemistry* **2004**, *65*, 1287–1290.
64. Kamel, S., Mohamed. Flavone C-glycosides from *Lupinus hartwegii. Phytochemistry* **2003**, *63*, 449-452.
65. Kemal, M., Khalil, S. K. W, Rao, N. G. S. Woolsey, N.F. Identification of cannabinoid-like compound from Amorpha species. *J. Nat. Prod*. **1979**, *42*, 463 – 468.
66. Khoo, B. Y., Chua, S. L., Balaram, P. Effect of chrysin in human cancer cell lines. *Int. J. Mol. Sci*. **2010**, *11*, 2188 – 2199.
67. Kikuzaki, H., Kawabata, M., Ishida, E., Akazawa, Y., Takei, Y., Nakatani, N. LC-MS analysis and structural determination of new amides from Javanese Long Pepper (*Piper retrofractum*). *Bios. Biotech. Biochem.* **1993,** *57*, 1329.
68. Kim, H. J., Ruszczycky, M. W., Choi, S. H., Liu, Y. N., Liu, H. W. Enzyme-catalysed [4+2] cycloaddition is a key step in the biosynthesis of spinosyn A. *Nature* **2011**, *473*, 109 – 112.
69. Kim, H. J., Lee, D. H., Hwang, Y. Y., Lee, K. S., Lee, J. S. Characterization of β-hydroxy-β-methylglutaryl coenzyme A reductase inhibitor from *Pueraria thunbergiana*. *J. Agric. Food Chem.* **2005**, *53*, 5882–5888.
70. Kim, K. J., Lee, M. S., Jo, K., Hwang, J. K. Piperidine alkaloids from *Piper retrofractum* Vahl. protect against high-fat diet-induced obesity by regulating lipid metabolism and activating AMP-activated protein kinase. *Biochem. Biophys. Res. Com***.** **2011**, *411*, 219-225.
71. Kim, Y. S., Ryu, Y. B., Curtis-Long, M. J, Yuk, H. J., Cho, J. K., Kim, J. Y., Kim, K. D., Lee, W. S**.,** Park, K. H. Flavanones and rotenoids from the roots of *Amorpha fruticosa* L that inhibit bacterial neuraminidase. *Food Chem Toxicol*. **2011**, *49*, 1849 – 1856.
72. Kinghorn, A. D., Balunas, M. J. Drug discovery from medicinal plants. *Life Sciences* **2005**, *78*, 431- 441.
73. Kirkpatrick, K. A., Siebert, M. R. Cation or radicals? Inherent reactivity of biosynthetic intermediates in the B-ring formation of rotenoids natural products. *J. Phys. Chem*. **2016**, *120*, 2372 – 2379.
74. Klas, K., Tsukamoto, S., Sherman, D. H., Williams, R. M. Natural Diels-alderases: elusive and irresistible. *J. Org. Chem*. **2015,** *80*, 11672 – 11685.
75. Konoshima, T., Terada, H., Kokumai, M., Kozuka, M. Studies on inhibitors of skin tumor promotion, XII. Rotenoids from *Amorpha fruticosa*. *J. Nat. Prod*. **1993**, *56*, 843 – 848.
76. Kostova, I., Berova, N., Ivanov, P., Mikhova, B., Rakovska, R. Stereochemical studies of some 12a-substituted rotenoid derivatives. *Croa. Chem. Acta*. **1991**, *64*, 637-647.
77. Kostova, I., Ognyanov, I. Preparation and stereochemistry of 12a-hydroxymethyl derivatives of rotenone and amorphigenin. *Z. Naturforsch., B: Anorg. Chem., Org. Chem.* **1983**, *38*, 761–763.
78. Kreuter, M. H., Robitzki, A., Chang, S., Steiffen, R., Michaelis, M., Kjajic, Z., Bachmann, M., Schroder, H.C., Müller, W. E. G. Production of cytotatic agent aeroplysinin by the

sponge *Verongia aerophoba* in *in vitro* culture. *Comp. Biochem. Physiol*. **1992**, *101C*, 183-187.

79. Kubitzki, K. The families and genera of Vascular Plants Vol. VI. flowering plants dicotyledons celastrales, oxalidales, rosales, cornales, ericales; Springer-Verlag: Berlin. **2004**. 287 – 288.
80. Kubo, M., Ishii, R., Ishino, Y., Harada, K., Matsui, N., Akagi, M., Kato, E., Hosoda, S., Fukuyama, Y. Evaluation of constituents of *Piper retrofractum* fruits on neurotrophic activity. *J. Nat. Prod*. **2013**, *76*, 769 – 773.
81. Lee, F. P., Chen, Y. C., Chen, J. J., Tsai, I. L., Chen, I. S. Cyclobutanoid amides from Piper arborescens. *Helv. Chim. Acta*. **2004**, *87*, 463 – 468.
82. Lee, H. J., Kang, H. Y., Kim, C. H., Kim, H. S., Kwon, M. C., Kim, S. M., Shin, I. S., Lee, H. Y. Effect of new rotenoids glycoside from the fruits of *Amorpha fruticosa* LINNE on the growth of human immune cells. *Cytotechnology* **2006**, *52*, 219 – 226.
83. Li, L., Wang, H. K., Chang, J., McPhail. A. T., McPhail, D. R., Terada, H. Antitumor agents, 138. Rotenoids and isoflavones as cytotoxic constituents from *Amorpha fruticosa*. *J. Nat. Prod*. **1993**, *56*, 690 – 698.
84. Li. L., Wang, H. K., Fujioka, T., Chang, J. J., Kozuka, M., Konoshima, T., Estes, J. A., McPhail, D. R., McPhail, A. T. Structure and stereochemistry of amorphispironone, a novel cytotoxic spironone type rotenoids from *Amorpha fruticosa*. *J. Chem. Soc. Chem. Comm*. **1991**, *22*, 1652 – 1653.
85. Li, W., Koike, K., Asada, Y., Hirotani, M., Rui, H., Yoshikawa, T., Nikaido, T. Flavonoids from *Glycyrrhiza pallidiflora* hairy root cultures. *Phytochemistry* **2002**, *60*, 351–355.
86. Liang, Y., Li, X., Gu, Z., Qin, P., Ji, M. Toxicity of amorphigenin from the seeds of *Amorpha fruticosa* against the Larvae of *Culex pipiens pallens* (Diptera; Culicidae). *Molecules*. **2015**, *20*, 3*238 – 3254.*
87. Lim, T.K. *Edible Medicinal and Non-medicinal Plants,* Springer Science & Business: Netherlands, **2012**, 4, 351.
88. Limyati, D. A., Juniar, B. L. L. Jamu gendong, a kind of traditional medicine in Indonesia, the microbial contamination of its materials and endprodutc. *J. Ethnopharmacol*. **1998**, *63*, 201 – 208.
89. Lin, L. J., Ruangrungsi, N., Cordell, G. A., Shieh, H. L., You, M., Pezzuto, J. M. 6-deoxyclitoriacetal from *Clitoria macrophylla*. *Phytochemistry* **1992**, *31*, 4329–4331.
90. Lis, A., Jozef, G. Essential oil of *Amorpha fruticosa*. *J. Essential Oil Res*. **2001**, 13 (5), 340 – 342.
91. Liu, R., Zhang, M., Wyche, T. P., Winston-McPherson, G. N., Bugni, T. S., Tang, W. Stereoselective preparation of cyclobutanes with four different substituents: Total synthesis and structural revision of pipercyclobutanamide A and piperchabamide G. *Angew. Chem*. **2012**, *124*, 7621 – 7624.
92. Lombó, F., Olano, C., Salas, J. A., Méndes, C Sugar biosynthesis and modification, in Methods in Enzymology, 1st ed. Elsevier. **2009,** 281.

93. Lukaseder, N., Vajrodaya, S., Hehenberger, T., Seger, C., Nagl, M., Lutz-Kutschera, G., Robien, W., Greger, H., Hofer, O. Prenylated flavanones and flavanoids as chemical markers in *Glycosmis* species (Rutaceae). *Phytochemistry* **2009**, *70*, 1030 – 1037.
94. Luyen, B. T. T., Tai, B. H., Thao, N. P.; Yang, S. Y., Cuong, N. M., Kwon, I. Y., Jang, H. D., Kim, Y. H. A new phenylpropanoid and alkylglycoside from *Piper retrofractum* leaves with their antioxidant and α-glucosidase inhibitory activity. *Biorg. Med. Chem. Lett*. **2014**, *24*, 4120 – 4124.
95. Maleck, M., Ferreira, B., Mallet, J., Guimaraes, A., Kato, M. Cytotoxicity of piperamides towards *Aedes aegypti* (Diptera: culicidae). *J. Med. Entolomol*. **2014**, *51*, 458 – 463.
96. Magalhaes, A. F., Tozzi, A. M. G. A., Sales, B. H. L. N., Magalhaes, E. G. Twenty-three flavonoids from *Lonchocarpus subglaucescens*. *Phytochemistry* **1996**, *42*, 1459–1471.
97. Mantoro, P., Carbone, V., Simone, F., Pizza, C., Tommasi, N. Studies on the constituents of *Cyclanthera pedata* Fruits: isolation and structure elucidation of new flavonoid glycosides and their antioxidant activity. *J. Agric. Food. Chem*. **2001,** 49, 5156-5160.
98. Marques, J. V., Kitamura, R. O. S., Lago, J. H. G., Young, M. C. M., Guimaraes, E. F., Kato, M. J. Antifungal amides from *Piper scutifolium* and *Piper hoffmanseggianum*. *J. Nat. Prod*. **2007**, *21*, 1807 – 1813.
99. Marques, J. V., Olievera, A., Raggi, L., Young,M. C. M., Kato, M. J. Antifungal activity of natural and synthetic amides from *Piper* species. *J. Braz. Chem. Soc*. **2010**, *21*, 1807 – 1813.
100. Marschal, K., Stamminger, T. Molecular targets for antiviral therapy of cytomegalovirus infections. *Future Microbiol*. **2009**, *4*, 731 – 742.
101. Matsuda, H., Ninomiya, K., Morikawa, T., Daisuke, Y., Yamaguchi, I., Yoshikawa, M. Hepatoprotective amide constituents from the fruit of *Piper chaba*: structural requirements, mode of action, and new amides. *Bioorg. Med. Chem.* **2009**, *17*, 7313 – 7323.
102. Mitscher, L. A., Park, Y. H., Al-Shamma, A., Hudson, P. B., Haas, T. Amorfrutin A and B, bibenzyl antimicrobial agents from *Amorpha fruticosa*. *Phytochemistry*. **1981**, *20*, 781 – 785.
103. Miyaichi, Y., Tomimori, T. Studies on the constituents of Scutellaria species XVI: on the phenol glycosides of the root of *Scutellaria baicalensis* Georgi. *Nat. Med*. **1994**, *48*, 215 – 218.
104. Mizokami, H., Yokotiani, K., Yoshitama, K. Flavonoids in the leaves of Oxalis corniculata and sequestration of the flavonoidsin the wing scales of the pale grass blue butterfly, *Pseudozizeeria maha*. *J. Plant. Res*. **2008**, 133 – 136.
105. Moresco, H. H., Queiroz, G. S., Pizzolatti, M. G., Brighente, I. M. Chemical constituents and evaluation of the toxic and antioxidant activities of *Averrhoa carambola* leaves. *Braz. J. Pharmacogn*. **2012**, *22*, 319-324.
106. Morikawa, T., Matsuda, H., Yamaguchi, I., Pongpiriyadacha, Y., Yoshikawa, M. New amides and gastroportective constituents from the fruit of *Piper chaba*. *Planta Med.* **2004**, *70*, 152-159.
107. Nakatani, N., Inatani, R. Isobutyl amides from Pepper (*Piper nigrum* L). *Agric. Biol. Chem*. **1981**, *45*, 1473 – 1476.

References

108. Nakatani, N., Matsui, M. Interconversion between rotenone and dalpanol. *Agr. Biol. Chem.* **1977**, *41*, 601–602.
109. Narui, T., Takeuchi, M., Ishii, R., Ishida, T., Okuyama, T. Studies on the constituents of *Piper hancei* of Spice from Okinawa. *Nat. Med.* **1995**. *49*, 438 – 441.
110. Navickiene, H. M. D., Alecio, A. L., Kato, M. J., Bolzani, V. S., Young, M. C. M., Cavalheiro, A. J., Furlan, M. Antifungal amides from *Piper hispidum* and *Piper tuberculatum*. *Phytochemistry* **2000**, *55*, 621 – 626.
111. Newman, D. J., Cragg, A. D. Natural products as sources of new drugs from 1981 to 2014. *J. Nat. Prod*. **2016**, *79*, 629 -621.
112. Nikolov, N., Seligmann, O., Wagner, H., Horowitz, R. M., Gentili, B. New flavonoid glycosides from *Crataegus monogyna* and *Crataegus pentagyna*. *Planta Med*. **1982,** *44*, 50-53.
113. Noboru, S., Akemi, U., Nobuaki, S., Tsunematsu, T., Akiko, K., Yasushi, O. Dehydropipernonaline, an amide possesingcoronary vasolidating activity, isolated from *Piper longum* L. *J. Pharm. Sci.* **1986**, *75*, 1188 – 1189.
114. Nohara, T., Kinjo, J., Furusawa, J., Sakai, Y., Inoue, M., Shirataki, Y., Ishibashi, Y., Yokoe, I., Komatsu, M. But-2-enolides from *Pueraria lobata* and revised structures of puerosides A,B, and sophoroside A. *Phytochemistry* **1993**, *33*, 1207 – 1210.
115. Oberholzer, M. E., Rall, G. J. H., Roux, D. G. The concurrence of 12a-hydroxy- and 12a-O-methylrotenoids, Isolation of the first natural of 12a-O-methylrotenoids. *Tetrahedron Lett*. **1974**, *25*, 2211 – 2214.
116. Omarim, A. P. de Oliveira., De Carvalho, A.R., Lopes, N. P. Jr., Castro, R. N., De Oliveira, M. C. C, De Cavalho, M.G.. Chemical compounds isolated from Talinum triangulare. *Food Chem*. **2014**, *160*, 204 – 208.
117. Ognyanov, I., Somleva, T. Rotenoids and 7,2′,4′,5′-tetramethoxyisoflavone in *Amorpha fruticosa* L. Fruits. *Planta Med.* **1980**, *38*, 279–280.
118. Okwute, S. K., Egharevba, H. O. Piperine-type amides: Review of the chemical and biological characteristics. *Int. J. Chem.* **2013**, *5*, 99 – 122.
119. Painuly, P., Tandon, J.S. Two new 3-C-methylflavone glycosides from Eugenia kurzii. Phytochemistry **1983**, *22*, 243 – 245.
120. Pan, Z., Ning, D., Wu, X., Huang, S., Li, D., Lv, S. New clerodane diterpenoids from the twigs and leaves of *Croton euryphyllus*. *Bioorg. Med. Chem. Lett*. **2015**, *25*, 1329 – 1332.
121. Pancheva, S., Manolova, N., Gagov, I., Maksimova, V. Antiviral effect of some rotenoids and their derivatives. *Acta Microbiol. Bulg*. **1982**, *10*, 1 – 14.
122. Paula, J. C. N. V. F., David, J. M., David, J. P. Occurrence, biological activity and ^{13}C NMR data of amides from *Piper* (Piperaceae). *Quim. Nova,* **2012**, *35*, 2288-2311.
123. Pelter, A., Ward, R. S., Bass, R. J. The carbon-13 nuclear magnetic resonance spectra of isoflavones. *J. Chem. Soc. Perkin Trans. 1* **1978**, 666–668.

References

124. Pham, C. D., Hartmmann, R., Bohler, P., Stork, B., Wesselborg, S., Lin, W., Lai, D., Proksch, P. Callyspongiolide, a cytotoxic macrolide from the marine sponge Callyspongia sp. *Organic Letters*. **2014**, *16*, 266-269.
125. Phillipson, J. D. Phytochemistry and medicinal plants. *Phytochemistry* **2001**, *56*, 237 – 243.
126. Pushvalli, G., Kalaiarasi, P., Veeramani, C., Pugalendi, K. V. Effect of chrysin on hepatoprotective and antioxidant status in D-galactosamine-induced hepatitis in rats. *Eur. J. Pharmacolog*. **2010**, *631*, 36 – 41.
127. Raina, M., Dhar, K., Atal, C. K. Occurrence of N-isobutyl eicosa-trans-2-trans-4-dienamide in *Piper nigrum*. *Planta Med.* **1976**, *30* (6), 198 – 200.
128. Rao, V. R. S., Suresh, G., Babu, K. S., Raju, S. S., Vardhan, M. V. P. S. V., Ramakrishna, S., Rao, J. M. Novel dimeric amide alkaloids from *Piper chaba* Hunter: isolation, cytotoxic activity, and their biomimetic synthesis. *Tetrahedron* **2011**, *67*, 1885 – 1892.
129. Rates, S. M. K. Plants as source of drugs. *Toxicon*. **2001**, *39*, 603 – 613.
130. Rayyan, S., Fossen, T., Andersen, Ø. M. Flavone C-glycosides from leaves of *Oxalis triangularis. J. Agric. Food. Chem.* **2005,** *53*, 10057-10060.
131. Rukachaisirikul, T., Prabpai, S., Champung, P., Suksamrarn, A. Chabamide, a novel piperine dimer from stems of *Piper chaba*. *Planta Med.* **2002**. *68*, 853-855.
132. Rukachaisirikul, T., Siriwattanakit, P., Sukcharoenphol, K., Wongvein, C., Ruttanaweang, Wongwattanavuch, P., Suksamrarn, A. Chemical constituents and bioactivity of *Piper sarmentosum*. *J. Ethnopharmacol*. **2004,** *93*, 173 – 176.
133. Ryoho, G., Masao, T. *Yakugaku Zasshi*. **1938**, *58*, 933 – 938.
134. Sasaki, H., Shibata, H., Imabayashi, K., Takaishi, Y., Kashiwada, Y. Prenylated flavonoids from the stems and leaves of *Desmodium caudatum* and evaluation of their inhibitory activity against the film-forming growth of *Zygosaccharomyces rouxii* F51. *J. Agric. Food Chem*. **2014**, *62*, 6345 – 6353.
135. Sauer, S. Amorfrutins: a promising class of natural products that are beneficial to health. *ChemBioChem*. **2014**, *15*, 1231 – 1238.
136. Savoia, D. Plant-derived antimicrobial compounds: alternative to antibiotics. *Future Microbiol*. **2012**, *7* (8), 979 – 990.
137. Seigler, D. S. Plant Secondary Metabolism. Springer Science + Bisnis Media, LLC. New York. **1998**, 250 – 251.
138. Shi, H., Ma, J., Mi, C., Li, J., Wang, F., Lee, J. J., Jin, X. Amorfrutin A inhibits TNF-α-induced NF-*κ*B activation and NF- *κ*B *regulated target gene products. Int Immunopharmacol*. **2014**, *21*, 56 – 62.
139. Siddiqui, B. S., Gulzar, T., Begum, S., Rasheed, M., Farhat, Noor, F. An Amide from fruits of *Piper nigrum*. *Phytochemistry* **1997**, *45*, 1617 – 1619.
140. Siddiqui, B. S., Gulzar, T., Begum, S., Rasheed, M., Sattar, F. A., Afshan, F. Two new insecticidal amides and a new alcoholic amide from *Piper nigrum*. *Helve. Chim. Acta.* **2003**, *86*, 2760 – 2767.

141. Singhal, A. K., Sharma, R. P., Baruah, J. N., Govindan, S. V., Herz, W. Rotenoids from roots of *Millettia pachycarpa*. *Phytochemistry* **1982**, *21*, 949–951.
142. Stierle, A., Strobel, G., Stierle, D. Taxol and taxane production by taxomyces andreanae, an endophytic fungus of Pacific Yew. *Science*. **1993**, *260*, 214 – 216.
143. Subehan, Usia, T., Kadota, S., Tezuka, Y. Mechanism-based inhibition of human liver microsomal cytochrome P450 2D6 (CYP2D6) by alkamides of *Piper nigrum*. *Planta Med.* **2006**, *72*, 527 – 532.
144. Sun, J., Gu, Y.F., Su, X.Q., Li, M.M., Huo, H.X., Zhang, J., Zeng, K.W., Zhang, Q., Zhao, Y.F., Li, J., Tu, P.F. Anti-inflammatory lignanamides from the roots of *Solanum melongena* L. *Fitoterapia* **2014**, 98, 110 – 116.
145. Sunila, E. S., Kuttan, G. Immunomodulatory and antitumor activity of *Piper longum* Linn and piperine. *J. Etnopharmacol*. **2004**, *90*, 339 – 346.
146. Sutthivaiyakit, S., Seeka, C., Wetprasit, N., Sutthivaiyakit, P. C-Methylated flavonoids from *Pisonia grandis* roots. *Phytochemistry Lett*. **2013**, *6*, 458 – 472.
147. Suzuki, R., Okada, Y., Okuyama, T. A new flavone C-glycoside from the style of *Zea mays* L. with glycation inhibitory activity. *Chem.Pharm. Bull*. **2003**, *51*, 1186-1188.
148. Tabuneng, W., Bando, H., Amiya, T. Studies on the constituents of the crude drug Piperis longi frutctus. On the alkaloids of fruits of *Piper longum* L. *Chem. Pharm.Bull.* **1983**, *31*, 3562 – 3565.
149. Takastsuki, A., Nakatani, N., Morimoto, M., Tamura, G., Matsui,M., Arima, K., Yamaguchi, I., Misato, T. XX. Effects of rotenone, degeulin, and related compounds on animal and plant viruses. *Applied Microbiol*. **1969**, 660 – 667.
150. Tanaka, T., Nakashima, T., Ueda, T., Tomii, K., Kouno, I. Facile discrimation of aldose enantiomers by reversed-phase HPLC. *Chem. Pharm. Bull*. **2007,** *55*, 899 – 901.
151. Terada, H., Kokumai, M., Konoshima, T., Kozuka, M., Haruna, M., Ito, K., Estes, J. R., Li, L., Wang, H. K., Lee, K. H. Structural elucidation and chemical conversion of amorphispironone, a novel spironone from *Amorpha fruticosa*, to Rotenoids. *Chem. Pharm. Bull*. **1993**, *4*, 187 – 190.
152. Ting, M., Wang, J., Gao, B., Zhang, I., Liu, X., Wang, X., Tu, P., Shi, S. Combinatorial synthesis of flavonoids and 4-hydroxy-δ-lactones by plant-originated enzymes. *Chin. J. Org. Chem*. **2015**, *35*, 1052 – 1059.
153. Townsend, C.A. A "Diels-Alderase" at last. *Chem.Bio.Chem*. **2011**, 12, 2267 – 2269.
154. Tsuji, P. A., Walle, T. Cytotoxic effects of dietary flavones chrysin and apigenin in a normal trout liver cell line. *Chem. Biol. Interact*. **2008**, *171*, 37 – 44.
155. Tsukamoto, S., Tomise, K., Miyakawa, K., Cha, B. C., Abe, T., Hamada, T., Hirota, H., Ohta, T. CYP3A4 inhibitory activity of new bisalkaloids, dipiperamides D and E, and cognates from white pepper. *Bioorg. Med. Chem.* **2002**, *10*, 2981 – 2985.
156. Ulrich, H., Rao, D. V., Stuber, F. A., Sayigh, A. A. The photodimerization of substituted stilbenes. *J. Org. Chem*. **1970**, *35*, 1121- 1125.

157. Veldkamp, J. F. A revision of *Sarcotheca* Bl and *Dapania* Korth (Oxalidaceae). *Blumea-Biodiversity, Evolution and Biogeography of Plants* **1967**, *15*, 519-543.
158. Vijay, G., Sayed, S. H. Alkaloids from *Piper hookeri*: revision of NMR assignments by the application of 2D NMR spectroscopy. *J. Pharm. Res*. **2011**, *4*, 4265 – 4267.
159. Vittorio, P. *Rend. R. Ist. Lomb. Sci. Lett.* **1904**, *31* (ii), 487 – 494.
160. Wang, S. F., Jiang, Q., Ye, Y. H., Li, Y., Tan, R. X. Genistein derivatives as selective estrogen receptor modulators: Sonochemical synthesis and in vivo anti-osteoporotic action. *Bioorg. Med. Chem.* **2005**, *13*, 4880–4890.
161. Wei, K., Li, W., Koike, K., Chen, Y., Nikaido, T. Nigramide A-S, dimeric amide alkaloids from the roots of *Piper nigrum*. *J. Org. Chem*. **2005**, *70*, 1164 – 1176.
162. Weidner, C., Rousseau, M., Micikas, R. J., Fischer, C., Plauth, A., Wowro, S. J., Siems, K., Hetterling, G., Kliem, M., Schroeder, F. C., Schauer, S. Amorfrutin C induces apoptosis and inhibits proliferation in colon cancer cells through targeting mitochondria. *J. Nat. Prod*. **2015**, *79*, 2 – 12.
163. Wu, X., Liao H. B., Li, G. Q., Liu, Y., Cui, L., Wu, K. F., Zhu, X. H., Zeng, X. B. Cytotoxic rotenoid glycosides from the seeds of *Amorpha fruticosa*. *Fitoterapia*. **2015,** *100*, 75-80.
164. Yan, R., Cao, Y., Chen, C., Dai, H., Yu, S., Wei, J., Hua, L., Yang, B., Antioxidant flavonoids from the seed of *Oroxylum indicum. Fitoterapia* **2011**, *82*, 841-848.
165. Ye, H., Chen, L., Li, Y., Peng, A., Fu, A., Song, H., Tang, M., Luo, H., Luo, Y., Xu, Y., Shi, J., Wei, Y. Preparative isolation and purification of three rotenoids and one isoflavone from the seeds of *Millettia pachycarpa* Benth by high-speed counter-current chromatography. *J. Chromatogr. A* **2008**, *1178*, 101–107.
166. Yan, X., Tang, J., Dos Santos Passos, C., Nurisso, A., Simoes-Pires, C.A, Ji, M., Lou, H., Fan, P. Characterization of lignanamides from Hemp (*Cannabis sativa* L.) seed and their antioxidant and acetylcholinesterase inhibitory activity. *J. Agri, Food Chem*. **2015**, *63*, 10611 – 10619.
167. Yang, Y., Zhang L.H., Yang, B.X., Tian, J.K., Zhang, L. Aurantiamide acetate suppresses the growth of malignant gliomas in vitro and in vivo by inhibiting autophagic flux. *J. Cell. Mol. Med*. **2015**, *19*, 1055 – 1064.
168. Yenesew, A., Kiplagat, J. T., Derese, S., Midiwo, J.O., Kabaru, J. M., Heydenreich, M., Peter, M. G. Two unusual rotenoid derivatives, 7a-O-methyl-12a-hydroxydeguelol and spiro-13-homo-13-oxaelliptone, from the seeds of *Derris trifoliate*. *Phytochemistry* **2006**, *67*, 988 – 991.
169. Yuk, H. J., Lee, J. H., Curtis-Long, M. J., Lee, J. W., Kim, Y. S., Ryu, H. W., Park, C. G., Jeong, T. S., Park, K. H. The most abundant polyphenol of soy leaves, coumestrol, display potent α-glucosidase inhibitory activity. *Food Chem.* **2011**, *126*, 1057–1063.
170. Zhang, J.X., Guan, S.H., Feng, R.H., Wang, Y., Wu, Z.Y., Chen, X.H., Bi, K.S., uo, D.A. Neolignanamides, lignanamides, and other phenolic compounds from the root bark of *Lycium chinense*. *J. Nat. Prod*. **2013**, *76*, 51 – 58.

References

171. Zhang, X., Chen, C., Li, Y., Chen, D., Dong, L., Na, W., Wu, C., Zhang, J., Li, Y. Tadehaginosides A-J, phenylpropanoid glucosides from *Tadehagi triquetrum*, enhance glucose uptake via the upregulation of PPARγ and GLUT-4 in C2C12 myotubes. *J. Nat. Prod*. **2016**, *79*, 1249 – 1258.
172. Zhang, Y. L., Luo, J. G., Wan, C. X., Zhou, Z. B., Kong, L. Y. Geranylated 2-arylbenzofurans from *Morus alba* var. *tatarica* and their α-glucosidase and protein tyrosine phosphatase 1B inhibitory activities. *Fitoterapia* **2014**, 116 – 126.

9. List of Abbreviations

$[\alpha]_D$	specific rotation at the sodium D-line
br	broad signal
CC_{50}	cytotoxicity concentration 50%
CD	Circular Dichroism
CH_2Cl_2	dichloromethane
$CHCl_3$	chloroform
COSY	correlation spectroscopy
d	doublet
DCM	dichloromethane
dd	double of doublet
DMSO	dimethyl sulfoxide
DNA	deoxyribonucleic acid
ECD	electronic circular dichroism
ED	effective dose
ESI	electrospray ionization
et al.	et altera (and others)
EtOAc	ethyl acetate
eV	electronvolt
g	gram
HMBC	Heteronuclear Multiple Bond Connectivity
HMQC	Heteronuclear Multiple Quantum Coherence
HSQC	Heteronuclear Single Quantum Coherence
H_2O	water
HPLC	High Pressure Liquid Chromatography
H_3PO_4	phosphoric acid
hr	hour
HR-ESIMS	High Resolution Electronspray Ionization Mass Spectrometry
Hz	Herz
L	liter
LC	liquid chromatography

Abbreviations

LC/MS	liquid chromatography-mass spectrometry
m	multiplet
M	Molar
MeOD	deuterated methanol
MeOH	methanol
mg	milligram
MHz	mega Herz
min	minute
mL	milliliter
mm	millimeter
MRC	Medical Research Council
MS	mass spectrometry
MTT	microculture tetrazolium assay
m/*z*	mass per charge
n-	normal-
μg	microgram
μL	microliter
μM	micromolar
NaCl	sodium chloride
NMR	Nuclear Magnetic Resonance
NOE	Nuclear Overhauser Effect
NOESY	Nuclear Overhauser and Exchange Spectroscopy
ppm	part per million
q	quartet
R	rectus (right)
ROESY	Rotating frame Overhauser Enhancement Spectrocopy
RP 18	reverse phase C 18
s	singlet
S	sinister (left)
sp.	species
t	triplet

Abbreviations

TFA	trifluoroacetic acid
THF	tetrahydrofuran
TLC	Thin Layer Chromatography
t_R	time retention
UV	Ultra Violet
VLC	Vacuum Liquid Chromatography

10. Research Contribution

Publications

Muharini, R., Wray, V., Lai, D., Proksch, P. New flavones C-glycosides from leaves *Sarcotheca griffithii* (Hook F) Hallier F. *Phytochemistry Lett*. **2014**, *9*, 26 – 32

Muharini, R., Liu, Z., Lin, W., Proksch, P. New Amides from the fruits of *Piper retrofractum*. *Tetrahedron Lett*. **2015**, *56*, 2521 – 2525.

Ancheeva, E., Daletos, D., Muharini, R., Lin, W. H., Teslov, L., Proksch, P. Flavonoids from *Stellaria nemorum* and *Stellaria holostea*. *Nat. Prod. Comm*. **2015**, *10*, 437–440.

Omeokoli, B.O., Muharini, R., Okoye, F.B., Ajiwe, V.I., Akpuaka, M.I.U., Lin, W., Liu, Z., Proksch, P., New C-methylated flavonoids and α-pyrone derivative from roots of *Talinum triangualare* growing in Nigeria. *Fitoterapia* **2016**, *109*, 169 – 173.

Muharini, R., Díaz, A., Ebrahim, W., Mándi, A., Kurtán, T., Rehberg, N., Kalscheuer, R., Hartmann, R., Orfali, R.S., Lin, W., Liu, Z., Proksch, P. Antibacterial and cytotoxic phenolic metabolites from fruits of *Amorpha fruticosa*. *Journal of Natural Products*. **2016** (submitted).

11. Curriculum Vitae

Name : Rini Muharini
Nationality : Indonesian
E-Mail Address : riniyansyah@yahoo.com, rinimuharini@chem.edu.untan.ac.id

Educational backgrounds

11.2012 – present	PhD student at the Institute of Pharmaceutical Biology and Biotechnology, Heinrich Heine University of Düsseldorf, Germany. Supervisor : Prof. Dr. Peter Proksch
09.1999 – 10.2002	Master of Science, Organic Natural Product Chemistry at Chemistry Department, Institute of Technology, Bandung (ITB), Indonesia. Supervisor : Prof. Dr. Euis Holisotan Hakim
09.1993 – 01.1999	Bachelor of Science, Chemistry Department, Institute of Technology Sepuluh November (ITS), Indonesia. Supervisor : Dr. Yulfi Zetra

Employment records

12.2008 – present	Educational Chemistry Department, Tanjungpura University, Indonesia
10.2002 – 10.2004	Agricultural Technology, State Polytechnic of Pontianak, Indonesia

Publications

Muharini R., Hakim EH., Achmad SA., Aimi N., Makmur L., Syah YM., Juliawati LD., Kitajima M., Takayama H. Davidiol A, A Stilbenoid Derivative from The Tree Bark of *Shorea guiso* Blume. *Bulletin of The Indonesian Society of Natural Products Chemistry*, **2002**, *2*, 37–40.

Muharini, R., Wray, V., Lai, D., Proksch, P. New flavones C-glycosides from leaves *Sarcotheca griffithii* (Hook F) Hallier F. *Phytochemistry Lett*. **2014**, *9*, 26 – 32

Muharini, R., Liu, Z., Lin, W., Proksch, P. New Amides from the fruits of *Piper retrofractum*. *Tetrahedron Lett*. **2015**, *56*, 2521 – 2525.

Ancheeva, E., Daletos, D., **Muharini, R**., Lin, W. H., Teslov, L., Proksch, P. Flavonoids from *Stellaria nemorum* and *Stellaria holostea*. *Nat. Prod. Comm*. **2015**, *10*, 437–440.

Omeokoli, B.O., **Muharini, R.**, Okoye, F.B., Ajiwe, V.I., Akpuaka, M.I.U., Lin, W., Liu, Z., Proksch, P., New C-methylated flavonoids and α-pyrone derivative from roots of Talinum triangualare growing in Nigeria. *Fitoterapia* **2016**, *109*, 169 – 173.

Curriculum Vitae

Muharini, R., Diaz, A. L., Liu, Z., Ebrahim, W., Mandi, A., Rehberg, N., Kurtán, T., Hartmann, R., Orfali, R.S., Kalscheuer, R., Proksch, P. Antibacterial and cytotoxic phenolic metabolites from fruits of *Amorpha fruticosa*. *J. Nat. Prod*, **2016** (subsmitted).

Conferences

23 - 24.10.2001	Third International Seminar on Tropical Rainforest Plants and Their Utilization for Development, Padang, Indonesia: α-Viniferin, A Trimer stilbenoid and related compounds from *Shorea guiso* Blume.
23 - 27.08.2015	63rd International Congress and Annual Meeting of the Society for Medicinal Plant and Natural Product Research, in Budapest, Hungary: New cytotoxic and antifungal amides from the fruits of *Piper retrofractum*.

Honor

Granted for Green Scouts Exchange Program, The 1st AusAID PCI Exchange Project in Australia Between Scouts of East Java Province and Scouts & Guides of Western Australia, 13th to 28th March 1999.

Granted a full scholarship for Doctoral study from Directorate General of Higher Education, The Ministry of Research, Technology and Higher Education of the Republic of Indonesia.

Society Member

2000 – present	The Indonesian of Natural Products Chemistry.
2014 – present	The Society for Medicinal Plant and Natural Products Research (GA).